





**FARRINGTON DANIELS  
J.W. WILLIAMS  
PAUL BENDER  
ROBERT A. ALBERTY  
C.D. CORNWELL**

**EXPERIMENTAL  
PHYSICAL  
CHEMISTRY**

## *Preface*

To illustrate the principles of physical chemistry, to train in careful experimentation, to develop familiarity with apparatus, to encourage ability in research—these are the purposes of this book, as stated in the first edition a third of a century ago. In each of the five revised editions an attempt has been made to keep pace with the new developments in physical chemistry and to have the book representative of the teaching of the laboratory course in physical chemistry at the University of Wisconsin.

There are many more experiments in this book than can be performed by any one student. Selection will be made on the basis of the time and apparatus available and on the capacity and ultimate aims of the student. If an experiment is too short, the student will find interesting projects under Suggestions for Further Work; if it is too long, the instructor may designate parts of the Procedure to be omitted.

The imperative is not used. Procedures are described, but orders are not given. The student studies the experiment first and then plans his work—a method which develops both his power and his interest.

The high cost of laboratory apparatus restricts the choice of experiments, particularly where classes are small. Nevertheless, there has been no hesitation in introducing advanced apparatus and concepts. If students are not given an opportunity to become familiar with a variety of modern developments and new techniques, they will be handicapped in their later practice of chemistry. Space for additional material has been obtained by abbreviating parts of the last edition and omitting some of the older classical experiments which have found their way into first- and second-year chemistry courses.

All the experiments previously given have been reviewed, and changes have been made, based on continuing class experience. Some experiments have been deleted. New experiments include Knudsen vapor-pressure measurements, X-ray diffraction studies, dielectric constants of solids, dielectric constants of pure polar liquids, kinetics of the bromination of acetone, azeotropic systems, determination of activity coefficients



from liquid-vapor equilibria and from freezing-point equilibria, thermodynamic analysis of the mechanical properties of rubber, and spectrophotometric studies of chemical equilibrium.

A new practice is introduced in this edition. Students should have experience in making detailed calculations from exact data obtained with expensive apparatus such as high-resolution infrared spectrometers, nuclear-magnetic-resonance spectrometers, and microwave spectrometers. Such elaborate equipment is not generally available in the teaching laboratories of physical chemistry. Accordingly, an experiment has been introduced in which the student does no experimental laboratory work but is provided instead with raw data and charts obtained with these instruments, from which he calculates various molecular parameters.

The second part of the book describes apparatus and techniques, particularly for more advanced work. It is designed not only to encourage students to undertake special work, but to aid them in later years in the solution of their laboratory problems. No claim whatsoever is made for completeness. In their selection of material the authors have been guided by their own experience. The difficulty of selection increases with each new edition because the literature on new apparatus and techniques is expanding at an explosive rate, and because commercial instrument manufacturers have developed so many new and improved products. Many comprehensive descriptions of experimental methods may be found in Weissberger's "Technique of Organic Chemistry."

This edition, like its predecessors, owes much to many people—colleagues at the University of Wisconsin, students, laboratory assistants, and teachers in other universities and colleges—who, over the years, have offered thoughtful criticisms and provided many worthwhile suggestions for improvements. The authors greatly appreciate this help and welcome further suggestions for future editions. They are indebted to Professors John D. Ferry, Lawrence F. Dahl, Edward O. Stejskal, Monroe V. Evans, John L. Margrave and other staff members for critical reading of parts of the manuscript. They wish to acknowledge the help of Lawrence Barlow, Lee Thompson, and others connected with the teaching of physical chemistry in this laboratory. They are indebted to Harry A. Schopler for many of the drawings retained from earlier editions, and to Mrs. Irene Frey for careful typing and preparation of the manuscript.

*Farrington Daniels*  
*John Warren Williams*  
*Paul Bender*  
*Robert A. Alberty*  
*C. Daniel Cornwell*

# Contents

<b>Preface</b> . . . . .	<b>v</b>
<b>Symbols</b> . . . . .	<b>xii</b>
<b>PART I. LABORATORY EXPERIMENTS</b>	
<b>Chapter 1. Gases</b> . . . . .	<b>3</b>
1. Gas Density 2. Vapor Density	
<b>Chapter 2. Thermochemistry</b> . . . . .	<b>15</b>
3. Heat of Combustion: Bomb Calorimeter 4. Heat of Solution 5. Heat of Reaction in Solution: Constant-pressure Calorimeter	
<b>Chapter 3. Vapor Pressures of Pure Substances</b> . . . . .	<b>39</b>
6. Vapor Pressure of a Pure Liquid 7. Knudsen Sublimation-pressure Measurement	
<b>Chapter 4. Solutions</b> . . . . .	<b>51</b>
8. Liquid-Vapor Equilibrium in Binary Systems 9. Fractional Distillation 10. Variation of Azeotrope Composition with Pressure 11. Elevation of the Boiling Point 12. Activities from Freezing-point Depression Data 13. Partial Molal Properties of Solutions	
<b>Chapter 5. Homogeneous Equilibria</b> . . . . .	<b>93</b>
14. Equilibrium in Solution 15. Dissociation of Nitrogen Tetroxide 16. Spectrophotometric Determination of an Equilibrium Constant 17. Acid Dissociation Constant of Methyl Red	
<b>Chapter 6. Heterogeneous Equilibria</b> . . . . .	<b>110</b>
18. Distribution of a Solute between Immiscible Solvents 19. Phase Diagram of a Binary Solid-Liquid System 20. Three-component Systems 21. Solubility as a Function of Temperature	
<b>Chapter 7. Chemical Kinetics</b> . . . . .	<b>129</b>
22. Hydrolysis of Methyl Acetate 23. Reaction of Ethyl Acetate with Hydroxyl Ion 24. Inversion of Sucrose 25. Bromination of Acetone	

<b>Chapter 8. Irreversible Processes in Solution . . . . .</b>	<b>147</b>
26. Viscosity of Liquids 27. Conductance Behavior of Weak and Strong Electrolytes 28. Transference Number of the Hydrogen Ion by the Moving-boundary Method 29. Transference Number of the Silver Ion by the Hittorf Method 30. The Dropping-mercury Electrode	
<b>Chapter 9. Electromotive Force . . . . .</b>	<b>183</b>
31. Single-electrode Potentials 32. The Hydrogen Electrode 33. The Glass Electrode 34. Free Energy and the Equilibrium Constant 35. Thermodynamics of Electrochemical Cells	
<b>Chapter 10. Dielectric and Optical Properties of Matter . . . . .</b>	<b>212</b>
36. Dipole Moment from Dielectric-constant Measurements on Solutions; Heterodyne-beat Method 37. Dielectric Constants of Polar Liquids; Resonance Method 38. Dielectric Constant of a Solid as a Function of Temperature 39. Optical Rotatory Dispersion	
<b>Chapter 11. Spectroscopy . . . . .</b>	<b>243</b>
40. Spectrometry and Spectrography 41. Raman Spectrum 42. Spectroscopic Methods for the Study of Molecular Structure	
<b>Chapter 12. Diffraction . . . . .</b>	<b>288</b>
43. X-ray Diffraction of Crystals	
<b>Chapter 13. Macromolecular Chemistry . . . . .</b>	<b>296</b>
44. Viscosity of High-polymer Solutions 45. Determination of the Osmotic Pressure of a Solution of High Polymer 46. Ion-exchange Chromatography 47. Sedimentation Rate and Particle Size Distribution 48. Thermodynamic Analysis of Rubberlike Elasticity	
<b>Chapter 14. Surface Chemistry . . . . .</b>	<b>321</b>
49. Surface Tension 50. Adsorption from Solution 51. Adsorption of Gases	
<b>Chapter 15. Photochemistry . . . . .</b>	<b>339</b>
52. Photohydrolysis of Monochloroacetic Acid	
<b>Chapter 16. Radioactive Isotopes and Tracers . . . . .</b>	<b>343</b>
53. Determination of Range and Energy 54. The Szilard-Chalmers Process and the Half-life of Radioiodine 55. Exchange Reactions with Deuterium Oxide	
<b>Chapter 17. General Experimental Techniques . . . . .</b>	<b>361</b>
56. Glassblowing 57. High Vacuum 58. Electronics	
<b>PART II. APPARATUS AND METHODS</b>	
<b>Chapter 18. Treatment of Experimental Data . . . . .</b>	<b>393</b>
Errors of Measurement . . . . .	393
Estimation of Experimental Errors—Influence of Experimental Errors	

on the Final Result—Addition and Subtraction—Multiplication or Division—Propagation of Probable Errors—Random Errors	
Significant Figures . . . . .	404
Representation of Data . . . . .	405
Tabular Representation—Representation of Data by Graphs—Representation of Data by Equations	
Error Problems. . . . .	414
<b>Chapter 19. Opticochemical Measurements . . . . .</b>	<b>418</b>
Refractometry . . . . .	418
Refractometers Measuring Critical Angle—Differential Instruments—Schlieren Techniques—Interferometric Methods	
Light Scattering . . . . .	422
Microscopy. . . . .	424
Light Microscope—Electron Microscope	
Polarimetry. . . . .	426
<b>Chapter 20. Thermal Measurements . . . . .</b>	<b>428</b>
Thermometry . . . . .	428
The International Temperature Scale—Mercury Thermometers—Other Liquid Thermometers—Bimetallic Thermometers—Gas Thermometers—Resistance Thermometers—Thermocouples—Optical Pyrometers	
Calorimetry. . . . .	437
<b>Chapter 21. Physical Properties of Fluids . . . . .</b>	<b>439</b>
Physical Properties of Gases . . . . .	439
Volume by Displacement—Flowmeters—Manometers—Bourdon Gauge—Deadweight Gauge—Pumps	
Determination of the Boiling Point . . . . .	445
Superheating—Ebullimeters	
Measurement of Vapor Pressure. . . . .	447
Dynamic Method—Static Method—Gas-saturation Method—Isopiestic Method	
Fractional Distillation. . . . .	449
High-vacuum Distillation	
Density . . . . .	452
Pycnometers—Buoyancy Methods—Floating Equilibrium—Falling Drop	
Viscometry . . . . .	456
Surface Tension . . . . .	457
Diffusion . . . . .	458
Free Diffusion—Restricted Diffusion—Steady-state Diffusion	
Osmotic Pressure . . . . .	460
<b>Chapter 22. Electrical Measurements . . . . .</b>	<b>463</b>
Galvanometers. . . . .	463
Measurement of Electromotive Force . . . . .	466
Potentiometers—Recording Potentiometers—Standard Cells—Standard Electrodes	
Measurement of Electrolytic Conductance. . . . .	471

Alternating-current Wheatstone Bridge—Conductivity Cells—Conductance of Potassium Chloride Solutions—Conductance Water	
Measurement of Current and Quantity of Electricity . . . . .	476
Measurement of Electrical Energy in Calorimetry . . . . .	477
Measurement of Transference Numbers and Ionic Mobilities . . . . .	479
Measurement of Dielectric Constant . . . . .	480
Measurements at Very High Frequencies	
<b>Chapter 23. Nuclear and Radiation Chemistry . . . . .</b>	<b>484</b>
Availability of Isotopes . . . . .	484
Analysis for Stable Isotopes . . . . .	485
Mass Spectrometry	
Analysis for Radioactive Isotopes . . . . .	486
Ionization Chambers—Proportional Counters—Geiger-Müller Counters—Scintillation Counters—Solid-state Detectors—Neutron Counters—Miscellaneous Methods	
Radiation Chemistry . . . . .	493
Radiation Safety	
<b>Chapter 24. Purification of Materials . . . . .</b>	<b>495</b>
Methods—Crystallization—Fractional Distillation—Azeotropic Distillation—Adsorption—Drying—Zone Refining—Criteria of Purity—Water—Mercury—Benzene—Hydrocarbons—Sodium Chloride—Sodium Hydroxide	
<b>Chapter 25. Photochemistry . . . . .</b>	<b>502</b>
Sources of Light . . . . .	502
Tungsten Filament—Mercury Arc—Other Arcs	
Techniques for Producing Atoms and Radicals . . . . .	505
Optical Filters . . . . .	506
Glass Filters—Solutions—Gelatin Filters—Interference Filters	
Monochromators . . . . .	508
Thermopiles . . . . .	508
Calibration	
Bolometers . . . . .	511
Photoelectric Cells . . . . .	511
Reaction Cells . . . . .	513
Photography . . . . .	514
<b>Chapter 26. Spectroscopy . . . . .</b>	<b>519</b>
Resolution—Sensitivity—Bandwidth and Response Time—Saturation Effect—Absorption and Dispersion	
Radiofrequency Spectrometer . . . . .	522
Microwave Spectrometer . . . . .	529
Infrared Spectrometer . . . . .	534
<b>Chapter 27. Electronics . . . . .</b>	<b>542</b>
Alternating-current Circuit Theory . . . . .	543
Basic Circuit Elements—Properties of Sinusoidal Waveforms—Impedance—Impedance of a Network	
Parallel Resonant Circuit . . . . .	550

Active Circuit Elements—Thévenin's Theorem—Impedance Matching—Magnetic Coupling—Response to Nonsinusoidal Excitation—Amplitude Modulation and Detection—Frequency Modulation—Mixing—Harmonic Generation—Bandwidth and Response Time	
Vacuum Tubes. . . . .	559
The Diode and Rectification—The Triode and Amplification—Graphical Analysis of Triode Amplifier—Dynamic Characteristics of Triodes—Gain of a Triode Amplifier—Equivalent Circuit—Practical Triode-amplifier Circuit—The Pentode	
Semiconductor Devices . . . . .	570
Semiconductors—Thermistors—Diodes—Transistors	
Noise . . . . .	577
Noise as the Ultimate Limit to Sensitivity—Frequency Distribution of Noise—Johnson Noise—Shot-effect Noise—Flicker-effect Noise—Current Noise—Noise in Transistors—Noise Figure—Noise Calculations	
Measurements and Test Equipment. . . . .	581
Multimeters—Vacuum-tube Voltmeters—Potentiometric Instruments—The Cathode-ray Oscilloscope—Measurement of Resistance, Capacitance, and Inductance—Measurement of Frequency—Time and Frequency Standards	
Miscellaneous Electronic Circuits . . . . .	588
Full-wave-rectifier Power Supply—Alternating-current Voltage Regulators—Direct-current Voltage Regulator—Constant Current Supply—Vacuum-tube Relay—Cathode Follower—Amplifier with Feedback—Amplifiers with Negative Feedback—Narrow-band (Frequency-selective) Audio Amplifier—Vacuum-tube Oscillator—Eccles-Jordan Trigger Circuit—Pulse-counting, or Scaling, Circuit—Phase-sensitive Detector	
Safety Precautions. . . . .	608

## APPENDIX

Algebra of Complex Numbers . . . . .	609
Physical-Chemical Constants . . . . .	610
Values of the Defined Constants. . . . .	610
Values of the Basic Constants . . . . .	611
Values of the Derived Constants. . . . .	611
Values of Certain Auxiliary Relations . . . . .	611
Reduction of Barometer Readings on a Brass Scale to 0° . . . . .	611
Vapor Pressure of Water . . . . .	612
Density of Water in Grams per Milliliter . . . . .	613
Concentration Scales . . . . .	614
Color-code Conventions for Electronic-circuit Components . . . . .	615
Schematic Symbols for Electronic-circuit Components. . . . .	617
Common Abbreviations of Electronics . . . . .	618
<b>Index.</b> . . . .	<b>619</b>

**International Atomic Weights, 1956–1957 (FRONT END PAPER)**

**Table of Logarithms (BACK END PAPER)**



## Symbols

<i>A</i>	reciprocal moment of inertia, absorbancy
<i>A</i>	angstrom
<i>B</i>	rotational constant, reciprocal moment of inertia
<i>C</i>	heat capacity, capacitance
<i>D</i>	diffusion coefficient
<i>E</i>	potential difference, voltage, electric field
<i>E<sub>a</sub></i>	Arrhenius activation energy
<i>F</i>	faraday
<i>G</i>	Gibbs free energy
<i>H</i>	enthalpy, magnetic field strength
<i>I</i>	ionic strength, moment of inertia, intensity of light, current, angular momentum (nuclear spin)
<i>J</i>	angular momentum (generalized), spin-spin coupling constant, rotational quantum number
<i>K</i>	equilibrium constant
<i>K</i>	Kelvin scale
<i>K<sub>b</sub></i>	boiling-point elevation constant
<i>K<sub>f</sub></i>	freezing-point depression constant
<i>L</i>	angular momentum (orbital)
<i>M</i>	molecular weight
<i>M</i>	molar scale
<i>N<sub>0</sub></i>	Avogadro's number
<i>P</i>	pressure, polarization, angular momentum (molecular rotation)
<i>R</i>	gas constant
<b>R</b>	Rydberg constant
<i>S</i>	entropy
<i>T</i>	absolute temperature, Kelvin scale
<i>T<sub>+</sub>, T<sub>-</sub></i>	transference number
<i>U</i>	internal energy, potential energy function for diatomic molecule
<i>V</i>	volume
<i>W</i>	energy
<i>X</i>	mole fraction
<i>Z</i>	compressibility factor
<i>G</i>	electrical conductance
<i>H, <math>\hat{H}</math></i>	Hamiltonian, Hamiltonian operator
<i>P</i>	molar polarization
<i>R</i>	molar refractivity

$a$	activity, lattice constant
$a_s$	absorbancy index
$c$	concentration in moles per liter, number of components in phase rule, velocity of light
$d$	distance
$e$	electronic charge, electron, voltage (time-dependent part)
ev	electron volts
$f$	fugacity, frequency
$g$	acceleration of gravity
$h$	Planck's constant
$i$	current (time-dependent part)
$k$	Boltzmann constant, reaction-rate constant cell constant
$l$	mean free path, ionic conductance
$m$	mass, molal concentration
m	molal scale
$n$	number of moles, refractive index
$p$	partial pressure, number of phases in phase rule, linear momentum
pH	measure of hydrogen-ion activity
$q$	quantity of heat absorbed
$r$	internuclear distance, particle radius
$t$	centigrade temperature, time
$v$	velocity, variance
$w$	work done
$y$	activity coefficient on molar scale
$\alpha$	degree of dissociation, angle of optical rotation, alpha particle
$\beta$	beta particle
$\gamma$	activity coefficient on the molal scale, gamma ray, surface tension, gyromagnetic ratio
$\epsilon$	dielectric constant, energy of a radiation quantum
$\eta$	viscosity
$\theta$	freezing-point depression, boiling-point elevation
$\varphi$	fugacity coefficient
$\kappa$	specific conductance
$\lambda$	wavelength
$\Lambda$	equivalent conductance
$\mu$	dipole moment, chemical potential, micron, reduced mass
$\nu$	frequency
$\bar{\nu}$	wave number
$\rho$	density
$\tau$	torque
$\Sigma$	summation

$\Phi$	quantum yield
$\omega$	angular velocity

A superscript zero on a symbol for a thermodynamic quantity means that the value given corresponds to standard-state conditions.

A symbol  $\Delta$ , as in  $\Delta H$ , indicates the increment in the thermodynamic quantity accompanying the change from the initial to the final state.

A bar over the symbol for a thermodynamic quantity designates the partial molal quantity (which for a pure substance is equal to the molar value of the quantity).

The notation used for vectors (quantities having magnitude and direction) is illustrated by the following example:

$\mathbf{A}$  = vector quantity

$A$  = magnitude of  $\mathbf{A}$

$A_x, A_y, A_z$  = components of  $\mathbf{A}$  along axes  $x, y, z$ , respectively.

**PART I**

***Laboratory Experiments***

## CHAPTER 1

# *Gases*

### 1. GAS DENSITY

This experiment illustrates the simplest and most direct method for determining the molecular weight of a gas. The density of a gas is determined also by means of a density balance.

**Theory.** According to the ideal-gas law,

$$PV = \frac{g}{M} RT \quad (1)$$

where  $P$  = pressure

$V$  = volume

$T$  = absolute temperature ( $t^{\circ}\text{C} + 273.15^{\circ}$ )

$g$  = weight of gas of molecular weight  $M$

For the evaluation of the ideal-gas constant  $R$ , measurements with a substance of known molecular weight are required. The chemical scale of atomic and molecular weights is defined by taking the molecular weight of atmospheric† oxygen as 32 g mole<sup>-1</sup>. Careful experiments have shown that the pressure-volume product for 32 g of oxygen at 0°C approaches 22.414 liter-atm as the pressure approaches zero, leading to the value of 0.08205 liter-atm mole<sup>-1</sup> deg<sup>-1</sup> for  $R$ . From measurements of  $P$  and  $V$  for a known weight  $g$  of gas at a known absolute temperature  $T$ , a value of an unknown molecular weight  $M$  may be calculated. For permanent gases and pressures of the order of atmospheric pressure, this value of  $M$  is reasonably accurate, but, strictly speaking, Eq. (1) is obeyed exactly only as the pressure approaches zero.

In the second part of the experiment the density of a gas is determined by means of a density balance. The principle of Archimedes is used, according to which the upward force is equal to the weight of the gas displaced. A large glass bulb on a balance beam is counterpoised

† By international agreement this definition of the chemical atomic-weight scale has recently been replaced by one in which the atomic weight of the isotope C<sup>12</sup> is taken as 12.000000. This lowers atomic weights by 43 ppm relative to the old chemical scale, but this change is not significant for most purposes.

with a weight. A reference gas such as oxygen is admitted, and its pressure adjusted. The density at this pressure  $P_1$  of the reference gas of molecular weight  $M_1$  may be written as

$$\left(\frac{g}{V}\right)_1 = \frac{P_1 M_1}{RT} \quad (2)$$

If the apparatus is evacuated and another gas admitted, the pressure has to be adjusted to a different value in order to obtain a zero reading on the balance. At this new pressure the density of the gas of molecular weight  $M_2$  is the same as that given by Eq. (2). If the temperature is constant

$$P_1 M_1 = P_2 M_2 \quad (3)$$

Thus, for gases which obey the ideal-gas law, this equation offers a convenient method for determining the molecular weight of an unknown gas.

**Apparatus.** A 200-ml thin-walled bulb with a small capillary stopcock; counterpoise of same volume; analytical balance; vacuum-pump and manometer assembly; gas-density balance; barometer; carbon dioxide; other gases.

**Procedure.** Gases are weighed in the glass bulb of the type shown in Fig. 1. The bulb is first weighed evacuated, and it is then weighed after filling to a known pressure with a gas the molecular weight of which is to be determined.

In weighing large glass vessels it is necessary to maintain uniform conditions. The bulb is wiped with a clean damp cloth and allowed to stand in the balance for 5 or 10 min to come to constant weight. A counterpoise, consisting of a closed glass bulb of practically the same volume, is used on the opposite balance pan to minimize errors due to adsorption of moisture and changes in buoyancy of the air due to barometric fluctuations.

The assembled apparatus is shown in Fig. 1. The pressure is read to a fraction of a millimeter on a closed-end manometer. The pressure inside the glass bulb  $B$ , in millimeters of mercury, is equal to the difference in height of the mercury menisci in the two limbs of the manometer. The tube at the base of the manometer has a small bore to prevent splashing the mercury when the pressure is raised or lowered suddenly.

The bulb is first evacuated to 1 mm or less with a motor-driven oil pump that is properly protected by use of a suitable trap. In order to obtain a steady pressure, it is important that the system be free of leaks, as proved by evacuating the bulb and observing that the mercury levels in the manometer remain constant when the connection to the pump is closed. Leaks at the rubber connections may be stopped by substituting new gum rubber which fits tightly over the glass tubes and



by winding wire around the connection, which is then painted with a solution of Glyptal resin.

The bulb is removed from the rubber connecting tube, wiped with a clean, damp (not wet), lintless cloth, and allowed to hang in the balance

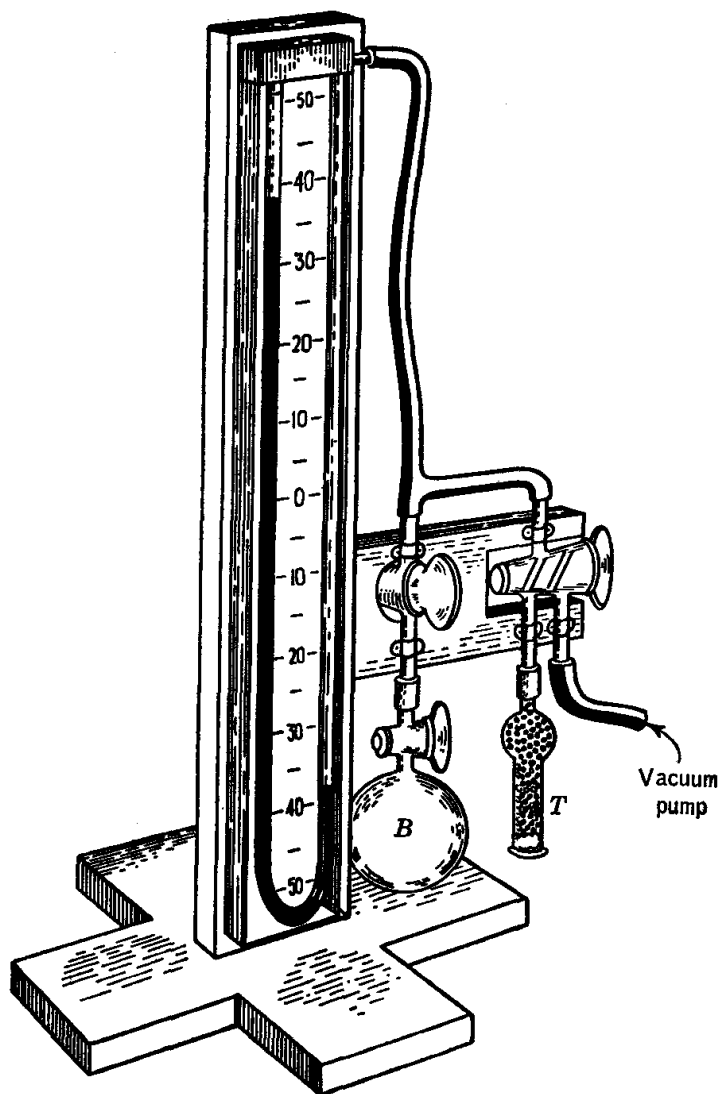


FIG. 1. Manometer and vacuum system for gas-density measurements.

for 5 or 10 min to come to constant weight. The counterpoise, wiped in the same way, is used on the opposite pan.

The bulb is replaced in the apparatus and subjected to a second evacuation, after which it is weighed again. If the two weights do not check, the process is repeated until they do check.

The evacuated bulb is now filled with carbon dioxide or other gas from a tank. A diaphragm regulator connected to the tank is used to regulate

the pressure. The bulb is returned to the vacuum system which has previously been evacuated. With the two-way stopcock closed, the stopcock on the bulb is opened and the pressure measured. The temperature of the air in the vicinity of the bulb is recorded. After wiping with a damp cloth and waiting for equilibrium in the balance case, the bulb of gas is weighed. After weighing, the bulb is again evacuated and filled cautiously with carbon dioxide, the measured temperature and pressure are recorded, and the bulb is weighed.

The weight of carbon dioxide is determined in the same manner at about  $\frac{3}{4}$  and again at about  $\frac{1}{2}$  atm pressure. It is essential in this work that there be no leaks.

The density of air or city gas or of some unknown gas or mixture of gases may be determined, introducing the gas through the drying tube *T*.

The volume *V* of the bulb in cubic centimeters is obtained by weighing it empty and filled with distilled water. The bulb is filled by evacuating it, closing the stopcock, immersing the end of the tube in a beaker of distilled water, and then opening it to permit the bulb to fill. A hypodermic syringe may be used to complete the filling of the bulb. The bulb is then emptied by use of a water aspirator and placed in a drying oven. It is evacuated several times while hot to remove the last traces of moisture.

In the second part of the experiment, the gas-density balance is used to determine the average molecular weight of dry air. A balance developed by Edwards<sup>5</sup> is illustrated in Fig. 2. The case of the balance is connected to a closed-end manometer and has connections for attaching a vacuum pump or tank of purified gas. The window at the end of the balance containing the counterpoise is marked so that the position of the pointer may be determined.

Several readings are made on gas of known molecular weight such as oxygen. The pressure necessary to bring the pointer to the zero point is determined.

The pressure required for a zero balance with air, which has been passed through a tower of soda lime to remove water vapor, is determined next. In order to fill the gas balance with a new gas, it is evacuated, filled with gas, evacuated, and refilled with gas to sweep out the last traces of the first gas. A second density reading is then taken after further sweeping out with the new gas. If the two readings do not agree, the sweeping process is continued until two successive readings agree closely.

**Calculations.** If the counterpoise has practically the same volume as the bulb, it is unnecessary to make a correction for the buoyancy of the air (see Appendix).

The weight *g* of the gas is obtained by subtracting the weight of the dry evacuated bulb from that of the bulb when filled with the gas.

If a closed-end manometer is used, the observed pressure in millimeters of mercury is corrected to 0° by use of the equation

$$P_0 = P - P \frac{\alpha t - \beta(t - t_s)}{1 + \alpha t} \quad (4)$$

where  $P_0$ ,  $P$  = corrected and observed pressures

$t$  = centigrade temperature of manometer

$t_s$  = temperature at which scale was calibrated, normally 20°C

$\alpha$  = mean cubical coefficient of expansion of mercury between 0 and 35°

$\beta$  = linear coefficient of expansion of scale material

The value of  $\alpha$  is  $181.8 \times 10^{-6}$ , and the value of  $\beta$  is  $18.4 \times 10^{-6}$  for brass.

If a wooden scale is used, taking the value of  $\beta$  equal to zero introduces a negligible error, since  $\beta$  for wood is about  $5 \times 10^{-6}$ .

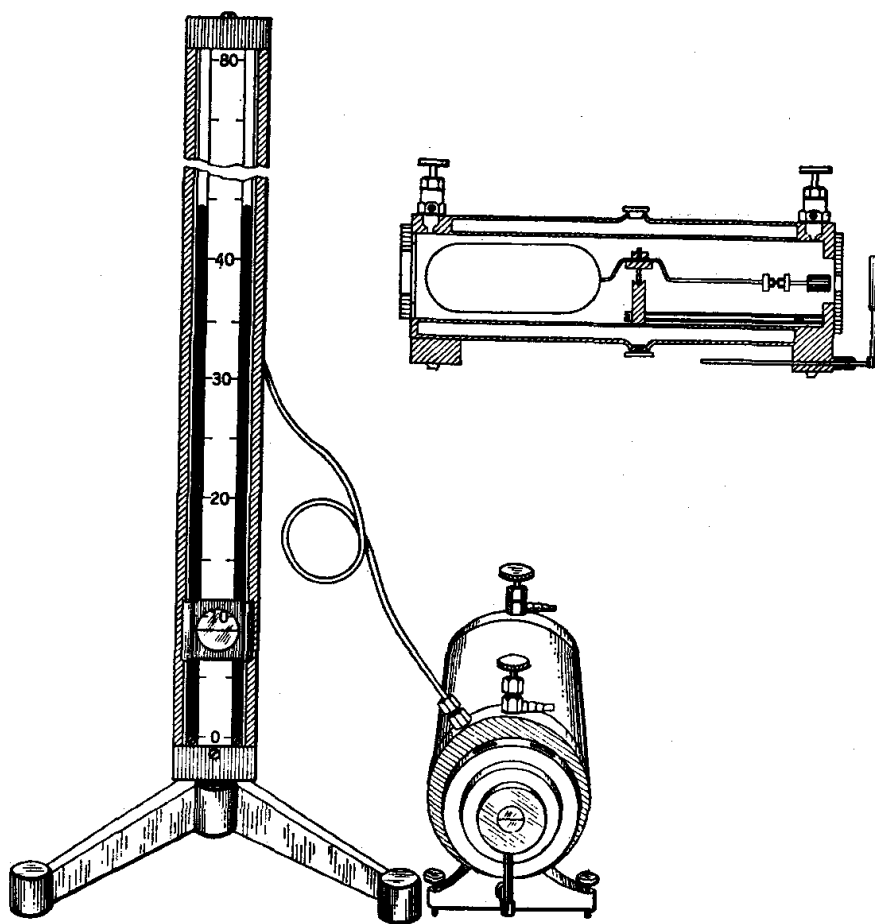


FIG. 2. Gas-density balance.

If an open-end manometer is used, the pressure in the bulb is equal to the difference between the corrected barometer pressure (see Appendix) and the manometer pressure corrected by use of Eq. (4).

The molecular weight of carbon dioxide is calculated at each pressure. If carbon dioxide were a perfect gas, the calculated molecular weight would be the same at all pressures. In determining the true molecular weight of a gas, it is necessary to plot the molecular weight obtained at different pressures and extrapolate to zero pressure. If the precision of the data warrants, a more accurate value of the molecular weight of carbon dioxide may be obtained in this way.

The mean molecular weight of air is calculated from measurements with the gas-density balance by using Eq. (3) and compared with the average molecular weight obtained from the known composition of air.

**Practical Applications.** The formula of a chemical compound may be calculated from the molecular weight, together with the atomic weights, and the percentage composition found by chemical analysis. In the most accurate work, globes of 8 to 20 liters have been used and corrections were made for the loss of buoyancy of the globe when it contracted on evacuation.<sup>1</sup> The determination of the density of ammonia gas by Dietrichson and coworkers<sup>4</sup> illustrates the experimental techniques used in accurate work. Birge and Jenkins<sup>2</sup> have discussed the methods for extrapolating to the limiting gas density and the errors involved. The work of Cady and Rarick<sup>3</sup> indicates the high precision with which molecular weights may be determined with a gas-density balance.

The chemical equilibrium between different gases may often be calculated from the density of the equilibrium mixture of gases.

**Suggestions for Further Work.** The accurate determination of the molecular weight of hydrogen gas by this method constitutes a real test of a student's care and skill.

The molecular weights of other gases may be determined. Small tanks of methane, ethylene, nitrous oxide, Freon, and other gases can be purchased.

The percentage composition of a mixture of two gases such as oxygen and carbon dioxide may be determined from the density of the mixture.

More exact values of the molecular weights may be calculated with equations of state such as those of Berthelot, van der Waals, or Beattie and Bridgman. However, the use of these equations requires a knowledge of certain constants characteristic of the gas which will not be available for an unknown gas.

The gas-density balance is well adapted to measuring the density of a mixture of gases. For example, the carbon dioxide content of the exhaled breath may be determined by blowing the breath through a calcium chloride drying tube and a cotton packing into the balance.

In the analysis of a mixture of gases, the density in grams per liter is determined with the balance, and the density of each pure gas at the same pressure is known. A formula is derived that will give the percentage composition corresponding to the observed density at the observed pressure. It is assumed that any interaction among the different gases leading to density changes is negligible in the experiments described here.

#### References

1. Baxter and Starkweather, *Proc. Natl. Acad. Sci. U.S.*, **12**, 699 (1926).
2. Birge and Jenkins, *J. Chem. Phys.*, **2**, 167 (1934).
3. Cady and Rarick, *J. Am. Chem. Soc.*, **63**, 1357 (1941).

4. Dietrichson, Bircher, and O'Brien, *J. Am. Chem. Soc.*, 50, 1-21 (1933).
5. Edwards, *Ind. Eng. Chem.*, 9, 790 (1917).

## 2. VAPOR DENSITY

This experiment illustrates a practical method for determining the molecular weight of a volatile material. It provides excellent practice in the use of physical-chemical apparatus, which demands some skill in manipulation.

**Theory.** The density of a vapor is more easily determined than the density of a gas because the substance may be weighed accurately when condensed to a liquid at room temperature. Very accurate vapor-density results can be obtained in this way. When only moderate accuracy is required, the Victor Meyer<sup>2,3</sup> method is one of the simplest, and it is still frequently used.

A known weight of liquid is vaporized in a chamber maintained at an appropriate and constant high temperature. The air displaced from the chamber is cooled to room temperature, and its volume carefully measured. Substitution of air for the actual vapor thus provides a means of determining the volume the known weight of vapor would occupy at room temperature if it could be cooled without condensation.

It should be noted that it is not necessary that the temperature of the vaporization chamber be known, but it must be constant.

**Apparatus.** Modified Victor Meyer apparatus; gas burette and leveling bulb; 1° thermometer; barometer; glass bulblets; carbon tetrachloride, benzene, acetone, or chloroform; water aspirator; large and small test tube.

**Procedure.** A modified form of the Victor Meyer apparatus is assembled as shown in Fig. 3. It consists essentially of four parts: (a) a small bulblet containing a weighed amount of a volatile liquid, (b) a vaporizer tube which contains the vapor after the bulblet is broken, (c) a gas burette for measuring the volume of air displaced by the formation of the vapor, and (d) a steam generator connected to a heating jacket surrounding the vaporizer tube.

The bulblets for containing the weighed samples of liquid are made by drawing out 4 mm soft glass as shown in Fig. 4. The tubing is rotated evenly during the heating operation. The micro flame shown is formed by a jet of gas issuing from a capillary section drawn at the end of a Pyrex tube. After drawing, bending, and sealing the right-angled tail, the bulblet is weighed on an analytical balance. About 0.1 ml of the liquid to be used is placed in a miniature test tube ( $\frac{3}{8}$  by 2 in.), and the latter is then placed in a large test tube (1 by 6 in.) with the open capillary of the bulblet dipping into the liquid. A stopper with outlet tube is

fitted to the test tube and attached by vacuum tubing to a water aspirator. The tube is evacuated, and some of the air contained in the bulblet bubbles out. The vacuum is then broken by suddenly removing the connecting tube, and the liquid is driven into the bulblet. The bulblet is then removed and inverted to drain the capillary, and the capillary is

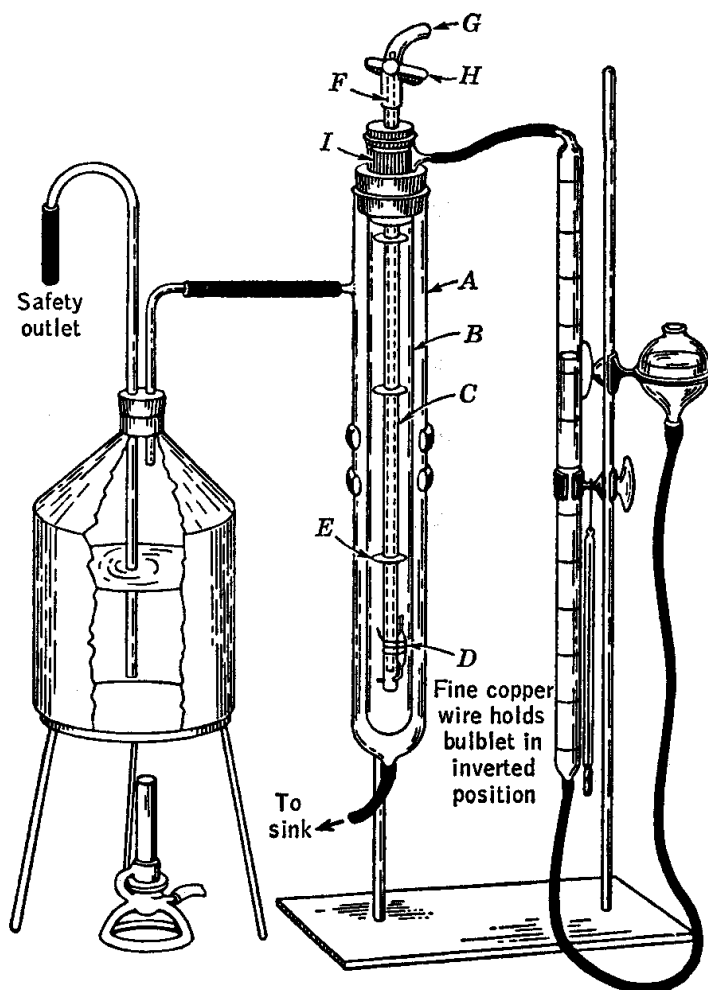


FIG. 3. Modified Victor Meyer apparatus.

sealed off with a small flame from a wing-top bunsen burner or a Pyrex capillary, about an inch from the end, care being taken that no liquid is present in the immediate area of heating and that the flame does not strike the open end of the capillary, where it can deposit condensed water. The sealed bulblet with its liquid and the remaining sealed-off end are then weighed again to obtain the weight of the liquid. Any liquid remaining in the open capillary tip which has been sealed off must be removed before weighing. Because leaking bulblets are the main cause of difficulty in this experiment, the quality of the seal should be tested. The bulblet, in a



*dry* miniature test tube, is returned to the filling apparatus, which is then evacuated as far as possible with the water aspirator. Any serious deficiency in the seals will become obvious by leakage.

The assembled apparatus is shown in Fig. 3. The inner vaporizer tube *B*, 40 cm in length and 2 or 3 cm in diameter, is provided with a

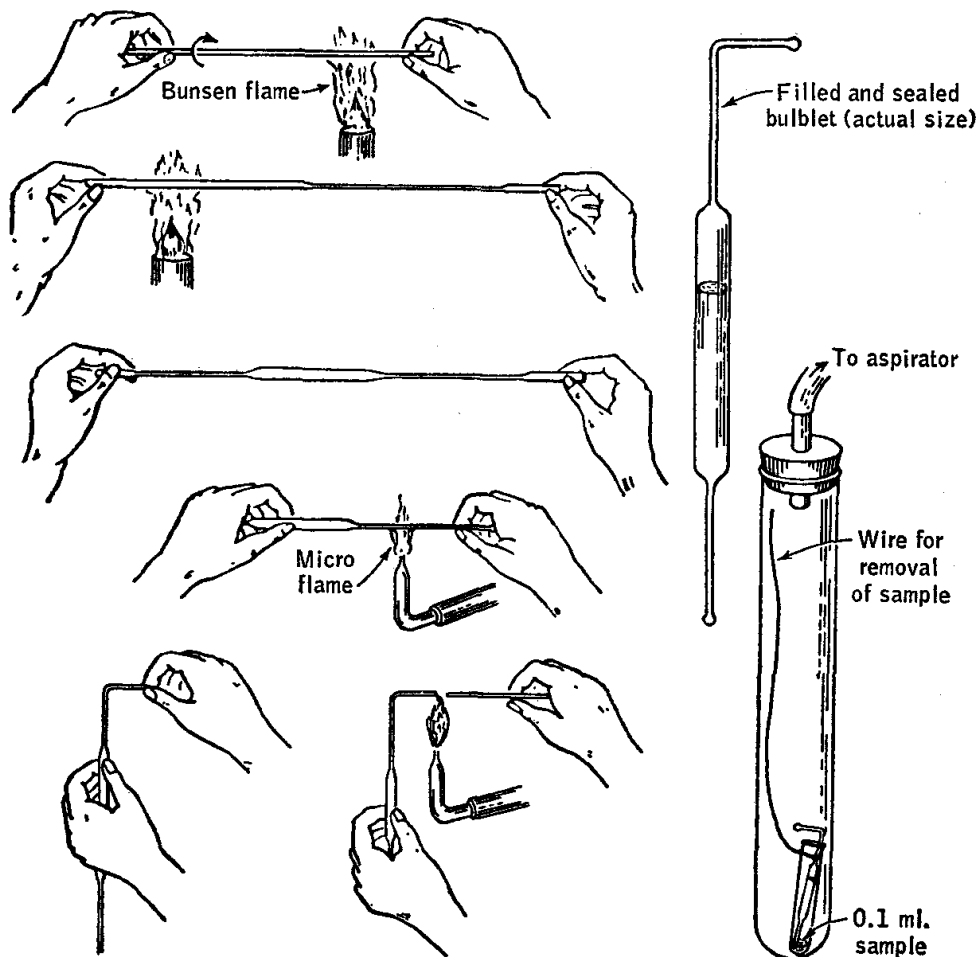


FIG. 4. Preparation and filling of Victor Meyer bulblet.

rubber stopper through which passes a brass tube *C*. At the bottom of the tube *C* a hole is bored through both walls to hold the bent tail of the bulblet *D*. Three or four metal disks, spaced along the brass tube *C* and somewhat smaller in diameter than the vaporizer tube, reduce the rate of upward progress of the vapor when the bulblet is broken and thus reduce the chance of condensing vapor. They are cut from thin metal and provided with a central hole so that they can be slipped along the tube and soldered in position. A loosely fitting cylinder *I* of suitable plastic or hard rubber is placed at the top of the tube to reduce the dead air space and hasten the attainment of thermal equilibrium.

A loosely fitting brass rod *F* passes through the tube *C* and ends just above the holes drilled in it for holding the bulblet. It is securely held at its upper end by a rubber tube *G* which passes around both the brass tube and the brass rod, thus providing a vertically adjustable but gas-tight joint. The rod is pushed down at the appropriate time to break the bent tail of the bulblet.

A side arm at the top of the vaporizer tube *B* leads through a rubber tube to a gas burette and leveling bulb, which is filled with water.

The vaporizer tube is surrounded by an outer jacket *A* of Pyrex which is about 40 cm long and 5 cm in diameter. It is centered in a ring stopper and is connected through a sidearm to a steam generator with a safety tube. The bottom of the jacket is provided with an outlet and rubber tube through which condensed water and excess steam pass to a sink.

When the bulblets have been filled and weighed and the steam jacket is operating, the vaporizer is swept out with a current of air to remove any condensible vapor from previous determinations. The rubber stopper containing the brass tube is loosened to provide air entrance, and the aspirator draws air through the vaporizer and the rubber tube *G*.

The apparatus is assembled with the sealed bulblet in an inverted position as shown in Fig. 3. After steam has passed through the jacket for at least 10 min, the stoppers are tightened and the screw clamp *H* is closed. The vaporizer is tested for leaks and thermal equilibrium by lowering the leveling bulb to create a pressure less than that of the atmosphere. If the water in the burette does not continue to fall when the leveling bulb is maintained at this lower level, the apparatus is air-tight and in thermal equilibrium. The apparatus is then in condition for the start of the experiment.

The reading of the gas burette is taken with the leveling bulb adjusted to make the liquid level the same in the bulb and in the burette. The pressure inside the system is then equal to atmospheric pressure. The brass rod is now pushed down sufficiently to break off the lower capillary tip of the bulblet, whereupon the heated liquid is rapidly vaporized. As the vaporization takes place, the leveling tube is lowered so as to maintain nearly equal pressure inside and outside the apparatus, to minimize leakage. When the hot air displaced into the gas burette cools, a slight contraction may be noted. When the level of the liquid in the burette ceases to change position, the levels of the liquid are carefully adjusted to exactly the same height, and the final reading of the volume is made. After the apparatus has stood for a longer time, the volume of the measured air may decrease, because of diffusion of the vapor from the vaporizer into the cooler parts of the apparatus where it condenses. The final reading is taken before such condensation occurs, just as soon as the level becomes constant. The temperature is taken from a thermometer hang-

ing close to the burette. For more precise work, the measuring tube may be jacketed with a concentric tube containing water and a thermometer.

Carbon tetrachloride, benzene, or any low-boiling liquid may be used. The material must be pure. Two or more determinations are made until satisfactory checks are obtained. After each determination the vapor is removed before a second experiment is started, for an excessive volume of vapor leads to condensation in the connecting tube.

The apparatus should not be dismantled until the calculations have been made and the results compared.

**Calculations.** The pressure is read from the barometer and corrected to 0°C, using tables or calculations (Appendix). The correction amounts to 2 or 3 mm. Another correction should be made for water vapor in the measured air volume. The partial pressure of water in the gas burette is equal to  $p_{\text{H}_2\text{O}}^\circ$ , the vapor pressure of water at the prevailing temperature. The air introduced from the vaporization tube has a partial pressure of water vapor,  $rp_{\text{H}_2\text{O}}^\circ$ , determined by the relative humidity  $r$  of the laboratory air. The latter may be determined with a sling psychrometer or, more conveniently, a hair hygrometer reading directly in relative humidity. The difference in partial pressure of water between saturated air and the unsaturated laboratory air is subtracted from the total pressure  $P$  in the burette, which is equal to the atmospheric pressure as recorded by the barometer. This correction assumes that no diffusion of water vapor into the vaporization tube occurs during the preliminary phases of the experiment, and it becomes less accurate if the experiment requires an extended period of time.

The molecular weight  $M$  of the vapor is calculated from the familiar equation

$$pV = \frac{g}{M} RT$$

where  $p$  = partial pressure, in burette, of air displaced by vapor  
 $= P - p_{\text{H}_2\text{O}}^\circ(1 - r)$

$V$  = volume of displaced air, ml

$T$  = absolute temperature at which volume is measured

$g$  = weight of liquid taken

$R$  = gas constant

Better results are obtained by using van der Waals' equation or Berthelot's equation. A convenient form of the latter is

$$M = g \frac{RT}{PV} \left[ 1 + \frac{9}{128} \frac{P}{P_c} \frac{T_c}{T_s} \left( 1 - 6 \frac{T_c^2}{T_s^2} \right) \right]$$

where  $P_c$  = critical pressure of compound used

$T_c$  = critical temperature of compound used

$T_s$  = temperature of steam jacket

Such an equation is obviously of no use in the case of an unknown compound, since the critical temperature and pressure will not be known. It is used, however, for testing the reliability of the apparatus on known substances.

**Practical Applications.** The determination of the molecular weight is useful in identifying a chemical compound and in establishing its formula.

When gases dissociate on heating, the equilibrium may be studied quantitatively through measurements of the gas densities.

**Suggestions for Further Work.** The densities of several organic or inorganic vapors may be measured. For substances having boiling points above 80°, some liquid boiling higher than water must be used to generate vapor for the jacket,<sup>2</sup> or a furnace may be used for extremely high temperatures.<sup>5</sup> The jacket should be at a temperature at least 20° above the boiling point of the substance whose vapor density is being determined, because of the failure of the gas laws to apply to vapors that are near the condensation point.

#### References

1. Evans, *J. Am. Chem. Soc.*, **35**, 958 (1913).
2. Harris and Meyer, *Ber.*, **27**, 1482 (1894), and earlier papers.
3. Kretschmer and Wiebe, *J. Am. Chem. Soc.*, **76**, 2579 (1954).
4. Meyer, *Ber.*, **11**, 1867 (1878).
5. Meyer and Meyer, *Ber.*, **12**, 1112 (1879).

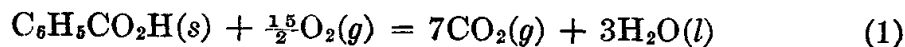
## CHAPTER 2

# Thermochemistry

### 3. HEAT OF COMBUSTION: BOMB CALORIMETER

The enthalpy of combustion is determined in this experiment by means of a bomb calorimeter.

**Theory.**<sup>3,5,8</sup> The standard enthalpy of combustion for a substance is defined as the enthalpy change,  $\Delta H_T^\circ$ , which accompanies a process in which the given substance undergoes reaction with oxygen gas to form specified combustion products [such as  $\text{CO}_2(g)$ ,  $\text{H}_2\text{O}(l)$ ,  $\text{N}_2(g)$ ,  $\text{SO}_2(g)$ ], all reactants and products being in their respective standard states at the given temperature  $T$ . Thus the standard enthalpy of combustion of benzoic acid at  $298.15^\circ\text{K}$  is  $\Delta H_{298.15^\circ}$  for the process



with reactants and products in their standard states for this temperature.

As will be shown below, the enthalpy of combustion can be calculated from the temperature rise which results when the combustion reaction occurs under adiabatic conditions in a calorimeter. It is important that the reaction in the calorimeter take place rapidly and completely. To this end, the material is burned in a steel bomb with oxygen under a pressure of about 25 atm. A special acid-resistant alloy is used for the construction of the bomb because water and acids are produced in the reaction.

In the adiabatic-jacket bomb calorimeter (Fig. 5) the bomb is immersed in a can of water, fitted with a precise thermometer. This assembly is placed within an outer water-filled jacket. Both before and after the combustion occurs, the jacket temperature is maintained (by external means) at the same value as that of the water in the can. If the temperatures are matched with sufficient accuracy, the can and contents do not gain or lose energy by radiation or conduction, and the process is therefore adiabatic.

This method affords convenience in work of moderate accuracy, but there is inevitably some error due to time lag in adjustment of the outer-

jacket temperature. For the most exacting research measurements, an isothermal jacket is used and accurate cooling corrections are made.<sup>3-5a, 5c, 8</sup>

It should be recognized that the process which actually takes place in the calorimeter does not correspond exactly to one of the type of Eq. (1). In the actual calorimeter process, the final and initial temperatures are not equal and the reactants and products are not in their standard states.

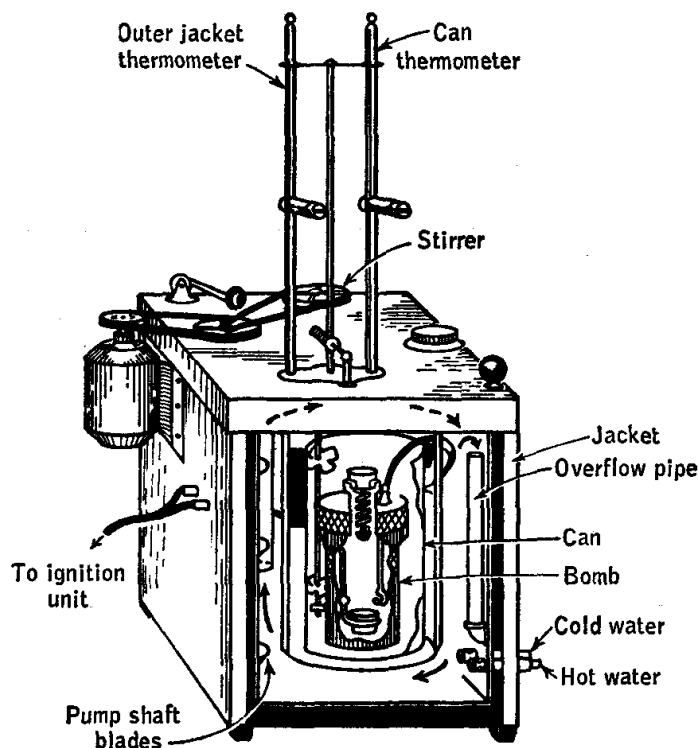


FIG. 5. Adiabatic combustion calorimeter (Parr series 1200 calorimeter with 1102 bomb).

The relationship of the calorimeter process to the isothermal standard-state process may be clarified by reference to Fig. 6. The initial and final temperatures in the calorimeter process are  $T_1$  and  $T_2$ , respectively. The various states of interest are shown, and on each arrow is written the energy change for the *can and contents* in going from one state to another in the direction indicated. Here  $\Delta U_c$  is the energy change for the actual calorimeter process, while  $\Delta U_{T_1}$  is the energy change for an imagined process in which the final state is at  $T_1$  rather than  $T_2$ . The heat capacity  $C$  is that for the can and its contents under the conditions of the experiment. The work of expansion of water in the can is entirely negligible.

The first law of thermodynamics,

$$\Delta U = q - w \quad (2)$$



where  $\Delta U$  = internal energy change for the system

$q$  = energy transfer into the system by heat flow

$w$  = work done by the system

may be applied to the actual calorimeter process, which is assumed to be adiabatic ( $q = 0$ ). In the present experiment,  $w$ , which consists mainly of the work of stirring, can be neglected,<sup>†</sup> and Eq. (2) then becomes

$$\Delta U_c = 0 \quad (3)$$

Since the energy change is independent of path, one has

$$\Delta U_c = \Delta U_{T_1} + \int_{T_1}^{T_2} C dT \quad (4)$$

Since the temperature change is small, it is usually valid to consider  $C$  to

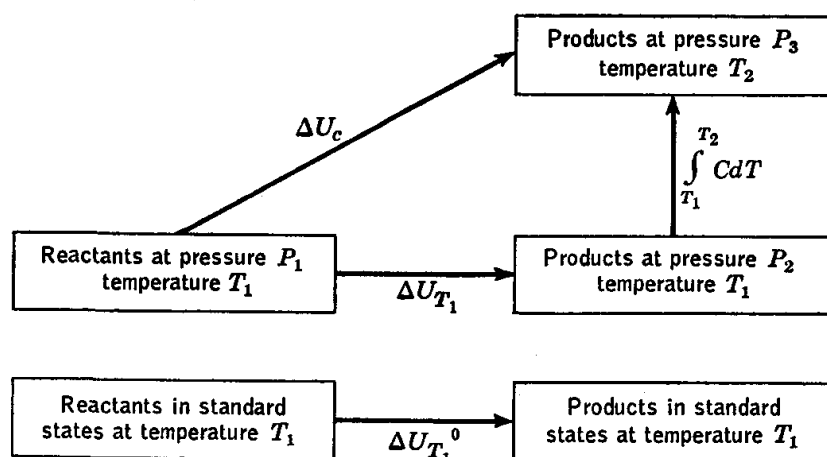


FIG. 6. Relationship among pertinent states of the calorimeter system (comprising the can and its entire contents). The energy change in going from one state to another is shown near the arrow connecting the states.

be constant, so that the integral becomes equal to  $C(T_2 - T_1)$ . One then obtains

$$\Delta U_{T_1} = -C(T_2 - T_1) \quad (5)$$

It may be observed that a temperature rise corresponds to a negative  $\Delta U_{T_1}$ , that is, to a decrease in energy for the imagined isothermal process.

The next step is to calculate  $\Delta U_{T_1}^0$  from  $\Delta U_{T_1}$ . Although the energy is not sensitive to changes in pressure, the correction to standard states, called the Washburn correction, may amount to several tenths of a per cent and is important in work of high accuracy.<sup>5b,9</sup> The principal Washburn correction terms allow for the changes in  $U$  associated with (a) changes in pressure, (b) mixing of reactant gases and separating

<sup>†</sup> In the isothermal-jacket method, mentioned above, the stirring term is not neglected, but rather is effectively eliminated along with the heat transfer by making a correction to the observed temperature rise.<sup>3,4,8</sup>

product gases, and (c) dissolving reactant gases in, and extracting product gases from, the water in the bomb.

The standard enthalpy change  $\Delta H_{T_1}^\circ$  may then be calculated. The definition of  $H$  leads directly to

$$\Delta H_{T_1}^\circ = \Delta U_{T_1}^\circ + \Delta(PV) \quad (6)$$

Since the standard enthalpy and energy for a real gas are so defined as to be the same, respectively, as the enthalpy and energy of the gas in the

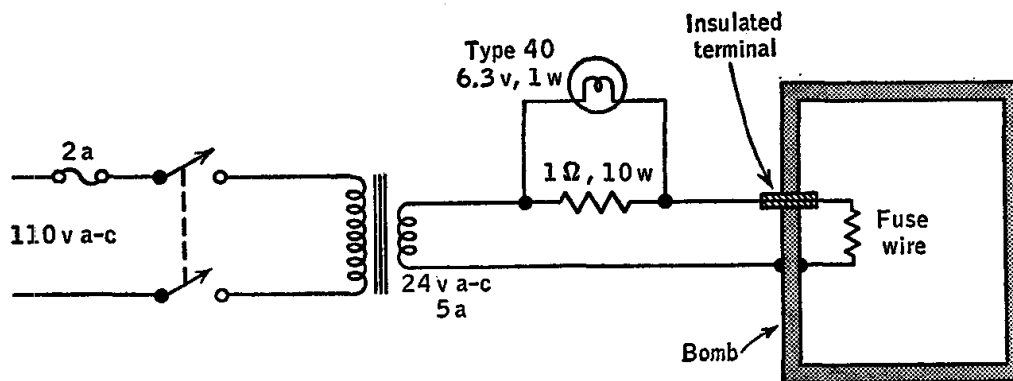


FIG. 7. Ignition circuit for bomb calorimeter. The fuse wire inside the bomb becomes hot and initiates combustion of the sample. The wire itself is oxidized, and the circuit thereby is opened. When this happens, the lamp ceases to glow. The switch is of the momentary contact type. The circuit as shown is suitable for use with a 10-cm length of Parr 45C10 fuse wire.

zero-pressure limit, the ideal-gas equation may be used to evaluate the contribution of gases to  $\Delta(PV)$  in Eq. (6). The result is

$$\Delta(PV) = (n_2 - n_1)RT \quad (7)$$

where  $n_2$  = number of moles of gaseous products

$n_1$  = number of moles of gaseous reactants

The contribution to  $\Delta(PV)$  from the net change in  $PV$  of solids and liquids in going from reactants to products is generally negligible.

**Apparatus.** Parr, Emerson, or other adiabatic calorimeter; pellet press; two thermometers graduated to  $0.01^\circ$ ; fuse wire, having a known heat of combustion per unit length; benzoic acid, naphthalene, or other samples.

**Procedure.** A Parr-type calorimeter† is shown in Fig. 5, and a suitable ignition circuit in Fig. 7. The outer jacket is heated by adding hot water. In an Emerson-type calorimeter, jacket heating is accomplished by passing alternating current directly through the water of the

† A calorimeter with semimicro bomb (22 ml) suitable for samples up to about 0.2 g is available from Parr Instrument Co., Moline, Ill., at a cost appreciably below that of the standard-size-bomb calorimeter described above.

outer jacket.<sup>1</sup> In either type, cooling of the jacket is accomplished by adding cold water.

The two thermometers read in the range 18 to 30°C or thereabouts and should be graduated to 0.01°. It is convenient to use a matched pair, although, as an alternative, one may be calibrated relative to the other; the correction may be assumed to be constant.

The following precautions must be followed if the danger of explosion is to be avoided:<sup>4</sup>

1. The amount of sample must not exceed 1 g.
2. The oxygen pressure must not exceed 30 atm.
3. The bomb must not be fired if gas bubbles are leaking from it when submerged in water.
4. The operator should stand back for at least 15 sec after igniting the sample and should keep clear of the top of the calorimeter. An explosion would be most likely to drive the top upward.
5. Much less than 1 g of sample should be used for testing materials of unknown combustion characteristics.
6. The use of high-voltage ignition systems is to be avoided. Arcing between electrodes may cause the electrode seals to fail and permit the escape of hot gases with explosive force.

A little less than 1 g of the sample is formed into a pellet by means of a pellet press; this is done to prevent scattering of material during the combustion, with consequent incompleteness of reaction. The pellet is weighed and placed in the sample pan. The fuse wire, of measured length about 10 cm and known heat of combustion per unit length, is attached to the two terminals and adjusted to give firm contact with the pellet. It is important to avoid getting kinks in the fuse wire since fusion may occur at such points before the portion of wire in contact with the pellet becomes hot enough to initiate combustion.

The surfaces at which closure of the bomb is to be effected must be kept scrupulously clean, and every precaution taken to avoid marring them. The parts of the dismantled bomb should be placed on a clean, folded towel.

The cover is carefully assembled with the bomb and tightened by means of a wrench (Emerson) or by hand (Parr). The bomb is then connected to the oxygen tank, and oxygen is admitted *slowly* until the pressure is 25 atm. The valves are then closed, the pressure in the line is relieved, and the bomb is removed.

About 2000 ml of water, the temperature of which has been adjusted so as to be at least several degrees below the upper limit of the thermometer range, and preferably close to room temperature, is weighed in the calorimeter can; the latter is then placed within the adiabatic jacket. The ignition leads are connected, and the bomb is immersed in the water.

(With the Parr bomb, one ignition wire is connected to the terminal on the cover, the other to the can, which makes electrical contact with the bomb.)

The water in the can must cover the bomb. If gas bubbles escape, the assembly ring may require tightening, or the gaskets may need to be replaced.

The cover of the adiabatic jacket is set in place, and the thermometers lowered into position. The stirrer is started, and the jacket temperature is then adjusted to within  $0.03^\circ$  of that of the water in the can. The thermometer in the can is read for a few minutes to be sure that equilibrium has been attained. This temperature is recorded as the initial temperature  $T_1$ . The ignition switch is then closed until fusion of the wire is indicated by glowing of the lamp (Fig. 7). However, the switch should not be held closed for more than about 5 sec, because damage to the ignition unit or undue heating by passage of current through the water may result.

If combustion has occurred, the temperature of the water in the can will be seen to rise within a few seconds. Otherwise the leads should be examined, the voltage output of the ignition circuit checked, or the bomb opened and examined for possible sources of trouble.

After a successful ignition, the temperature of the calorimeter rises quickly. The jacket temperature should be kept as close as possible to that of the can. After several minutes the rate of change of the temperature becomes sufficiently small that the difference between the can and jacket temperatures can be reduced to a few hundredths of a degree. The final steady temperature of the can is then recorded as  $T_2$ .

Next, the bomb is removed, the pressure relieved by opening the valve, and the cover removed. If the sample contained nitrogen, the acid residue in the bomb is washed quantitatively with water into a flask and titrated with 0.1 N NaOH. However, the nitric acid titration may be omitted in work of moderate accuracy if the only source of nitrogen is the air initially present in the bomb. In any case, the length of the residue of unoxidized fuse wire is measured. The bomb and calorimeter are carefully cleaned and dried after each experiment.

Two runs are made with benzoic acid for determination of the heat capacity of the calorimeter, and two with naphthalene (or other sample) for determination of the enthalpy of combustion.

**Calculations.** The heat capacity  $C$  may be written as

$$C = mC_{\text{H}_2\text{O}} + C_0 \quad (8)$$

where  $m$  = mass of water in can

$C_{\text{H}_2\text{O}}$  = heat capacity of water per gram =  $0.999 \text{ cal deg}^{-1} \text{ g}^{-1}$  at room temperature

Here  $C_0$  represents the heat capacity of the calorimeter (bomb and contents, can, immersed portion of thermometer, etc.). The value of  $C_0$  may be assumed to be the same for all four runs.

For the benzoic acid runs,  $\Delta U_{T_1}$  is considered to be known and  $C_0$  may be calculated from the temperature rise. The value of  $\Delta U_{T_1}$  is calculated by allowing<sup>3</sup>  $-6318 \text{ cal g}^{-1}$  of benzoic acid burned and the value specified by the manufacturer† for the wire burned. The contribution from nitric acid formed may be calculated when necessary as  $-13,800 \text{ cal}$  per mole of  $\text{HNO}_3$  produced.

The data for the naphthalene runs are used to calculate  $\Delta U_{T_1}^\circ$  and the standard heat of combustion  $\Delta H_{T_1}^\circ$ ; for student work, the difference between  $\Delta U_{T_1}$  and  $\Delta U_{T_1}^\circ$  may be considered negligible. The values of  $\Delta U_{T_1}^\circ$  and  $\Delta H_{T_1}^\circ$  should be reported for one mole of sample.

The standard enthalpy of formation of naphthalene is then calculated from the values  $-94.05$  and  $-68.32 \text{ kcal mole}^{-1}$  for the standard enthalpies of formation of  $\text{CO}_2(g)$  and  $\text{H}_2\text{O}(l)$ , respectively, at  $25^\circ$ . If the experimental values of  $T_1$  are within a few degrees of  $25^\circ$ , the correction of the enthalpy of combustion from  $T_1$  to  $25^\circ$  may be omitted.

**Practical Applications.** For many modern technological developments, such as rocket-propulsion systems, it is obviously necessary to have good thermochemical data.

**Suggestions for Further Work.** The enthalpy of combustion of a liquid sample may be determined. The sample is sealed off in a thin-walled glass bulb.<sup>8</sup> A weighed quantity of naphthalene or paraffin oil is placed around the bulb. When ignited, this will break the glass and start combustion of the liquid.

Solid samples which cannot be formed easily into pellets are placed in the sample pan around the fuse wire. The oxygen must be admitted slowly to prevent scattering of the powder.

#### References

1. Daniels, *J. Am. Chem. Soc.*, **38**, 1473 (1916).
2. International Critical Tables, Vol. V, p. 162, McGraw-Hill Book Company, Inc., New York (1928).
3. Jessup, Precise Measurement of Heat of Combustion with a Bomb Calorimeter, *Natl. Bur. Standards (U.S.), Monograph*, **7** (1960).
4. Oxygen Bomb Calorimetry and Combustion Methods, Parr Instrument Co., Tech. Manual 130, Moline, Ill. (1960).
5. Rossini (ed.), "Experimental Thermochemistry," Interscience Publishers, Inc., New York (1956). (a) Chap. 3 by Coops, Jessup, and van Nes. (b) Chap. 5 by Hubbard, Scott, and Waddington. (c) Chap. 6 by Prosen.
6. Selected Values of Chemical Thermodynamic Properties, *Natl. Bur. Standards (U.S.), Circ.*, **500** (1952).
7. "Selected Values of Physical and Thermodynamic Properties of Hydrocarbons and Related Compounds," American Institute Research Project 44 Report, Carnegie Press, Pittsburgh (1955).

† For example,  $-2.3 \text{ cal cm}^{-1}$  for Parr 45C10 (No. 34 B & S gauge Chromel C).

8. Sturtevant in Weissberger (ed.): "Technique of Organic Chemistry," 3d ed., Vol. I, Pt. I, Chap. 10, Interscience Publishers, Inc., New York (1959).
9. *Ibid.*, pp. 597-598.

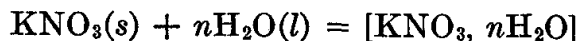
#### 4. HEAT OF SOLUTION

The integral heat of solution of potassium nitrate in water is determined as a function of concentration. From these data differential heats of solution and integral heats of dilution are calculated.

**Theory.** The quantitative study of the thermal effects which accompany the solution of a solute in a pure solvent or a solution has been systematized through the introduction of the concepts of the integral and differential heats of solution.

The *integral heat of solution*  $\Delta H_{I.S.}$  at a particular concentration is the heat of reaction† at a specified temperature and pressure when *one mole of solute* is dissolved in enough pure solvent to produce a solution of the given concentration.

Thus  $\Delta H_{I.S.}$  for  $\text{KNO}_3$  in water equals the enthalpy change for the process‡



For example, if one mole of solute is dissolved in 500 g of water at constant  $T$  and  $P$ , the heat of reaction gives the value of the integral heat of solution at the concentration 2 molal.

The *differential heat of solution* of the solute is defined as

$$\left[ \frac{\partial(\Delta H_s)}{\partial n_2} \right]_{T,P,n_1}$$

where  $\Delta H_s$  is the enthalpy change for the dissolving, at constant  $T$  and  $P$ , of  $n_2$  moles of solute in  $n_1$  moles of solvent. The differential heat of solution may be visualized as the enthalpy change for the addition, at constant  $T$  and  $P$ , of a *mole of solute* to so large a quantity of *solution* that the addition of one more mole of solute does not change the molality appreciably. Now the addition, at constant  $T$  and  $P$ , of  $dm$  moles of solute to a solution already containing  $m$  moles of solute in 1000 g of solvent (hence, of molality  $m$ ) produces the enthalpy change  $d(m\Delta H_{I.S.})$ ; hence the differential heat of solution of the solute is given by

$$\left[ \frac{\partial(\Delta H_s)}{\partial n_2} \right]_{T,P,n_1} = \left[ \frac{\partial(m\Delta H_{I.S.})}{\partial m} \right]_{T,P} \quad (1)$$

† Because the processes considered here take place at constant pressure and only pressure-volume work is involved, the heats of reaction are given by the corresponding enthalpy changes.

‡ The symbol on the right-hand side of this equation refers to a solution consisting of one mole of  $\text{KNO}_3$  in  $n$  moles of water.

The differentiation indicated on the right side of Eq. (1) may be carried out explicitly to obtain

$$\left(\frac{\partial \Delta H_s}{\partial n_2}\right)_{T,P,n_1} = \Delta H_{\text{I.S.}} + m \left(\frac{\partial \Delta H_{\text{I.S.}}}{\partial m}\right)_{T,P} \quad (2)$$

Note that all the quantities on the right side of Eq. (2) are dependent on molality, so that the differential heat of solution also is a function of molality.

The magnitudes of these heats of solution depend specifically on the solute and solvent involved. The value of the heat of solution at high dilutions is determined by the properties of the pure solute and by the interactions of the solute with the solvent. As the concentration of the solution increases, the corresponding changes in the differential and integral heats of solution reflect the changing solute-solvent and solute-solute interaction effects.

For the interpretation of heat-of-solution data for some systems, it is instructive to compare the results with the behavior predicted for ideal solutions. An ideal solution may be defined as one which obeys Raoult's law over the entire range of concentrations being considered. It can be shown<sup>3</sup> that the mixing, at constant  $T$  and  $P$ , of pure liquid solvent with such a solution produces no change in enthalpy. From this it follows that for the case of a *liquid* solute, dissolving to form an ideal solution,  $\Delta H_{\text{I.S.}} = 0$ . For the case of a *solid* solute which dissolves to form an ideal solution,  $\Delta H_{\text{I.S.}}$  equals the molar heat of fusion to give the (super-cooled) liquid at the temperature of the solution. Such behavior is approximated in some actual cases, which involve nonelectrolyte solutes and nonpolar solvents (e.g., naphthalene in benzene). For electrolyte solutes the actual behavior is very different from the ideal case, because of marked solute-solvent and solute-solute interactions.

The *integral heat of dilution*  $\Delta H_{D,m_1 \rightarrow m_2}$  between two molalities  $m_1$  and  $m_2$  is defined as the heat effect, at constant temperature and pressure, accompanying the addition of enough solvent to a quantity of solution of molality  $m_1$  containing *one mole of solute* to reduce the molality to the lower value  $m_2$ . The process to which the integral heat of solution at molality  $m_2$  refers is equivalent to the initial formation of the more concentrated solution of molality  $m_1$  followed by its dilution to the lower molality  $m_2$ ; the integral heat of dilution is thus equal to the difference of the integral heats of solution at the two concentrations involved:

$$\Delta H_{D,m_1 \rightarrow m_2} = \Delta H_{\text{I.S.}}(m_2) - \Delta H_{\text{I.S.}}(m_1) \quad (3)$$

**Apparatus.** Heat-of-solution calorimeter; sensitive mercury thermometer (18 to 31° in 0.01° divisions); potentiometer and potential divider; thermistor thermometer with Wheatstone bridge and lamp and scale galvanometer; calibrated ammeter with

1-amp scale; 6-volt d-c power supply; stop watch or electric timer; six weighing bottles or 10-ml Erlenmeyer flasks with stoppers; potassium nitrate; switch and wire.

**Procedure.**<sup>5</sup> This experiment illustrates the special advantage that endothermic reactions offer for calorimetric measurements. When the reaction absorbs heat, the cooling effect may be balanced with electrical

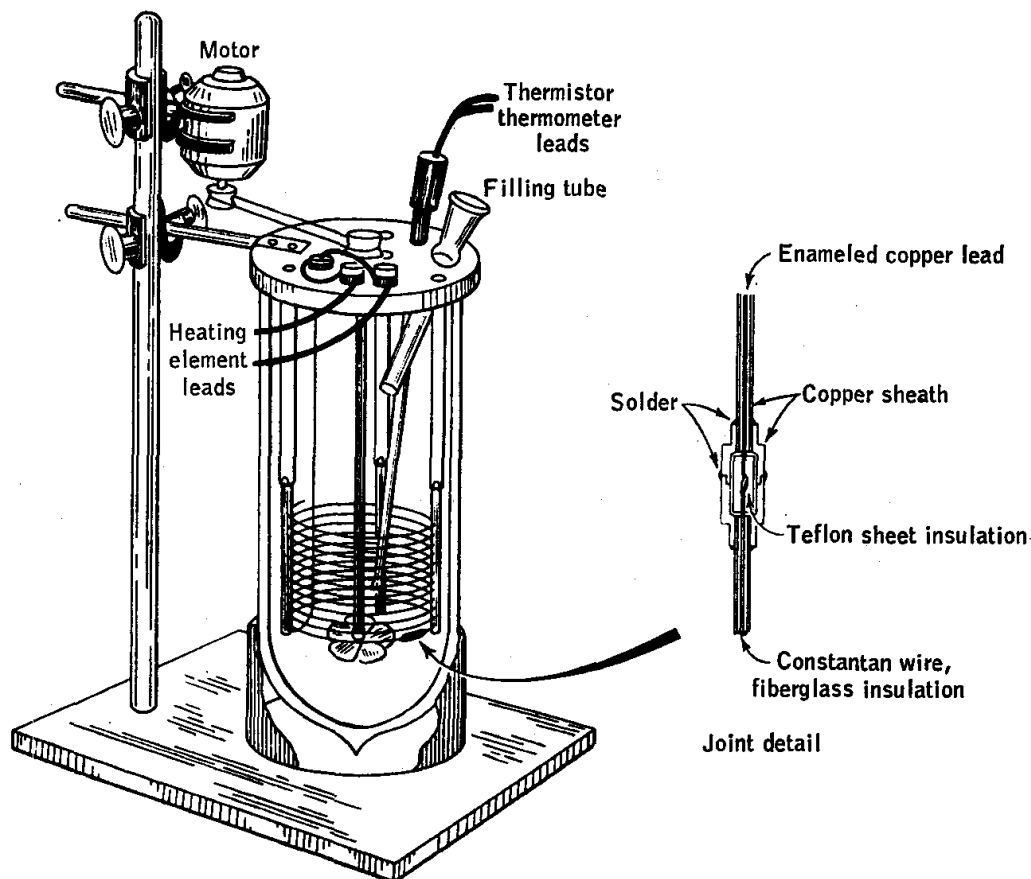


FIG. 8. Calorimeter for measuring heats of solution.

heating to prevent any change of temperature. It thus becomes unnecessary to know the heat capacity of the calorimeter or of the solution being studied. No cooling correction is necessary, and the method is simpler than the ordinary adiabatic method.

The essential features of a suitable calorimeter for work of moderate precision are shown in Fig. 8. The vacuum bottle minimizes heat exchange between the solution and the surroundings. A mechanical stirrer is used to provide the efficient and uniform stirring essential to the rapid solution of the solute. The rate of stirring, however, should be kept as low as efficiency permits to minimize the energy introduced by stirring. The stirrer shaft should be of a poor heat conductor, and proper bearings must be provided to eliminate as far as is possible heat



generation by friction. (The shaft bearings should be located above the calorimeter proper.) A belt-and-pulley drive is used to keep the heat transfer by conduction and radiation from the motor at a minimum.

The calorimeter heating element should have a low temperature coefficient of resistance and a low time lag in transferring heat to the solution and must be electrically insulated from the solution. These requirements can conveniently be met by use of copper-sheathed Fiber-glas-insulated constantan wire.† The copper sheath, soldered to the resistance wire at one end, serves as one electrical lead. At the other end, the sheath is cut back to expose a short section of the wire, to which an enameled copper lead wire is then soldered. A section of copper sheath from which the resistance wire has been removed is slipped over the lead wire, and a water-tight joint‡ is made between the two sections, as shown, for example, in Fig. 8. The heater-coil assembly should remain immersed for some distance past the joint to ensure its temperature equilibration with the solution. A heater resistance of about 7 ohms, as given by about 5 ft of 24-gauge constantan wire, is recommended because the current obtained by use of a 6-volt storage battery or regulated d-c supply§ can be determined accurately with a 1-amp ammeter.

As temperature indicator, a sensitive mercury thermometer may be used, but a thermistor (page 571) is recommended because of its rapid and sensitive response to temperature changes. A conventional student d-c Wheatstone bridge with lamp and scale galvanometer readily makes available a thermometric sensitivity of the order of a millidegree.

A schematic diagram of the electrical circuits involved is given in Fig. 9. The timer is actuated by a ganged switch so that the time that current flows through the heating coil will be measured. Temperature indication is achieved by means of a thermistor immersed in the solution. The resistance  $R_t$  of the thermistor varies rapidly with temperature (about 80 ohms  $\text{deg}^{-1}$  near room temperature with  $R_t$  about 2000 ohms).

The resistance of the heating coil  $R_h$  must be measured with the current flowing since its resistance increases with increasing temperature. This is accomplished by measuring the potential drop across  $R_h$  by means of a potentiometer while a known current is passing. The value of  $R_h$  is then calculated by using Ohm's law. Since the potential drop across  $R_h$  is about 7 volts, it is necessary to use a potential divider if the ordinary type of laboratory potentiometer is to be used. The potential-divider

† This wire assembly is made by the Precision Tube Company, Inc., North Wales, Pennsylvania, under the name Precision Coaxitube.

‡ The brass fittings can be prepared at any machine shop.

§ A compact, regulated transistorized supply convenient for this application is available from Sorensen and Company, Inc., South Norwalk, Conn. (Q.M. Series D.C. Power Supplies).

ratio  $(R_1 + R_2)/R_2$  is chosen to be 10:1. Since the current may change somewhat during the balancing process, the current should be noted at a time when the potentiometer is in balance. For the calculation of  $R_h$ , it is to be noted that the current indicated by the ammeter includes a current through the potential divider as well as the current through the heating coil.

The calibration of the ammeter is checked by measuring the potential drop across a standard resistance  $R_s$  in series with the heater.

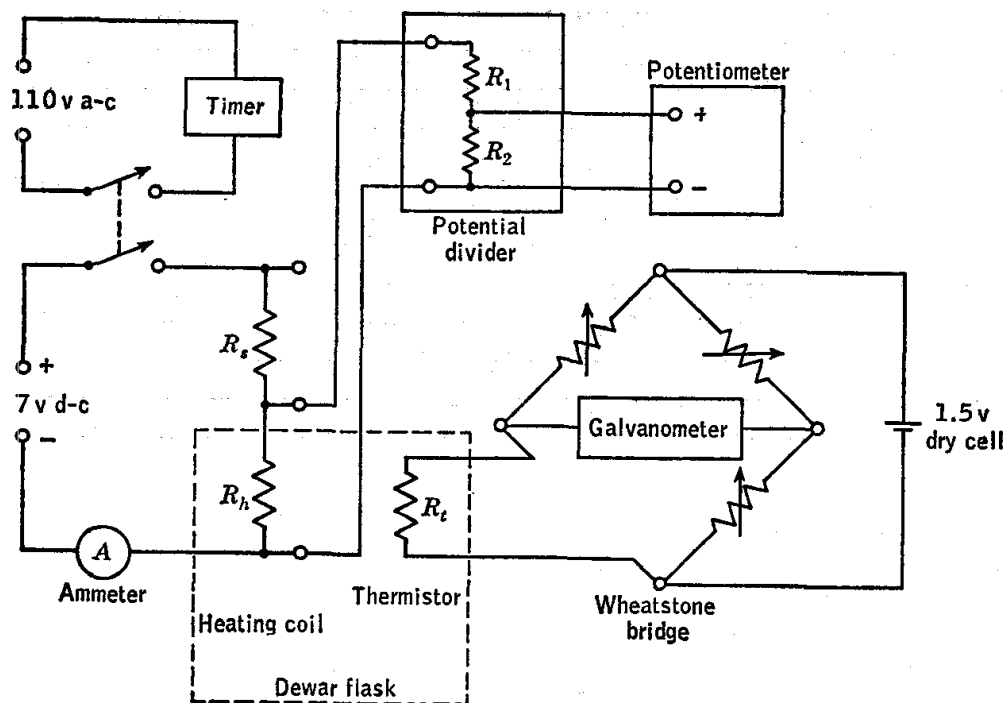


FIG. 9. Schematic diagram of electrical circuits for measurement of heat of solution.

Six samples of finely pulverized potassium nitrate, three of about 8 g and one each of 3, 4, and 5 g, are transferred to numbered weighing bottles, which are then stoppered and weighed. About 200 ml of distilled water, which has been carefully adjusted to room temperature, is weighed into the vacuum bottle, and the calorimeter assembled. The thermistor thermometer is connected to the Wheatstone bridge, and the stirrer is started. The time that the stirrer is on must be recorded. The thermometer resistance is checked by means of the bridge; if the water temperature was properly adjusted, the resistance will soon show only a very slow decrease due to the temperature rise caused by stirring.

When this condition has been reached, the position of the galvanometer light balance is noted as a reference point for later use, and the first determination is started by adding the 3-g sample of potassium nitrate

through the sample tube. The emptied weighing bottle is set aside to be reweighed later. The heating-circuit switch is then closed. The heating current is recorded, and any salt adhering to the surface of the filling tube is pushed down with a blunt glass rod or a camel's-hair brush.

The galvanometer deflection is checked at frequent intervals; *the bridge dial settings are not changed*. When the unbalance has been reduced far enough so that the galvanometer light spot remains on the scale, the galvanometer circuit switch is closed and the heating current and timer are turned off. The number  $n$  of scale divisions traversed thereafter by the spot due to the lag in the heater and thermometer is noted. The heating current and timer are switched on again and turned off when the light spot has reached the point  $n$  scale divisions short of the initial balance reference point. The spot will then come to rest very close to the latter, and in this way the final temperature of the solution is matched to the initial temperature. The total heating time is recorded.

The thermometer bridge balance is checked, and the second determination is made as above with the addition of the 4-g sample. Since heat exchange with the surroundings is influenced by the magnitude of the temperature differential between the calorimeter and the room, the solute may profitably be added gradually during the heating period rather than all at once. The remaining samples are used in turn to extend the concentration range studied to near 2 molal. The empty weighing bottles are then reweighed.

To determine the work of stirring per second, the solution is stirred for a time of the order of 15 min and the resulting change in the thermistor resistance,  $\Delta R_t$ , is noted. Next, a measured current is passed through the heating coil for about one minute, and the change  $\Delta R_t$  again noted. From these data, the work of stirring per second may be calculated if it is assumed that the resistance of the thermistor  $R_t$  varies linearly with temperature. This assumption is entirely satisfactory over the very small temperature intervals involved.

It is wise to make one or two test experiments to learn the proper technique.

**Calculations.** For this experiment the first law of thermodynamics leads to

$$\Delta H = q - w_s \quad (4)$$

The work of stirring  $w_s$  is negative because work is done on the system. The heat absorbed by the solution,  $q$ , is equal to the electrical energy dissipated in the resistor of resistance  $R$  due to passage of current  $I$  for time  $t$ . Hence

$$\Delta H = I^2 R t - w_s \quad (5)$$

If  $I$  is expressed in amperes,  $R$  in ohms, and  $t$  in seconds, the energy dissipated is given in joules; to convert to calories the energy in joules is divided by 4.184.

For each solution the total number of moles of solute present and the corresponding total enthalpy change  $\Delta H$  are calculated. The molality of the solution and the integral heat of solution at that concentration are then calculated. The integral heat of solution  $\Delta H_{\text{I.S.}}$  is plotted against the molality, and the differential heat of solution is evaluated at 0.5 and 1.5 molal by use of Eq. (2). This method is employed, rather than direct use of Eq. (1), to minimize the uncertainty in the calculated values due to the difficulty of determining accurately the slope of a curve.

The integral heats of solution at 0.5, 1, and 1.5 molal are obtained by interpolation, and the integral heats of dilution from 1.5 to 1 molal and 1 to 0.5 molal are evaluated. The various experimental results are compared with accepted values.<sup>4</sup> For comparison with literature data it should be remembered that the enthalpy of formation of a solute is defined as the enthalpy change for formation of the solution from the solvent and the elements of the solute, each in its standard state (pages 31–32).

**Practical Applications.** Integral-heat-of-solution data are often required in energy-balance calculations for chemical processes for engineering purposes. They are also used in the indirect evaluation of standard heats of formation of compounds for which heats of reaction in solution must be utilized. Measurements of the integral heat of solution may be used for the calculation of integral heats of dilution when no direct determinations of the latter are available. The differential heat of solution at saturation determines the temperature coefficient of solubility of the solute<sup>6</sup> (cf. Exp. 21).

**Suggestions for Further Work.** The method here described is suitable for measurements on most endothermic reactions. The apparatus may be used for exothermic reactions by determining the temperature rise due to the reaction, then cooling the system to the initial temperature and reheating it through the identical temperature range by means of the electrical heating coil.

The heat of solution of urea may be determined as typical of a nonelectrolyte. The individual samples used should be larger (about 15 g) because of the smaller heat of solution. The heats of solution of urea, phenol, and the compound  $(\text{NH}_2)_2\text{CO} \cdot 2\text{C}_6\text{H}_5\text{OH}$  are measured separately, and the heat of formation of the compound calculated.<sup>2</sup> The compound is prepared by fusing 9.40 g of phenol with 3 g of urea in a test tube immersed in boiling water.

The heat of hydration of calcium chloride may be determined indirectly from measurements of the endothermic heat of solution of  $\text{CaCl}_2 \cdot 6\text{H}_2\text{O}$  and the exothermic heat of solution of  $\text{CaCl}_2$ . A test of the equipment and operating technique may be made by measuring the relatively small heat of solution of sodium chloride. Comparison data for concentrations up to 1.3 molal have recently been given by Benson and Benson.<sup>1</sup>

The heat of mixing of organic liquids may be determined with the same apparatus.<sup>7</sup> The results for chloroform-acetone and carbon tetrachloride-acetone may be discussed on the basis of hydrogen bonding.

## References

1. Benson and Benson, *Rev. Sci. Instr.*, **26**, 477 (1955).
2. Campbell and Campbell, *J. Am. Chem. Soc.*, **62**, 291 (1940).
3. Lewis and Randall, "Thermodynamics," 2d ed., rev. by Pitzer and Brewer, McGraw-Hill Book Company, New York (1961).
4. Selected Values of Chemical Thermodynamic Properties, *Natl. Bur. Standards (U.S.), Circ.*, **500** (1952).
5. Sturtevant in Weissberger (ed.): "Technique of Organic Chemistry," 3d ed., Vol. I, Pt. I, Chap. 10, Interscience Publishers, Inc., New York (1959).
6. Williamson, *Trans. Faraday Soc.*, **40**, 421 (1944).
7. Zaslow, *J. Chem. Educ.*, **37**, 577 (1960).

### 5. HEAT OF REACTION IN SOLUTION: CONSTANT-PRESSURE CALORIMETER

The enthalpy change for a reaction in solution at constant pressure and temperature is found from the measured temperature change which occurs when the reaction takes place in a thermally insulated vessel.

**Theory.** The present experiment is concerned with the determination of the enthalpy change for a chemical reaction in solution. As an example, consider the reaction



where the symbol  $\text{Hg}^{++}(\text{aq})$  means one mole of  $\text{Hg}^{++}$  in an infinitely dilute solution in water solvent, and  $\text{HgCl}_2(\text{aq})$  refers to a mole of undissociated  $\text{HgCl}_2$  in solution at infinite dilution. The value of  $\Delta H$  for process (1) at a given temperature is practically equal to  $\Delta U$ , the difference in energy between reactants and products. Because of the specification attached to Eq. (1) that reactants and products be at infinite dilution, the enthalpy change equals  $\Delta H^\circ$ , the standard-state enthalpy change for the given temperature.

As the measurement cannot actually be performed on infinitely dilute solutions, recourse is had to a scheme such as that depicted in Fig. 10.

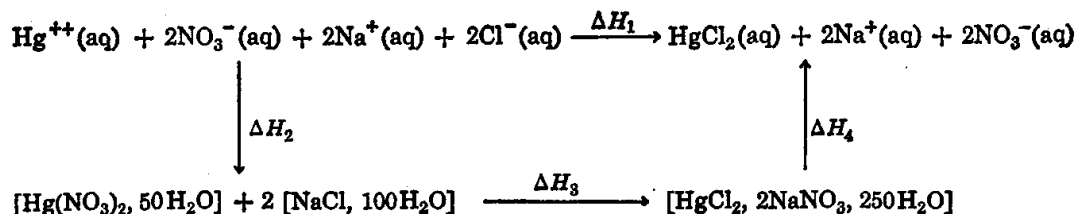


FIG. 10. Outline of steps for determination of  $\Delta H$  for reaction (1) in the text, equivalent to process 1 in the figure. Since  $\Delta H$  is independent of path,

$$\Delta H_1 = \Delta H_2 + \Delta H_3 + \Delta H_4$$

The symbol  $[\text{Hg}(\text{NO}_3)_2, 50\text{H}_2\text{O}]$  represents a solution containing one mole of  $\text{Hg}(\text{NO}_3)_2$  dissolved in 50 moles of  $\text{H}_2\text{O}$ . The quantity  $\Delta H_3$  is accurately measurable; steps 2 and 4 correspond to dilution processes for which  $\Delta H$  values may be obtained from heat-of-dilution data, which are tabulated for many common solutes and can otherwise be obtained from auxiliary experiments (Exp. 4).

The principles involved in the measurement of  $\Delta H$  for a process at finite concentrations of the type



of which Fig. 10, step 3, is an example, may now be considered. It is to be noted that in Eq. (2), reactants and products are specified to be at the same temperature; the enthalpy change for a reaction process of this type will be designated  $\Delta H_T$ .

The method of measurement involves a simple application of two important properties of the enthalpy function:

1. The energy transfer to the system by heat flow,  $q$ , is given by

$$q = \Delta H \quad (3)$$

for any process carried out in such a manner that the conditions  $P = \text{constant}$  and  $w = \int P dV$  hold.

2. The enthalpy is a function of state; hence  $\Delta H$  is independent of path, while  $q$  in general is not.

The present method is particularly well suited to the determination of  $\Delta H_T$  for reactions involving solutions. The reaction is carried out under a constant (atmospheric) pressure in a vacuum bottle, which is an excellent thermal insulator. Therefore the actual calorimeter process is adiabatic ( $q = 0$ ) rather than isothermal ( $T = \text{constant}$ ). The relationship between the calorimeter process and an isothermal process of the type of Eq. (2) is shown in Fig. 11. Clearly,

$$\Delta H_c = \Delta H_{T_1} + \int_{T_1}^{T_2} C_P dT \quad (4)$$

where  $\Delta H_c$  = enthalpy change for calorimeter process

$T_1$  = initial temperature

$T_2$  = final temperature

$C_P$  = heat capacity, at constant pressure, of contents and inner wall of vacuum flask after reaction has occurred

The temperature interval is generally sufficiently small that  $C_P$  may be considered constant, and the integral in Eq. (4) then becomes  $C_P(T_2 - T_1)$ . Furthermore, one has from Eq. (3), applied to the calorimeter process,

$$\Delta H_c = q = 0 \quad (5)$$

and combining this with Eq. (4) yields

$$\Delta H_{T_1} = -C_P(T_2 - T_1) \quad (6)$$

It may be noted that if the temperature *rises* in the adiabatic calorimeter process, then  $\Delta H_{T_1}$  is *negative*; in this case, heat would be evolved, according to Eq. (3), were the same reaction to be carried out isothermally at temperature  $T_1$ .

In order that Eq. (6) may be used to calculate  $\Delta H_{T_1}$  from the measured temperature change, it is necessary to determine  $C_P$  for the product

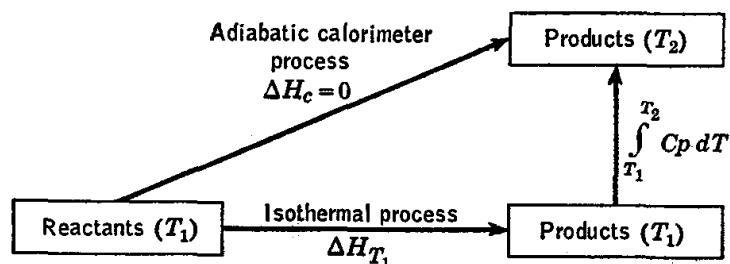


FIG. 11. Relationship between the actual adiabatic calorimeter process and the imagined isothermal process for which  $\Delta H_T$  is to be determined. Near each arrow is written the enthalpy change in going from one state to another in the direction indicated.

system. This is best done by an electrical method. Shortly after the reaction has occurred, a current is passed through the coil of wire immersed in the solution and the resulting temperature rise ( $T_4 - T_3$ ) is measured. The enthalpy change for the system in this process is  $\Delta H = C_P(T_4 - T_3)$ . Since electrical work  $I^2 R_h t$  is done on the system, Eq. (3) does not apply and must be replaced by

$$q - w_{el} = \Delta H \quad (7)$$

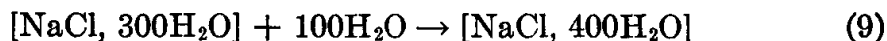
with  $q = 0$  and  $w_{el} = -I^2 R_h t$ . Here  $R_h$  stands for the resistance of the heater coil and  $t$  for the time of current flow. Hence,  $C_P$  may be calculated from

$$C_P(T_4 - T_3) = \Delta H = I^2 R_h t \quad (8)$$

For the calculation of  $\Delta H$  for the dilution steps, enthalpy-of-formation tables<sup>4</sup> may be used. The true enthalpy of formation,  $\Delta H_{f,T}$ , for a *solution* would be  $\Delta H$  for the formation of the specified solution from the *elements of all components* in their standard states at the given temperature. However, when one component is designated as solvent, it is conventional to define an enthalpy of formation for a *solute* as  $\Delta H$  for the formation of the specified solution from the pure *solvent* and *elements of the*

solute in their standard states at the given temperature. An enthalpy of formation for a solute in the latter sense will be denoted by  $\Delta H_{f',T}$ . Figure 12 may serve to clarify the distinction between  $\Delta H_{f,T}$  and  $\Delta H_{f',T}$ .

From the definition it is easily shown that  $\Delta H$  for a dilution process such as



is found by subtracting the heats of formation  $\Delta H_{f',T}$  for the solute at the

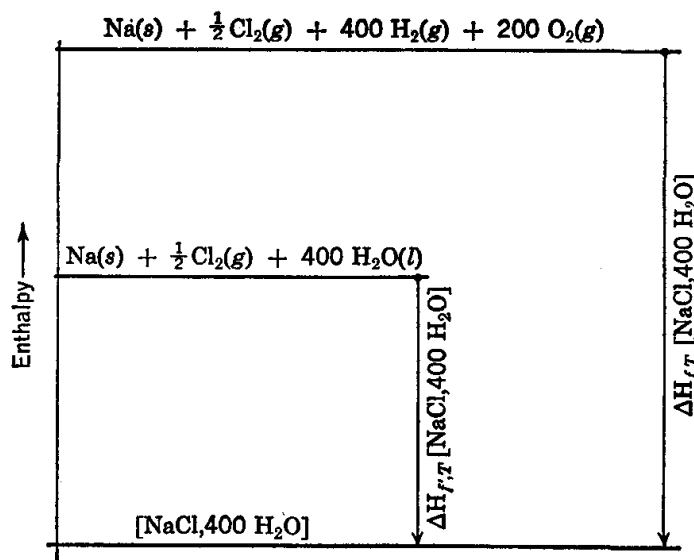
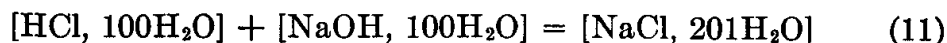


FIG. 12. Diagram illustrating the distinction between  $\Delta H_{f,T}$  and  $\Delta H_{f',T}$  for the solution  $[\text{NaCl}, 400\text{H}_2\text{O}]$ .

two concentrations. If  $\Delta H_T$  for a reaction is to be calculated from solute enthalpies of formation by the equation

$$\Delta H_T = \Sigma \Delta H_{f,T}(\text{products}) - \Sigma \Delta H_{f,T}(\text{reactants}) \quad (10)$$

an explicit term involving  $\Delta H_{f,T}(\text{H}_2\text{O})$  must be included if the number of moles of solvent, here considered to be water, changes in the reaction; for example, for the reaction



$\Delta H_T$  is given by

$$\begin{aligned} \Delta H_T = & \Delta H_{f',T}[\text{NaCl}, 201\text{H}_2\text{O}] + \Delta H_{f,T}(\text{H}_2\text{O}) \\ & - \Delta H_{f',T}[\text{NaOH}, 100\text{H}_2\text{O}] - \Delta H_{f',T}[\text{HCl}, 100\text{H}_2\text{O}] \end{aligned} \quad (12)$$

It may be desired to calculate  $\Delta H_{f,T}^\circ$  for a temperature  $T_0$  different from that at which the measurement was made. This calculation is most efficiently accomplished through introduction of partial molar quantities



(page 87). For the  $k$ th component of a solution, the partial molar enthalpy  $\bar{H}_k$  is defined by

$$\bar{H}_k = \left( \frac{\partial H}{\partial n_k} \right)_{T, P, n_1, \dots} \quad (13)$$

where  $H$  = enthalpy of solution

$n_k$  = number of moles of component  $k$

$n_1, \dots$  = numbers of moles of all other components

For a reaction,

$$\Delta H_T = \sum_j \nu_j \bar{H}_j - \sum_i \nu_i \bar{H}_i \quad (14)$$

where  $\nu_i$  is the coefficient of the  $i$ th reactant, and  $\nu_j$  that of the  $j$ th product, in the chemical equation for the reaction as written;  $\Sigma_j$  and  $\Sigma_i$  denote summation over products and reactants, respectively. The validity of Eq. (14) may be verified by considering the occurrence of an infinitesimal amount of reaction by removal of differential quantities of reactants and introduction of differential quantities of products in amounts consistent with the stoichiometry of the reaction.

To differentiate Eq. (14) with respect to  $T$ , we use

$$\frac{\partial \bar{H}_k}{\partial T} = \frac{\partial}{\partial T} \left( \frac{\partial H}{\partial n_k} \right) = \frac{\partial}{\partial n_k} \left( \frac{\partial H}{\partial T} \right) = \frac{\partial}{\partial n_k} C_P \equiv \bar{C}_{P,k} \quad (15)$$

and obtain

$$\frac{\partial \Delta H_T}{\partial T} = \sum_j \nu_j \bar{C}_{P,j} - \sum_i \nu_i \bar{C}_{P,i} \quad (16)$$

Integration of Eq. (16) from  $T_1$  to  $T_0$  yields

$$\Delta H_{T_0} - \Delta H_{T_1} = \int_{T_1}^{T_0} \left( \sum_j \nu_j \bar{C}_{P,j} - \sum_i \nu_i \bar{C}_{P,i} \right) dT \quad (17)$$

If the temperature interval ( $T_0 - T_1$ ) is only a few degrees so that the partial-molar-heat capacities may be considered to be constant, and if specialization is made to the standard-state case, Eq. (17) becomes

$$\Delta H_{T_0}^\circ = \Delta H_{T_1}^\circ + \left( \sum_j \nu_j \bar{C}_{P,j}^\circ - \sum_i \nu_i \bar{C}_{P,i}^\circ \right) (T_0 - T_1) \quad (18)$$

Values of  $\bar{C}_P^\circ$  for a number of solutes in water may be found in the National Bureau of Standards tables.<sup>4</sup>

Clearly, the solvent terms in Eq. (18) will cancel unless the number of moles of solvent changes in the reaction. If the standard state for the solvent is taken to be the pure solvent at temperature  $T$ , as is generally

the case, then  $\bar{C}_P^\circ$  for the solvent is just its molar heat capacity. For pure water, this is

$$C_P^\circ = (0.9989)(18.016) = 17.996 \text{ cal deg}^{-1} \text{ mole}^{-1} \text{ at } 25^\circ\text{C}$$

**Apparatus.** Calorimeter (Fig. 13) consisting of 500-ml vacuum bottle, sensitive ( $0.01^\circ$ ) thermometer, stirrer, special inner flask, and 15-watt heater coil; source of water-saturated, pressurized air; 6 or 12 volts d-c supply for heater; heater timer; double-pole double-throw switch controlling both heater and heater timer; additional timer or clock with sweep second hand; calibrated ammeter; potentiometer; precision potential divider; reactant solutions, 500 ml of  $[\text{NaCl}, 100\text{H}_2\text{O}]$ , 100 ml of  $[\text{Hg}(\text{NO}_3)_2, 50\text{H}_2\text{O}]$ .

**Procedure.** The calorimeter is shown in Fig. 13. A vacuum bottle provides a simple yet effective means of keeping the rate of heat exchange

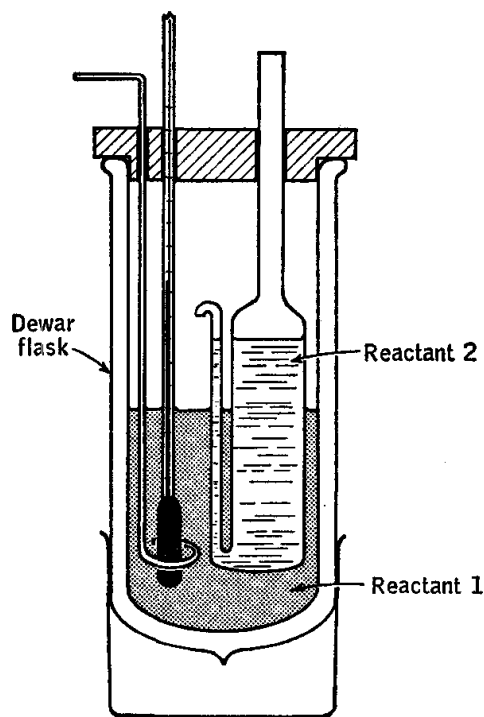


FIG. 13. Vacuum-flask calorimeter for solution reactions.

with the environment to a very low value. The cover is fitted with a thermometer† sensitive to  $0.01^\circ$  and a polystyrene stirrer. The inner Pyrex vessel serves to hold one reactant separate from the other, while permitting the two solutions to come to the same temperature before the reaction takes place. At the proper time, air pressure is used to force the reactant out of the inner flask. Water-saturated air should be used to minimize the cooling effect of evaporation.

A simpler method which yields satisfactory though somewhat less accurate results is to place the reactants initially in separate Dewar flasks, in one of which a heating coil is immersed, and to mix the two solutions at the proper time by pouring one reactant into the other. The product mixture should then be in the Dewar with the heater coil. An advantage of this procedure is that it allows greater flexibility in the choice of relative volumes of the two reactant solutions.

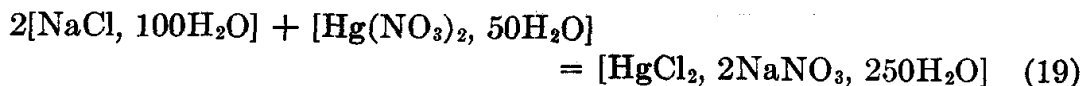
† A thermistor may be used in place of the mercury-in-glass type of thermometer shown in Fig. 13. The thermistor offers the advantages of smaller size, lower heat capacity, and more rapid response and is therefore particularly appropriate if it is desired to use small quantities of reactants. Suitable apparatus and calibration techniques for use with a thermistor are described in Exps. 4 and 12, respectively.

The heater coil, used in the determination of heat capacity, may be of the same design as that described in Exp. 4. The power required is of the order of 15 watts. A 6- or 12-volt d-c power supply is convenient. A regulated supply is preferable to a storage battery because the voltage of the latter will drop slightly even in the course of a single run. A calibrated ammeter serves to indicate the heater current, and a timer actuated by the switch which controls the heater current (Fig. 9 on page 26) measures the period of current flow.

In addition to the heater timer, a timing device is needed which will operate continuously over the duration of the run. A clock with sweep second hand will serve for this purpose if a second laboratory timer is not available.

Effective stirring is essential. For the outer solution, a motor-driven stirrer is to be recommended. This must be positioned with care if the thermometer is to survive the experiment. A simple glass or plastic rod stirrer may be used for the inner flask.

Several factors are involved in selecting the reactant concentrations to be used. The concentrations should be large enough to give an accurately measurable temperature rise, of the order of several degrees, and the relative volumes of the two reactants should be appropriate for the calorimeter. For the study of reaction (1), a suitable choice is



where the concentrations indicated correspond to relative reactant volumes of about 4:1.

The reactant solutions may be prepared by standard volumetric procedures. The amount of solute which reacts must be accurately known; the proportion of solvent to solute should correspond nominally to the chemical equation as written. Thus the NaCl solution of Eq. (19) is approximately 0.55 M, the  $\text{Hg}(\text{NO}_3)_2$  solution, about 1.1 M. The concentration of the former must be accurately known, as it is the limiting reactant; the concentration of the  $\text{Hg}(\text{NO}_3)_2$  need be known only to about 1 per cent. To prevent hydrolysis of the  $\text{Hg}(\text{NO}_3)_2$ , a dilute nitric acid solvent is used instead of pure water. This solvent, prepared by dilution of concentrated nitric acid about 1:10 with water, should be mixed *before* it is combined with the solute.†

An accurately known quantity, say 200 ml, of the first reactant is placed in the vacuum bottle. The amount of the second reactant placed in the inner flask is chosen such that the amount delivered will correspond

† If the two-Dewar procedure is followed, with equal volumes for the two reactants, suitable concentrations are 0.73 M for the NaCl and 0.37 M for the  $\text{Hg}(\text{NO}_3)_2$  solution, corresponding to  $[\text{NaCl}, 75 \text{H}_2\text{O}]$  and  $[\text{Hg}(\text{NO}_3)_2, 150 \text{H}_2\text{O}]$ , respectively.

to an excess of the order of 2 per cent over the stoichiometric amount. Preliminary testing may be necessary to learn the volume retained in the second flask. It is important that an excess be delivered if the amount reacted is to be accurately known.

When the apparatus is ready for a run, it is assembled with reactant solutions in place. The solutions are stirred until the system has reached thermal equilibrium. Then the temperature is noted, the second reactant is forced out of its flask to mix with the first, and the timer is started (or

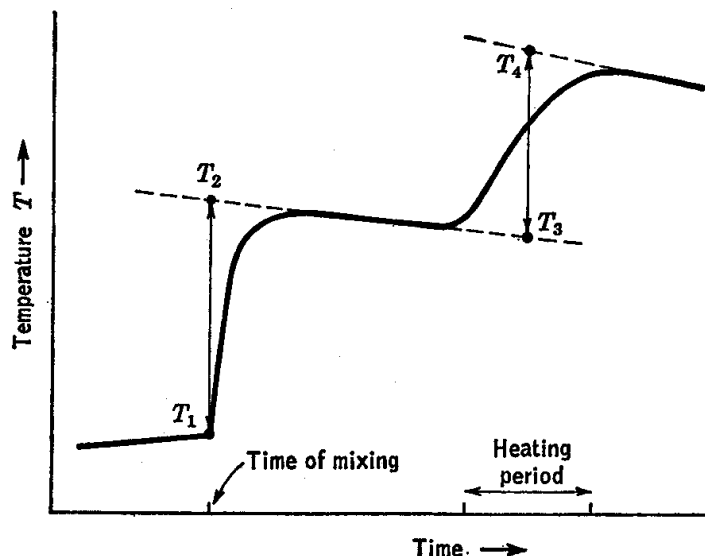


FIG. 14. Typical time-temperature graph.

the time noted if a clock is used). Temperature readings are taken at about one-minute intervals until a constant rate of change has been reached. (This slow change is due to heat exchange with the surroundings and to work of stirring.)

Next, the heater is turned on for a measured interval of time, such as to produce a rise of the order of 1 or 2° in temperature. (With a 15-watt heater, the time required for this would be of the order of several minutes.) After the current has stopped, time-temperature readings are again taken until the rate of change becomes constant, as shown in Fig. 14.

Finally, the resistance of the heater is measured. The measurement must be made with the usual heater current flowing, because the resistance changes with temperature. A satisfactory procedure is to measure the voltage at the heater terminals, by means of a potentiometer, and simultaneously note the current. If the voltage exceeds the range of the potentiometer, a precision potential divider is used (cf. Fig. 4).

At least two determinations should be made on each reaction system studied.

**Calculations.** Time-temperature curves are plotted (Fig. 14). The nearly straight line obtained a short time after mixing is extended back to the time of mixing to obtain  $T_2$ . One seeks with this procedure to find the temperature which would have been reached if the mixing of reactants and the subsequent thermal equilibration of solution and thermometer had occurred instantaneously, i.e., in too short a time for heat exchange with the environment to have occurred.

In this calculation it is implicitly assumed that the rate of heat transfer between system and surroundings is constant from the time of mixing until the linear rate of change is reached. This assumption would not be acceptable if the solution temperature actually changed as slowly after mixing as the graph would seem to indicate. For typical ionic reactions in solution, however, the temperature rise of the solution itself probably occurs almost as quickly as the reactants can be mixed, and the slower rise in observed readings is then due mainly to lag in the thermometer response. When this is the case, the method given above for determining  $T_2$  will be valid.

The temperature rise ( $T_4 - T_3$ ) produced by electrical heating is found by drawing, on the time-temperature graph, straight lines through the linear portions which precede and follow the passage of the current and extending these forward and backward, respectively, beyond the middle of the heating period. The temperature rise produced by the electrical heating alone is the vertical distance between these nearly parallel lines, measured at the midpoint of the electrical-heating period.

The enthalpy change due to electrical heating is  $\Delta H = I^2 R_h t$ , where  $I$  is the current,  $t$  the time, and  $R_h$  the resistance of the heating coil. In the calculation of  $R_h$ , one must take into account the fact that the current indicated by the ammeter includes not only the current through the heater coil, but also that through the potential divider used for the voltage measurement.

The remainder of the calculation of  $\Delta H_T$  is straightforward. The value reported should be for the amounts shown in the chemical equation as written, and the temperature should be specified.

If the necessary data are available, the value of  $\Delta H_T$  for the reaction at infinite dilution at 298.15°K should be calculated. For the case of reaction (19), it may be assumed that the value of  $\Delta H$  for the dilution of the solution  $[\text{HgCl}_2, 2\text{NaNO}_3, 250\text{H}_2\text{O}]$  is equal to that for the solution  $2[\text{NaNO}_3, 125\text{H}_2\text{O}]$ ; this amounts to assuming that the heat of dilution of the  $\text{HgCl}_2$  (undissociated) is negligible, while that of the  $\text{NaNO}_3$  is not negligible and furthermore is not affected by the presence of the  $\text{HgCl}_2$ . It will usually be true that the heats of dilution of ionized solutes are much larger than those of un-ionized solutes at comparable concentrations.

**Practical Applications.** The study of heats of reaction in solution has contributed to an understanding of the behavior of some systems, particularly electrolytes. Enthalpy data for reactions are used extensively for calculating the rate of change of equilibrium constant with temperature, through the relation  $\partial \ln K / \partial T = \Delta H^\circ / RT^2$ . Enthalpy data may also be combined with entropy data for the calculation of  $K$  at a single temperature by use of the relation  $-RT \ln K = \Delta G^\circ = \Delta H^\circ - T\Delta S^\circ$ .

**Suggestions for Further Work.** It is interesting to study heats of neutralization of a series of weak acids by NaOH. Miller, Lowell, and Lucasse<sup>2</sup> suggest the acids sulfamic, acetic, monochloroacetic, oxalic, and tartaric. The results may be combined with the accurately known enthalpy change for the process



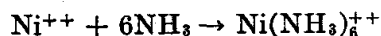
to obtain the enthalpy changes for dissociation of the acids at infinite dilution. While the association of ions to form the weak acids could be studied directly by the use of reactions of the sodium or potassium salts with a strong acid, the neutralization reactions offer the advantage of not involving ternary (three-component) solutions, for which heat-capacity and heat-of-dilution data are usually not available.

Pattison, Miller, and Lucasse<sup>3</sup> describe procedures for determining heats of several types of reactions. A few examples are:

1. Gas evolution: decomposition of  $\text{H}_2\text{O}_2$
2. Oxidation-reduction: reaction of  $\text{KBrO}_3$  with  $\text{HBr}$
3. Precipitation: reaction of  $\text{MgSO}_4$  with  $\text{NaOH}$
4. Dilution:  $\text{H}_2\text{SO}_4$  with water; ethyl alcohol with water
5. Organic reaction: reaction of hydroxylamine with acetone

An instructive exercise is the following. Given<sup>4</sup> the enthalpy of formation of  $\text{PbI}_2(c)$ , devise a suitable procedure and then use it to determine the enthalpy of formation of the dissolved, ionized salt at infinite dilution in water,  $\text{Pb}^{++}(\text{aq}) + 2\text{I}^-(\text{aq})$ . The symbol  $(c)$  indicates the crystalline state.

Approximate values can be obtained in favorable cases for the heat of formation of a complex ion from its constituents even though the stability of the complex ion is not high. An illustration is the determination of  $\Delta H$  for the reaction



by Yatsimirskii and Grafova.<sup>6</sup> A large excess of  $\text{NH}_3$  is used, and the heat of reaction is measured as a function of the concentration of  $\text{NH}_3$  in the final solution. Care must be taken in interpreting such data if there is any possibility that several species of complex ions are present in significant amounts.

### References

1. Mathews and Germann, *J. Phys. Chem.*, **15**, 73 (1911).
2. Miller, Lowell, and Lucasse, *J. Chem. Educ.*, **24**, 121-122 (1947).
3. Pattison, Miller, and Lucasse, *J. Chem. Educ.*, **20**, 319-326 (1943).
4. Selected Values of Chemical Thermodynamic Properties, *Natl. Bur. Standards, (U.S.), Circ.*, **500** (1952).
5. Sturtevant in Weissberger (ed.): "Technique of Organic Chemistry," 3d ed., Vol. I, Pt. I, Chap. 10, Interscience Publishers, Inc., New York (1959).
6. Yatsimirskii and Grafova, *Zhur. Obshchei Khim.*, **22**, 1726 (1952); **23**, 717 (1953). See also *Chem. Abstracts*, **47**, 2030c, 10327e (1953).

## *Vapor Pressures of Pure Substances*

### 6. VAPOR PRESSURE OF A PURE LIQUID

In this experiment the vapor pressure of a liquid is measured at several temperatures. The enthalpy of vaporization is calculated using the Clausius-Clapeyron equation.

**Theory.** When the temperature is raised, the vapor pressure of a liquid increases, because more molecules gain sufficient kinetic energy to break away from the surface of the liquid. When the vapor pressure becomes equal to the pressure of the gas space, the liquid boils. The temperature at which the vapor pressure reaches 760 mm Hg is the *standard* boiling point.

According to the Clapeyron equation, the temperature coefficient of the vapor pressure of a liquid is given by

$$\frac{dP}{dT} = \frac{\Delta \bar{H}_{\text{vap}}}{T(\bar{V}_v - \bar{V}_l)} \quad (1)$$

where  $\Delta \bar{H}_{\text{vap}}$  = enthalpy of vaporization at temperature  $T$

$\bar{V}_v, \bar{V}_l$  = molar volumes of vapor and liquid

The Clausius-Clapeyron equation

$$\ln P = - \frac{\Delta \bar{H}_{\text{vap}}}{RT} + \text{constant} \quad (2)$$

is derived from this exact equation with the following three assumptions: (a) the volume of a mole of liquid may be neglected in comparison with a mole of vapor at its saturation pressure; (b) the vapor behaves as an ideal gas; and (c) the enthalpy of vaporization is independent of temperature. Although Eq. (2) leads to a very simple interpretation of experimental data, the values of  $\Delta \bar{H}_{\text{vap}}$  calculated in this way may disagree significantly with the directly determined calorimetric values. Better values may be obtained by use of a more complete equation derived in the following way.<sup>1</sup>

The volume factor in the Clapeyron equation may be written

$$\bar{V}_v - \bar{V}_l = \bar{V}_v \left( 1 - \frac{\bar{V}_l}{\bar{V}_v} \right) = \frac{ZRT(1 - \bar{V}_l/\bar{V}_v)}{P} \quad (3)$$

where  $Z$  is the compressibility factor for the vapor. The expression on the right is introduced in the Clapeyron equation, which can then be rearranged to yield

$$\frac{d \ln P}{d(1/T)} = - \frac{\Delta \bar{H}_{\text{vap}}}{ZR(1 - \bar{V}_l/\bar{V}_v)} \quad (4)$$

or

$$\ln P = \frac{-\Delta \bar{H}_{\text{vap}}}{ZR(1 - \bar{V}_l/\bar{V}_v)T} + \text{constant} \quad (5)$$

This is an exact equation, but it involves three quantities which are functions of the temperature,  $\Delta \bar{H}_{\text{vap}}$ ,  $Z$ , and  $(1 - \bar{V}_l/\bar{V}_v)$ . When  $P$ - $V$ - $T$  data on the compound being studied are available, the enthalpy of vaporization may be calculated from the slope of the plot of  $\ln P$  versus  $1/T$  using Eq. (5). If  $P$ - $V$ - $T$  data are not available, a good estimate of the required quantities may often be made using the Berthelot equation, if the critical constants are known.

**Apparatus.** Vacuum system consisting of water aspirator, ballast tank, mercury manometer, and connections; Ramsay-Young vapor-pressure tube; one or more liquids chosen from carbon tetrachloride, acetone, chloroform, benzene, or other liquid boiling below  $100^\circ$ ; autotransformer and heating mantle.

**Procedure.** This experiment may be carried out using the classical Ramsay-Young<sup>2</sup> apparatus or, preferably, the Tobey<sup>4</sup> modification. In the usual Ramsay-Young apparatus the organic liquid to be studied is allowed to drip from a dropping funnel and down the thermometer to a hygrometer wick or layer of muslin cloth around the thermometer bulb. The temperature measured is that of the liquid in equilibrium with the vapor at the pressure indicated by the manometer. In the Tobey modification shown in Fig. 15, the dropping funnel is replaced by a cold finger, and the liquid is vaporized at the lower end of the long column and recondensed at the upper end. Thus there is no loss of material during the experiment as with the Ramsay-Young apparatus, and the difficulties of adjusting the flow rate, which are characteristic of that apparatus, are avoided.

A long Pyrex tube  $A$ , about 25 mm in diameter, is sealed to a 200-ml round-bottom flask, and a 29/42 standard taper joint is fastened to the top. The flash guard at the bottom of the column prevents liquid from bumping up into the column, with consequent superheating of the thermometer bulb. The cold finger should be sufficiently long so that a negligible amount of organic liquid escapes into the vacuum system. The dimensions in the diagram are recommended. The thermometer  $C$  is a  $0.0$  to  $110.0^\circ\text{C}$  complete-immersion precision type graduated to  $0.1^\circ$ . The bulb is wrapped with a hygrometer wick or layer of muslin cloth.



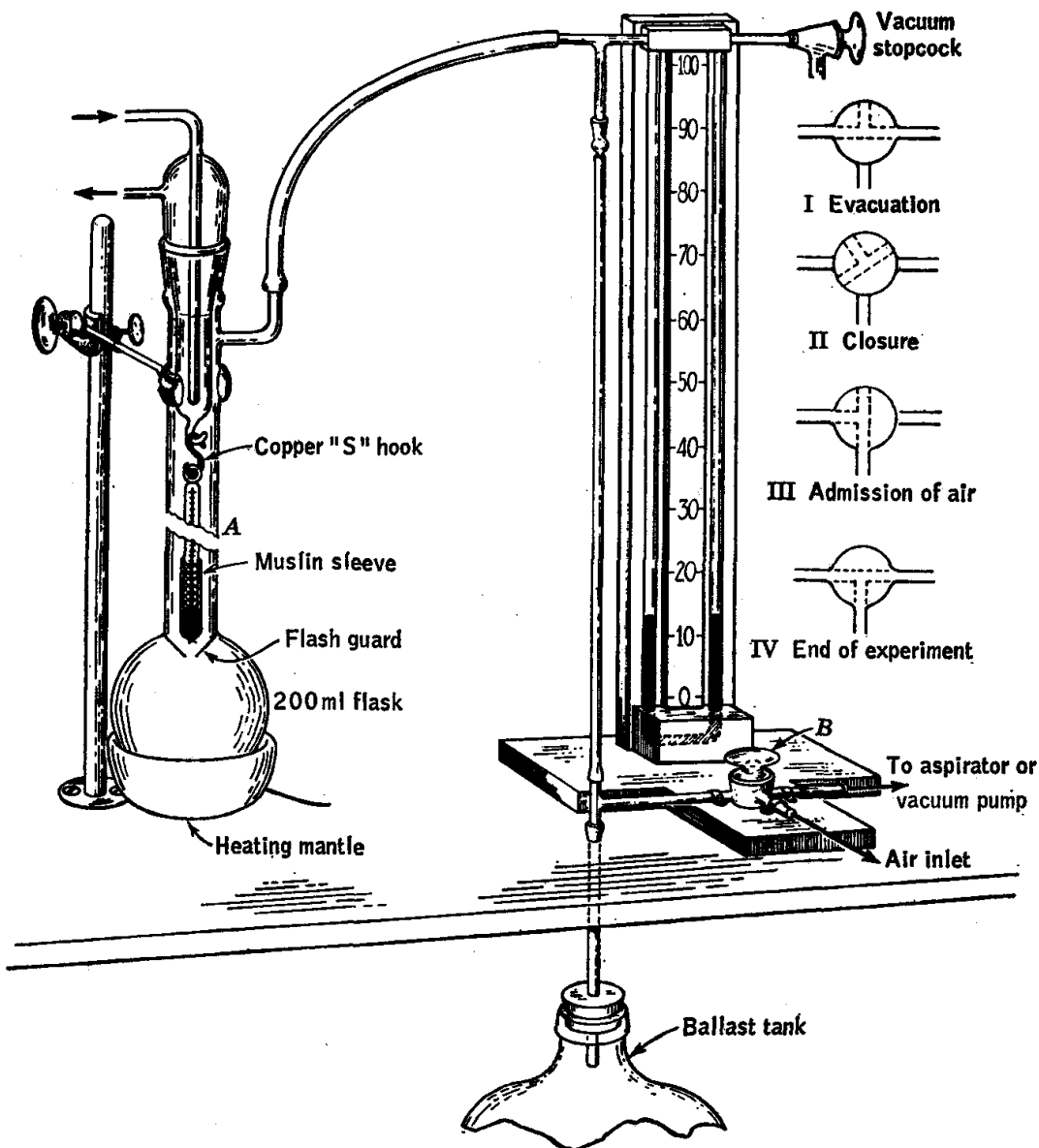


FIG. 15. Vapor-pressure apparatus.

The vacuum system consists of an aspirator connected through a three-way T stopcock *B* to a ballast tank of 10 liters or more capacity.† This tank prevents sudden pressure surges from disturbing the equilibrium. Connections between the various parts of the apparatus can be made with rubber vacuum hose, but Tygon tubing is better. The

† Stainless-steel tanks which are widely used by the Army air forces for breathing oxygen make excellent ballast tanks. These may be available at surplus-property supply houses. If an ordinary glass bottle is used, it should be wrapped in heavy wire mesh or placed in a wooden box to eliminate hazards due to flying glass in case of breakage when evacuated.

stopcocks and the glass joints are greased, if this has not already been done.

The bulb at the bottom of the column is filled approximately half full with the liquid to be studied. If a liquid different from the one being studied has been used previously in the apparatus, the system must be cleaned out and the liquid completely removed.

The experiment may be performed using either a closed-end or open-end manometer, but closed-end manometers have the advantage that they read the pressure, rather than the difference from atmospheric pressure.

If a manometer of the closed-end type is used, the manometer is connected to the atmosphere by use of stopcock *B* to see if the indicated pressure agrees with that given by the precision barometer in the laboratory. If the difference is greater than 1 mm, the instructor should be consulted.

The cooling water for the reflux head is turned on. With stopcock *B* in position I, the system is pumped down until the manometer indicates approximately 100 mm pressure in the system, or until the liquid in the bulb begins to boil. To test for leaks, stopcock *B* is closed (position II) to disconnect the aspirator, and the mercury meniscus in the manometer is watched. If it rises continuously, there is a leak in the system. If there is leakage, the source must be located and eliminated.

An autotransformer connected to the heating mantle is turned on, the dial is set at about 30 volts, and the heater is allowed to come to temperature. When steady-state conditions within the system are reached, there will be a steady flow of liquid back into the pot through the hole in the flash guard and a drop of liquid should drop off the thermometer bulb about every 5 to 10 sec. The thermometer bulb is heated by condensation of vapor and by radiation from the flask and cooled by evaporation until a steady temperature is registered. This is the boiling temperature of the liquid at the pressure registered on the manometer, unaffected by superheating. When the temperature registered by the thermometer reaches a steady value, the temperature and pressure are recorded.

The pressure in the system is then raised slightly by turning stopcock *B* gradually toward position III. Sufficient air is introduced to increase the pressure in the system so that the temperature indicated by the thermometer rises about 5°C, or the pressure is increased about 100 mm. The stopcock is then closed, and the system allowed to come to a steady state as before. This process is continued until the pressure in the system is returned to atmospheric. As the pressure is raised, it will be necessary to advance the setting of the Variac to obtain a suitable rate of reflux.

The pressure is now successively reduced in steps, and another series of data points is taken on a descending run. To lower the pressure, stop-

cock *B* is opened briefly so that air is pumped out of the system. The Variac is turned back as required to maintain a suitable rate of reflux.

At the close of the experiment, stopcock *B* is turned to position IV, the Variac is turned off, and the cooling water is shut off.

**Calculations.** Two types of graphs are plotted. In one the vapor pressures are plotted against the temperatures, and in the second the logarithms of the vapor pressures are plotted against the reciprocals of the *absolute* temperatures. Values taken from the literature are plotted also.

The values of the constants *A* and *B* in the equation

$$\log P = \frac{A}{T} + B \quad (6)$$

are determined by two methods.

First, the best straight line is drawn through the points by eye, and the constants *A* and *B* are calculated for this straight line. This may be done by using two points on the line which are far apart and solving the two simultaneous equations for *A* and *B*. Alternatively, the slope *A* may be calculated, and then *B* calculated, using  $\log P$  at some particular temperature.

Second, more objective values of *A* and *B* are calculated using the method of least squares. As explained in Chap. 18, this method yields the values of *A* and *B* such that the sum of the squares of the deviations of the experimental points from the theoretical line is a minimum. The details of the method are given on page 413. The first step is to tabulate  $\log P$ ,  $1/T$ ,  $(1/T)^2$ , and  $(1/T) \log P$ . In carrying out these calculations a desk calculator is required since the calculations must be carried out with several more figures than represented by the number of significant figures in the experimental results.

The heat of vaporization  $\Delta H_{\text{vap}}$  is then calculated from the values of *A* obtained by using the two methods. By comparison of Eqs. (2) and (6) it can be seen that

$$A = \frac{-\Delta H_{\text{vap}}}{2.303R} \quad (7)$$

The assumptions made in the derivation of the Clausius-Clapeyron equation limit the accuracy of the heats of vaporization calculated in this way.

Better values may be calculated using Eq. (5). The compressibility factor may be obtained directly from *P-V-T* data for the compound under study if they are available. When *P-V-T* data are not available, the compressibility factor may be estimated using the Berthelot equation, which may be written

$$Z = 1 + \frac{9}{128} \frac{P}{P_c} \frac{T_c}{T} \left( 1 - 6 \frac{T_c^2}{T^2} \right) \quad (8)$$

where  $T_c$  is the critical temperature. The compressibility factor is calculated for a particular point on the vapor-pressure curve, and the slope of the plot of  $\ln P$  versus  $1/T$  at that point is used. The ideal-gas law is used to calculate  $V_v$  in the factor  $(1 - V_l/V_v)$ .

**Practical Applications.** Vapor-pressure measurements are important in all distillation problems and in the calculation of certain other physical properties. They are used in the correction of boiling points and in the recovery of solvents. The concentration of vapor in a gas space may be regulated nicely by controlling the temperature of the evaporating liquid. Humidity conditions, which are so important in many manufacturing processes, depend largely on the vapor pressure of water.

**Suggestions for Further Work.** The vapor pressures of other liquids may be determined, using, if possible, liquids whose vapor pressures have not yet been recorded in tables. The sublimation temperature of a solid may be obtained by covering the thermometer bulb with a thin layer of the solid.

The vapor pressure may be determined by an entirely different method, evaluating the amount of liquid evaporated by a measured volume of air, as described in Chap. 21.

#### References

1. Brown, *J. Chem. Educ.*, **28**, 428 (1951).
2. Ramsay and Young, *J. Chem. Soc.*, **47**, 42 (1885).
3. Thomson in Weissberger (ed.): "Physical Methods of Organic Chemistry," Vol. I, Pt. I, Chap. 9, Interscience Publishers, Inc., New York (1959).
4. Tobey, *J. Chem. Educ.*, **35**, 352 (1958).
5. Willingham, Taylor, Pignocco, and Rossini, *J. Research, Natl. Bur. Standards (U.S.)*, **35**, 219 (1945).

### 7. KNUDSEN SUBLIMATION-PRESSURE MEASUREMENT

This experiment illustrates a method for the determination of the sublimation pressure of a solid and provides experience in the use of high-vacuum equipment.

**Theory.** The rate of escape of molecules of a gas through a small hole into a vacuum is directly proportional to the pressure under certain conditions, and the proportionality constant may be calculated from kinetic theory.<sup>4,5,8</sup> In order to obtain a simple relation it is necessary that the pressure outside of the hole be sufficiently low so that the mean free path of the molecules, the average distance traversed by a molecule between collisions, is long compared with the diameter of the hole and the thickness of the foil through which the hole is punched. For an ideal gas of rigid spherical molecules, the mean free path  $l$  is given by

$$l = \frac{1}{\sqrt{2} \pi \sigma^2 n} = \frac{kT}{\sqrt{2} \pi \sigma^2 P} \quad (1)$$

where  $\sigma$  = collision diameter for gas molecule (e.g.,  $3.75 \times 10^{-8}$  cm for  $N_2$  and  $4.63 \times 10^{-8}$  cm for  $CO_2$ )

$n$  = number of molecules per  $cm^3$

$P$  = pressure

$k$  = Boltzmann constant =  $R/N_0$

When the mean free path on the low-pressure side is large compared with the diameter of the hole, the number of molecules passing through the hole is equal to the number of molecules that would collide with the corresponding area of wall. The kinetic-theory result for the number of gas molecules  $\nu$  colliding with a square centimeter of wall in a second is

$$\nu = n \left( \frac{RT}{2\pi M} \right)^{1/2} \quad (2)$$

where  $R$  = ideal-gas constant

$M$  = molecular weight of gas

Since the rate of escape depends upon the number  $n$  of molecules per cubic centimeter, it may be expressed in terms of the pressure by introducing  $P = nRT/N_0$ , where  $N_0$  is Avogadro's number. The effusion rate is conveniently expressed in terms of the mass  $m$  of gas passing through the hole per  $cm^2$  area per sec.

$$m = \frac{M\nu}{N_0} \quad (3)$$

Eliminating  $\nu$  between Eqs. (2) and (3) and introducing the ideal-gas law yields

$$P = m \left( \frac{2\pi RT}{M} \right)^{1/2} \quad (4)$$

If  $m$  is expressed in  $g\ cm^{-2}\ sec^{-1}$  and  $R$  is written as  $8.314 \times 10^7$  erg deg $^{-1}$  mole $^{-1}$ ,  $P$  comes out in dynes  $cm^{-2}$ . The pressure in atmospheres may then be obtained by dividing by

$$(76\ cm)(13.595\ g\ cm^{-3})(980.7\ cm\ sec^{-2}) = 1.013 \times 10^6\ dynes\ cm^{-2}\ atm^{-1}$$

Equation (4) is often referred to as the Herz-Knudsen equation.

By measuring the rate of escape of gas from a saturated vapor through a small hole into a vacuum, the vapor pressure may be obtained. This method was developed by Knudsen<sup>4,5</sup> and is useful for the measurement of the sublimation pressures of relatively nonvolatile solids at high temperatures. The range of sublimation pressures which may be studied is about  $10^{-9}$  to  $10^{-3}$  atm. A number of refinements of this method have been developed.<sup>7</sup>

**Apparatus.** Mechanical vacuum pump; mercury diffusion pump to reduce the pressure to about one micron ( $1 \mu = 10^{-3}$  mm) of mercury; McLeod gauge; Knudsen cell; brass shim stock (0.002 in. thick); cold trap and chamber for Knudsen cell; thermostat, 10 to 50°; naphthalene.

**Procedure.** The Knudsen cell is shown in Fig. 16a. In order to get accurate results with the Knudsen method, the pressure outside the

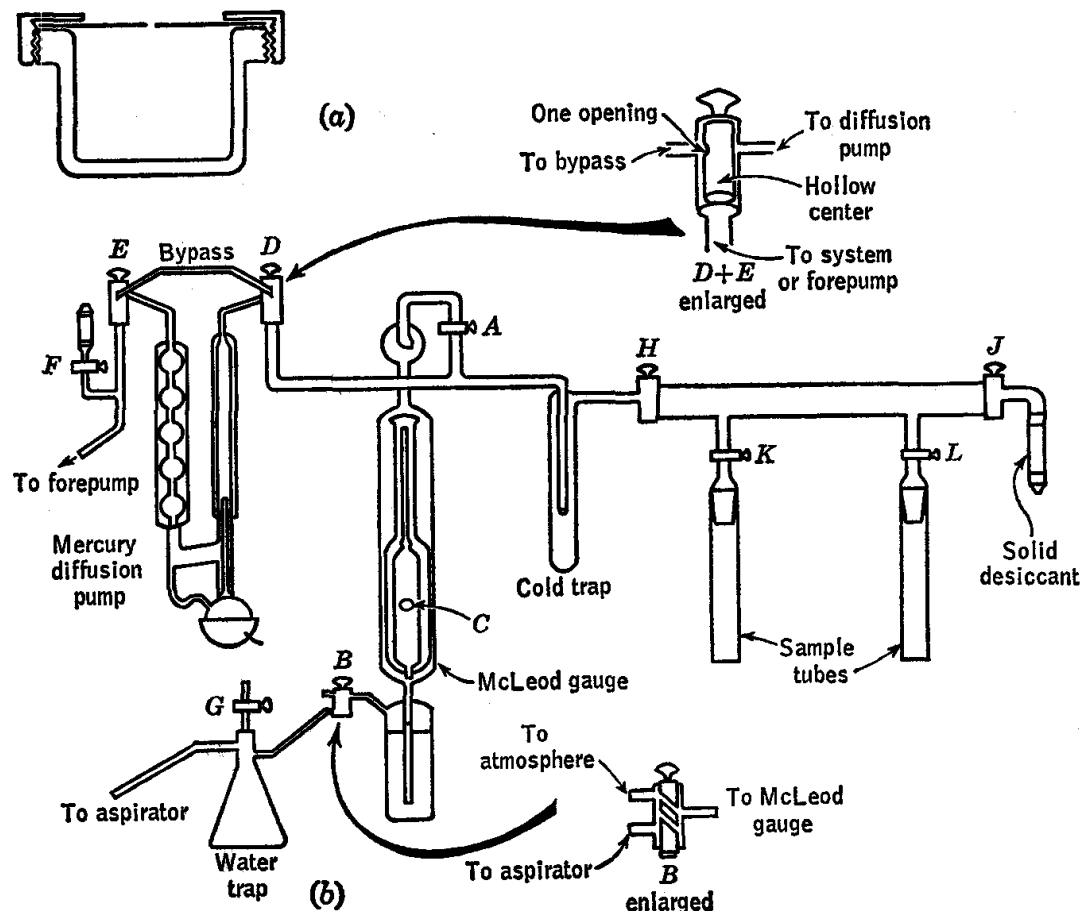


FIG. 16. (a) Diagram of Knudsen cell; (b) vacuum system for measurement of vapor pressure by Knudsen method. The vacuum line should be at least 76 cm above the mercury level.

Knudsen cell should be maintained at about  $10^{-3}$  mm of mercury or less. In the laboratory this is accomplished with a mechanical vacuum pump and a mercury diffusion pump. The pressure is measured with a McLeod gauge. *Before starting this experiment, the student should study the principles of operation of the rotary vacuum pump, mercury diffusion pump, and McLeod gauge (see Exp. 57).*

The vacuum system to be used is shown in Fig. 16b.

**A. Turning on the Vacuum System.** The vacuum system is turned on, and the pressure measured by the following procedure:

1. The water to the condenser of the mercury diffusion pump is turned on.
2. Stopcock *G* is opened, the water aspirator is turned on full force, and then stopcock *G* is closed.
3. A slush of finely powdered dry ice in trichloroethylene is prepared in the Dewar flask. The dry ice, as obtained from the mechanical crusher, is too coarse for this purpose and should be reduced to fine powder by placing a cupful at a time in a towel and beating it with a hammer. The final mixture should contain enough liquid so that it can be placed around the cold trap without danger of breakage. The Dewar flask should be almost half filled. When the bath has been prepared, it is placed very carefully around the cold trap.
4. Initially stopcocks *A*, *D*, *E*, *F*, *H*, *J*, *K*, and *L* should be closed. The forepump is started. *E* and then *D* are opened to bypass the diffusion pump. Pumping is continued for about one minute, until the pump is relatively quiet. It is well to listen to the pump while opening stopcock *H*. If the right-hand portion of the system was full of air initially, the characteristic sound of large quantities of air passing through the forepump will be heard. This sound should be remembered.
5. A test is carried out to see what the pressure is after the forepump has been running about 10 to 15 min:

The stopcock *A* to the McLeod gauge is opened cautiously.

  - a. If the mercury begins rising in the McLeod gauge, this stopcock is closed and an instructor is consulted.
  - b. If the mercury does not begin rising into the gauge, stopcock *B* is slowly opened to the atmosphere. The mercury will then begin to rise in the McLeod. The stopcock is left open until the mercury is about 2 cm above the midpoint of the large glass tube marked *C* on the diagram. The stopcock *B* is closed. The mercury will continue to rise until it reaches the capillaries. The pressure can now be read.

To pull the mercury down, stopcock *B* is opened to the aspirator. (The aspirator is left on throughout the experiment.) Then stopcock *A* is closed. When the mercury is down, stopcock *B* is closed.
6. When the pressure is below 100  $\mu$ , stopcock *E* is turned to open the diffusion pump to the forepump. By listening to the forepump the presence of air in the diffusion pump is checked. If air is present, it should be pumped out before turning stopcock *D* to open the diffusion pump to the rest of the system. The diffusion pump is turned on. The Variac which controls the diffusion-pump heater should be set at the optimum value for operation of the pump.
7. When the mercury in the diffusion pump has been distilling for about 10 min, the pressure is checked again as above. If the pressure is not below 1  $\mu$ , an instructor should be consulted; the difficulty could

result from a leak, from faulty operation of the pumps, or from outgassing. If the pressure is below  $1\ \mu$ , the experiment is continued. The mercury level is lowered and the McLeod gauge is closed off by shutting stopcocks *A* and *B*. These are *not* opened again during the experiment.

*B. Preparing the Knudsen Cells.* Two Knudsen cells are used. A sketch showing the design of a Knudsen cell appears in Fig. 16a. The top plate is a thin disk of brass (about 0.002 in. thick) with an orifice in the center. The orifice can best be fabricated by means of a drill press, with the top plate sandwiched between two  $\frac{1}{16}$ -in. plates of brass the upper of which has a pilot hole to guide the drill.

Because of a tendency for the orifice to collect obstructing particles of dust, it should be washed with acetone and carefully blown out with filtered compressed air before the plate is inserted into the effusion cell. Furthermore, just before introducing each cell into the vacuum system, its orifice should be cleaned by inserting a fine wire and *very* lightly rubbing it against the edges.

The Knudsen cells are carefully cleaned and dried and are half filled with finely powdered naphthalene. Top plates having the desired orifice sizes (see below) are placed on top of the Knudsen cells, and the caps are screwed on. Fingerprints are wiped off the cells, and the filled cells are weighed to 0.1 mg.

*C. Placing the Knudsen Cell in the Vacuum System.* Observations are to be made at four different temperatures, for which four different top plates (three orifice sizes) are provided. The largest orifice size is used at  $0^{\circ}\text{C}$ , the medium size at  $15^{\circ}$ , and the two smallest sizes at  $30$  and  $45^{\circ}$ .

The two higher temperatures may be attained in the regulated water baths, the two lower in Dewar flasks containing water to which ice may be added from time to time as required. Two runs may be made on each day.

The following procedure is suitable for introduction of the Knudsen cell:

1. Stopcock *H* is closed.
2. Stopcocks *K* and *L* are opened. Then *J* is opened slowly to admit dry air.
3. The sample tubes are removed.
4. The Knudsen cells are placed in the sample tubes. A long spring clamp may be used to facilitate this operation. The glass sample tubes should be clean because any dirt or grease transferred to the Knudsen cell will cause an error in the weight loss.
5. The standard taper connections are regreased if necessary, and the sample tubes reconnected to the vacuum system. Small springs or rubber bands may be used to support the sample tubes.
6. The water baths are put into place.



7. Stopcock *J* is closed.
8. Stopcocks *K* and *L* are opened.
9. Stopcock *H* is opened. The time is recorded, as the vaporization begins at this time.

*D. Closing Down the Vacuum System.* After 2 or 3 hr, the cells are removed and the vacuum system closed down according to the following procedure.

1. Stopcock *H* is closed.
2. Stopcock *J* is opened to the atmosphere. The time at which this is done is recorded.
3. Stopcocks *K* and *L* to the sample tubes are closed; *then* the samples are removed. (*K* and *L* are closed to prevent moist laboratory air from entering the manifold.)
4. Stopcocks *D* and *E* are closed to prevent the vacuum from being lost in the diffusion pump.
5. Stopcock *F* is opened to the atmosphere. Then the forepump is promptly turned off.
6. Stopcock *G* on the water trap leading to the aspirator is opened. Then the water aspirator is turned off.
7. The diffusion pump heater is turned off.
8. The cooling water to the diffusion pump is turned off.
9. Stopcocks *F* and *J* are closed.

*E. Weighing the Knudsen Cells.* If the cell has been at a temperature appreciably different from room temperature, it must be allowed to come to the temperature of the balance case before weighing.

**Calculations.** The vapor pressure of naphthalene is calculated from the rate of weight loss, using Eq. (4). The reliability of the calculated vapor pressure is estimated.

The experimental vapor pressures are compared with literature values by means of a plot of  $\log P$  versus  $1/T$ . The heat of sublimation per mole  $\Delta\bar{H}$  is calculated from the slope of this plot, assuming  $\Delta\bar{H}$  is independent of temperature.

**Suggestions for Further Work.** Other compounds which may be studied are benzoic acid, *d*-camphor, acetamide, and hexachlorobenzene.

If the vapor pressure is determined over a sufficiently wide range of temperature, it will be found that the plot of  $\log P$  versus  $1/T$  is not straight. This is primarily a result of the change in heat of sublimation with temperature. If the temperature range is not too large, the change in heat of sublimation with temperature is given by

$$\Delta\bar{H}_{T_2} = \Delta\bar{H}_{T_1} + \Delta\bar{C}_P(T_2 - T_1) \quad (5)$$

where  $\Delta\bar{C}_P$  is the difference in molar heat capacity of the vapor and solid at constant pressure. Actually, the total pressure varies over the range of temperature, but this causes little error. The enthalpies of sublimation are calculated at two widely

separated temperatures from the slope of tangents to the  $\log P$  versus  $1/T$  plot. Then  $\Delta\bar{C}_P$  is calculated using Eq. (5).

This method is especially useful for the determination of sublimation pressures at high temperatures.<sup>7</sup> The measurement of the sublimation pressures of tungsten<sup>6</sup> and beryllium<sup>8</sup> are examples.

#### References

1. Daniels and Alberty, "Physical Chemistry," John Wiley & Sons, Inc., New York (1961).
2. Hirschfelder, Curtiss, and Bird, "Molecular Theory of Gases and Liquids," John Wiley & Sons, Inc., New York (1954).
3. Holden, Speiser, and Johnson, *J. Am. Chem. Soc.*, **70**, 3897 (1948).
4. Knudsen, *Ann. Phys.*, **28**, 75, 299 (1909); **29**, 179 (1909).
5. Knudsen, "Kinetic Theory of Gases," Methuen & Co., Ltd., London (1934).
6. Langmuir, *Phys. Rev.*, **2**, 329 (1913).
7. Margrave in Bockris, White, and MacKenzie: "Physico-chemical Measurements at High Temperatures," Academic Press, Inc., New York (1959).
8. Present, "Kinetic Theory of Gases," McGraw-Hill Book Company, Inc., New York (1958).

## CHAPTER 4

# Solutions

### 8. LIQUID-VAPOR EQUILIBRIUM IN BINARY SYSTEMS

Boiling-point and vapor-composition data for a binary solution system at constant pressure may be correlated in a graph of temperature versus composition. Data for such a plot are obtained in this experiment, in which the liquid and vapor compositions are determined refractometrically. The calculation of the activity coefficients for the components in the liquid phase and their representation by the van Laar equation are considered.

**Theory.**<sup>2,3,8</sup> The relation between the composition of a liquid solution (phase *l*) of two volatile liquids and that of the vapor (phase *v*) in equilibrium with it at a given temperature and pressure may be established by use of the thermodynamic requirement that the chemical potential  $\mu_i$  for component *i* have a common value for the two equilibrium phases

$$\mu_{i,l} = \mu_{i,v}$$

The fugacity  $f_i$  for component *i*, irrespective of the phase in which it is present, is defined by the relation

$$\mu_i = \mu_i^* + RT \ln f_i \quad (1)$$

where  $\mu_i^*$  corresponds to the chemical potential that component *i* would have as an ideal gas at one atmosphere pressure at the temperature *T*. This definition makes the fugacity of a component of an ideal-gas mixture identical with its formal partial pressure  $P_i = X_{i,v}P$ , where  $X_{i,v}$  is the mole fraction of constituent *i* present, and *P* the total pressure of the gas phase. For a real-gas mixture,  $f_{i,v} = \vartheta_i P_i = \vartheta_i X_{i,v}P$ , where the *fugacity coefficient*  $\vartheta_i$  is a function of temperature, pressure, and composition which can be calculated from the equation of state of the gas phase. For a condensed phase, the fugacity of a constituent can be found by determining its value for the equilibrium vapor phase. Condensed phases are of interest, however, under conditions in which no such calculation is possible, as, for example, a solid of unmeasurably low vapor pressure, or a

solution of a nonvolatile solute such as sodium chloride in aqueous solution. It is thus convenient to introduce the *thermodynamic activity*  $a_i$  for a constituent of a given phase by the relation

$$\mu_i = \mu_i^\circ + RT \ln a_i = \mu_i^\circ + RT \ln \frac{f_i}{f_i^\circ} \quad (2)$$

where  $f_i^\circ$  is the fugacity for a selected standard state for which the chemical potential is  $\mu_i^\circ$ . The activity  $a_i$  is a ratio of two fugacities, which may readily be determined even when the individual fugacities involved cannot be. The standard state employed may be selected arbitrarily on a basis of practical convenience, but will normally be so chosen as to provide the simplest possible relation between the activity and the concentration of the constituent in the phase concerned. It thus becomes common to select a different standard state for a component for each phase in which it is present, so that the activity, unlike the fugacity, usually does not have a common value for different equilibrium phases.

For nonelectrolytic solutions the standard state for each component is normally taken to be the pure liquid at the temperature and pressure of the solution, and the activity is correlated with the concentration on the mole-fraction scale by means of the *activity coefficient*  $\gamma$ .

$$a_i = \frac{f_{i,l}}{f_{i,l}^\circ} = \gamma_i X_{i,l} \quad (3)$$

For what is called an *ideal* solution,  $\gamma_i$  as defined above is identically equal to unity for any component at any concentration. For real solutions the activity coefficients must be determined by experiment.

The fugacity  $f_{i,l}^\circ$  for this standard state is calculated as follows. The vapor pressure  $P_i^*(T)$  of pure liquid  $i$  at the given temperature is multiplied by the fugacity coefficient  $\vartheta_i^*(P_i^*, T)$  of the vapor as calculated from the equation of state of the vapor to obtain the fugacity of the saturated vapor at the temperature  $T$ . This then gives the fugacity of pure liquid  $i$  for temperature  $T$  and pressure  $P_i^*$ . The fugacity  $f_{i,l}^\circ = f_{i,l}(P_i^*, T)$  may then be calculated by taking into account the difference between  $P_i^*$  and  $P$ , using the thermodynamic relation

$$\ln f_{i,l}^\circ = \ln f_{i,l}(P, T) = \ln \vartheta_i^* P_i^* + \int_{P_i^*}^P \frac{\bar{V}_i^*}{RT} dP \quad (4)$$

where  $\bar{V}_i^*$  = molar volume of pure liquid  $i$ . The integral in Eq. (4) will be negligible if  $(P - P_i^*)$  is not large.

For liquid-vapor equilibrium, since the fugacity of each constituent must have a common value for both phases,

$$f_{i,l} = \gamma_i f_{i,l}^\circ X_{i,l} = f_{i,v} = \vartheta_i X_{i,v} P \quad (5)$$

Assuming the effect of pressure on the fugacity of the pure liquid to be negligible,  $f_{i,l}^\circ = \vartheta_i^* P_i^*$  and

$$X_{i,l} = \frac{1}{\gamma_i} \frac{\vartheta_i}{\vartheta_i^*} \frac{P}{P_i^*} X_{i,v} \quad (6)$$

If the gas phases involved are considered to behave ideally,

$$X_{i,l} = \frac{1}{\gamma_i} \frac{P}{P_i^*} X_{i,v} \quad (7)$$

For ideal liquid solutions, this desired relation between the liquid and vapor compositions further simplifies to

$$X_{i,l} = \frac{P}{P_i^*} X_{i,v} \quad (8)$$

For real solutions the activity coefficients are functions of concentration, temperature, and pressure. For a binary nonelectrolytic solution system the concentration dependence may often be represented to a good degree of approximation by the van Laar equations, which have been written as follows by Carlson and Colburn:<sup>2</sup>

$$\log \gamma_1 = \frac{A_1}{\left(1 + \frac{A_1 X_1}{A_2 X_2}\right)^2} \quad \log \gamma_2 = \frac{A_2}{\left(1 + \frac{A_2 X_2}{A_1 X_1}\right)^2} \quad (9)$$

The van Laar coefficients  $A_1$ ,  $A_2$  are functions of temperature and pressure. Even substantial changes in pressure have only a small effect. The dependence on temperature is more important, but over a range of ten or twenty degrees the resultant change in a typical activity coefficient will usually be only a few per cent.

Real solution systems vary widely in their degree of departure from the ideal-solution rule, for which the boiling points of the solutions are always intermediate between those of the pure liquids. In many cases, however, the deviation from ideality becomes so great that a minimum or maximum results in the plot of boiling point versus liquid or vapor composition. At such a maximum or minimum, the equilibrium vapor and liquid compositions are identical. Such solutions are called *azeotropes*. A comprehensive description of methods for the experimental study of vapor-liquid equilibria and for the correlation of the results has been given by Hala *et al.*<sup>6</sup> An extensive table of azeotropes has been prepared by Horsley *et al.*,<sup>7</sup> and data for many binary solution systems have been summarized by Timmermans.<sup>14</sup>

**Apparatus.** Distilling apparatus as illustrated in Fig. 17; pipette of about 1 ml; resistance wire for electric heater; step-down transformer (110 to 6 volts); thermometer graduated to  $0.1^\circ$ ; refractometer with thermostated prism; weighing bottle; benzene; ethanol.

**Procedure.** The apparatus which is shown in Fig. 17 may be readily constructed from a 50-ml distilling flask. Superheating is avoided by internal electrical heating with a resistance coil. An alternative apparatus is described by Rogers, Knight, and Choppin.<sup>11</sup>

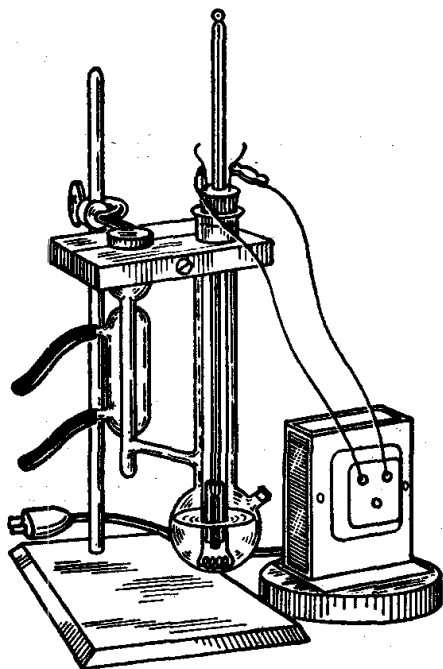


FIG. 17. Apparatus for determining liquid and vapor compositions of binary systems as a function of temperature.

The heating coil of No. 26 nichrome wire about 14 cm long is wound in the form of a helix about 3 mm in diameter. It is brazed to No. 14 copper wire leads set into the cork. The coil should touch the bottom. A small step-down transformer capable of at least 25 watts output is used.

Other types and sizes of resistance wire may be used, but the current should be such that the wire is heated to a dull red heat when out in the open air. A heater of 2 ohms operating at 6 volts is satisfactory.

A thermometer graduated to  $0.1^\circ$  and reading from 50 to  $100^\circ$  serves very well, but any accurate thermometer with large  $1^\circ$  divisions will do. A short length of glass tubing surrounds the bulb of the thermometer; this enables the boiling liquid to circulate over the entire thermometer bulb. The bulb must not touch the heating coil.

The arm of the distilling flask is bent upward to act as a reflux condenser; at the bottom of the bend is a bulb of about 1 ml capacity to act as a pocket for retaining condensed distillate as it flows down from the short condenser.

The transformer is adjusted so that the liquid boils vigorously at a constant rate, and the vapor condenses in the reflux condenser. Additional regulation may be accomplished with a rheostat, if necessary. The boiling is continued until the pocket below the reflux condenser has been thoroughly rinsed out with condensed liquid and the thermometer reading has become constant. The approach to equilibrium is hastened by stirring the liquid in the pocket with a long glass rod. The current is then turned off, and samples of about 1 ml are taken with a small tube

or pipette from the distillate in the pocket and then from the residue in the flask through the sidearm. The sample of distillate is removed by inserting the end of the pipette through the open end of the reflux condenser directly into the pocket below. A dry pipette should be used for taking the samples. The refractive indices of the samples are determined with a refractometer. Samples for this determination may be preserved

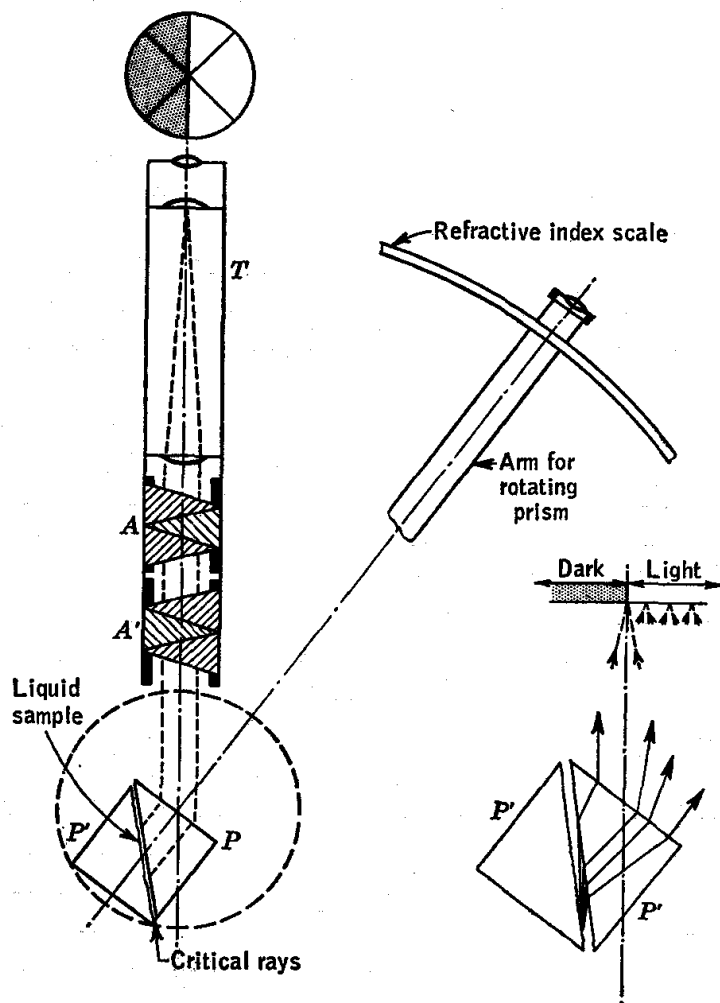


FIG. 18. Optical path in Abbe refractometer.

for a short time in small *stoppered* vials or test tubes, but errors caused by partial evaporation of the samples must be considered. It is important to close the jaws of the refractometer quickly to avoid evaporation from the liquid film on the prism.

The Abbe refractometer, illustrated in Fig. 18, makes use of the principle of the grazing angle. The field in the telescope will show a light region and a dark region, the sharp line of demarcation between which corresponds to the grazing angle.

White light from a frosted electric-light bulb is used for convenience, and if it were not for the compensating Amici prism of different kinds of glass in the telescope, the line of demarcation between the dark and light fields would be colored and indistinct because the refraction of light is different for different wavelengths. The light of different wavelengths is dispersed by the refractometer prism, by the first compensating prism  $A'$ , and by the sample of liquid. Since the extent of the dispersion differs for each liquid, the second compensating prism  $A$  is adjusted manually so that its dispersion is exactly equal and opposite to the dispersion produced by the refractometer and the liquid. A knurled ring in the middle of the telescope barrel is turned until the compensation is complete and the color fringes disappear, leaving a sharp line of demarcation between the two parts of the field.

Although white light is used, the refractive index measured,  $n_D$ , is for the D line, 5893 Å, because the Amici compensating prisms are constructed with special glasses so that light of this wavelength is not deviated but all other light is deviated.

The Abbe refractometer has two prisms, the first of which,  $P'$ , has a ground-glass face. It is used to confine the thin sample of liquid and to illuminate it with scattered light. The upper prism  $P$  is the refracting prism. The prisms are jacketed so that the temperature may be controlled to  $0.2^\circ$  with water from a thermostat. The refractometer prism is rotated by a protruding arm so as to set the edge of the shadow directly on the intersection of the cross hairs as shown in Fig. 18.

The prisms are opened like jaws after turning the lock nut, and they are wiped with lens tissue paper, care being taken not to scratch the prism surfaces. A few drops of liquid are placed on the face of the lower prism, and the prism jaws are then closed and locked. The compensating ring is turned to eliminate color fringes. The telescope is set in a convenient position, and the mirror is adjusted to reflect the light from a frosted electric lamp into the refractometer. The prism is rotated by means of the arm until the border between the dark and light fields passes exactly through the intersection of the cross hairs. The telescope eyepiece is adjusted until the cross hairs are in good focus, and the eyepiece on the movable arm is adjusted to give a sharp focus on the scale. The scale is graduated directly in terms of refractive index calculated for the glass used in the prism as shown on page 419. The reproducibility of the individual readings on the scale is  $\pm 0.0002$  in refractive index. Accurate temperature control is important because the refractive indices of many organic liquids change 0.0004 per degree. After a liquid is used, it is absorbed with lens paper or rinsed off with a volatile liquid in which it is soluble.

About 25 ml of benzene is measured into the flask, and its boiling point



is determined. Boiling points and refractive indices of the residue and distillate are then determined after successive additions of 0.2, 0.5, 1, 5, 5, and 5 ml of ethanol. The refractive indices are used to obtain the mole fractions of ethanol in these solutions.

In order to construct a plot of refractive index versus mole per cent ethanol, the refractive indices are determined for the pure benzene and ethanol and for a series of solutions containing accurately known weights of benzene and ethanol. Mixtures about 5 ml in volume containing approximately 1 volume of ethanol to 1, 3, and 6 volumes of benzene are convenient.

The boiling flask is drained and dried, and about 25 ml of ethanol is introduced for a boiling-point determination. Boiling points and compositions of the residue and distillate are then determined after successive additions of benzene as, for example, 2, 4, 5, 7, and 10 ml.

The barometer should be read occasionally. In case the atmospheric pressure changes considerably, it is necessary to estimate a correction for the boiling point, taking an average correction for the two liquids as an approximation. Such a correction may usually be avoided by performing all the distillation experiments within a few hours.

**Calculations.** The refractive indices of the weighed samples and the pure liquids are plotted against the compositions of the solutions expressed in mole fractions of ethanol. The composition of each sample of distillate and residue may then be determined by interpolation on this graph. In a second graph three sets of curves are plotted:

I. The boiling-point diagram for the system as determined experimentally. Two curves are plotted, one in which boiling temperature is plotted against the mole fraction of ethanol in the residue; in the other, the same boiling temperatures are plotted against the mole fraction of ethanol in the distillate. The composition as mole-fraction ethanol is plotted along the horizontal axis. Different symbols should be used for the two sets of points. The significance of this graph is discussed with respect to the feasibility of separating benzene and ethanol by fractional distillation.

II. The boiling-point diagram for the system as predicted by the ideal-solution rule. Points for the two curves involved may be calculated as follows for a given pressure  $P$ . A temperature  $T$  is selected between the boiling points of the two pure liquids as *calculated* from accurate relations such as those given below. The terms  $P_1^*(T)$ ,  $P_2^*(T)$  represent the calculated vapor pressures of the pure liquids at this temperature.

$$P = P_1 + P_2 = X_{1,i}P_1^*(T) + X_{2,i}P_2^*(T) \\ = P_1^*(T) + X_{2,i}[P_2^*(T) - P_1^*(T)] \quad (10)$$

From Eq. (10) there is then calculated the mole fraction  $X_{2,i}$  of component

2 in the solution having vapor pressure  $P$  at temperature  $T$ . Then the mole fraction  $X_{2,v}$  for the equilibrium vapor phase is given by

$$X_{2,v} = \frac{P_2}{P} = \frac{X_{2,l}P_2^*(T)}{P} \quad (11)$$

III. The boiling-point diagram for the system as predicted by the van Laar equations for values of  $A_1, A_2$  consistent with the experimentally determined azeotrope temperature and composition. In this calculation it will be necessary to assume that the activity coefficients are functions of composition only (that is,  $A_1, A_2 = \text{constants}$ ), an approximation justified by the small temperature range involved.

The activity coefficient  $\gamma_i$  is given by the relation (7) (for the *ideal-gas* approximation).

$$\gamma_i = \frac{X_{i,v}}{X_{i,l}} \frac{P}{P_i^*(T)}$$

For the azeotropic solution, the mole fraction of each component has the same value for the liquid and vapor phases; hence the activity coefficients  $\gamma_{1,az}$  and  $\gamma_{2,az}$  for the azeotropic solution are given by

$$\gamma_{1,az} = \frac{P}{P_1^*(T)} \quad \gamma_{2,az} = \frac{P}{P_2^*(T)} \quad (12)$$

From the pair of activity coefficients so calculated and the composition of the azeotrope, the van Laar coefficients may be calculated. It is convenient first to calculate the ratio  $A_2/A_1$ .

$$\frac{A_2}{A_1} = \frac{X_{1,l}^2 \log \gamma_1}{X_{2,l}^2 \log \gamma_2} \quad (13)$$

$$\text{Then} \quad A_2 = \left(1 + \frac{A_2}{A_1} \frac{X_{2,l}}{X_{1,l}}\right)^2 \log \gamma_2 \quad A_1 = \frac{A_2}{A_2/A_1} \quad (14)$$

Now select some concentration  $X_{2,l}, X_{1,l} = 1 - X_{2,l}$ , and calculate from the van Laar equations  $\gamma_2$  and  $\gamma_1$ .

$$P = P_1 + P_2 = \gamma_1 X_{1,l} P_1^*(T) + \gamma_2 X_{2,l} P_2^*(T) \quad (15)$$

By successive approximation, determine the temperature  $T$  for which this equation is satisfied for the known pressure  $P$ . Then

$$X_{2,v} = \frac{P_2}{P} = \frac{\gamma_2 X_{2,l} P_2^*(T)}{P} \quad (16)$$

Several sets of points should be calculated in this way for compositions on each side of the azeotropic composition.

The required data on the vapor pressures of benzene and ethanol may be calculated from the following relations:

$$\text{Benzene (Ref. 12): } \log P = 6.90522 - \frac{1211.215}{t + 220.87}$$

$$\text{Ethanol (Ref. 8): } \log P = 8.11576 - \frac{1595.76}{t + 226.5}$$

These equations give the vapor pressure in standard millimeters of mercury for temperature in degrees centigrade.

**Practical Applications.** Vapor-composition curves are necessary for the efficient separation of liquids by distillation. Fractional distillation under controlled conditions is essential in the purification of liquids and in many industries, such as the petroleum industry and solvent industries.

**Suggestions for Further Work.** Solutions of chloroform and acetone, giving a maximum in the boiling-point curve, may be studied in exactly the same manner as described for ethanol and benzene.

The maximum in the boiling-point curve of hydrochloric acid and water occurs at 108.5° and a composition of 20.2 per cent hydrochloric acid at a pressure of 760 mm. The distillate at the maximum boiling point is so reproducible in composition at a given pressure and so easily obtained that it may be used to prepare solutions of HCl for volumetric analysis. A solution of hydrochloric acid is made up roughly to approximate the constant-boiling composition, and after boiling off the first third, the remaining distillate is retained. The barometer is read accurately, and the corresponding composition is obtained from the literature.<sup>1,5,7</sup>

Solutions of chloroform and methanol, giving a minimum in the boiling-point curve, may be studied by using a Westphal density balance for determining the compositions instead of a refractometer. A density-mole-fraction curve is plotted, and the compositions of the samples are determined by interpolation. Since larger samples are needed for the density measurements, more material and a larger flask are required.

The gas-saturation method for vapor-pressure measurements may be used in studying binary liquids. Using this technique, Smyth and Engel<sup>13</sup> have determined vapor-pressure-composition curves for a number of ideal and nonideal types.

Vapor-liquid equilibria at different total pressures provide an interesting study. The acetonitrile-water system has an azeotrope which varies considerably in composition as the pressure is reduced.<sup>9</sup> Othmer and Morley<sup>10</sup> describe an apparatus for the study of vapor-liquid compositions at pressures up to 500 psi. The earlier papers of Othmer may be consulted for a number of binary vapor-liquid equilibria.

#### References

1. Bonner and Branting, *J. Am. Chem. Soc.*, **48**, 3093 (1926).
2. Carlson and Colburn, *Ind. Eng. Chem.*, **34**, 581 (1942).
3. Daniels and Alberty, "Physical Chemistry," 2d ed., John Wiley & Sons, Inc., New York (1961).
4. Dodge, "Chemical Engineering Thermodynamics," Chaps. XII, XIII, McGraw-Hill Book Company, Inc., New York (1944).
5. Foulk and Hollingsworth, *J. Am. Chem. Soc.*, **45**, 1220 (1923).

6. Hala, Pick, Fried, and Vilim, "Vapor-Liquid Equilibrium," Pergamon Press, New York (1958).
7. Horsley and coworkers, "Azeotropic Data," American Chemical Society, Advances in Chemistry Series, Washington, D.C. (1952); Tables of Azeotropes and Non-azeotropes, *Anal. Chem.*, **19**, 508-600 (1947).
8. Kretschmer and Wiebe, *J. Am. Chem. Soc.*, **71**, 1793 (1949).
9. Othmer and Josefowitz, *Ind. Eng. Chem.*, **39**, 1175 (1947).
10. Othmer and Morley, *Ind. Eng. Chem.*, **38**, 751 (1946).
11. Rogers, Knight, and Choppin, *J. Chem. Educ.*, **24**, 491 (1947).
12. Smith, *J. Research, Natl. Bur. Standards (U.S.)*, **26**, 129 (1941).
13. Smyth and Engel, *J. Am. Chem. Soc.*, **51**, 2646, 2660 (1929).
14. Timmermans, "Physico-chemical Constants of Binary Systems in Concentrated Solutions," Interscience Publishers, Inc., New York (1959).

## 9. FRACTIONAL DISTILLATION

In this experiment the efficiencies of packed and unpacked columns are compared at total reflux. The separation of a binary mixture by fractional distillation is studied by using refractive-index measurements to analyze the distillate.

**Theory.** The separation of liquids by distillation is one of the oldest and most important operations of chemistry, but considerable improvement has been made in the design of apparatus for fractional distillation. The developments in petroleum refining and the need for increased efficiency in laboratory operations and purification have been largely responsible for these improvements. The concentration of isotopes has made still greater demands on fractional distillation.

The separation of two liquids which is obtained by a simple vaporization and condensation is not effective except in the case of liquids with widely differing boiling points. Greater separation may be achieved by a series of simple distillations, but this is laborious. The same result is obtained by using a fractionating column through which the vapor is passed and brought into contact with part of the condensate flowing down the column. The less volatile components in the ascending vapor are condensed in such a column, and the more volatile components are boiled out of the descending liquid phase, so that distillation through the column is equivalent to a number of successive simple distillations. Greater separation is obtained in a fractionating column if most of the vapor condensed at the top of the column is returned as reflux. The reflux ratio is defined as the ratio of the volume of liquid flowing back into the column to the volume of liquid removed as distillate.

It is necessary to insulate or heat a fractionating column so that the net condensation in the column will not be too great. The temperature will be lower at the top of the column, where the more volatile component is concentrated, than at the bottom. The purpose of the packing is to

provide good contact between the vapor and liquid phases in the column, but it is undesirable for the packing to hold a large fraction of the batch being distilled because of the resulting decrease in sharpness of separation. A number of types of packing are listed on page 450.

The effectiveness of a distilling column is expressed in terms of the theoretical plate. The *theoretical plate* is a hypothetical section of

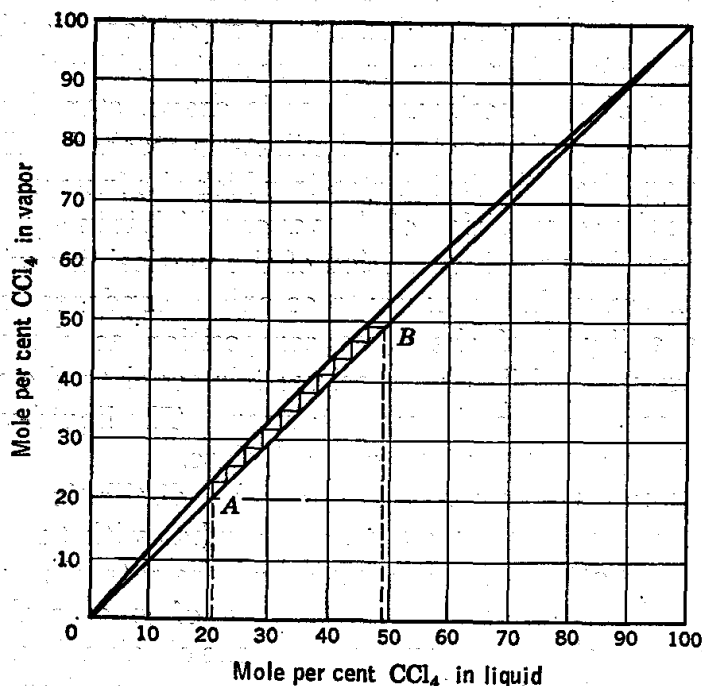


Fig. 19. Vapor-liquid graph for calculating the number of theoretical plates.

column which produces a separation of components such that the vapor leaving the top of the section has the composition of the vapor which is in equilibrium with the liquid leaving the bottom of the section. A column consisting of a simple 1-cm tube 1 m long might be equivalent to only 1 theoretical plate, whereas the same tube filled with adequate packing can give the equivalent of 20 or more theoretical plates. A column with 12 theoretical plates is adequate for the practical separation of benzene (bp 80.1°) and toluene (bp 110.8°). The number of theoretical plates required for a given separation increases when the reflux ratio is decreased.

The number of theoretical plates cannot be determined from the geometry of the distilling column; it is calculated from the separation effected with a liquid mixture for which the liquid-vapor equilibrium data are fully known. As an example, the determination of the number of theoretical plates in a column by a distillation of a mixture of carbon tetrachloride and benzene is illustrated in Fig. 19.

The ordinates of the upper curve give the experimentally determined

mole per cent of carbon tetrachloride in the vapor which is in equilibrium with the liquid having the composition given on the abscissa. Along the lower line, making an angle of  $45^\circ$ , the compositions of the vapor and liquid are the same. Temperatures are not involved in this diagram. They vary from the boiling point of pure benzene to that of pure carbon tetrachloride.

Suppose, for example, that a sample of the distillate obtained under conditions of practically total reflux had composition *B* and the residue in the distilling flask had composition *A*, as indicated by the dotted lines. A series of vertical and horizontal lines is drawn stepwise from *A* as shown until the composition of the distillate is reached. Each vertical line represents an ideal distillation step in which the intersection with the upper line gives the composition of the vapor which is in equilibrium with the liquid indicated by the intersection of the vertical line with the lower line. Each horizontal line represents complete condensation of all the vapor to give a liquid of the same composition as the vapor. The number of these vertical-line steps minus 1 is equal to the number *n* of theoretical plates in the fractionating column. The liquid-vapor surface in the distillation pot acts as 1 theoretical plate.

Depending upon the construction of the distillation column, the number of theoretical plates may vary somewhat with the rate of entry of vapor into the bottom of the column and the rate of return of liquid from the top of the column. In the case of small-scale laboratory columns, it is found that the actual separations obtainable at finite reflux ratios are, in general, lower than would be predicted from the number of theoretical plates determined at total reflux.

The number of theoretical plates in a column under actual operating conditions may be determined by the method of McCabe and Thiele.<sup>5</sup> In this method the number of theoretical plates is obtained by plotting a curve representing mole fraction of the more volatile component in the binary mixture in the vapor phase versus its mole fraction in the liquid phase and counting steps between this curve and the *operating line*, rather than the  $45^\circ$  line, which is used for the calculation of theoretical plates at total reflux. The operating line is a straight line drawn through the  $45^\circ$  line at the composition of the distillate with a slope equal to  $R/(1 + R)$ , where *R* is the reflux ratio. The student is referred to chemical engineering texts<sup>1,8</sup> for a complete description of the use of this important concept in actual separations by fractional distillation.

**Apparatus.** Vigreux column; vacuum-jacketed packed columns; still head with cold thumb and thermometer; glass-cloth-covered heating mantle; variable auto-transformer; distilling flask; 100-ml graduated cylinder; small test tubes and corks; Abbe refractometer; carbon tetrachloride; chloroform; benzene.

**Procedure.** Two types of fractionating columns are to be employed, such as unpacked columns of the Vigreux type and vacuum-insulated columns of the bubble-plate type or columns packed with double cones of metal screen (Stedman), stainless-steel saddles, or glass helices. A distillation apparatus with a vacuum-jacketed fractionating column is illustrated in Fig. 20. The unpacked column and one of the packed columns are compared by determining the number of theoretical plates for each at total reflux, using solutions of benzene and carbon tetrachloride. Samples from the distilling pot and distillate are to be analyzed, and measurements of refractive index with an Abbe refractometer are convenient for this purpose.

About 10 ml of carbon tetrachloride and 40 ml of benzene are mixed and placed in the distillation pot, which is attached to the Vigreux column. The distilling pot is heated with an electrical heating mantle controlled with a variable autotransformer. The liquid is boiled vigorously until condensation takes place in the top of the distilling column, and then the heating is decreased so that the column does not become flooded. The cold-thumb condenser should be in such a position that all the condensate is returned to the column.

After equilibrium is attained, as indicated by the fact that the thermometer reading is constant, a sample of the material is taken from the top of the column. The cold-thumb condenser is withdrawn to a position such that the condensed liquid drips into the graduated cylinder and is collected. The first two or three drops are discarded, and then a 1-ml sample is collected for analysis with the Abbe refractometer (page 55). The electrical heater is then turned off, and a sample of the liquid (about 1 ml) is removed through the sidearm of the distillation pot, using a pipette or tube. It is to be emphasized that the efficiency of the column

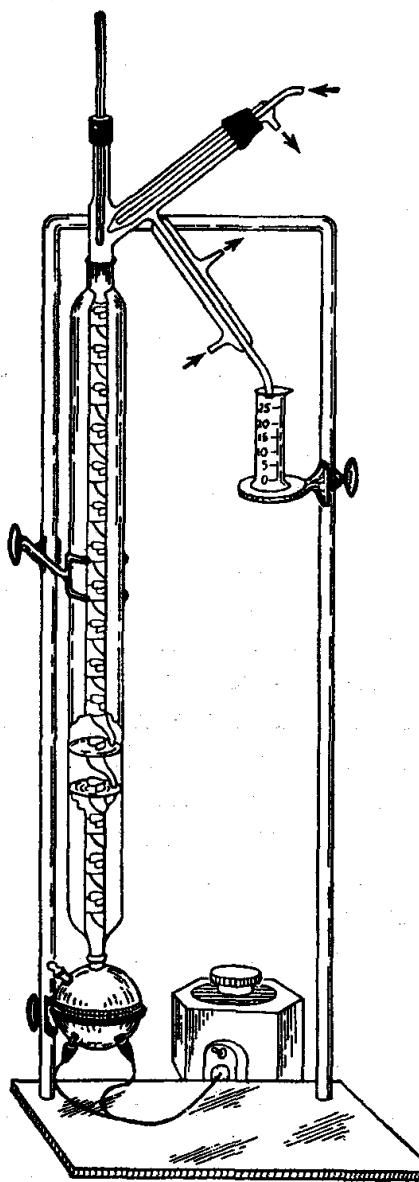


FIG. 20. Bubble-plate fractionating column.

determined by use of these two samples is the efficiency essentially at total reflux, since the column is brought to equilibrium at total reflux and only a small sample is withdrawn from the column. A finite reflux ratio is necessarily used in collecting the sample, but it has a negligible effect on the composition of the sample as long as the sample taken is small.

The above procedure is repeated using a packed fractionating column or a bubble-plate column rather than the Vigreux column. The packed column requires a longer time to come to equilibrium.

While equilibrium is being established in the fractionating column, refractive-index measurements with an Abbe refractometer are made on pure benzene, pure carbon tetrachloride, and two or three mixtures of known composition. These measurements are used for the determination of the compositions of samples of distillate and residue.

The packed column is used next to demonstrate the separation of two liquids. The column and distilling pot are emptied and dried, and 30 ml of chloroform and 30 ml of benzene are introduced. The reflux condenser is set for a reflux ratio of from 5:1 to 10:1, as estimated from the rates of dripping from the reflux condenser and from the distillation tube. The distillate is collected in the graduated cylinder. A 1-ml sample of the distillate is collected in a small stoppered bottle after every 3 ml of distillate, and the samples are then used for refractive-index measurements. A record is kept of the total volume of liquid distilled and the thermometer reading at the time of taking each sample. The final total volume of the distillate is also recorded.

**Calculations.** The refractive indices of benzene, of carbon tetrachloride, and of the known mixtures of the two are plotted on coordinate paper against the mole per cent of carbon tetrachloride. A smooth curve is drawn to represent these data and used to determine the composition of an unknown liquid mixture by interpolation of the refractive index.

The numbers of theoretical plates effective in the Vigreux column and in the packed column at total reflux are calculated with the help of a large graph in which the mole per cent of the more volatile component in the vapor is plotted against the mole fraction of this component in the liquid, as indicated in Fig. 19. The data required for the benzene-carbon tetrachloride system are given in Table 1.

The efficiency of various types of packing and construction of the fractionating column may be compared by calculating the length equivalent to 1 theoretical plate. The length of column per theoretical plate is called the *height equivalent per theoretical plate* (H.E.T.P.). This value is calculated for the various columns used.

The effectiveness of the chloroform-benzene distillation is illustrated by



plotting the temperatures of the condensing distillate against the percentage of the total volume of the mixture distilled. The refractive indices of the samples of distillate are also plotted on the same graph against the percentage of the total volume of liquid distilled. For a column with a very large number of theoretical plates operated at a high reflux ratio, a square step-shaped curve is obtained. The refractive index of the distillate changes abruptly from that of the more volatile to that of the less volatile component when the former has all distilled out. Likewise, the temperature of distillation rises abruptly when the more volatile component is distilled out.

TABLE 1. LIQUID AND VAPOR COMPOSITION OF MIXTURES OF CARBON TETRACHLORIDE AND BENZENE AT 760 MM AND AT TEMPERATURES BETWEEN THE BOILING POINTS<sup>7</sup>

Mole per cent CCl <sub>4</sub> in liquid.....	0	13.64	21.57	25.73	29.44	36.34	40.57	52.69	62.02	72.2
Mole per cent CCl <sub>4</sub> in vapor.....	0	15.82	24.15	28.80	32.15	39.15	43.50	54.80	63.80	73.3

**Suggestions for Further Work.** Additional pairs of liquids may be separated by fractionation with an efficient column. A mixture of carbon tetrachloride and toluene may be used to determine the number of theoretical plates. The data for this system are given in Table 2.

TABLE 2. LIQUID AND VAPOR COMPOSITIONS OF MIXTURES OF CARBON TETRACHLORIDE AND TOLUENE<sup>7</sup>

Mole per cent CCl <sub>4</sub> in liquid...	0	5.75	16.25	28.85	42.60	56.05	64.25	78.20	94.55
Mole per cent CCl <sub>4</sub> in vapor...	0	12.65	31.05	49.35	64.25	75.50	81.22	89.95	97.35

Some of the various types of packing referred to in Chap. 21 may be compared by determining the H.E.T.P. for each.

The value of a fractionating column depends not only on the number of theoretical plates, but also on the amount of liquid held up by the packing.<sup>4,8</sup> Equilibrium conditions are attained more rapidly if the holdup of the column is small. The amount of liquid held up may be determined at the end of an experiment by removing the heating bath, taking out the column and blowing dry air through it, and condensing the material in a weighed U tube surrounded by a freezing bath of dry ice. When the packing is completely dry, the increase in weight of the U tube gives the weight of the liquid held up in the column.

#### References

1. Badger and Banchero, "Introduction to Chemical Engineering," McGraw-Hill Book Company, Inc., New York (1955).
2. Bowman in Gruse and Stevens: "Chemical Technology of Petroleum," 3d ed., McGraw-Hill Book Company, Inc., New York (1960).
3. Carney, "Laboratory Fractional Distillation," The Macmillan Company, New York (1949).

4. Collins and Lantz, *Ind. Eng. Chem. Anal. Ed.*, **18**, 673 (1946).
5. McCabe and Thiele, *Ind. Eng. Chem.*, **17**, 605 (1925).
6. Morton, "Laboratory Techniques in Organic Chemistry," McGraw-Hill Book Company, Inc., New York (1938).
7. Perry, "Chemical Engineers' Handbook," 3d ed., Sec. 9, McGraw-Hill Book Company, Inc., New York (1950).
8. Robinson and Gilliland, "Elements of Fractional Distillation," 4th ed., McGraw-Hill Book Company, Inc., New York (1950).
9. Williams and Glazebrook in Weissberger (ed.): "Technique of Organic Chemistry," 3d ed., Vol. IV, Chap. 2, "Distillation," Interscience Publishers, Inc., New York (1960).

## 10. VARIATION OF AZEOTROPE COMPOSITION WITH PRESSURE

The variation of azeotrope composition with pressure is determined for a binary system, and the results compared with predictions based on thermodynamic principles. Measurements of heats of mixing of the two pure liquids are made, and their relation to the effect of temperature on the activity coefficients is considered.

**Theory.**<sup>1-3</sup> The Gibbs free energy  $G$  of a single homogeneous phase containing two components is a function of temperature, pressure, and the numbers of moles  $n_1$ ,  $n_2$  of the two components. For a change of state the differential change in Gibbs free energy is given by

$$dG = -SdT + VdP + \mu_1 dn_1 + \mu_2 dn_2 \quad (1)$$

where  $S$  is the entropy of the phase,  $V$  its volume, and  $\mu_1$ ,  $\mu_2$  the chemical potentials of its two components. Since at any temperature and pressure the free energy of the phase is given by

$$G = n_1\mu_1 + n_2\mu_2 \quad (2)$$

the differential  $dG$  is also given by

$$dG = n_1 d\mu_1 + n_2 d\mu_2 + \mu_1 dn_1 + \mu_2 dn_2 \quad (3)$$

Combination of Eqs. (1) and (3) yields the Gibbs-Duhem equation,

$$SdT - VdP + n_1 d\mu_1 + n_2 d\mu_2 \equiv 0 \quad (4)$$

which interrelates the changes in the temperature, the pressure, and the chemical potentials of the components for the given change of state. This relation may be written in terms of intensive quantities by dividing by  $(n_1 + n_2)$ , the total number of moles, to obtain

$$\bar{S}dT - \bar{V}dP + X_1 d\mu_1 + X_2 d\mu_2 \equiv 0 \quad (5)$$

where  $\bar{S}$ ,  $\bar{V}$  are entropy and volume per mole of solution, respectively, and  $X_i$  is the mole fraction of component  $i$ .

Consider now the simultaneous application of this relation to a liquid phase (subscript  $l$ ) and the vapor phase (subscript  $v$ ) in equilibrium with it:

$$\bar{S}_l dT - \bar{V}_l dP + X_{1,l} d\mu_{1,l} + X_{2,l} d\mu_{2,l} \equiv 0 \quad (6)$$

$$\bar{S}_v dT - \bar{V}_v dP + X_{1,v} d\mu_{1,v} + X_{2,v} d\mu_{2,v} \equiv 0 \quad (7)$$

Since for equilibrium the chemical potential for each component must have a common value for both phases,

$$\mu_{1,v} = \mu_{1,l} = \mu_1 \quad \mu_{2,l} = \mu_{2,v} = \mu_2$$

and Eqs. (6) and (7) may be combined to give

$$(\bar{S}_v - \bar{S}_l) dT - (\bar{V}_v - \bar{V}_l) dP + (X_{2,l} - X_{2,v})(d\mu_1 - d\mu_2) \equiv 0 \quad (8)$$

This equation determines the relation between the changes in temperature, in pressure, and in chemical potentials in going from one vapor-liquid equilibrium condition to another. Now consider a variation in composition at constant temperature ( $dT = 0$ ) away from a state for which the equilibrium vapor and liquid compositions are identical (the azeotropic condition), so that  $(X_{2,l} - X_{2,v}) = 0$ . Since in general  $(\bar{V}_v - \bar{V}_l)$  is not zero, it follows that  $dP = 0$  for the indicated differential change, and hence there must be a minimum or maximum in the plot of equilibrium pressure versus composition, at constant temperature, at the azeotrope composition. Similarly, for a shift in composition at constant pressure, since  $(\bar{S}_v - \bar{S}_l) \neq 0$ , there must be a maximum or minimum at the azeotrope composition in the plot of equilibrium temperature versus composition at constant pressure (the boiling-point diagram).

The azeotrope composition changes as the equilibrium temperature and pressure are changed. If the composition is known for one pressure, the corresponding azeotrope composition for another pressure can be estimated in the following way. As shown in Exp. 8, to the ideal-gas approximation for the vapors involved, the activity coefficient for a component in the liquid phase is given by

$$\gamma_i = \frac{X_{i,v} P}{X_{i,l} P_i^*(T)} \quad (9)$$

where  $P$  = pressure of equilibrium vapor phase

$P_i^*(T)$  = vapor pressure of pure-liquid component  $i$  at temperature involved

$X_{i,v}$ ,  $X_{i,l}$  = mole fractions of component  $i$  in vapor and liquid phases, respectively

Let  $P_{\text{az}}$  represent the vapor pressure of the azeotrope (this of course corresponds to the constant pressure  $P$  for a boiling-point diagram), for

which  $X_{i,l} = X_{i,v}$ . Then for the azeotropic solution

$$\gamma_{1,az} = \frac{P_{az}}{P_1^*(T)} \quad \gamma_{2,az} = \frac{P_{az}}{P_2^*(T)} \quad (10)$$

and hence

$$\frac{\gamma_{1,az}}{\gamma_{2,az}} = \frac{P_2^*(T)}{P_1^*(T)} \quad (11)$$

The azeotrope composition thus is that composition for which the ratio of the activity coefficients of the two components is equal to the inverse ratio of the vapor pressures of the two pure liquids at the temperature concerned. If the azeotrope composition and pressure are known for one temperature, the coefficients  $A_1$ ,  $A_2$  can be calculated for the given  $T$ ,  $P$ , for the van Laar equations:

$$\log \gamma_1 = \frac{A_1}{\left(1 + \frac{A_1 X_{1,l}}{A_2 X_{2,l}}\right)^2} \quad \log \gamma_2 = \frac{A_2}{\left(1 + \frac{A_2 X_{2,l}}{A_1 X_{1,l}}\right)^2} \quad (12)$$

If  $A_1$  and  $A_2$  as thus determined are assumed to be independent of temperature and pressure, i.e., if the activity coefficients are considered to be functions of composition only, then it is possible to calculate the mole fraction of component 1 for the azeotrope at a different temperature as the value of  $X_{1,l}$  for which Eq. (11) is satisfied at this new temperature. The new azeotrope pressure  $P_{az}$  can be calculated by use of the relation

$$\gamma_{1,az} = \frac{P_{az}}{P_1^*(T)}$$

The accuracy of the prediction so made necessarily depends on how well the van Laar equations express the concentration dependence of the activity coefficients at a given temperature and pressure; for satisfactory results the azeotropes involved should be reasonably intermediate in composition.

There remains the question of the validity of the assumption that the activity coefficients are insensitive to changes in temperature and pressure at constant composition. From Eq. (12) it is seen that

$$A_1 = \lim_{X_{1,l} \rightarrow 0} (\log \gamma_1) \quad A_2 = \lim_{X_{2,l} \rightarrow 0} (\log \gamma_2) \quad (13)$$

Hence

$$\left(\frac{\partial A_1}{\partial T}\right)_P = \left[\left(\frac{\partial \log \gamma_1}{\partial T}\right)_P\right]_{X_{1,l} \rightarrow 0} \quad (14)$$

From the basic relation between the activity coefficient, concentration, and chemical potential,

$$RT \ln \gamma_1 X_{1,l} = \mu_{1,l} - \mu_{1,l}^\circ$$

and thus

$$\left(\frac{\partial \log \gamma_1}{\partial T}\right)_{P, X_{1,l}} = -\frac{1}{2.303R} \frac{\bar{H}_1 - \bar{H}_1^\circ}{T^2} \quad (15)$$

where the term  $\bar{H}_1 - \bar{H}_1^\circ$  actually represents the differential heat of solution (cf. Exp. 4) of pure-liquid component 1 in the solution of concentration  $X_{1,l}$  at the given temperature and pressure. The temperature coefficient of  $A_1$  is thus determined by the limiting value of the differential heat of solution of component 1 at infinite dilution in component 2 as solvent.

$$\left(\frac{\partial A_1}{\partial T}\right)_P = \frac{-1}{2.303RT^2} [\bar{H}_1(X_{1,l}) - \bar{H}_1^\circ]_{X_{1,l} \rightarrow 0} \quad (16)$$

The bracketed enthalpy term can be calculated from integral-heat-of-solution data; it can be approximated by measuring the heat of solution per mole of component 1 in a sufficiently large excess of component 2 to give a very dilute product solution. Its value may be as large as several kilocalories per mole or more, particularly when hydroxylic compounds, such as alcohols, are involved. Similarly, the pressure coefficient of  $A_1$  is found as follows:

$$\left(\frac{\partial \log \gamma_1}{\partial P}\right)_T = \frac{1}{2.303RT} \left[ \left(\frac{\partial \mu_{1,l}}{\partial P}\right)_{T, X_{1,l}} - \left(\frac{\partial \mu_{1,l}^\circ}{\partial P}\right)_{T, X_{1,l}} \right] \quad (17)$$

$$= \frac{1}{2.303RT} [\bar{V}_1(X_{1,l}) - \bar{V}_1^\circ] = \frac{1}{2.303RT} [\bar{V}_1(X_{1,l}) - V_1^*] \quad (18)$$

and

$$\left(\frac{\partial A_1}{\partial P}\right)_T = \frac{\bar{V}_1(X_{1,l} \rightarrow 0) - V_1^*}{2.303RT} \quad (19)$$

where  $\bar{V}_1^\circ = V_1^*$ , the molar volume of pure liquid 1 at the temperature and pressure of the solution. The partial molar volume of component 1 at infinite dilution in component 2 as solvent,  $\bar{V}_1(X_{1,l} \rightarrow 0)$ , can be calculated from density measurements on the solutions (cf. Exp. 13). Since for solutions of this type  $\bar{V}_1$  changes but slightly with concentration and is usually not much different from  $V_1^*$ , the pressure coefficient of  $A_1$  will be very small.

**Apparatus.** Fractional distillation column equipped for vacuum distillations; distilling flask; heating mantle and autotransformer; pressure-control system; pycnometers or Westphal balance; sample vials; Dewar calorimeter, thermistor thermometer, or sensitive mercury thermometer; distilled water; acetonitrile, ethanol.

**Procedure.** An aqueous solution containing acetonitrile at a mole fraction of approximately 0.75 is prepared. The quantity of solution required will depend upon the holdup of the fractionating column used, but should not exceed 150 ml. The solution is placed in the distilling

flask, which is then connected to the fractionating column. The water valve is opened *slowly* to start the flow of cooling water through the distilling head, which is set for total reflux. The autotransformer switch is turned on, and the control knob advanced from zero as required to raise the temperature of the solution to the boiling point. The boil-up rate is increased until condensation takes place in the distilling head, with a steady but not excessive stream of condensate returned to the column. When the temperature shown by the thermometer immersed in the vapor at the top of the column has become constant, indicating that equilibrium has been reached, a preliminary sample of condensate is drained into the first receiver (and subsequently discarded) and the sample collector is rotated to obtain a sample for analysis in the second receiver. The barometric pressure and condensation temperature are recorded. Analysis of this sample gives the azeotrope composition for the measured temperature and pressure, since the fractionating column separates out the minimum-boiling azeotrope due to its high volatility. If the analysis is not made immediately, the sample container should be tightly stoppered.

The head is again set for total reflux, and the autotransformer is turned off. The sample collecting unit is removed, and the container holding the azeotrope sample is tightly stoppered and set aside for later analysis. The sample collector is cleaned, dried, reassembled, and put back in place on the column, which is then connected to the pressure-control system. The pressure in the column is then *gradually* reduced to about 500 mm and maintained there. The liquid boil-up rate is increased, and the column is brought to equilibrium as before. A sample for analysis is then obtained as described above; the pressure and condensation temperature are recorded. The column is reset to total reflux, and the heating mantle turned off. The pressure in the system is now raised slowly to atmospheric. The second azeotrope sample is set aside for analysis, and the apparatus prepared for the next run. Further determinations are then made for pressures of approximately 350 and 200 mm. Care should be taken to record the condensation temperature and pressure for each azeotropic solution collected.

The densities of the samples are measured by means of the Westphal balance (page 454) or by the pycnometric method (page 90), and their concentrations are determined by reference to a working curve of density versus mole fraction of acetonitrile as found for samples of known composition. The data for this curve may be obtained during the periods in which the column is coming to equilibrium.

A measurement is made of the integral heat of solution of liquid acetonitrile in water to give a product solution in which the mole fraction of acetonitrile is 0.05 or less. A Dewar calorimeter of the type used in Exp. 4 or 5 may be used. Fifty milliliters of distilled water (or other

accurately measured quantity, as required to cover the thermometer bulb completely) is placed in the calorimeter. The thermometer reading is noted, and a sample of acetonitrile is adjusted to the same temperature level by warming or cooling in a water bath. Ten milliliters of acetonitrile is then pipetted into the calorimeter, the solution is stirred to make it homogeneous, and the change in temperature is determined as described under Exp. 5. In this case the temperature change will be small. The temperature change observed and the quantities of reactants used are recorded.

In a second experiment the same procedure is followed with 100 ml of acetonitrile as solvent and 1 ml of water added as solute.

The heat capacity of the calorimeter used may be determined as described under Exp. 5, if the value is not given for the unit provided.

**Calculations.** From the experimentally determined azeotrope composition at atmospheric pressure, the van Laar coefficients are calculated (cf. Exp. 8). The necessary vapor-pressure data for acetonitrile may be taken from the work of Heim as summarized by Timmermans,<sup>8</sup> and for water from handbooks or the International Critical Tables.<sup>4</sup> The ratio  $\gamma_1/\gamma_2$  is calculated for various values of  $X_{1,l}$ , the mole fraction of acetonitrile, from 0.6 to 0.9. The ratio  $P_2^*(t)/P_1^*(t)$  of the vapor pressures of the two pure liquids is calculated for a series of temperatures in the range from 30 to 90°C. On the same piece of graph paper two curves are plotted, with the same vertical scale in each case:

1.  $\gamma_1/\gamma_2$  as ordinate versus  $X_{1,l}$  as abscissa
2.  $P_2^*(t)/P_1^*(t)$  as ordinate versus  $t$  as abscissa

For a selected temperature  $t'$  the predicted azeotrope composition is found by reading off the value of  $X_{1,l}$  for which  $\gamma_2/\gamma_1 = P_2^*(t)/P_1^*(t)$ . For this composition the activity coefficient  $\gamma_{1,az}$  for acetonitrile in the azeotropic solution is calculated from the van Laar equation, and the azeotrope pressure  $P_{az}(t')$  is predicted from the relation

$$\gamma_{1,az} = \frac{P_{az}(t')}{P_1^*(t')}$$

In this way, results are obtained for a comparison with the experimentally determined combinations of azeotrope pressure, temperature, and composition, which is prepared in tabular form.

The heat of solution, for the common temperature of the reactants, of the species added as solute in a given case is calculated from the relation (cf. Exp. 5)

$$\Delta H = -C_P \Delta T$$

where  $\Delta T$  = observed change in temperature

$C_P$  = total heat capacity of system

Here  $C_P$  is the sum of the heat capacities of the product solution and calorimeter. The former is to be calculated as the sum of the heat capacities<sup>4</sup> of the pure liquids, an approximation which is adequate for the present purposes. The latter will be furnished for the unit provided. The integral heat of solution is then calculated by dividing the observed  $\Delta H$  by the number of moles of solute added. It is now assumed that the product solution is sufficiently dilute so that the integral heat of solution and differential heat of solution differ negligibly and their common value would not change significantly for work at lower concentrations. The temperature coefficient of the van Laar parameter  $A_1$  is then calculated by use of Eq. (16). In a similar fashion the temperature coefficient for the quantity  $A_2$  is calculated. The implications of these results (concerning the assumption earlier made that the activity coefficients are functions of composition only) are considered. It should be recognized that the heat-of-solution data, here obtained at room temperature, are subject to some change with temperature.

A summary of experimental results for the acetonitrile-water system has been given by Timmermans.<sup>9</sup> Of particular pertinence are the papers of Othmer and Josefowitz,<sup>6</sup> Maslan and Stoddard,<sup>5</sup> and Vierk.<sup>9,10</sup> The heat-of-mixing data given in the latter reference were calculated from temperature-pressure-composition data for the system and do not result from direct calorimetric measurements.

**Practical Applications.** The prediction of the behavior of real-solution systems from a minimum of experimental data is a common problem in modern technology.

**Suggestions for Further Work.** The heat-of-solution measurements may be made for a range of concentrations to permit a more accurate estimation of the differential heats of solution at infinite dilution. Similar measurements may be made for the system acetonitrile-ethanol, and the results compared with those calculated from the heats of mixing given by Thacker and Rowlinson.<sup>7</sup> The term *heat of mixing*,  $\Delta H_m$ , as regularly employed in solution thermochemistry, refers to the increase in enthalpy in the formation of one mole of *solution* from the pure-liquid components at the temperature and pressure of the solution.

### References

1. Guggenheim, "Thermodynamics," pp. 188-190, Interscience Publishers, Inc., New York (1949).
2. Hala, Pick, Fried, and Vilim, "Vapor-Liquid Equilibrium," transl. by G. Standart, Pergamon Press, New York (1958).
3. Hougen and Watson, "Chemical Process Principles," Chap. XV, John Wiley & Sons, Inc., New York (1949).
4. International Critical Tables, McGraw-Hill Book Company, Inc., New York (1928).
5. Maslan and Stoddard, Jr., *J. Phys. Chem.*, **60**, 1147 (1956).
6. Othmer and Josefowitz, *Ind. Eng. Chem.*, **39**, 1175 (1947).
7. Thacker and Rowlinson, *Trans. Faraday Soc.*, **50**, 1036 (1954).



8. Timmermans, "Physico-chemical Constants of Pure Organic Compounds," Elsevier Press, Inc., Houston, Tex. (1950).
9. Timmermans, "Physico-chemical Constants of Binary Systems," Vol. IV, Interscience Publishers, Inc., New York (1960).
10. Vierk, *Z. anorg. Chem.*, **261**, 283 (1950).

## 11. ELEVATION OF THE BOILING POINT

The boiling points of a solution and of the pure solvent are determined and used for calculating the molecular weight of a nonvolatile solute.

**Theory.** When a *nonvolatile* solute is dissolved in a solvent, the vapor pressure of the latter is decreased; as a consequence, the boiling point of the solution is higher than that of the pure solvent. The extent of the elevation  $\theta$  depends upon the concentration of the solute, and for *dilute*, *ideal* solutions it may be shown that

$$T_b - T_0 = \theta = K_b m \quad (1)$$

where

$$K_b = RT_0^2/1000\lambda_v \quad (2)$$

and  $T_0$  = boiling point of pure solvent

$T_b$  = boiling point of solution of molality  $m$ , at same pressure

$\lambda_v$  = enthalpy of vaporization of pure solvent *per gram* at temperature  $T_0$

$K_b$  = molal boiling-point elevation constant

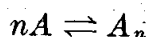
Note that  $K_b$  is a constant characteristic of the solvent. Relation (1) permits calculation of the molecular weight of the solute, since it may be transformed into the equivalent form

$$M = \frac{1000K_b g}{G\theta} \quad (3)$$

where  $\theta$  is the elevation of the boiling point for a solution containing  $g$  grams of solute of molecular weight  $M$  in  $G$  grams of solvent of boiling-point elevation constant  $K_b$ .

It should be noted that even for ideal solutions the foregoing relations are valid only if the solution is also dilute, i.e., if the mole fraction of solute is small.

One of the more interesting applications of this equation is in the study of solutes which can form dimers, trimers, etc. The position of equilibria of the type



may be strongly dependent on the solvent. Examination of the derivation which leads to Eqs. (1) to (3) will show that if several solute species

are present, the value of  $M$  (now the *apparent molecular weight*) found by naïve application of Eq. (3) is actually the average for the species present; i.e.,

$$M = \sum_i X_i M_i \quad (4)$$

where  $X_i$  is the mole fraction of species  $i$ , and  $M_i$  its molecular weight. Although the position of equilibrium cannot be found with accuracy by this method, it is possible to characterize systems in which the solute is mainly of a single species by comparing the apparent molecular weight with the known formula weight.

More rigorous thermodynamic equations are required for the analysis of boiling-point elevation data on solutions which deviate markedly from ideal behavior. The effort is rewarded, however, because one gains additional information in such cases, pertaining to the nonideal properties of these solutions.<sup>3,8</sup> For example, activity coefficients for sodium chloride in aqueous solution have been determined in this way by Smith<sup>9</sup> over the range 60 to 100°C. Thus boiling-point data represent potentially a valuable source of information concerning electrolyte solutions.

For the determination of the boiling temperature of a solution, the thermometer must be in contact with solution rather than condensed vapor as in the case of a pure liquid. The elimination of superheating of the liquid phase is therefore particularly important and is usually accomplished by means of the vapor lift pump described below; electrical heating may be used to minimize the initial degree of superheating of the solution. The method of Landsberger,<sup>5</sup> preferably as modified by McCoy,<sup>6</sup> may also be used; solvent vapor is passed into the solution, where it condenses, and raises the solution to the boiling point. In this arrangement there is no radiation or conduction of heat from a body at a higher temperature and superheating is eliminated.

**Apparatus.** Boiling-point apparatus of the Cottrell type; Beckmann thermometer or other thermometer graduated to 0.01°; carbon tetrachloride; benzoic acid.

**Procedure.** The elevation of the boiling point of carbon tetrachloride produced by dissolved benzoic acid is to be measured.

A commercially available boiling-point apparatus of the Cottrell type<sup>1,2,11</sup> is shown in Fig. 21. A known quantity of solvent is placed in the tube, and a Beckmann thermometer or other thermometer graduated to 0.01° is put into place. The liquid level must be below the lower end of the glass thermometer shield. The apparatus is clamped in a vertical position and heated with a small gas flame or, preferably, an electrical heater. The external shield shown in Fig. 21 is a convenient means of keeping drafts of air away. The purpose of the small inverted funnel, which is raised above the bottom on small projections, is to catch

the bubbles of vapor and direct them through the center tube and three vertical spouts. As the bubbles discharge through these outlets, they direct three sprays of liquid and vapor against the thermometer; any superheated solution comes to equilibrium with the vapor by the time it gets to the thermometer bulb.

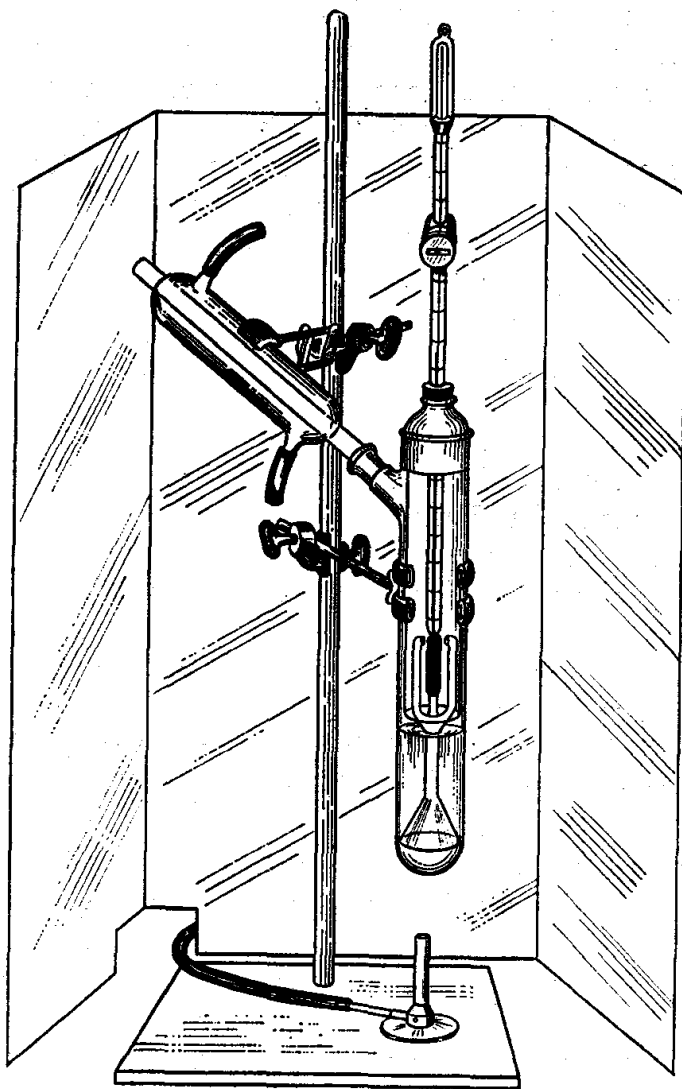


FIG. 21. Cottrell boiling-point apparatus.

An inner glass shield, concentric with the outer tube but fastened at the top, improves the efficiency of the pumping system and also serves to shield the thermometer from the cold solvent returning from the condenser. A somewhat more rugged design is one in which the funnel unit is firmly attached by three short pieces of glass rod to the lower end of the inner glass shield.†

† An apparatus of this design is obtainable on special order from the Scientific Glass Apparatus Co., Bloomfield, N.J., as Model J-2098-1 (modified, Print 577996).

If the liquid does not pump steadily over the thermometer bulb, the rate of heating is changed. The rate should be adjusted so that ebullition takes place primarily within the funnel in order to produce the most efficient pumping action. The rate of heating should be steady and should not be so great as to drive the liquid condensate film too close to the upper end of the condenser, since this may result in loss of solvent and also cause superheating. A metal chimney placed around the burner helps to reduce fluctuations in the rate of heating.

An absolutely constant boiling-point reading cannot be expected, but when equilibrium has been reached, the observed temperature will fluctuate slightly around a mean value and in particular will not show a slow drift except when there is a corresponding drift in barometric pressure. The thermometer, which must be handled carefully, is tapped gently before a reading is taken. Since the boiling point is sensitive to changes in pressure, the barometer should be read just after the temperature reading is recorded.

After the boiling point of the pure solvent has been determined, the liquid is allowed to cool. The condenser is then removed, and a weighed quantity of benzoic acid sufficient to produce a 2 to 3 per cent solution is added. To prevent loss, the benzoic acid is made up into a pellet in a pellet machine or is placed in a short glass tube and rammed tight with a central rod acting as a plunger.

After the boiling point of the pure solvent has been determined, the liquid is allowed to cool, the condenser is removed, and the first solute sample is added; alternatively, if it is feasible to do so, the pellets may be dropped in through the condenser. The steady boiling point of the solution is then determined in the manner previously described. Additional determinations are made by adding more pellets. In each case, the barometric pressure is recorded just after the temperature reading has been made.

When possible, a second series of measurements should be made, starting again with pure solvent and covering the same general range of concentrations as before. In this way, a valuable check is obtained on reproducibility.

Serious error can result from failure to wait for equilibrium to be attained. Other experimental errors may be caused by fluctuations in atmospheric pressure, or by appreciable holdup of solvent in the condenser or escape of solvent vapor. The first difficulty may be met by making corrections for pressure changes, by employing a manostat to maintain a constant pressure, or by using two sets of apparatus at the same time, one for solvent and one for solution. Errors from loss or holdup of solvent are tolerable in student work provided reasonable care is

taken to minimize these effects. For work of highest accuracy, one may use an apparatus† in which provision has been made for withdrawing a sample of the liquid just after the temperature measurement has been made. The molality is then found by weighing this sample, evaporating the solvent, and then weighing the residue.

**Calculations.** The molecular weight is calculated by means of Eq. (3), from the values for  $K_b$  shown in Table 1, corrected by use of the pressure coefficient given in the last column, unless the correction is negligible.

TABLE 1. MOLAL BOILING-POINT ELEVATION CONSTANTS<sup>4</sup>

Solvent	Boiling point, °C at 760 mm	$K_b$ at 760 mm	$\frac{\Delta K_b}{\Delta P \text{ (mm)}}$
Acetone.....	56.0	1.71	0.0004
Benzene.....	80.2	2.53	0.0007
Bromobenzene.....	155.8	6.20	0.0016
Carbon tetrachloride....	76.7	5.03	0.0013
Chloroform.....	60.2	3.63	0.0009
Ethanol.....	78.3	1.22	0.0003
Ethyl ether.....	34.4	2.02	0.0005
Methanol.....	64.7	0.83	0.0002
Water.....	100.0	0.51	0.0001

The necessary correction to  $\theta$  required by a difference in the barometric pressures at the times the boiling points of the solvent and solution were recorded may be made by use of Eq. (1) of Exp. 6. For this purpose, it is assumed that  $dp/dT$  may be set equal to  $\Delta p/\Delta T$ . The value of  $\lambda_v$  may be values taken from a handbook.

The calculated apparent molecular weight values are graphed against molality and compared with the formula weight. Any discrepancies among these values should be discussed in the light of the estimated experimental error.

**Practical Applications.** Many materials cannot be vaporized for direct determinations of the vapor density without decomposition. In such cases the material is dissolved in a suitable solvent, and the elevation of the boiling point furnishes a rapid and convenient method for determining the molecular weight. Molecular weights of substances in solution, however, may be different from the values found from vapor-density measurements.

**Suggestions for Further Work.** A more elaborate and accurate method may be used in which a thermocouple gives directly the difference in boiling point between

† The Washburn and Reed<sup>11</sup> modification of the Cottrell boiling point apparatus is available from several commercial sources.

the solvent and solution in two different vessels. This method has been described by Mair.<sup>7</sup> Data of sufficient accuracy may be obtained in this way for extrapolation of the apparent molecular weights to infinite dilution. Only in this way can an accurate value be obtained.<sup>7</sup>

The molecular weight of benzoic acid in a polar solvent such as ethanol may be determined, and the result compared with that obtained with the nonpolar solvent.

*Caution is required when an inflammable solvent is used.*

### References

1. Cottrell, *J. Am. Chem. Soc.*, **41**, 721 (1919).
2. Davis, *J. Chem. Educ.*, **10**, 47 (1933).
3. Harned and Owen, "Physical Chemistry of Electrolyte Solutions," 3d ed., Reinhold Publishing Corporation, New York (1958).
4. Hoyt and Fink, *J. Phys. Chem.*, **41**, 453 (1937).
5. Landsberger, *Ber.*, **31**, 458 (1898).
6. McCoy, *Am. Chem. J.*, **23**, 353 (1900).
7. Mair, *J. Research, Natl. Bur. Standards (U.S.)*, **14**, 345 (1935).
8. Robinson and Stokes, "Electrolyte Solutions," 2d ed., Academic Press, Inc., New York (1959).
9. Smith, *J. Am. Chem. Soc.*, **61**, 497, 500 (1939).
10. Swietoslawski and Anderson in Weissberger (ed.): "Technique of Organic Chemistry," 3d ed., Vol. I, Pt. I, Chap. 8 (1959).
11. Washburn and Read, *J. Am. Chem. Soc.*, **41**, 729 (1919).

### 12. ACTIVITIES FROM FREEZING-POINT DEPRESSION DATA

The freezing point of a solution is lower than that of the pure solvent. Freezing-point depression data are of considerable value in the thermodynamic study of solutions. In particular, activity coefficients of both solvent and solute can be determined as a function of concentration to a high degree of accuracy.

**Theory.** The activity  $a_1$  of solvent† in a solution at temperature  $T$  is defined by

$$\bar{G}_1 = \bar{G}_1^\circ + RT \ln a_1 \quad (1)$$

where  $\bar{G}_1$  = partial molar Gibbs free energy of solvent in solution at temperature  $T$

$\bar{G}_1^\circ$  = molar Gibbs free energy of pure liquid solvent at temperature  $T$

For a solution at the temperature  $T_0$  of freezing of the pure solvent, Eq. (1) is equivalent to

$$\bar{G}_1 = \bar{G}_1^c + RT \ln a_1 \quad (2)$$

where  $\bar{G}_1^c$  = molar free energy of pure crystalline solvent at temperature  $T_0$

† Solvent properties are designated throughout by subscript 1, and solute properties by subscript 2.

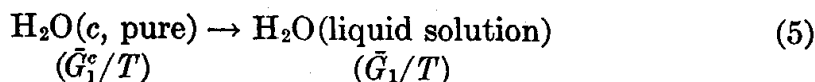
because at  $T_0$  the equilibrium condition

$$\bar{G}_1^o = \bar{G}_1^c \quad (3)$$

is satisfied. Therefore  $a_1$  for a solution at temperature  $T_0$  can be calculated from

$$R \ln a_1 = \left( \frac{\bar{G}_1}{T_0} - \frac{\bar{G}_1^c}{T_0} \right) = \Delta \left( \frac{\bar{G}_1}{T_0} \right) \quad (4)$$

Here, and throughout this discussion, the increment symbol  $\Delta$  will refer to a change in a function of state for solvent in going from the pure crystalline solid to a solution at the *same temperature*  $T$ ; e.g., for water solvent,



For a series of solutions it is desired to calculate, by Eq. (4), the activity of the solvent at the temperature  $T_0$ . To evaluate the right side of Eq. (4), consider the function

$$\Delta \left( \frac{\bar{G}_1}{T} \right)$$

for general  $T$ ; this may be expanded in a Taylor series about  $T_0$  to obtain

$$\begin{aligned} \Delta \left( \frac{\bar{G}_1}{T} \right) = & \left[ \Delta \left( \frac{\bar{G}_1}{T} \right) \right]_0 + \left[ \frac{\partial(\Delta \bar{G}_1/T)}{\partial T} \right]_0 (T - T_0) \\ & + \frac{1}{2} \left[ \frac{\partial^2(\Delta \bar{G}_1/T)}{\partial T^2} \right]_0 (T - T_0)^2 + \cdots \end{aligned} \quad (6)$$

The functions in square brackets in Eq. (6) are to be evaluated at  $T = T_0$ . The series-expansion coefficients are

$$\left[ \Delta \left( \frac{\bar{G}_1}{T} \right) \right]_0 = R[\ln a_1]_0 \quad (7a)$$

$$\left[ \frac{\partial(\Delta \bar{G}_1/T)}{\partial T} \right]_0 = - \left[ \frac{\Delta \bar{H}_1}{T_0^2} \right]_0 \quad (7b)$$

$$\frac{1}{2} \left[ \frac{\partial^2(\Delta \bar{G}_1/T)}{\partial T^2} \right]_0 = - \frac{1}{2} \left[ \frac{\partial}{\partial T} \left( \frac{\Delta \bar{H}_1}{T^2} \right) \right]_0 = \left[ \frac{\Delta \bar{H}_1}{T_0^3} - \frac{\Delta \bar{C}_P}{2T_0^2} \right]_0 \quad (7c)$$

where again all quantities in square brackets are to be evaluated at  $T = T_0$ .

Now if  $T$  in Eq. (6) is specified to be the freezing point of the solution,  $T_f$ , the left side of Eq. (6) becomes zero because of the basic requirement for equilibrium, namely, that  $\bar{G}_1$  have the same value for both phases.

Combining Eqs. (7) and (6) for  $T = T_f$  then yields

$$0 = R[\ln a_1]_0 - \left[ \frac{\Delta \bar{H}_1}{T_0^2} \right]_0 (T_f - T_0) + \left[ \frac{\Delta \bar{H}_1}{T_0^3} - \frac{\Delta \bar{C}_P}{2T_0^2} \right]_0 (T_f - T_0)^2 + \dots \quad (8)$$

With the freezing-point depression designated as  $\theta = T_0 - T_f$ , Eq. (8) leads to

$$-R[\ln a_1]_0 = \left[ \frac{\Delta \bar{H}_1}{T_0^2} \right]_0 \theta + \left[ \frac{\Delta \bar{H}_1}{T_0^3} - \frac{\Delta \bar{C}_P}{2T_0^2} \right]_0 \theta^2 + \dots \quad (9)$$

Since  $\Delta \bar{H}_1 = \bar{H}_1 - \bar{H}_1^c$  will often be close to  $\Delta \bar{H}_f^\circ \equiv \bar{H}_1^\circ - \bar{H}_1^c$ , the heat of fusion of the pure solvent, it is convenient to write

$$\Delta \bar{H}_1 = \Delta \bar{H}_f^\circ + \bar{L}_1 \quad (10)$$

where  $\bar{L}_1$  is defined by  $\bar{L}_1 = \bar{H}_1 - \bar{H}_1^\circ$  at any given temperature. Introduction of Eq. (10) into (9) then yields

$$-R[\ln a_1]_0 = \left[ \frac{\Delta \bar{H}_f^\circ}{T_0^2} \right]_0 \left\{ \left[ 1 + \frac{\bar{L}_1}{\Delta \bar{H}_f^\circ} \right]_0 \theta + \left[ \frac{1}{T_0} - \frac{\Delta \bar{C}_P^\circ}{2\Delta \bar{H}_f^\circ} \right]_0 \theta^2 + \dots \right\} \quad (11)$$

where  $\bar{L}_1$  and  $\partial \bar{L}_1 / \partial T$  are neglected in comparison with  $\Delta \bar{H}_f^\circ$  and  $\Delta \bar{C}_P^\circ$ , respectively, in the  $\theta^2$  term.

Thus from Eq. (11) the activity coefficient of solvent in a solution at temperature  $T_0$ —the freezing point of the pure solvent—may be found from a measurement of the freezing-point depression  $\theta$  for the given solution.†

For solutions of moderate or low concentration, the simple equation

$$-R[\ln a_1]_0 = \left[ \frac{\Delta \bar{H}_f^\circ}{T_0^2} \right]_0 \theta \quad (12)$$

will often be sufficiently accurate.‡ However, one cannot really use Eq. (12) with confidence unless the higher-order terms in Eq. (11) have been estimated for the most concentrated solution being considered and found to be less than experimental error.

† An equation for  $\ln a_1$  is sometimes given in a somewhat simpler form, with the small but concentration-dependent  $\bar{L}_1$  term absent; in this case, however,  $a_1$  is specified to be the activity at temperature  $T_f$  (rather than at  $T_0$ ); for a series of measurements on solutions of various concentrations, the calculated activities then refer to different temperatures. Equation (11) is given above in the same form as in Reference 2, although a slightly different method of derivation has been used.

‡ Physically, Eq. (12) corresponds to the case  $\Delta \bar{H}_1 = \Delta \bar{H}_f^\circ$ ,  $\Delta \bar{C}_P = 0$ ,  $\theta \ll T_f$ .



For water as solvent at 0°C, the factor in braces in Eq. (11) becomes

$$\left\{ \left[ 1 + \frac{\bar{L}_1}{1436} \right]_0 \theta + [4.9 \times 10^{-4}] \theta^2 + \dots \right\} \quad (13)$$

with  $\bar{L}_1$  in calories per mole and  $\theta$  in degrees. The quantity  $\bar{L}_1$  may be evaluated experimentally from heat-of-dilution data or calculated from

$$\bar{L}_1 = \frac{\partial \Delta H_{1.s.}}{\partial n_1} \quad (14)$$

where  $\Delta H_{1.s.}$  is the integral heat of solution (page 22) for one mole of solute in  $n_1$  moles of solvent. It may also be calculated from solute heats of formation,  $\Delta H_f$  (pages 31–32), which are tabulated for many substances.

A familiar equation for the freezing-point depression for an *ideal*, *dilute* solution is obtained by introducing into Eq. (12) the approximations

$$a_1 \cong X_1 \quad \text{ideal solution} \quad (15)$$

$$\ln X_1 = \ln (1 - X_2) \cong -X_2 \cong -\frac{mM_1}{1000} \quad \text{dilute solution} \quad (16)$$

where  $m$  = molality = number of moles of solute in 1000 g of solvent

$M_1$  = molecular weight of solvent

$X_1, X_2$  = mole fractions of solvent and solute, respectively

The result is

$$\theta = \frac{RT_0^2 M_1}{1000 \Delta \bar{H}_f} m = K_f m \quad (17)$$

where

$$K_f = \frac{RT_0^2 M_1}{1000 \Delta \bar{H}_f} = \frac{RT_0^2}{1000 \lambda_f} \quad (18)$$

where  $\lambda_f$  = heat of fusion of pure solvent, *per gram*, at temperature  $T_0$

$K_f$  = molal freezing-point depression constant

Observe that  $K_f$  is a property of the pure solvent and as such does not depend on the nature of the solute.

If the solute is associated or dissociated in solution, the ideal equations can be expected to serve as useful approximations only if the association or dissociation is recognized explicitly. Thus, consider a solution containing  $n_1$  formula-weight units of solvent and  $n_2$  formula-weight units of solute;  $n_1$  and  $n_2$  are the weights divided by the respective formula weights. Now suppose that, in solution,  $n_2$  formula-weight units of solute actually form  $\nu n_2$  moles of solute, with  $\nu > 1$  for dissociation and  $\nu < 1$  for association. Then the actual mole fraction of solvent,  $X'_1$ , calculated with the association or dissociation explicitly recognized, is

$$X'_1 = \frac{n_1}{n_1 + \nu n_2} = 1 - \frac{\nu n_2}{n_1 + \nu n_2} \cong 1 - \nu \frac{n_2}{n_1} \quad (19)$$

where the last form is valid for dilute solutions. For a solution of stoichiometric molality  $m$  (i.e., with  $m$  formula-weight units of solute per 1000 g of solvent), Eq. (16) becomes

$$\ln X'_1 \cong - \left( \nu \frac{n_2}{n_1} \right) = - \left( \frac{\nu m M_1}{1000} \right) \quad (20)$$

and Eq. (17) becomes

$$\theta = K_f \nu m \quad (21)$$

with  $K_f$  defined as before.

An important use of Eq. (21) is the determination of  $\nu$ . Since the equation holds for the ideal, dilute case only, Eq. (21) might more appropriately be written

$$\nu = \lim_{m \rightarrow 0} \frac{\theta}{K_f m} = \frac{1}{K_f} \lim_{m \rightarrow 0} \frac{\theta}{m} \quad (22)$$

It should be recognized that the limit in Eq. (22) is to be evaluated from experimental data for a number of solutions at finite concentrations; the value of  $\nu$  obtained therefore reflects the behavior of the given solute at the lower end of the concentration range studied.

If the data are accurate enough, *solute* activities may also be calculated from the freezing-point data. The only case to be considered in detail here will be that of a solute which is neither associated nor dissociated at the lower end of the concentration range studied. For this case, the activity  $a_2$  and activity coefficient  $\gamma_2$  of the solute are defined by†

$$\bar{G}_2 = \bar{G}_2^\circ + RT \ln a_2 \quad (23)$$

$$= \bar{G}_2^\circ + RT \ln \gamma_2 m \quad (24)$$

with  $\bar{G}_2^\circ$  defined by specifying  $\gamma_2 \rightarrow 1$  as  $m \rightarrow 0$  or, equivalently, by

$$\bar{G}_2^\circ = \lim_{m \rightarrow 0} (\bar{G}_2 - RT \ln m) \quad (25)$$

The equation for calculating  $\gamma_2$  for a given solution of molality  $m$  at temperature  $T_0$ , based on Eqs. (24) and (25), is

$$\ln \gamma_2 = (\phi_m - 1) + \int_0^m \left( \frac{\phi_m - 1}{m} \right) dm \quad (26)$$

where  $\phi_m$  is the osmotic coefficient at molality  $m$ , defined by

$$\phi_m = - \frac{X_1}{X_2} \ln a_1 = - \left( \frac{1000}{m M_1} \right) \ln a_1 \quad (27)$$

† The molality scale for  $\gamma_2$  is used here. Alternative scales<sup>1-4</sup> are sometimes used and lead to different equations and different numerical values for  $\gamma_2$ .

The derivation of Eq. (26) may be found in a number of texts on chemical thermodynamics.<sup>1-4</sup> When Eq. (12) is applicable,  $\phi_m$  and  $\phi_m - 1$  may be calculated from

$$\phi_m = \frac{\theta}{K_f m} \quad (28)$$

$$\phi_m - 1 = \frac{(\theta/m) - K_f}{K_f} \quad (29)$$

A suitable procedure is first to prepare a graph of  $\theta/m$  versus  $m$  to see whether the data indicate either association or dissociation at the low-concentration end; if, to within experimental error,  $\nu = 1$ , then Eqs. (26) and (29) may be used to find  $\gamma_2$  for any  $m$  in the range studied. The integral is evaluated graphically from a plot of  $(\phi_m - 1)/m$  versus  $m$ .

If an attempt is made to use Eq. (26) for a solute which is associated or dissociated at the lower end of the concentration range studied, the integrand will seem to increase without limit as  $m$  approaches zero; the integral will therefore be indeterminate. This observation reflects the fact that the limit in Eq. (25) either does not exist (dissociation case) or is not being approached even at the lowest concentrations studied (association case). One is therefore compelled to modify the definition of  $\bar{G}_2^\circ$ , and hence also that of  $\gamma_2$  in order to be able to obtain meaningful results for such systems.<sup>1-4</sup>

**Apparatus.** Vacuum bottle with cork and stirrer; precision (calorimeter-type) thermometer ( $+0.5^\circ$  to  $-5.0^\circ$ , graduated to  $0.01^\circ$ ), or differential thermometer with  $5^\circ$  range, or thermistor and bridge (Exp. 4); five 6-in. test tubes with tight stoppers; density balance precise to  $\pm 0.0002$  g/ml with a 10-ml sample, or a set of 5-ml pycnometers and an analytical balance; 100 ml of a suitable solute sample such as isopropyl alcohol, *n*-propyl alcohol, or acetonitrile.

**Procedure.** A suitable apparatus, shown in Fig. 22, consists of a vacuum bottle (1 pt) fitted with a cork, polystyrene† stirrer, and thermometer. A convenient type of thermometer for this experiment is one having a range of  $0.5$  to  $-5.0^\circ\text{C}$  with  $0.01^\circ$  graduations. If a Beckmann thermometer is used, it is adjusted so that the mercury comes near the top of the scale at the freezing point of the pure solvent.

A thermistor‡ offers definite advantages as an alternative to a mercury thermometer: the thermistor has a relatively low time lag and, being physically smaller, does not conduct heat from the room as rapidly into the freezing solution. Thus thermal equilibration can be achieved more

† Polystyrene is thermoplastic and can be bent when heated in a drying oven or above a bunsen-burner flame.

‡ A suitable thermistor and bridge assembly is available as Model S-81601 from E. H. Sargent & Co., Chicago, Illinois.

efficiently. If a thermistor is used, the resistance measurement may be made by means of a d-c Wheatstone bridge and sensitive galvanometer, as outlined in Exp. 4. The temperature dependence of the thermistor resistance may be assumed to have the form

$$R = Be^{\beta/T} \quad (30)$$

where  $R$  is the resistance of the thermistor at the temperature  $T$ . The parameters  $B$  and  $\beta$  may be evaluated by measurement of  $R$  at several known temperatures, which for convenience may be chosen in the range 0 to 25°C.

To the vacuum bottle is added distilled water and an equal volume of clean cracked ice. The water used should be prechilled, to minimize the amount of impurities set free by melting of ice. The freezing mixture should cover the thermometer bulb or thermistor without being too close to the cork. If the ice is not of adequate purity, the observed freezing point will slowly decrease with time as occluded impurities are freed by melting; in this event, it may be necessary to prepare ice by freezing distilled water.

The ice and water are stirred vigorously until a steady temperature is attained. This value is then recorded. If a mercury thermometer is used, it should be gently tapped before being read.

The water is drained off and replaced by a chilled solution of the specified solute in distilled water at a concentration of about 3 molal. The solution and ice are stirred vigorously until a constant temperature is reached, whereupon the temperature is recorded and a sample is with-

drawn quickly with a 10-ml pipette; the tip of the pipette should be held near the bottom of the flask to avoid getting pieces of ice. The pipette is used here only as a matter of convenience, as the sample volume need not be accurately known. To obtain a sample with minimal disturbance of the equilibrium system, the sample should be taken rapidly. The sample is discharged into a 6-in. test tube, which is then stoppered and set aside.

The temperature will appear to rise slightly when the stirring is interrupted for sample-taking, but this apparent rise can be ignored because it results mainly from the warming of the thermometer or thermis-

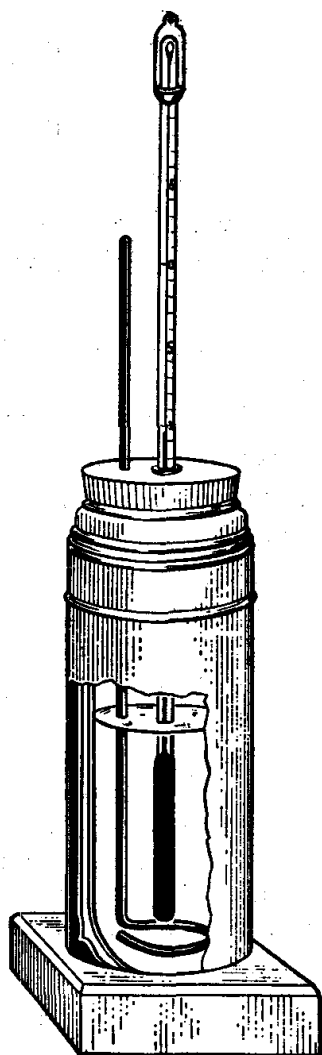


FIG. 22. Freezing-point apparatus.

tor itself and does not indicate a change in temperature of the solution. After the sample has been withdrawn, vigorous stirring may be resumed and a second temperature reading taken. The temperatures recorded for the stirred system immediately before and after sampling should agree to within about  $0.01^{\circ}\text{C}$ , and these values may be averaged for the subsequent calculations.

In a similar fashion, additional samples are taken from equilibrium freezing systems with progressively more dilute solutions, obtained by adding each time an appropriate amount of ice (to replace ice melted in the flask) and ice-cold distilled water. Some allowance should be made for dilution by melting of ice. In all, measurements should be made for about six different concentrations, ranging downward from 3 molal in roughly equal steps of about 0.5 molal each. A convenient way of obtaining well-spaced points covering the desired range of molalities is to adjust the concentration each time to bring the freezing point to the desired region.

The molalities of the samples are determined by careful measurement of density. The precision required is of the order of  $\pm 0.0002$  g/ml. If a density balance is used, the measurements can be made with the samples still in the original test tubes if a device is provided to support them in the balance. The temperatures of the samples should be noted at the time of the density measurements, and the density values corrected to a common temperature by assuming that the thermal coefficient of expansion of a dilute aqueous solution is about the same as that of pure water, for which  $(1/V)(\partial V/\partial T)_P$  is  $2.6 \times 10^{-5} \text{ deg}^{-1}$  at  $25^{\circ}\text{C}$ . Alternatively, 5-ml pycnometers may be filled with the samples at a known temperature and subsequently weighed.

The data needed for preparing a calibration graph of density versus molality are obtained by measuring densities of pure solvent and of four or five solutions of known composition made up by mixing known volumes of the two components.

**Calculations.** If a thermistor is used for temperature measurement, the constant  $\beta$  may be found from a plot of  $\log R$  versus  $1/T$ . As neither this graph nor Eq. (30) is particularly well suited to the accurate calculation of small temperature increments, it is preferable, provided the range of freezing points does not exceed a few degrees, to calculate the freezing-point depressions from the expansion

$$\theta = \frac{T_0^2}{\beta} \left[ \frac{R_f - R_0}{R_0} - \left( \frac{1}{2} + \frac{T_0}{\beta} \right) \left( \frac{R_f - R_0}{R_0} \right)^2 + \cdots \right] \quad (31)$$

where  $R_0$  = resistance at freezing point  $T_0$  of pure solvent

$R_f$  = resistance at freezing point  $T_f$  of solution

Equation (31) is obtained by expanding  $T$  as a function of  $R$  in a Taylor series about  $T_0$ ; the derivatives required are most easily calculated from

$$\frac{dR}{dT} = -\frac{R\beta}{T^2} \quad (32)$$

etc. The first neglected term inside the brackets is of the order of  $[(R_f - R_0)/R_0]^3$ .

The molalities and freezing-point depressions for the various samples are then tabulated. A graph of  $\theta/m$  versus  $m$  is prepared to illustrate the determination of  $\nu$  from Eq. (22). The solvent activity and the osmotic coefficient are calculated for each molality and graphed as functions of  $m$ . For this calculation it is convenient to express the coefficient in Eq. (12) in terms of  $K_f$ . Values of  $K_f$  and of several other pertinent quantities appear in Table 1. For most nonelectrolyte solutions in the concentration range considered here, the  $\bar{L}_1$  term in Eq. (13) is quite negligible.

TABLE 1. FREEZING-POINT DEPRESSION CONSTANTS AND RELATED DATA

Solvent	Freezing point, $t^\circ\text{C}$	$\lambda_f$ , cal/g	$K_f$	$\Delta\bar{C}_P^\circ$ , cal/deg mole
Acetic acid <sup>a</sup> .....	16.61	46.6	3.58	9.4
Benzene <sup>b</sup> .....	5.5	30.1	5.12	
<i>tert</i> -Butanol <sup>c</sup> .....	25.1	21.88	8.37	
Carbon tetrachloride <sup>a</sup> .....	-22.9	3.9	32	
Cyclohexane <sup>b</sup> .....	6.5	7.4	20.0	1.1
Cyclohexanol <sup>d</sup> .....	25.1	4.27	37.7	
Water <sup>a</sup> .....	0.00	79.72	1.860	

<sup>a</sup> Selected Values of Chemical Thermodynamic Properties, *Natl. Bur. Standards (U.S.), Circ., 500* (1952).

<sup>b</sup> Lange, "Handbook of Chemistry," 8th ed., Handbook Publishers, Inc., Sandusky, Ohio (1952).

<sup>c</sup> Getman, *J. Am. Chem. Soc.*, **62**, 2179 (1940).

<sup>d</sup> Wilson and Heron, *J. Soc. Chem. Ind. (London)*, **60**, 168 (1941).

The calculation of solute activities from these data is outlined below.

**Practical Applications.** Equation (17) is often used for the determination of molecular weights of solutes, since it may be written in the equivalent form

$$M_2 = \frac{1000K_f g}{G\theta} \quad (33)$$

where  $\theta$  is the freezing-point depression for a solution containing  $g$  grams of solute of molecular weight  $M_2$  in  $G$  grams of solvent of molal freezing-point depression constant  $K_f$ . Association or dissociation, if complete, leads to values of  $M_2$  which are multiples or submultiples of the formula weight. By an extension of Eq. (33), ionization

constants of weak acids can be found from freezing-point data, since the apparent molecular weight  $M_2$  can be expressed in terms of the fraction dissociated.

**Suggestions for Further Work.** If the data are sufficiently accurate, *solute* activities may be calculated from the data obtained in this experiment; Eq. (26) is applicable provided the graph of  $\theta/m$  versus  $m$  indicates  $\nu = 1$  to within experimental error. It may be desirable to draw a smooth curve, representing the data, on the  $\theta/m$  versus  $m$  graph and to use selected points from this curve (rather than raw data points) for the calculation of solute activities. In any case, the quantities  $(\phi_m - 1)$  and  $(\phi_m - 1)/m$  are tabulated and graphed against  $m$ . For selected values of  $m$ , the integral in Eq. (26) is evaluated from the graph, and  $\gamma_2$  is calculated from Eq. (26).

A good example of a dissociated solute which is readily studied is KCl. In this case, the samples, after being withdrawn into a 5-ml pipette, should be discharged into previously weighed bottles and then weighed. The weight of KCl in each sample is subsequently found by titrating the samples with 0.1 N  $\text{AgNO}_3$ , with about 0.2 ml of 5 per cent potassium chromate solution added as indicator. The  $\text{AgNO}_3$  solution is standardized with weighed samples of KCl.

### References

1. Harned and Owen, "Physical Chemistry of Electrolyte Solutions," 3d ed., Reinhold Publishing Corporation, New York (1958).
2. Lewis and Randall, "Thermodynamics," 2d ed., pp. 404-409, 412-413, rev. by Pitzer and Brewer, McGraw-Hill Book Company, Inc., New York (1961).
3. Robinson and Stokes, "Electrolyte Solutions," 2d ed., Academic Press, Inc., New York (1959).
4. Wall, "Chemical Thermodynamics," pp. 353-355, 357-358, W. H. Freeman and Company, San Francisco (1958).

## 13. PARTIAL MOLAL PROPERTIES OF SOLUTIONS

The accurate determination of the density of a liquid and the precise mathematical treatment of the properties of solutions are studied.

**Theory.**<sup>3-5,7</sup> The quantitative study of solutions has been greatly advanced by the introduction of the concept of partial molal quantities. A property of a solution, e.g., the volume of a mixture of alcohol and water, changes continuously as the composition is changed, and considerable confusion existed formerly in expressing these properties as a function of composition. A *partial molal property* of a component of a solution is defined as follows. Let  $Y$  represent any extensive property of a binary solution; at constant temperature and pressure,  $Y$  then will be a function of the two independent variables  $n_1$  and  $n_2$ , which represent the numbers of moles of the two components present. The partial molal property of component 1 is then defined by the relation

$$\bar{Y}_1 = \left( \frac{\partial Y}{\partial n_1} \right)_{n_2, T, P} \quad (1a)$$

Similarly for component 2,

$$\bar{Y}_2 = \left( \frac{\partial Y}{\partial n_2} \right)_{n_1, T, P} \quad (1b)$$

The partial molal quantity may be designated by a bar above the letter representing the property, and by a subscript, which indicates the component to which the value refers. The usefulness of the concept of partial molal quantities lies in the fact that it may be shown mathematically<sup>3,4,7</sup> that

$$Y(n_1, n_2) = n_1 \bar{Y}_1 + n_2 \bar{Y}_2 \quad (T, P \text{ constant}) \quad (2)$$

Any extensive property of the solution may be expressed in this manner in terms of partial molal properties, which themselves are functions of the concentration of the solution, the temperature, and the pressure and must be evaluated by means of experimental measurements. The activity  $a_i$  of a component of a solution is defined in terms of its relative partial molal free energy  $\bar{G}_i - \bar{G}_i^\circ$ , and the calculation of heats of reaction for solution systems requires a knowledge of the relative partial molal enthalpies  $\bar{H}_i - \bar{H}_i^\circ$  for all the components. The superscript  $^\circ$  refers to the standard state.

In the case of the volume of the solution, Eq. (2) gives directly

$$V = n_1 \bar{V}_1 + n_2 \bar{V}_2 \quad (T, P \text{ constant})$$

The partial molal volumes  $\bar{V}_1$  and  $\bar{V}_2$  may be evaluated from density measurements on the solutions. The graphical methods described fully by Lewis and Randall<sup>4</sup> may be used in the treatment of the data; of these, the use of the apparent molal volume  $\phi_V$  is particularly convenient for binary solutions.

The apparent molal volume is defined by the relation

$$\phi_V = \frac{V - n_1 \bar{V}_1^\circ}{n_2} \quad (T, P \text{ constant}) \quad (3)$$

where  $V$  = volume of solution containing  $n_1$  moles of component 1 and  $n_2$  moles of component 2

$\bar{V}_1^\circ$  = molar volume of component 1 at given  $T, P$

Since  $V = n_2 \phi_V + n_1 \bar{V}_1^\circ$ ,

$$\bar{V}_2 = \left( \frac{\partial V}{\partial n_2} \right)_{n_1, T, P} = \phi_V + n_2 \left( \frac{\partial \phi_V}{\partial n_2} \right)_{n_1, T, P} \quad (4a)$$

$$\text{and} \quad \bar{V}_1 = \frac{V - n_2 \bar{V}_2}{n_1} = \frac{1}{n_1} \left[ n_1 \bar{V}_1^\circ - n_2^2 \left( \frac{\partial \phi_V}{\partial n_2} \right)_{n_1, T, P} \right] \quad (4b)$$

In terms of the experimentally measured density  $\rho$  and the molecular weights  $M_1$  and  $M_2$  of the two components,

$$\phi_V = \frac{1}{n_2} \left( \frac{n_1 M_1 + n_2 M_2}{\rho} - n_1 \bar{V}_1^\circ \right) \quad (5)$$



When the molal concentration scale is used,  $n_2 = m$ , the molality, and  $n_1$  is equal to the number of moles of component 1 in 1000 g of solvent, so that

$$\phi_v = \frac{1}{m} \left( \frac{1000 + mM_2}{\rho} - \frac{1000}{\rho_1} \right) = \frac{1000}{m\rho\rho_1} (\rho_1 - \rho) + \frac{M_2}{\rho} \quad (6)$$

where  $\rho_1$  = density of pure component 1

$\rho$  = density of solution of molality  $m$  of component 2 having molecular weight  $M_2$

The second expression is particularly convenient for actual calculations.

The use of the apparent molal volume in this determination is advantageous because the error involved in the graphical determination of the derivative of a function is encountered only in the evaluation of the term giving the difference between the partial molal volume and the apparent molal volume.

The partial molal volume may be visualized by considering a large reservoir of a solution of given composition, so large that the addition of one more mole of a component will not appreciably alter the concentration. If now one mole of component 1 is added to this large reservoir of solution, the increase in the volume of the solution is equal to the partial molal volume of component 1 at the indicated concentration, temperature, and pressure. The magnitude of the partial molal volume depends upon the nature of the interactions between the components of the solution under the given conditions; the effects of these interactions are difficult to predict theoretically, but the over-all result is readily expressed mathematically, as already shown. In the special case of an ideal solution, the partial molal volume of any component at any concentration is equal to the molar volume of the pure liquid component at the temperature and pressure of the solution.

The concept of the partial molal quantity may, of course, be applied to solutions containing more than two components. The extension of Eqs. (1) and (2) to the general case is discussed in detail elsewhere.<sup>3,4,7</sup>

**Apparatus.** Pycnometers; thermostat; rapid analytical balance; six small glass-stoppered bottles or flasks; sodium chloride.

**Procedure.**<sup>1</sup> Solutions of sodium chloride in water containing approximately 2, 4, 8, 12, and 16 per cent sodium chloride by weight are prepared. The salt and water are weighed out accurately into a weighing bottle or glass-stoppered flask, care being taken to prevent evaporation of the volatile solvent. A total volume of about 75 ml of each solution is required for the execution of duplicate determinations.

The density of each solution is determined accurately at 25.0°C. A

pycnometer of the Weld or Ostwald-Sprengel type shown in Fig. 23 may be used. The pycnometer is dried carefully, weighed, then filled with distilled water, and placed in the thermostat for 10 or 15 min.

The Weld pycnometer is initially filled to bring the liquid level about halfway up the throat  $T$  of the reservoir  $R$ . The pycnometer is placed in the thermostat with the cap  $C$  in position to prevent evaporation from the exposed liquid surface. When temperature equilibrium has been reached, the cap  $C$  is removed and the plug  $P$  is inserted. A moderate

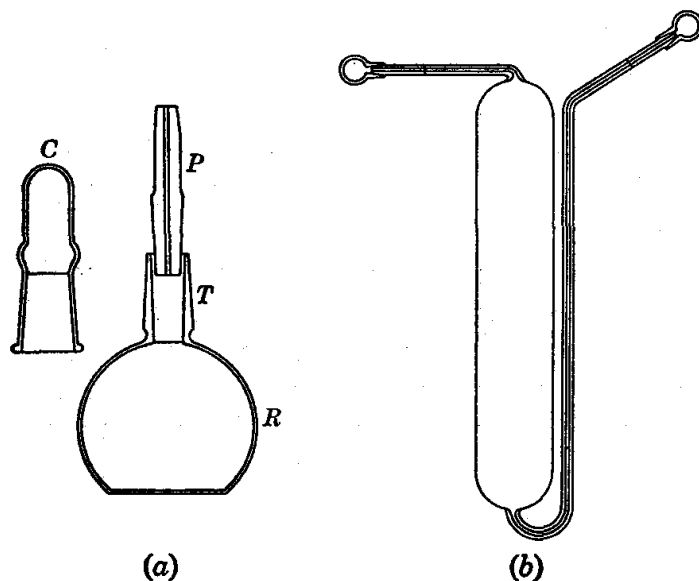


FIG. 23. (a) Weld pycnometer; (b) Ostwald-Sprengel pycnometer.

pressure is sufficient to seat the plug firmly. Any excess liquid on the tip of the plug is wiped off with a piece of filter paper, care being taken to avoid removing liquid from the plug capillary in the process. The pycnometer is then removed from the thermostat, wiped dry with a lintless cloth, and the (dried) cap  $C$  put in place. It is allowed to stand in the balance case for a few minutes before being weighed.

With the Ostwald-Sprengel pycnometer, the quantity of liquid is adjusted so that the liquid meniscus is at the mark on the horizontal capillary when the other capillary arm is filled. This adjustment may be made by tilting the completely filled unit slightly and withdrawing liquid slowly from the other capillary by touching a piece of filter paper to it. The pycnometer is removed from the thermostat and wiped dry with a lintless cloth, and the caps placed on the capillary arms. It is allowed to stand in the balance case for a few minutes before being weighed.

For the best results, it is suggested that the temperature of the balance room be not much above that of the thermostat. Also, there is often

difficulty with "creeping" of the salt solutions during storage. It is preferable to make up the solutions and measure the densities on the same day.

In this fashion, duplicate determinations are made of the weight of liquid required to fill the pycnometer at the thermostat temperature, for water and for each of the solutions previously prepared. Two pycnometers may be used to advantage, so that one may be weighed while the other is in the thermostat.

**Calculations.** The weights of the water and of the various salt solutions held by the pycnometers are corrected to vacuum as described in Chap. 21. The density of water at 25°C is taken as 0.99707 g ml<sup>-1</sup> for the calculation of the volumes of the pycnometers. The density of each solution is then calculated by dividing its vacuum weight by the appropriate pycnometer volume.

The concentration of each solution is expressed in terms of the molal concentration scale, and the apparent molal volume is determined at each concentration. The uncertainty in the apparent molal volume introduced by an uncertainty of 0.02 per cent in the density is computed for each solution.

By means of Eqs. (4a) and (4b) the partial molal volumes of solute and solvent are evaluated at each concentration. In this case  $n_2 = m$ , the molality, and  $n_1$ , the number of moles of solvent associated with  $n_2$  moles of solute, is equal to 55.51, that is, 1000/18.016. It is convenient in the case of an electrolytic solution to plot  $\phi_v$  against  $m^{1/2}$  instead of against  $m$  and to utilize the relationship

$$\left(\frac{\partial \phi_v}{\partial m}\right)_{n_1, T, P} = \frac{1}{2m^{1/2}} \left[ \frac{\partial \phi_v}{\partial (m^{1/2})} \right]_{n_1, T, P} \quad (7)$$

A second method is also used for the evaluation of  $\bar{V}_2$ . The volume of solution containing 1000 g of solvent is plotted against the molality  $m$ . The slope of the tangent to the curve at any chosen concentration gives directly the value of  $\bar{V}_2$  (Ref. 3). The values given by this method are compared with those obtained by the preceding method.

**Practical Applications.** The use of partial molal quantities is fundamental in the application of thermodynamics to solution systems.

**Suggestions for Further Work.** Other solutions may be investigated. The system benzene-carbon tetrachloride<sup>8</sup> exhibits nearly ideal behavior. The system ethanol-water<sup>8</sup> provides an example of nonideal behavior and is particularly interesting in the region from 0 to 15 mole per cent ethanol.

#### References

1. Bauer and Lewin in Weissberger (ed.): "Technique of Organic Chemistry," 3d ed., Vol. I, Pt. I, Chap. 4, Interscience Publishers, Inc., New York (1959).

2. Gucker, *J. Phys. Chem.*, **38**, 307 (1934).
3. Klotz, "Chemical Thermodynamics," Prentice-Hall, Inc., Englewood Cliffs, N.J. (1950).
4. Lewis and Randall, "Thermodynamics," 2d ed., rev. by Pitzer and Brewer, McGraw-Hill Book Company, Inc., New York (1961).
5. MacDougall, "Thermodynamics and Chemistry," 3d ed., pp. 23ff., John Wiley & Sons, Inc., New York (1939).
6. Osborne, McKelvey, and Bearce, *Natl. Bur. Standards (U.S.), Bull.*, **9**, 424 (1913).
7. Wall, "Chemical Thermodynamics," W. H. Freeman and Company, San Francisco (1958).
8. Wood and Brusie, *J. Am. Chem. Soc.*, **65**, 1891 (1943).

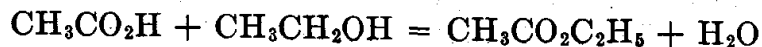
## CHAPTER 5

# Homogeneous Equilibria

### 14. EQUILIBRIUM IN SOLUTION

This experiment illustrates the determination of the equilibrium constant for a solution reaction.

**Theory.** The thermodynamic equilibrium constant  $K$  for a solution reaction is expressed in terms of the activities of the reactants and products at equilibrium. The specific example to be considered here is the formation of ethyl acetate from acetic acid and ethanol.



The thermodynamic equilibrium constant may be expressed in terms of activities on the mole-fraction scale ( $X$  = mole fraction and  $\gamma$  = activity coefficient).

$$K = \frac{\gamma_{\text{CH}_3\text{CO}_2\text{C}_2\text{H}_5} X_{\text{CH}_3\text{CO}_2\text{C}_2\text{H}_5} \gamma_{\text{H}_2\text{O}} X_{\text{H}_2\text{O}}}{\gamma_{\text{CH}_3\text{CO}_2\text{H}} X_{\text{CH}_3\text{CO}_2\text{H}} \gamma_{\text{CH}_3\text{CH}_2\text{OH}} X_{\text{CH}_3\text{CH}_2\text{OH}}} \quad (1)$$

In the absence of detailed information about the activity coefficients of the various components of the solutions, it is necessary to use the apparent equilibrium constant  $K'$ , which is defined simply in terms of the mole fractions of the reactants and products.

$$K' = \frac{X_{\text{CH}_3\text{CO}_2\text{C}_2\text{H}_5} X_{\text{H}_2\text{O}}}{X_{\text{CH}_3\text{CO}_2\text{H}} X_{\text{CH}_3\text{CH}_2\text{OH}}} \quad (2)$$

By comparison of these equations it can be seen that the apparent equilibrium constant  $K'$  is related to the thermodynamic equilibrium constant  $K$  by

$$K' = K \frac{\gamma_{\text{CH}_3\text{CO}_2\text{H}} \gamma_{\text{CH}_3\text{CH}_2\text{OH}}}{\gamma_{\text{CH}_3\text{CO}_2\text{C}_2\text{H}_5} \gamma_{\text{H}_2\text{O}}} \quad (3)$$

These activity coefficients could be determined by use of vapor-pressure measurements.<sup>6</sup> For many practical purposes apparent equilibrium constants are used since they may be reasonably constant over a range of concentrations.

The equilibrium is sometimes reached very slowly, and it may be necessary to raise the temperature or to use a catalyst to hasten the approach to equilibrium. In this experiment the reaction is catalyzed by hydrochloric acid. Its concentration is great enough to change the character of the water and alter the numerical value of the equilibrium constant,<sup>5</sup> but the results are fairly constant for a given concentration of hydrochloric acid. The hydrochloric acid is added merely as a catalyst to hasten the reaction, and it takes no part in the stoichiometric reaction.

**Apparatus.** Burette; 5-ml pipette; 2-ml pipette; 1-ml pipette; fourteen 50-ml glass-stoppered bottles; 0.5 N sodium hydroxide; phenolphthalein, ethyl acetate, concentrated hydrochloric acid, glacial acetic acid, absolute ethanol.

**Procedure.** The following solutions are prepared in 50-ml glass-stoppered bottles.

- a. 5 ml 3 N HCl + 5 ml water
- b. 5 ml 3 N HCl + 5 ml ethyl acetate
- c. 5 ml 3 N HCl + 4 ml ethyl acetate + 1 ml water
- d. 5 ml 3 N HCl + 2 ml ethyl acetate + 3 ml water
- e. 5 ml 3 N HCl + 4 ml ethyl acetate + 1 ml ethanol
- f. 5 ml 3 N HCl + 4 ml ethyl acetate + 1 ml acetic acid
- g. 5 ml 3 N HCl + 4 ml ethanol + 1 ml acetic acid

Duplicate determinations are made. Each of the bottles is stoppered immediately and allowed to stand in the desk for at least 48 hr and preferably for a week, with occasional shaking. It is necessary that the stoppers fit tightly to prevent evaporation. A thermostat is unnecessary because this equilibrium is affected only slightly by temperature changes.

The weight of each reactant is determined by discharging the pipette directly into a glass-stoppered weighing bottle and weighing. In this way the following weighings are made:

- 5 ml 3 N hydrochloric acid
- 5 ml and 2 ml ethyl acetate
- 1 ml and 4 ml ethanol
- 1 ml acetic acid
- 5 ml, 3 ml, and 1 ml water

The drainage of the pipettes will not always be uniform, but the error involved in using a pipette is not serious for the present work. Since the equilibrium shifts slowly, the equilibrium concentrations may be determined by titration.

After standing, each solution is titrated with the 0.5 M sodium hydroxide, using phenolphthalein as an indicator.

**Calculations.** The weight of water in each bottle is obtained by adding the weight of pure water to the water contained in the 3 N hydrochloric acid. The latter is calculated by subtracting the weight of the hydrochloric acid, obtained by titration, from the weight of the 5 ml of hydrochloric acid solution.

The amount of acetic acid at equilibrium in each bottle is obtained by subtracting the number of milliliters of sodium hydroxide used in solution *a* from that used for the titration of the equilibrium solution. In solutions *f* and *g*, acetic acid is added to the original solution, and this amount must be used in calculating the equilibrium amounts of the other reactants. For every mole of acetic acid produced in the reaction, 1 mole of ethanol is produced, 1 mole of water disappears, and 1 mole of ethyl acetate disappears.

If the number of moles of each of the four reactants in the original mixture and the number of moles of acetic acid produced in the reaction are known, the apparent equilibrium constant  $K'$  may be computed. It is defined by Eq. (2).

As indicated in the opening paragraph, the value of  $K'$  obtained in this way is somewhat dependent on the various concentrations.

**Practical Applications.** In planning any chemical synthesis, it is desirable to know what yield of material may be expected from a given concentration of reactants. Such a calculation may be made when the value of the equilibrium constant is known, provided that the reaction is fast enough to come to equilibrium in the time allowed.

**Suggestions for Further Work.** Similar experiments may be carried out with other esters.

In the absence of catalyst, it is necessary to heat the mixture to about 150° in sealed tubes to effect an equilibrium within a couple of days. If sufficient precautions are taken to avoid danger from bursting tubes, the equilibrium constant may be determined by titrating mixtures that have been weighed out, sealed off in small glass tubes, and heated.<sup>3</sup>

The equilibrium involved in the reaction between acetaldehyde and alcohol to give acetal and water may be studied.<sup>2</sup> A little hydrochloric acid is used as a catalyst, and the equilibrium concentration of the acetaldehyde is determined volumetrically by the sulfite method,<sup>1</sup> with thymolphthalein as indicator.<sup>4</sup>

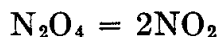
#### References

1. Adams and Adkins, *J. Am. Chem. Soc.*, **47**, 1358 (1925).
2. Adkins and Adams, *J. Am. Chem. Soc.*, **47**, 1368 (1925).
3. Berthelot and St. Gilles, *Ann. chim. et phys.* (3), **65**, 385 (1862); **68**, 225 (1863).
4. Deyrup, *J. Am. Chem. Soc.*, **56**, 60 (1934).
5. Jones and Lapworth, *J. Chem. Soc.*, **99**, 1427 (1911).
6. Lewis and Randall, "Thermodynamics," 2d ed., rev. by Pitzer and Brewer, McGraw-Hill Book Company, Inc., New York (1961).

## 15. DISSOCIATION OF NITROGEN TETROXIDE

The equilibrium constant for a reaction is determined as a function of temperature, and the corresponding heat of reaction is calculated.

**Theory.** Nitrogen tetroxide dissociates in accordance with the reaction



If the equilibrium degree of dissociation is represented by  $\alpha$ , an initial one mole of  $\text{N}_2\text{O}_4$  gives  $2\alpha$  moles of  $\text{NO}_2$  and  $1 - \alpha$  mole of  $\text{N}_2\text{O}_4$  at equilibrium. The total number of moles is thus  $1 + \alpha$ , and the mole fraction of  $\text{NO}_2$  is  $2\alpha/(1 + \alpha)$ , and that of  $\text{N}_2\text{O}_4$  is  $(1 - \alpha)/(1 + \alpha)$ . When the partial pressure  $p$  of each constituent is set equal to the product of its mole fraction and the total pressure  $P$ , the equilibrium constant for the reaction takes the form

$$K_p = \frac{p_{\text{NO}_2}^2}{p_{\text{N}_2\text{O}_4}} = \frac{\left(\frac{2\alpha}{1 + \alpha} P\right)^2}{\frac{1 - \alpha}{1 + \alpha} P} = \frac{4\alpha^2 P}{1 - \alpha^2} \quad (1)$$

Experimentally,  $\alpha$  is found by measuring  $M$ , the average molecular weight of the equilibrium gas mixture. One mole of undissociated  $\text{N}_2\text{O}_4$ , of molecular weight  $M_0 = 92.06$ , dissociates to form  $1 + \alpha$  moles in the equilibrium mixture. Since the total weight is unchanged, the average molecular weight is

$$M = \frac{M_0}{1 + \alpha} \quad \text{or} \quad \alpha = \frac{M_0 - M}{M} \quad (2)$$

Equation (2) is used to calculate  $\alpha$  from  $M$ . Equations (1) and (2) apply when the gas mixture is considered to be an ideal mixture of perfect gases.

The standard Gibbs free-energy change for a reaction can be calculated from the thermodynamic equilibrium constant.

$$\Delta G^\circ = -RT \ln K = -2.303RT \log K \quad (3)$$

The determination of the equilibrium constant at a series of temperatures permits the evaluation of the standard heat of reaction by application of the Gibbs-Helmholtz equation in the form

$$\Delta H^\circ = -T^2 \left( \frac{\partial \Delta G^\circ / T}{\partial T} \right)_P = 2.303RT^2 \frac{d \log K}{dT} = -2.303R \frac{d \log K}{d(1/T)} \quad (4)$$

When the plot of  $\log K$  versus  $1/T$  is a straight line, the standard heat of reaction is constant over the temperature range involved and may be calculated from the slope of the line. When the line is not straight, the heat of reaction depends on the temperature, but the slope of a tangent



drawn at a point corresponding to any temperature will give the heat of reaction at that temperature.

**Apparatus.** Two gas-density bulbs; counterpoise bulb of same capacity; small adjustable thermostat; cylinder of nitrogen tetroxide, gas-filling apparatus with stopcocks.

**Procedure.** Pyrex bulbs of about 200 ml capacity with capillary glass stopcocks are used for determining the density of the dissociation

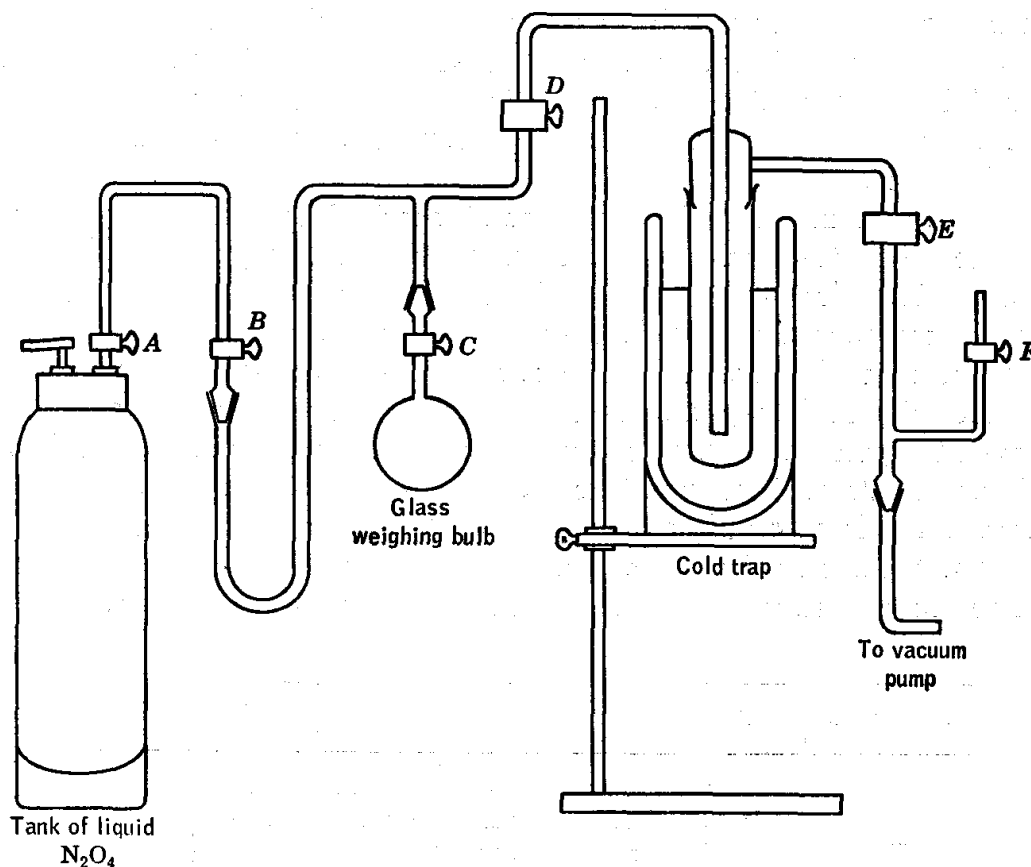


FIG. 24. Apparatus for filling bulbs with nitrogen tetroxide.

mixture. Nitrogen tetroxide attacks ordinary stopcock greases, but its effect on silicone grease is negligible during the period of the experiment if a minimum amount is used in lubricating the plug.

Two bulbs are evacuated to 1 mm or less with the vacuum system described in Exp. 1 and weighed to 0.1 mg, with a bulb of similar volume used as counterpoise. The student should refer to Exp. 1 for comments concerning the weighing procedure.

The weighed bulbs are filled from a small cylinder of nitrogen tetroxide.

**Caution:** Nitrogen tetroxide is corrosive and very poisonous. All operations should be carried out in a well-ventilated hood.

The arrangement of stopcocks and traps shown in Fig. 24 is used for

filling the bulbs with dry nitrogen tetroxide (in equilibrium with nitrogen dioxide). The tank of liquid  $\text{N}_2\text{O}_4$  and the train of glass tubes are set up permanently on a rack in a ventilated hood.

The steel valve *A* on the nitrogen tetroxide tank is connected with a small, slightly flexible stainless-steel tube and stopcock *B*. The outlet from this stopcock is attached with inert cement to the inner half of a standard tapered ground-glass joint. The outer part of the joint is connected to the glass system of tubes and stopcocks including a standard tapered ground-glass joint into which the weighed bulb for holding the  $\text{N}_2\text{O}_4$  is inserted. This bulb is provided with stopcock *C*, and the ground-glass joint is lubricated with only a trace of silicone grease because the bulb is to be weighed and it must not have uncertain weights of grease clinging to it.

The tube from the tank extends to stopcock *D* of large diameter and then to a cold trap containing trichloroethylene and dry ice in a vacuum bottle. The dry ice is added in small pieces, slowly at first, to prevent frothing of the liquid over the top of the vacuum bottle. The bottle is partially filled and then raised on a ring stand and holder to immerse the cold trap and freeze out the nitrogen tetroxide and thus protect the pump and pump oil from nitrogen tetroxide and prevent back diffusion of atmospheric moisture. Stopcock *E* of large bore permits the pump to be closed off after the system has been evacuated, and stopcock *F* allows the access of air at atmospheric pressure.

The filling operation is carried out, in steps I to V, as follows:

Stopcocks	<i>A</i>	<i>B</i>	<i>C</i>	<i>D</i>	<i>E</i>	<i>F</i>
I	Closed	Closed	Closed	Closed	Closed	Open
II	Closed	Closed	Open	Open	Open	Closed
III	Closed	Open	Open	Open	Open	Closed
IV	Open	Open	Open	Closed	Open	Closed
V	Closed	Closed	Closed	Closed	Open	Closed

The vacuum oil pump is started with stopcocks arranged as indicated in step I.

The system is evacuated as shown at step II.

Evacuation is continued with stopcocks set as shown in step III.

Then the stopcocks are turned as shown at step IV, and the bulb is filled with nitrogen tetroxide at a pressure equal to its vapor pressure. The temperature of the tank must be higher than  $21.5^\circ$ , the boiling point, in order to have the gas in the bulb slightly above atmospheric pressure.

Steps III and IV are then repeated to eliminate residual air.

The stopcocks are then closed as indicated at step V, and the bulb is removed for weighing.

A second bulb is filled using the same sequence of operations. When there are no more bulbs to be filled, stopcock *F* is opened and the pump is turned off. Then the freezing bath is lowered, the trichloroethylene is stoppered and saved, and the lower part of the trap is removed. The frozen nitrogen tetroxide is flushed out with an excess of water.

A small thermostat which permits rapid setting is used for measurements at successively higher temperatures.

The bulb is placed in the small thermostat, which is first set at the lowest temperature to be used (about 30°). The stopcock is opened momentarily at intervals of 2 or 3 min during the period of thermostating, and the gas is allowed to escape until no more brown fumes are seen to issue from the opening. The bulb is closed and again weighed;† care must be taken to ensure uniform weighing technique. Time should be allowed for moisture equilibrium between the bulb and the air in the balance case to be attained and for the bulb to cool to the temperature of the balance.

The bulb is then placed in a thermostat at a temperature approximately 10° higher, and the above procedure repeated. The same measurements are made every 10° up to 60°.

The volume of the bulb may be determined from the weight of water it can hold. The bulb is evacuated two or three times with a water aspirator in order to remove all corrosive nitrogen tetroxide. It is then evacuated with the aspirator, the stopcock is closed, and the end of the tube is immersed in a beaker of distilled water. The stopcock is then opened to permit the bulb to fill. A hypodermic syringe with a long needle, passing through the stopcock bore, may be used to complete the filling of the bulb. The bulb is then weighed, and from the weight of water it holds, the volume is calculated by use of the data on the density of water given in the Appendix.

The bulb is then emptied for later experiments, with the help of the water aspirator, and placed in a drying oven. It is evacuated several times, while hot, to assist in the drying process.

The barometric pressure must be taken at the time of the experiment for use in subsequent calculations.

**Calculations.** The average molecular weight of the gas at each temperature is computed by use of the ideal-gas law (cf. Exp. 1). The corresponding values of the degree of dissociation and the equilibrium constant are calculated by application of Eqs. (2) and (1). A plot is

† After removing the bulb from the thermostat, the temperature regulator should be reset to a point approximately 10° higher. The thermostat will then be approaching the new temperature while weighings are being made.

made of  $\log K$  versus  $1/T$ , and the equation is found for the line considered to best represent the set of points. The standard heat of reaction, the standard free-energy change, and the entropy change for the reaction are calculated for 25°C.

**Practical Applications.** The determination of equilibrium constants is of fundamental importance in industrial work, where the yield under specified conditions must be known.

**Suggestions for Further Work.** A glass-diaphragm manometer may be used for studying this equilibrium at various pressures.<sup>5</sup>

A simple photometer may be used for determining the partial pressure of  $\text{NO}_2$  in the mixture.<sup>3</sup>

The dissociation of  $\text{N}_2\text{O}_4$  in carbon tetrachloride solution may be studied.<sup>1</sup>

Other rapid reversible dissociations such as that of phosphorus pentachloride and ammonium chloride may be studied at higher temperatures. The method of Victor Meyer (Exp. 2) is suitable for these determinations.

### References

1. Atwood and Rollefson, *J. Chem. Phys.*, **9**, 506 (1941).
2. Giauque and Kemp, *J. Chem. Phys.*, **6**, 40 (1938).
3. Harris and Siegel, *Ind. Eng. Chem., Anal. Ed.*, **14**, 258 (1942).
4. Lewis and Randall, "Thermodynamics," 2d ed., p. 561, rev. by Pitzer and Brewer, McGraw-Hill Book Company, Inc., New York (1961).
5. Verhoek and Daniels, *J. Am. Chem. Soc.*, **53**, 1250 (1931).

## 16. SPECTROPHOTOMETRIC DETERMINATION OF AN EQUILIBRIUM CONSTANT

The equilibrium constant for a reaction in solution is determined from a study of the concentration dependence of an absorption band in the spectrum of the solution.

**Theory.**<sup>1,2</sup> The present experiment illustrates an important method for the study of chemical equilibrium in solution. The method utilizes differences in the light-absorbing properties of reactants and products and is particularly appropriate for systems in which the reaction is so rapid that classical methods of chemical analysis cannot be used to find the concentrations of the various species present.

The optical absorption spectrum, i.e., the percentage transmission of light as a function of wavelength, has been investigated for iodine in a variety of solvents. Associated with the color of the solutions is a strong absorption in the neighborhood of 500  $\text{m}\mu$ .† In certain solvents, especially aromatic compounds, a new absorption band appears in the violet or ultraviolet region. The new band has been explained as being due to a complex (a molecular combination of iodine with solvent) existing in equilibrium with uncomplexed iodine and solvent. By means of a quanti-

† The wavelength unit millimicron ( $\text{m}\mu$ ) is equivalent to 10 Å, or  $10^{-7}$  cm.

tative study of the intensity of absorption at the peak of this band, as a function of concentration, it is possible to test this interpretation and to obtain a value for the equilibrium constant for the formation of the complex.

The study is best carried out with iodine and the complexing organic substance, mesitylene in this experiment, both present as solutes in dilute solution in an inert solvent such as  $\text{CCl}_4$ . (The inertness of  $\text{CCl}_4$ , expected on chemical grounds, is verified by the absence of new absorption bands in solutions of  $\text{I}_2$  in  $\text{CCl}_4$ .) The initial step involves the measurement of the percentage transmission, over the appropriate wavelength range, of three solutions: one containing  $\text{I}_2$  solute only, one containing mesitylene solute only, the third containing both  $\text{I}_2$  and mesitylene as solutes. An absorption band present only in the spectrum of the third solution is attributed to a 1:1 complex,  $\text{M} \cdot \text{I}_2$ , existing in equilibrium with free mesitylene (M) and  $\text{I}_2$ ,

$$\begin{aligned} \text{M} + \text{I}_2 &= \text{M} \cdot \text{I}_2 \\ K &= \frac{x}{(c_1 - x)(c_2 - x)} \end{aligned} \quad (1)$$

where  $c_1$  = total concentration of mesitylene

$c_2$  = total concentration of  $\text{I}_2$

$x$  = concentration of complex at equilibrium

$K$  = equilibrium constant

The task remaining is to verify that an equilibrium condition of the form of Eq. (1) is actually consistent with the concentration dependence of the absorption intensity, and to evaluate  $K$ . The new absorption band occurs in a wavelength region in which absorption by uncomplexed iodine and mesitylene is very slight; the investigation can therefore proceed without serious interference from absorption due to uncomplexed solutes.

Let  $I$  and  $I_0$  be intensities of light of a specified wavelength transmitted, respectively, by solution and by pure solvent. Then the optical absorbancy  $A$ , defined by

$$A = -\log \frac{I}{I_0} \quad (2)$$

is given by the Beer-Lambert law, for the case in which only one solute absorbs at the given wavelength, by

$$A = abc$$

where  $a$  = molar absorbancy index of absorbing solute

$b$  = length of light path in cell

$c$  = concentration of absorbing solute

The molar absorbandy index depends on the wavelength, temperature, and solvent.

If several solutes absorb independently, the absorbances are additive. Thus

$$A = A_1 + A_2 + A_3 \quad (3)$$

$$A_1 = a_1 b(c_1 - x) \quad (4)$$

$$A_2 = a_2 b(c_2 - x) \quad (5)$$

$$A_3 = a_3 b x \quad (6)$$

where  $a_1$  = molar absorbandy index of mesitylene

$a_2$  = molar absorbandy index of  $I_2$

$a_3$  = molar absorbandy index of complex

Hence, in the present case, measurement of absorbandy does not lead directly to values for the concentration of complex.  $A_1$  and  $A_2$ , though smaller than  $A_3$  at the wavelength of the peak of the new complex band, may not always be negligible; also,  $a_3$  is initially unknown. However, the following indirect procedure yields values for  $a_3$  as well as for  $K$ .

A considerable simplification in the work results from restricting the investigation to solutions in which mesitylene is present in large excess. Thus

$$c_1 \gg c_2 > x \quad (7)$$

Accordingly, for the calculation of  $A_3$  from  $A$ , the approximations

$$A_1 = a_1 b c_1$$

$$A_2 = 0$$

may be used, with  $a_1$  calculated from the absorbandy measured at the given wavelength for a solution containing only mesitylene as solute at a known concentration.

The equilibrium condition (1), with the approximation (7), simplifies to

$$K = \frac{x}{c_1(c_2 - x)} \quad (8)$$

Upon replacement of  $x$  by  $A_3/a_3 b$  and rearrangement, this becomes

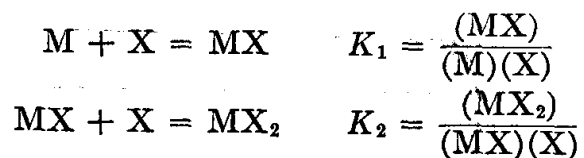
$$\frac{A_3}{c_1 c_2} = b a_3 K - \frac{A_3}{c_2} K \quad (9)$$

Absorbancies are measured for a series of solutions made up with various known values of  $c_1$  and  $c_2$ , and values of  $A_3/c_1 c_2$  plotted against  $A_3/c_2$ . If the data are well represented by a straight line, the slope and intercept lead to values for  $a_3$  and  $K$ .

The inclusion of a correction for absorption due to uncomplexed  $I_2$  may be warranted if the data are of sufficient accuracy. A procedure for

carrying out this refinement is outlined under Suggestions for Further Work.

A word of caution is in order with regard to the interpretation of the results. While it is possible by the procedure outlined here to learn whether or not the absorbancies are consistent with the postulated reaction equilibrium, linearity of the graph does not of itself constitute proof that Eq. (1) represents the true state of affairs. It has in fact been shown<sup>3,4</sup> that a functional relationship among  $c_1$ ,  $c_2$ , and  $A_3$  identical with that of Eq. (9) will exist for a system described by two stages of complex formation,



if the ratio of the molar absorbancies of MX and MX<sub>2</sub> happens to satisfy a certain condition. (In this case  $A_3$ , found experimentally as before, stands for the total absorbancy due to complexed M.) The best procedure, therefore, when it can be used, is to make measurements on more than one of the absorption bands due to the complex. The necessary condition on the ratio of the absorbancies is likely not to be satisfied at each of several widely different wavelengths, so that it will then become obvious if the system is not obeying the equilibrium equations corresponding to Eq. (1).

Finally, a few comments will be made about the principle and operation of the spectrophotometer. The function of a spectrophotometer is to produce monochromatic light of a selected wavelength and to measure the intensity of light transmitted by a solution relative to that transmitted by a sample of the pure solvent. The essential elements of a typical spectrophotometer are shown in Fig. 25. The source is a tungsten lamp. The wavelength to be used is selected by turning a knob which moves the prism until light of the desired wavelength is directed toward the slit. The wavelength scale is mechanically coupled to the same shaft. The slit, an aperture of adjustable width, serves to admit only light of a narrow band of wavelengths; at the same time, it necessarily determines the intensity of light passed. As the slit is widened to provide greater intensity of light for the measurement, a wider range of wavelengths is permitted to pass through. At wavelengths where the transmission of a sample varies rapidly with wavelength, the slit width should be kept as narrow as possible, consistent with the need for adequate intensity.

In the unit shown, any one of four samples may be placed in the light path by manually shifting an external shaft. With the shutter closed, the so-called dark current of the phototube is balanced out so as to give a

meter deflection corresponding to zero per cent transmission. With the shutter open, and the pure solvent sample in the light path, the sensitivity and slit-width controls are adjusted to give a deflection corresponding to 100 per cent transmission. Finally, with the solution sample in the light path, the deflection indicates directly the per cent transmission. The output meter scale is also calibrated directly in absorbancy. If the solution transmission is low, better accuracy may be attained by increasing the sensitivity control by one or more steps; if this is done, the

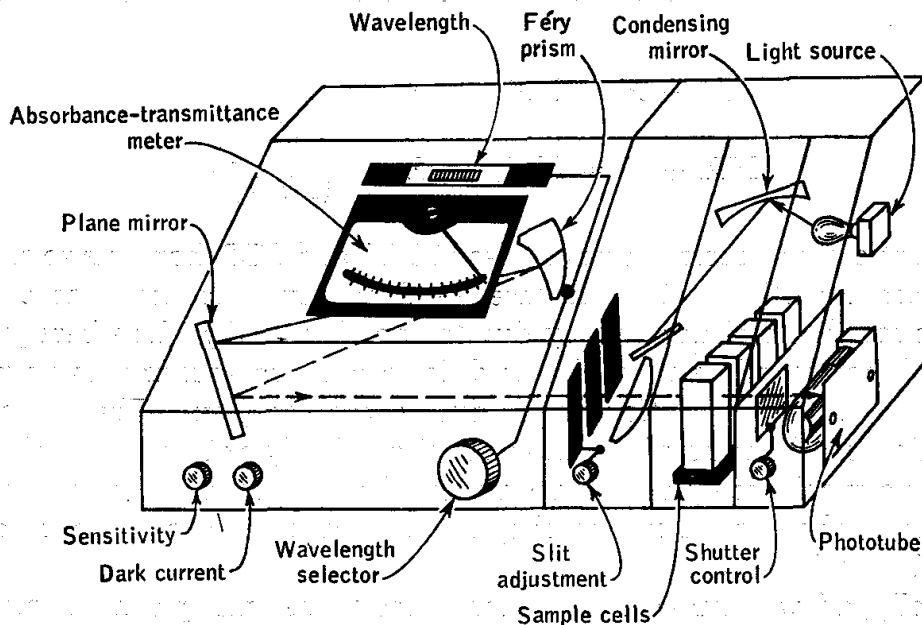


FIG. 25. Diagram of Beckman Model B spectrophotometer. The wavelength range is 320 to 1000  $m\mu$ .

scale is of course altered: for the Beckman Model B spectrophotometer, 0.5 must be added to the absorbancy scale reading for each step by which the sensitivity control has been advanced above that at which the reference setting was made with the pure solvent.

For accurate work it is necessary to take into account differences among spectrophotometer sample cells. The first to be considered is that resulting from imperfections in the cell windows. To determine the correction for this effect, the cells are cleaned and filled with nonabsorbing solvent. It is convenient to select the cell with the highest transmission as the reference cell. The slit width is adjusted to give a deflection corresponding to 100 per cent transmission with this cell in the light path. The other cells are then placed in turn in the light path, and the absorbancies, designated  $A_c$ , noted. The value of  $A_c$  for a particular cell is called the cell correction;  $A_c$  may vary with wavelength. In subsequent measurements with solutions, the true sample absorbancy is then found by sub-



tracting the value of  $A_c$  for the cell used from the measured absorbancy of the cell filled with the solution sample.

Secondly, the optical path lengths may be different for two cells of nominally the same thickness. The path lengths for two cells can most easily be compared by measuring the transmission for both filled with a series of absorbing solutions. The manufacturing tolerances on cell thickness are sufficiently close so that the path-length correction need not be made in most student work.

If much spectrophotometric work is to be done, it will be worth the modest added expense of obtaining a matched set of cells; with such a set, the cell corrections will be quite small and the path-length corrections negligible.

**Apparatus.** Spectrophotometer; set of four cells, preferably matched; special mixing cell; reagent grade  $\text{CCl}_4$ ; 1 ml of 0.04 M  $\text{I}_2$  in  $\text{CCl}_4$ ; 8 ml mesitylene (1,3,5-trimethylbenzene); 25-ml volumetric flask.

**Procedure.** Two solutions are prepared: (a) 100 ml of 0.0004 M  $\text{I}_2$  in  $\text{CCl}_4$  and (b) 25 ml of 2 M mesitylene in  $\text{CCl}_4$ . The first is prepared by dilution of a more concentrated solution, which in turn is made up by dissolving a weighed quantity of  $\text{I}_2$  in a measured volume of solution. The second is made up by weighing approximately 8 ml of mesitylene in a 25-ml volumetric flask and filling to the mark with solvent. The concentration of the  $\text{I}_2$  solution may be determined by standard titration methods or may be calculated from the measured absorbancy at the peak of the band near 500  $\text{m}\mu$ ; the molar absorbancy index for  $\text{I}_2$  in  $\text{CCl}_4$  solvent at the wavelength of the peak of this band is 900 liters/mole-cm (Ref. 5).

The spectra of three solutions are to be obtained:

- a. 0.0002 M  $\text{I}_2$  in  $\text{CCl}_4$
- b. 1 M mesitylene in  $\text{CCl}_4$
- c. 0.0002 M  $\text{I}_2$ , 1 M mesitylene, in  $\text{CCl}_4$

Each of these is placed in a spectrophotometer cell, and pure solvent is placed in a fourth cell to serve as reference. The percentage transmission is measured at convenient intervals from 320 to 700  $\text{m}\mu$ . The manufacturer's instructions for the operation of the spectrophotometer should be consulted, but it is to be noted especially that the slit width must be adjusted at each wavelength for a meter deflection of 100 per cent for the pure solvent and that, where recommended, a suitable filter should be used. The data may be plotted while the measurements are being made in order that sufficiently closely spaced points may be taken to assure adequate delineation of the spectral curves.

The three cells used for the solutions may then be filled with solvent, and their transmission measured relative to that of the reference cell at several wavelengths. A cell correction can be applied to the data previously obtained if there is an appreciable difference between any cell and the reference cell.

Absorbancies of a number of solutions are to be measured at a wavelength at which the complex absorbs strongly while uncomplexed  $I_2$  and mesitylene do not. For these measurements, a special spectrophotometer cell† (Fig. 26) is employed, together with an ordinary cell containing pure solvent as reference. The entire series of measurements is to be taken without altering the wavelength setting.

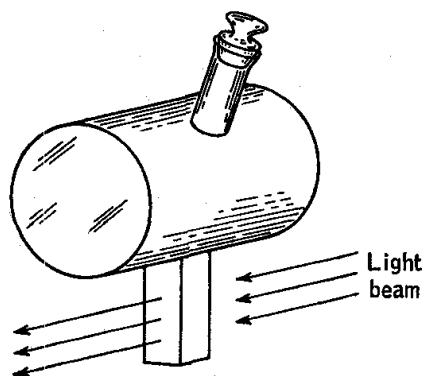


FIG. 26. Special mixing cell for spectrophotometer. The lower portion is a Pyrex spectrophotometer cell.

First, pure solvent is placed in the special cell and the cell correction relative to the reference cell determined. Next, a sample of the 0.0004 M  $I_2$  solution is placed in the special cell and its absorbance noted. For best results in the measurements to follow, the absorbance of the iodine solution should not exceed 0.02 with the proper cell correction; a larger absorbance may indicate the presence of impurities due to aging of the solution or to the use of impure solvent in its preparation.

After careful rinsing and drying of the special cell, a 5-ml sample of the 2 M mesitylene solution is placed in it and the absorbance measured. To this are added one 1-ml portion and then in succession five 5-ml portions of the  $I_2$  solution, the absorbance being measured after each addition. Care must be taken to avoid error due to evaporation of solvent. The solutions should be mixed by gently rocking the cell, and not by shaking it, because loss of solution at the top will cause error.

Finally, the temperature of the solution is recorded.

**Calculations.** Percentage transmission is plotted versus wavelength for each of the three solutions and the significance of the curves briefly discussed.

The absorbance data obtained in the final series of measurements may be treated by the graphical procedure outlined in the theory section to determine  $a_3$  and  $K$  for the temperature of the run.

The validity of the approximation  $c_1 \gg x$  should be checked by calculating  $c_1$  and  $x$  for the least favorable case.

† Available commercially from Norman D. Erway, Oregon, Wisconsin.

**Suggestions for Further Work.** Combination of Eq. (8) with (5) gives an expression which may be used to calculate values of  $A_2$  for each solution after the first approximation to  $K$  has been obtained by the procedure given above. Improved values of  $A_2$  may then be calculated, and a new series of points plotted on the original graph. The cycle may be repeated if the new value for  $K$  leads to appreciably different estimates for values of  $A_2$ . A value for  $a_2$  at the appropriate wavelength may be obtained from measurements on the stock  $I_2$  solution.

### References

1. Andrews and Keefer, *J. Am. Chem. Soc.*, **74**, 4500 (1952).
2. Benesi and Hildebrand, *J. Am. Chem. Soc.*, **71**, 2703 (1949).
3. Kruh, *J. Am. Chem. Soc.*, **76**, 4865 (1954).
4. Newton and Baker, *J. Phys. Chem.*, **61**, 934 (1957).
5. Walker, *Trans. Faraday Soc.*, **31**, 1432 (1935).
6. West in Weissberger (ed.): "Technique of Organic Chemistry," 3d ed., Vol. I, Pt. III, Chap. 28, Spectroscopy and Spectrophotometry, Interscience Publishers, Inc., New York (1960).

## 17. ACID DISSOCIATION CONSTANT OF METHYL RED

The spectrophotometric determination of the acid dissociation constant of a dye is illustrated.

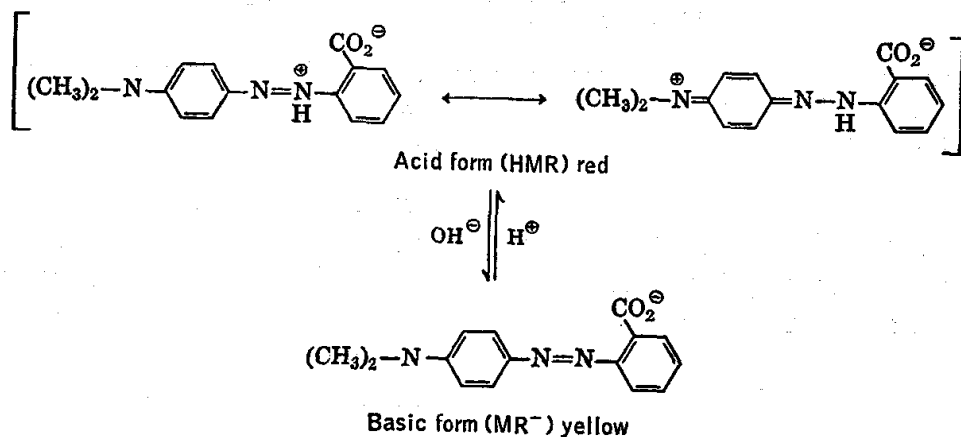


Fig. 27. HMR and  $MR^-$  forms of methyl red.

**Theory.** In aqueous solution methyl red is a zwitter ion and has a resonance structure somewhere between the two extreme forms shown in Fig. 27. This is the red form HMR in which methyl red exists in acid solutions. When base is added, a proton is lost and the yellow anion  $MR^-$  of methyl red has the structure shown in Fig. 27. The basic form is yellow because it absorbs blue and violet light. The equilibrium constant for the ionization of methyl red is

$$K = \frac{(H^+)(MR^-)}{(HMR)} \quad (1)$$

It is convenient to use this equation in the form

$$pK = pH - \log \frac{(\text{MR}^-)}{(\text{HMR})} \quad (2)$$

The ionization constant may be calculated from measurements of the ratio  $(\text{MR}^-)/(\text{HMR})$  at known pH values.

Since the two forms of methyl red absorb strongly in the visible range, the ratio  $(\text{MR}^-)/(\text{HMR})$  may be determined spectrophotometrically. The absorption spectra of methyl red in acidic and basic solutions are determined, and two wavelengths are selected for analyzing mixtures of the two forms. These two wavelengths,  $\lambda_1$  and  $\lambda_2$ , are chosen so that at one, the acidic form has a very large absorbancy index (page 101) compared with the basic form, and at the other, the situation is reversed. The absorbancy indices of HMR and  $\text{MR}^-$  are determined at both of these wavelengths, using several concentrations to determine whether Beer's law is obeyed.

The composition of a mixture of HMR and  $\text{MR}^-$  may be calculated from the absorbancies  $A_1$  and  $A_2$  at wavelengths  $\lambda_1$  and  $\lambda_2$  using

$$A_1 = a_{1,\text{HMR}}(\text{HMR}) + a_{1,\text{MR}^-}(\text{MR}^-) \quad (3)$$

$$A_2 = a_{2,\text{HMR}}(\text{HMR}) + a_{2,\text{MR}^-}(\text{MR}^-) \quad (4)$$

**Apparatus.** Spectrophotometer for measuring absorbancies in the visible range; pH meter; methyl red; sodium acetate; acetic acid; hydrochloric acid; 95 per cent ethanol; volumetric flasks and pipettes for preparing solutions.

**Procedure.** The procedure for this experiment has been described by Tobey.<sup>4</sup> The methyl red is conveniently supplied as a stock solution made by dissolving 1 g of crystalline methyl red in 300 ml of 95 per cent ethanol and diluting to 500 ml with distilled water. The standard solution of methyl red for use in this experiment is made by adding 5 ml of the stock solution to 50 ml of 95 per cent ethanol and diluting to 100 ml with water.

The absorption spectrum of methyl red is determined in hydrochloric acid solution as solvent to obtain the spectrum of HMR and in sodium acetate solution as solvent to obtain the spectrum of  $\text{MR}^-$ . Distilled water is used in the reference cell. The procedure for using the spectrophotometer is described in Exp. 16. Since the equilibrium to be studied is affected by temperature, it is important that all the spectrophotometric and pH measurements be made at the same temperature. If the cell compartment of the spectrophotometer is slightly above room temperature, the filled cells should be placed in the spectrophotometer just before making the measurements. In order to obtain the best results, the cell compartment should be thermostated. The acidic solution is

conveniently prepared by diluting a mixture of 10 ml of the standard methyl red solution and 10 ml of 0.1 M hydrochloric acid to 100 ml. The basic solution is conveniently prepared by diluting a mixture of 10 ml of the standard methyl red solution and 25 ml of 0.04 M sodium acetate to 100 ml.

From the plots of absorbancy versus wavelength, two wavelengths are selected for analyzing mixtures of the acidic and basic forms of methyl red. Further spectrophotometric measurements over a range of concentration are made at these two wavelengths with both acidic and basic solutions to check whether Beer's law is obeyed. The solutions are diluted with 0.01 N hydrochloric acid or 0.01 N sodium acetate, respectively, so that the medium is held constant.

In order to determine the ionization constant of the dye, spectrophotometric analyses are carried out on solutions containing 0.01 N sodium acetate, a constant total concentration of dye, and various concentrations of acetic acid. The pH values of these solutions are measured at the same temperature as the spectrophotometric measurements. For methyl red it is convenient to use acetic acid concentrations ranging from 0.001 to 0.05 N.

**Calculations.** Plots are prepared of absorbancy versus wavelength and absorbancy versus concentration of dye in acidic and basic solutions at  $\lambda_1$  and  $\lambda_2$ . The values of the various absorbancy indices are calculated.

The concentrations of the acidic and basic forms of the dye in the various buffer solutions are calculated by using Eqs. (3) and (4).

Equation (2) is used to calculate the pK value for the dye. As a means of testing and averaging the data  $\log [(MR^-)/(HMR)]$  may be plotted versus the pH. An average value from the literature<sup>3</sup> is  $5.05 \pm 0.05$  for the 25 to 30° temperature range.

**Practical Applications.** This method is useful for studying dyes for use as indicators in acid-base titrations, or by an analogous procedure for indicators for oxidation-reduction titrations.

**Suggestions for Further Work.** The pK values for other common dyes may be determined.

#### References

1. Bell, "Acids and Bases: Their Quantitative Behavior," Methuen & Co., Ltd., New York (1952).
2. Bell, "The Proton in Chemistry," Cornell University Press, Ithaca, N.Y. (1959).
3. Kolthoff, "Acid-Base Indicators," The Macmillan Company, New York (1953).
4. Tobey, *J. Chem. Educ.*, **35**, 514 (1958).

## *Heterogeneous Equilibria*

### 18. DISTRIBUTION OF A SOLUTE BETWEEN IMMISCIBLE SOLVENTS

Studies are made of the equilibrium distributions of a solute between two immiscible solvents. Such experiments give evidence of association or dissociation of the solute in one of the phases. They provide information as to the nature of complex ions and their dissociation constants. Distribution-coefficient data are of value in the design and operation of solvent-extraction equipment.

**Theory.** When two liquid phases are in equilibrium with each other, a dissolved substance will distribute itself between the two according to a definite equilibrium. If we represent the two solvents in contact as being the  $\alpha$  and  $\beta$  phases, and the solute which is present in each layer as  $i$ , then at equilibrium the chemical potentials of  $i$  in the two phases will be equal; thus  $\mu_i^\alpha = \mu_i^\beta$ . In general, and on the  $C$ , or volume-based, concentration scale, we then have

$$(\mu_i^\alpha)^\circ + RT \ln y_i^\alpha C_i^\alpha = (\mu_i^\beta)^\circ + RT \ln y_i^\beta C_i^\beta$$

where the activity coefficients are represented by  $y_i$ . Thus

$$\ln \frac{y_i^\beta C_i^\beta}{y_i^\alpha C_i^\alpha} = \frac{(\mu_i^\alpha)^\circ - (\mu_i^\beta)^\circ}{RT} = \text{constant at constant } T, P \quad (1)$$

Hence the distribution coefficient  $K$ , defined by

$$\frac{C_i^\beta}{C_i^\alpha} = K \quad (2)$$

is a function of solute concentrations only to the extent that the activity coefficients are concentration-dependent.

In this simplest form the behavior of a neutral solute molecule has been considered. However, the relationship  $\mu_i^\alpha = \mu_i^\beta$  is a perfectly general one, and it is necessary only to use proper descriptions of these chemical potentials when the solute ionizes or associates in either of the two solvent mediums. For a substance which ionizes, the logarithmic relation of

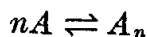
chemical potential to concentration applies in the limit of zero concentration to each ionic species, so that the chemical potential of a salt is obtained by adding the chemical potentials of the ions. If, for example, the equilibrium distribution of hydrochloric acid between benzene and water were being studied,<sup>5</sup> one would write for the chemical potential of the acid in the aqueous phase,  $\alpha$ ,

$$\mu_{\text{HCl}} = (\mu_{\text{H}^+})^\circ + (\mu_{\text{Cl}^-})^\circ + 2RT \ln C_{\text{HCl}} + 2RT \ln y_{\pm}^\dagger$$

Equating this to the chemical potential of the acid in the benzene phase,  $\beta$ , written in a similar form yields

$$\frac{C_i^\beta}{(C_i^\alpha)^2} = K \quad (3a)$$

If, on the other hand, the solute is associated to form an  $n$ -mer in the organic, or  $\beta$ , phase according to the reaction



it can be shown in the same way that

$$\frac{C_i^\beta}{(C_i^\alpha)^n} = K \quad (3b)$$

If the association is not complete, the value of  $n$  computed from Eq. (3b) will not be an integer and it may vary with concentration.

The carboxylic acids are suitable for a study of an association because they generally form double molecules in nonpolar solvents or in the gas phase but exist as single molecules in polar solvents such as water. Some carboxylic acids, e.g., acetic acid, are so weak that their ionization in water can be practically neglected, but others, e.g., trichloroacetic acid, are almost entirely ionized.

It follows directly from the distribution law that extraction with several portions of solvent is more efficient than with a single portion of the same total volume. In the case of phase distributions which satisfy Eq. (2), it is possible to derive a generalized formula which will show the amount remaining unextracted after a given number of operations. If  $V$  milliliters of solution initially containing  $x_0$  grams (or equivalents) of a substance is repeatedly extracted with  $v$  milliliters of an immiscible solvent,

† When a salt (or strong acid or base) is dissolved in water, a system of three chemically different species is formed. The logarithmic relation of chemical potential to concentration applies to each species, so that in this instance the chemical potentials of hydrogen and chloride ions are to be added to give the chemical potential of the acid. Perhaps it should be noted that this is a system of two components rather than of three, because the concentration of one of the ions is known from that of the other, for the system as a whole is electrically neutral.

we may calculate the number of grams  $x_n$  remaining unextracted after  $n$  extractions as follows. After one extraction, the concentration in the original solution will be  $x_1/V$  and in the extracting phase  $(x_0 - x_1)/v$ . Therefore the distribution coefficient is

$$\frac{x_1/V}{(x_0 - x_1)/v} = K \quad (4)$$

and

$$x_1 = x_0 \left( \frac{KV}{KV + v} \right) \quad (5)$$

After a second extraction,  $x_2$  grams (or equivalents) remains in the original solvent. Thus

$$x_2 = x_1 \left( \frac{KV}{KV + v} \right) = x_0 \left( \frac{KV}{KV + v} \right)^2 \quad (6)$$

The last term is obtained by substituting for  $x_1$  its equivalent as given by Eq. (5).

After  $n$  extractions, the quantity remaining in the original solvent is

$$x_n = x_0 \left( \frac{KV}{KV + v} \right)^n \quad (7)$$

Craig and others<sup>1,3</sup> have designed various pieces of apparatus for carrying out multiple extractions conveniently. A countercurrent-distribution apparatus is analogous to a distillation column in that separation is achieved by many two-phase distributions. Such countercurrent-distribution experiments may be used not only for the purpose of fractionation, but also for the characterization of unknown organic compounds.

Since the distribution coefficients for organic acids and bases between aqueous solutions and immiscible organic solvents depend markedly on the pH of the aqueous phase, multiple extractions with various buffer solutions may be used to separate various organic acids, such as the penicillins.

In still another application, distribution experiments may be used to investigate the nature of a complex ion and to make estimates of its dissociation constant. We consider the triiodide ion. With pure water and carbon tetrachloride as the immiscible solvents, the distribution coefficient  $K$  for iodine,  $I_2$ , between them is determined. Then, if instead of pure water, solutions of potassium iodide are used as one of the phases, there will be an apparent increase in the solubility of the iodine which may be attributed to the rapidly reversible reaction





for which the apparent equilibrium constant is

$$K_e = \frac{C_{I_3^-}}{C_{I^-} \cdot C_{I_2}} \quad (8)$$

The amount of free iodine in aqueous iodide solution cannot be determined by direct titration with standard thiosulfate solution, because as soon as the iodine is removed, the complex triiodide ion which is present dissociates to give more iodine. However, the concentration of uncombined iodine in this aqueous phase can be obtained by titrating the carbon tetrachloride layer and making use of the known distribution coefficient for iodine between the two pure liquids.

The total iodine present,  $I_2$  and  $I_3^-$ , may be obtained by the thiosulfate titration, so it becomes possible to compute by difference the triiodide-ion concentration. The total iodide-ion concentration is known from the manner in which the experiment is designed.

#### PART A

**Apparatus.** Three 100-ml separatory funnels; three 100-ml Erlenmeyer flasks; 100-ml volumetric flask; 25-ml pipette; 10-ml pipette; 1.0 N acetic acid or trichloroacetic acid or other acid; glacial acetic acid; carbon tetrachloride; ether; 0.5 N sodium hydroxide; 0.01 N sodium hydroxide.

**Procedure.** One hundred milliliters each of approximately 0.50 N, 1 N, and 2 N solutions of acetic acid in water is prepared. Twenty-five milliliters of each of the three solutions is pipetted into closed 100-ml separatory funnels, and to each is added 25 ml of diethyl ether. Closed rubber tubes are put over the outlets to keep out the water of the thermostat, and the separatory funnels are set in a thermostat at 25° for 20 min or more, with frequent shaking.

After the solutions have come to equilibrium, the separatory funnels are removed from the thermostat and the lower layers run out into beakers, care being taken to let none of the upper layer go through. Ten-milliliter samples of each of the lower layers are taken rapidly and drained into Erlenmeyer flasks for titration with sodium hydroxide, using phenolphthalein as an indicator. Samples of the upper layers are removed from the separatory funnels with 10-ml pipettes, care being taken to avoid taking up any of the lower layer. The aqueous and ether solutions are titrated with 0.5 N NaOH. Check titrations should be made in each case.

A second set of experiments is carried out in the same way, using 25-ml aliquots of carbon tetrachloride instead of ether. Ten-milliliter aliquots of the  $CCl_4$  phases are measured rapidly in order to prevent loss due to evaporation. The  $CCl_4$  phases are titrated with 0.01 N sodium hydroxide.

In titrating the acid dissolved in carbon tetrachloride or ether, an equal volume of water is added initially, and it is necessary to shake vigorously to accelerate the passage of dissolved acid across the surface and into the water layer and thus reduce the time required for elimination of the fading (phenolphthalein) end point.

**Calculations.** The concentrations of acid in the two layers in the distribution experiments are calculated in moles per liter, and the distribution coefficients are calculated with Eq. (2). Plots of  $\log C_A^B$  versus  $\log C_A^A$  are also constructed, and  $n$  of Eq. (3b) calculated. If the value of  $n$  is not equal to unity, a hypothesis is suggested to explain the results.

As an illustration of the application of the distribution coefficient, the concentration of acetic acid remaining in the ether phase is calculated for the following cases:

- a. 50 ml of 1.0 N acetic acid in ether is extracted with 50 ml of water.
- b. 50 ml of 1.0 N acetic acid in ether is extracted with five 10-ml portions of water.

#### PART B

**Apparatus.** Glass-stoppered bottles of 250 ml capacity; beakers, burettes, and pipettes; starch indicator; 0.02 and 0.1 N thiosulfate solutions; 0.1 N potassium iodide; carbon tetrachloride saturated with iodine.

**Procedure.** In this section we investigate the triiodide equilibrium. To do so, the distribution of iodine between carbon tetrachloride and three different aqueous phases is studied. These aqueous phases are (a) pure water, (b) 0.01 N potassium iodide solution, and (c) 0.1 N potassium iodide solution. To each of six of the glass-stoppered bottles is added 35 ml of the carbon tetrachloride saturated with iodine. The bottles are then segregated in pairs to provide duplicate experiments. To each of the first pair is added 100 ml pure water; to each of the second pair, 75 ml of 0.01 N potassium iodide solution; and to each of the third pair, 35 ml of 0.1 N potassium iodide solution. The bottles are thoroughly shaken from time to time and at frequent intervals for half an hour; otherwise they are to remain immersed to the neck in a 25°C thermostat.

After the several systems have come to equilibrium, time is permitted for complete phase separation. Then samples may be removed by pipetting directly from the bottles in the thermostat. In pipetting out samples of the carbon tetrachloride phase, the inside of the pipette may be kept dry as it passes through the aqueous phase by placing a finger tightly over the upper end of the pipette. The concentration of iodine in each of the solutions is determined by titration with one of the thiosulfate solutions, using the starch indicator.

In order to achieve the necessary accuracy, it is suggested that the dilute thiosulfate solution be used for the titration of measured volumes of

the aqueous phases, 75 ml, 50 ml, and 25 ml being used in order of increasing potassium iodide concentration, including the water phase. For the carbon tetrachloride layers, 25 ml is a suitable volume and the more concentrated thiosulfate solution is used as the analytical reagent.

The titration of the carbon tetrachloride layer presents some problems. In the first place, it is slow, because the iodine must be extracted into the aqueous solution which is being added. The starch-indicator solution is used in small volume only as the end point is approached, as judged by the near disappearance of the iodine color from the carbon tetrachloride phase. It is difficult to avoid overtitration. The addition of a small volume of 10 per cent KI solution is of aid in the titration.

**Calculations.** The concentrations of iodine in the two pure-solvent layers, water and carbon tetrachloride, are calculated in moles per liter, and the distribution coefficient is computed with the aid of Eq. (2). Now, with the use of this coefficient, the concentration of molecular iodine,  $C_{I_2}$ , in the two potassium iodide solutions is calculated, it being assumed that

$$\frac{C_{I_2}^{\alpha}}{C_{I_2}^{\beta}} = \text{constant}$$

These values, when subtracted from the total iodine concentration of the solution, provide data for the computation of the concentrations of the  $I_3^-$  in the two aqueous potassium iodide systems. The iodide-ion concentrations,  $C_{I^-}$ , are obtained by subtracting the values for  $C_{I_3^-}$  from the original potassium iodide concentrations.

With these data, values for the equilibrium constant for the reaction  $I^- + I_2 = I_3^-$ , as defined by Eq. (8), are computed for the two different potassium iodide systems. They are compared with data in the literature.<sup>6</sup>

**Practical Applications.** Extraction of a solute by shaking a solution with an immiscible solvent is an operation that is used extensively in organic chemistry. The efficiency of any such operation may be calculated when the distribution coefficient is known.

The chemical potential of a solute determines its distribution into a second solvent; thus the activity of the solute may be calculated from distribution data.

In some cases, the degree of hydrolysis of a salt may be determined by measuring the distribution ratio of the acid or base when shaken with an immiscible solvent.

The extraction of uranium from its ores and the separation of uranium from its fission products in atomic-energy operations often make use of solvent extraction with an organic solvent which is immiscible with water.

The coloring of polyethylene terephthalate fibers by nonionic dyes is another example of the practical use of a distribution coefficient.<sup>7</sup>

**Suggestions for Further Work.** Other distribution systems may be studied, such as the following:

Hydrochloric acid between water and benzene.<sup>5</sup>

Salicylic acid or picric acid between water and benzene, and between water and chloroform as a function of the pH of the aqueous phase.

Uranyl nitrate between water and ether or between water and tributyl phosphate. The extraction of uranyl nitrate into the organic phase is improved by the addition of nitric acid.

As an example of the distribution of an inorganic salt between immiscible solvents, the distribution of ferric chloride between ether and water may be studied. The salting-out effect is illustrated by the addition of excess sodium chloride or calcium chloride to the aqueous phase.

#### References

1. Craig, *J. Biol. Chem.*, **155**, 519 (1944).
2. Craig and Craig in Weissberger (ed.): "Technique of Organic Chemistry," 2d ed., Vol. III, Pt. I, Interscience Publishers, Inc., New York (1956).
3. Craig, Golumbic, Mighton, and Titus, *J. Biol. Chem.*, **161**, 321 (1945).
4. Craig, Hogeboom, Carpenter, and du Vigneaud, *J. Biol. Chem.*, **168**, 665 (1947).
5. Hinshelwood and Knight, *J. Chem. Soc.*, 466 (1927).
6. Jones and Kaplan, *J. Am. Chem. Soc.*, **50**, 1845 (1928).
7. Schuler and Remington, *Faraday Soc., Discussions*, **16**, 201 (1954).

### 19. PHASE DIAGRAM OF A BINARY SOLID-LIQUID SYSTEM

This experiment illustrates the use of cooling curves to establish the phase diagram for a binary system. It illustrates also the use of the thermocouple.

**Theory.**<sup>1</sup> The purpose of the experiment is to obtain data by thermal analysis for constructing a phase diagram which indicates the solid and liquid phases that are present at each temperature and composition. The temperatures at which solid phases appear upon cooling various solutions of the two components are detected by observation of the changes in slope of the plot of temperature versus time. A slower rate of cooling is obtained while a solid phase is separating out because the heat evolved by solidification partly offsets the heat lost by radiation and conduction to the colder surroundings.

#### A. AN ALLOY SYSTEM

**Apparatus.** Six Pyrex test tubes fitted with thermocouple wells and spacers; tin, lead, and their binary mixtures; benzoic acid; bismuth; chromel-alumel thermocouple and potentiometer; electric furnace or Méker burner; large test tube, spacer, and rack; aluminum foil; watch or electric clock; vacuum bottle. (Recording potentiometer is recommended.)

**Procedure.** A suggested sample tube and cooling jacket are shown in Fig. 28. A brass spacer centers the thermocouple well in the sample tube, and a second spacer centers the sample tube in the outer Pyrex tube. Bright aluminum foil is rolled into a cylinder and placed between the

sample tube and the cooling jacket to reduce radiation losses and extend the time of cooling. The metal to be melted is placed in a steel cup made by drilling out a short piece of steel rod. It is set in the Pyrex tube on a wad of glass wool. If the metals are melted and frozen directly in the glass sample tube, the tube is apt to break because of the differences in thermal expansion. The tube containing a particular sample is heated† until the material has just melted completely. If the tube is markedly overheated, oxidation may be more serious, and furthermore a large number of readings of no practical value will be required at the beginning of the measurements. The Pyrex tube containing the metal cup is then transferred to the outer cooling jacket, and the time-temperature curve determined.

One junction of the thermocouple is placed in the thermocouple well of the sample tube; the other is placed in a tube in an ice bath contained in a vacuum bottle. The thermocouple leads are connected to a potentiometer designed for thermocouple use; for the present application the commonly available 0-to-16-millivolt range is appropriate. The potentiometer is adjusted as required to balance the changing electromotive force of the thermocouple as the sample cools. Time and voltage (temperature) readings are recorded approximately every quarter minute, until the results indicate that the freezing point (or, for a mixture, the eutectic temperature) has been reached as illustrated in Fig. 29.

The chromel-alumel thermocouple is calibrated by taking cooling curves with solids of known melting points: benzoic acid ( $121.7^{\circ}$ ), tin ( $232^{\circ}$ ), bismuth ( $271^{\circ}$ ), and lead ( $327^{\circ}$ ).

† The Fieldner volatile-matter furnace, obtainable at supply houses, is recommended for this experiment. The furnace temperature may be controlled conveniently by use of a Variac or other variable autotransformer. A bunsen burner may be used.

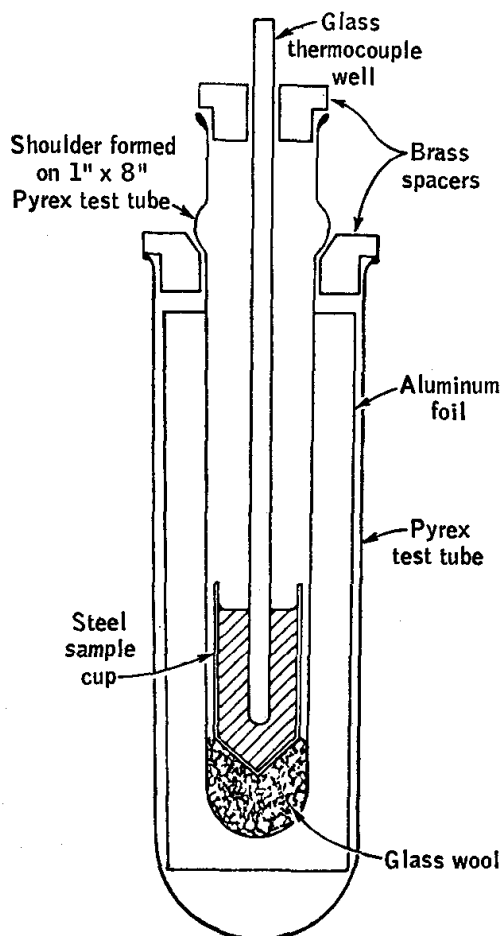


FIG. 28. Sample tube and cooling jacket.

Cooling curves are then determined for the following mixtures:

1. Lead, 90 per cent; tin, 10 per cent
2. Lead, 80 per cent; tin, 20 per cent
3. Lead, 60 per cent; tin, 40 per cent
4. Lead, 40 per cent; tin, 60 per cent
5. Lead, 20 per cent; tin, 80 per cent

It is convenient to have each of the samples in a separate sample holder with thermocouple well. This collection of samples is kept in a metal

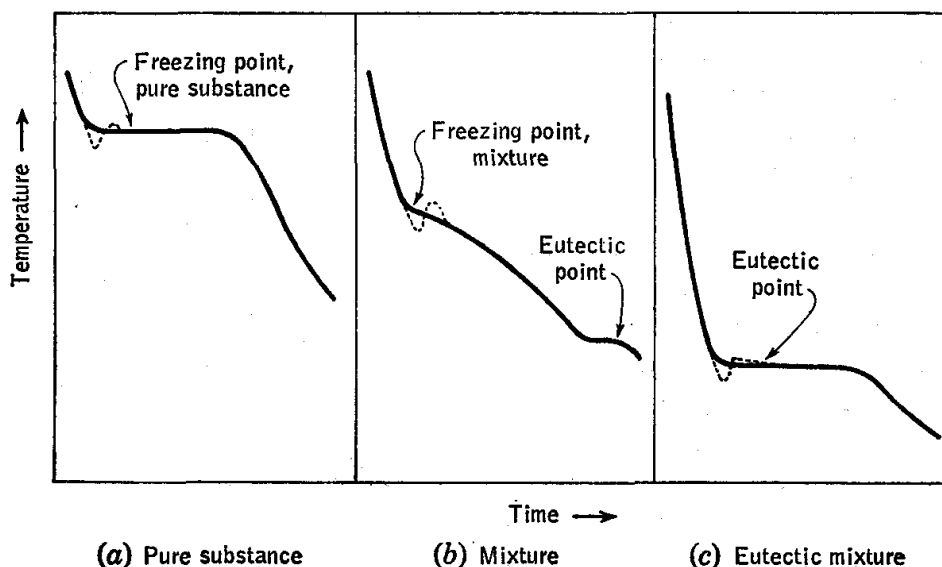


FIG. 29. Typical cooling curves (dashed portions illustrate supercooling effects).

test-tube rack, and the thermocouple is transferred to a new, heated well when one cooling curve is completed. A thin layer of graphite is placed over the samples to minimize air oxidation. When a sample becomes extensively oxidized, it is replaced with fresh material. Cooling curves obtained with impure or oxidized samples will often fail to exhibit the distinct breaks which are sought.

The experiment is greatly facilitated by a recording potentiometer, which automatically graphs the voltage of the thermocouple against time. The range of the recorder is set to obtain full deflection at the highest temperature.

#### B. AN ORGANIC COMPOUND SYSTEM

**Apparatus.** Ten Pyrex tubes with varying compositions of phenol and *p*-toluidine; larger tube for slow cooling; recording potentiometer, or 0 to 50° thermometer with 0.1 or 0.2° divisions.

**Procedure.** Phase relationships can be illustrated by use of mixtures of organic compounds as well as metal-alloy systems. For example, compound formation between the components is shown by the system phenol-*p*-toluidine. *These compounds must be handled with great care to avoid contact with the skin.*

For the system assigned, a set of about 10 freezing-point tubes should be prepared to cover the composition range from one pure component to the other. The compounds are weighed out carefully into  $\frac{1}{2}$ - by 6-in. test tubes; about 6 g total mixture weight is sufficient. One of the tubes is heated with hot water or a bunsen burner until the mixture is barely, but completely, melted. It is then inserted in a larger test tube, with the help of a cork ring, to reduce the rate of cooling. A small glass tube, closed at the bottom, is fitted into a cork and set so that it reaches near the bottom of the melted material. The thermocouple junction fits into this well, and a little oil is added to improve the thermal conductance. The alumel-chromel thermocouple and recorder used in Part A may be used here, or at these lower temperatures a more sensitive couple of copper-constantan may be used. The thermocouple is calibrated with ice and boiling water, making correction for barometer, and with one or two other materials with sharp melting points at intermediate temperatures.

If a recording potentiometer is not available, a 0 to 50° thermometer graduated to 0.1° may be used in place of the thermocouple and well.

A ring stirrer is used to keep the cooling mixture at a uniform temperature. The stirrer may be made from thin glass rod or nichrome wire or other chemically inert wire. It was unnecessary to stir the metals and alloys in the procedure of Part A because their thermal conductance is so high.

A time-temperature graph is obtained as described under the procedure of Part A, and the readings are continued until the sample has completely solidified.

The mixture may be melted again, and a check determination made. The thermocouple well is then removed *carefully* and thoroughly cleaned before inserting in the next sample. The procedure is repeated with each of the mixtures. It is important to use pure materials for preparing the mixtures.

For mixtures with low freezing points the test tube and its outer jacket may be immersed in an ice bath or an ice-salt mixture. If the compounds are subject to air oxidation or tend to absorb moisture or carbon dioxide from the air, they may be sealed off in an all-glass tube. The thermometer well is sealed into the top of the tube and extends nearly to the bottom of the tube. The sample is introduced through a side tube, which is then sealed off. It is more difficult to avoid supercooling in this apparatus in which shaking is the means of stirring.

A major experimental problem in all this work is supercooling, i.e., failure of crystallization to take place at the proper temperature. Actually, a *small* extent of supercooling is useful, since then, when crystallization does start, the crystals formed are dispersed widely through the liquid, and equilibrium between the solid and liquid phases is more easily maintained. If supercooling seems too great, the experiment is repeated, with more vigorous stirring at the appropriate stages. Supercooling may usually be avoided by dropping in a "seed crystal" of the solid material.

**Calculations.** In the interpretation of actual time-temperature graphs, care must be taken that spurious irregularities, due to instrumental and other experimental errors, are avoided.

The various experimental cooling curves are drawn as plots of potentiometer readings versus times of observation. The voltages corresponding to the freezing points of the substances used as calibration standards are determined (Fig. 29a). A thermocouple calibration curve is constructed from the voltage-temperature points thus obtained, and voltages are then converted into temperatures by interpolation on this curve. For each mixture studied, the temperatures at the characteristic transformation points (initial crystallization of solid, crystallization of eutectic mixture, etc.) can then be obtained from its cooling curve (Fig. 29).

A third graph is then prepared by plotting these transformation temperatures against the compositions of the mixtures. Lines are drawn through the points to complete a phase diagram. Each area, line, and invariant point on the diagram is discussed briefly in terms of the phase rule.

**Practical Applications.** The method of thermal analysis illustrated in this experiment is a basic procedure in the study of phase relationships. A maximum in the freezing-point-composition curve indicates the existence of an intermediate compound, and the composition of the compound is given by the highest point on the composition-temperature curve, for this represents the melting point of the pure compound.

Temperature-composition curves and other phase diagrams are of great value in the technical study of alloys and ceramics and in the recovery of a salt by crystallization from a mixture of salts.

**Suggestions for Further Work.** The following pairs of organic compounds are suitable for study: urea-phenol, naphthalene-nitrophenol, acetamide- $\beta$ -naphthol,  $\beta$ -naphthol-*p*-toluidine, phenol- $\alpha$ -naphthylamine, diphenylamine-naphthalene. A number of phase diagrams in organic systems are discussed by Kofler<sup>3</sup> and by Skau and Wakeham.<sup>4</sup> Interesting inorganic systems may be selected by reference to the diagrams given in the International Critical Tables.<sup>2</sup>

Fractional crystallization is an effective method of purification.

The constancy of the freezing point through the whole solidification from start to finish is one of the best criteria for purity. If the substance is impure, the impurities become concentrated in the mother liquor as the liquid freezes out, and the freezing point is lowered more and more by the impurities.



## References

1. Findlay, Campbell, and Smith, "The Phase Rule and Its Applications," Dover Publications, New York (1951).
2. International Critical Tables, Vols. II, IV, McGraw-Hill Book Company, Inc., New York (1928).
3. Kofler, "Thermo-Mikro-Methoden," Verlag Chemie, G.m.b.H., Weinheim/Bergstrasse, Germany (1954).
4. Skau and Wakeham in Weissberger (ed.): "Technique of Organic Chemistry," 3d ed., Vol. I, Pt. I, Chap. 3, Interscience Publishers, New York (1959).

## 20. THREE-COMPONENT SYSTEMS

Solubility and tie-line data for a three-component system are plotted in a triangular graph.

**Theory.** According to the phase rule of Gibbs, the variance  $v$  (number of degrees of freedom) of a system at equilibrium is equal to the number of components  $c$  minus the number of phases  $p$  plus 2, provided that the equilibrium is influenced only by temperature, pressure, and concentration.

$$v = c - p + 2 \quad (1)$$

The variance  $v$  is the smallest number of independent variables required to completely describe the state of the system.

This experiment is carried out at constant temperature and pressure so that these are not variables. Thus Eq. (1) becomes

$$v = c - p \quad (2)$$

so that for a three-component system  $v = 3 - p$ . Thus the variance is 2 if a single phase is present and 1 if two phases are present.

It is convenient to represent a three-component system on a triangular diagram such as that illustrated in Fig. 30.

In an equilateral triangle, the sum of the perpendiculars from a given point to the three sides is a constant. The perpendicular distance from each apex, representing a pure compound, to the opposite side is divided into 100 equal parts, corresponding to per cent, and labeled along the side at the right of the perpendicular. A point situated on one of the sides of the triangle indicates that there are two components with the percentage composition indicated. The composition corresponding to any point within the triangle is obtained by measuring on these coordinates the distance toward apex  $A$ , the distance toward  $B$ , and the distance toward  $C$ . These three distances representing percentages always add up to 100. For example, point  $M$  represents the composition 30 per cent  $A$ , 60 per cent  $B$ , and 10 per cent  $C$ .

Several different types of ternary systems are possible, depending upon whether one, two, or three pairs of the liquids are partially miscible in each other. In the system illustrated in Fig. 30, *A* and *C* are partially miscible while pair *A* and *B* and pair *B* and *C* are completely miscible. Mixtures having compositions lying below the curve will separate into two phases, while all other mixtures form homogeneous solutions. For example, mixture *O* will separate into two phases *K* and *L*, and the line

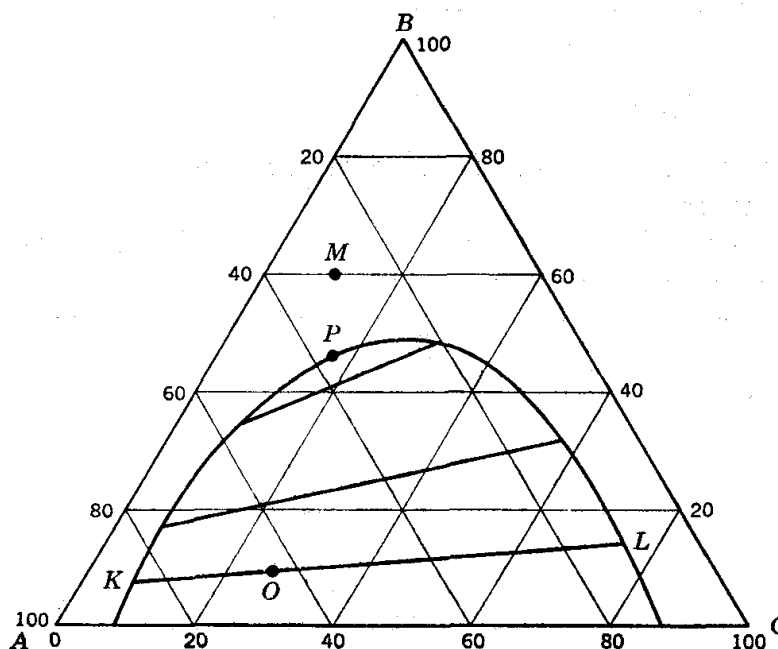


FIG. 30. Phase diagram for a three-component system.

connecting these conjugate ternary solutions in equilibrium with each other is called a tie line. It is an important characteristic of a ternary diagram that the relative amounts of phases *K* and *L* are proportional to the lengths *OL* and *OK*, respectively. These tie lines slope upward to the right, indicating that component *B* is relatively more soluble in the phase rich in *C* than it is in the phase rich in *A*.

As the amount of component *B* is increased, the compositions of the conjugate solutions approach each other. At point *P* the two conjugate solutions have the same composition, so that the two layers have become one: this is called the *plait point*.

**Apparatus.** Thermostat (25°); three burettes (25 ml); six glass-stoppered bottles (50 ml); one 5-ml pipette; small separatory funnel; Westphal density balance; chloroform; glacial acetic acid; 0.5 N sodium hydroxide.

**Procedure.** The solubility relations of the three-component system chloroform-acetic acid-water are studied in this experiment. The tie

lines may be determined conveniently by titrating the acetic acid in the two separate liquid phases, which are separated after they have come into equilibrium with each other.

Three burettes are set up containing water, chloroform, and acetic acid. Nonaq† grease should be used for the burette containing chloroform. The density of each liquid is determined with the Westphal balance, and solutions of accurately known concentration are prepared containing approximately 10, 25, 40, and 60 per cent by weight acetic acid in water. About 20 g of each is sufficient. These four solutions are placed in 50-ml glass-stoppered bottles and set in a thermostat at 25°. After coming to temperature, they are removed as necessary and titrated with chloroform. During the titration, the bottle is shaken vigorously after each addition of chloroform, and the end point is taken as the first perceptible cloudiness.

Samples of approximately 10, 25, 40, and 60 per cent acetic acid in chloroform are then prepared and titrated to cloudiness with water at the thermostat temperature. The percentage by weight of each component present at the appearance of the second phase is calculated, and the compositions are plotted on the ternary diagram.

The tie lines are determined by preparing about 40 ml each of mixtures of accurately known concentrations containing approximately 10, 20, 30, or 40 per cent acetic acid with 45 per cent chloroform in each case, the remainder being water. These two-phase mixtures are prepared in the glass bottles and are allowed to equilibrate in the 25° thermostat. After equilibrium has been reached and the phases have been separated by means of a separatory funnel, the density of each phase is determined with the Westphal balance, and 5-ml aliquots are titrated with 0.2 N sodium hydroxide, using phenolphthalein as indicator.

**Calculations.** The percentage by weight of chloroform, acetic acid, and water for each of the mixtures that showed the first indication of turbidity is plotted on triangular graph paper.

The determination of the acetic acid concentrations allows the compositions of the conjugate phases to be located on the two-phase curve. It may be assumed that the more dense phase is the one rich in chloroform. The gross compositions of the two-phase mixtures are also plotted on the triangular graph, and the tie lines should pass through these points.

The phases present at each area and line are recorded, and the effect of adding more of the components at significant points is described.

**Practical Applications.** The increase in mutual solubility of two liquids due to the addition of a third is of practical as well as theoretical importance. Calculations in two-phase extraction processes may be carried out, using triangular diagrams.

**Suggestions for Further Work.** The solubility and tie-line determinations may be repeated at a different temperature. As the temperature is raised, the area under

† Eimer and Amend, New York.

the curve corresponding to the region of two liquid phases becomes smaller, because the liquids become more soluble in each other. Several isothermal lines may be drawn on the same diagram, or a space model may be constructed with temperature as the vertical axis and the triangular diagrams lying in horizontal planes. A triangular-prism space model may be made for the liquid-solid phases in the system diphenyl-diphenylamine-benzophenone.<sup>3</sup>

The systems benzene-water-alcohol and cyclohexane-water-alcohol studied by Washburn and his associates illustrate the effect of increasing the hydrocarbon-chain length in the alcohol-homologous series.<sup>5</sup>

The system water-ether-succinic nitrile furnishes an example of a three-component system containing three pairs of partially miscible liquids. The system water-methyl acetate (or ethyl acetate)-*n*-butyl alcohol is an example of a system in which two of the pairs of liquids are partially miscible while the third pair is completely miscible.

A three-component system involving two solids and a liquid which is suitable for a laboratory experiment<sup>2</sup> is provided by lead nitrate-sodium nitrate-water. Data are obtained by evaporating the water from saturated solutions of known weight.

### References

1. Findlay, Campbell, and Smith, "The Phase Rule," Dover Publications, New York (1951).
2. Heric, *J. Chem. Educ.*, **35**, 510 (1958).
3. Lee and Warner, *J. Am. Chem. Soc.*, **55**, 4474 (1933).
4. Rhodes, "Phase Rule Studies," Chaps. V and VI, Oxford University Press, New York (1933).
5. Washburn *et al.*, *J. Am. Chem. Soc.*, **53**, 3237 (1931); **54**, 4217 (1932); **56**, 361 (1934); **57**, 303 (1935); **59**, 2076 (1937); **61**, 1694 (1939); **68**, 235 (1946).

## 21. SOLUBILITY AS A FUNCTION OF TEMPERATURE

The determination of solubility and the calculation of the differential heat of solution at saturation are illustrated in this experiment.

**Theory.** One of the simplest cases of equilibrium is that of a saturated solution in contact with excess solute; molecules leave the solid and pass into solution at the same rate at which molecules from the solution are deposited on the solid. The term *solubility* refers to a measure, on some arbitrarily selected scale, of the concentration of the solute in the saturated solution. Here the molal concentration scale will be used, and the solubility then becomes equal to the molality  $m_s$  of the solute in the saturated solution.

An equilibrium-constant relation may be written for the equilibrium considered:

$$K = \frac{a_2}{a_2^*} \quad (1)$$

Here  $a_2$  represents the activity of the solute in the saturated solution, and  $a_2^*$ , the activity of the pure solid solute. The conventional choice of standard state for the latter is the pure solute itself at the temperature

and pressure involved, making  $a_2^*$  identically equal to unity. The activity  $a_2$  is related to the molality  $m$  of the solute by means of the activity coefficient  $\gamma$ , a function of  $T$ ,  $P$ , and composition which approaches unity as  $m$  approaches zero. Then

$$K = a_2(m_s) = \gamma_s m_s \quad (2)$$

where the subscript  $s$  indicates that the relation applies to the saturated solution. The symbol  $a_2(m_s)$  denotes the value of the activity  $a_2$  for the saturated solution.

The change in  $K$  with temperature at constant pressure reflects a change in  $m_s$ , and also the change in  $\gamma_s$ , which is affected by both the variations in temperature and concentration of the solution. The van't Hoff equation requires that

$$\left( \frac{\partial \ln K}{\partial T} \right)_P = \frac{\Delta H^\circ}{RT^2} \quad (3)$$

where  $\Delta H^\circ$  = standard enthalpy change for solution process. This quantity should not be confused with any actual experimentally measurable heat of solution; it can be determined indirectly, however.

Taking into account the effects of temperature and concentration on  $\gamma_s$  (Ref. 7), there results for constant pressure

$$\left[ 1 + \left( \frac{\partial \ln \gamma}{\partial \ln m} \right)_{T, P, m=m_s} \right] \frac{d \ln m_s}{dT} = \frac{\Delta H_{D.S.}(m_s)}{RT^2} \quad (4)$$

Here  $\Delta H_{D.S.}(m_s)$  is the *differential heat of solution* at saturation at the given temperature and pressure (cf. Exp. 4). For cases in which the activity coefficient  $\gamma$  for the solute changes only slightly with concentration in the immediate neighborhood of saturation, the bracketed term in Eq. (4) becomes equal to unity, and

$$\frac{d \ln m_s}{dT} = \frac{\Delta H_{D.S.}(m_s)}{RT^2} \quad (5)$$

or

$$\frac{d \log m_s}{d(1/T)} = \frac{-\Delta H_{D.S.}(m_s)}{2.303R} \quad (6)$$

In this approximation, then, the differential heat of solution at saturation may be calculated at a given temperature  $T$  by multiplying by  $-2.303R$  the slope corresponding to this temperature of the plot of  $\log m_s$  versus  $1/T$ .

If it is assumed in addition that  $\Delta H_{D.S.}(m_s)$  is independent of  $T$ , an assumption which in general is better for nonelectrolytic solutes than for

electrolytic types, then integration of Eq. (5) leads to

$$\log \frac{m_s(T_2)}{m_s(T_1)} = \frac{\Delta H_{D.S.}(T_2 - T_1)}{2.303RT_2T_1} \quad (7)$$

The heat of solution with which we are concerned here is the heat absorbed when 1 mole of the solid is dissolved in a solution that is already practically saturated. It differs from the heat of solution at infinite dilution, which is the heat of solution often given in tables, by an amount equivalent to the heat of dilution from saturation to infinite dilution.

**Apparatus.** Ice bath at 0°; large test tube; 0.5 N sodium hydroxide; oxalic acid; 0.1° thermometer; 10-ml pipette; 10-ml weighing bottle.

**Procedure.** The solubility of oxalic acid is determined at 25, 20, 15, and 0°, or at other convenient temperatures below room temperature; the temperature is read to 0.1° with a thermometer immersed in the solution. The 15° temperature is achieved by adding small amounts of ice or ice water as necessary to the thermostat.

For the solubility determinations a test tube fitted with a thermometer and stirrer is used. The stirrer is made from a small rod of glass or polystyrene, bent into a ring of such size that it cannot hit the thermometer bulb. It is moved up and down vigorously by hand. The air jacket between the test tubes is provided to reduce the rate of cooling or heating. A simple thermostat improvised from a large beaker and a small motor-driven stirrer may be used. A 10-ml sample is removed with a pipette, drained into a weighing bottle, and weighed to 0.01 g.

Distilled water in large test tubes is saturated with oxalic acid by dissolving crystals at a higher temperature and then cooling to the required temperature so that some of the dissolved material is crystallized out. When the equilibrium is approached in this way, from the side of supersaturation rather than from the crystal side, the equilibrium is attained rapidly. For this reason, if the thermostat temperature is not constant, a falling temperature may not be serious, but a rising temperature may introduce a considerable error.

To prevent drawing small crystals into the pipette along with the solution, a filter such as shown in Fig. 31 may be used. Alternatively, a small piece of filter paper may be wrapped around the tip of the pipette and fastened with thread or a small rubber band. The filter is removed before draining the pipette. The solution is then titrated with 0.5 N sodium hydroxide, using phenolphthalein as an indicator.

Duplicate determinations are made at each temperature.

**Calculations.** The solubility in moles per 1000 g of solvent is calculated at each of the four temperatures and compared with the accepted values. It is interesting to compare these values with the solubilities calculated in moles per liter.

The logarithm of the solubility in moles per 1000 g of solvent is plotted against the reciprocal of the absolute temperature, and a smooth curve is drawn through the four points. If the heat of solution were constant, the line would be straight. Tangents are drawn at 25 and 0°, and the heat of solution is determined at the two temperatures with the help of Eq. (6).

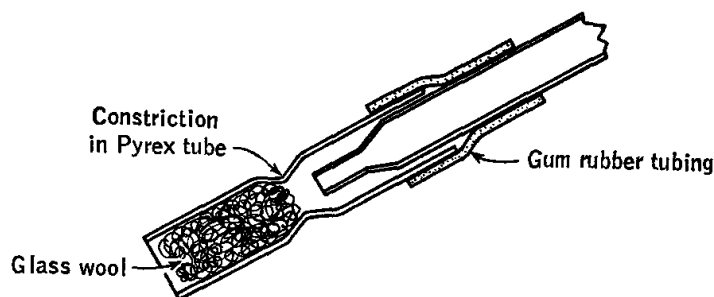


FIG. 31. Filter for use in solubility determinations.

**Practical Applications.** The solubility of a substance may be calculated at other temperatures when it has been determined at two different temperatures. The results are more accurate when the heat of solution is not affected by temperature or when the temperature range is small. Solubility may be used as a criterion of purity and as a means of studying intermolecular forces.<sup>6</sup>

**Suggestions for Further Work.** The solubility of other materials may be determined in a similar way, benzoic acid or succinic acid, for example, or other solids having low solubility and easy methods of analysis. Nonaqueous solvents may be used also.

Boric acid may be used instead of oxalic acid for this experiment. It is titrated by using phenolphthalein as an indicator and adding 10 to 20 ml of neutral glycerin to give a sharp end point.

The solubility-product rule and the effect of other salts on solubility may be illustrated by determinations of the solubility of a slightly soluble salt such as silver bromate in the presence of common ions, ammonium hydroxide, and other salts.

The influence of salts in reducing the solubility of benzoic acid may be determined.<sup>1</sup> The salting-out constant thus obtained can be used for calculating activity coefficients.

In Eq. (2) it is assumed that the heat of solution is independent of temperature, but this assumption is not often justified. The equation may be made exact by introducing terms for the heat capacity of the solute and solvent and for the solution.

#### References

1. Goeller and Osol, *J. Am. Chem. Soc.*, **50**, 2132 (1937).
2. Hildebrand and Scott, "Solubilities of Non-electrolytes," American Chemical Society Monograph, Reinhold Publishing Corporation, New York (1950).

3. Seidell, "Solubilities of Inorganic and Metal Organic Compounds," 3d ed., Vol. I, D. Van Nostrand Company, Inc., Princeton, N.J. (1940).
4. Seidell, "Solubilities of Organic Compounds," 3d ed., Vol. II, D. Van Nostrand Company, Inc., Princeton, N.J. (1941).
5. Seidell and Linke, "Supplement to Solubilities of Inorganic and Organic Compounds," 3d ed., Vol. III, D. Van Nostrand Company, Inc., Princeton, N.J. (1952).
6. Mader, Vold, and Vold in Weissberger (ed.): "Technique of Organic Chemistry," 3d ed., Vol. I, Pt. I, Chap. 11, Interscience Publishers, Inc., New York (1959).
7. Williamson, *Trans. Faraday Soc.*, **40**, 421 (1944).



## CHAPTER 7

# Chemical Kinetics

### 22. HYDROLYSIS OF METHYL ACETATE

From experimental data on the rate of a chemical reaction the reaction-rate constant is calculated for two different temperatures, and from these the energy of activation is determined.

**Theory.**<sup>1,4</sup> In chemical kinetics the term *rate of reaction* refers to the time rate of change,  $dc/dt$ , of the concentration of one of the reactants or products. The *reaction-rate constant*  $k$  is a proportionality factor which relates the rate of reaction to the concentrations of the reactants.

A *first-order reaction* is one whose rate is found by experiment to be proportional to the concentration of the reacting substance:

$$-\frac{dc}{dt} = kc \quad (1)$$

Integration of this equation gives the equivalent expressions

$$-2.303 \log c = kt + \text{constant} \quad (2)$$

$$k = \frac{2.303}{t_2 - t_1} \log \frac{c_1}{c_2} \quad (3)$$

$$k = \frac{2.303}{t} \log \frac{c_0}{c} \quad (4)$$

where  $c$  = concentration of reactant at time  $t$

$c_0, c_1, c_2$  = concentrations at times  $t = 0, t_1$ , and  $t_2$ , respectively

For the first-order reaction,  $k$  is numerically equal to the fraction of the substance which reacts per unit time, usually expressed in reciprocal seconds (or minutes). It should be noted that for a first-order reaction the reaction rate can be determined without information on the initial reactant concentration or even as to the absolute concentrations at various times, provided that a quantity directly proportional to the concentration can be determined.

The kinetics of a *second-order reaction* is described by the equation

$$-\frac{dc_A}{dt} = kc_A^2 \quad (5)$$

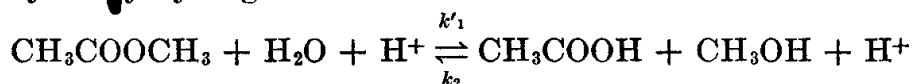
where  $c_A$  is the concentration of the reactant A, or

$$-\frac{dc_A}{dt} = kc_Ac_B \quad (6)$$

where  $c_A$  and  $c_B$  represent the concentrations of two reactants A and B. The numerical value of the rate constant  $k$  for a second-order reaction depends on the units in which the concentrations are expressed. In a second-order reaction, if one reactant is present in sufficiently large excess, its concentration will remain essentially constant while that of the other constituent undergoes a marked change, and the reaction will then appear to be first-order.

From the kinetic viewpoint, most chemical reactions are complex, the reaction mechanism consisting of several successive steps, each of which will normally be either first- or second-order. Another typical complication arises with reactions which proceed to an equilibrium state appreciably short of completion; in these cases the reverse reaction becomes important as equilibrium is approached. The concentration of a catalyst may also be an important variable.

The hydrolysis of methyl acetate presents a number of interesting kinetic aspects. The reaction, which is extremely slow in pure water, is catalyzed by hydrogen ion:



The reaction is reversible, so the net rate of hydrolysis at any time is the difference between the rates of the forward and reverse reactions, each of which follows the simple rate law given by Eq. (6). Thus

$$-\frac{dc_{\text{CH}_3\text{COOCH}_3}}{dt} = k'_1c_{\text{H}_2\text{O}}c_{\text{CH}_3\text{COOCH}_3} - k_2c_{\text{CH}_3\text{COOH}}c_{\text{CH}_3\text{OH}} \quad (7)$$

where  $k'_1$  is the rate constant for the forward reaction and  $k_2$  for the reverse reaction. For dilute solutions, water is present in such large excess that its concentration undergoes a negligible proportional change while that of the methyl acetate is changed considerably. For this case Eq. (7) may be written

$$-\frac{dc_{\text{CH}_3\text{COOCH}_3}}{dt} = k_1c_{\text{CH}_3\text{COOCH}_3} - k_2c_{\text{CH}_3\text{COOH}}c_{\text{CH}_3\text{OH}} \quad (8)$$

In the early stages of the hydrolysis, the concentrations of acetic acid and methanol remain small enough so that the term involving them is negligible, and the reaction appears to be of first order:

$$-\frac{dc_{\text{CH}_3\text{COOCH}_3}}{dt} = k_1c_{\text{CH}_3\text{COOCH}_3} \quad (9)$$

The value of  $k_1$  can then be determined by one of the methods conventional for first-order reactions.

Evaluation of  $k_1$  at the different temperatures permits the calculation of the *Arrhenius heat of activation*,  $\Delta H_a$ , for the forward reaction:

$$\frac{d \ln k_1}{dT} = \frac{\Delta H_a}{RT^2} \quad (10)$$

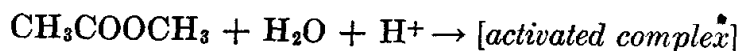
$$\log \frac{k_{1,T_2}}{k_{1,T_1}} = \frac{\Delta H_a}{2.303R} \left( \frac{T_2 - T_1}{T_2 T_1} \right) \quad (11)$$

In obtaining the integrated form, it is assumed that  $\Delta H_a$  is a constant. The heat of activation is usually expressed in calories per mole and is interpreted as the amount of energy the molecules must have in order to be able to react.

A more accurate calculation of the influence of temperature may be made on the basis of the Eyring equation,

$$k = \kappa \left( \frac{kT}{h} \right) e^{\Delta S^\ddagger/R} e^{-\Delta H^\ddagger/RT} \quad (12)$$

where  $\Delta S^\ddagger$  and  $\Delta H^\ddagger$  are the standard entropy and enthalpy changes for formation of the activated complex from the reactants



and  $\kappa$  is a constant, of the order of  $\frac{1}{2}$ , defined as the probability that an activated complex will decompose to form product species (rather than regenerating reactant species). Thus  $\Delta H^\ddagger$  may be determined from measurements of  $k$  at two or more temperatures, on the assumption that  $\Delta S^\ddagger$ ,  $\Delta H^\ddagger$ , and  $\kappa$  are independent of temperature.

$$\frac{k_{1,T_2}}{k_{1,T_1}} = \frac{T_2}{T_1} \exp \left[ - \frac{\Delta H^\ddagger}{R} \left( \frac{1}{T_2} - \frac{1}{T_1} \right) \right] \quad (13)$$

$$\Delta H^\ddagger = \frac{RT_1 T_2}{T_2 - T_1} 2.303 \log \frac{(k_{1,T_2}) T_1}{(k_{1,T_1}) T_2} \quad (14)$$

Although  $\Delta S^\ddagger$  cannot be determined from these data, for want of a knowledge of the value of  $\kappa$ , it is sometimes possible to gain some information about the magnitude of  $\Delta S^\ddagger$  by making a guess as to the value of  $\kappa$ . In ordinary cases, a value of  $\frac{1}{2}$  to 1 is considered a reasonable estimate, but under certain circumstances  $\kappa$  may be very small. The value of  $\Delta H^\ddagger$  can be used, of course, to calculate the value of  $k_1$  at any temperature (over the range in which  $\Delta H^\ddagger$  and  $\Delta S^\ddagger$  remain constant) from a knowledge of  $k_1$  at one temperature.

An explicit solution to the kinetic equation may also be written for the case where the reverse reaction cannot be ignored. If the concen-

tration of methyl acetate is  $a$  moles per liter initially, and  $(a - x)$  moles per liter at time  $t$ , then Eq. (8) can be written as

$$-\frac{d(a-x)}{dt} = \frac{dx}{dt} = k_1(a-x) - k_2x^2 \quad (15)$$

since for each mole  $x$  of methyl acetate hydrolyzed, one mole  $x$  of acetic acid and one mole of methanol are produced. Integration of this relation gives

$$t = \frac{1}{k_1 \left( \frac{4ak_2}{k_1} + 1 \right)^{1/2}} \ln \frac{2a+x \left[ \left( \frac{4ak_2}{k_1} + 1 \right)^{1/2} - 1 \right]}{2a-x \left[ \left( \frac{4ak_2}{k_1} + 1 \right)^{1/2} + 1 \right]} \quad (16)$$

Making use of the relation that the equilibrium constant  $K_h$  for the hydrolysis reaction is given by the expression

$$K_h = \frac{c_{\text{CH}_3\text{COOH}}c_{\text{CH}_3\text{OH}}}{c_{\text{CH}_3\text{COOCH}_3}c_{\text{H}_2\text{O}}} = \frac{k'_1}{k_2} = \frac{k_1}{k_2c_{\text{H}_2\text{O}}}$$

one obtains

$$t = \frac{1}{k_1 \left( \frac{4a}{K_h c_{\text{H}_2\text{O}}} + 1 \right)^{1/2}} \ln \frac{2a+x \left[ \left( \frac{4a}{K_h c_{\text{H}_2\text{O}}} + 1 \right)^{1/2} - 1 \right]}{2a-x \left[ \left( \frac{4a}{K_h c_{\text{H}_2\text{O}}} + 1 \right)^{1/2} + 1 \right]} \quad (17)$$

Here  $c_{\text{H}_2\text{O}}^\circ$  represents the concentration of water present, which is treated as a constant in accordance with the assumption made in obtaining Eq. (8) from Eq. (7).

**Apparatus.** Thermostats at 25 and 35°; three 250-ml, two 125-ml Erlenmeyer flasks; 5-ml pipette; 100-ml pipette; stop watch or electric timer; methyl acetate; 2 liters 0.2 N sodium hydroxide; phenolphthalein indicator; 500 ml of standardized 1 N hydrochloric acid; distilled water; ice.

**Procedure.** The concentration of methyl acetate at a given time is determined through titration of samples with a standard sodium hydroxide solution; the experimental accuracy depends chiefly on the care used in pipetting and titrating. The sodium hydroxide solution used should be prepared by dilution of a *saturated* stock solution to minimize the amount of carbonate present, and hence to reduce the fading of the phenolphthalein end point. It is not necessary, however, to use  $\text{CO}_2$ -free distilled water, because the amount of carbonate introduced in air-saturated water is negligible when titrating with 0.2 N sodium hydroxide.

A test tube containing about 12 ml methyl acetate is set into a thermostat at 25°C. Approximately 250 ml of standardized 1 N hydrochloric

acid is placed in a flask clamped in the thermostat. After thermal equilibrium has been reached (10 or 15 min should suffice), two or three 5-ml aliquots of the acid are titrated with the standard sodium hydroxide solution to determine the exact normality of the sodium hydroxide in terms of the standardized hydrochloric acid. Then 100 ml of acid is transferred to each of two 250-ml flasks clamped in the thermostat and 5 min allowed for the reestablishment of thermal equilibrium. Precisely 5 ml of methyl acetate is next transferred to one of the flasks with a clean, dry pipette; the timing watch is started when the pipette is half emptied. The reaction mixture is shaken to provide thorough mixing.

A 5-ml aliquot is withdrawn from the flask as soon as possible and run into 50 ml of distilled water. This dilution slows down the reaction considerably, but the solution should be titrated at once; the error can be further reduced by chilling the water in an ice bath. The time at which the pipette has been half emptied into the water in the titration flask is recorded, together with the titrant volume. Additional samples are taken at 10-min intervals for an hour; then at 20-min intervals for the next hour and a half. A second determination is started about a quarter hour after the first one to provide a check experiment.

In similar fashion, two runs are made at a temperature of 35°. Because of the higher rate of reaction, three samples are first taken at 5-min intervals, then several at 10-min intervals, and a few at 20-min intervals. It is convenient to start the check determination about a half hour after the first experiment is begun.

**Calculations.** The titrant volume at time  $t$ ,  $V_t$ , measures the number of equivalents of hydrochloric acid and acetic acid then present in the 5-ml reaction-mixture aliquot. Let  $V_T$  represent what the titrant volume per 5-ml aliquot would be if the hydrolysis were complete. Then  $V_T - V_t$  measures the number of equivalents of methyl acetate remaining per 5-ml aliquot at time  $t$ , because one molecule of acetic acid is produced for each molecule of methyl acetate hydrolyzed. The corresponding concentration of methyl acetate in moles per liter is  $N(V_T - V_t)/5$ , where  $N$  is the normality of the sodium hydroxide solution.

If the reaction actually proceeded to completion,  $V_T$  could be measured directly by titration of an aliquot from the equilibrium mixture. An appreciable amount of unhydrolyzed methyl acetate is present at equilibrium, however, so  $V_T$  must be *calculated*.

The volume of the solution initially formed on mixing the 100 ml of 1 N hydrochloric acid with 5 ml of methyl acetate is designated by  $V_s$ . At 25°C,  $V_s$  is 104.6 ml rather than 105 ml because the solution is not ideal. Let the number of milliliters of sodium hydroxide solution required to neutralize a 5-ml aliquot of the original 1 N hydrochloric acid be  $V_x$ . The number of milliliters required to neutralize the hydrochloric acid in

5 ml of the reaction mixture at any time is  $V_x (100/V_s)$ , on the assumption that the total volume of the reaction mixture remains constant as the hydrolysis proceeds.

The weight of the 5 ml of methyl acetate is  $5\rho_2$ , where  $\rho_2$  is the density of methyl acetate (0.9273 g ml<sup>-1</sup> at 25° and 0.9141 at 35°), and the number of moles in this 5-ml sample is  $5\rho_2/M_2$ , where  $M_2$  is the molecular weight, 74.08. The number of moles of methyl acetate initially present in any 5-ml aliquot of the reaction mixture is  $(5\rho_2/M_2)(5/V_s)$ .

Since 1000/ $N$  ml of sodium hydroxide of normality  $N$  is required to titrate the acetic acid produced by the hydrolysis of one mole of methyl acetate,  $(1000/N)(25\rho_2/M_2V_s)$  ml will be required for the titration of the acetic acid produced by the complete hydrolysis of the methyl acetate originally contained in any 5-ml sample of the reaction mixture. The total number of milliliters of sodium hydroxide solution  $V_T$  required to titrate both the hydrochloric acid and the acetic acid produced by the complete hydrolysis of the methyl acetate in a 5-ml sample of the reaction mixture is

$$V_T = V_x \frac{100}{V_s} + \frac{1000}{N} \frac{25\rho_2}{M_2V_s} \quad (18)$$

The value of  $V_T$  is calculated for each experiment by means of Eq. (18). For each run a tabulation is made of the times of observation and the corresponding values of  $V_t$  and  $V_T - V_t$ .

Two graphs are then prepared. For each temperature a plot is made of  $\log (V_T - V_t)$  versus  $t$ ; the points obtained in the two runs can be identified by use of circles and squares. The straight line which is considered to best represent the experimental results is drawn for each set of points, and the rate constants for the two temperatures are calculated from the slopes of the two lines, in accordance with Eq. (2). It is not necessary to calculate the actual concentrations of methyl acetate, since a plot of  $\log (V_T - V_t)$  versus  $t$  has the same slope as a plot of  $\log [(V_T - V_t)(N/5)]$ .

Comparison values of  $k_1$  are calculated at each temperature from several sets of points by use of Eq. (3), to illustrate the dependence of the calculated rate constant on the particular pair of points chosen, and hence emphasize the advantages of the averaging achieved in the graphical method. It should be noted that it is not significant to substitute an explicit averaging of the values of  $k$  obtained from the successive observations by means of Eq. (3).<sup>7</sup>

From the rate constants found for the two temperatures, the heat of activation is calculated by use of Eq. (11).

**Practical Applications.** The rate of a chemical reaction is important in determining the efficiency of many industrial reactions. In organic reactions particularly,

where there is the possibility of several reactions going on simultaneously, the kinetic considerations will often be no less important than the equilibrium relationships.

**Suggestions for Further Work.** The integration of Eq. (15) to give Eqs. (16) and (17) may be checked to illustrate a typical transformation in chemical kinetics. The integral involved is given in mathematical tables.

Instead of estimating by eye the "best" straight-line representation of the plot of  $\log (V_T - V_\infty)$  versus time, the method of least squares may be used (Chap. 18).

Different acid concentrations or other acids may be used;<sup>5</sup> the influence of neutral salts may be studied.<sup>2</sup> Nonaqueous solvents may be used,<sup>3</sup> and methyl acetate may be replaced by other esters,<sup>6</sup> higher temperatures being used if necessary.

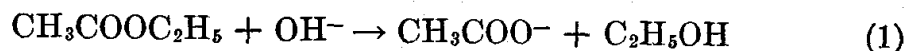
### References

1. Amis, "Kinetics of Chemical Change in Solution," The Macmillan Company, New York (1949).
2. Duboux and deSousa, *Helv. Chim. Acta*, **23**, 1381 (1940).
3. Friedman and Almore, *J. Am. Chem. Soc.*, **63**, 864 (1941).
4. Frost and Pearson, "Kinetics and Mechanisms," John Wiley & Sons, Inc., New York (1961).
5. Griffith and Lewis, *J. Chem. Soc.*, **109**, 67 (1916).
6. Harned and Pfansteil, *J. Am. Chem. Soc.*, **44**, 2193 (1922).
7. Roseveare, *J. Am. Chem. Soc.*, **53**, 1651 (1931).

### 23. REACTION OF ETHYL ACETATE WITH HYDROXYL ION

This experiment illustrates the determination of order and the calculation of the rate constant for a reaction of second order.

**Theory.** The reaction studied in this experiment is



Since the actual reaction mechanism may involve several steps, the equation for the over-all reaction does not necessarily suggest the correct form for the rate law. However, it has been found that reaction (1) does follow the second-order equation (page 130),

$$\frac{dx}{dt} = k_1(a - x)(b - x) \quad (2)$$

where  $t$  = time elapsed from initiation of reaction

$x$  = number of moles per liter reacted at time  $t$

$a$  = initial molar concentration of  $\text{CH}_3\text{COOC}_2\text{H}_5$

$b$  = initial molar concentration of  $\text{OH}^-$

$k_1$  = rate constant for reaction (1)

provided the reaction mixture is not so close to its equilibrium state as to require inclusion in Eq. (2) of a term for the reverse reaction.

Integration of Eq. (2) for the case  $a \neq b$  leads to the result

$$\ln \frac{b(a - x)}{a(b - x)} = k_1(a - b)t \quad (3)$$

For the case  $a = b$  one obtains

$$\frac{x}{a - x} = k_1 a t \quad (4)$$

The temperature dependence of  $k_1$  can be related to  $\Delta S^\ddagger$  and  $\Delta H^\ddagger$  for the formation of the activated complex from reactants (page 131). From measurement of  $k_1$  at two or more temperatures,  $\Delta H^\ddagger$  can be found with the use of Eq. (14) of the preceding experiment.

The experimental problem is to determine  $x$  as a function of  $t$  for a solution in which reaction proceeds at a constant temperature. The reaction mixture undergoes a marked decrease in conductance with time as hydroxyl ion is replaced by acetate ion. The progress of the reaction can therefore be followed by measurement of conductance.

**Apparatus.** Two 250-ml glass-stoppered volumetric flasks; modified 250-ml Erlenmeyer flask; conductance bridge; conductance cell; glass-stoppered weighing bottle; ethyl acetate; standardized NaOH; 25-ml burette; 1-ml graduated pipette; 25-ml pipette; 50-ml pipette; thermostats at 25 and 35°; stop watch or timer.

**Procedure.** Chapter 22 may be consulted for information on the theory and practice of conductance measurements. The bridge selected for the present experiment should be of a type which can be balanced and read rapidly; for this reason, a bridge having a continuously adjustable dial of rather wide range is to be preferred to the decade step-switch type, even at some sacrifice in accuracy. The Freas type of conductance cell shown in Fig. 38 (page 163) is suitable.

As some of the experiments are to be based on Eq. (4), solutions of NaOH and of ethyl acetate of equal normality, nominally 0.02 N, are prepared; 250 ml of each is required.

The ethyl acetate solution must be prepared on the day on which it is to be used, because a slow reaction occurs even in the absence of  $\text{OH}^-$ . A technique which reduces error from volatilization of the ethyl acetate is to weigh the latter in a weighing bottle containing some water (the bottle and water having previously been weighed) and then transfer the sample quantitatively to the volumetric flask for preparation of the final solution. The solution of NaOH of the same normality is prepared by quantitative dilution of standardized stock solution.

Three runs are to be made at 25°C:

$$a = 2b \quad 2a = b \quad a = b$$

and one at 35°C:

$$a = b$$

Each is to be preceded by a measurement of resistance of the cell containing NaOH solution diluted with water in such proportion that the concen-



tration of NaOH is equal to that initially present in the *reaction mixture* for that run. The bridge setting so obtained will be very close to that corresponding to zero time in the subsequent run. A prior knowledge of this setting will facilitate finding the balance point after the reaction has started, and provides also a valuable check on the extrapolation to zero time required for calculation of the rate constant.

It is essential that the reactants be mixed rapidly and the timer started simultaneously. The use of a special mixing flask† (Fig. 32) will facilitate carrying out this operation. Initially, 25 ml of one reactant is placed in the central compartment, and 25 or 50 ml of the other reactant, as the case may be, is placed in the outer compartment. When the flask, solutions, and empty cell have reached thermal equilibrium with the thermostat, the timer is started and the flask is inverted several times to ensure thorough mixing. A small portion of the reaction mixture is poured into the conductance cell, shaken, and discarded. Then the cell is filled to the mark with the reaction mixture and is returned to the thermostat. The cell resistance  $R_t$  is measured at intervals of several minutes over a period of about an hour.

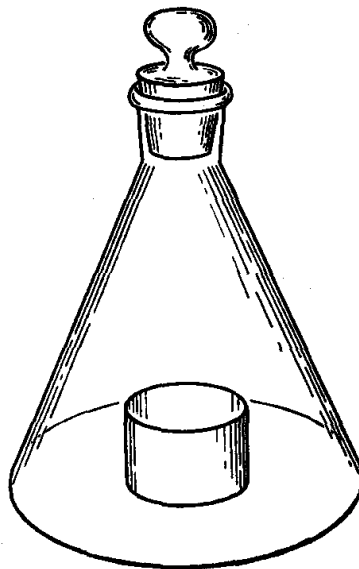


FIG. 32. Special mixing flask.

For runs 1 and 2 it is necessary to determine  $R_e$ , the resistance which the cell would have if the reaction were to reach completion. While  $R_e$  can be found by actual measurement with solutions of NaOH and  $\text{CH}_3\text{COONa}$  made up to the appropriate concentrations, it is more easily obtained by calculation as described below.

**Calculations.** For the calculation of  $x$  from the conductance data, it is assumed that the conductance of the solution,  $\mathcal{G}_t$ , at time  $t$ , obeys the equation

$$\begin{aligned}\mathcal{G}_t &= \frac{1}{1000K} \sum_j c_j l_j \\ &= \frac{1}{1000K} [(b - x)l_{\text{OH}^-} + xl_{\text{CH}_3\text{COO}^-} + bl_{\text{Na}^+}]\end{aligned}\quad (5)$$

where  $l_j$  = equivalent ionic conductance of species  $j$

$c_j$  = concentration of species  $j$  in equivalents/liter

$K$  = cell constant (page 158)

The solutions employed are sufficiently dilute to justify the further

† Available commercially from Norman D. Erway, Oregon, Wisconsin.

assumption that  $l_{\text{OH}^-}$  and  $l_{\text{CH}_3\text{COO}^-}$  are constant even though the concentrations change during the run.

The value of  $x$  ranges from  $x = 0$  to  $x = c$ , where  $c$  is  $a$  or  $b$ , whichever is the smaller. Hence Eq. (5) leads, in either case, to

$$\mathcal{G}_0 - \mathcal{G}_t = \frac{x(l_{\text{OH}^-} - l_{\text{CH}_3\text{COO}^-})}{1000K} \quad (6)$$

$$\mathcal{G}_0 - \mathcal{G}_c = \frac{c(l_{\text{OH}^-} - l_{\text{CH}_3\text{COO}^-})}{1000K} \quad (7)$$

Thus  $x$  is given by

$$\frac{x}{c} = \frac{\mathcal{G}_0 - \mathcal{G}_t}{\mathcal{G}_0 - \mathcal{G}_c} = \frac{(1/R_0) - (1/R_t)}{(1/R_0) - (1/R_c)} \quad (8)$$

By substituting Eq. (8) into (3) and rearranging, one obtains the working equations for the runs with unequal concentrations.

For  $b > a$ ,

$$\frac{k_1(b-a)t}{2.303} + \log \frac{bf}{a} = \log \frac{fR_c - R_t}{R_c - R_t} \quad (9a)$$

where

$$f = \left[ \frac{b}{a} + \left( 1 - \frac{b}{a} \right) \frac{R_c}{R_0} \right]^{-1}$$

For  $a > b$ ,

$$\frac{k_1(a-b)t}{2.303} + \log \frac{ag}{b} = \log \frac{gR_c + R_t}{R_c - R_t} \quad (9b)$$

where

$$g = \left[ \left( \frac{a}{b} - 1 \right) \frac{R_c}{R_0} - \frac{a}{b} \right]^{-1}$$

A plot of resistance versus time is prepared and extrapolated to zero time to obtain the value of  $R_0$ . As a check, the value available from the preliminary measurement on the NaOH solution may be placed on the same graph. The value of  $R_c$ , if not measured directly, is obtained from  $R_0$  and the ratio  $R_c/R_0 = \mathcal{G}_0/\mathcal{G}_c$ , the latter being calculated from Eq. (5), with published values for the ionic conductances at infinite dilution used as approximations to  $l_{\text{Na}^+}$ ,  $l_{\text{OH}^-}$ , and  $l_{\text{CH}_3\text{COO}^-}$ .

Plots of  $\log [(fR_c - R_t)/(R_c - R_t)]$  or  $\log [(gR_c + R_t)/(R_c - R_t)]$  versus  $t$  are prepared. If the data are consistent with Eq. (9), values for the rate constant  $k_1$  may be derived from these graphs.

For the two runs with equal concentration, Eq. (4) is applicable. Introduction of Eq. (8) into (4) leads to

$$\frac{\mathcal{G}_0 - \mathcal{G}_t}{\mathcal{G}_t - \mathcal{G}_c} = k_1at \quad (10)$$

Rearrangement of Eq. (10) then yields

$$g_t = g_c + \frac{1}{k_1 a t} (g_0 - g_t) \quad (11)$$

The rate constant  $k_1$  is calculated from a plot of  $g_t$  versus  $(g_0 - g_t)/t$ .

The enthalpy of activation,  $\Delta H^\ddagger$ , is calculated from the values of  $k_1$  at 25 and 35°C. Two values for  $\Delta S^\ddagger$  may be calculated by assuming  $\kappa = \frac{1}{2}$  and  $\kappa = 1$ , to see the effect on  $\Delta S^\ddagger$  of a given uncertainty in  $\kappa$ .

**Suggestions for Further Work.** As an alternative to the conductimetric method, a procedure which may be used to follow the progress of the reaction is to withdraw samples from the reaction mixture at definite intervals, discharge them into excess standard HCl to arrest the reaction, and back-titrate with NaOH. For best results, CO<sub>2</sub>-free water should be used to prepare the NaOH solutions. In other respects, the procedure followed may be similar to that described above. A suitable equation for graphical analysis of the data for the case  $a \neq b$  is obtained by expressing  $(a - x)$  and  $(b - x)$  as functions of the titration volumes and substituting into Eq. (3); the result of this is

$$\log \left\{ \frac{[V_a(N'/N) + v(a - b)/N] - V_t}{V_a(N'/N) - V_t} \right\} + \log \frac{b}{a} = \frac{k_1(a - b)}{2.303} t \quad (12)$$

where  $V_t$  = volume of NaOH solution required to titrate sample in which reaction was stopped at time  $t$

$V_a$  = volume of HCl into which samples were discharged

$N$  = normality of NaOH solution used for titrations

$N'$  = normality of HCl solution

$v$  = volume of each sample taken

It should be noted that, for a given run, the only time-dependent quantity in the first term on the left side of Eq. (12) is  $V_t$ .

### References

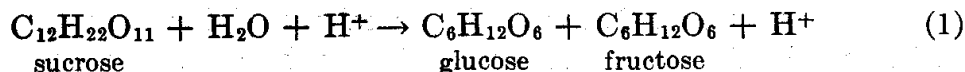
1. Amis, "Kinetics of Chemical Change in Solution," The Macmillan Company, New York (1949).
2. Benson, "Foundations of Chemical Kinetics," McGraw-Hill Book Company, Inc., New York (1960).
3. Frost and Pearson, "Kinetics and Mechanism," John Wiley & Sons, Inc., New York (1961).
4. Laidler, "Chemical Kinetics," McGraw-Hill Book Company, Inc., New York (1950).
5. Moelwyn-Hughes, "Kinetics of Reactions in Solution," Oxford University Press, New York (1947).
6. Tables of Chemical Kinetics, Homogeneous Reactions, *Natl. Bur. Standards (U.S.), Circ.*, 510 (1951). Supplement 1 (1956).
7. Walker, *Proc. Roy. Soc. (London)*, A78, 157 (1906).

## 24. INVERSION OF SUCROSE

This experiment illustrates the use of the polarimeter and the calculation of reaction-rate constants. The catalysis of a hydrolytic reaction by hydrochloric acid and monochloroacetic acid is studied.

**Theory.** The kinetic equations are discussed in Exp. 22.

The inversion of cane sugar can be followed without disturbing the system. The angle of rotation of polarized light passing through the solution is measured with a polarimeter. The reaction is



Sucrose is dextrorotatory, but the resulting mixture of glucose and fructose is slightly levorotatory because the levorotatory fructose has a greater molar rotation than the dextrorotatory glucose. As the sucrose is used up and the glucose-fructose mixture is formed, the angle of rotation to the right (as the observer looks into the polarimeter tube) becomes less and less, and finally the light is rotated to the left. The rotation is determined at the beginning ( $\alpha_0$ ) and at the end of the reaction ( $\alpha_\infty$ ), and the algebraic difference between these two readings is a measure of the original concentration of the sucrose. It is assumed that the reaction goes to completion so that practically no sucrose remains at "infinite" time. At any time  $t$ , a number proportional to the concentration  $c$  of sucrose is obtained from the difference between the final reading (which has a negative value in this case) and the reading of  $\alpha_t$  at the time  $t$ .

The reaction proceeds too slowly to be measured in pure water, but it is catalyzed by hydrogen ions. The water is in such large excess that the reaction follows the equation for a first-order reaction, although two kinds of molecules are involved in the reaction. Thus the reaction-rate constant may be calculated from the equation

$$k = \frac{2.303}{t} \log \frac{\alpha_0 - \alpha_\infty}{\alpha_t - \alpha_\infty} \quad (2)$$

Guggenheim<sup>6</sup> has described a method for calculating the rate constant of a first-order reaction without an infinite time value. This method is useful if the reaction does not go to completion in one laboratory period and has the added advantage that each plotted point does *not* depend upon a *single* observation of the reading at time infinity.

The Guggenheim method may be applied directly if data are taken at equal time intervals. However, the reaction rate changes so rapidly that the procedure calls for shorter time intervals at the beginning. Accordingly, the values of  $\alpha_t$  are plotted as a function of time. The data are then interpolated from the smoothed curves at constant time intervals.

The data are arranged in two sets. For each observation  $c_1$  at time  $t$  in the first set, another observation  $c_2$  is taken at time  $t + \Delta t$ , where  $\Delta t$  is a fixed time interval. If a plot of  $\log (c_1 - c_2)$  versus  $t$  is prepared, the points will fall on a straight line of slope  $-k/2.303$ . The constant time

interval  $\Delta t$  may be taken as approximately one-half the duration of the experiment. If  $\Delta t$  is too small, there will be a large error in  $c_1 - c_2$ .

The equation for this method may be derived as follows. From the integrated form of the first-order-reaction differential equation,

$$c = c_0 e^{-kt} \quad (3)$$

The concentrations  $c_1$  and  $c_2$  at two times differing by  $\Delta t$  are

$$c_1 = c_0 e^{-kt} \quad (4)$$

$$c_2 = c_0 e^{-k(t+\Delta t)} \quad (5)$$

Subtracting,

$$c_1 - c_2 = c_0 e^{-kt} (1 - e^{-k\Delta t}) \quad (6)$$

Taking logarithms,

$$\log (c_1 - c_2) = \frac{-kt}{2.303} + \log [c_0 (1 - e^{-k\Delta t})] \quad (7)$$

Thus the slope of a plot of  $\log (c_1 - c_2)$  versus  $t$  is  $-k/2.303$ .

If instead of measuring concentration directly, some linear function  $X$  of the concentration, say, optical rotation, is measured, an equation of the same form as Eq. (7) applies. For example, if

$$X = ac + b \quad (8)$$

$$c_1 - c_2 = \frac{X_1 - X_2}{a} \quad (9)$$

$$\text{and} \quad \log (X_1 - X_2) = \frac{-kt}{2.303} + \log [ac_0 (1 - e^{-k\Delta t})] \quad (10)$$

The slope is the same as it would be if actual concentration differences had been plotted.

**Apparatus.** Polarimeter (described on page 238); mercury-vapor lamp with filters (Chap. 25) or sodium-vapor lamp; thermostat and circulating pump; two water-jacketed polarimeter tubes; pure sucrose; 100 ml of 4 N hydrochloric acid; 100 ml of 4 N monochloroacetic acid; three 25-ml pipettes.

**Procedure.** Twenty grams of pure cane sugar (sucrose) is dissolved in water (filtered, if necessary, to give a clear solution) and diluted to 100 ml. The sucrose solution, the 4 N hydrochloric acid solution, and the 4 N monochloroacetic acid are placed in the 25° thermostat and allowed to stand a few minutes to come to temperature.

Two jacketed polarimeter tubes, filled with water, are connected in series with the circulating water from a thermostat at 25°. A zero reading is taken with a mercury-vapor lamp and Corning glass filters arranged to transmit only the green light (Chap. 25). A sodium-vapor lamp is equally satisfactory.

Twenty-five milliliters of the sucrose solution is thoroughly mixed with 25 ml of the 4 N monochloroacetic acid solution, and small portions of the solution are used to rinse out one polarimeter tube. The tube is then filled and stoppered. The second polarimeter tube is filled in a similar manner after rinsing, using 25 ml of the sugar solution and 25 ml of the 4 N hydrochloric acid solution. The tubes are filled rapidly, and readings are taken as soon as possible after mixing. The first reading is taken on the hydrochloric acid solution and recorded, and subsequent measurements are recorded about every 10 min for the first hour or so. As the reaction slows down, the observations may be taken less frequently. The observations should extend over a period of 3 hr or more. The reaction goes much more slowly with the monochloroacetic acid, and the readings are taken less frequently. They are taken at convenient intervals of time when the polarimeter is not being used for readings on the solution containing hydrochloric acid.

The final readings ( $\alpha_\infty$ ) are taken after the solutions have stood in a tightly stoppered flask long enough for the reaction to be completed, at least 2 days for the hydrochloric acid and a week for the monochloroacetic acid. A second reading is taken at a later time to be sure that the reaction has been completed. If it is not convenient to obtain the final reading for the monochloroacetic acid, it may be assumed that  $\alpha_\infty$  will be the same as for the hydrochloric acid.

**Calculations.** The concentrations of sucrose in terms of  $\alpha_t - \alpha_\infty$  are plotted against time in minutes. Then the values of  $\log (\alpha_t - \alpha_\infty)$  are plotted against time. The best straight lines are drawn through the points for each reaction. The reaction-rate constants  $k$  are calculated from the slopes of the lines.

In calculating the results of this experiment, at least one set of data is treated by the Guggenheim method for comparison with the usual method. If the reading at infinite time cannot be obtained conveniently, this method may be used exclusively.

**Practical Applications.** These are discussed under Exp. 22.

**Suggestions for Further Work.** Some suggestions for further work are discussed under Exp. 22.

Trichloroacetic acid and sulfuric acid, and other acids, each 4 N, may be used as catalysts. Trichloroacetic acid is about as strongly dissociated as hydrochloric acid. (**Caution:** It is corrosive.) The relative acid strengths of monochloroacetic acid and trichloroacetic acid are to be explained on the basis of molecular structure.

The activation energies may be obtained by running a second set of determinations, using water pumped from a thermostat at 35° or at 15°, and comparing them with those at 25°.

The effect of ionic strength on the rate of this reaction<sup>2</sup> may be investigated. The effect of changing the dielectric constant may be investigated by adding ethanol or dioxane.<sup>1</sup>

Volume changes as measured continuously in a dilatometer may be used to follow the course of a reaction. The hydrolysis of acetal<sup>3,4</sup> is a good example. At 25°, 0.005 M HCl is mixed quickly with enough acetal from a graduated pipette to make the solution 0.15 M with respect to acetal. The solution is transferred immediately to a dilatometer through a tightly fitting stopcock, and the rise of the liquid in the capillary is recorded at frequent intervals. The logarithm (of the final reading minus the reading at time  $t$ ) is plotted against time, and the rate constant is calculated. A second experiment may be carried out with 0.05 M acetic acid instead of the hydrochloric acid.

The method of least squares (Chap. 18) may be used for calculating the best straight line which represents  $\log (\alpha_t - \alpha)$  plotted versus time.

### References

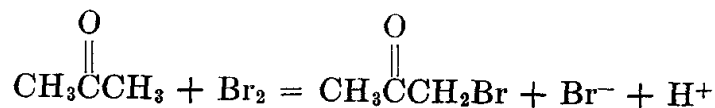
1. Amis and Holmes, *J. Am. Chem. Soc.*, **63**, 2231 (1941).
2. Amis and Jaffe, *J. Chem. Phys.*, **10**, 598 (1942).
3. Brønsted and Wynne-Jones, *Trans. Faraday Soc.*, **25**, 59 (1929).
4. Ciapetta and Kilpatrick, *J. Am. Chem. Soc.*, **70**, 639 (1948).
5. Frost and Pearson, "Kinetics and Mechanism," John Wiley & Sons, Inc., New York (1961).
6. Guggenheim, *Phil. Mag.* (7), **2**, 538 (1926).
7. Pennycuik, *J. Am. Chem. Soc.*, **48**, 6 (1926).
8. Scatchard, *J. Am. Chem. Soc.*, **48**, 2259 (1926).

## 25. BROMINATION OF ACETONE

The form of the rate law for the bromination of acetone using an acid catalyst is determined. This experiment illustrates the fact that the rate law does not necessarily bear any simple relationship to the stoichiometric equation for the reaction.

**Theory.**<sup>6</sup> The rate law for a reaction cannot be predicted from the balanced equation for the reaction. The rate law can only be determined experimentally. From the form of the rate law certain conclusions can be reached about the mechanism of the reaction.

The stoichiometric equation for the bromination of acetone is



The reaction rate increases with the concentration of  $\text{H}^+$  in acidic solution or with the concentration of  $\text{OH}^-$  in basic solution. The balanced equation for the reaction occurring in acidic solution involves hydrogen ion as a product, and one would anticipate, therefore, an increasing reaction rate in the course of an experiment carried out in unbuffered solutions.

The rate of halogenation of acetone is independent of the concentration of halogen, except at very high acidities.<sup>10</sup> The rates of reaction with





This is in accord with the observation that the over-all reaction is first-order in ketone and acid but independent of the concentration of halogen. It can be seen that in general the apparent second-order rate constant is made up of a combination of  $k_1$  and the equilibrium constant  $K$  for the formation of ion I.

A great deal of research has been carried out on this particular reaction, and the above mechanism can be extended to include racemization, deuterium exchange,<sup>8</sup> and catalysis by bases.<sup>1</sup> The over-all reaction does not stop with the monobromo-acetone, but it is not necessary to consider the subsequent reactions if only *initial* reaction rates are studied.

**Apparatus.** Bromine, water, acetone, standard hydrochloric acid (1 M or 2 M); spectrophotometer; pipettes; volumetric flasks.

**Procedure.** Since bromine absorbs strongly at the blue end of the visible spectrum, this reaction may be studied conveniently with a spectrophotometer such as that described in Exp. 16. The absorbancy indices of  $\text{Br}_2$  dissolved in distilled water are  $160 \text{ M}^{-1} \text{ cm}^{-1}$  at  $400 \text{ m}\mu$ ,  $100 \text{ M}^{-1} \text{ cm}^{-1}$  at  $450 \text{ m}\mu$ ,  $30 \text{ M}^{-1} \text{ cm}^{-1}$  at  $500 \text{ m}\mu$ , and  $8 \text{ M}^{-1} \text{ cm}^{-1}$  at  $550 \text{ m}\mu$ . The solubility of  $\text{Br}_2$  in water is about 0.2 M at  $25^\circ$ , and it is more convenient to use water saturated with  $\text{Br}_2$  in preparing solutions than to use pure liquid bromine. The concentration of the stock bromine solution is determined, using the absorbancy indices given above. In accurate work it is necessary to determine cell corrections by intercomparing the various cells filled with solvent. In order to obtain the greatest percentage accuracy in the determination of concentration, the absorbancy should be in the range of about 0.2 to 0.7 (per cent transmission of about 60 to 20). The spectrophotometer cells and all bromine solutions should be kept covered.

Hydrochloric acid is a convenient catalyst, and a suitable concentration range is 0.05 to 0.5 M. It is desired to determine the initial rate law, i.e., the order of the reaction with respect to acetone, hydrogen ion, and bromine, and the rate constant. In order to avoid complications, only initial velocities are used. A series of experiments is designed to determine the concentration effects. The acetone concentration may be varied in the range 0.1 to 2 M. The bromine concentration may be varied in the range 0.001 to 0.01 M. Some of the higher concentrations should be run first because the initial velocities can be determined in a shorter time. Using a cell holder for four cells, three kinetic experiments can be run simultaneously. In order to obtain accurate results, the spectrophotometer should be equipped with a thermostating arrangement so that the reacting solutions can be held at the desired constant temperature. In the absence of this equipment, the temperatures of the solutions should be measured at the beginning and end of the experiment.

This reaction can also be studied titrimetrically. The reaction is stopped by pipetting aliquots into sodium acetate solution to raise the pH. Potassium iodide is added, and the  $I_2$  formed is titrated with sodium thiosulfate.

**Calculations.** The reaction rates in moles per liter of  $Br_2$  reacting per second are calculated for each reaction mixture, and the approximate uncertainty is estimated. It is the initial velocity which is desired in each case. Plots of initial velocity *versus* (acetone),  $(H^+)$ , and  $(Br_2)$  are prepared to determine the order with respect to each of these substances. After the form of the rate law has been determined, the best value of the rate constant is calculated.

**Suggestions for Further Work.** The reaction of acetone with iodine may be studied. Because of the low solubility of iodine in water, a 0.1 M KI solution may be used as solvent.

The catalysis of the reaction by acetate-acetic acid buffers may be studied.<sup>3,5</sup> Since the acetate ion is also a catalyst, there will be terms in the rate law for both acetate ion and acetic acid. There is also a term proportional to the product of these concentrations. The reaction is subject to general acid-base catalysis.<sup>4</sup>

The catalysis of the reaction by bases such as pyridine or hydroxyl ion may also be studied.<sup>1</sup>

#### References

1. Bartlett, *J. Am. Chem. Soc.*, **56**, 967 (1934).
2. Bartlett and Stauffer, *J. Am. Chem. Soc.*, **57**, 2580 (1935).
3. Bell and Jones, *J. Chem. Soc.*, **88** (1953).
4. Dawson, Haskins, and Smith, *J. Chem. Soc.*, 1884 (1929).
5. Dawson and Spivey, *J. Chem. Soc.*, **2180** (1930).
6. Hammett, "Physical Organic Chemistry," McGraw-Hill Book Company, Inc., New York (1940).
7. Hsui and Wilson, *J. Chem. Soc.*, **623** (1936).
8. Hsui, Ingold, and Wilson, *J. Chem. Soc.*, **78** (1938).
9. Ingold and Wilson, *J. Chem. Soc.*, **773** (1934).
10. Zucker and Hammett, *J. Am. Chem. Soc.*, **61**, 2791 (1939).

## *Irreversible Processes in Solution*

### 26. VISCOSITY OF LIQUIDS

Liquid viscosities are measured in this experiment by the capillary-flow method and by the falling-ball method.

**Theory.** The flow of a fluid is said to be *laminar* if points fixed in the fluid move smoothly in layers, one layer (lamina) sliding relative to another. The elementary process involved in laminar flow is pictured in Fig. 33, which represents a small region of the fluid. The  $x$  axis is

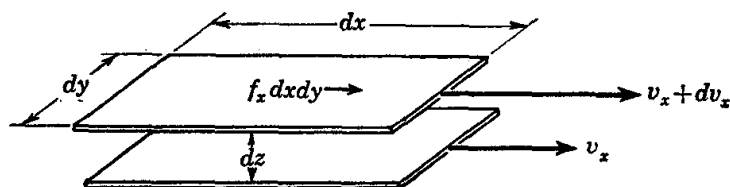


FIG. 33. Diagram illustrating the quantities involved in Eq. (1), defining the coefficient of viscosity. Acting on the plane of area  $dxdy$  is the shearing force  $f_x dxdy$ , which maintains the velocity gradient  $dv_x/dz$ . The shearing force per unit area,  $f_x$ , is proportional to  $dv_x/dz$ .

chosen to lie in the local direction of flow, the  $z$  axis perpendicular to the laminae;  $v_x$  represents the velocity of fluid in the  $x$  direction. Viscous effects come into play if an element of the fluid is caused to change its shape as it moves. The coefficient of viscosity,  $\eta$ , is defined by the equation

$$f_x = \eta \left( \frac{\partial v_x}{\partial z} \right) \quad (1)$$

where  $f_x$  is the shearing force per unit area exerted in the direction of flow on the element of fluid between two planes at the plane of larger  $z$  (an equal and opposite shearing force acts on the opposite face), and  $(\partial v_x / \partial z)$  is the velocity gradient in the  $z$  direction. Equation (1) simply expresses the proportionality between the velocity gradient and the shearing force which produces it. The coefficient  $\eta$  depends on temperature, pressure,

and composition. A fluid is said to be a *Newtonian fluid* if, in laminar flow,  $\eta$  is a constant independent of the velocity gradient; common liquids under ordinary circumstances behave in this way. The cgs unit for viscosity ( $\text{g cm}^{-1} \text{sec}^{-1}$ ) is called the *poise*.

A very satisfactory method for determining  $\eta$  consists of measuring the volume rate of flow of the fluid through a long cylindrical tube of circular cross section. The required equation is obtained by application of Eq. (1). To make the problem tractable, certain simplifying assumptions are introduced:

1. The fluid is assumed to be a Newtonian, incompressible fluid.
2. It is assumed that the flow is laminar, with flow lines parallel to the walls. Hence the laminae consist of concentric cylinders coaxial with the tube.
3. The layer next to the wall is assumed to stick to the wall, so that its velocity is zero.
4. The flow is assumed to be steady, in the sense that the velocity of the fluid at any fixed point in the tube is constant in time.

Let  $\Delta P$  be the pressure increment (in the direction of flow) between the ends of the tube of length  $l$  when the fluid flows at a certain constant rate, and let  $\Delta P_0$  be the pressure increment which would exist between the same two points if the fluid were not moving. Then the driving pressure  $\mathcal{P}$  is defined by

$$\mathcal{P} = \Delta P_0 - \Delta P \quad (2)$$

and may be thought of as the additional pressure drop (beyond the hydrostatic value) which exists while the fluid is flowing. In the case of steady-state flow through a long cylindrical tube, the fluid is not accelerated and the added pressure drop  $\mathcal{P}$  is attributable entirely to the shearing work which must be done on the viscous fluid to maintain a steady rate of flow. The shearing force acting on a layer of fluid between two concentric cylinders of radii  $s$  and  $s + ds$ , respectively, is  $\pi s^2 \mathcal{P}$ . The force in the direction of flow acts on the surface of smaller radius  $s$ . From Eq. (1), with  $dz = -ds$ ,

$$\frac{\pi s^2 \mathcal{P}}{2\pi s l} = -\eta \left( \frac{\partial v}{\partial s} \right) \quad (3)$$

where  $v$  is the velocity of the fluid in the layer of radius  $s$ . The velocity is considered to be positive in the direction of flow. Separating variables  $s$  and  $v$  and integrating from the wall ( $s = r, v = 0$ ) to an arbitrary radius, one gets

$$\int_0^v dv = -\frac{\mathcal{P}}{2\eta l} \int_r^s s ds \quad (4)$$

$$v = \frac{\mathcal{P}}{4\eta l} (r^2 - s^2) \quad (5)$$

giving  $v$  at radius  $s$ . Thus the velocity profile is parabolic. The volume of fluid which flows past any cross section per second ( $dV/dt$ ) is found by integration over the cross section:

$$\frac{dV}{dt} = \int_0^r 2\pi s v ds = \frac{\pi \mathcal{P} r^4}{8\eta l} \quad (6)$$

Provided  $\mathcal{P}$  is constant in time, the total volume  $V$  which flows past any cross section in time  $t$  is

$$V = \frac{\pi \mathcal{P} r^4 t}{8\eta l} \quad (7)$$

This is known as the Hagen-Poiseuille equation.

In the Ostwald viscometer (Fig. 34), the liquid flows through a vertical capillary tube from a reservoir of well-defined, fixed volume at the top into a second reservoir at the lower end. The driving pressure  $\mathcal{P}$ , defined by Eq. (2) with increments taken between the reservoir surfaces, is  $\rho gh$ , where  $h$  is the difference in height of the surfaces of the two reservoirs,  $\rho$  is the density of the fluid, and  $g$  is the acceleration of gravity; this is so because  $\Delta P = 0$ , both reservoirs being under atmospheric pressure, while  $\Delta P_0 = \rho gh$ , the latter being the pressure difference which would have to be applied to maintain hydrostatic equilibrium. Thus Eq. (7) solved for  $\eta$  becomes

$$\eta = \frac{\pi r^4 g h}{8 V l} \rho t \quad (8)$$

To avoid the complications implicit in direct and accurate measurement of the various apparatus dimensions appearing in Eq. (8), and the further problem of a small variation in  $h$  during each run, it is common to assume that the equation

$$\eta = A \rho t \quad (9)$$

holds where  $A$  is a constant for a given viscometer. Since  $l$  is the capillary length, Eq. (8) neglects the driving pressure drops in the reservoirs.

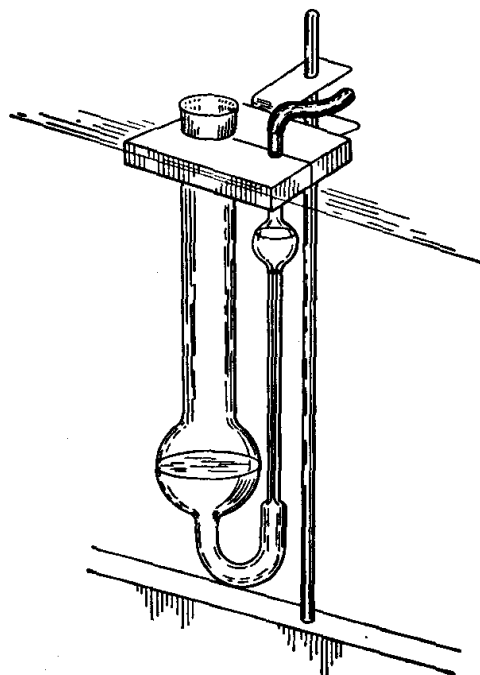


FIG. 34. Ostwald viscometer.

The assumption that the flow is laminar can be checked by calculating the Reynolds number  $\mathcal{R}$ , which in general is defined by

$$\mathcal{R} = \frac{v\rho a}{\eta} \quad (10)$$

where  $v$  = velocity of fluid

$a$  = characteristic dimension of flow system

For the capillary-flow case,  $v$  may be taken as the mean fluid velocity  $\langle v \rangle$  in the tube,

$$\langle v \rangle = \frac{1}{\pi r^2} \int_0^r (v) 2\pi s \, ds = \frac{\mathcal{O}r^2}{8\eta l} = \frac{V}{\pi r^2 t} \quad (11)$$

and  $a$  as the tube diameter. The flow may safely be assumed to be laminar for  $\mathcal{R} < 2000$ ; the onset of turbulence usually occurs somewhere within the range 2000 to 10,000.

Provided the flow is laminar, the various assumptions used in obtaining Eq. (8) hold quite well in the interior of the capillary tube, but not at the ends. The most important end effect is that which arises from the fact that work must be done on the fluid to accelerate it as it approaches and enters the capillary tube from the entrance reservoir. The driving pressure  $\mathcal{O}$  properly includes not only the Hagen-Poiseuille pressure drop

$$\mathcal{O}' = \frac{8Vl\eta}{\pi r^4 t} \quad (12)$$

but in addition a term from the work done in accelerating the fluid. If viscous effects are neglected in calculating the latter term, one may use the Bernoulli equation<sup>7</sup>

$$P + \rho gh + \frac{1}{2}\rho v^2 = \text{constant along a streamline} \quad (13)$$

which expresses the principle that the work done on an element of volume of an incompressible fluid moving along a streamline equals the total increase in potential and kinetic energy. (The internal energy is assumed to be constant.) Associated with this increase in fluid velocity is a pressure drop

$$\Delta P = -\Delta \frac{1}{2}\rho \langle v^2 \rangle_m \quad (14)$$

where  $\langle v^2 \rangle_m$  is the mass-averaged value of  $v^2$  (over a cross section), which is zero initially and has the value

$$\langle v^2 \rangle_m = \frac{1}{\rho(dV/dt)} \int_{s=0}^r (v^2) 2\pi s v \rho \, ds = \frac{1}{2} \left( \frac{\mathcal{O}'}{4\eta l} \right)^2 r^4 = 2 \left( \frac{V}{\pi r^2 t} \right)^2 \quad (15)$$

within the capillary beyond the point at which the velocity profile of

Eq. (5) has become established. The increment  $\Delta \frac{1}{2} \rho \langle v^2 \rangle_m$  must be added to the Hagen-Poiseuille pressure drop to give the total driving pressure.

$$\mathcal{P} = \frac{8Vl\eta}{\pi r^4 t} + \frac{1}{2} \rho \langle v^2 \rangle_m \quad (16)$$

It may be asked whether a similar application of the Bernoulli theorem should not be made at the exit reservoir; if it were, the deceleration of the fluid would require a pressure increase exactly canceling the decrease of Eq. (14). The answer is that the Bernoulli pressure rise at the exit is neglected, it being assumed that the kinetic energy of the fluid issuing into the exit reservoir is dissipated entirely through viscous effects in the reservoir and passes by heat flow into the surroundings, instead of producing a pressure rise and thereby being transferred to the environment through performance of work. The assumption that the Bernoulli pressure change is the dominant effect at the entrance to the capillary but negligible at the exit is not unreasonable, because the flow scheme is quite different in the two reservoirs, as one may easily verify by adding a dye to the fluid in one reservoir and then observing the flow.<sup>4</sup> While there is no rigorous basis for this assumption, the essential correctness of the kinetic-energy term, as the last term in Eq. (16) is called, is well established experimentally for the usual conditions of measurement.<sup>5, 11-13</sup>

The equation for  $\eta$  with the kinetic-energy correction included,

$$\eta = \frac{\pi \mathcal{P} r^4 t}{8Vl} - \frac{\rho V}{8\pi l t} \quad (17)$$

is obtained by solving Eq. (16) for  $\eta$  and using Eq. (15) to eliminate  $\langle v^2 \rangle_m$ . Applied to the Ostwald viscometer, for which  $\mathcal{P}$  equals  $\rho gh$ , Eq. (17) becomes

$$\eta = A \rho t - B(\rho/t) \quad (18)$$

where

$$A = \frac{\pi r^4 gh}{8Vl} \quad B = \frac{V}{8\pi l} \quad (19)$$

The apparatus constant  $B$  can be estimated reasonably well from the viscometer dimensions, or it can be determined empirically, along with  $A$ , from measured flow times and densities for two or more liquids of accurately known viscosity.<sup>†</sup>

† Additional end effects for which corrections are sometimes made arise from the viscous pressure drop in the reservoirs and from the fact that the viscous pressure drop in the capillary tube near the entrance, where the velocity profile is not yet parabolic, is slightly larger than the Hagen-Poiseuille value. Corrections for these effects are made by replacing  $l$  in both Eqs. (19) by  $l' \cong l + 0.5r$  and inserting a numerical factor  $m \cong 1.1$  in the numerator of the expression for  $B$ . These corrections are not accurate, but will serve as a useful means for gauging the general magnitude of these effects. The numerical constants are often found empirically.<sup>12, 13</sup>

The capillary-flow method has been found useful, with appropriate choice of capillary dimensions, for fluids of viscosity up to 100 poises. For viscosities in a higher range, say, 10 to 10,000 poises, the falling-ball method is generally suitable.

If a spherical body is caused to move at a sufficiently low velocity  $v$  through a fluid, laminar flow takes place. For the case of an incompressible, unbounded Newtonian fluid with viscosity coefficient  $\eta$ , the retarding force  $f$  exerted on the body at low velocities is given by Stokes' equation,

$$f = 6\pi r\eta v \quad (20)$$

where  $r$  is the radius of the sphere. If the body falls freely through the fluid, the velocity asymptotically approaches that velocity (the *terminal velocity*) at which the sphere suffers no further acceleration because the retarding force exerted by the fluid exactly cancels the gravitational force. With allowance for buoyancy, the equation for this balance of forces is

$$\frac{4}{3}\pi r^3(\rho - \rho_0)g = 6\pi r\eta v \quad (21)$$

where  $\rho$  = density of falling body

$\rho_0$  = density of fluid

$g$  = acceleration of gravity

The falling-ball viscometer (Fig. 35, page 155) consists of a cylindrical tube filled with the fluid of unknown viscosity. A ball of suitable density and radius is allowed to fall along the axis of the tube. The times at which the ball passes regularly spaced horizontal calibration marks are recorded. In the present experiment, the apparatus is constructed from a graduated cylinder, and steel bearing balls are used.

The hydrodynamic equation for this system is complicated by the presence of the walls and by the fact that the velocity may be large enough for Stokes' equation to fail even though the flow remains laminar. A satisfactory solution, in the form of a power series expansion, has been derived theoretically by Faxen and tested experimentally by Bacon.<sup>1</sup> The equation for  $\eta$ , with only the leading terms included explicitly here, is

$$\eta = \frac{2gr^2(\rho - \rho_0)}{9v} \left[ 1 - 2.104 \left( \frac{r}{R} \right) + 2.09 \left( \frac{r}{R} \right)^3 + \dots \right] \quad (22)$$

where  $R$  is the radius of the cylinder. The reason for the existence of the wall effect is that the boundary conditions are different for the cylinder from those for an unbounded medium. A layer of fluid adjacent to the surface of the ball moves with the ball, and fluid farther from the surface moves in such a fashion as to transport fluid upward, from the region ahead of the ball, to its wake. In an unbounded medium, this flow occurs to an appreciable extent throughout a region extending outward from the



ball a distance of many times the ball diameter. The presence of the cylinder walls modifies the flow, because the fluid at the walls is at rest.

The most important terms in the Faxen equation after those given in Eq. (22) involve the Reynolds number. For Eq. (22) to be accurate, with these terms neglected, the condition

$$R^2 \ll \frac{r}{R} \quad (23)$$

must be met, where now

$$R = \frac{2v\rho r}{\eta} \quad (24)$$

The molecular theory of viscosity of liquids has not been developed to the point where accurate predictions can be made for liquids of polyatomic molecules. However, the Eyring theory of absolute reaction rates<sup>6</sup> provides a useful basis for correlation of viscosity data and certainly represents a valuable first step toward understanding the molecular processes involved. Applied to the case of viscous flow, the Eyring equation is

$$\eta = \left( \frac{hN_0}{V} \right) e^{\Delta G^\ddagger/RT} \quad (25)$$

where  $h$  = Planck's constant

$N_0$  = Avogadro's number

$V$  = molar volume =  $M/\rho$

$M$  = molecular weight

$\Delta G^\ddagger$  = standard free energy of activation for viscous flow

The exponential dependence on  $T$  is typical for processes which require activation. The activation process to which  $\Delta G^\ddagger$  refers cannot be precisely described, but in general terms it corresponds to the passage of the system into some relatively unfavorable configuration, from which it can then easily go on to the final state of the molecular-flow process. For example, in normal liquids, the activation step may be the creation within the body of the liquid of a vacancy or hole into which an adjacent molecule can move; for associated liquids, it might be the breaking of enough intermolecular bonds to permit a molecule to move into an available vacancy.<sup>10</sup>

The temperature dependence of  $\eta$  implied by Eq. (25) is found by making use of the rigorously exact equation

$$\left[ \frac{\partial(\Delta G^\ddagger/T)}{\partial T} \right]_P = - \frac{\Delta H^\ddagger}{T^2} \quad (26)$$

where  $\Delta H^\ddagger$ , the enthalpy change for the activation process, is related to  $\Delta G^\ddagger$  through

$$\Delta G^\ddagger = \Delta H^\ddagger - T\Delta S^\ddagger \quad (27)$$

$\Delta S^\ddagger$  being the entropy of activation for viscous flow. The result is

$$\left[ \frac{\partial \ln (\eta/\rho)}{\partial (1/T)} \right]_P = \frac{\Delta H^\ddagger}{R} \quad (28)$$

where the temperature dependence of  $V$  has been acknowledged by replacing  $V$  by  $(M/\rho)$  and transferring  $\rho$  to the left side before differentiating. Thus, from values of  $\eta$  and  $\rho$  at several temperatures, one may calculate  $\Delta G^\ddagger$ ,  $\Delta H^\ddagger$ , and  $\Delta S^\ddagger$ .

Equation (25) has been generalized for solutions. Of particular interest are those cases in which mixtures of a pair of liquids show a maximum or minimum in viscosity as a function of mole fraction. Vapor-pressure data for such pairs often show very marked departures from Raoult's law. An equation which ties together these two types of anomalous behavior has been given by Kincaid, Eyring, and Stearn.<sup>6,9</sup>

**Apparatus.** Ostwald viscometer; stop watch or timer; thermostat with glass window; 10-ml graduated pipette; density balance or other means for determining densities; acetone, chloroform, or other liquids.

Falling-ball viscometer filled with fluid† of known density; precision chrome-steel bearing balls of several diameters (e.g.,  $\frac{1}{16}$  in.,  $\frac{5}{64}$  in.,  $\frac{3}{32}$  in.); two timers; switching circuit; micrometer; scale for measurement of fluid height and calibration spacing; forceps; magnet for recovery of balls; hypodermic syringe.

**Procedure.** The Ostwald viscometer is shown in Fig. 34. Since the glassware itself is very easily broken, the method of clamping shown is highly recommended.

The value of the constant  $B$  is to be calculated from Eq. (19). A value for  $V$  sufficiently accurate for the calculation of  $B$  may be obtained with the aid of a hypodermic syringe. The length  $l$  may be measured directly with a steel scale. Then the constant  $A$  is to be determined from measurement of the time of flow with water.

After the viscometer has been thoroughly cleaned with *hot* sulfuric acid-potassium dichromate solution, it is thoroughly rinsed by drawing water through it, followed by acetone, and finally is dried by aspirating *clean* air through it. Compressed air is not used because foreign particles or traces of oil may cause serious errors. The viscometer is clamped vertically in the thermostat, and a specified quantity of sample is added from a pipette. The volume of sample used should be such that the liquid surface in the lower reservoir is in the widest part in order that the change in  $h$  during a run will be minimized. The same volume of sample is used for all samples. A dust-free rubber tube is attached to the smaller tube, and by means of a rubber suction bulb the liquid is drawn up into the enlarged bulb and above the upper mark.

† Fluid materials having viscosities in the appropriate range are available from Dow Chemical Company, Midland, Michigan.

The liquid is then allowed to flow down through the capillary. The timer is started when the meniscus passes the upper mark and is stopped when it passes the lower mark. If several check determinations on the time of flow do not agree closely, the tube should be cleaned again.

The viscosities of acetone, chloroform, and of about four binary mixtures of acetone and chloroform (about equally spaced on a mole-fraction basis) are measured. The solutions may conveniently be made up by volumetric techniques, since density data for the pure liquids may later be used to calculate the mole fractions.

For Eq. (9) or (18) to be used, the density and the time of flow must be measured at the same temperature. The density measurements are most easily made with a density balance, although a pycnometer method (page 90) may be used.

Next, the viscosity of a pure liquid such as *n*-butyl alcohol is determined at a number of temperatures over the range 0 to 45°C in order to find the activation energy for viscous flow. The required density data may be taken from published tables. For the time of flow measurements, it is important to have a thermostat which maintains the temperature reasonably steady over a sufficiently long period for the sample to reach thermal equilibrium and for several flow determinations to be made. Measurements at 0°C may be made with a large unsilvered Dewar flask containing an ice-water bath. The Dewar should be surrounded with a sheet of heavy celluloid or other suitably strong and transparent material to provide protection against the danger of flying glass from an implosion. It is imperative that glasses or safety goggles, preferably of a type having side shields, be worn while this work is being done.

Finally, the viscosity of a polymer liquid is measured by means of the falling-ball viscometer, shown in Fig. 35.† The outermost cylinder is a section of 60-mm Pyrex tubing which is placed around the viscometer to protect it from air drafts. The inner cylinder, which holds the sample, is a standard 100-ml graduated cylinder, having a diameter of roughly 30 mm. The graduated cylinder is mounted perpendicular to the base plate, and a small bubble level fastened to the latter is used to facilitate getting the cylinder vertical. A thermometer (not shown) is taped to the outside wall of the inner cylinder.

The cylinder must be filled well in advance and allowed to stand for hours (or days!) until the bubbles have all escaped. A satisfactory

† The glass parts for a viscometer of this type are available from Norman D. Erway, Oregon, Wisconsin.

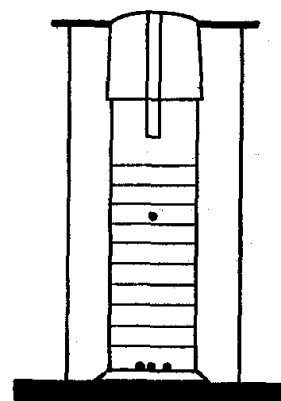


FIG. 35. Falling-ball viscometer.

procedure for determining the density of the fluid is to calibrate the cylinder before filling, weigh the cylinder before and after filling, and note the level of the fluid after it has become clear of bubbles and has reached the temperature at which the viscosity is to be measured.

The apparatus must be vertical, so that the balls travel along the axis of the tube. Adequate time should be allowed for the fluid to come to a

uniform temperature if the ambient temperature is different from that at which the unit was stored.

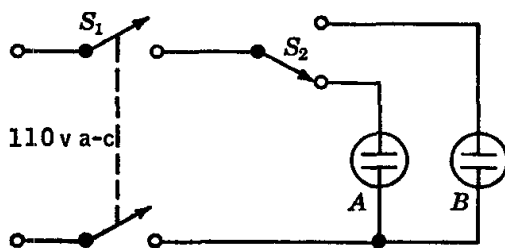


FIG. 36. Switching circuit for falling-ball viscometer. The two electric timers are plugged into the outlets A and B.

Three steel balls of each size to be used are rinsed in benzene, dried on a towel, and not subsequently handled with the fingers. The average weight per ball is found by weighing a set of several of the same size. The diameters of the balls may be taken from the manufacturer's speci-

fication or measured carefully with a micrometer, and the densities calculated later from the measured weights. After a practice run, data are obtained for at least two balls of each size.

Since the 10-ml calibration lines of the graduated cylinder run the full circumference, parallax error may be avoided in determining the times at which the ball passes these lines. With the timer switches in the positions shown in Fig. 36, and both timers set to zero, a ball is dropped through the aligning tube at the top. As it crosses the first line, one timer is started by closing switch  $S_1$ . As the ball crosses each subsequent line, switch  $S_2$  is thrown to stop one timer and start the other. After each such change, the reading of the stopped timer is recorded, and this timer is then reset to zero. At the end of the run, switch  $S_1$  is opened. The temperature of the fluid is noted. The average distance between calibration lines is measured. The mean cylinder radius may be calculated from the spacing of calibration lines on the assumption that the column has a uniform circular cross section.

After a number of balls have been accumulated, they may be drawn up along the wall by the action of a small magnet.

**Calculations.** The viscosities of the solutions are calculated and plotted against mole fraction. Viscosity and density data for water are available in a number of standard references.

Values of  $\Delta G^\ddagger$ ,  $\Delta H^\ddagger$ , and  $\Delta S^\ddagger$  are calculated from the data for *n*-butanol with the aid of a plot of  $\log (\eta/\rho)$  versus  $1/T$ .

The falling-ball data should be examined carefully to determine the average velocity of fall in that region of the tube in which the velocity is sensibly uniform. The viscosity may be calculated from this average.

Comparison of results for different ball diameters provides a valuable check on the accuracy of the wall correction.

**Practical Applications.** Studies of the viscosities of high polymers and of solutions of macromolecules have provided interesting information as to the structure and motions of these molecules. Non-Newtonian behavior is not uncommon among these systems.

**Suggestions for Further Work.** The equation of Kincaid, Eyring, and Stearn<sup>6,9</sup> for nonideal mixtures is not difficult to use. In addition to the viscosity and density data for the two pure liquids and their mixtures, the only additional quantities required are the excess free energies of mixing (i.e., above the ideal values). These are easily calculated from vapor-pressure data<sup>8</sup> for the mixtures, provided it is assumed that nonideality in the vapor can be neglected.

Several liquids of widely different viscosity may be used to verify that Eq. (18) fits the data satisfactorily and to determine the constants  $A$  and  $B$  empirically. Obviously, the data must be of good accuracy, and reasonable care must be taken to obtain samples of good purity. A graphical procedure should be used for analyzing these data.

#### References

1. Bacon, *J. Franklin Inst.*, **221**, 251 (1936).
2. Bird, Stewart, and Lightfoot, "Transport Phenomena," John Wiley & Sons, Inc., New York (1960).
3. Chu, Wang, Levy, and Paul, "Vapor-Liquid Equilibrium Data," J. W. Edwards, Publisher, Inc., Ann Arbor, Mich. (1956).
4. Dorsey, *Phys. Rev.*, **28**, 833 (1926).
5. Erk, "Zahigkeitsmessungen," in "Handbuch der Experimentalphysik," Vol. 4, Pt. 4, pp. 465-468, Akademie-Verlags. G.m.b.H., Berlin (1932).
6. Glasstone, Laidler, and Eyring, "The Theory of Rate Processes," pp. 480-516, McGraw-Hill Book Company, Inc., New York (1941).
7. Halliday and Resnick, "Physics," Combined Ed., pp. 376-378, John Wiley & Sons, Inc., New York (1960).
8. International Critical Tables, McGraw-Hill Book Company, Inc., New York (1928).
9. Kincaid, Eyring, and Stearn, *Chem. Revs.*, **28**, 301 (1941).
10. Powell, Roseveare, and Eyring, *Ind. Eng. Chem.*, **33**, 430 (1941).
11. Schiller, "Stromung in Rohren," in "Handbuch der Experimentalphysik," Vol. 4, Pt. 4, pp. 39-57, Akademie-Verlags. G.m.b.H., Berlin (1932).
12. Swindells in Weissberger (ed.): "Technique of Organic Chemistry," 3d ed., Vol. I, Pt. I, Chap. 12, Interscience Publishers, Inc., New York (1959).
13. Swindells, Coe, and Godfrey, *J. Research, Natl. Bur. Standards (U.S.)*, **48**, 1 (1952).

#### 27. CONDUCTANCE BEHAVIOR OF WEAK AND STRONG ELECTROLYTES

In this experiment practice is obtained in the measurement of the electrical conductance of solutions. The influence of concentration on the conductance of weak and strong electrolytes is studied, and the apparent dissociation constant of a weak acid is determined.

**Theory.**<sup>4,6,7</sup> The specific resistance of an electrolytic solution is defined as the resistance in ohms of a column of the solution 1 cm long and 1 cm<sup>2</sup> in cross section. The specific conductance  $\kappa$  is the reciprocal of the specific resistance and could be evaluated from a resistance measurement with a cell having a volume of 1 cm<sup>3</sup> and constructed with plane-parallel electrodes 1 cm<sup>2</sup> in area and 1 cm apart. The usual conductance cell does not satisfy these requirements, but it is possible to determine the value of a constant and characteristic factor  $k$  called the *cell constant*, such that

$$k = \kappa R \quad (1)$$

where  $R$  is the resistance of the actual cell containing an electrolytic solution of specific conductance  $\kappa$ . The numerical value of  $k$  for a particular cell is determined experimentally by use of a standard solution of known specific conductance. For this purpose a solution of potassium chloride of accurately known specific conductance<sup>3</sup> is used; for 0.02 N KCl, for example, the specific conductance  $\kappa$  is 0.002768 ohm<sup>-1</sup> cm<sup>-1</sup> at 25°C. The observed resistance  $R$  for the potassium chloride solution is multiplied by the known specific conductance to obtain the cell constant. The specific conductance of any solution may be then calculated by using the same equation and substituting the known value of the cell constant and the observed resistance.

The equivalent conductance  $\Lambda$ , which is the conductance in reciprocal ohms of a solution containing 1 g-equiv of solute when placed between plane-parallel electrodes of suitable area 1 cm apart, is calculated from the relation

$$\Lambda = \kappa V \quad (2)$$

where  $V$  is the volume of solution in cubic centimeters which contains 1 g-equiv weight of solute.

In general, pure solvents are poor conductors of electricity, but when acids, bases, or salts are dissolved in them, the conductance is greatly increased.

The conductance of these solutions is the result of the movement of ions through the solution to the electrodes. When two electrodes of an electrical circuit are placed in a solution, the cations (+) are attracted to the negative pole (cathode), and the anions (−) are attracted to the positive pole (anode). Changes in the equivalent conductance of an electrolytic solution due to variations in concentration may result from changes both in the number and in the mobility of the ions present.

The difference in behavior between a weak and a strong electrolyte becomes evident when the equivalent conductances of their solutions are plotted as a function of the concentration, especially in the dilute region. The equivalent conductance for the strong electrolyte approaches a

definite value at infinite dilution, but that of the weak electrolyte cannot be extrapolated to a definite value because the slope of the curve is still changing appreciably at the lowest concentrations at which accurate experimental measurements can be made. When the electrolyte is weak, the increase observed in the equivalent conductance on dilution is due mainly to an increase in the number of ions present, corresponding to a higher degree of dissociation as the solution is diluted. This is the basis of the theory of Arrhenius, proposed in 1887, which has been so successful in describing quantitatively the behavior of solutions of weak electrolytes.

The increase of the equivalent conductance of solutions of strong electrolytes with dilution in the low-concentration range is not due to an increase in dissociation, because the dissociation is already complete, but to an increased mobility of the ions. In a concentrated solution of a highly ionized strong electrolyte, the ions are close enough to one another so that any one of them in moving is influenced not only by the electrical field impressed across the electrodes, but also by the field of the surrounding ions. The ionic velocities are, then, dependent upon both forces. Arrhenius attempted to treat the electrolytic-conductance behavior of the strong electrolytes in the way in which he had successfully treated the weak electrolytes; such a treatment is, however, inconsistent with the experimental fact discovered by Kohlrausch that a plot of the equivalent conductance of a strong electrolyte against the square root of the concentration is very nearly linear. More recently Debye and Hückel and Onsager have been able to calculate the effect of the surrounding ions on the mobility of any given ion and, for dilute solutions, have obtained results entirely consistent with the experimental facts. Complete dissociation is here assumed.

The apparent dissociation constant for a typical *weak* electrolyte such as acetic acid may be calculated as

$$K_a = \frac{\alpha^2 C}{1 - \alpha} = \frac{C_{H^+} \cdot C_{A^-}}{C_{HA}} \quad (3)$$

where  $\alpha$  = degree of dissociation

$C$  = concentration of solute, moles/liter

According to the Arrhenius theory, the value of  $\alpha$  at any concentration is given by the relation

$$\alpha = \frac{\Lambda}{\Lambda_0} \quad (4)$$

where  $\Lambda$  = equivalent conductance at concentration  $C$

$\Lambda_0$  = equivalent conductance at infinite dilution

In the case of a weak electrolyte the value of  $\Lambda_0$  cannot be obtained by the extrapolation to infinite dilution of results obtained at finite concen-

trations, but must be calculated from results obtained with strong electrolytes by means of the law of Kohlrausch concerning the additivity of ionic conductances at infinite dilution. Thus, for a weak acid HR, the value of  $\Lambda_0$  may readily be determined from a knowledge of the values of  $\Lambda_0$  for HCl, NaCl, and the sodium salt, NaR, of the weak acid:

$$\Lambda_{0,HR} = \Lambda_{0,HCl} + \Lambda_{0,NaR} - \Lambda_{0,NaCl}$$

Alternatively, the relation

$$\Lambda_{0,HR} = l_{0,H^+} + l_{0,R^-}$$

may be used directly. The value of  $l_{0,H^+}$ , the limiting conductance of the hydrogen ion, is obtained as the product of  $\Lambda_0$  for HCl and the limiting value of the transference number at infinite dilution of the hydrogen ion in HCl solutions. For the evaluation of  $l_{0,R^-}$  similar measurements on solutions of the sodium salt of the weak acid are used. The  $\Lambda_0$  values for the *strong* electrolytes are obtained by extrapolating to infinite dilution values of the equivalent conductance versus square root of the concentration.

The relation expressed by Eq. (3) is derived by assuming that the ions and undissociated molecules behave as ideal solutes. The calculation of the degree of dissociation by means of Eq. (4) would be accurate if the ionic mobilities were independent of the concentration. Where really high accuracy is attainable, a more elaborate method<sup>4,7</sup> of calculation is employed and additional useful data are provided. For example, we are aware that electrically charged solutes deviate widely from the ideal behavior even in dilute solution. Precise conductance measurements provide an approach to measure this nonideality as an activity coefficient in solutions of weak electrolytes. The thermodynamic ionization constant, as contrasted with the apparent one as defined by Eq. (3), may be written as

$$K = \frac{C_{H^+} y_{H^+} \cdot C_{A^-} y_{A^-}}{C_{HA} \cdot y_{HA}} \quad (5)$$

where  $y$  is an activity coefficient on the volume concentration scale (page 110).

From Eqs. (3) and (5) we now have

$$\log K_a = \log K - \log \frac{y_{H^+} y_{A^-}}{y_{HA}} \quad (6)$$

$$\text{and} \quad \lim_{C \rightarrow 0} K_a = K \quad (6a)$$

So from a series of conductance measurements at different solute concentrations,  $C$ , we may estimate the value of this limit. Having deter-



mined a value for  $K$ , the experimental value of  $K_a$  at any concentration allows one to compute the factor  $y_{H^+} \cdot y_{A^-} / y_{HA}$ . To a good approximation  $y_{HA}$  can be considered as unity. The square root of  $y_{H^+} y_{A^-}$  is, by definition, the mean ionic activity coefficient for the weak electrolyte. MacInnes and Shedlovsky<sup>5</sup> give  $K = 1.752 \times 10^{-5}$  for acetic acid in aqueous solution at 25°C.

**Apparatus.** Wheatstone-bridge assembly; conductance cell; oscillator with a frequency of about 1000 cycles/sec; earphones; conductance water; platinizing solution; 0.02000 N potassium chloride solution; 0.05 N solution of acetic acid; 0.02 N solution of hydrochloric acid; thermostat at 25°C; 50- and 100-ml volumetric flasks.

**Procedure.** The conductance assembly for this experiment consists of a vacuum-tube oscillator to provide an input voltage at 1000 cycles/sec

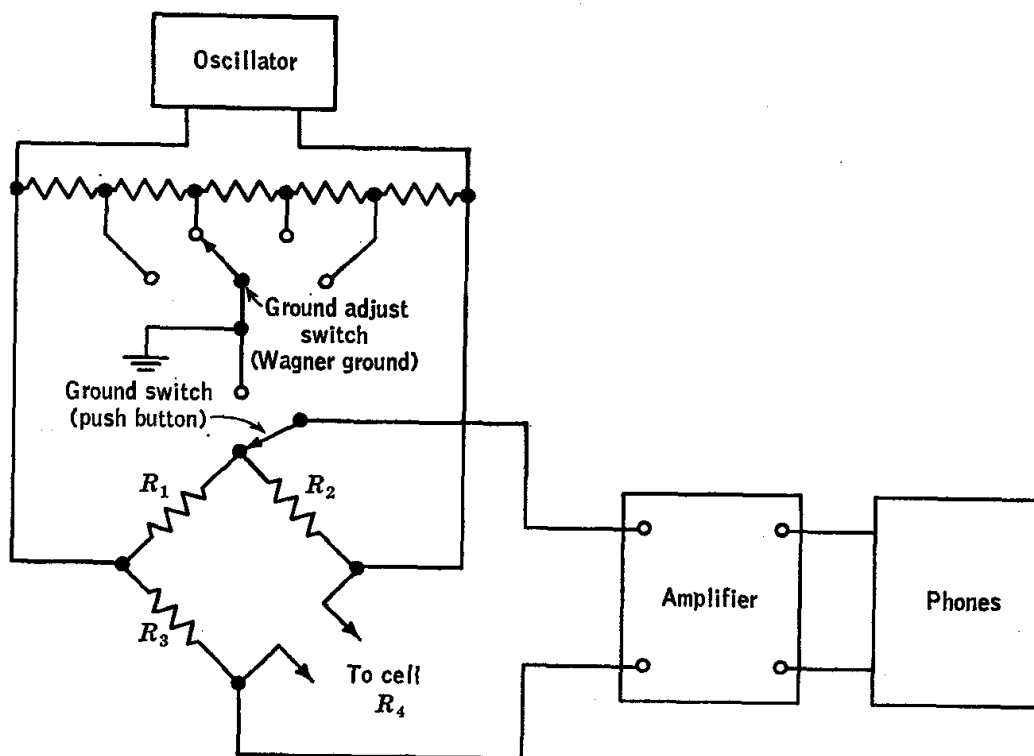


Fig. 37. Bridge circuit for conductance measurements.

for the bridge, a Wheatstone bridge, an amplifier connected to the output terminals of the bridge, and a Wagner grounding circuit, all shown diagrammatically in Fig. 37.

When the bridge has been balanced by adjustment of the resistance  $R_3$  and the ratio  $R_2/R_1$ , as indicated by a minimum output, the cell resistance  $R_4$  is given as  $R_4 = (R_2/R_1)R_3$ . The ratio  $R_2/R_1$  is adjustable

in decimal steps and appears directly on the dial marked with the word "multiply." The resistance  $R_3$  is read in ohms from the four dials.

There is usually some uncertainty in the balance point because of the presence of a background tone, which results from the flow of alternating currents through stray capacitances not shown in Fig. 37. This effect is considerably reduced, and the sharpness of balance correspondingly improved, by the proper adjustment of the Wagner grounding circuit, controlled by a switch.

The amplitude of the input voltage may be varied by means of the gain control on the oscillator.

The conductance cell is filled with the solution whose conductance is to be measured. After the elimination of any bubbles in the cell, the latter is placed in the thermostat. While the solution is coming to the desired temperature, a test measurement on a resistor may be made for practice. The resistance to be measured is to be connected to the terminals marked  $X$  on the Wheatstone-bridge box.

The following directions may be of use in finding the balance point of the bridge; they assume the use of a typical "student-type" Wheatstone bridge with a Wagner ground auxiliary circuit.

1. The amplifier gain is set to give a tone well below the maximum obtainable.

2. With the  $X1000$  dial not at zero, that position of the "multiply" switch is selected which gives the minimum intensity, and the  $X1000$  dial is then adjusted for a minimum. If a minimum is not obtained, it may be necessary to try an adjacent position of the "multiply" switch.

3. The push-button "ground" switch is depressed, and the best "Wagner ground" switch position is selected. The push-button switch is then released.

4. Adjustment of the bridge is continued for minimum intensity, taking the four decade resistors in decreasing order. It is essential that at each step the setting is verified by approach from both the high- and low-resistance sides; proper execution of this step may require thought when the balance point appears to correspond to a dial setting of 0 or 9.

5. An estimate of uncertainty is recorded for each measurement. This should not exceed 0.3 per cent, except for pure water.

The Freas-type conductance cell shown in Fig. 38 is particularly suitable for the conductance measurements. The four corners of the thin platinum squares are anchored to a glass frame. The cell is readily filled and emptied, and the volume of solution required is small. For all conductance measurements the cell is immersed in a thermostat, preferably at  $25^{\circ}\text{C}$  regulated to  $0.02^{\circ}$ .

The electrodes of the conductance cell must have an adherent coating of platinum black and should be immersed in distilled water whenever

the cell is not in use. If the electrodes are allowed to dry out, it is difficult to rinse out electrolytes from them, and it is advisable to dissolve off the coating with aqua regia (under the hood) and plate out a fresh deposit. The electrodes and cell are rinsed out thoroughly, first with distilled water and then with conductance water, which is especially pure water prepared by multiple distillations. The conductance cells must be handled with great care; the electrodes must not be touched, and they must not be moved with respect to each other during the course of an experiment.

The cell is filled with conductance water, inspected to make sure there are no air bubbles at the electrodes, and its resistance is measured; it is then rinsed and refilled, and the resistance is measured again. This process is repeated until the resistance has become essentially constant, showing that contaminating electrolytes in the cell have been rinsed out. The cell resistance will not become absolutely constant because the conductance water is very pure and traces of electrolytes insignificant in the later measurements will produce noticeable fluctuations. The specific conductance of the water used should be about  $5 \times 10^{-6} \text{ ohm}^{-1} \text{ cm}^{-1}$  or less, corresponding to a resistance of 200,000 ohms or more in a cell of unit cell constant. At these high resistances an accuracy of more than two significant figures is difficult to obtain without special precautions. For the other solutions studied, a precision of the order of a few tenths of a per cent should be obtained in the resistance measurements.

When the cell is clean, as shown by a reasonably constant high resistance with conductance water, it is rinsed two or three times with 0.02 N potassium chloride solution, and the resistance is then determined with this solution filling the cell. Additional measurements are made on fresh samples of the solution until successive determinations agree closely. The purpose of these measurements is to secure data for the calculation of the cell constant.

The cell is emptied and rinsed with the next solution for which the conductance is to be measured. It is advisable to make check determinations on each solution to make sure that the cell was thoroughly rinsed.

One hundred milliliters of 0.05 N acetic acid is prepared by quantitative dilution of 1 N stock solution with conductance water, and its concentration is verified by titration with standard sodium hydroxide. After the conductance of this solution has been determined, a 0.025 N solution is

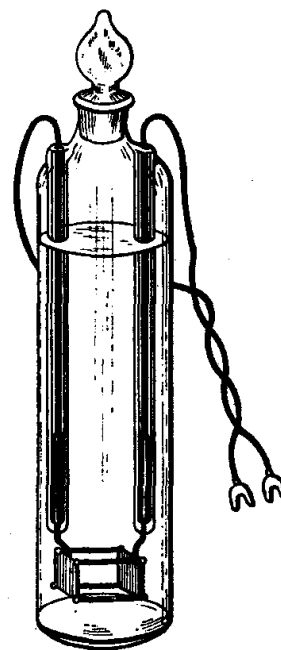


FIG. 38. The Freas-type conductance cell.

prepared by quantitative dilution of the 0.05 N acetic acid for a second conductance measurement. In this fashion, conductance measurements are made on 0.05, 0.025, 0.0125, 0.00625, 0.00312, and 0.00156 N acetic acid solutions. The successive dilutions must be made with great care; otherwise the propagation of error will become excessive. They may be made by using a 100-ml calibrated flask and a 50-ml calibrated pipette.

Conductance measurements are then made on solutions of hydrochloric acid, at concentrations of 0.02, 0.01, 0.005, 0.0025, and 0.00125 N. The solutions are prepared as above by quantitative dilution of a stock solution with conductance water. These measurements provide data illustrating the conductance behavior of solutions of strong electrolytes and data for the calculation of the equivalent conductance at infinite dilution for acetic acid.

**Calculations.** The cell constant for the conductance cell is determined by means of Eq. (1) and the known specific conductance of the potassium chloride solution. The specific conductances of the conductance water and of the various solutions are then calculated. The specific conductance of the solute in each case is evaluated as the difference between the specific conductance of the particular solution and that of the solvent used. The equivalent conductance of the solute is then calculated for each solution.

For each of the solutes a plot is made of equivalent conductance versus the square root of the concentration; for the hydrochloric acid an extrapolation† of the experimental data to zero concentration is made for the evaluation of the equivalent conductance at infinite dilution. The value so obtained is combined with values of  $\Lambda_0$  for sodium chloride and sodium acetate taken from the literature to give the equivalent conductance at infinite dilution for the acetic acid. A second calculation of this quantity is made by use of the values of  $\Lambda_0$  for the sodium acetate and hydrochloric acid solutions and the values 0.449 and 0.821, respectively, for the transference numbers at infinite dilution of the acetate ion of sodium acetate and the hydrogen ion of hydrochloric acid at 25°.

The apparent dissociation constant  $K_a$  for the acetic acid is then calculated at each concentration by use of Eqs. (3) and (4), with the value of  $\Lambda_0$  for acetic acid obtained as described above. No such calculations should be carried out for strong electrolytes, since these equations are without significance for them.

The data and the results of this experiment may be conveniently tabulated under the following column headings: concentration, milliliters containing 1 g-equiv of solute, resistance in ohms, specific conductance,

† The reliability of the various experimental points should be considered in making this extrapolation.

equivalent conductance, degree of dissociation, and dissociation constant. Wherever possible the results are compared with accepted values,<sup>4,6,7</sup> and any discrepancies arising are discussed in the light of the sources of experimental error.

**Practical Applications.** Some examples of the use of conductance measurements in the solution of chemical problems are indicated in the following paragraph. To illustrate their application to engineering chemistry, it may be mentioned that observations of this sort have been used to measure the flow of water in streams, to determine the total solids in water, and to test for pollution of water.

**Suggestions for Further Work.** The influence of substitution and structure on the apparent dissociation constants of organic acids may be studied. For example, the dissociation constants of mono- and dichloroacetic acids and propionic acid may be determined and compared with the dissociation constant of acetic acid. In the same way the influence of substituting amino or nitro groups into benzoic acid may be studied.

The end point of a neutralization reaction involving a strong acid and a strong base may be determined by observations of electrical conductance. When the base is added gradually to the acid solution, the hydrogen ions of very high mobility are replaced by the cations of the base, which have normal mobilities, so a change in conductance arises from the difference in the mobilities of the ions. The conductance decreases until the hydrogen ions have disappeared; it then increases as excess base is added, since now hydroxyl ions of higher mobility are accumulating.

The conductometric test for an end point is not limited to neutralization reactions. It can be used with reactions which involve the precipitation of an insoluble salt or the formation of complex ions.

#### References

1. Harned and Owen, "The Physical Chemistry of Electrolytic Solutions," 3d ed., Reinhold Publishing Corporation, New York (1958).
2. International Critical Tables, Vol. VI, pp. 229ff., McGraw-Hill Book Company, Inc., New York (1928).
3. Jones and Bradshaw, *J. Am. Chem. Soc.*, **55**, 1780 (1933).
4. MacInnes, "The Principles of Electrochemistry," Reinhold Publishing Corporation, New York (1939).
5. MacInnes and Shedlovsky, *J. Am. Chem. Soc.*, **54**, 1429 (1932).
6. Robinson and Stokes, "Electrolyte Solutions," 2d ed., Academic Press, Inc., New York (1959).
7. Shedlovsky in Weissberger (ed.): "Technique of Organic Chemistry," 3d ed., Vol. I, Pt. IV, Chap. 45, Interscience Publishers, Inc., New York (1960).

#### 28. TRANSFERENCE NUMBER OF THE HYDROGEN ION BY THE MOVING-BOUNDARY METHOD

The moving-boundary method offers the most accurate method for the determination of transference numbers of both cations and anions, and such a determination, together with a measurement of specific conductivity, may be used to calculate ionic mobilities.

**Theory.** In the moving-boundary method, an initially sharp boundary between two electrolyte solutions having either the same anion or the same cation is subjected to an electric field. If the two solutions have different cations, a boundary will move toward the cathode with the velocity of the cation in the solution into which the boundary moves. In order to obtain a sharp moving boundary, it is necessary that the boundary be made to move into the solution containing the cation with

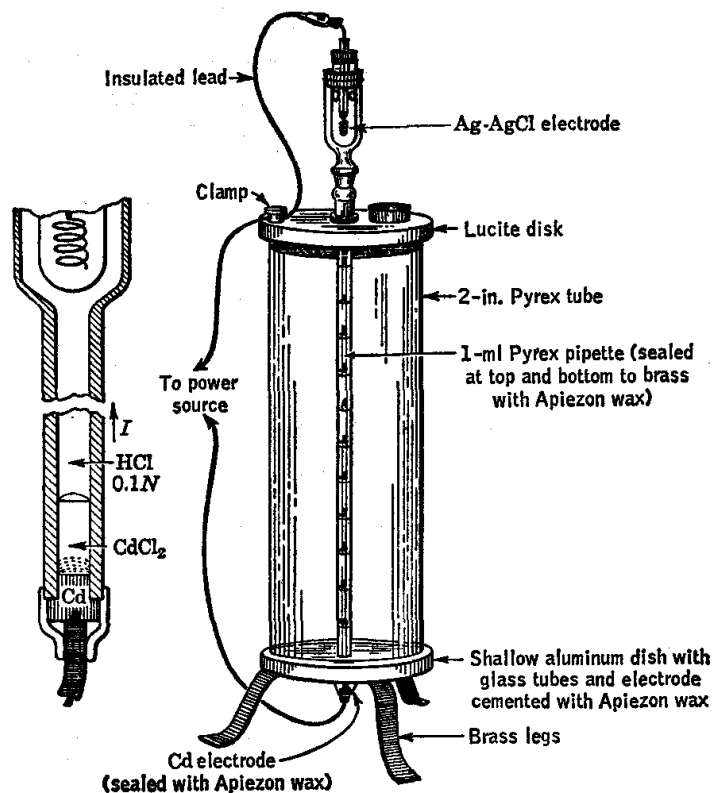


FIG. 39. Apparatus for the moving-boundary method for the determination of transference numbers.

the higher mobility. The latter solution is called the *leading* solution, and the other solution, the *indicator* solution.

In this experiment electrolysis is used to form the indicator solution. The anode in the moving-boundary apparatus is made of metallic cadmium, so that  $\text{CdCl}_2$  is formed by the passage of current. A boundary between the solutions of cadmium chloride and hydrochloric acid will leave the face of the electrode and move up the tube as illustrated in Fig. 39. Since the cadmium ion has a much lower mobility than the hydrogen ion, this moving boundary is very sharp. As the boundary moves upward, the chloride ion moves downward across the boundary and eventually accumulates around the anode. Electrical neutrality is preserved

in the solution near the electrode because only a fraction of the cadmium ions which are formed by the electrolysis of the anode is necessary for the maintenance of the growing column of indicator solution. This concentrated solution of cadmium chloride which accumulates at the anode may be seen at the conclusion of the experiment by tipping the tube so that the heavy solution falls down the tube.

When one faraday  $F$  of electricity passes through a tube containing such a boundary, there will be a movement of one equivalent of electrolyte through a hypothetical plane in the solution. The transference number  $T_c$  of the cation is, by definition, the fraction of the current carried by the cation. Thus  $T_c$  equivalents of the cation will move through a plane toward the cathode per faraday of electricity passing through this plane.

The charge carried past a plane by current  $I$  in time  $dt$  is  $I dt$ . The charge carried past a plane in the HCl solution by cations, if the boundary sweeps out a volume  $dV$  in the time interval  $dt$ , is

$$\frac{C}{1000} F dV$$

where  $C$  is the concentration in equivalents per liter.

The ratio of the charge carried through a plane by cations to the total charge transported through the plane is  $T_c$ .

$$T_c = \frac{CF}{1000I} \left( \frac{dV}{dt} \right) \quad (1)$$

One faraday  $F$  is equivalent to 96,490 coulombs (or amp-sec). The same equation may be used to calculate anion transference numbers if the solutes forming the boundary have the same cation but different anions.

The ionic mobility  $u$ , which is the ratio of the ion velocity to the electric field strength, may be calculated from the data of a moving-boundary experiment as follows. The electric field strength  $dE/dx$  is given in volts per centimeter by

$$\frac{dE}{dx} = \frac{I}{A\kappa} \quad (2)$$

where  $A$  = cross-sectional area of tube,  $\text{cm}^2$

$\kappa$  = specific conductivity of leading solution,  $\text{ohm}^{-1} \text{cm}^{-1}$

The mobility  $u$  (in  $\text{cm}^2 \text{sec}^{-1} \text{volt}^{-1}$ ) of an ion is calculated by means of the equation

$$u = \frac{\Delta x / \Delta t}{dE/dx} = \frac{A\kappa \Delta x}{I \Delta t} = \frac{\kappa \Delta V}{I \Delta t} \quad (3)$$

In our experiment, the  $\text{CdCl}_2$  solution below the boundary has a specific conductivity  $\kappa$ , which is lower than that of the hydrochloric acid solution, because it is more dilute, and the  $\text{Cd}^{++}$  ion has a lower mobility than the  $\text{H}^+$  ion. By reference to Eq. (2) it is seen that the electric field strength is greater in the  $\text{CdCl}_2$  solution below the moving boundary than in the  $\text{HCl}$  solution above the boundary. Therefore, if  $\text{H}^+$  ions diffuse into the  $\text{CdCl}_2$  solution below the boundary, they will encounter a high field strength and will be rapidly sent up to the boundary. On the other hand, if  $\text{Cd}^{++}$  ions diffuse ahead of the boundary, they will have a lower velocity than the hydrogen ions because of their lower mobility and will soon be overtaken by the boundary. This so-called "adjusting effect" keeps the boundary sharp.

**Apparatus.** Glass assembly shown in Fig. 39 fitted with cadmium and silver-silver chloride electrodes; d-c power supply; 0.1 N  $\text{HCl}$  solution; methyl violet indicator.

**Procedure.** The adaptation of this method for use as a laboratory experiment is described by Longworth.<sup>5</sup> The glass capillary tube is made of a 1-ml Pyrex pipette graduated every 0.1 ml and having an inside diameter of about 2 mm. The capillary is rinsed several times with 0.1 N hydrochloric acid containing methyl violet indicator. Only enough methyl violet to give a distinguishable color in the capillary tube is required. The indicator should be added to the acid just before the start of the experiment, because the color will fade. The rinsing of the capillary may be aided by the use of a wood or glass rod which just fits in the capillary and is used as a plunger. It is important to dislodge any bubbles at the lower end of the tube. Next the electrode chamber is filled with hydrochloric acid, and the silver-silver chloride electrode is inserted.

It is necessary to immerse the tube in which the boundary moves in a water bath, in order to dissipate the heat which is developed in the tube by the passage of the electric current.

The electrodes are connected to a source of direct current capable of delivering 2 to 4 milliamp. It is most convenient if the current through the capillary is kept constant during the experiment. If the applied voltage is constant, the current through the capillary will decrease during the experiment, because as the boundary ascends the tube, the length of the column of indicator electrolyte increases correspondingly, and this solution is a poorer conductor than the one it replaces. The potential applied to the cell must therefore be continually increased in order to maintain a constant current. This may be done by one of two methods: (a) part of the current supply may be shunted across a rheostat which has a sliding contact, and by manual adjustment of this contact a con-



stant current through the cell may be maintained; (b) a power supply designed to produce a constant current with minimum adjustment, such as that of Bender and Lewis,<sup>1</sup> may be used. This method has the advantage that attention may be focused on the determination of the boundary velocity. The current may be measured by means of a low-range milliammeter, or if greater accuracy is required, by measuring the potential drop across an accurately known series resistance with a potentiometer.

The time, to the nearest second, at which the boundary crosses successive graduations is obtained with the aid of a stop watch.

A second experiment is performed at a different current.

**Calculations.** Values of the transference number of the hydrogen ion are calculated by the use of Eq. (1) and a plot of  $V$  versus  $t$ . In the regions of the tube near the cadmium electrode, the movement of the hydrogen ion may be retarded because of the diffusion of the  $\text{CdCl}_2$  solution.

The specific conductivity of 0.1 N hydrochloric acid is  $0.03913 \text{ ohm}^{-1} \text{ cm}^{-1}$  at  $25^\circ$ . The specific conductivity of a solution slightly different from 0.1 N may be calculated by assuming that the specific conductivity is directly proportional to concentration. The hydrogen-ion mobility is calculated from the experimental data by using Eq. (3). The chloride-ion transference number and mobility are calculated by using the relation  $T_{\text{H}^+} + T_{\text{Cl}^-} = 1$ .

**Practical Applications.** The moving-boundary method for the determination of ionic mobilities has been particularly useful in the study of proteins.<sup>2</sup> Electromigration methods have been used for the separation of isotopes.<sup>3</sup>

**Suggestions for Further Work.** If the current is regulated very closely and the moving-boundary tube is calibrated, the variation of the transference number and mobility of hydrogen ion may be determined, using 0.01 and 0.05 N hydrochloric acid. The apparatus may also be used to determine the transference number of cations which yield colored solutions.

The transference number of potassium ion in 0.1 N potassium chloride may be determined with the same apparatus. In this case, the boundary is visible only because of the difference in the refractive indices of the two solutions. Longworth<sup>5</sup> has described a simple optical arrangement for the location of the boundary.

### References

1. Bender and Lewis, *J. Chem. Educ.*, **24**, 454 (1947).
2. Bier, *Electrophoresis*, Academic Press, Inc., New York (1959).
3. Brewer, Madorsky, Taylor, Dibeler, Bradt, Parham, Britten, and Reid, *J. Research, Natl. Bur. Standards (U.S.)*, **38**, 137 (1947).
4. Daniels and Alberty, "Physical Chemistry," John Wiley & Sons, Inc., New York (1961).
5. Longworth, *J. Chem. Educ.*, **11**, 420 (1934).
6. Robinson and Stokes, "Electrolyte Solutions," 2d ed., Academic Press, Inc., New York (1959).

### 29. TRANSFERENCE NUMBER OF THE SILVER ION BY THE HITTORF METHOD

The transference number of the silver ion may be determined by chemical analysis of solutions before and after electrolysis. High accuracy is required in the analytical procedure.

**Theory.** When an electric current is passed through an electrolyte solution, the current is carried by ions, and an oxidation reaction occurs at the anode while reduction occurs at the cathode. If the electrolysis

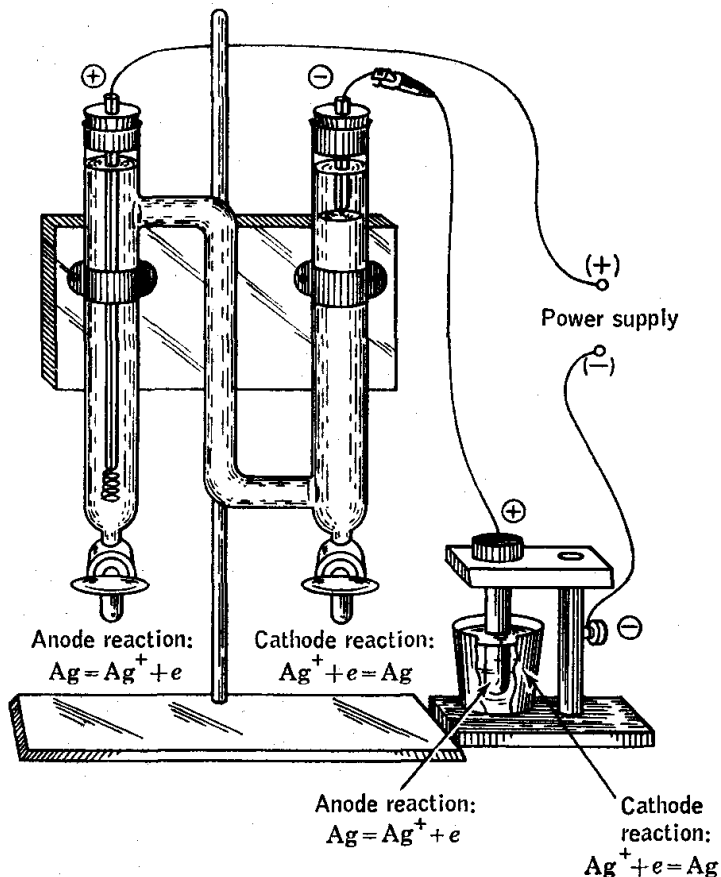


FIG. 40. Hittorf apparatus for the determination of transference numbers.

of silver nitrate solution is carried out by using silver electrodes, the number of equivalents of silver ion formed at the anode (+) is equal to the number of gram atoms of metallic silver formed at the cathode (-). However, the concentration of silver ions in the regions surrounding the two electrodes depends not only upon the duration of electrolysis and upon the current used, but also upon the mobilities of the silver and nitrate ions. Hittorf (1853) was the first to make use of this fact to determine transference numbers.

The construction of the electrolysis cell used in this experiment is illustrated in Fig. 40. At the anode an equivalent of silver ion goes into

solution per faraday of current passed and less than one equivalent of silver ions is transported out of the arm by ion migration. Therefore the solution around the anode becomes more dense during electrolysis, and so the anode is placed at the bottom of the chamber and the connecting arm is placed at the top. On the other hand, silver is plated out on the cathode faster than it migrates into the cathode chamber, so that the solution in the surrounding region becomes lighter than the initial solution and tends to rise to the top. Therefore the cathode is placed at the top of its chamber and the connecting arm is placed at the bottom. When the apparatus is constructed in this way, the concentration changes are restricted to as small as possible volumes in the anode and cathode chambers, and the concentration of the solution in the connecting arm is unchanged if the duration of the electrolysis is not too long.

The transference number of an ion may be defined as the fraction of the total current through the solution carried by that ion. If  $x$  faradays of charge are passed between the electrodes, then  $x$  equivalents of silver ion would disappear from the cathode chamber if there were no migration of silver ion. However, if only  $y$  equivalents of silver disappear from the cathode chamber,  $y$  being less than  $x$  because of migration of silver ions toward the negative electrode,  $x - y$  is the number of equivalents of silver ion which have migrated into the cathode chamber during the passage of  $x$  faradays of charge. Thus the fraction of the current carried by silver ions is

$$T_+ = \frac{x - y}{x} \quad (1)$$

The transference number of the silver ion,  $T_+$ , may also be calculated from the change in concentration in the anode chamber. Here  $x$  equivalents of silver ion are formed by the electrode reaction, but the increase in the number of equivalents of silver ion in this compartment is only  $z$  because of the migration of silver ions away from the positive electrode. The number of equivalents of silver ion which have migrated out of the anode chamber is  $x - z$ , so that the fraction of the current carried by the silver ions is

$$T_+ = \frac{x - z}{x} \quad (2)$$

If analyses were simultaneously carried out for nitrate ion, it would be found that the nitrate concentration would have increased in the anode chamber and decreased in the cathode chamber. The transference number of the anion may also be calculated from

$$T_+ + T_- = 1 \quad (3)$$

since the sum of the transference number of anion and cation must be unity.

In order to calculate the ionic mobilities, it is also necessary to have information concerning the specific conductance of the solution as discussed in Exp. 27.

**Apparatus.** Transference-number cell with silver electrodes; source of 90 to 110 volts direct current; milliammeter; 0.05 molal silver nitrate; 0.02 N potassium thiocyanate; silver coulometer; ferric sulfate.

**Procedure.** The transference number of silver ion in 0.05 molal silver nitrate solution is to be determined in this experiment, and the transference number of the nitrate ion calculated, using Eq. (3). The apparatus which is illustrated in Fig. 40 is filled with a 0.05 molal solution of silver nitrate, and the silver electrodes are put in place.

The silver coulometer is filled with a solution containing 15 per cent by weight of silver nitrate in water. The silver anode is wrapped in filter paper to prevent particles from falling from the anode onto the cathode. The platinum crucible is cleaned with dilute nitric acid, rinsed thoroughly, heated at  $110^{\circ}$ , cooled in a desiccator, and weighed. The silver crystals deposited on the cathode will not adhere unless the surface is clean.

The electrical connections are made as illustrated in the figure, and a current of 0.01 amp is passed through the solution for a period of time of 120 min or more, accurately measured by means of an electric clock. Currents of greater magnitude should not be used on account of the heating effect of the current, which causes convection currents. It is convenient to use a current-regulated power supply, since then the total quantity of electricity involved is accurately given by the product of current and time.

While the electrolysis is in progress, 10-ml aliquots of the 0.05 molal silver nitrate solution are titrated, using a standard solution of KCNS (about 0.02 N). This solution may be standardized against a weighed quantity of  $\text{AgNO}_3$ . A few milliliters of ferric sulfate solution made slightly acid with nitric acid is used as an indicator.

For the computations it is the change in total amount of the solute in each compartment which is required. The concentration analyses serve to demonstrate that data representative of the whole compartment have been obtained.

The necessary data are obtained in the following manner. After the current has been turned off, slightly more than 50 ml of solution is withdrawn from the *anode* chamber by means of the stopcock at its bottom. Of this volume exactly 50 ml is measured into a flask, which is then stoppered for later titration. Then some five successive 10-ml portions are removed. All these samples are now titrated in order, stopping when the titer of a 10-ml portion reaches that of the original silver nitrate

solution. Since the concentration changes in the electrode compartments are small, it is necessary that these analyses be performed with utmost care.

Solutions from the *cathode* chamber are removed for titration by means of pipettes. A 50-ml pipette is inserted under the surface of the solution just far enough to remove 50 ml of solution. This is then emptied into a beaker for titration. A 10-ml pipette is then inserted into the cathode solution just far enough to remove 10 ml of solution. The pipette is drained, and the solution titrated. This procedure is repeated until the titer of two of these 10-ml aliquots agrees within the experimental error with that of the initial solution. If the titrations cannot be completed in one laboratory period, the solutions should be withdrawn from the Hittorf apparatus as described and placed in separate closed flasks for titration during the next period.

The silver nitrate solution from the coulometer is then poured into the silver residue bottle, and the crucible is washed carefully with distilled water. Then it is heated in an oven at  $110^{\circ}$ , cooled in a desiccator, and weighed.

If possible, the electrolysis experiment should be repeated.

**Calculations.** The transference number of the silver ion is calculated from the analyses of the solutions in both the anode and cathode compartments. The quantity of electricity in faradays ( $x$ ) is obtained from the weight of silver deposited in the coulometer and from the product of current and time. One faraday (96,490 coulombs) corresponds to 107.88 g of silver.

The decrease ( $y$ ) in the number of equivalents of silver ion in the cathode compartment is calculated. The total number of equivalents of silver in the aliquots titrated is computed, and subtracted from the number of equivalents of silver ion in the same volume of the initial solution. This calculation involves an approximation since it is assumed that equal volumes of the various solutions contain equal weights of water. The transference number of silver ion is computed by use of Eq. (1).

The increase ( $z$ ) in the number of equivalents of silver ion in the anode compartment is calculated. The total number of equivalents of silver in the aliquots titrated is computed, and from this number is subtracted the number of equivalents of silver ion in the same volume of the initial solution. The transference number of silver ion is calculated by use of Eq. (2).

The nitrate-ion transference number is calculated by using Eq. (3).

**Practical Applications.** Transference numbers have an important application to the so-called "electromotive-force cells with transference." In this type of cell, there is a potential difference, which cannot be directly measured, established at the surface of contact of the two solutions of different concentration. This potential

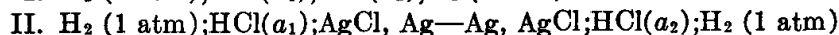
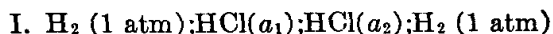
difference is due to a migration of the ions from the concentrated to the dilute solution, and it becomes zero only when the anion and cation have the same velocity. It is, however, possible to approximate the magnitude of this potential by certain formulas which have been proposed and which always involve a knowledge of the magnitude of the transference numbers. For further details, Reference 5 may be consulted.

A less general application is the use of transference data to obtain information concerning the composition of complex ions. For example, if a solution of  $\text{KAg}(\text{CN})_2$  is electrolyzed, it is found that the concentration of the silver actually increases in the anode compartment, showing that the silver is contained in a complex negative ion.

**Suggestions for Further Work.** The transference number of cupric ion may be determined by the Hittorf method, using the same apparatus, by substituting copper electrodes and filling the apparatus with 0.05 M cupric sulfate solution. After the experiment, the anode and cathode solutions are analyzed for copper. One convenient method is to add ammonium hydroxide drop by drop until the precipitate just clears and then add 5 ml of glacial acetic acid and 3 g of potassium iodide. The iodine liberated is titrated with thiosulfate, using soluble starch as an indicator. Each mole of iodine ( $\text{I}_2$ ) formed corresponds to 2 moles of copper.

This experiment is sometimes performed in a single vertical tube with stopcock at the bottom and with copper anode and cathode placed at its lower and upper ends, respectively. The connections to the coulometer are again in series. At the completion of the experiment, anode, middle, and cathode solutions are successively removed through the stopcock for analysis.

In certain cases transference numbers may be determined by electromotive-force measurements. Mason and Mellon<sup>4</sup> have shown that this method may be used as a convenient laboratory experiment to determine the cation transference number in HCl solutions. The cells used are:



Cell I involves transference, whereas cell II does not. The electromotive forces of these cells are:

$$\text{I. } E_t = 2T_+ \frac{RT}{F} \ln \frac{a_2}{a_1}$$

$$\text{II. } E = 2 \frac{RT}{F} \ln \frac{a_2}{a_1}$$

The transference number of the cation is obtained by division.

$$T_+ = \frac{E_t}{E}$$

### References

1. Harned and Owen, "The Physical Chemistry of Electrolytic Solutions," 3d ed., Reinhold Publishing Corporation, New York (1958).
2. MacInnes, "The Principles of Electrochemistry," Reinhold Publishing Corporation, New York (1939).
3. MacInnes and Longworth, *Chem. Revs.*, **11**, 171 (1932), and preceding papers.
4. Mason and Mellon, *J. Chem. Educ.*, **16**, 512 (1939).
5. Pearce and Mortimer, *J. Am. Chem. Soc.*, **40**, 509 (1918).

6. Robinson and Stokes, "Electrolyte Solutions," 2d ed., Academic Press, Inc., New York (1959).
7. Spiro in Weissberger (ed.): "Physical Methods of Organic Chemistry," 3d ed., Vol. I, Pt. IV, Interscience Publishers, Inc., New York (1960).

### 30. THE DROPPING-MERCURY ELECTRODE

This experiment illustrates the use of the current-voltage curves obtained with the dropping-mercury electrode in the qualitative and quantitative analysis of reducible and oxidizable solutes. Both the diffusion current and the decomposition potentials are involved.

**Theory.**<sup>3-5</sup> In electrolysis a potential difference is impressed between two electrodes immersed in a solution. The decomposition potential is defined as the potential difference required to cause continuous electrolysis to take place. This potential depends not only on the standard electrode potentials involved, but also on the composition of the solution and on surface effects. In ordinary electrolysis the current which flows increases continuously as the voltage is increased beyond the decomposition potential, but as originally shown by Heyrovsky, if one electrode is a microelectrode, i.e., of very small dimensions, such as the dropping-mercury electrode, current-voltage curves can be obtained whose unusual characteristics lead to important practical applications.

In the dropping-mercury electrode, mercury flows through a section of fine-bore capillary tubing in a succession of small drops which grow to a maximum diameter of about 0.5 mm before breaking away.

Now, as a continuously increasing potential difference is applied to the cell, the current through it will be very small until the voltage drop at the mercury-drop cathode is large enough to cause reduction of the constituent with the lowest reduction potential. The current then rises rapidly, but it is again limited by concentration polarization at the small cathode. When there is present a large amount of supporting electrolyte which is not involved in the cathode reaction, the rate of diffusion of the reducible reactant to the electrode and its concentration determine the limiting current.

For the cathode a small mercury drop is suspended from a capillary tube, in turn connected to a reservoir of mercury. Fresh drops are being continually formed, and conditions vary during the formation and detachment cycle of the drop; however, on the average, they are constant over longer periods of time. The diffusion current has been shown to be proportional to the maximum surface of the drop and to the square root of the rate of drop formation. A theoretical equation describing the average diffusion current was derived by Ilkovic:<sup>2</sup>

$$I_D = knD^{1/2}m^{2/3}t^{1/6}C$$

where  $I_D$  = diffusion current,  $\mu\text{amp}$

$n$  = number of electrons transferred in electrode reaction

$k$  = constant = 607 when  $I_D$  is mean diffusion current

$D$  = diffusion coefficient of reducible species,  $\text{cm}^2/\text{sec}$

$m$  = rate of flow of mercury from tip,  $\text{mg}/\text{sec}$

$t$  = drop time,  $\text{sec}$

$C$  = concentration of reactant, millimoles/liter

Thus the current  $I_D$  varies according to the product  $m^{3/2}t^{1/2}$ . The proportionality between  $I_D$  and  $C$  is a direct consequence of the concentration polarization of the dropping-mercury electrode.

The *half-wave potential*  $E_{1/2}$  for the current-voltage "wave" for a particular constituent is the value of the applied voltage for which the current (corrected for the residual-current contribution) is equal to one-half the limiting diffusion current. When the electrode reaction is reversible, a study of the effect on the half-wave potential of variation in the composition of the solution has been made to yield information of thermodynamic interest on complex ions, etc.,<sup>3,4</sup> through consideration of the system as a special type of electromotive-force cell. For simple ions, such as  $\text{Tl}^+$ ,  $\text{Zn}^{++}$ , etc., which are reduced rapidly and reversibly at the dropping-mercury electrode with the formation of an *amalgam* at the drop surface, the half-wave potential is constant and independent of the concentration of the reducible ion when the temperature and supporting electrolyte concentration are constant. In principle, the half-wave potential in such cases thus provides a means of identifying the material responsible for a wave, but in practice this is of little value unless auxiliary information is available to limit the possibilities.

**Practice.** The experimental arrangement used in the determination of current-voltage curves with the dropping-mercury electrode is shown in Fig. 41. Variation of the resistance  $R$  in series with the battery  $B$  permits adjustment of the potential drop, measured by the voltmeter  $V$ , across the precision voltage divider  $D$ . Any desired fraction of this potential drop then can be applied across the electrolysis cell by adjustment of the setting of  $D$ . The resulting current is measured by the galvanometer  $G$ ; the shunt  $S$  is used to bypass current around the galvanometer when reduced current sensitivity is required. For a given applied voltage, the current increases to a maximum value as the drop grows in size. The average current during the life of the drop is the important quantity measured; a long-period galvanometer is used to facilitate the determination of this average current.

Following the terminology introduced by Heyrovsky, the current-voltage curve obtained with the dropping-mercury electrode is commonly called a *polarogram*, and the instrument used in its determination a *polarograph*. The latter term applies in particular to the automatic



instruments in which the applied potential is gradually changed by use of a motor-driven potential divider, and the corresponding galvanometer deflections are recorded on photographic paper mounted on a drum whose rotation is coupled mechanically to that of the potential divider. Alternatively, the galvanometer is replaced by a strip-chart recorder. The various commercial instruments and their characteristics are described in several places.<sup>3-5</sup>

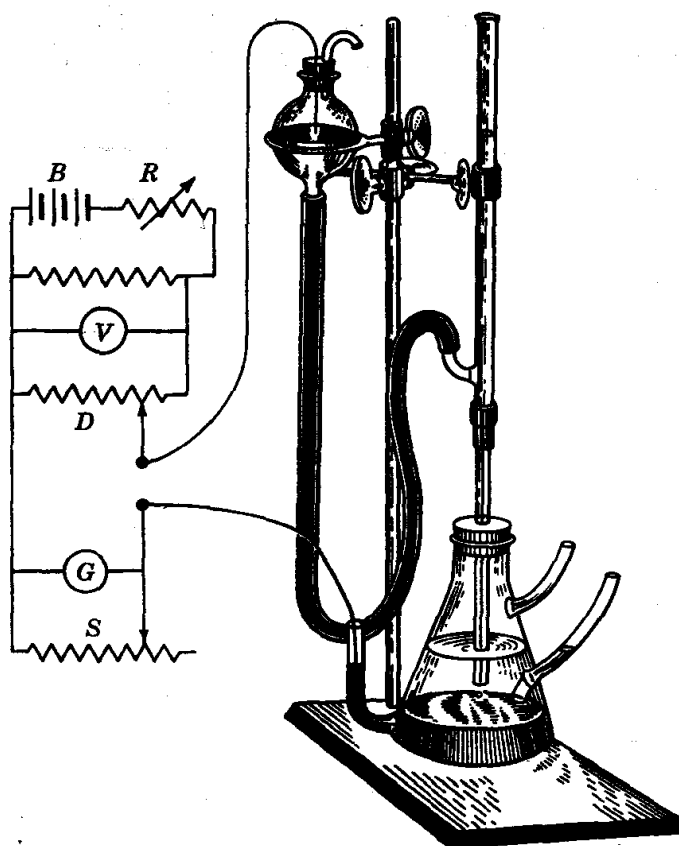


FIG. 41. Schematic diagram of a cell to obtain current-voltage curves with the dropping-mercury electrode.

A typical average current-voltage curve obtained with a solution 0.001 M in  $\text{ZnSO}_4$  and 0.1 N in KCl is shown in Fig. 42. For low applied voltages only a very small current results, called the *residual current*. This current includes contributions from the *condenser current*, the current required to charge the individual drop to the applied potential, and the *electrolysis*, or *faradaic*, *current*, resulting from the reduction of impurities such as traces of dissolved oxygen, mercury ions, etc. It should be noted that the applied voltage is the potential relative to the anode. A mercury-pool electrode in a 0.1 N KCl solution assumes a potential essentially equal to that of the decinormal calomel electrode. As may be seen from a table of standard electrode potentials, an electrode

potential of  $-1.0$  volt relative to the decinormal calomel electrode corresponds at  $25^{\circ}\text{C}$  to  $-0.665$  volt relative to the standard hydrogen electrode, or  $-0.910$  volt versus the saturated calomel electrode (s.c.e.). The latter is commonly used in accurate work as the reference electrode in reporting the potential of the dropping-mercury electrode.

After the decomposition potential is passed, the current first increases rapidly with increasing voltage, then levels off at an essentially constant value because a state of extreme concentration polarization is reached at the dropping-mercury electrode. We have noted that the two processes which can bring zinc ions to the electrode are migration and diffusion.

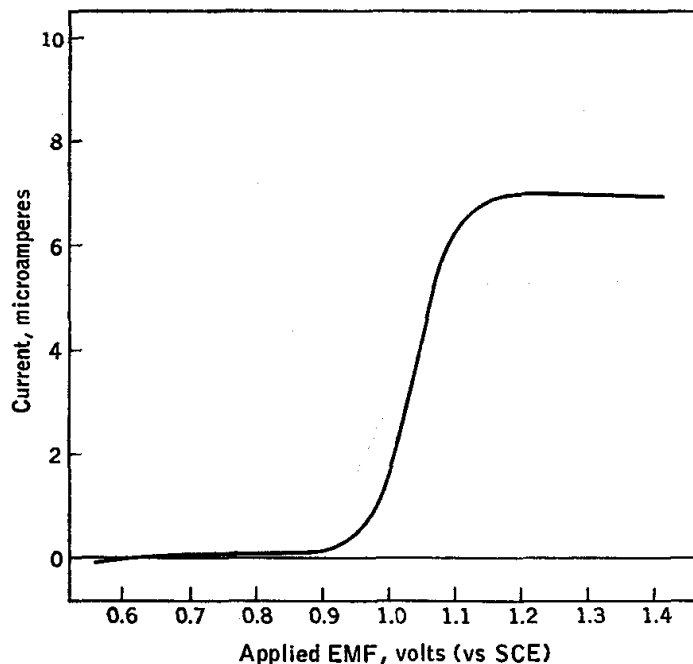


Fig. 42. Current-voltage curve for reduction at the dropping-mercury cathode.

The large excess of the supporting electrolyte, potassium chloride, reduces the transference number of the zinc ion to such a low value that transport of zinc ion by migration is made negligible. The zinc ions thus move to the electrode by diffusion, for which the number arriving per unit time is determined by the concentration gradient from the body of the solution to the mercury-drop surface and by the diffusion coefficient  $D$ . As the applied electromotive force is increased, the electrolysis current increases, and correspondingly the concentration of the reducible ion at the electrode surface is decreased below the value for the body of the solution. The concentration difference so produced increases with increased applied voltage until the concentration of reducible ions at the electrode surface becomes negligible. The cathode is then said to be "concentration-polarized." At this point the average rate of diffusion of reducible ions

to the electrode becomes constant, because the driving force for diffusion, the concentration difference between the body of the solution and at the electrode surface, has become constant. The average electrolysis current therefore remains constant as the applied voltage is further increased, except for a slight increase due to a change in the residual current, until the voltage becomes large enough to produce another chemical reaction at the cathode.

It is the diffusion-limited contribution to the electrolysis current which is called the *diffusion current* for the ion. It may be best determined by subtracting from the total current at a voltage on the flat part of the curve the corresponding residual current evaluated in a control experiment with a solution identical with the first except for the omission of the reducible ion in question. Alternatively, the residual-current contribution may be found by extrapolation to the appropriate voltage of the residual-current line determined at lower applied voltages.

Since oxygen is readily reduced at the dropping-mercury electrode and thus interferes with the current-voltage curves of other substances, it must ordinarily be removed from the solution to be electrolyzed. This may be accomplished by bubbling an inert gas such as nitrogen through the solution before (but not during) the electrolysis. Oxygen interference may also be eliminated by addition of sodium sulfite to neutral or alkaline solutions, to the extent of about 1 g per 100 ml of solution.

Another complication encountered is the appearance of a maximum in the current-voltage wave. The maximum is caused by a streaming of the solution past the drop surface; this stirring effect destroys the concentration polarization of the electrode, and consequently the current can increase beyond the diffusion-limited value. These maxima may usually be eliminated by the addition to the solution of small amounts of adsorbable materials such as gelatin, dyes, etc., which are not reduced at the given potential. Such maximum suppressors may produce undesirable effects as well, however, so that their characteristics should be carefully checked in each pertinent case.

In analytical work the optimum concentration range extends from about  $10^{-2}$  to  $10^{-5}$  M. The dropping-mercury electrode may be used at potentials from approximately +0.2 to -2.0 volts versus the saturated calomel electrode. On the positive side the limit is set by the anodic dissolution of mercury; the extended negative range is made possible by the high overvoltage of hydrogen on mercury. An additional advantage results from the amalgamation of most metals by mercury, which permits their reduction at the dropping-mercury electrode at less negative potentials than otherwise would be required.

Initial work in polarography was centered on the obvious analytical applications. The continuing development of the field, however, has

included significant contributions to problems of physical-chemical interest, and it forms an important aspect of modern electrochemistry. An excellent introduction to the theory and practice of polarography has been given by Meites,<sup>4</sup> while the monograph and review article of Kolthoff and Lingane<sup>3</sup> provide another comprehensive survey of the field. Applications to organic chemistry in particular are treated by Müller,<sup>5</sup> and Delahay<sup>1</sup> has given a definitive treatment of the newer instrumental methods in electrochemistry.

**Apparatus.** Dropping-mercury electrode and circuit elements; gelatin or Triton X-100 solution; KCl; ZnCl<sub>2</sub>; CdCl<sub>2</sub>; MnCl<sub>2</sub>; nitrogen tank or sodium sulfite; unknown.

**Procedure.** Directions will be provided by the instructor for the operation of the polarograph to be used. The recommended cell assembly is shown in Fig. 41. The capillary tip is about 5 or 10 cm long. The appropriate tubing is available from supply houses, or an adequate substitute may be obtained by drawing out a section of ordinary capillary tubing and cutting it off in the constricted section. The mercury used must be of high purity (Chap. 24), and a connecting tube of polyethylene is recommended. If rubber tubing is substituted, pure gum tubing should be used. It should be boiled with concentrated sodium hydroxide solution, to remove sulfur compounds, and carefully rinsed before use.

The mercury flow should be started, by increasing the height of the mercury column, *before* the electrode is immersed in any solution. It is best to allow the mercury to flow continuously through the whole laboratory period rather than to stop it and clean the tip between determinations. The electrode is then immersed in the first solution to be studied, and the mercury height adjusted to give a drop time between 3 and 6 sec. The electrodes are then connected to the polarograph, and a series of current-voltage readings made for the applied potential range 0 to -2 volts. The current will rise sharply in the neighborhood of -2 volts because the decomposition potential for potassium ion has been reached. For each voltage setting the *average* galvanometer deflection is recorded. The galvanometer shunt is adjusted as required to give an accurately measurable deflection for the current involved. The actual electrolysis current is obtained as follows:

$$I = asg^\circ$$

where  $I$  = current,  $\mu\text{amp}$

$a$  = galvanometer deflection, mm

$g^\circ$  = basic galvanometer deflection sensitivity,  $\mu\text{amp mm}^{-1}$

$s$  = shunt reduction factor

The value of  $g^\circ$  is characteristic of the galvanometer used; if it is not specified for the instrument employed, it can be calculated by determining

the deflection obtained for a known voltage with a known resistance of about 100,000 ohms substituted for the electrolysis cell.

Solutions of  $\text{CdCl}_2$ ,  $\text{ZnCl}_2$ , and  $\text{MnCl}_2$  are first studied, with potassium chloride as the supporting electrolyte. The solutions are made 0.1 N in KCl and 0.001 N in the reducible ion. To suppress maxima, 0.1 ml of a 0.2 per cent stock solution of Triton X-100† is added for each 10 ml of solution being analyzed. Gelatin may also be used as a maximum suppressor; it should be used in amounts not exceeding 0.01 per cent by addition of the necessary quantity of a *fresh* 0.5 per cent stock solution prepared from high-quality gelatin.

A sample of the first solution is placed in the working cell containing a large mercury-pool electrode, and nitrogen is bubbled through the solution to remove dissolved air. The dropping-mercury electrode is then inserted to complete the cell assembly, and the current-voltage curve determined. The other two solutions are then treated similarly.

Measurements are next made on a series of solutions of  $\text{CdCl}_2$  to test the relation between the concentration and the diffusion current. Concentrations of  $10^{-2}$ ,  $5 \times 10^{-3}$ ,  $10^{-3}$ ,  $5 \times 10^{-4}$ , and  $10^{-4}$  equiv of  $\text{CdCl}_2$  per liter are used, with 0.1 N KCl as supporting electrolyte. A maximum suppressor is not required in this case. An appropriate voltage is selected on the basis of the previous work, and the corresponding residual current is determined by a measurement on the supporting electrolyte solution itself. The diffusion current is also determined for an unknown solution of  $\text{CdCl}_2$  in 0.1 N KCl.

Finally, a polarogram is obtained for a solution prepared by mixing equal volumes of the 0.001 N  $\text{CdCl}_2$  and  $\text{ZnCl}_2$  solutions prepared earlier, to illustrate the successive discharge of two different reducible ions. A maximum suppressor is required here.

The cell is then removed, and a beaker placed below the electrode to catch the flowing mercury. The electrode is rinsed with distilled water, then dried carefully with filter paper, care being taken to remove water from the end of the capillary. The mercury flow is permitted to continue for several minutes, and the reservoir is then lowered to stop the flow.

**Calculations.** The several complete current-voltage curves are plotted; the half-wave potentials are determined for the various ions, and the results compared with accepted values.<sup>3</sup>

A graph of diffusion current versus concentration is prepared for the  $\text{CdCl}_2$  solutions, and the concentration of  $\text{CdCl}_2$  in the unknown solution is obtained by its use.

**Practical Applications.** A knowledge of the decomposition potential is important in the calculation of the energy requirements in an electrolytic process such as electroplating.

† Manufactured by the Rohm and Haas Co., Philadelphia.

The dropping-mercury electrode has been applied in analysis for a large variety of substances, both inorganic and organic. The analyses can be made quickly, and often with very small quantities of material. Each analysis, however, must be regarded as empirical and reliable only when checked against known concentrations of the same material.

The polarographic determination of dissolved oxygen has proved useful in respiration studies and various biological investigations.<sup>6</sup>

**Suggestions for Further Work.** The reduction of oxygen at the dropping-mercury electrode may be investigated, and the efficiency of the methods previously recommended for the removal of oxygen from the solutions studied may be checked. Oxygen is reduced irreversibly at the dropping-mercury electrode in two steps; the first wave is associated with the reduction of oxygen to hydrogen peroxide, and the second corresponds to the reduction of hydrogen peroxide. The marked maximum otherwise associated with the first wave is readily suppressed in the conventional fashion.

The influence of complex ion formation may be illustrated by comparison of the polarograms obtained for lead ion in 1 N NaOH and 0.1 N KCl as supporting electrolyte. The following reference reduction potentials are pertinent: Hg,Hg<sub>2</sub>Cl<sub>2</sub>; KCl (0.1 N), 0.355 volt, and Hg,HgO;NaOH (1 N), 0.140 volt. The values given are for 25°C and are referred to the standard hydrogen electrode.

Directions for a number of other interesting experiments have been given by Meites.<sup>4</sup>

#### References

1. Delahay, "New Instrumental Methods in Electrochemistry," Interscience Publishers, Inc., New York (1954).
2. Ilkovic, *Collection Czech Chem. Commun.* **6**, 498 (1934).
3. Kolthoff and Lingane, *Chem. Revs.*, **24**, 1-94 (1939); "Polarography," 2d ed., Interscience Publishers, Inc., New York (1952).
4. Meites, "Polarographic Techniques," Interscience Publishers, Inc., New York (1955).
5. Müller in Weissberger (ed.): "Technique of Organic Chemistry," 3d ed., Vol. I, Pt. IV, Chap. 48, Interscience Publishers, Inc., New York (1960).
6. Petering and Daniels, *J. Am. Chem. Soc.*, **60**, 2796 (1938).

## CHAPTER 9

# *Electromotive Force*

### 31. SINGLE-ELECTRODE POTENTIALS

In this experiment determinations are made of the electrode potentials of several metals. Experience is gained in the use of the potentiometer and electrochemical conventions.

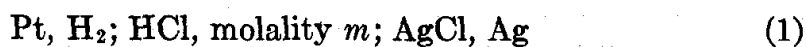
**Theory.** An electrochemical cell is a device whereby the decrease in free energy of a system in a spontaneous process may be made a source of electrical work. The process involved may be an ordinary chemical reaction, the transfer of a constituent from one concentration level to another, etc.; the essential requirement is that it must be possible to accomplish it as the resultant of an oxidation step and a reduction step, each of which takes place separately at an appropriate electrode. The electromotive force of the cell depends upon the change of state of the cell system, and also upon the closeness of approach to reversibility permitted by the intrinsic characteristics of the electrode processes themselves and by the degree of irreversibility introduced by the manner in which the cell is used. In the present case we shall be concerned with cells which are considered capable of reversible performance and shall assume that the electromotive-force measurements are made by the potentiometric method, which permits the current drawn from the cell in the voltage measurement to be reduced to a level for which an adequate approach to reversible cell performance is obtained. It also permits a true test of reversibility, since the direction of the cell reaction and current flow can be changed at will.

In order to correlate a cell voltage with a cell reaction as written on paper, it is necessary to follow certain conventions. For a given cell reaction, the corresponding cell is designated by specifying, at the left, the electrode at which oxidation takes place and, at the right, the electrode at which reduction takes place when the reaction takes place in the direction specified. (For a given cell expression, the conventional cell reaction can be written down directly in terms of these same requirements.) If the spontaneous cell reaction actually takes place in the

direction specified, the right-hand electrode will necessarily be the positive electrode. Correspondingly, in this case, a positive sign is required for the voltage of the cell, since the electrical work, which is proportional to the cell voltage, is done at the expense of the free energy of the cell system. Conversely, if the right-hand electrode is found to be negative, the cell electromotive force should be given a negative sign, and the cell reaction postulated does not take place spontaneously.

The voltage of the cell may be considered to be the resultant of two single-electrode potentials. By convention, the voltage is then calculated as the single-electrode potential for the electrode written at the right minus the single-electrode potential for the electrode written at the left in the cell expression. These conventional electrode potentials are then reduction potentials. The absolute values of such electrode potentials cannot be determined, so the hydrogen electrode with hydrogen gas at unit fugacity and hydrogen ion at unit activity is taken as the reference electrode with a defined potential of zero. A comprehensive summary of theoretical and experimental information on this and other reference electrodes has been provided by Ives and Janz.<sup>8</sup>

For unit activity of all species taking part in the cell reaction, the electromotive force is designated as  $E^\circ$  and is called the standard electromotive force. This standard electromotive force then can be expressed in terms of two standard electrode potentials. The determination of the standard electrode potential for a given electrode then requires a knowledge of the value of  $E^\circ$  for a cell containing this electrode and a second electrode for which the standard potential is known. Thus, for the cell



the standard electromotive force  $E^\circ$  is equal to the standard electrode potential of the silver-silver chloride electrode, since the standard electrode potential of the hydrogen electrode is zero. Extensive tabulations of standard electrode potentials are available.<sup>3,9</sup>

The calomel electrode, often used as a reference electrode, does not conform completely to the conventional standard-state specifications. The mercury and mercurous chloride are present as the pure liquid and solid, respectively, and thus are at unit activity relative to the ordinary standard-state choice. The activity of the chloride ion is not unity, however, but varies with the concentration of potassium chloride used. This variation is then accounted for in the different reference electrode potentials given for the calomel electrode for different potassium chloride concentrations.

The electrode potential changes with the activities of the ions. The fundamental equation governing the effect of activity of ions on the



voltage is

$$E = E^\circ - \frac{RT}{nF} \ln Q \quad (2)$$

where  $R$  = gas constant, 8.314 joules deg<sup>-1</sup> mole<sup>-1</sup>

$F$  = faraday, 96,490 coulombs equiv<sup>-1</sup>

$n$  = number of faradays for reaction as written

$Q$  = activity quotient

$$Q = \frac{a_G^g a_H^h}{a_A^a a_B^b} \quad (3)$$

for the generalized reaction  $aA + bB = gG + hH$ .

The type of cell used in the laboratory may be written as follows for a monovalent metal ion:



The electromotive force of this cell is given by

$$E = -E_{M^+,M}^\circ - \frac{RT}{F} \ln a_{M^+} + E_{\text{KCl(sat)}; \text{Hg}_2\text{Cl}_2, \text{Hg}}^\circ + E_j \quad (5)$$

where  $E_{M^+,M}^\circ$  is the standard electrode potential for the metal electrode;  $E_{\text{KCl(sat)}; \text{Hg}_2\text{Cl}_2, \text{Hg}}^\circ$  is the electrode potential for the saturated calomel electrode; and  $E_j$  is the liquid-junction potential which is made small by the action of the KCl salt bridge which couples the calomel electrode to the solution in which it is immersed.

For the cells involving divalent metal ions,



the electromotive force is given by

$$E = -E_{M^{++},M}^\circ - \frac{RT}{2F} \ln a_{M^{++}} + E_{\text{KCl(sat)}; \text{Hg}_2\text{Cl}_2, \text{Hg}}^\circ + E_j \quad (7)$$

Irrespective of the accuracy of the electromotive-force measurements, an exact value for a single-electrode potential cannot be calculated from measurements on a cell of type (4), because the salt bridge does not completely eliminate the liquid-junction potential.

In Eqs. (5) and (7), the activities may be expanded in terms of activity coefficients and molalities by use of the relations

$$a_i = \gamma_i m_i \quad (8)$$

where  $a_i$  = activity of species  $i$

$\gamma_i$  = activity coefficient of species  $i$

$m_i$  = molality of species  $i$

For a typical strong electrolyte  $A_{\nu_+}B_{\nu_-}$  which dissociates into  $\nu_+$  positive ions A and  $\nu_-$  negative ions B, the mean ionic activity coefficient  $\gamma_{\pm}$  is defined by

$$\gamma_{\pm} = (\gamma_A^{\nu_+} \gamma_B^{\nu_-})^{1/\nu} \quad (9)$$

where  $\nu = \nu_+ + \nu_-$ . This mean ionic activity coefficient is measurable; individual ionic activity coefficients  $\gamma_A$  and  $\gamma_B$  cannot be separately determined from thermodynamic experiments. In Eqs. (5) and (7) it is usual to substitute  $\gamma_{\pm}$  for  $\gamma_+$ ; this is actually only an approximation.

**Apparatus.** Potentiometer; electrodes of cadmium, copper, lead, silver, zinc; electrode vessels; calomel electrode (saturated potassium chloride); standard cell; dry cells; key; 0.100 M solutions of cadmium chloride, copper sulfate, lead nitrate, silver nitrate, zinc sulfate; 2 N ammonium nitrate solution; 100-ml volumetric flask; one 10-ml pipette.

**Procedure.** In this experiment, the single-electrode potentials of cadmium, copper, lead, silver, and zinc are to be determined using 0.1 and 0.01 M solutions. The 0.1 M solutions are prepared carefully by weighing out the salts with due allowance for water of crystallization, or better, by determining the concentration by analytical methods. The 0.01 M solutions may be prepared by pipetting exactly 10 ml of the 0.1 M solution into a 100-ml volumetric flask and diluting with distilled water.

The electrodes of zinc and lead are prepared by pouring the molten metal from a small porcelain crucible into a glass tube and setting a copper wire into the upper end for a terminal. When cold, the glass tube is broken and removed. For the copper electrode a wire of large diameter is used. The electrodes may be amalgamated, to give a steady potential, less affected by mechanical strains. It should be remarked, however, that the potential of an amalgamated electrode is not necessarily exactly that of the pure metal. The electrode is placed in a beaker of dilute acid with a drop of mercury, and a small brush or cloth is used to spread the mercury over the surface of the electrode.

The silver electrode may be prepared by electroplating spongy silver on a platinum-wire cathode in a silver cyanide (**caution**) solution, using a silver or platinum anode. A single dry cell gives sufficient voltage. Pure silver wire or strip may also be used for the cathode. The silver electrode is not amalgamated.

For best results the aqueous solutions should be bubbled out with a stream of hydrogen or purified nitrogen, to remove dissolved oxygen.

The experimental assembly is shown in Fig. 43.

The electrodes are mounted in rubber stoppers and set tightly into vessels having sidearms to provide liquid contact with a reference electrode. The snugly fitting stopper prevents the solution from siphoning out of the electrode vessel.

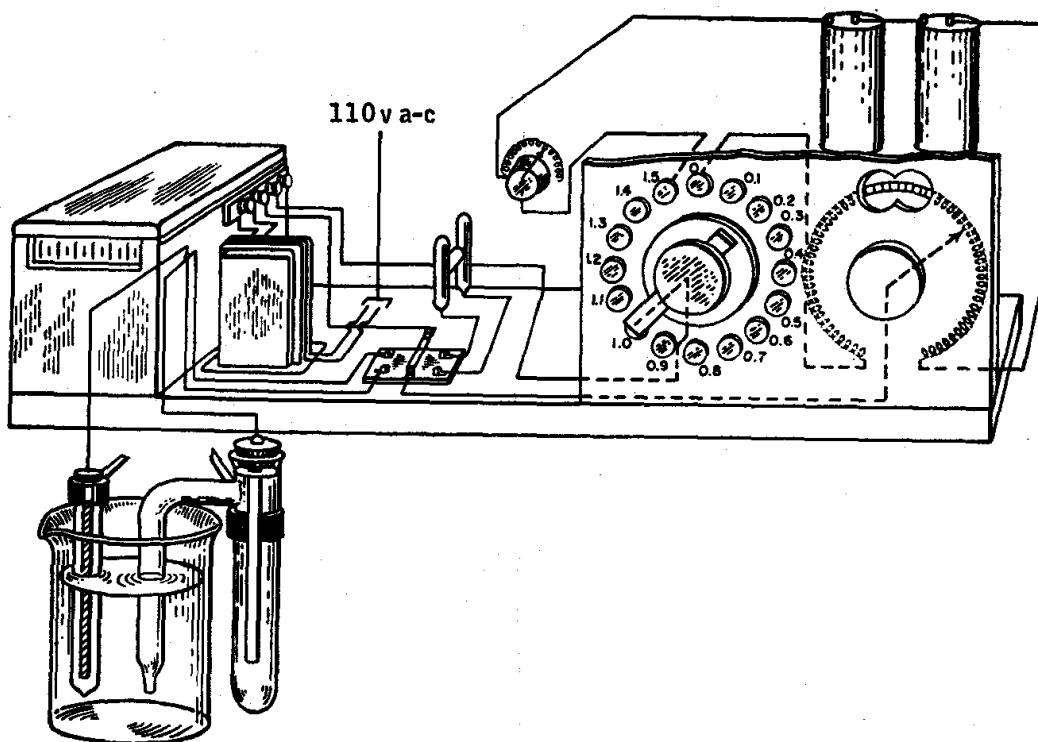


FIG. 43. Measurement of electrode potentials with the potentiometer.

A saturated calomel electrode is used for the reference electrode. In the commercially available type shown later in Fig. 47, a thread of glass fibers wet with KCl solution performs the function of a salt bridge to minimize the liquid-junction potential. In the case of the silver electrode, it is necessary to connect the silver and calomel electrodes through a beaker of 2 N ammonium nitrate which is set between the silver electrode and the calomel cell to act as an auxiliary salt bridge which prevents precipitation of silver chloride.

The electromotive force of this cell, with the metal electrode and calomel cell, is determined by means of the potentiometer. The principle of the potentiometer is shown in Fig. 44, in which the electromotive forces, or potentials, of two cells *A* and *B* may be balanced. A wire *RS*, of uniform and high resistance, is stretched along a linear scale. The current is supplied by cell *B*, whose electromotive force is larger than that of cell *A*. Since the wire is of uniform resistance and the same current passes through each section of it, there will be a uniform fall of potential

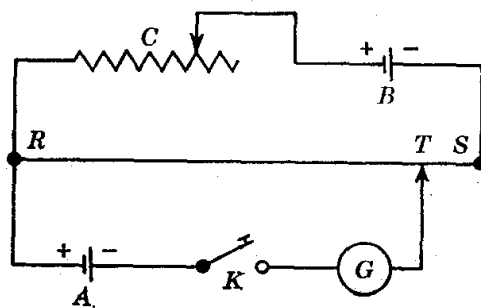


FIG. 44. Simple potentiometer circuit.

per unit length in the direction  $R$  to  $S$ . To measure an unknown electromotive force (cell  $A$ ), a second circuit containing a key, galvanometer, and sliding contact is necessary. The positive terminal of cell  $A$  is connected opposite the positive terminal of cell  $B$ , at  $R$ . The sliding contact  $T$  is moved along the wire, until there is no deflection of the galvanometer  $G$  when the key  $K$  is pressed. If the sliding contact is moved too far to the right, the galvanometer will deflect in one direction; if too far to the left, the galvanometer will deflect in the other direction. If the potential drop per unit length of the slide wire is known from the potential difference between  $R$  and  $S$  and the distance between  $R$  and  $S$ , the electromotive force of cell  $A$  may be determined directly from the length  $RT$ . Then, when the setting at  $T$  gives no galvanometer deflection, the ratio  $RT/RS$  gives the ratio of the voltage of cell  $A$  to the potential difference between  $R$  and  $S$ .

Potentiometers are designed so that the fall of potential per unit length of wire is adjusted to some decimal fraction of a volt, and the unknown voltage is then read directly from the scale. This reading is accomplished by means of the rheostat  $C$ , using a Weston cell (page 468) in place of cell  $A$ . The Weston standard cell has a voltage of 1.0186 volts at  $20^\circ$ . The point  $T$  is moved to a position such that there are 1018.6 divisions of the wire between  $R$  and  $S$ . The current from the cell  $B$  through the wire is then changed by the adjustable resistance  $C$  until the galvanometer shows no deflection, signifying that the fall of potential along  $RT$  is 1.0186 volts and the difference of potential per unit length is 1 millivolt. Having once adjusted the potentiometer with the rheostat  $C$  against the standard cell, the readings thereafter are given directly in voltages.

It is important to record which is the positive electrode, i.e., the electrode connected to the positive terminal of the potentiometer when the circuit is balanced. If there is any doubt as to which is positive, the circuit may be compared with one in which an ordinary dry cell is used. In this cell the zinc is negative and the carbon electrode is positive. The negative terminal is the one that gives a blue color when the wires are both touched to a piece of moist litmus paper. If the galvanometer always deflects in the same direction no matter how the potentiometer is set, the terminals of the unknown cell must be reversed to obtain a point of balance.

**Calculations.** For a particular cell, a cell reaction and the corresponding cell expression as in Eq. (1) are written. The appropriate electromotive-force expression is written in accordance with Eqs. (5) and (7). The electromotive force measured for the cell is given the proper sign, determined as the sign of the right-hand electrode in the cell expression used. The necessary mean-ionic-coefficient data are given in Table 1. The standard electrode potential of the metal electrode is

then computed on the basis of the value 0.2444 volt (Ref. 8) for the reference potential for the saturated calomel electrode, and the value obtained compared with the accepted value as given in reference tables.

TABLE 1. MEAN ACTIVITY COEFFICIENTS OF ELECTROLYTES AT 25°C

Electrolyte	Concentration		
	0.001 M	0.01 M	0.1 M
Cadmium chloride.....	0.819	0.524	0.228
Copper sulfate.....	0.69	0.40	0.16
Lead nitrate.....	0.89	0.69	0.37
Silver nitrate.....	0.95	0.90	0.731
Zinc sulfate.....	0.700	0.387	0.150
Sodium chloride.....	.....	0.9032	0.7784
Hydrochloric acid.....	0.9656	0.9048	0.7964

**Practical Applications.** A knowledge of the value of  $E^\circ$  is essential in the calculation of mean ionic activity coefficients and other thermodynamic properties for solutions of electrolytes from electromotive-force measurements on suitable cells.

**Suggestions for Further Work.** It is of interest to study the effect of continued dilution of the metallic ions surrounding an electrode upon its potential. It has been suggested in the experiment that 0.01 M and 0.1 M salt concentrations be used. By making further careful dilutions of these solutions, it is possible in principle to extrapolate to zero concentration where the activity coefficients approach unity. However, the experimental errors become very large at these high dilutions. For evaluating  $\gamma_{\pm}$  and  $E^\circ$ , it is necessary to use some function of the molality which will give a straight line when plotted against the molality and thus permit accurate extrapolations to infinite dilution from data at moderate concentrations where the accuracy is good.

The values of  $E^\circ$  and  $\gamma_{\pm}$  for hydrochloric acid are determined in Exp. 32.

The effect on the single-electrode potential of bending or straining the electrode is sufficient to be measured by means of the student potentiometer, except in the case of the softest of the metals.

### References

1. Bockris, "Electrochemistry," Academic Press, Inc., New York (1954).
2. Conway, "Electrochemical Data," Elsevier Press, Inc., Houston, Tex. (1952).
3. Daniels and Alberty, "Physical Chemistry," 2d ed., Chap. XIV, John Wiley & Sons, Inc., New York (1961).
4. Dole, "Principles of Experimental and Theoretical Electrochemistry," McGraw-Hill Book Company, Inc., New York (1935).
5. Glasstone, "Introduction to Electrochemistry," D. Van Nostrand Company, Inc., Princeton, N.J. (1942).
6. Harned and Ehlers, *J. Am. Chem. Soc.*, **54**, 1350 (1932).
7. Harned and Owen, "The Physical Chemistry of Electrolytic Solutions," 3d ed., Reinhold Publishing Corporation, New York (1958).
8. Ives and Janz, "Reference Electrodes," Academic Press, Inc., New York (1961).

9. Latimer, "The Oxidation States of the Elements and Their Potentials in Aqueous Solutions," Prentice-Hall, Inc., Englewood Cliffs, N.J. (1952).
10. Lewis and Randall, "Thermodynamics," 2d ed., rev. by Pitzer and Brewer, McGraw-Hill Book Company, Inc., New York (1961).
11. MacInnes, "The Principles of Electrochemistry," Reinhold Publishing Corporation, New York (1939).

### 32. THE HYDROGEN ELECTRODE

This experiment illustrates the use of the hydrogen electrode, which is the basic reference electrode for electromotive-force studies. A cell consisting of a hydrogen electrode and a silver-silver chloride electrode is used to determine the standard potential of the silver-silver chloride electrode and the activities of hydrochloric acid solutions.

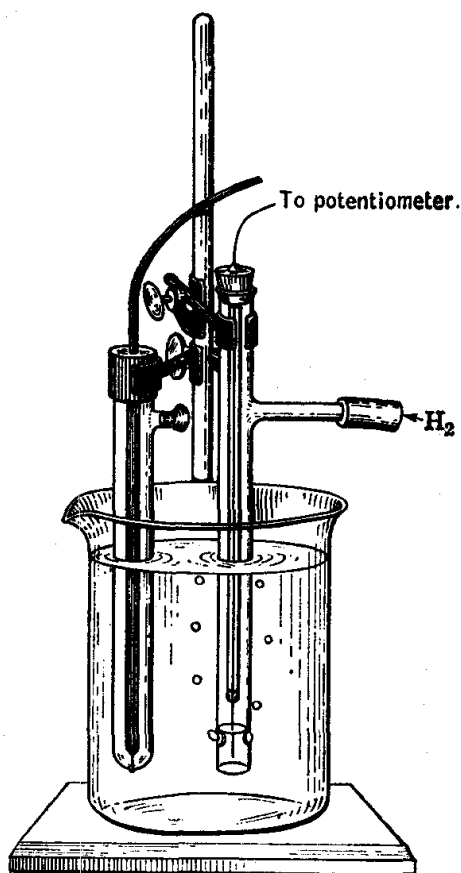


FIG. 45. Hydrogen electrode and calomel electrode.

#### A. HYDROGEN ELECTRODE

**Theory.** A cell involving a hydrogen electrode is illustrated in Fig. 45. A hydrogen electrode is formed by bubbling pure hydrogen gas over a wire or small foil with a specially prepared surface which is able to catalyze the reaction



thus establishing equilibrium between hydrogen molecules and the hydrogen ions in the solution in which the electrode is immersed. The hydrogen electrode is designed so that a platinized platinum wire is partly covered by the solution. As hydrogen is passed into the sidearm and bubbles out into the solution, the level of the solution at the wire rises and falls so that the wire is alternately bathed in hydrogen and in the

solution. The hydrogen electrode cannot be used in the presence of certain substances like  $\text{H}_2\text{S}$ , cyanides, and arsenic compounds which inhibit the catalysis of the electrode process.

Because hydrogen gas at pressures near one atmosphere shows only a slight deviation from ideality, its activity can be set equal to the magnitude of its partial pressure in standard atmospheres. Since the standard potential of the hydrogen electrode is conventionally assigned the

value zero at all temperatures, the potential of a hydrogen electrode half-cell is given by

$$E = -\frac{RT}{F} \ln \frac{a_{H^+}}{p_{H_2}^{1/2}} \quad (1)$$

When used in conjunction with a saturated calomel electrode as illustrated in Fig. 45, the cell may be represented by



where there is a liquid junction between the saturated KCl solution and the acid solution. This cell operates spontaneously, with oxidation occurring at the left electrode. Thus this electrode is connected to the negative terminal of the potentiometer, and the electrode at the right is connected to the positive terminal. The electromotive force of this cell is given by

$$E = E_{\text{KCl(sat)}; \text{Hg}_2\text{Cl}_2, \text{Hg}}^\circ - \frac{RT}{F} \ln \frac{a_{H^+}}{p_{H_2}^{1/2}} + E_j \quad (2)$$

where  $E_{\text{KCl(sat)}; \text{Hg}_2\text{Cl}_2, \text{Hg}}^\circ$  is the standard electrode potential of the saturated calomel electrode, and  $E_j$ , the potential caused by the liquid junction, is assumed to be independent of the concentration of the acid solution. Equation (2) may be rearranged to

$$-\log a_{H^+} + \frac{1}{2} \log p_{H_2} = \frac{E - E_{\text{KCl(sat)}; \text{Hg}_2\text{Cl}_2, \text{Hg}}^\circ - E_j}{2.303RT/F} \quad (3)$$

The activity of hydrogen ions may be expressed in terms of the pH, which is  $-\log a_{H^+}$ . Thus

$$\text{pH} = \frac{E - E_{\text{KCl(sat)}; \text{Hg}_2\text{Cl}_2, \text{Hg}}^\circ - E_j}{2.303RT/F} - \frac{1}{2} \log p_{H_2} \quad (4)$$

where the partial pressure of hydrogen above the solution,  $p_{H_2}$ , is given in atmospheres. For the saturated calomel electrode,  $E_{\text{KCl(sat)}; \text{Hg}_2\text{Cl}_2, \text{Hg}}^\circ + E_j$  is taken to have the value 0.2444 volt at 25°. A value of 0.2802 volt would be used for the calomel electrode containing 1 N KCl at 25°. Values for other temperatures and other reference electrodes are given by Bates.<sup>1</sup>

Since it is not possible to measure individual ion activities, the pH scale is a conventional one.<sup>1</sup> Although glass electrodes are widely used for the determination of pH, the hydrogen electrode is the standard in this field.

**Apparatus.** Potentiometer and accessories; hydrogen electrode; calomel electrode; 0.5 N hydrochloric acid (with normality accurately known); 0.5 N (approximate) sodium hydroxide.

**Procedure.** A known volume of 0.5 N hydrochloric acid (say, 25 ml) is placed in a beaker, and the hydrogen electrode and saturated calomel electrode are immersed as illustrated in Fig 45. Hydrogen from a tank is allowed to bubble slowly through the glass hood of the hydrogen electrode. For research purposes it is necessary to remove any oxygen and carbon dioxide in the hydrogen. Unless found to be free from sulfur, all the rubber tubing used should be boiled in concentrated sodium hydroxide solution and thoroughly rinsed.

The student should be familiar with the principle and operation of the potentiometer before starting the experiment (see Exp. 31 and Chap. 22). Since the cell operates spontaneously with oxidation occurring at the hydrogen electrode, the hydrogen electrode is connected to the negative terminal of the potentiometer and the calomel electrode to the positive terminal. The circuit is closed only momentarily with the tapping key to find the point of balance because any appreciable passage of current will polarize the electrodes.

The initial voltage should be approximately 0.26 volt; otherwise the electrode is not functioning properly. Replatinizing the electrode will usually correct faulty behavior of a hydrogen electrode. When the electrode is properly platinized, a steady voltage should be reached in half a minute or so. After adding a drop of phenolphthalein solution, approximately 0.5 N sodium hydroxide is added slowly from a burette, and the solution is stirred after each addition. At first about 5 ml is added at a time, but as the neutral point is approached, readings are taken more frequently, and after passing the end point, larger amounts can again be added. The exact end point should be found by accurate drop-by-drop titrations, so that the pH at which the phenolphthalein changes color can be calculated. The addition of alkali is continued until the voltage has become practically constant.

The barometric pressure is read so that the partial pressure of hydrogen above the solution may be calculated.

To prepare the hydrogen electrode, it is wiped as clean as possible and dipped for a few seconds into warm aqua regia, under the hood. The electrode is then platinized, i.e., coated with a deposit of platinum black, by electrolyzing the electrode as the negative pole in a 1 per cent solution of platinic chloride. Another platinum wire serves as the anode, and the potential is supplied by two dry cells connected in series. The electrolysis is allowed to continue for several minutes. The electrodes are then placed in a small beaker of distilled water to which a drop of concentrated sulfuric acid has been added, and the electrolysis is allowed to proceed as before. This treatment produces hydrogen and removes any impurities. The electrode should be kept in distilled water until used; it should never be allowed to dry out. Electrodes must be replati-

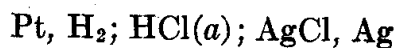


nized from time to time, as the coating of platinum black becomes "poisoned" with use.

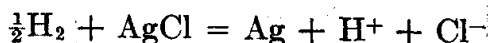
**Calculations.** Graphs are drawn in which the numbers of milliliters of sodium hydroxide solution added are plotted as abscissas with voltages as ordinates. The steepest part of the curve corresponds to the end point. The corresponding volume is used for calculating the normality of the sodium hydroxide from the known normality of the original hydrochloric acid solution. The hydrogen-ion activity of a given solution is calculated by means of Eq. (4) from the observed voltage  $E$  of the cell. The partial pressure of hydrogen above the solution is calculated by subtracting the vapor pressure of water from the corrected barometric pressure. The hydrogen-ion activity and pH value corresponding to the voltage at which phenolphthalein changes color may now be calculated.

#### B. ELECTROMOTIVE-FORCE CELL WITHOUT TRANSFERENCE

The liquid junction in the cell used in the first part of this experiment contributes a potential difference which cannot be determined with exactness. Such cells are therefore not suitable for accurate thermodynamic measurements. The problem of the liquid-junction potential is avoided in cells such as



which contain a single electrolyte solution. The cell reaction is



and the electromotive force of the cell is given by

$$E = E^\circ - \frac{RT}{F} \ln \frac{a_{\text{H}^+} a_{\text{Cl}^-} a_{\text{Ag}}}{a_{\text{AgCl}} a_{\text{H}_2}^{1/2}} \quad (5)$$

where  $E^\circ$  is the standard reduction potential for the silver-silver chloride electrode. The activities of Ag and AgCl are unity because of the presence of the solid phases, and  $a_{\text{H}^+} a_{\text{Cl}^-}$  may be written as  $\gamma_{\pm}^2 m^2$ , where  $\gamma_{\pm}$  is the mean ionic activity coefficient and  $m$  is the molality.

$$E = E^\circ - \frac{RT}{F} \ln \frac{\gamma_{\pm}^2 m^2}{p_{\text{H}_2}^{1/2}} \quad (6)$$

At atmospheric pressures it is satisfactory to assume that the activity of hydrogen gas is given by its pressure in standard atmospheres.

The value of the standard potential for the silver-silver chloride electrode has been determined<sup>2,3</sup> in very careful research in which the Debye-Hückel theory is used to guide the extrapolation of experimental values

to  $m = 0$ , where  $\gamma_{\pm}$  is taken to be unity. The values of the reduction potential at 20, 25, and 30° are 0.22557, 0.22234, and 0.21904 volt, respectively. Thus a measurement of the electromotive force of a cell at a particular hydrogen pressure and molality of hydrochloric acid makes it possible to calculate the mean ionic activity coefficient of hydrochloric acid by use of Eq. (6).

**Apparatus.** Potentiometer and accessories; hydrogen electrode and tank of hydrogen; silver-silver chloride electrode; approximately 2 N HCl of accurately known molality.

**Procedure.** The construction of the cell is illustrated in Fig. 46. If silver-silver chloride electrodes are not available, they may be prepared

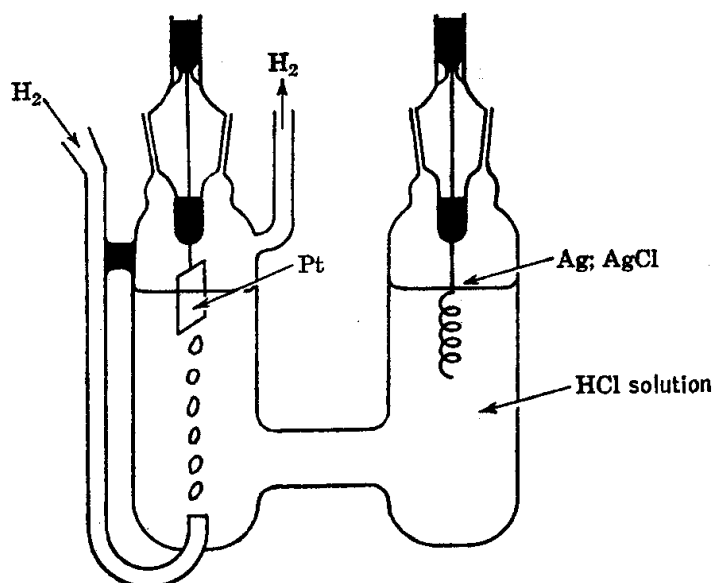
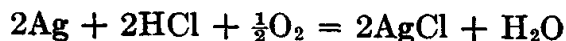


FIG. 46. Cell without transference for the determination of the activity of the hydrochloric acid in solution.

from a piece of platinum wire (No. 26) about 7 mm in length coiled into a helix and sealed into a glass tube as illustrated in Fig. 46. The electrode is cleaned in warm 6 N nitric acid, and silver is electrodeposited from a silver nitrate solution. The surface of the deposit is then converted to silver chloride by electrolysis as the anode in 1 N HCl solution. Too thick a coat of silver chloride will make the electrode response sluggish. The electrodes are immersed in distilled water for storage.

These electrodes are subject to an aging effect during the first 20 to 30 hr after preparation and are sensitive to traces of bromide in the solutions. In the presence of air the potential is slightly more positive than for an air-free solution, probably because of a slight decrease in the concentra-

tion of chloride ion within the interstices of the electrode by the reaction



These effects all have to be taken into account in work of the highest precision.

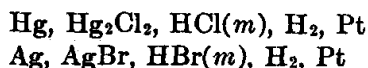
The electromotive forces of the cell containing 2 N, 1 N, 0.5 N, 0.25 N, and 0.125 N hydrochloric acid are measured at a constant temperature, preferably 25°. The barometric pressure is recorded.

**Calculations.** The molalities of the hydrochloric acid solutions are calculated from the known normalities by use of density data which may be obtained from a handbook. Since several solutions are involved, it will be convenient to prepare a plot of molality against normality.

The partial pressure of hydrogen above the solution is taken to be equal to the difference between the barometric pressure and the vapor pressure of water. In more accurate work the vapor pressure of the solution would have to be known. The pressure in Eq. (6) must be expressed in standard atmospheres.

The mean ionic activity coefficients of the various hydrochloric acid solutions are calculated by use of Eq. (6). A plot of activity coefficient versus molality is prepared, and a comparison with the literature values is made.

**Suggestions for Further Work.** Measurements may be made in the concentration range 0.005 to 0.05 molal, and the data extrapolated by use of the Debye-Hückel theory to obtain a value of  $E^\circ$ . Other cells suitable for study are



#### References

1. Bates, "Electrometric pH Determinations," p. 201, John Wiley & Sons, Inc., New York (1954).
2. Daniels and Alberty, "Physical Chemistry," pp. 385, 406, John Wiley & Sons, Inc., New York (1961).
3. Harned and Owen, *J. Am. Chem. Soc.*, **55**, 1350, 2179 (1933).
4. Harned and Owen, "The Physical Chemistry of Electrolytic Solutions," 2d ed., Reinhold Publishing Corporation, New York (1950).
5. MacInnes, "The Principles of Electrochemistry," Reinhold Publishing Corporation, New York (1939).
6. Pinching and Bates, *J. Research, Natl. Bur. Standards (U.S.)*, **37**, 311 (1946).
7. Ricci, "Hydrogen Ion Concentration," Princeton University Press, Princeton, N.J. (1952).

### 33. THE GLASS ELECTRODE

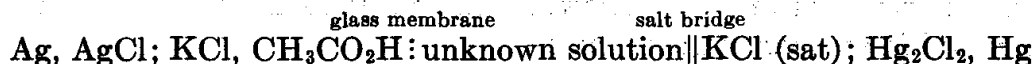
The use of the glass electrode for the determination of pH is illustrated by the titrations of phosphoric acid and glycine. The preparation

of buffers of given pH and the determination of buffer capacity are introduced.

**Theory.** The theory of pH measurements is discussed in Exp. 32.

The glass electrode has several advantages over the hydrogen electrode for the measurement of pH. The glass electrode functions in both oxidizing and reducing media and in the presence of proteins and sulfur compounds, all of which interfere with the use of platinized platinum.

The glass electrode consists of a thin membrane of soft glass enclosing a dilute solution of potassium chloride and acetic acid in which is immersed a platinum wire coated with Ag-AgCl. The variation of the potential of a glass electrode with varying hydrogen-ion concentration is the same as that of a hydrogen electrode.† A number of theories for the action of a glass electrode have been proposed.<sup>1</sup> A saturated calomel electrode is used in conjunction with the glass electrode, so that the cell may be represented diagrammatically as follows:



The construction of commercially available electrodes is illustrated in Fig. 47. The electromotive force of this cell cannot be measured with a potentiometer because of the high resistance of the glass membrane. For this reason an electronic voltmeter is used. The glass-electrode potential changes 0.0591 volt/pH unit at 25°C, and pH meters are graduated directly in terms of pH. According to the simplified theory, two solutions of the same hydrogen-ion activity, with the glass membrane interposed, should show no potential difference. However, glass electrodes usually do show a small potential (asymmetry potential) under these conditions, and for this reason it is necessary to set the pH meter periodically by using a buffer of known pH. Some useful buffers for this purpose studied by MacInnes<sup>5</sup> are given in Table 1.

TABLE 1. pH VALUES OF STANDARD BUFFERS

Buffer	12°C	25°C	38°C
CH <sub>3</sub> CO <sub>2</sub> H(0.1 N), CH <sub>3</sub> CO <sub>2</sub> Na(0.1 N).....	4.650	4.640	4.635
Potassium acid phthalate (0.05 M).....	4.000	4.000	4.015

The pH of a mixture of a weak acid or base and its salt may be calculated with a reasonable degree of precision from the ordinary mass-action equilibrium formulation

$$K = \frac{[\text{H}^+][\text{A}^-]}{[\text{HA}]} \quad (1)$$

† At pH's above 10 it is necessary to correct for response to Na<sup>+</sup> ions unless special glasses are used.

in which HA represents a weak acid. Taking the logarithm of this equation and rearranging, we obtain

$$\text{pH} = \text{pK} + \log \frac{[\text{A}^-]}{[\text{HA}]} \quad (2)$$

where  $\text{pK}$  is equal to  $-\log K$ . Note that if the concentrations of the acidic and basic forms of the buffer are equal,  $[\text{A}^-] = [\text{HA}]$ , and

$$\text{pH} = \text{pK} = -\log K$$

This fact may be used to determine ionization constants of rather weak acids and bases. The pH of the buffer depends upon the ratio of the

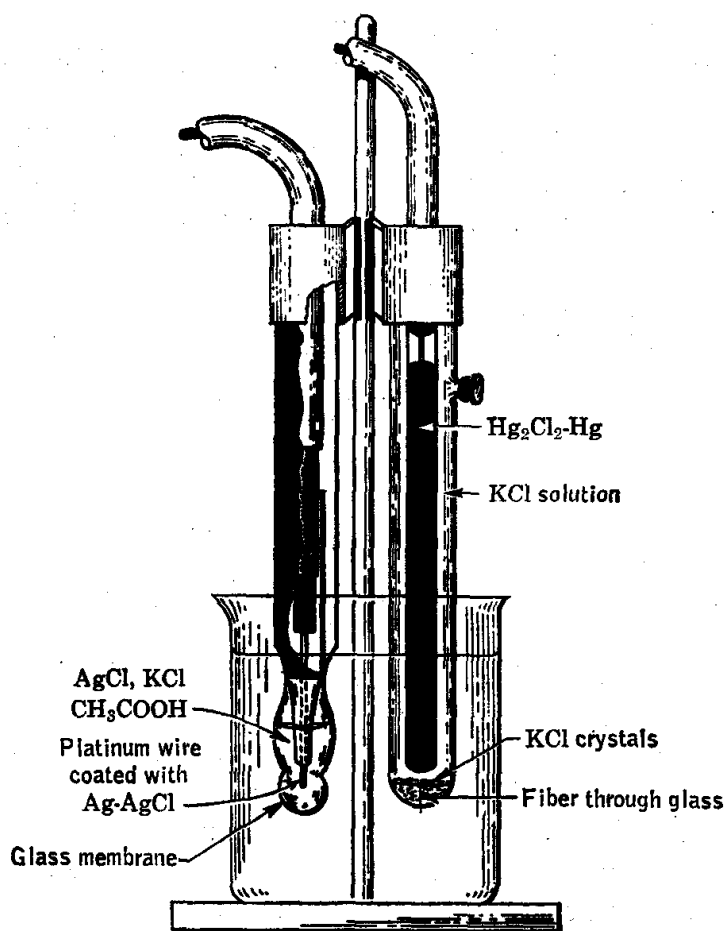


FIG. 47. Glass-electrode-calomel-electrode assembly.

concentrations of these two forms, and not on the total amounts. However, the capacity of a buffer to resist changes of pH produced by the addition of acid or alkali depends upon the concentrations of the two forms present. The slope of a plot of equivalents of acid or base added per liter of buffer versus pH is sometimes called the *buffer capacity*. The

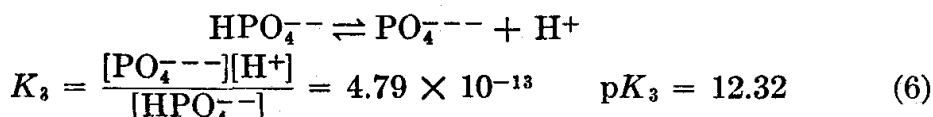
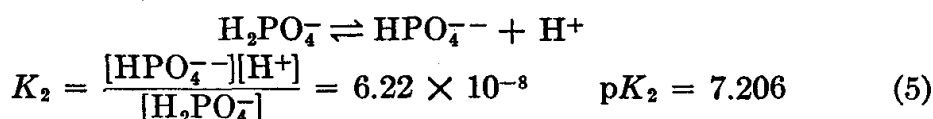
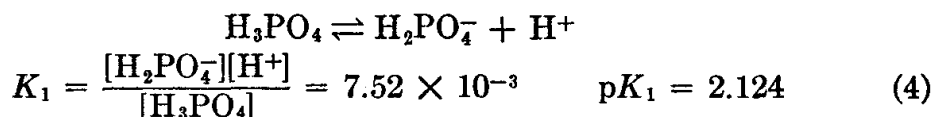
buffer capacity may be calculated from the concentrations of the salt and undissociated acid, using Eq. (3) (see Ref. 7):

$$\frac{dB}{d(\text{pH})} = \frac{2.3 [A^-][HA]}{[A^-] + [HA]} \quad (3)$$

where  $B$  represents the number of equivalents of acid or base added per liter of buffer. The buffer capacity is a maximum at  $\text{pH} = \text{p}K$ . At 1 pH unit away from the  $\text{p}K$ , a buffer is about 33 per cent as effective.

The  $\text{p}K$  value of a weak acid determined with Eq. (2) depends upon the salt concentration, since the equilibrium expression (1) has been written in terms of concentrations rather than activities. The value of the ionization constant of a weak acid or base determined by titration is referred to as the apparent ionization constant, to distinguish it from the thermodynamic ionization constant obtained by extrapolation to infinite dilution.

The titration of a polybasic acid such as phosphoric acid, using a pH meter, may be used to evaluate the ionization constants. The successive ionizations of phosphoric acid may be represented as follows:



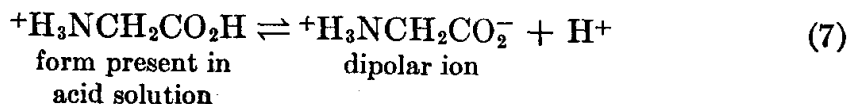
The third dissociation takes place at such a high pH that it cannot be studied in dilute aqueous solutions. The first two end points can be recognized by the large change in pH for a small addition of base.

At the pH at which the second acid group is half neutralized, the hydrogen-ion activity is equal to the equilibrium constant  $K_2$ .

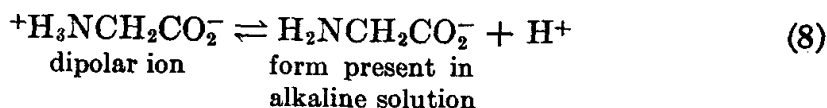
The  $\text{p}K$  values for ionizations (4), (5), and (6) are the thermodynamic values.<sup>3</sup> At 0.1 ionic strength the value of  $\text{p}K_2$  is 6.80. The ionic strength is half the sum of the concentrations of the ions, each multiplied by their valence squared.

In aqueous solution pure glycine exists as a dipolar ion (zwitter ion), as evidenced by the high dielectric constant which is measured for such a solution. When glycine is titrated with acid, the hydrogen ions react with the carboxyl group as illustrated by the reverse of Eq. (7). When half the carboxyl groups have reacted, the hydrogen-ion activity is

equal to the equilibrium constant  $K_1$ . The equivalent pH is  $-\log K_1 = 2.35$ . When neutral glycine is titrated with sodium hydroxide, the hydrogen on the amino group is titrated as indicated by Eq. (8). The equilibrium expressions for these reactions are written as follows:



$$K_1 = \frac{[+\text{H}_3\text{NCH}_2\text{CO}_2^-][\text{H}^+]}{[+\text{H}_3\text{NCH}_2\text{CO}_2\text{H}]} = 4.47 \times 10^{-3} \quad \text{p}K_1 = 2.35$$



$$K_2 = \frac{[\text{H}_2\text{NCH}_2\text{CO}_2^-][\text{H}^+]}{[+\text{H}_3\text{NCH}_2\text{CO}_2^-]} = 1.66 \times 10^{-10} \quad \text{p}K_2 = 9.78$$

The three dissociable hydrogens of phosphoric acid are equivalent in  $\text{H}_3\text{PO}_4$ , and so the question as to which  $\text{H}^+$  dissociates first does not arise. In the case of glycine, there are two possibilities, and various types of evidence, including the high dielectric constant of neutral solutions of glycine, indicate that the carboxyl group is the stronger acid group.

**Apparatus.** pH meter with glass electrode and calomel electrode; bottle of standard buffer; 0.1 N acetic acid; 0.1 N sodium acetate; 0.1 M phosphoric acid; glycine.

#### A. TITRATION OF PHOSPHORIC ACID

**Procedure and Calculations.** The Beckman Model H pH meter is a convenient one for the experiment. The two electrodes, glass and calomel, are fragile and must be handled with great care. The electrodes are mounted on the meter, and the leads to them are inserted at the rear of the instrument. There is a push-button switch above the electrode terminals which is to be locked in the "in" position, except when the pH is being actually read, otherwise the glass electrode will become polarized.

The instrument is connected to the 110-volt a-c line with the main switch at the "start" position and the push-button switch at "in." After some minutes to warm up, the instrument is ready for use. The electrodes are then inserted in a beaker which contains a standard buffer solution. The main switch is turned to pH 0-7. The push-button switch is let out, and the standardization control is used to bring the meter needle to the pH of the standard buffer.

The push-button switch is now locked at the "in" position, and the pointer is set to mark the position of the meter needle. If the meter reads off scale, one switches to the other scale before setting the pointer.

The meter is now ready for use. The electrodes are rinsed with dis-

tilled water and then immersed in the solution of unknown pH. The push-button switch is let "out," and the pH is read on the proper scale. When not in use the electrodes are immersed in distilled water.

Twenty-five milliliters of 0.1 M  $\text{H}_3\text{PO}_4$  is titrated with 0.1 N NaOH. The pH is measured after each addition of about 5 ml of base, except near the end points, where more readings are taken. In order to determine the pH range for the color change of a typical indicator, a few drops of phenolphthalein solution are added before the titration. The color change of the indicator is noted during the titration. The pH of the solution is plotted versus volume of sodium hydroxide added, and the ionization constant  $K_2$  is calculated.

#### B. BUFFERS

**Procedure and Calculations.** The following buffer solutions are carefully prepared, using volumetric equipment:

Solution	ml 0.10 N HAc	ml 0.10 N NaAc
1	95	5
2	50	50
3	5	95

The pH of each solution is determined with the pH meter and compared with the values calculated from Eq. (2). Since acetic acid is a weak acid, it does not contribute appreciably to the acetate concentration of these buffers, so that the acetate-ion concentration is determined only by the amount of sodium acetate added. Four milliliters of 0.1 N sodium hydroxide is added to each of the above buffers, and the pH again measured. Four milliliters of 0.1 N sodium hydroxide is added to 100 ml of distilled water, and the pH change noted. The ratios  $\Delta B/\Delta(\text{pH})$  of the numbers of equivalents of base added per liter of buffer to the changes in pH are calculated and compared with the buffer capacities calculated by using Eq. (3).

#### C. TITRATION OF GLYCINE

**Procedure and Calculations.** Two approximately 250-mg portions of glycine are weighed and dissolved in 30 ml of distilled water. One portion is titrated with 0.1 N NaOH, and the other with 0.1 N HCl, the pH being recorded at six to eight intervals. No definite end points are obtained, however, since they occur in such strongly acidic or basic solutions that a large amount of the added acid or base is required to change the pH.



The titration curves are plotted by graphing the volume of acid added to the left of the origin on the horizontal axis and the volume of base added to the right with the pH plotted as ordinate. In a second figure the pH is plotted versus the number of equivalents of acid or base which have reacted per mole of glycine. The number of equivalents of hydrogen ion or hydroxyl ion which have reacted with glycine is the difference between the number of equivalents of acid or base added and the number of equivalents remaining free in solution (calculated from the pH and the volume of solution being titrated). The calculations are most conveniently arranged in tabular form. The corrected titration curve is plotted, and the  $pK$  values of glycine calculated from it.

**Practical Applications.** The rates of many reactions depend markedly upon the pH, and therefore solutions in which such reactions are carried out must be buffered. Industrially, pH is frequently controlled by automatic devices which add acid or base, depending upon the potential of a glass electrode. The pH meter is particularly important in biological research.

**Suggestions for Further Work.** The glass electrode may be used for the measurement of the pH of a wide variety of miscellaneous substances, e.g., milk, sour milk, blood, orange juice, lemon juice, water extract of soil, tap water, tap water from which carbon dioxide has been expelled. If a mixture of acids which have  $pK$ 's differing by about 2 (e.g., hydrochloric acid, acetic acid, and lactic acid) is titrated with the pH meter, it is possible to determine the amount of each acid present.

Measurements of pH may be used to determine the degree of hydrolysis of salts, provided the salts have been carefully purified and pure water is used. While aqueous solutions of salts of strong acids and strong bases are neutral, solutions of salts of strong acids and weak bases are acidic, and solutions of salts of weak acids and strong bases are basic. To illustrate this, the pH values of solutions of sodium chloride, sodium acetate, ammonium acetate, and aniline hydrochloride may be measured. The degree of hydrolysis  $x$  is calculated from  $x = (OH^-)/c$  or  $x = (H^+)/c$ , depending upon whether the solution is basic or acidic. The concentration of the salt in equivalents per liter is represented by  $c$ . The experimentally determined degrees of hydrolysis are compared with the values calculated from the ionization constants in the literature.

#### References

1. Bates, "Electrometric pH Determinations," John Wiley & Sons, Inc., New York (1954).
2. Daniels and Alberty, "Physical Chemistry," 2d ed., John Wiley & Sons, Inc., New York (1961).
3. Hammett, "Introduction to the Study of Physical Chemistry," pp. 335 ff., McGraw-Hill Book Company, Inc., New York (1952).
4. Harned and Owen, "The Physical Chemistry of Electrolytic Solutions," 3d ed., Reinhold Publishing Corporation, New York (1958).
5. MacInnes, "The Principles of Electrochemistry," Chap. 15, p. 258, Reinhold Publishing Corporation, New York (1939).
6. Tanford and Wawzonek in Weissberger (ed.): "Technique of Organic Chemistry," 3d ed., Vol. I, Pt. IV, Chap. 44, Interscience Publishers, Inc., New York (1960).
7. Van Slyke, *J. Biol. Chem.*, **52**, 525 (1922).

### 34. FREE ENERGY AND THE EQUILIBRIUM CONSTANT

This experiment illustrates the important relation between free energy and the equilibrium constant and interrelates chemical and electrical measurements through thermodynamics.

**Theory.** One of the most important equations of physical chemistry is that which interrelates the standard-free-energy change  $\Delta G^\circ$  and the thermodynamic equilibrium constant  $K$  for a chemical reaction:

$$\Delta G^\circ = -RT \ln K \quad (1)$$

This equation is exact only if the equilibrium constant  $K$  is expressed in terms of activities; it is often useful as an approximation when activities are replaced by concentrations or partial pressures.

The standard state for a gas is the pure gas in the hypothetical ideal-gas state at one atmosphere pressure at the given temperature; for a pure liquid or solid, it is usually the pure condensed phase at the given temperature and a pressure of one atmosphere. For a solution constituent considered to act as a solvent, the standard state is taken as the pure liquid at the temperature and pressure of the solution; for a constituent treated as a solute, it is so selected that the activity coefficient, defined as the ratio of activity  $a_2$  to the concentration  $x_2$  on the scale chosen, will approach unity as  $x_2$  approaches zero.

The standard-free-energy change for a reaction may be calculated indirectly by addition of the standard-free-energy changes for any sequence of reactions which together are equivalent to the total reaction. This procedure may be facilitated by the tabulation of the standard free energy of formation, which for a particular compound is the free-energy change for the given temperature and for standard-state conditions for all species involved, for the reaction in which one mole of the compound in question is formed from its elements. It is rather more common, however, to calculate the standard-free-energy change for a given temperature from the relation

$$\Delta G^\circ = \Delta H^\circ - T\Delta S^\circ \quad (2)$$

The standard heat of reaction  $\Delta H^\circ$  is calculated from tabulated standard heats of formation, and the standard entropy change  $\Delta S^\circ$  from standard entropies obtained by use of the third law of thermodynamics. An important modern application of such indirect calculations of equilibrium constants is in the prediction of the performance to be expected from proposed rocket propellants, in which the calculation of the equilibrium composition for complex reaction systems plays an important part.<sup>2</sup> It should be understood, however, that kinetic as well as thermodynamic

considerations may be important in determining the composition of a system.

The free-energy change for a chemical reaction may be determined most directly, and frequently with high accuracy, if the reaction may be made to take place reversibly in an electrochemical cell for which the electromotive force can be measured. For a reversible process at constant temperature and pressure, the decrease in free energy of the system,  $-\Delta G$ , is equal to  $w_{\text{net}}$ , the work other than  $PV$  work done on the surroundings. For the cell,  $w_{\text{net}}$  is the electrical work and is equal to  $nFE$ , when  $E$  is the electromotive force of the cell,  $F$  is the faraday, and  $n$  is the number of faradays of electricity which flow through the cell circuit for completion of the cell reaction as written. Letting  $a_j$ ,  $\nu_j$  represent the activity and number of moles of typical product  $j$ , with  $a_i$ ,  $\nu_i$  playing parallel roles for typical reactant  $i$ , for the cell reaction

$$\Delta G = \Delta G^\circ + RT \ln \frac{\prod_j a_j^{\nu_j}}{\prod_i a_i^{\nu_i}} \quad (3)$$

The symbol  $\Pi$  denotes a product of factors. Since  $\Delta G = -nFE$ , and defining  $\Delta G^\circ = -nFE^\circ$ ,

$$E = E^\circ - \frac{RT}{nF} \ln \frac{\prod_j a_j^{\nu_j}}{\prod_i a_i^{\nu_i}} \quad (4)$$

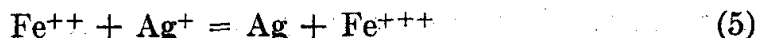
The calculation of the standard electromotive force  $E^\circ$ , which corresponds to standard-state conditions for all species involved, requires a knowledge of the thermodynamic activities of all species taking part in the reaction as well as the actual electromotive force  $E$ .

The electromotive force of a cell may be resolved into the algebraic difference of two electrode potentials, each of which is set equal to a standard electrode potential (evaluated on a scale established by setting the standard potential of the hydrogen electrode equal to zero) plus the appropriate term involving the activities of the species taking part in the pertinent electrode reaction. If one of the electrodes is the calomel electrode, the activity of the chloride ion does not appear in the expression for the electromotive force; while it is not unity, it is accounted for in the numerical value of the electromotive force recorded as "standard" for this electrode.

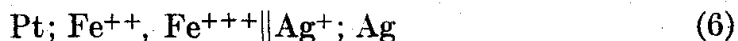
Cells with liquid junctions between the different electrolytes cannot be given exact thermodynamic treatment, but they can give a useful result

if the liquid junctions have been practically eliminated by a salt bridge. Such cells are used widely in pH measurements; they are to serve in another way in this experiment.

The reaction



is particularly suitable for testing Eq. (1), because the equilibrium is quickly reached, the equilibrium constant is easily obtained by volumetric analysis, and the free-energy change may be calculated from the voltage of the cell



**Apparatus.** Two 150-ml glass-stoppered bottles; platinum electrode; silver electrode; two half-cells (Fig. 48); crystallizing dish; calomel cell; potentiometer assembly; 0.1 M ferric nitrate in 0.5 M nitric acid; 0.1 M silver nitrate; 0.1 M potassium thiocyanate, ferrous sulfate, barium nitrate; purified nitrogen or carbon dioxide.

#### A. TITRATION METHOD

**Procedure.** Precipitated silver is prepared by dissolving about 7 g of silver nitrate in water and adding an excess of copper wire. The precipitate of silver is filtered and rinsed with distilled water until the rinsings give no test for copper ion with ammonia solution. The yield is split between the two glass-stoppered bottles, to each of which is added 100 ml of a solution which is 0.100 M in ferric nitrate and 0.05 M in nitric acid. The nitric acid reduces hydrolysis of the ferric salt. Purified nitrogen (page 470) or carbon dioxide is bubbled slowly through the solution for a few minutes to sweep out dissolved oxygen; the glass joint is greased, and the bottle tightly stoppered. Oxidation of ferrous ions by dissolved air constitutes one of the greatest difficulties in this experiment.

The two bottles are heated to about 50°; they are removed and shaken at frequent intervals and then set aside to stand for at least 24 hr. Procedure B may be performed while equilibrium is being attained.

When equilibrium has been reached, the solutions are analyzed for silver ions. A 25-ml sample of the solution is titrated with 0.1 M potassium thiocyanate, the ferric nitrate already in solution serving as an indicator. The potassium thiocyanate solution is standardized with the 0.1 M silver nitrate solution, an equal volume of the ferric nitrate solution being added as indicator.

The titrations should be made as soon as the stoppers are removed in order to avoid air oxidation of ferrous ion.

#### B. POTENTIOMETRIC METHOD

**Procedure.** Twenty milliliters of 0.1 M ferric nitrate in 0.05 M nitric acid is mixed with 20 ml of freshly prepared ferrous nitrate solution.

The latter is prepared by mixing equal portions of 0.2 M ferrous sulfate and 0.2 M barium nitrate. The barium sulfate is allowed to settle for a few minutes in a stoppered vessel; the resulting solution is decanted into one of the half-cells, and the rubber stopper which holds the platinum electrode is sealed tightly in place. It is just as important to prevent air oxidation here as in the procedure for method A, and to this end the use of purified nitrogen or carbon dioxide over the solutions may be advisable.

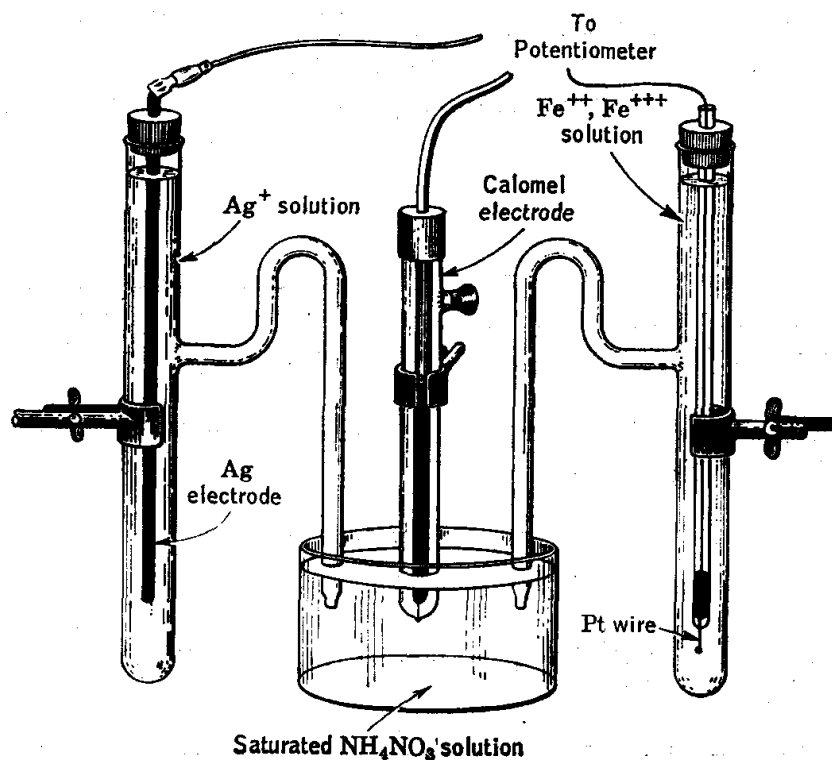


FIG. 48. Measurement of electrode potentials for calculating the free-energy change in chemical reactions.

The presence of a small amount of suspended barium sulfate in the solution should not affect the results.

Into the other half-cell are placed 0.1 M silver nitrate and the silver electrode, with the rubber stopper seating tightly. The sidearms in both half-cells must be completely filled.

The two half-cells and the calomel cell are now set up as shown in Fig. 48. The crystallizing dish contains saturated ammonium nitrate solution, which acts as a salt bridge.

The principle of the potentiometer should be fully understood (Exp. 31 and Chap. 22).

Three potentials are determined between the following pairs of electrodes: silver against calomel, ferrous-ferric against calomel, and silver

against ferrous-ferric. In each case, time should be allowed for a steady potential to be reached. The sign of the cell voltage should be recorded as the sign of the right-hand electrode for the cell as written (page 183).

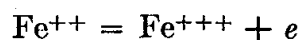
The silver residues from both procedures are to be placed in a special recovery bottle.

**Calculations.** The concentration of silver ion in the equilibrium solution is calculated from the potassium thiocyanate titration. The concentration of the ferrous ion is the same as that of the silver ion, and the concentration of ferric ion is calculated by subtracting the concentration of ferrous ion from the concentration of ferric ion originally present. The apparent equilibrium constant  $K'_{app}$  is then calculated as follows:

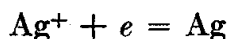
$$K'_{app} = \frac{c_{Fe^{+++}}}{c_{Fe^{++}} \cdot c_{Ag^+}}$$

The term "apparent equilibrium constant" is used because concentrations rather than activities are used except for the metallic silver, whose activity does not appear explicitly since it is unity for this pure solid phase.

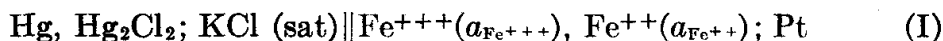
The electrochemical reactions at the two electrodes corresponding to the cell given by Eq. (6) are



and



The reduction potential  $E^\circ_{Fe^{+++}, Fe^{++}; Pt}$  may be calculated from the electromotive force  $E_I$  of the cell



Assuming that the junction potential is negligible,

$$E_I = -E^\circ_{KCl(sat); Hg_2Cl_2, Hg} + E^\circ_{Fe^{+++}, Fe^{++}; Pt} - 0.0591 \log \frac{a_{Fe^{++}}}{a_{Fe^{+++}}}$$

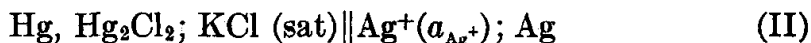
where  $E^\circ_{KCl(sat); Hg_2Cl_2, Hg}$  is the reduction potential for the saturated calomel electrode.

If  $a_{Fe^{++}}$  is set equal to  $a_{Fe^{+++}}$  when  $c_{Fe^{++}} = c_{Fe^{+++}}$ ,

$$E^\circ_{Fe^{+++}, Fe^{++}; Pt} = E_I + E^\circ_{KCl(sat); Hg_2Cl_2, Hg}$$

The value of  $E^\circ_{Fe^{+++}, Fe^{++}; Pt}$  found is compared with that given in tables.

The reduction potential  $E^\circ_{Ag^+; Ag}$  may be calculated from the electromotive force  $E_{II}$  of the cell

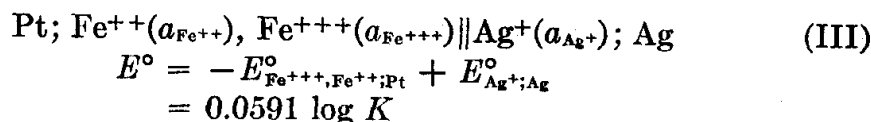


Assuming that the junction potential is negligible,

$$E_{II} = -E_{\text{KCl(sat)}; \text{Hg}_2\text{Cl}_2, \text{Hg}}^\circ + E_{\text{Ag}^+; \text{Ag}}^\circ - 0.0591 \log \frac{1}{a_{\text{Ag}^+}}$$

Thus 
$$E_{\text{Ag}^+; \text{Ag}}^\circ = E_{II} + E_{\text{KCl(sat)}; \text{Hg}_2\text{Cl}_2, \text{Hg}}^\circ + 0.0591 \log \frac{1}{a_{\text{Ag}^+}}$$

Then for the cell

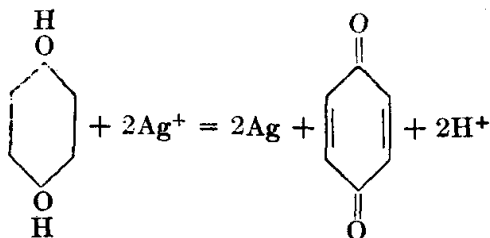


The value of  $K$  is calculated from this equation and compared with the value of  $K$  obtained by direct analysis. The agreement can be only approximate, because analytically determined concentrations, rather than activities, are used for calculating  $K$  from the equilibrium mixture and for determining  $E_{\text{Fe}^{+++}, \text{Fe}^{++}; \text{Pt}}^\circ$ , but since the solutions are fairly dilute, the error is not great. The contact potential between the unlike solutions is another source of considerable error.

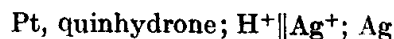
**Practical Applications.** An equilibrium constant for a chemical reaction can be calculated when the free-energy change is known. In accumulating tables of free energies for this purpose, the direct electromotive-force measurement of reversible cells constitutes one of the most valuable methods. The equilibrium constants for various reactions may be calculated from the oxidation-reduction potentials.

**Suggestions for Further Work.** The results may be made considerably more accurate by carrying out the measurements with a series of more dilute solutions and evaluating  $\log K$  and  $E^\circ$  by extrapolation to infinite dilution, where the concentrations and activities become identical. More accurate determination of ferric iron is advisable, using reduction with zinc and titration with potassium permanganate.

The oxidation of hydroquinone by silver ion is an excellent reaction<sup>3</sup> to study because the equilibrium constant can be determined accurately by iodimetric titration, and because dissolved oxygen from the air does not affect the results. The reaction is



and the cell by which the equilibrium constant can be calculated is



The dissociation pressure of copper oxide or mercuric oxide may be calculated from electromotive-force measurements of suitable cells.

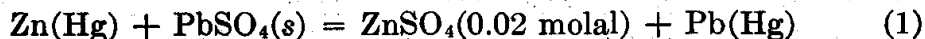
## References

1. Lewis and Randall, "Thermodynamics," 2d ed., rev. by Pitzer and Brewer, McGraw-Hill Book Company, Inc., New York (1961).
2. Brinkley in Lewis, Pease, and Taylor (eds.): "Combustion Processes," Princeton University Press, Princeton, N.J. (1956).
3. Livingston and Lingane, *J. Chem. Educ.*, **15**, 320 (1938).

## 35. THERMODYNAMICS OF ELECTROCHEMICAL CELLS

The electromotive force of a cell is measured at different temperatures, and the heat of the reaction is calculated by means of the Gibbs-Helmholtz equation.

**Theory.** The following reaction<sup>2</sup> is studied:†



The enthalpy change for this reaction may be measured by combining the reactants in a calorimeter under conditions where only work of expansion is performed, or it may be calculated indirectly from electrical measurements. Since the measurement of electrical quantities is very precise, the latter method is often more accurate than the direct calorimetric method.

Instead of placing zinc amalgam directly in contact with lead sulfate and carrying out the reaction irreversibly, the reaction may be brought about reversibly in the electrochemical cell



The cell represented by (2) is particularly suited for experimental study. It is a cell *without transference*; i.e., it has no liquid junction and therefore no uncertain junction potential, provided the effect of the slight solubility of lead sulfate is considered negligible.

Electrical work is equal to the product of the potential and the charge carried through the circuit. When the cell operates reversibly, the electrical work done is determined by the Gibbs free-energy change accompanying the cell reaction:

$$\Delta G = -nFE \quad (3)$$

where  $E$  = cell electromotive force for reversible operation

$n$  = number of faradays transferred in cell reaction as written

$F$  = faraday, 96,490 coulombs equiv<sup>-1</sup>

$nF$  = charge flow, coulombs, accompanying cell reaction as written

† The symbol (s) refers to the solid state. Zn(Hg) and Pb(Hg) are two-phase systems consisting of a solid intermetallic compound, for example, Pb<sub>2</sub>Hg, in equilibrium with a saturated liquid amalgam.



Thus, for the above reaction,  $\Delta G$  is the Gibbs free-energy change attending the reaction of 1 mole of zinc in accordance with Eq. (1). It can be determined by measuring the cell potential for reversible operation, such as is adequately approached in voltage measurements with a potentiometer. The use of the potentiometer is described under Exp. 31.

At constant temperature and pressure, the heat effect accompanying the direct irreversible reaction, in which only  $PV$  work is done, is equal to  $\Delta H$ , the change in enthalpy for the process; while for the reversible execution of the reaction it is equal to  $T\Delta S$ , where  $\Delta S$  is the corresponding change in entropy. The difference in these two quantities determines the electrical work done in the reversible process, since for the specified conditions of constant temperature and pressure  $\Delta G = \Delta H - T\Delta S$ . If  $\Delta S > 0$ , the electrical work done is greater than that equivalent to  $\Delta H$ ; the energy balance is achieved through heat absorbed by the cell from its surroundings in constant-temperature operation. If  $\Delta S < 0$ , heat is given up to the surroundings in the reversible operation of the cell at constant temperature and the electrical work becomes less than that equivalent to  $\Delta H$ .

Values of  $\Delta G$ ,  $\Delta S$ , and  $\Delta H$  for the cell reaction are calculated from Eqs. (3), (4), and (5)

$$\Delta S = - \left( \frac{\partial \Delta G}{\partial T} \right)_P = nF \left( \frac{\partial E}{\partial T} \right)_P \quad (4)$$

$$\Delta H = \Delta G + T\Delta S = -nFE + nFT \left( \frac{\partial E}{\partial T} \right)_P \quad (5)$$

from measured values of  $E$  and  $(\partial E/\partial T)_P$ .

**Apparatus.** H-type cell, preferably with sintered-glass disk in connecting arm; mercury; granular zinc; granular lead; zinc sulfate; lead sulfate; mortar and pestle; thermostats at several temperatures from 0 to 40°, or rapidly adjustable thermostat in this range; potentiometer assembly.

**Procedure.** The H-type cell is shown in Fig. 49. For preparing these cells, sintered-glass disks sealed into straight tubes are available from supply houses. The coarse grade of sintered glass is preferred. Alternatively, an open tube plugged with clean glass wool may be used. The purpose of this disk, or plug, is to prevent solid lead sulfate from contaminating the zinc half-cell. Contact with the amalgam electrode is obtained by platinum wires sealed into the end of a glass tube. Mercury is placed in this tube, and the leads from the potentiometer dip into the mercury.

About 500 ml of 0.02 *molar*  $\text{ZnSO}_4$  is prepared. To 100 ml of this solution is added about 2 g of lead sulfate, and the mixture is shaken vigorously.

In all precise work with electrochemical cells, oxygen must be carefully excluded from the cell. If a nitrogen tank and purification train (page

470) are available, the solutions of  $\text{ZnSO}_4$  and of  $\text{ZnSO}_4$  saturated with  $\text{PbSO}_4$  are swept out with nitrogen while the amalgams are being prepared.

The amalgams are prepared by grinding the granular metal with mercury under a little dilute (0.5 N)  $\text{H}_2\text{SO}_4$  in a mortar. The amalgams should contain about 6 per cent of Zn or Pb by weight. The sulfuric acid prevents an oxide scum from forming on the surface and hastens the amalgamation.

Some grinding of the zinc with mercury should be done before adding the acid; otherwise the granules will tend to float on the acid. The amalgams are carefully rinsed with distilled water and with three or four portions of  $\text{ZnSO}_4$  solution; they are then transferred to their respective arms of the cell. If the zinc amalgam has thickened to form a sludge, moderate warming will render it mobile.

The  $\text{ZnSO}_4$  solution is placed over the zinc amalgam, and the  $\text{ZnSO}_4$  solution saturated with  $\text{PbSO}_4$  is placed over the lead amalgam, care being taken not to allow excessive mixing of the two solutions. The platinum leads are then introduced, with the platinum completely immersed in the amalgam.

The potential is to be determined at several temperatures in the range 0 to 40°. Temperature intervals of 10 or 15° are convenient. For careful work the cell should be placed in a thermostat. The cell may take so long to reach equilibrium that a manually

controlled bath cannot be recommended. A well-stirred ice bath in an insulated jacket is used for the 0° measurement.

Readings of the potential at each temperature are taken at intervals until a value constant within a few tenths of a millivolt is obtained; this value is taken to be the cell potential for reversible operation at the particular temperature. If erratic operation or continual drift of the cell voltage occurs, a new cell should be set up.

The first set of readings may be recorded starting at 0° and increasing the temperature. A check run is then made with descending temperature, starting at the highest point in the previous set.

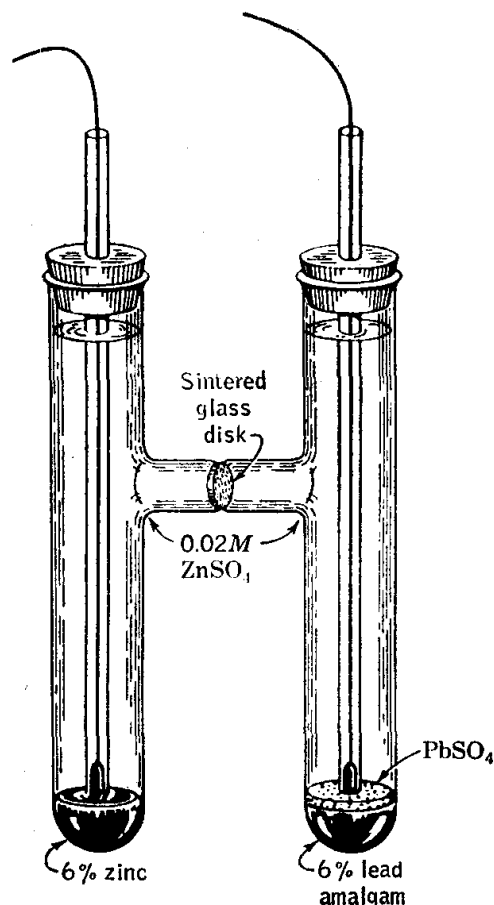


FIG. 49. Electrochemical cell for determination of thermodynamic functions.

**Calculations.** The potential is plotted against the absolute temperature, and  $(\partial E/\partial T)_P$  is obtained by drawing a tangent to the curve. The estimated reliability of the voltage measurements should be considered in drawing the curve.

Values of  $\Delta G$ ,  $\Delta S$ , and  $\Delta H$  are calculated for 25°C by use of Eqs. (3) to (5), for both joules and calories as the energy unit. The heat for the direct irreversible reaction is compared with that for the reversible case.

The value obtained for  $\Delta H$  is compared with that obtained from the heats of formation.<sup>8</sup> The heats of formation of the saturated zinc and lead amalgams and the heat of dilution of 0.02 M  $\text{ZnSO}_4$  may be neglected<sup>1,3,8</sup> in this calculation.

**Practical Applications.** The relation between  $\Delta G$  and  $\Delta H$  discussed in this experiment was studied down to low temperatures by Richards and led to the first expression of what is now known as the third law of thermodynamics.

**Suggestions for Further Work.** Various other cells may be studied, including a copper-zinc cell, in which  $\Delta H$  and  $\Delta G$  are nearly equal, a copper-lead cell, where  $\Delta H$  is less than  $\Delta G$ , and a silver-zinc cell, where  $\Delta H$  is greater than  $\Delta G$ .

Cadmium and cadmium sulfate may be used in place of zinc and zinc sulfate in the apparatus of this experiment.<sup>5</sup>

By extending these measurements to several different concentrations, it is possible to obtain the  $E^\circ$  of the cell, the activity coefficients, heats of transfer, and the partial and integral heats of dilution of  $\text{ZnSO}_4$  (Refs. 2, 4) or of  $\text{CdSO}_4$  (Ref. 6).

In the case of the cadmium-lead system, thermodynamic data may be obtained for reactions involving the pure metals, using measurements of the electromotive force of the Cd-Cd amalgam couple by LaMer and Parks<sup>7</sup> and of the Pb-Pb amalgam couple by Gerke.<sup>3</sup> The latter reference contains a wealth of practical information on the techniques of precise potential measurements.

### References

1. Clayton and Vosburgh, *J. Am. Chem. Soc.*, **58**, 2093 (1936).
2. Cowperthwaite and LaMer, *J. Am. Chem. Soc.*, **53**, 4333 (1931).
3. Gerke, *J. Am. Chem. Soc.*, **44**, 1684 (1922).
4. LaMer and Cowperthwaite, *J. Am. Chem. Soc.*, **55**, 1004 (1933).
5. LaMer and Parks, *J. Am. Chem. Soc.*, **53**, 2040 (1931).
6. LaMer and Parks, *J. Am. Chem. Soc.*, **55**, 4343 (1933).
7. LaMer and Parks, *J. Am. Chem. Soc.*, **56**, 90 (1934).
8. Selected Values of Chemical Thermodynamic Properties, *Natl. Bur. Standards (U.S.), Circ.*, **500** (1952).

## *Dielectric and Optical Properties of Matter*

### 36. DIPOLE MOMENT FROM DIELECTRIC-CONSTANT MEASUREMENTS ON SOLUTIONS; HETERODYNE-BEAT METHOD

The heterodyne-beat method is one of the most commonly used by chemists for dipole-moment studies. The reason for this is that it is the most accurate method for determining the dielectric constants of fluids having very low conductance and is therefore particularly well suited to the measurements on gases or on dilute solutions in nonpolar solvents required for the determination of dipole moment with the Debye equations. In this experiment the solution procedure is used.

**Theory.** It was pointed out by Debye that molecules of the so-called *polar* substances, though electrically neutral, possess a nonvanishing electric dipole moment even in the absence of applied fields and that the magnitude of the molecular dipole moment could be found from dielectric-constant data. The measurement and study of molecular dipole moments continues to be an important step in characterizing the properties of molecules.

Let us begin by defining the term dipole moment. To do so, we consider a cluster of charges for which the net charge is zero. The dipole moment  $\mathbf{p}$  of such a group of charges is a vector quantity,\* the components of which are defined by

$$p_x = \sum_i q_i x_i \quad p_y = \sum_i q_i y_i \quad p_z = \sum_i q_i z_i$$

where  $x_i$ ,  $y_i$ ,  $z_i$  are the coordinates of charge  $q_i$ . It is easily shown that  $\mathbf{p}$  is independent of the location of the origin of the coordinate system if the net charge  $\sum_i q_i$  is zero.

It is usual to recognize two distinct processes which may occur when a substance is subjected to the influence of an electric field: (a) conduction and (b) polarization. Conduction is the transport of charged particles

\* The notation used for vectors is illustrated in the Appendix.

over relatively large distances (i.e., large compared with molecular dimensions). The term polarization refers to the displacement over relatively short distances (of the order of a molecular diameter or less) of charges which are bound within some more or less permanent, though not rigid, aggregate of charged particles such as a neutral molecule. The charge displacements involved in the polarization process never carry a charge very far from the position it would have in the absence of the field.

The state of polarization of a substance is characterized by a vector quantity  $\mathbf{P}$ , called the polarization. The vector  $\mathbf{P}$  can be defined as the average resultant dipole moment per unit volume due to bound charge, this average being taken over an element of volume which, though small by ordinary standards, nevertheless contains a relatively large number of molecules. The value of  $\mathbf{P}$  in a given small region of the substance depends on the electric field  $\mathbf{E}$  in the same region.

The concept of the field  $\mathbf{E}$  within matter requires clarification. The field  $\mathbf{E}$  at any point *in a vacuum* is defined by the statement that  $\mathbf{E}dq$  is the force which would be exerted on a "test" charge  $dq$  of infinitesimal magnitude placed at the given point. The field defined in exactly this same way within matter fluctuates wildly over atomic-scale dimensions. The macroscopic field  $\mathbf{E}$  at a point *within matter* is therefore defined as the average of this atomic-scale field over a small region in the neighborhood of the given point, this region being chosen small by ordinary standards, yet large enough to contain many molecules.

For *isotropic* substances,  $\mathbf{P}$  lies in the same direction as  $\mathbf{E}$ , and for this case the susceptibility  $\chi$  is defined by

$$P = \chi E \quad (1)$$

where  $P$  and  $E$  are the magnitudes of  $\mathbf{P}$  and  $\mathbf{E}$ , respectively. The dielectric constant  $\epsilon$  is†

$$\epsilon = 1 + 4\pi\chi \quad (2)$$

Subsequent discussion will be limited to the isotropic case.

† Maxwell's displacement field vector  $\mathbf{D}$  at any point is related to  $\mathbf{E}$  and  $\mathbf{P}$  by

$$\mathbf{D} = \mathbf{E} + 4\pi\mathbf{P} \quad (3a)$$

For isotropic substances,  $\mathbf{D}$ ,  $\mathbf{E}$ , and  $\mathbf{P}$  all have the same direction at any point and Eq. (3a) may be replaced by an equation relating the magnitudes,

$$D = E + 4\pi P \quad (3b)$$

The dielectric constant  $\epsilon$  is usually defined for the isotropic case by  $D = \epsilon E$ , which then leads directly to Eq. (2). These equations are in the cgs-esu system of units.

Two equations for  $P$  are fundamental for the interpretation of dielectric constants:

$$P = N\langle p_E \rangle \quad (4)$$

$$= \frac{\epsilon - 1}{4\pi} E \quad (5)$$

where  $P$  = polarization (in the direction of the field  $E$ )

$N$  = number of molecules per unit volume

$p_E$  = component of the total dipole moment of a molecule in the direction of  $E$

The angle brackets mean that the quantity enclosed is to be averaged over the thermal motions of the molecules, and also over the different species of molecules present in the case of a mixture. Equation (4), it should be noted, relates  $P$  to molecular properties, while Eq. (5), which follows from Eqs. (1) and (2), relates  $P$  to the directly measurable macroscopic quantity  $\epsilon$ .

When the field  $E$  is applied suddenly, a certain amount of time is required before the equilibrium degree of polarization becomes established. The static dielectric constant  $\epsilon_s$  is the value of  $\epsilon$  measured in either a constant field  $E$  or in a field changing slowly enough that the substance is essentially at equilibrium at every instant.† We shall consider this case first.

Three contributions to  $\langle p_E \rangle$  are to be considered. The first arises if the molecule has a dipole moment even in the absence of an applied field. This moment is called the *permanent* dipole moment, and its magnitude is represented by the symbol  $\mu$ . Let this dipole moment lie in a direction which makes an angle  $\vartheta$  with the field direction. Then the contribution of the permanent dipole term to  $\langle p_E \rangle$  is

$$\mu\langle \cos \vartheta \rangle \quad (6)$$

Because of thermal agitation, a single molecule will in a period of time assume all possible orientations with reference to a fixed direction. In the absence of an applied field, these orientations have equal probabilities and  $\langle \cos \vartheta \rangle$  vanishes. In the presence of a field, however, orientations in which the dipole is close to alignment with the field will be favored over those in which the dipole is opposed to the field. The average value of  $\cos \vartheta$  in a field  $E_i$  is

$$\langle \cos \vartheta \rangle = \frac{\mu E_i}{3kT} \quad (7)$$

† For most liquids or gases at ordinary temperatures, this criterion still permits  $\epsilon_s$  to be measured at rather high frequencies. In the present experiment, for example, measurement of  $\epsilon$  at roughly 1 Mc/sec (megacycle/sec) yields  $\epsilon_s$  to all intents and purposes.

where  $k$  = Boltzmann constant

$T$  = absolute temperature

Here the average field acting on the given molecule has been designated  $E_i$ . It is related to, but is not equal to, the field  $E$  defined above. The field  $E_i$ , called the *internal*, or *local*, field, may be visualized as the average field at the location of a molecule, produced by all charges except those of the given molecule.

For typical values of the quantities in Eq. (7), this average is of the order of  $1 \times 10^{-5}$ . It is clear, therefore, that the alignment is far from being complete; rather there is only a very slight degree of preference shown for orientation with the field. Nevertheless, for polar molecules, this mechanism gives the dominant contribution to  $\langle p_E \rangle$ , of magnitude

$$\frac{\mu^2}{3kT} E_i \quad (8)$$

In addition to this term, associated with orientation of the permanent molecular dipole moments, additional polarization results from distortion of the molecule produced by the externally applied field. Specifically, this distortion includes (a) deformation of the same sort as that involved in vibrational motions, namely, changes in bond lengths and angles, and (b) displacement of the average positions of the electrons relative to the nuclear framework. The field-dependent part of the molecular dipole moment produced in this way is called the *induced* moment. When averaged over all orientations of the molecule, it lies in the same direction as, and is closely proportional to,  $E_i$ . These terms in  $\langle p_E \rangle$  are therefore written as

$$(\alpha_v + \alpha_e) E_i \quad (9)$$

where  $\alpha_v$  = mean molecular vibrational or atomic polarizability

$\alpha_e$  = mean molecular electronic polarizability

The complete expression for  $\langle p_E \rangle$  is therefore

$$\langle p_E \rangle = \left( \frac{\mu^2}{3kT} + \alpha_v + \alpha_e \right) E_i \quad (10)$$

Before Eq. (10) can be used, it is necessary to have a relation between  $E_i$  and  $E$ . Debye used an expression, derived earlier by Lorentz,

$$E_i = \frac{\epsilon + 2}{3} E \quad (11)$$

which is satisfactory only if the concentration of polar molecules is very low. Therefore the following equations are accurate for gases and are reasonably satisfactory for very dilute solutions of polar molecules in nonpolar solvents, but are not useful for polar liquids. Substitution of

(11) in (10) and of the resulting expression for  $\langle p_E \rangle$  into (4) yields

$$P = N \left( \frac{\mu^2}{3kT} + \alpha_v + \alpha_e \right) \frac{\epsilon_s + 2}{3} E \quad (12)$$

Then equating the right sides of (12) and of (5), eliminating  $N$  through the substitution

$$NV = N_0 = \text{Avogadro's number}$$

where  $V = M/\rho = \text{molar volume}$

$\rho = \text{density}$

$M = \text{molecular weight}$

and collecting the measurable quantities on the left side leads to

$$\frac{\epsilon_s - 1}{\epsilon_s + 2} V = \frac{4\pi N_0}{3} \left( \frac{\mu^2}{3kT} + \alpha_v + \alpha_e \right) \quad (13)$$

A quantity called the molar polarizability,  $\mathcal{P}$ , is defined as

$$\mathcal{P} = \frac{\epsilon - 1}{\epsilon + 2} \frac{M}{\rho} = \frac{\epsilon - 1}{\epsilon + 2} V \quad (14)$$

The left side of Eq. (13) is the static value of  $\mathcal{P}$ .

Equation (13) has been found to be quite accurate for most gases. Thus measurements of dielectric constant and density of a polar gas as a function of temperature may be combined to permit a determination of both the permanent dipole moment  $\mu$  and the mean total polarizability  $(\alpha_v + \alpha_e)$ . From Eqs. (13) and (14), a graph of  $\mathcal{P}_s$  versus  $1/T$  will give a straight line with slope  $4\pi N_0 \mu^2 / 9k$  and intercept  $(4\pi N_0 / 3)(\alpha_v + \alpha_e)$ .

Since gas-phase measurements are not always practicable for the substance of interest, Debye extended Eq. (13) to cover the case of a solute in dilute solution in a nonpolar solvent. If reasoning similar to that leading to Eq. (13) is repeated, there is obtained for the solution case the equation

$$\mathcal{P} = X_1 \mathcal{P}_1 + X_2 \mathcal{P}_2 \quad (15)$$

$$\text{with} \quad \mathcal{P} = \frac{\epsilon_s - 1}{\epsilon_s + 2} V = \frac{\epsilon_s - 1}{\epsilon_s + 2} \left( \frac{X_1 M_1 + X_2 M_2}{\rho} \right) \quad (16)$$

$$\mathcal{P}_1 = \frac{4\pi N_0}{3} (\alpha_{v_1} + \alpha_{e_1}) \quad (17)$$

$$\mathcal{P}_2 = \frac{4\pi N_0}{3} \left( \frac{\mu_2^2}{3kT} + \alpha_{v_2} + \alpha_{e_2} \right) \quad (18)$$

where  $X_1, X_2 = \text{mole fractions}$

$M_1, M_2 = \text{molecular weights}$

Subscript 1 refers to the solvent, and 2 to the solute, while  $\epsilon_s$ ,  $V$ , and  $\rho$



are the static dielectric constant, average molar volume, and density of the solution, respectively. The quantity  $\Phi$  is expressed in Eq. (16) in terms of directly measurable quantities, and for dilute solutions,  $\Phi_1$  is approximated by the molar polarization of the pure solvent,

$$\Phi_1^o = \frac{\epsilon_1 - 1}{\epsilon_1 + 2} \frac{M_1}{\rho_1} \quad (19)$$

so that  $\Phi_2$  may be calculated from the expression

$$\Phi_2 = \frac{\Phi - X_1 \Phi_1^o}{X_2} \quad (20)$$

However, as a result mainly of interactions among polar solute molecules,  $\Phi_2$  calculated from Eq. (20) is found to vary with concentration. Since the magnitude of this interaction depends on the distance between the polar solute molecules, extrapolation of  $\Phi_2$  to zero solute mole fraction yields a value  $\Phi_2^o$  which is free from the effect of such interactions. (This procedure is comparable to the use of the method of limiting densities for the accurate determination of the molecular weight of a real gas.) Formally,  $\Phi_2^o$  may be written as

$$\Phi_2^o = \lim_{X_2 \rightarrow 0} \frac{\Phi - X_1 \Phi_1^o}{X_2} \quad (21)$$

Then Eq. (18) is replaced by

$$\begin{aligned} \Phi_2^o &= \frac{4\pi N_0}{3} \left( \frac{\mu^2}{3kT} + \alpha_v + \alpha_e \right) \\ &= \Phi_{2\mu}^o + \Phi_{2v}^o + \Phi_{2e}^o \end{aligned} \quad (22)$$

where  $\mu$ ,  $\alpha_v$ , and  $\alpha_e$  pertain to the solute molecule at infinite dilution in the given solvent.

Before  $\mu$  can be calculated from  $\Phi_2^o$ , it is necessary to separate the dipole term in Eq. (22) from the others. In the solution case, the temperature method of determining  $\mu$  is found to be unreliable, presumably because of temperature-dependent interactions between solute and solvent. Another method is therefore used, which depends on the behavior of  $\epsilon$  as a function of frequency.

Figure 50 shows qualitatively how  $\epsilon$  varies with frequency for a typical polar substance. The frequency dependence of  $\Phi$  is similar. Equation (13) holds in region A. Beyond the upper end of this region, the field is alternating so rapidly that there is not time in the period of a cycle for the molecular-orientation polarization to develop. In the relatively flat region B, where the value of  $\epsilon$  is usually denoted by  $\epsilon_\infty$ , there is no appreciable contribution to  $\langle p_E \rangle$  from dipolar orientation and Eq. (13) is

replaced by

$$\frac{\epsilon_{\infty} - 1}{\epsilon_{\infty} + 2} V = \frac{4\pi N_0}{3} (\alpha_v + \alpha_e) = \mathcal{P}_v + \mathcal{P}_e \quad (23)$$

In region *C*, only the electronic contribution remains.

In the infrared and visible regions,  $\epsilon$  can be measured by optical methods through application of the equation

$$\epsilon = n^2 \quad (24)$$

where  $n$  is the index of refraction, and  $\epsilon$  and  $n$  are to be measured at one and the same frequency. To find  $\mathcal{P}_v + \mathcal{P}_e$ , it would therefore be appropriate to measure  $\epsilon_{\infty}$  or  $n^2$  at far-infrared frequencies, but this is at present

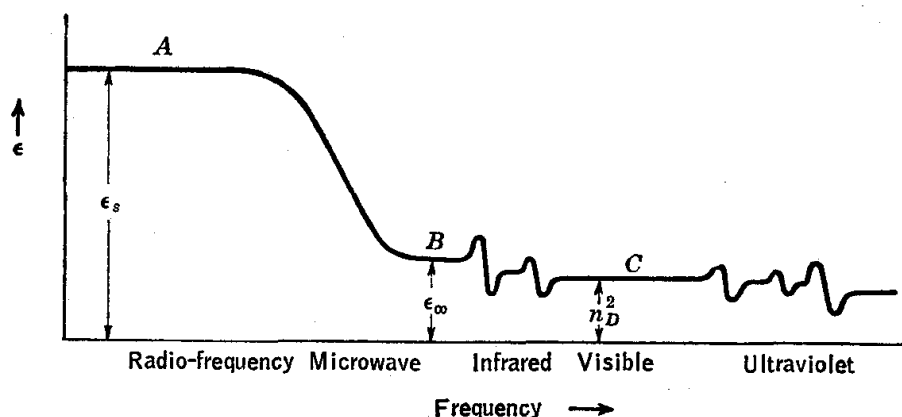


FIG. 50. Frequency dependence of  $\epsilon$  for a typical polar molecule. The frequency scale is only qualitative.

a rather difficult type of measurement. On the other hand,  $n$  is easily measured at the frequency of the sodium D line to obtain

$$\left( \frac{n_D^2 - 1}{n_D^2 + 2} \right) V = \frac{4\pi N_0}{3} \alpha_e = \mathcal{P}_e \quad (25)$$

where  $n_D$  is the index of refraction measured with light of the sodium D line.

The quantity on the left-hand side of Eq. (25) is called the molar refractivity; though it is best to measure it, this quantity can be estimated from tables of atomic refractivities. For the solution quantity  $\mathcal{P}_{2e}^o$ , it is satisfactory to use the value of  $\mathcal{P}_e$  calculated from  $n_D$  for the pure liquid, so long as  $\mathcal{P}_e$  is reasonably small compared with the dipole term, though in principle one should determine refractive indices for the solutions and use an equation similar to Eq. (21).

As  $\mathcal{P}_v$  is at present so difficult to measure and is often quite small, the common practice is to neglect it. For small rigid molecules this pro-

cedure probably does not introduce much error. However, for large or rather flexible molecules, or those having relatively small  $\mu$ , the neglect of  $\Phi_v$  is not justifiable.

In summary, then, the Debye equation for the solution case, as usually applied, is

$$\frac{4\pi N_0}{3} \frac{\mu^2}{3kT} = \Phi_2^o - \Phi_{2v}^o - \Phi_{2e}^o = \Phi_{2\mu}^o \quad (26)$$

or

$$\mu = 0.0127 \times 10^{-18} \sqrt{\Phi_{2\mu}^o T}$$

where  $\Phi_2^o$  is evaluated from Eq. (21),  $\Phi_{2e}^o$  from (25), and  $\Phi_{2v}^o$  is neglected. With the quantities of Eq. (26) expressed in cgs units, the value of  $\mu$  is obtained in esu units. The Debye unit often used for  $\mu$  is equivalent to  $10^{-18}$  esu.

Finally, we look into the question as to how  $\epsilon_s$  is to be measured. The basic equation used is  $\epsilon = C_x/C_0$ , where  $C_x$  is the capacitance of a capacitor filled with the substance and  $C_0$  that of the same capacitor evacuated. This relation follows from the definition of  $\epsilon$ , given after Eq. (3), upon straightforward application of principles of electrostatics. It is assumed that the sample is isotropic, homogeneous, and linear ( $\epsilon$  independent of  $E$ ) and that it completely fills the region in which the condenser field exists.

To minimize the error due to stray capacitance, it is best to use a cell consisting of a variable capacitor, designed to give a convenient difference in capacitance between maximum and minimum settings. The cell described in Exp. 37 (page 229) is satisfactory for this purpose. Two sturdy pins in the top plate serve as positive stops to guarantee that the maximum and minimum settings will be completely reproducible. To eliminate disturbances from stray fields and from variations in stray capacitance, the cell is enclosed within a heavy metal shield, and coaxial cable is used for the connection to the oscillator. The entire assembly should be well constructed mechanically to avoid any undesired relative motion of parts of the cell.

The dielectric constant is calculated as the ratio of two capacitance increments,

$$\epsilon = \frac{C_{b,liq} - C_{a,liq}}{C_{b,air} - C_{a,air}} \quad (27)$$

where  $C_{b,liq} - C_{a,liq}$  is the difference in cell capacitance for the two settings with the sample present, and  $C_{b,air} - C_{a,air}$  is the corresponding difference with air as dielectric. The dielectric constant of air is here being considered to be unity, as it virtually is in comparison with values for liquids.

For the accurate measurement of capacitance required for determination of dipole moments, the heterodyne-beat method is probably the best available. The samples encountered in using the Debye method will usu-

ally meet the requirement of having very low conductance.† However, the resonance apparatus of Exp. 37 is capable of giving satisfactory results, at least for substances with reasonably large dipole moments, and is usable with samples having a somewhat larger specific conductance.

The principle on which the heterodyne-beat method is based is schematically represented in Fig. 51. A radiofrequency signal of constant frequency  $f_0$ , generated by a fixed-frequency oscillator, and a second signal of frequency  $f$ , generated by a variable-frequency oscillator, are fed into a mixer (page 557), whose function is to produce in its output voltage a component of frequency  $|f - f_0|$ . This difference frequency, or beat

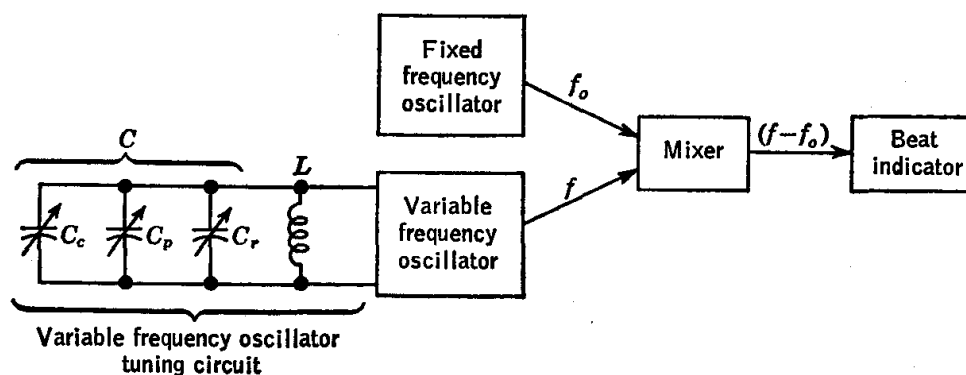


FIG. 51. Principle of the heterodyne-beat method.  $C_c$ , dielectric-constant cell;  $C_p$ , precision capacitor;  $C_r$ , rough-tuning capacitor.

frequency, will be in the audio range when  $f$  and  $f_0$  are nearly equal and can then be detected by earphones or other suitable means.

The frequency of the variable oscillator will be given very closely by the relation

$$f = \frac{1}{2\pi \sqrt{LC}}$$

where  $L$  and  $C$  represent the inductance and total capacitance,

$$C = C_c + C_p + C_r$$

of the variable-frequency-oscillator tank circuit (Fig. 51). Since  $L$  is fixed, the frequency is determined by  $C$ . For an arbitrary setting of  $C_p$ , the beat frequency  $|f - f_0|$  will usually be above the audio range. As  $C_p$  is then varied, a beat note will first be heard as a high-pitched tone when the difference  $|f - f_0|$  enters the audio range. As  $C_p$  is further changed, the beat frequency continuously decreases through the audio range until it becomes too low to be heard, passes through zero, and then

† At 1 Mc/sec, the precision is impaired if the specific conductance exceeds about  $10^{-8}$  ohm $^{-1}$  cm $^{-1}$ .

again increases on the other side. For precise location of the setting of  $C_p$  corresponding to zero beat, it is necessary also to have a meter, tuning eye, or other device capable of indicating the beats when the beat frequency is too low to be audible.

Provided  $f_0$  and  $L$  are constant and other factors† having incidental effects on  $f$  are sufficiently stable, the condition for zero beat is equivalent to

$$C_c + C_p + C_r = \text{constant}$$

Thus changes in  $C_c$  are accurately measured by finding the change in  $C_p$  required to restore a condition of zero beat. The capacitor  $C_r$  is adjusted as may be necessary to bring the zero-beat settings within the calibrated range of  $C_p$ , but  $C_r$  must obviously not be changed when an increment in  $C_c$  is being measured.

The potential accuracy of the heterodyne-beat method is very high. Differentiation of the frequency-determining relation gives, for constant  $L$ ,

$$\frac{\Delta f}{f} = -\frac{1}{2} \frac{\Delta C}{C}$$

If  $f_0$  is 1 Mc/sec and a beat frequency of 1 cycle/sec can be distinguished from zero beat, the detectable change of capacitance in the circuit is 1 part in 500,000.

**Apparatus.** The heterodyne-beat circuit of Chien<sup>5</sup> has been found very satisfactory for dipole-moment studies. A number of suitable circuits are described in the LeFevre<sup>7</sup> and Smyth<sup>8</sup> monographs. Additional requirements are an analytical balance, a refractometer, a sample of the substance (such as nitrobenzene or acetonitrile) whose dipole moment is to be determined, and about 500 ml of a suitable nonpolar solvent (such as benzene).

**Procedure.** Dielectric-constant measurements are made on benzene and on dilute solutions of acetonitrile in benzene. Concentrations suggested for the work are 1, 2, 3, and 4 mole per cent of solute.

Each solution is made up by weighing the solute in a 100-ml volumetric flask, adding solvent to the calibration mark, and then weighing the solution. The weight of the flask filled with pure solvent should also be obtained. These weighings should be made with an analytical balance. Both mole fractions and densities are to be found from these data. It is best to perform the weighings for all samples in the same volumetric flask, since in this way the normal calibration error in the flask will cause

† The factors most likely to lead to frequency instability are variation in the plate or filament supply voltages and changes in the temperature of critical circuit components. In addition, poor mechanical construction or inadequate shielding may lead to erratic behavior of the oscillator.

a practically constant error in the density which will not appreciably affect the final results with the method of calculation outlined below.

The sample temperature should be controlled to within a few tenths of a degree, as it is important that all measurements of  $\epsilon_s$  and of  $\rho$  be made at the same temperature.

Finally, the refractive index of the pure solute liquid is measured, and its density is either measured (with a pycnometer or density balance) or obtained from the literature.

**Calculations.** For the computation of the molecular dipole moment, it is necessary first to evaluate the molar polarization of the solute at infinite dilution,  $\mathcal{P}_2^\circ$ . One could in principle calculate  $\mathcal{P}_2$  by Eqs. (16), (19), and (20), plot these values against  $X_2$ , and extrapolate to  $X_2 = 0$ . This procedure is not satisfactory, however, because the curvature of the graphs, together with the increasing effect of experimental error on the points as  $X_2$  becomes small, makes the extrapolation unreliable.

The evaluation of  $\mathcal{P}_2^\circ$  may be accomplished analytically with good accuracy by a procedure due to Hedestrand.<sup>4</sup> Assume that, for the dilute solutions involved,  $\epsilon_s$  and  $\rho$  can be accurately expressed as linear functions of  $X_2$

$$\epsilon_s = \epsilon_1 + aX_2 \quad (28)$$

$$\rho = \rho_1 + bX_2 \quad (29)$$

where  $\epsilon_1$  and  $\rho_1$  are the static dielectric constant and the density of the actual solvent sample used, at the temperature at which the measurements have been made. The values of the coefficients  $a$  and  $b$  may be obtained from plots of  $\epsilon_s$  and  $\rho$  against  $X_2$ .

Expressions (28) and (29) may be substituted into the equation

$$\mathcal{P}_2 = \frac{1}{X_2} \left( \frac{\epsilon_s - 1}{\epsilon_s + 2} \frac{X_1 M_1 + X_2 M_2}{\rho} - X_1 \frac{\epsilon_1 - 1}{\epsilon_1 + 2} \frac{M_1}{\rho_1} \right) \quad (30)$$

which is an explicit form of Eq. (20). In this way there is obtained an equation for  $\mathcal{P}_2$  as a function of  $X_2$  which is valid in the dilute-solution range. The limiting value of  $\mathcal{P}_2$ , that is,  $\mathcal{P}_2^\circ$ , may then be evaluated by setting  $X_2$  equal to zero; the result is

$$\mathcal{P}_2^\circ = A(M_2 - Bb) + Ca \quad (31)$$

where

$$A = \frac{\epsilon_1 - 1}{\epsilon_1 + 2} \frac{1}{\rho_1}$$

$$B = \frac{M_1}{\rho_1}$$

$$C = \frac{3M_1}{(\epsilon_1 + 2)^2 \rho_1}$$

A discussion of this and of several other analytical extrapolation procedures is given by Böttcher.<sup>1</sup>

The orientation polarization  $\mathcal{O}_{2\mu}^0$  is then calculated, and from it the value of the dipole moment of the molecule is obtained from Eq. (26).

**Practical Applications.** The introduction of the heterodyne-beat method for the determination of the dielectric constant made possible for the first time really accurate determinations of the electric moments of gaseous molecules.<sup>2,11</sup> With the increased accuracy obtainable in the case of liquids, it is possible to study the effect of a change of nonpolar solvent on the magnitude of the measured electric moment of a given solute molecule.<sup>9</sup>

**Suggestions for Further Work.** The dipole moment of a less polar molecule such as chloroform may be determined. Careful attention to detail is required for accurate results in such work. Different extrapolation procedures may be tried with one set of data.<sup>1,3,6,9</sup>

### References

1. Böttcher, "Theory of Electric Polarisation," Elsevier Press, Inc., Houston, Tex. (1952).
2. Debye, "Polar Molecules," Reinhold Publishing Corporation, New York (1929); Dover Publications, Inc., New York (1929).
3. Halverstadt and Kumler, *J. Am. Chem. Soc.*, **64**, 2988 (1942).
4. Hedestrand, *Z. physik. Chem.*, **B2**, 428 (1929).
5. Chien, *J. Chem. Educ.*, **24**, 494 (1947).
6. Kwestroo, Meijer, and Havinga, *Rec. trav. chim.*, **73**, 717 (1954).
7. LeFevre, "Dipole Moments," 3d ed., Methuen & Co., Ltd., London (1954).
8. Smyth in Weissberger (ed.): "Technique of Organic Chemistry," 3d ed., Vol. I, Pt. III, Chap. 29, Interscience Publishers, Inc., New York (1960).
9. Smyth, "Dielectric Behavior and Structure," McGraw-Hill Book Company, Inc., New York (1955).
10. Wesson, "Tables of Electric Dipole Moments," Technology Press, Massachusetts Institute of Technology, Cambridge, Mass. (1948).
11. Zahn, *Phys. Rev.*, **24**, 400 (1924).

### 37. DIELECTRIC CONSTANTS OF POLAR LIQUIDS; RESONANCE METHOD

The dielectric constants and refractive indices of a number of pure liquids are measured. The results are interpreted with the Onsager equation. The resonance method is used for the dielectric-constant measurements.

**Theory.**<sup>†</sup> The Debye theory relating the dielectric properties of a substance to the molecular dipole moment is outlined in the preceding experiment. A major limitation of the Debye theory is that it is applicable only when the concentration of polar molecules is low—thus,

<sup>†</sup> The present discussion necessarily assumes that the reader is familiar with the basic principles outlined in Exp. 36, especially pages 212-219.

only to polar gases and to dilute solutions of polar solutes in nonpolar solvents.

A significant advance in dielectric theory was made by Onsager, who obtained an equation which is found to be remarkably good even for pure polar liquids, with the exception of associated liquids such as alcohols or water.

It is useful for purposes of comparison to write several equations which would follow from Debye's theory if it *were* to be applied to the case of a pure polar liquid:

$$\frac{\epsilon_s - 1}{\epsilon_s + 2} V = \frac{4\pi N_0}{3} \left( \frac{\mu^2}{3kT} + \alpha_v + \alpha_e \right) \quad (1)$$

$$= \frac{4\pi N_0}{3} \frac{\mu^2}{3kT} + \frac{\epsilon_\infty - 1}{\epsilon_\infty + 2} V \quad (2)$$

or 
$$\frac{4\pi N_0}{3} \frac{\mu^2}{3kT} = \left( \frac{\epsilon_s - 1}{\epsilon_s + 2} - \frac{\epsilon_\infty - 1}{\epsilon_\infty + 2} \right) V \quad (3)$$

where  $N_0$  = Avogadro's number

$\mu$  = molecular permanent dipole moment

$\alpha_v$  = molecular vibrational polarizability

$\alpha_e$  = molecular electronic polarizability

$\epsilon_s$  = static (equilibrium) dielectric constant

$\epsilon_\infty$  = "high-frequency" dielectric constant (page 218)

$V$  = molar volume =  $M/\rho$

$M$  = molecular weight

$\rho$  = density

$k$  = Boltzmann constant

The chief limitation of the Debye equation arises from the use of the Lorentz equation for the internal field (page 215). It is assumed in Debye's derivation that a given polar molecule is acted on by a constant field which is the time average of the field at a molecule due to all charges outside this molecule.

Onsager improved the calculation of the field acting on a molecule by taking into account the fact that the local field at a given polar molecule is a function of the orientation angle  $\vartheta$  (page 214) of the given molecule. The reason for this is that the given molecule influences the polarization of its neighbors, which in turn make important contributions to the field at the given molecule. To see this more clearly, one may visualize calculating the local field at a given polar molecule by holding this molecule at a particular value of  $\vartheta$  and averaging over the thermal motions of all the other molecules, and then repeating this process for various different values of  $\vartheta$ ; if account is taken of the effect of the given molecule on its neighbors, the resulting local field will be found to depend on  $\vartheta$ . Thus the Onsager theory leads to a different expression for  $\langle \cos \vartheta \rangle$  from



that of Debye. Also, explicit allowance is made in Onsager's derivation for the fact that the apparent permanent dipole moment of a molecule immersed in the liquid is slightly different from that of an isolated molecule. Onsager's equation replacing Eq. (3) may be written as

$$\begin{aligned} \frac{4\pi N_0}{3} \frac{\mu^2}{3kT} &= \frac{(2\epsilon_s + \epsilon_\infty)(\epsilon_s + 2)}{3\epsilon_s(\epsilon_\infty + 2)} \left( \frac{\epsilon_s - 1}{\epsilon_s + 2} - \frac{\epsilon_\infty - 1}{\epsilon_\infty + 2} \right) V \\ &= \frac{(\epsilon_s - \epsilon_\infty)(2\epsilon_s + \epsilon_\infty)}{\epsilon_s(\epsilon_\infty + 2)^2} V \end{aligned} \quad (4)$$

where  $\mu$  is the dipole moment of the isolated molecule. Since in most cases  $\epsilon_\infty$  can be replaced by  $n_D^2$  (page 218) without serious error, the quantities on the right side are all readily measurable. Equation (4) has been tested by calculating values of  $\mu$  from it for a large number of polar liquids and comparing these with values found by the gas or the solution method of Debye, or by spectroscopic methods; very good agreement has regularly been found for "normal" liquids, but not for those liquids which from other properties had already been identified as "associated" liquids.

Thus for normal liquids, Eq. (4) offers an attractive means of finding  $\mu$ , since it requires only a single measurement of  $\epsilon_s$  of moderate accuracy, whereas either the gas or the solution method of Debye calls for a series of measurements of high accuracy. The resulting values of  $\mu$ , while not as reliable as those found by measurements on the gas, are probably not significantly inferior to solution values provided the given substance is not associated.

The chief importance, however, of Onsager's equation is not so much in providing a short cut to finding molecular dipole moments as in offering an insight into the nature of molecular interactions in liquids. Whereas the Debye equation neglects the correlation between the orientation of a molecule and that of its neighbors, Onsager's equation takes account of this correlation to the extent that it is due to dipole-dipole interactions. The wide success of Onsager's equation for normal liquids is evidence that in such liquids the dipole-dipole interaction is the dominant one producing correlation in orientation of neighboring molecules. If for a given liquid Onsager's equation does not give the correct value for  $\mu$ , one has strong evidence that there exists in this liquid some specific type of interaction, such as hydrogen bonding or complex formation, which has an important influence on the relative orientation of neighboring molecules.

**Apparatus.** Resonance-type apparatus for measurement of dielectric constant; pycnometer or density balance; refractometer; series of pure-polar-liquid samples, about 100 ml of each.

**Procedure.** The dielectric constants, refractive indices, and densities are to be found for a number of pure liquids at 25°C. A suitable list is

chloroform, methyl ethyl ketone, ethanol, acetone, acetonitrile, trichloroethylene, *n*-propyl alcohol, toluene.

The refractive indices may be measured with an Abbe refractometer (page 55). The densities may be found from the literature or measured by means of a pycnometer or density balance.

The dielectric-constant measurements are based on the equation  $\epsilon = C/C_0$  (page 219). In order to circumvent difficulties due to stray capacitance, it is convenient to use a dielectric cell which is arranged so that measurements are made of capacitance differences between two fixed positions (*a* and *b*) of the rotor plates of a variable capacitor. The dielectric constant of the liquid sample is then obtained from the equation

$$\frac{\epsilon_{\text{liq}}}{\epsilon_{\text{ref}}} = \frac{C_{b,\text{liq}} - C_{a,\text{liq}}}{C_{b,\text{ref}} - C_{a,\text{ref}}} \quad (5)$$

where  $C_{b,\text{liq}} - C_{a,\text{liq}}$  = capacitance increment between positions *a* and *b* measured with plates immersed in liquid sample

$C_{b,\text{ref}} - C_{a,\text{ref}}$  = corresponding increment measured with plates immersed in a reference substance of known dielectric constant

The reference measurements are usually made either with air, for which the value of  $\epsilon$  at 0°C, 760 mm, is 1.00058, which may be considered unity for the present purpose, or with benzene, for which the value of  $\epsilon$  at temperature *t*°C is  $\epsilon = 2.274 + 0.0020(25 - t)$  (Ref. 8). The sample of benzene must be of high purity if a really accurate measurement is involved. The advantage of using benzene rather than air is that the former gives a much larger difference ( $C_{b,\text{ref}} - C_{a,\text{ref}}$ ), which is therefore measurable with greater fractional accuracy.

In this experiment, the capacitance increments are to be measured by a resonance method.† Its chief advantage lies in the fact that the apparatus is relatively simple and can easily be used over a wide frequency range. On the other hand, it is less accurate than the heterodyne-beat method and, at a given frequency, cannot be used with solutions having as high a conductance as can the bridge method.

The standard apparatus assembly for the resonance method is schematically represented in Fig. 52. The dielectric-constant cell forms a part of a resonant circuit comprising a coil *L* and a parallel combination of capacitors: the dielectric-constant cell  $C_e$ , a calibrated precision condenser  $C_p$ , and a coarse-tuning range condenser  $C_r$ . This circuit is coupled inductively (page 553) to the coil  $L_0$  of an oscillator which gen-

† The heterodyne-beat method of Exp. 36 is also very satisfactory for the present experiment; in general, the sample cell should have a somewhat lower capacitance increment ( $C_{b,\text{air}} - C_{a,\text{air}}$ ) than that used for Exp. 36 because much larger values of  $\epsilon$  are encountered.

erates an a-c voltage at a frequency  $f$ . (The frequency is commonly in the radiofrequency region, say 1 Mc/sec, though a wide range of frequencies can be used.) The voltage  $e_s$  induced in the secondary coil  $L$  depends on the current  $i_0$  through the oscillator coil  $L_0$  and on the coefficient of mutual inductance  $M$  (page 553). The equation in terms of a complex  $e_s$  and  $i_0$  is  $e_s = -iM\omega i_0$ , where  $\omega = 2\pi f$ . For loose coupling, the oscillator frequency  $f$  and current  $i_0$  remain constant when the capacitors in the secondary circuit are tuned. Furthermore,  $M$  depends only on the

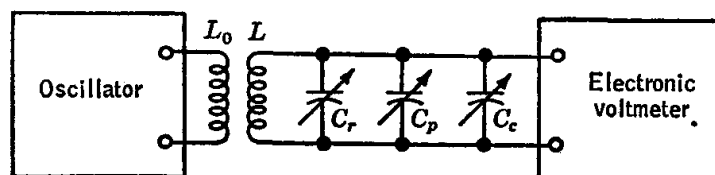


FIG. 52. Schematic representation of standard resonance apparatus. The electronic voltmeter must be of a type which has a high input impedance at the frequency of the oscillator in order that it not load the circuit.

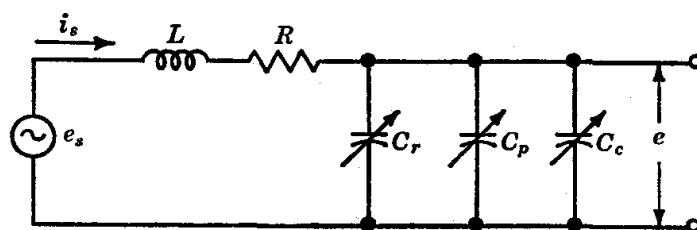


FIG. 53. Equivalent of the resonance circuit, for the case of loose coupling, with induced voltage  $e_s$  and measured voltage  $e$  indicated.

geometry of the coils. Therefore  $e_s$  is practically unaffected by tuning of the capacitors.

The equivalent of the secondary circuit is shown in Fig. 53 for the case of loose coupling. We now examine the behavior of this circuit as the capacitors are tuned. The following relations involving the secondary circuit current  $i_s$  and series impedance  $Z$  (page 547) hold:

$$i_s = \frac{e_s}{Z} \quad (6)$$

$$Z = i\omega L + R + \frac{1}{i\omega C} \quad (7)$$

where  $C$  = parallel combination =  $C_c + C_p + C_r$

$\omega = 2\pi f$

$R$  = effective series resistance, mainly that in the coil

Hence

$$i_s = \frac{e_s}{R + i(\omega L - 1/\omega C)} \quad (8)$$

The voltage across the capacitor is

$$e = i_s \frac{1}{i\omega C} \quad (9)$$

$$= \frac{e_s/i\omega C}{R + i(\omega L - 1/\omega C)} \quad (10)$$

A vacuum-tube voltmeter placed across the capacitors measures  $|e|$ , the magnitude of  $e$ , given by

$$|e|^2 = ee^* = \left(\frac{e_s}{\omega C}\right)^2 \left[ R^2 + \left(\omega L - \frac{1}{\omega C}\right)^2 \right]^{-2} \quad (11)$$

where  $e^*$  is the complex conjugate of  $e$ . Hence

$$|e| = \frac{e_s/\omega C}{[R^2 + (\omega L - 1/\omega C)^2]^{1/2}} \quad (12)$$

As  $C$  is varied,  $|e|$  goes through a maximum when the condition  $\omega L = 1/\omega C$  is met, provided  $R$  is small ( $R \ll \omega L$ ).

So long as  $e_s$ ,  $\omega$ , and  $L$  are held constant, the resonance condition then corresponds to a constant value for  $C = C_c + C_p + C_r$ . If the system is initially at resonance, and then  $C_c$  is changed, the change in  $C_c$  can be measured by finding the change in  $C_p$  required to restore the condition of resonance.

An alternative circuit is shown in Fig. 54. The 6E5 tuning-eye tube acts both as an oscillator tube and as a resonance indicator. The piezo-electric quartz crystal in the grid circuit acts like a very sharply resonant circuit.

As the capacitance in the plate tuning circuit is increased from below the resonance value, oscillations begin when the natural frequency of the plate circuit approaches that of the quartz crystal. The d-c plate current then decreases, the d-c plate voltage rises, and the tuning eye of the tube begins to close. As the capacitance is further increased, a point is reached at which oscillation ceases abruptly, with a corresponding sudden increase in the shadow angle. The critical capacitance setting at which the shadow angle abruptly widens is quite reproducible and is taken as the reference point for capacitance measurements. As the crystal resonance frequency is very stable and  $L$  is practically constant, this critical condition of resonance again corresponds to  $C = C_c + C_p + C_r = \text{constant}$ .

Instead of the tuning-eye tube, a milliammeter which indicates the plate current of the oscillator tube may be used to find the critical capacitance setting corresponding to resonance. As the resonance condition is approached with a gradually increasing value of capacitance, the tube

current gradually decreases to a minimum value, and then very suddenly jumps to a large value as the oscillation stops.

Whichever method is used to indicate the resonance condition, the measuring procedure is essentially the same. The rotor of the dielectric cell containing the reference substance is set in position *a* (minimum capacitance). The precision condenser is set near the upper limit of its range, and the range condenser is tuned to bring the circuit close to resonance, as shown by the response of the electronic voltmeter, tuning eye, or plate current meter, as the case may be. The precision condenser

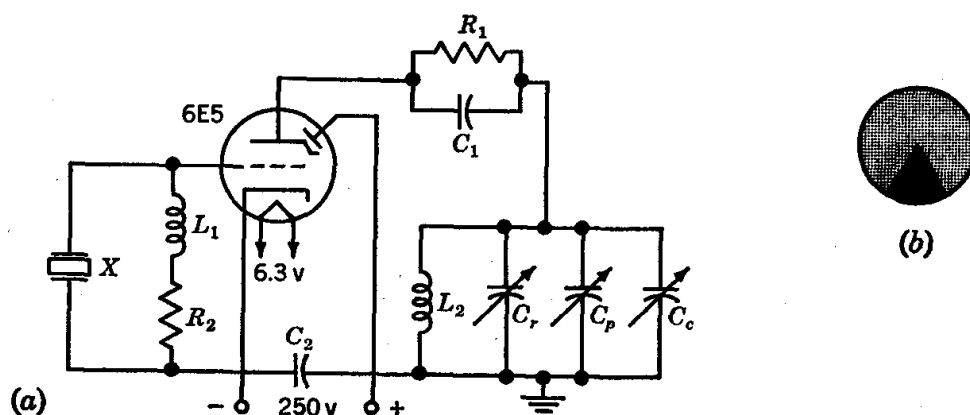


FIG. 54. (a) Resonance circuit for measurement of dielectric constants:  $R_1 = 150,000$  ohms;  $R_2 = 40,000$  ohms;  $L_1 = 2.5$ -millihenry radiofrequency choke;  $X$  = one-megacycle quartz crystal;  $C_p = 150\text{-}\mu\mu\text{f}$  variable air capacitor, calibrated, precision type;  $L_2$  = oscillator tank inductance: 60 turns No. 25 enameled wire, close wound on  $1\frac{1}{2}$ -in.-diameter coil form;  $C_1 = 0.001\text{-}\mu\text{f}$  450 W.V.D.C. (working voltage d-c);  $C_2 = 0.01\text{-}\mu\text{f}$  450 W.V.D.C.;  $C_c$  = dielectric-constant cell;  $C_r = 150\text{-}\mu\mu\text{f}$  variable air capacitor. (b) Face of 6E5 tuning-eye tube. The shadow angle (blackened area) widens as the d-c plate potential increases. As an alternative to the magic-eye indicator, a milliammeter may be inserted in the plate circuit.

is then adjusted carefully to locate the critical capacitance setting. The dielectric-cell rotor is then set to position *b* (maximum capacitance), and the condition of resonance is reestablished by setting the precision condenser, *the range condenser remaining unaltered*. The capacitance increment of the cell,  $\Delta C_c = C_{b,\text{ref}} - C_{a,\text{ref}}$ , is equal to the decrease in the capacitance of the precision condenser required to compensate for it. These same operations are carried out with the liquid sample as dielectric, and the dielectric constant calculated by means of Eq. (5). For accurate work the precision capacitor must be carefully calibrated.

A suitable dielectric-constant cell may be made from a small variable condenser, the number of rotor and stator plates of which is chosen to give a convenient capacitance increment. The guiding consideration here

is that the capacitance increment with a sample having the highest dielectric constant to be measured must not exceed the range of the precision condenser. The condenser, which should have two rotor bearings, is mounted below the metal plate which forms the top of the cell; the stator plates are insulated, and the rotor plates are grounded. An insulated arm is fastened to the rotor shaft, and two brass pins are driven into the supporting plate to provide reproducible minimum and maximum capacitance settings. To minimize pickup of stray voltages and to guard against disturbing effects of variations in stray capacitance between the capacitor and exterior objects, the cell should be surrounded by a grounded metal shield, fastened to the top plate for support, and the connection to the oscillator should be made with coaxial cable. The liquid sample is contained in a lipless beaker or a truncated polyethylene bottle which fits closely inside the shield can.

**Calculations.** Molecular dipole moments are calculated from Eq. (4) and, for comparison, from Eq. (3). The Onsager values are compared with reported<sup>7,9,10</sup> values of  $\mu$ , based on measurements by the Debye gas or solution methods or by spectroscopic methods, and any discrepancies are discussed with due regard for the estimated experimental uncertainty.

**Practical Applications.** The principle of the resonance method is employed in a number of common electronic instruments such as the grid-dip meter and the Q meter. These can be used for rapid measurement of dielectric properties over a wide range of frequencies when high accuracy is not required.

**Suggestions for Further Work.** Onsager<sup>5</sup> gives an equation for a solution of a polar solute in a nonpolar solvent. This equation may be tested by making appropriate measurements on solutions. It may be applied to the case of a solute which is associated as a pure liquid to determine the degree to which such association is important in the solutions.

For accurate measurements, the precision capacitor must be calibrated. It is an instructive exercise to perform this calibration after devising a suitable procedure. The method used will depend on the equipment available. If a precision capacitor and a sensitive bridge are available, the calibration may be made at audio frequencies with satisfactory results. Smyth<sup>7,8</sup> describes a procedure for use with the heterodyne-beat method which may be adapted for use with resonance equipment.

### References

1. Bender, *J. Chem. Educ.*, **23**, 179 (1946).
2. Böttcher, "Theory of Electric Polarisation," Elsevier Press, Inc., Houston, Tex. (1952).
3. Hartshorn, "Radio-frequency Measurements by Bridge and Resonance Methods," John Wiley & Sons, Inc., New York (1941).
4. Maryott and Smith, Table of Dielectric Constants of Pure Liquids, *Natl. Bur. Standards (U.S.), Circ.*, **514** (1951).
5. Onsager, *J. Am. Chem. Soc.*, **58**, 1486 (1936).
6. Pauling, "Nature of the Chemical Bond," 3d ed., Cornell University Press, Ithaca, N.Y. (1960).

7. Smyth, "Dielectric Behavior and Structure," McGraw-Hill Book Company, Inc., New York (1955).
8. Smyth in Weissberger (ed.): "Technique of Organic Chemistry," 3d ed., Vol. I, Pt. III, Chap. 29, Interscience Publishers, Inc., New York (1960).
9. Townes and Schawlow, "Microwave Spectroscopy," Appendix VI, McGraw-Hill Book Company, Inc., New York (1955).
10. Wesson, "Tables of Electric Dipole Moments," Technology Press, Massachusetts Institute of Technology, Cambridge, Mass. (1948).

### 38. DIELECTRIC CONSTANT OF A SOLID AS A FUNCTION OF TEMPERATURE

**Theory.** The dielectric constant of a substance may be defined as

$$\epsilon = \frac{C}{C_0} \quad (1)$$

where  $C$  = capacitance between a pair of conductors immersed in the substance

$C_0$  = capacitance for same arrangement of conductors *in vacuo*

The change in capacitance from  $C_0$  to  $C$  is due to the polarization of the substance under the influence of the field present when the capacitor plates are charged. Polarization is brought about by shifts, over distances of the order of molecular dimensions, in the average positions of the charged particles of which the substance is constituted. Thus  $\epsilon - 1$  is a measure of the extent of such polarization per unit field.

For polar liquids, the dominant contribution to the polarization is generally that due to a slight alignment in the field direction, on the average, of molecules possessing permanent dipole moments. Smaller contributions arise from field-induced distortion of bond lengths and bond angles and from shifts in the electron charge distribution relative to the nuclear framework. These three contributions, it may be noted, are associated, respectively, with rotational, vibrational, and electronic coordinates of the molecule.

As the temperature is lowered, most polar liquids show a gradual increase in dielectric constant, due partly to an increased degree of alignment in the field and partly to an increase in density. Upon freezing, there is observed in most cases an abrupt decrease in dielectric constant because freedom of the molecules to rotate in the field is lost. The small remaining dielectric effect is due to vibrational and electronic terms, which are often not much changed by a change in state, and to lattice polarizability.

It is not uncommon, however, for a polar liquid to exhibit only a small change in dielectric constant upon freezing, and then to show a marked

drop at some lower temperature. This phenomenon is attributed to the retention in the solid state of sufficient rotational freedom to allow reorientation of molecular dipoles in a field. This freedom is lost only at a lower temperature at which a crystalline phase transition takes place. To affect the dielectric constant appreciably, the rotation, whether it involves all or only a part of the molecule, must be such as to cause a change in the orientation or magnitude of the molecular dipole moment. The general correctness of this interpretation has been verified by the study of other properties of the same solids.<sup>1-4</sup> For example, an increase in rotational freedom is often accompanied by a marked increase in entropy and in heat capacity, an increase in symmetry of the crystal

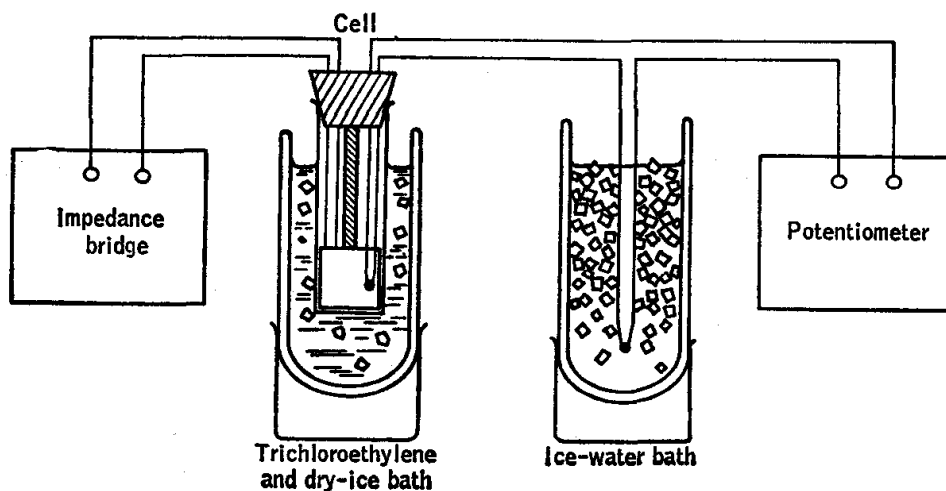


FIG. 55. Apparatus for measurement of dielectric constant as a function of temperature. The thermocouple junctions are shown as solid black circles.

structure, and a decrease in the width of lines in the nuclear-magnetic-resonance spectrum of the solid.

Such rotational effects are observed most often for substances the molecules of which are approximately spherical or cylindrical in shape. Thus, if there are attached, to a single carbon atom, four atoms or groups not all the same but of approximately the same size, the molecule will be polar and yet may exhibit rotation in the solid phase. For example, as a substituent in an organic molecule, a methyl group has about the same effective size as a chlorine or bromine atom. Thus rotation is observed in solid phases of  $\text{C}(\text{CH}_3)_3\text{Cl}$  and  $\text{C}(\text{CH}_3)_3\text{Br}$ .

In the present experiment, the dielectric constant of a polar substance is measured over a range of temperatures above and below the freezing point. The experimental arrangement is shown in Fig. 55. At a series of temperatures, established by a bath of dry ice in trichloroethylene, the capacitance  $C$  of the cell and connecting leads is measured by means of



an impedance bridge. Then  $\epsilon$  is calculated from

$$C = C_1 + \epsilon C_2 \quad (2)$$

where  $C_1$  = capacitance of connecting leads

$C_2$  = capacitance of empty cell alone

The quantities  $C_1$  and  $C_2$  are determined by two measurements of  $C$ , one with the cell empty and one with it filled with a liquid of known dielectric constant. The temperature is measured by means of a thermocouple immersed in the sample.

The sample under investigation, particularly while in the liquid state, may have an appreciable conductance. The cell will be equivalent electrically to a network (Fig. 56) consisting of a resistor in *parallel* with a capacitor. The equivalent resistance  $R$  and capacitance  $C$  depend only on properties of the medium (specific conductance and dielectric constant) and the geometry of the cell. The resistance is given by Eq. (1) of Exp. 27,

$$R = \frac{k}{\kappa} \quad (3)$$

where  $k$  = cell constant

$\kappa$  = specific conductance of medium

while the capacitance, including that of the connecting leads, is given by Eq. (2). The cell impedance  $Z$  for a given frequency  $f$  is determined by  $R$  and  $C$  through the relation (page 550)

$$\frac{1}{Z} = \frac{1}{R} + i\omega C \quad (4)$$

where  $\omega = 2\pi f$ .

The measurement of  $R$  and  $C$  may be accomplished by means of an impedance bridge, which is a generalized Wheatstone bridge having impedances (page 547) rather than resistances as branch elements. A typical bridge for measurement of resistance and capacitance is shown in Fig. 57. The device whose impedance is to be measured constitutes branch 4; the unknown impedance is  $Z_4$ . The input to the bridge is a sinusoidal (sine-wave) voltage, typically at a frequency of 1000 cycles/sec

The operation of balancing the bridge consists of adjusting  $R_1$ ,  $R_2$ , and  $R_3$  for zero output voltage (or, practically, for minimum output) as indicated by the detector. The condition for null output is

$$\frac{Z_1}{Z_2} = \frac{Z_3}{Z_4} \quad (5)$$

where  $Z_1$ ,  $Z_2$ ,  $Z_3$ ,  $Z_4$  are the branch impedances. For the type of bridge

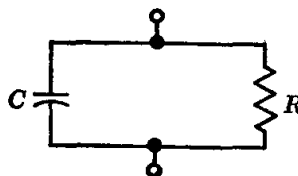


FIG. 56. Network equivalent to cell filled with sample.

shown, the known impedances are

$$Z_1 = R_1 \quad Z_2 = R_2 \quad Z_3 = R_3 + \frac{1}{i\omega C_3}$$

It is convenient to write  $Z_4$  formally as

$$Z_4 = R_4 + \frac{1}{i\omega C_4} \quad (6)$$

$$= \frac{1}{i\omega C_4} (1 + iD) \quad (7)$$

where

$$D = \omega R_4 C_4 \quad (8)$$

One may visualize  $R_4$  and  $C_4$  as the parameters of a fictitious resistor and capacitor which, connected in *series*, would give the total impedance

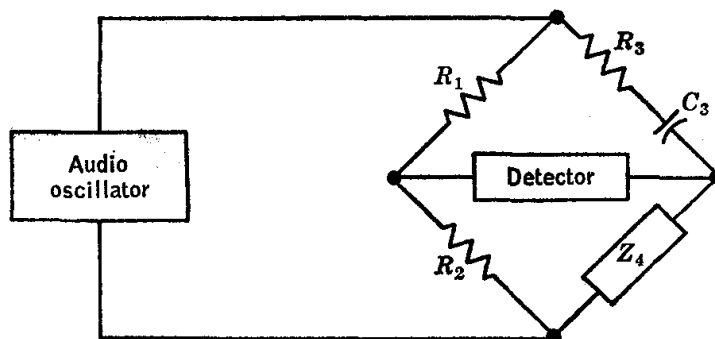


FIG. 57. Schematic diagram of impedance bridge used for dielectric constant measurements. The cell is branch 4.

$Z_4$ . The dissipation factor, as  $D$  is called, is seen to be the ratio of  $R_4$  to  $1/\omega C_4$ , the latter being the magnitude of the reactance of capacitor  $C_4$  at the frequency of measurement.

In principle, from the values of  $R_1$ ,  $R_2$ ,  $R_3$ , and  $C_3$  at balance, one could calculate  $R_4$  and  $C_4$ , or alternatively,  $C_4$  and  $D$ . The bridge dials are usually calibrated in terms of the latter pair of variables. The equations required for calculation of  $R$  and  $C$  from the measured quantities  $C_4$  and  $D$  may be obtained from the equation

$$Z = Z_4$$

where  $Z$  is given by Eq. (4) and  $Z_4$  by Eq. (7). The result is

$$R = R_4 \frac{(1 + D^2)}{D^2} \quad C = \frac{C_4}{1 + D^2} \quad (9)$$

The value of  $R$  is often not of interest because it is sensitive to the presence of impurities in the sample.

**Apparatus.**† Dielectric-constant cell; impedance bridge; thermocouple; potentiometer; samples (e.g., 1,1,1-trichloroethane); Dewar flask; trichloroethylene; dry ice; Variac-controlled electric heater (200-watt radiant immersion type recommended).

**Procedure.** The dielectric constant of 1,1,1-trichloroethane,  $\text{CCl}_3\text{CH}_3$ , is to be measured over the temperature range  $-70$  to  $0^\circ\text{C}$ . It is recommended that a graph of electromotive force versus temperature for the thermocouple be prepared in advance from handbook data.

The apparatus shown in Fig. 55 is assembled with the trichloroethylene‡ bath initially at room temperature. The ground terminal of the bridge should be connected to the outer electrode if the cell electrodes have a coaxial cylindrical arrangement. For the determination of  $C_1$  and  $C_2$ , the capacitance  $C$  is measured with the cell empty and with the cell filled with benzene at room temperature. The temperature of the bath is noted.

The bath is removed, and finely powdered dry ice is added, a few grams at a time, with stirring, until there is an excess. (Rather violent ebullition of bath liquid is apt to occur.)

The sample is placed in the cell, and the cold bath slowly raised into place. The object is to freeze the sample from the bottom upward in such a way as to avoid the formation of air bubbles, cracks, or voids within the solid sample. For highest accuracy, the cell should be fitted with a stopcock and standard taper connection so that it may be attached to a vacuum manifold, and the sample distilled into it with air completely excluded. This refinement can be omitted in student work.

The heater is turned on to produce a slow rate of rise of temperature. The capacitance  $C$  is measured at approximately  $5^\circ$  intervals. For each measurement, the electric heating is stopped and the temperature monitored until both temperature and capacitance are reasonably steady. Near phase changes, additional points should be recorded; to hold the temperature steady for this purpose it may be necessary to add a few grams of dry ice. It is desirable to obtain values of  $C$  intermediate between the values for the pure phases on either side of the transition.

† The design of the cell must be such as to prevent entrance of moist air from the room. A suitable cell available commercially is Type 2TN50 conductance cell manufactured by J. C. Balsbaugh, Marshfield Hills, Mass. This cell requires about 40 ml of sample and has an air capacity of  $50\ \mu\text{mf}$ . It may be modified by a glass blower to permit insertion of the thermocouple leads through the top. The thermocouple may be soldered to the ground electrode of the cell for mechanical support and improved thermal contact.

Coaxial thermocouple wire, well suited to this application, is manufactured by the Precision Tube Co., North Wales, Pa.

The impedance bridge available in kit form from the Heath Company, Benton Harbor, Mich., is satisfactory for this experiment.

‡ Trichloroethylene is mildly toxic; inhalation of appreciable amounts of the vapor is to be avoided.

For best results, the final experiment should be preceded by a preliminary trial, the object of which is to acquire facility with the apparatus and to locate approximately the temperatures at which phase changes occur.

If the conductance of the sample exceeds a certain level, it becomes difficult or even impossible to balance the bridge precisely.<sup>†</sup> The best procedure in such cases is to employ a higher frequency, say 20 kc/sec. This can be done by using an external oscillator as generator for the bridge. As a rule, the conductance of the sample decreases rapidly as the temperature is lowered.

After the conclusion of the work, the cell should be rinsed with a solvent and dried with a current of air.

**Calculations.** The dielectric-constant data are tabulated, and  $\epsilon$  plotted as a function of temperature. The results are interpreted qualitatively and correlated with other available data, such as heat capacities,<sup>2</sup> crystal-structure data,<sup>5</sup> or nuclear-magnetic-resonance-line widths,<sup>3</sup> which have a bearing on the question of rotation in the solid state.

**Practical Applications.** The study of dielectric properties has contributed much to our understanding of the structure and behavior of solids.

**Suggestions for Further Work.** Data may be taken with a slowly falling temperature. Since supercooling is common, it is often possible to obtain dielectric data for the supercooled liquid for a considerable range below the melting point.

It is instructive to calculate the concentration of an ionized impurity which would be needed to give a value of 0.1 for  $D$  for the case of the liquid phase of the sample studied. The correct order of magnitude will be obtained if the equivalent conductance of the impurity is taken as  $50 \text{ cm}^2 \text{ ohm}^{-1} \text{ equiv}^{-1}$ .

The relationship  $4\pi kC_0 = 1$  (esu units) or  $kC_0 = \epsilon_0 = 8.854 \times 10^{-12} \text{ farads/meter}$  (mks-coulomb units), easily derived for the parallel plate case but actually valid for any cell geometry, is useful for estimating effects of sample conductance.

### References

1. Böttcher, "Theory of Electric Polarisation," pp. 399-409, Elsevier Press, Inc., Houston, Tex. (1952).
2. Kushner, Crowe, and Smyth, *J. Am. Chem. Soc.*, **72**, 1091, 4009 (1950).
3. Powles and Gutowsky, *J. Chem. Phys.*, **21**, 1695 (1953).
4. Smyth, "Dielectric Behavior and Structure," McGraw-Hill Book Company, Inc., New York (1955).
5. Wyckoff, "Crystal Structures," Interscience Publishers, Inc., New York (1948-1959).

### 39. OPTICAL ROTATORY DISPERSION

The rotation of plane-polarized light may be determined by the use of a polarimeter. The variation of rotation with wavelength is called

<sup>†</sup> The null becomes broad unless  $D \ll 1$ . For small  $D$ , Eq. (9) leads to  $D \cong 1/\omega RC$ . Thus, for example, to obtain a sharp null with  $C = 100 \mu\text{f}$  and  $f = 1 \text{ kc/sec}$  requires  $R \gg 1.6 \text{ megohms}$ .

optical rotatory dispersion, and the study of this effect may be used to obtain information on molecular structure.

**Theory.**<sup>7</sup> Electromagnetic radiation consists of sinusoidally varying electric and magnetic fields, the directions of which lie in mutually perpendicular planes. The oscillations are transverse; those in the electric and magnetic fields are perpendicular to the direction of propagation. If the electric component, for example, is restricted to a single plane (as illustrated in Fig. 58a), the light is said to be plane-polarized. In ordinary light the electric component has all possible orientations, and none is preferred. This is because the individual atoms and molecules which are radiating act independently. Such unpolarized light may also

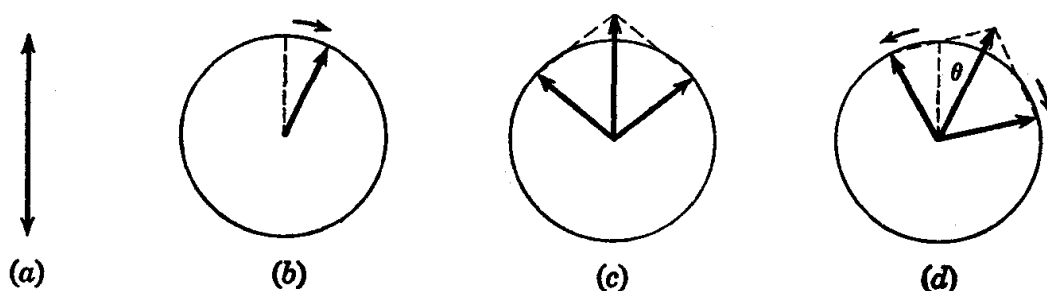


FIG. 58. (a) Electric vector of plane-polarized light moving in a direction perpendicular to the page; (b) circularly polarized light in which the electric vector rotates around the direction of propagation; (c) plane-polarized light considered to be the resultant of two vectors representing circularly polarized light with opposite senses of rotation; (d) rotation of the plane of polarization of plane-polarized light due to the fact that one type of circularly polarized light is propagated through the medium at a higher velocity than the other.

be considered to consist of two plane-polarized waves which are at right angles to each other and have a completely random phase relationship; that is, at any instant the phase difference between the two waves is equally likely to have any value between 0 and  $2\pi$ .

In optically *isotropic* crystals the index of refraction is independent of the direction of propagation of the light through the crystal. In *anisotropic* crystals, such as calcite ( $\text{CaCO}_3$ ), an incident beam of unpolarized light is split into two beams in the crystal. It is found that these two beams are plane-polarized, their planes of vibration being at right angles. The velocities of propagation of these two components through the crystalline medium are different because of the difference in the index of refraction of the medium for the two differently polarized rays. This makes possible the elimination of one component, so that plane-polarized light is obtained. A Nicol prism is constructed by cutting a calcite prism in half along a suitable diagonal plane and cementing the sections together with Canada balsam. At the calcite-Canada balsam interface,

one component is totally reflected to the side, where it is absorbed by a black coating applied to the prism. The other component, for which the refractive index of the balsam and the calcite are almost equal, is freely transmitted.

In order to get a better understanding of the rotation of the plane of polarization of light by certain solutions and crystals, it is useful to consider circularly polarized light. If plane-polarized light is allowed to pass into a suitably cut slab of calcite, the light will be separated into two waves which are plane-polarized at right angles to each other and have equal amplitudes, but are propagated in the same direction through the crystal. The waves travel through the crystal at different speeds, and so there will be a phase difference between them when they emerge from the crystal. If the thickness of the crystal is chosen so that this angle is  $90^\circ$ , the emerging light is circularly polarized and the ground crystal is referred to as a quarter-wave plate. Such a combination of two plane-polarized waves can be represented by a vector rotating about the direction of propagation as shown in Fig. 58*b*. Plane-polarized light may be considered to be made up of two oppositely rotating circularly polarized beams which are in phase. As shown in Fig. 58*c*, the resultant of the addition of these two vectors remains in a single plane.

The optical rotation by a gas, liquid, or solid may be considered to arise from a difference in the velocity of clockwise and counterclockwise circularly polarized light. As shown in Fig. 58*d*, the resultant of the addition of the two vectors representing circularly polarized light is rotated through an angle  $\theta$  if one component travels more rapidly than the other.

Molecules which can be distinguished from their mirror images are able to rotate the plane of polarized light when it passes through them. The presence in the molecule of an asymmetric carbon atom (one for which all four attached groups are different) leads to such a structure and is the most common, but not the only, cause of optical activity. Optical activity is found, for example, in inorganic compounds;  $[\text{Rh}\{(\text{HN})_2\text{SO}_2\}_2(\text{H}_2\text{O})_2]^-$ , an inorganic ion, has been resolved into its two optically isomeric forms.

The magnitude of the optical rotation is measured with a source of monochromatic light and a polarimeter which consists primarily of two Nicol prisms, between which the optically active substance is placed. When the second Nicol, known as the *analyzer*, is placed at right angles to the first, no light can pass through if the cell contains an optically inactive substance. When a substance that is capable of rotating the plane of polarized light is inserted between the Nicols, light can again be seen through the analyzer. The angle through which the analyzer must be turned to darken the field again is represented by  $\alpha$ . If the

analyzer is turned clockwise (as seen by the observer) to restore darkness, the substance is said to be dextrorotatory. If darkness is restored when the analyzer is turned counterclockwise, it is levorotatory.

Because of the error inherent in locating the point of minimum intensity, it is better to employ a scheme in which the eye is required only to compare one field with another field of nearly the same intensity, as is done in half-shadow and triple-shadow polarimeters.

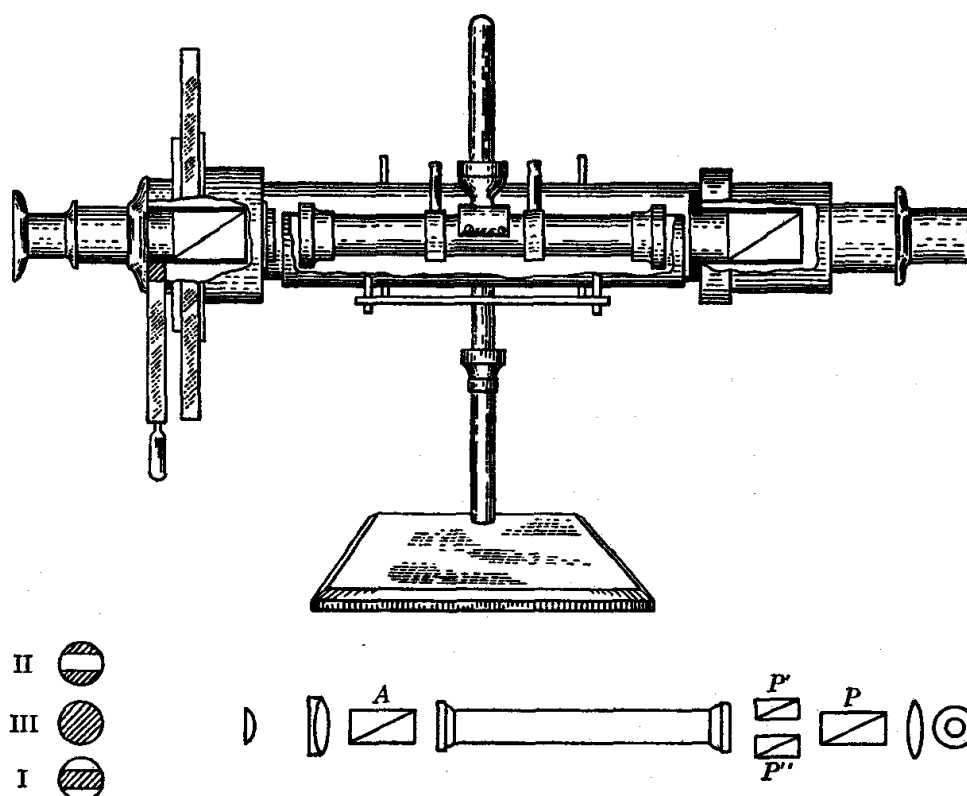


FIG. 59. Polarimeter.

The principle of the Landolt-Lippich triple-shadow polarimeter is illustrated in Fig. 59. Behind the large polarizing Nicol prism  $P$  are placed two auxiliary Nicols,  $P'$  and  $P''$ , whose planes of polarization have been adjusted to make an angle  $\theta$  with that of the principal polarizing prism  $P$ . The angle  $\theta$  may be adjusted to optimum conditions, which will depend on the intensity of the light and the transparency of the liquid. When the analyzer  $A$ , whose orientation is indicated by the instrument scale, is turned so that it is at right angles with the main polarizing Nicol, the central strip of the field, as viewed through the magnifying eyepiece, is dark and the sides are lighter, as shown at I. When the analyzer is turned through the small angle  $\theta$  to cross with the smaller Nicols, the sides are dark and the central strip is lighter, as shown

at II. When the analyzing Nicol is turned back through half of this small angle, it gives a uniform field as shown at III. This proper setting is readily found, and the corresponding reading of the scale is recorded. The double-field polarimeter (Laurent type) employs only one auxiliary Nicol prism, which covers half the field of the polarizing prism. The field of view is thus divided into two parts, and the reference analyzer setting is again that which gives a uniformly illuminated field. The scale is usually graduated directly into quarters of degrees, and with the aid of verniers and a magnifying lens, the angles may be read to  $0.01^\circ$ .

The magnitude of the optical rotation is affected by the concentration of the solution, the length of the path of the light in the solution, the wavelength of the light, the temperature, and the nature of the solvent. The specific rotation  $[\alpha]_\lambda^t$  for a given wavelength  $\lambda$  at a given temperature  $t$  is defined by the relation

$$[\alpha]_\lambda^t = \frac{\alpha}{lc} = \frac{\alpha}{l\rho p}$$

where  $\alpha$  = observed angle of rotation

$l$  = length of light path, *decimeters*

$c$  = concentration of solute, g solute/ml solution

$p$  = concentration of solute, g solute/g solution

$\rho$  = density of solution, g/ml

The specific rotation depends upon the wavelength of the light, and this dependence is called optical rotatory dispersion. The dispersion of optical rotation is closely related to light absorption; in the vicinity of absorption bands, the optical rotation usually increases rapidly and then decreases through zero to give an opposite rotation as the wavelength is changed. This is referred to as the Cotton effect. These changes are more sensitive than most properties to changes in molecular conformation. This tool has recently been developed into a very powerful one for studying molecular structures of complicated organic molecules.<sup>2</sup>

**Apparatus.** Polarimeter; sodium-vapor lamp and mercury-vapor lamp or other sources of monochromatic light; sugar solutions; filters.

**Procedure.** Solutions containing approximately 5, 10, and 15 g of sugar per 100 ml are prepared using volumetric flasks. The crystallized sucrose should be heated to  $105^\circ$ , cooled in a desiccator, and weighed out accurately.

Monochromatic light sources must be used with the polarimeter because of optical rotatory dispersion. To demonstrate this phenomenon for sucrose, the sodium-vapor lamp is supplemented as a light source



by a mercury-vapor lamp, such as Type H-4, with which filters† are used to isolate the strong lines in the visible region at 5780 Å (yellow), 5460 Å (green), and 4358 Å (blue). For this purpose it would be advantageous to use a monochromator by which the wavelength could be varied continuously. The light source should be placed at the proper focal distance from the end of the polarimeter (about 20 cm) and should not be close enough to heat the instrument. It must be carefully positioned on the optical axis of the instrument to ensure uniform illumination of the polarizer.

The polarimeter tube is rinsed and filled with distilled water, as full as possible, and the cap is screwed on, not tightly enough to cause strain, as this would produce an additional optical rotation. Any small air bubble remaining is driven up into an enlargement, above the line of vision. The glass plates at the ends must be clean, and the exposed surface must be dry. The analyzer is rotated until the field is uniformly illuminated, and several readings are taken. The average gives the zero point. The setting of the analyzer should always be approached from the same direction in order to avoid backlash. The zero reading is subtracted from the readings on the optically active material. It should be taken at the beginning and end of each set of determinations.

The tube is next rinsed two or three times with a sugar solution and filled as before; three or more readings are taken. For each solution the rotation is measured for each wavelength of light available.

**Calculations.** The specific rotation of sucrose is calculated from the observed optical rotations for each of the wavelengths employed. The results are compared with the values given in tables.<sup>6</sup> The change with temperature of the specific rotation of sucrose in water solution is approximately  $-0.02$  per cent/°C in the neighborhood of room temperature and is essentially independent of wavelength.

Plots are made of optical rotation versus concentration for each wavelength and of specific rotation versus wavelength.

**Practical Applications.** Optical rotation is used in identifying materials and in determining the structure of organic compounds.<sup>2,4</sup> It finds important applications in quantitative analysis, as, for example, in the determination of the concentration of sugar in solutions.<sup>1</sup> Certain chemical changes may be followed without disturbing the system, as, for example, in the rate of inversion of cane sugar by catalysts (described in Exp. 24). The helix-coil transformation in polypeptides may be studied by measurements of optical rotation.<sup>3</sup>

† Wratten filters may be obtained from the Eastman Kodak Co., for the yellow line No. 22, for the green line No. 77, for the blue line No. 40. The glass-filter combinations supplied by the Corning Glass Works may also be used, as described in Chap. 25. An excellent liquid filter solution for the 4358 Å line is described in Exp. 41. Some polarimeters are equipped with a removable glass filter, for use with the sodium D line source, which must be removed when other wavelengths are employed.

**Suggestions for Further Work.** Other substances which are optically active, such as tartaric acid, may be studied in the same manner as sugar. Nonaqueous solutions may be used, e.g., camphor in benzene, carbon tetrachloride, and acetone.

#### References

1. Bates *et al.*, *Polarimetry, Saccharimetry and Sugars, Natl. Bur. Standards (U.S.), Circ., C440* (1942).
2. Djerassi, "Optical Rotatory Dispersion," McGraw-Hill Book Company, Inc., New York (1960).
3. Doty and Yang, *J. Am. Chem. Soc.*, **78**, 498 (1956).
4. Gilman, "Organic Chemistry," 2d ed., John Wiley & Sons, Inc., New York (1943).
5. Heller and Fitts in Weissberger (ed.): "Technique of Organic Chemistry," 3d ed., Vol. I, Pt. III, Chap. 33, Interscience Publishers, Inc., New York (1960).
6. International Critical Tables, Vol. II, McGraw-Hill Book Company, Inc., New York (1928).
7. Kauzmann, "Quantum Chemistry," Chaps. 15 and 16, Academic Press, Inc., New York (1957).
8. Klyne and Parker in Weissberger (ed.): "Technique of Organic Chemistry," 3d ed., Vol. I, Pt. III, Chap. 33, Interscience Publishers, Inc., New York (1960).

## *Spectroscopy*

### 40. SPECTROMETRY AND SPECTROGRAPHY

The calibration and use of a spectrometer or spectrograph are illustrated in this experiment. The study of typical emission spectra is used to emphasize theoretical and practical applications.

**Theory.**<sup>1,3,4</sup> The passage of polychromatic light through a prism or its reflection from a ruled grating results in the dispersion of the light into its various wavelengths. The visible range of the spectrum so produced extends from the violet at about 4000 Å to the deep red at about 7500 Å. The angstrom unit, named after the Swedish physicist, was originally defined as  $10^{-8}$  cm. It is now defined as  $1/6438.4696$  of the wavelength of the cadmium red line, under carefully specified conditions, which thus becomes the primary standard of wavelength, and is designated as Å. Wavelengths of other lines used as secondary standards have been measured relative to the primary standard with a precision as high as 0.0001 Å, and the primary standard is known in terms of the standard meter bar to about 1 part in 10,000,000. For all but the most accurate work, 1 Å can still be taken to be  $10^{-8}$  cm.

For many purposes it is convenient to characterize spectral lines in terms of *wave number*,  $\tilde{\nu}$ , which is the reciprocal of the wavelength in centimeters. For example, the wave number of the green line in the mercury arc spectrum is  $1/(5460.73 \times 10^{-8} \text{ cm})$ , or  $18,312.6 \text{ cm}^{-1}$ .

A sketch of a simple spectrograph is shown in Fig. 60. The collimator renders the rays of light parallel; the prism refracts them to an extent depending on their wavelength; and the spectrum is observed at the focal plane of the camera lens. The collimator is essentially a tube provided with a convex lens at one end and a narrow adjustable slit at the other, the slit being at the principal focus of the lens, so that the light enters the prism as a parallel beam. The prism illustrated is of the constant-deviation type and can be regarded as built up of two 30-60° prisms, which perform the separation of the rays, and a 90° totally reflecting prism. The prism is rotated by means of the screw *A*, which moves a lever arm fastened to the prism table. A scale, also driven by the screw, indicates the wavelength centered in the field.

Specially sensitized photographic plates, made by the Eastman Kodak Co., are available for overlapping wavelength ranges from the far ultraviolet to the near infrared; for the visible spectrum panchromatic film is also useful. Glass prisms and lenses restrict observations to wavelengths from about 3600 to 10,000 Å. For the ultraviolet region quartz or fluorite optics are used, while infrared prism spectrometers employ NaCl, KBr, and CsBr prisms with special detectors. Reflection gratings avoid the problem of light absorption by prisms and can provide high dispersion and resolution of the spectrum.

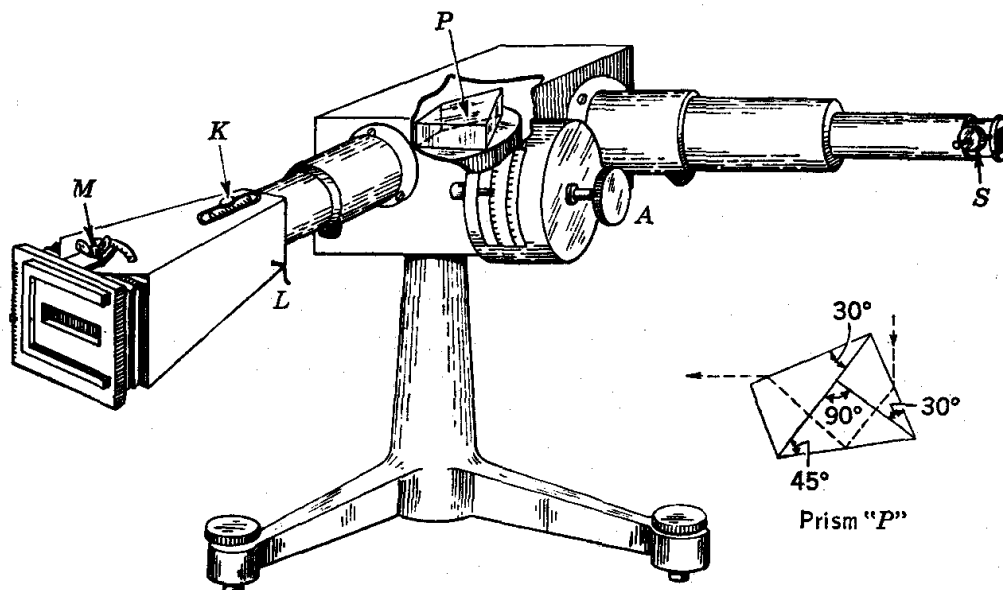


FIG. 60. Constant-deviation spectrograph: A, wavelength control; K, focusing adjustment; L, shutter; M, plate adjustment; P, prism; S, slit.

The instrument shown in Fig. 60 can be used as a spectrometer for visual work by replacement of the camera by an eyepiece assembly containing a cross hair. The wavelength of a spectral line brought to the cross hair is read directly on the wavelength scale. In another common type of spectrometer the spectrum lines are seen superimposed on an illuminated scale, relative to which the various line positions are read. The scale must be calibrated by use of lines of known wavelength.

The conditions required for the production of emission spectra (high-temperature-low-voltage arc, or high-voltage discharge) are such that only for atoms and very simple molecules can the emission spectrum be studied; for complex molecules the methods of absorption spectroscopy must be used. For atoms the emission lines originate in a change in the electronic energy of the atom. According to the quantum theory, the electronic energy of a particular kind of atom can have only certain discrete and characteristic values. For a gas such as helium, under ordinary

conditions all but a negligible fraction of the atoms will be in the lowest electronic-energy state. In the high-voltage gas discharge tube, however, atoms are raised to various high energy states. When such an excited atom drops back to a lower energy level, the energy balance is maintained by the emission of radiation, which is observed as one of the characteristic emission lines of the atom. The frequency of the emitted radiation is given by the quantum condition

$$h\nu = hc\bar{\nu} = E_2 - E_1 \quad (1)$$

where  $h$  = Planck's constant

$\nu$  = frequency

$E_2$  = energy of higher energy state

$E_1$  = energy of lower energy state

$c$  = velocity of light

$\bar{\nu}$  = wave number

The emission spectrum of a diatomic molecule, as obtained from a discharge tube, is a superposition of the spectra of the molecule and of the atoms produced by its dissociation. Because changes in quantized energies of vibration and rotation are possible for molecules as well as changes in electronic energy, the emission spectrum of a diatomic molecule is quite complex. It consists of a series of bands of lines, each band corresponding to a particular change in electronic energy combined with various smaller changes in rotational and vibrational energies.

The theoretical calculation of the electronic energy levels of complex atoms is quite difficult, but for atomic hydrogen, the simplest atom, the following result has been obtained for the wave numbers  $\bar{\nu}$  of the emission lines:

$$\bar{\nu} = R \left( \frac{1}{n_1^2} - \frac{1}{n_2^2} \right) \quad (2)$$

where  $R$  = Rydberg constant,  $109,677.76 \text{ cm}^{-1}$

$n_1, n_2$  = integral quantum numbers characterizing initial and final energy states

For a given value of  $n_1$ , successive higher values of  $n_2$  produce a series of lines. For  $n_1 = 2$ , this series of lines lies in the visible region of the spectrum. The Lyman series, for which  $n_1 = 1$ , is found in the ultraviolet range, and other series corresponding to  $n_1 = 3, 4$ , etc., lie in the infrared region. It is interesting to note that the relation expressed by Eq. (2) was found empirically by Balmer to represent the visible emission lines of atomic hydrogen long before the first theoretical derivation of the formula was achieved by Bohr.

**Apparatus.** Spectrograph; panchromatic film; plateholder; mercury-vapor lamp; argon, helium, hydrogen, nitrogen, and mercury-argon discharge tubes; discharge-tube

transformer; photographic developer and fixer solutions; sample undeveloped film; microscope comparator.

**Procedure.** The spectrograph focusing is checked by examination of the spectrum from a mercury-vapor lamp† placed in front of the slit. The slit width should be set to give a narrow line (about 0.1 mm) but should not be so small as to require inconveniently long exposures; a slit height of about 8 mm is recommended. The lines should be in good focus in all parts of the spectrum; if this is not the case, further adjustment of the instrument should be made in accordance with the instructions furnished by the manufacturer, or with *expert* assistance.

The panchromatic film, which is employed because of its sensitivity to the entire visible range of the spectrum, must be handled in complete darkness. The film is placed in the holder with the emulsion side out; this operation is facilitated by preliminary examination of a sample undeveloped film. Some holders are designed for use with cut film only, but others accommodate film or plates. In the latter case the film is placed in a metal film sheath for support before being put into the plateholder.

The spectrograph shutter is closed, the holder is attached to the camera, and the black slide covering the film is withdrawn. By means of the rack-and-pinion control provided, the plateholder position is adjusted so that the top edge of the film is in position for the first exposure. The shutter is then opened, and the spectrum of the mercury-vapor lamp is recorded. The proper exposure times for this and the other spectra studied depend on the characteristics of the particular spectrograph and light sources used. Approximate exposure times for the various spectra should be specified by the instructor as reference data for this experiment. For a new source, a set of trial exposures varying between wide limits may first be taken, and the optimum exposure time selected on the basis of these results.

The plateholder is moved up 1 cm, as indicated on the adjacent scale, and the next spectrum recorded. Exposures are thus taken of the argon, helium, hydrogen, and nitrogen discharge-tube spectra. The discharge tubes should be placed in position immediately in front of the slit. **Cau-tion:** The operating voltage for these tubes is several thousand volts. A switch in the transformer primary circuit is used to control the discharge tube; the intensity can be varied by a resistance connected in the primary circuit. Alternatively, an autotransformer may be used to supply the primary voltage.

A second mercury spectrum is recorded as the last exposure on the film. The order in which the spectra are taken is recorded.

† The General Electric H-2 or H-4 mercury-vapor lamp is recommended. Either lamp requires a special transformer for its operation.

The plateholder is taken to the darkroom. Three trays containing, respectively, D-19 developer solution, distilled water, and F-5 acid fixing solution are placed in a sequential order, and their positions memorized. In total darkness, the film is developed, with sensitized side facing upward, for 5 min, carefully rinsed in the distilled water tray, and then fixed for 15 min with frequent agitation. Care should be taken to avoid scratching the sensitized side. The film is then washed in running water for 30 min and air-dried. Further details of the practice and theory of the photographic process are given on page 514.

A straight line is marked on the film with a needle, connecting a sharp line in the upper mercury spectrum with the corresponding line in the lower. The distance of each of the mercury lines from this reference line is obtained using a comparator; the film is mounted between two pieces of *plate glass*, to keep it flat, with the emulsion side up. A preliminary dispersion curve is drawn through a plot of wavelength versus displacement in millimeters from the reference line; the wavelengths of the mercury lines are obtained from Fig. 133 (page 503). With this curve, lines in the helium spectrum listed in handbooks are identified; their positions relative to the reference line provide additional points to define the dispersion curve more accurately.

The displacements of several lines in the argon spectrum from the reference line are determined, together with those of the several lines of the Balmer series identified in the hydrogen spectrum. The comparator settings should all be approached from the same direction to eliminate difficulties from backlash and looseness in adjustment.

If a comparator is not available, an enlargement of the film may be made and the line positions measured with an accurate steel rule.

**Calculations.** The wavelengths found for the argon lines by means of the dispersion curve are compared with literature values. The wavelengths for the Balmer lines are calculated by use of the theoretical formula of Eq. (2) and compared with those found experimentally. No measurements on the nitrogen spectrum are made, but the features of the spectrum are carefully noted.

**Practical Applications.** The spectrograph has been one of the most useful tools in the advancement of science, particularly in the fields of chemistry, physics, and astronomy. With it, most of the elements and many compounds may be identified and a quantitative analysis obtained, even with minute quantities. It has aided in establishing the structure of organic compounds. It has been responsible for the discovery of many of our elements. It has made possible a determination of the composition and temperature of the sun and stars. Even the velocities of some of the stars have been calculated with its help. Intelligent advances in photochemistry demand a complete knowledge of absorption spectra, and a spectrometer furnishes the best source of monochromatic illumination for controlled experiments in that branch of physical chemistry.

The nature of the absorption spectrum, whether continuous or discontinuous, is of value in interpreting the mechanism of the molecular absorption and the nature of certain photochemical reactions.

**Suggestions for Further Work.** The absorption spectrum of potassium permanganate or of a dye solution may be obtained by placing an absorption cell in front of the slit and illuminating it with a small frosted electric-light bulb. Potassium permanganate and especially salts of neodymium and praseodymium give fairly sharp bands in sufficiently dilute solutions.

Several suitable experiments on band spectra of diatomic molecules have been suggested by Davies.<sup>2</sup>

#### References

1. Brode, "Chemical Spectroscopy," John Wiley & Sons, Inc., New York (1947).
2. Davies, *J. Chem. Educ.*, **28**, 474 (1951).
3. Harrison, Lord, and Loofbouro, "Practical Spectroscopy," Prentice-Hall, Inc., Englewood Cliffs, N.J. (1948).
4. Herzberg, "Atomic Spectra and Atomic Structure," 2d ed., Dover Publications, New York (1944).

#### 41. RAMAN SPECTRUM

The Raman spectra of chloroform and benzene are obtained, using the 4358 Å mercury line for excitation. The Raman frequency shifts are measured and compared with the infrared absorption frequencies of the compounds.

**Theory.**<sup>8,9,15</sup> When a transparent and homogeneous medium is traversed by a beam of light, laterally diffused radiation may be observed. This phenomenon, termed the scattering of light by the medium, is a universal property of matter and had been under experimental and theoretical investigation for a number of years when in 1928 Raman discovered, in the scattered light, weak radiation of discrete frequencies not present in the monochromatic incident light and characteristic of the material under investigation. The term *Raman effect* refers to the production of these altered frequencies, whose complement constitutes the Raman spectrum.

The Raman effect arises from an exchange of energy between the scattering molecule and a photon of the incident radiation, which results in a transition of the molecule from one of its discrete energy states to another and a compensating change in the energy, and hence in the frequency, of the photon. The fundamental equation is

$$h\nu + E_1 = h\nu' + E_2 \quad (1)$$

where  $h$  = Planck's constant

$\nu$  = frequency of incident photon

$\nu'$  = frequency of scattered photon

$E_1, E_2$  = initial and final energies of molecule



The Raman line of frequency  $\nu'$  is called a Stokes line, if  $\nu > \nu'$ , and an anti-Stokes line, if  $\nu' > \nu$ . The Stokes lines correspond to transitions in which the molecule is raised from a lower to a higher energy state at the expense of the photon, the anti-Stokes lines to transitions in which the molecule drops from an excited state to a lower energy level and gives up energy to the photon. Hence any permitted transition can give rise to both a Stokes and an anti-Stokes line, of which the former will be stronger because of the relatively small number of molecules in the higher energy states. Theory and experiment are in good agreement on the ratio of the intensities of the Stokes and anti-Stokes lines corresponding to a given transition.<sup>1</sup>

The difference in frequency between the Raman line and the exciting line is independent of the frequency of the incident light and is a measure of the separation of two energy states of the molecule. It is called the Raman frequency shift, or Raman frequency, and is ordinarily expressed in wave numbers  $\bar{\nu}$ , or  $\text{cm}^{-1}$  (page 243). Thus

$$\Delta\bar{\nu} = \frac{\nu - \nu'}{c} = \frac{E_2 - E_1}{hc} \quad (2)$$

where  $c$  is the velocity of light. For polyatomic molecules, only changes in the vibrational contributions to the energy are ordinarily observed in the Raman effect. The total vibrational contribution is the sum of the contributions of all the vibrational degrees of freedom of the molecule; for a particular vibrational degree of freedom, this contribution can have only values given by

$$E_i = (n + \frac{1}{2})hc\bar{\nu}_i \quad n = 0, 1, 2, 3, \dots \quad (3)$$

where  $\bar{\nu}_i$  = corresponding fundamental vibrational frequency,  $\text{cm}^{-1}$

$n$  = vibrational quantum number

It follows from Eqs. (2) and (3) that in the Raman spectrum of a polyatomic molecule there will be found:

1. Frequency shifts equal to fundamental vibrational frequencies of the molecule, corresponding to transitions between adjacent energy levels associated with a single vibrational frequency. These lines are ordinarily the strongest Raman lines.

2. Frequency shifts equal to linear combinations (sums and differences) of several fundamental frequencies, due to simultaneous changes in the energy associated with the several modes of vibration concerned.

3. Frequency shifts equal to integral multiples of the fundamental vibrational frequencies, due to the less common transitions between non-adjacent levels associated with a single frequency. These lines are usually very weak.

Corresponding to each fundamental vibrational frequency there is a

"normal mode of vibration," the complete description of which involves the specification of the motion undergone by each atom in the molecule. Any vibrational motion of the molecule can be represented as a superposition of the different normal modes with appropriate amplitudes. In general, *all* the atoms in the molecule are involved in each normal mode of vibration, but it has been found experimentally and explained theoretically that the presence of various groups in the molecule can give rise to characteristic vibrational frequencies irrespective of the nature of the rest of the molecule.<sup>8</sup> Thus all aliphatic nitriles have a characteristic frequency of approximately  $2100\text{ cm}^{-1}$  which is associated with the stretching of the carbon-nitrogen triple bond. These group frequencies are often useful in the identification of structural features through the Raman spectrum.

Significant results can be obtained from a study of the Raman lines obtained with appropriate excitation conditions. Let the incident light be nonpolarized and confined to a beam traveling in the  $XY$  plane and perpendicular to the axis of the Raman tube, which is considered to coincide with the  $X$  axis. Let the scattered light be resolved into components  $I_{\perp}$  polarized perpendicular to the  $XZ$  plane and  $I_{\parallel}$  polarized parallel to the  $XZ$  plane. Then the *depolarization factor*  $\rho$  for the Raman line is the ratio  $I_{\perp}/I_{\parallel}$ . Considering lines associated with the fundamental transition from the ground state to the first excited vibrational level for a single mode of vibration, the depolarization factor will be less than  $\frac{8}{7}$  if the symmetry of the equilibrium configuration of the molecule is preserved throughout the whole cycle of the vibrational motion involved; otherwise  $\rho$  will be equal to  $\frac{8}{7}$  (Ref. 8). For the totally symmetric modes of molecules such as carbon tetrachloride and sulfur hexafluoride which belong to cubic point groups, the depolarization factor is zero; for the totally symmetric modes of other molecules, it will be greater than zero but less than  $\frac{8}{7}$ . The determination of the polarization states of Raman lines is thus of great help in the assignment of frequencies to particular modes of vibration.<sup>8</sup>

Details of the single-exposure method, in which the two components of the scattered light are recorded simultaneously, have been given by Cleveland.<sup>3</sup> A two-exposure method in which polarized incident radiation is employed has been described by Crawford and Horowitz.<sup>4</sup> The recent improvements in photoelectric detection systems make it possible to avoid the problems of quantitative photographic photometry.

Intramolecular vibrations also give rise to absorption bands in the infrared region of the spectrum at frequencies equal to fundamental vibrational frequencies and their harmonics and combinations. The quantum theory permits a prediction from the structure of a molecule of the number of fundamental vibrational frequencies, etc., that will be observed in the

Raman spectrum and in the infrared absorption spectrum. Different rules are found to apply to the two different types of spectra, which thus yield complementary information in the study of molecular vibrations. A given vibrational frequency may be detected only in the Raman effect, only in the infrared spectrum, or in both. Conversely, from a comparison of the infrared and Raman spectra of a compound, important information concerning the structure of the molecule may be obtained.

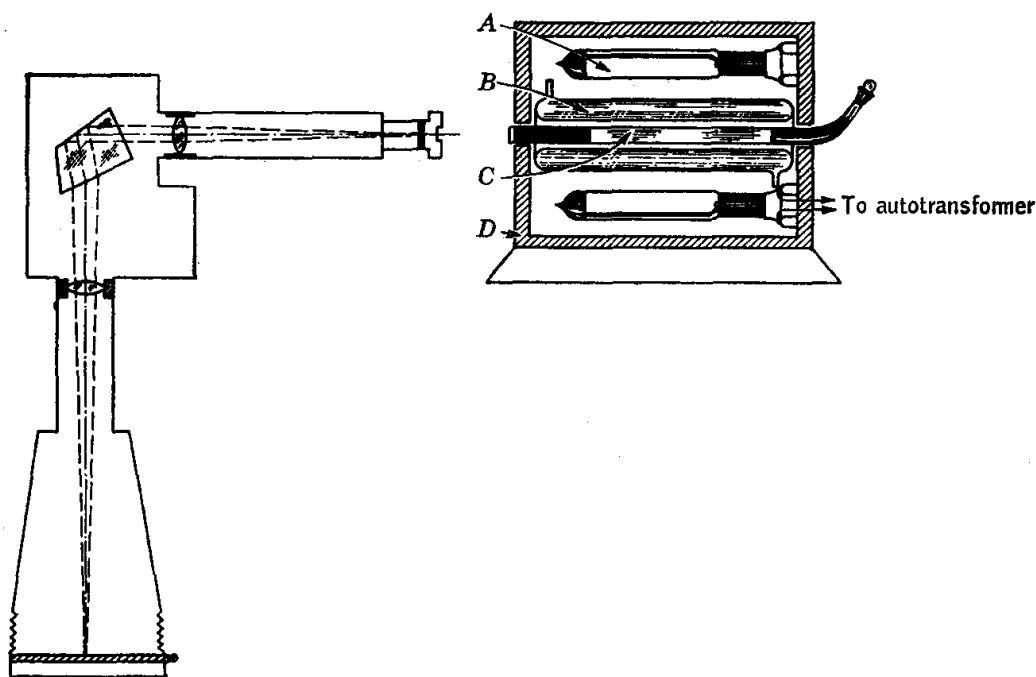


FIG. 61. Apparatus for Raman spectra.

Most studies of Raman spectra have been made on materials in the liquid state. The introduction of special techniques for the Raman spectroscopy of gases<sup>14,17</sup> has been an important recent development in this field.

**Apparatus.** Spectrograph; photographic plate or film; AH-2 mercury-vapor lamps and transformers; Raman tube; glass water jacket; chloroform and benzene; filter jacket; filter solution; argon-mercury tube, helium tube; transformer.

**Procedure.** A typical apparatus assembly is shown in Fig. 61. A spectrograph of fairly large aperture is preferable, but the common wavelength spectrometer of aperture about  $f/16$  gives satisfactory results with a slit width of 0.1 to 0.2 mm. Eastman Type 103a-J spectrographic plates are recommended, although the slower panchromatic film can also be used.

The intense source of light necessary is conveniently provided by a bank of AH-2 mercury-vapor lamps, A, which yield sharp lines and com-

paratively little continuous background in the visible region. A separate transformer is required for each lamp, and a 15-min warm-up period is required to bring the lamps to maximum brilliance.

In research apparatus d-c mercury-arc lamps with water-cooled electrodes<sup>16</sup> are used to give sharp lines of high intensity with favorable line to continuous background intensity ratio. Microwave excitation of alkali metal vapors has been recommended<sup>6</sup> where wavelengths other than those of the mercury spectrum are useful. The maser promises to become of increasing importance as a Raman excitation source.

The liquid to be examined is contained in the Raman tube *C*, of diameter approximately 16 mm and with a plain glass window sealed on the front end.† Except for the window and the section directly opposite the lamps, the tube is painted black to minimize the amount of light reflected rather than scattered into the spectrograph. The Raman tube is protected from the heat generated by the lamps by the glass water jacket *B*, through which tap water is circulated. The entire excitation unit is enclosed in a light-tight box *D*, to keep stray light from entering the spectrograph.

The Raman tube is filled with the desired liquid and placed in the jacket, which should be so adjusted that the axis of the tube coincides with the optic axis of the spectrograph collimator. Improper alignment of the Raman tube is the greatest source of trouble in this experiment. The exposure times required may be minimized by use of a suitable condensing lens selected in accordance with the recommendations of Nielsen.<sup>11</sup> After the two Raman exposures have been made, several reference spectrum exposures are made by means of a mercury-argon discharge tube, placed immediately in front of the spectrograph slit, for use in the construction of a dispersion curve for the spectrograph. Greater accuracy in the latter task is facilitated by superposition of a helium spectrum on the mercury-argon spectrum. The exposure times required for the several spectra depend upon the apparatus used, for which specific recommendations must be provided.

An unfiltered mercury-lamp source will yield spectra clearly showing the excitation of Raman lines by both the 4047 and 4358 Å mercury lines. An effectively monochromatic 4358 Å light source may be obtained by use of a filter solution‡ in a filter jacket surrounding the Raman tube but inside the water jacket. Alternatively, a filter jacket may be ring-sealed to the Raman tube, or an appropriate coating may be applied to the Raman tube itself.<sup>5</sup>

† Such tubes are readily available on special order from manufacturers of scientific glassware.

‡ A solution containing 0.01 per cent crystal violet and 4 per cent *p*-nitrotoluene in ethyl alcohol is recommended. (**Caution:** Fire hazard.)

**Calculations.** The Raman lines, which do not appear on the simple spectrum of the mercury lamp, may be seen at the sides of the 4358 Å exciting line. Their wavelengths are determined, as described on page 247, by means of a dispersion curve based on the standard values for the wavelengths of the mercury, argon, and helium lines; the photographic enlargement method mentioned can facilitate measurements on the weaker Raman lines, which often are difficult to see under the magnification given by a comparator. The frequencies, expressed in wave numbers, of the Raman lines and of the exciting line are calculated. The Raman frequency shifts for the compounds are then determined and compared with the principal infrared absorption frequencies given in Table 1.

For chloroform, agreement is obtained between the Raman shifts and the infrared absorption frequencies listed. For benzene, no such coincidences actually occur; this is an example of the so-called "mutual-exclusion rule" for molecules which, like benzene, possess a center of symmetry. In such a case, the Raman-active fundamentals are not infrared-active, and vice versa. It is readily seen that the application of this rule can be complicated by the experimental uncertainties in the Raman and infrared data.

TABLE 1. PRINCIPAL INFRARED ABSORPTION FREQUENCIES OF CHLOROFORM AND BENZENE<sup>a</sup>  
( $\bar{\nu}_{\text{vacuum}}$ ,  $\text{cm}^{-1}$ )

$\text{CHCl}_3$	$\text{C}_6\text{H}_6$
260	671
364	1,037
667	1,485
760	1,807
1,205	1,964
3,033	3,045
	3,099

<sup>a</sup> Herzberg, "Infra-red and Raman Spectra of Polyatomic Molecules," D. Van Nostrand Company, Inc., Princeton, N.J. (1945).

**Practical Applications.** Many uses have been discovered for the Raman spectra, and these are described in the voluminous literature published since the effect was discovered in 1928. A knowledge of the fundamental vibrational frequencies of the molecules is required for the theoretical calculation of the thermodynamic properties of gases by statistical methods, and the structures of molecules can be deduced through a study of the Raman and infrared spectra. Raman spectra have also found application in the qualitative<sup>2</sup> and quantitative<sup>13</sup> analysis of multicomponent systems and in the determination of the degree of dissociation of strong electrolytes in aqueous solution.<sup>12</sup>

**Suggestions for Further Work.** The Raman spectra of other liquids may be determined. A comparison of the Raman spectra of the two geometric isomers *cis*-

and *trans*-dichloroethylene provides an interesting study. Infrared data are available for these compounds.<sup>8</sup>

The marked difference between the depolarization factor of the  $\Delta\bar{\nu} = 459 \text{ cm}^{-1}$  line of carbon tetrachloride ( $\rho \sim 0$ ) and those of the other Raman lines ( $\rho = \frac{2}{3}$ ) may be shown.<sup>3,4</sup>

#### References

1. Chien and Bender, *J. Chem. Phys.*, **15**, 376 (1947).
2. Cleveland, *J. Am. Chem. Soc.*, **63**, 622 (1941).
3. Cleveland, *J. Chem. Phys.*, **13**, 101 (1945); see also Bender and Lyons, *ibid.*, **18**, 438 (1950).
4. Crawford and Horowitz, *J. Chem. Phys.*, **15**, 268 (1947).
5. Glockler and Haskin, *J. Chem. Phys.*, **15**, 759 (1947).
6. Ham and Walsh, *Spectrochim. Acta*, **12**, 88 (1958).
7. Herzberg, "Molecular Spectra and Molecular Structure," Vol. I, "Diatomic Molecules," 2d ed., D. Van Nostrand Company, Inc., Princeton, N.J. (1950).
8. Herzberg, "Infra-red and Raman Spectra of Polyatomic Molecules," D. Van Nostrand Company, Inc., Princeton, N.J. (1945).
9. Murphy, *J. Opt. Soc. Am.*, **30**, 396 (1940).
10. Murray and Stevenson, *J. Am. Chem. Soc.*, **66**, 812 (1944).
11. Nielsen, *J. Opt. Soc. Am.*, **20**, 701 (1930); **37**, 494 (1947).
12. Redlich and Biegeleisen, *J. Am. Chem. Soc.*, **65**, 1883 (1943).
13. Rosenbaum, Martin, and Lauer, *Ind. Eng. Chem., Anal. Ed.*, **18**, 731 (1946).
14. Stoicheff in Thompson (ed.): "Advances in Spectroscopy," Interscience Publishers, Inc., New York (1959).
15. Sutherland, "Infra-red and Raman Spectra," Methuen & Co., Ltd., London (1936).
16. Welsh, Crawford, Thomas, and Love, *Can. J. Phys.*, **30**, 577 (1952).
17. Welsh, Stansbury, Romanko, and Feldman, *J. Opt. Soc. Am.*, **45**, 338 (1955).

#### 42. SPECTROSCOPIC METHODS FOR THE STUDY OF MOLECULAR STRUCTURE

The use of physical methods for the determination of molecular structure continues to grow in importance as improvements in apparatus facilitate more accurate and detailed observations. The following three procedures provide experience in the use of results obtained with modern research instruments.

##### A. THE NEAR-INFRARED ABSORPTION SPECTRUM OF A HETERONUCLEAR DIATOMIC MOLECULE

**Theory.**<sup>2,3,6</sup> The determination of the characteristic energy levels for a diatomic molecule such as hydrogen chloride requires consideration of a complex dynamical system of electrically interacting particles consisting of two nuclei and a large number of electrons. The quantum-mechanical problem is simplified by the acceptance of the principle known as the Born-Oppenheimer approximation. Because of the marked difference in mass between the electron and even the smallest nucleus, the electrons

in a molecule complete many cycles of their motion in any time interval long enough to permit the more slowly moving nuclei to achieve a finite change in their positions. It is thus possible to consider the electron motion as establishing a potential function which determines the motion of the nuclei. This electronic potential function,  $U(r)$ , may be constructed by solving the Schrödinger wave equation for the electron motion for each of a continuous succession of fixed configurations of the nuclei, corresponding in turn to different values of  $r$ , the internuclear distance. A typical potential-energy curve for the ground electronic-energy state of a stable diatomic molecule is shown in Fig. 62. For this curve the value  $U(r)$  corresponding to a particular internuclear distance  $r$  is found as the lowest energy value for the system consistent with the Schrödinger wave equation for the motion of the electrons for fixed distance  $r$  between the nuclei. In principle, then, the potential-energy curve  $U(r)$  can be calculated theoretically for a molecule, but in practice its form must be established experimentally except for the simplest cases, such as  $\text{H}_2$ . It should be noted, however, that the function  $U(r)$  will be precisely the same for different isotopic species of the same compound, such as  $\text{HCl}^{35}$  and  $\text{HCl}^{37}$ .

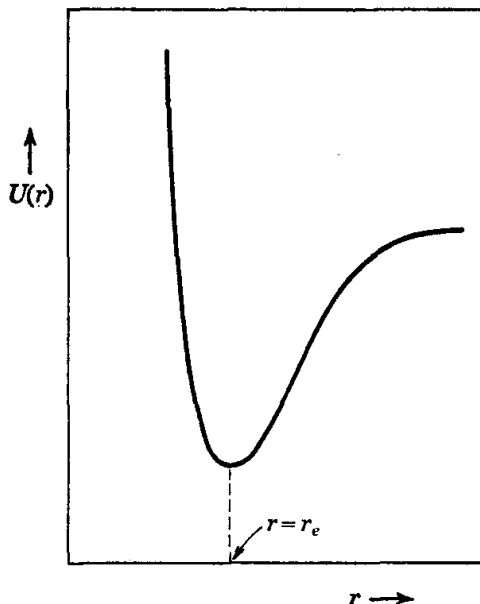


FIG. 62. Potential-energy curve for ground electronic state of a stable diatomic molecule.

The determination of the permitted energy levels ultimately reduces to finding the values of  $W$  for which the radial equation

$$\frac{1}{r^2} \frac{d}{dr} \left[ r^2 \frac{dR(r)}{dr} \right] + \frac{8\pi^2\mu}{h^2} \left[ W - \frac{J(J+1)h^2}{8\pi^2\mu r^2} - U(r) \right] R(r) \equiv 0 \quad (1)$$

admits of solutions for  $R(r)$ , the radial factor in the wave function for the system, which are single-valued, continuous, quadratically integrable, etc., as required for the interpretation of wave functions as probability distribution functions. In this equation  $\mu$ , the *reduced mass* of the two-particle system, is calculated from the masses  $M_1$ ,  $M_2$  of the two atoms as

$$\frac{1}{\mu} = \frac{1}{M_1} + \frac{1}{M_2} \quad (2)$$

The quantity  $h^2 J(J+1)/8\pi^2\mu r^2$ , in which  $J$  is a quantum number which takes on the values 0, 1, 2, 3, etc., may be regarded as a centrifugal-

energy term arising from the rotational motion of the system; the product  $\mu r^2$  is the moment of inertia of the system for internuclear distance  $r$ . Since the precise form of the function  $U(r)$  is not known, it is convenient to introduce a Taylor's series expansion about the equilibrium internuclear distance  $r = r_e$ , corresponding to the minimum in  $U(r)$ , for both it and the centrifugal-energy term. For a function  $f(x)$  the expansion about the point  $x = x_0$  is given by

$$f(x) = f(x_0) + f'(x_0)(x - x_0) + \frac{1}{2!}f''(x_0)(x - x_0)^2 + \frac{1}{3!}f'''(x_0)(x - x_0)^3 + \frac{1}{4!}f''''(x_0)(x - x_0)^4 + \dots \quad (3)$$

It follows that for  $(r - r_e) = \xi$ ,

$$U_J \equiv U(r) + \frac{h^2 J(J+1)}{8\pi^2 \mu} \frac{1}{r^2} = U(r_e) + \frac{h^2 J(J+1)}{8\pi^2 \mu r_e^2} + 2\pi^2 \mu \nu_e^2 \xi^2 + a\xi^3 + b\xi^4 - \frac{h^2 J(J+1)}{4\pi^2 \mu r_e^3} \xi + \frac{3h^2 J(J+1)}{8\pi^2 \mu r_e^4} \xi^2 + \dots \quad (4)$$

where the frequency  $\nu_e$  is defined by the relation

$$2\pi^2 \mu \nu_e^2 = \frac{1}{2} \left[ \frac{d^2 U(r)}{dr^2} \right]_{r=r_e}$$

and the coefficients  $a, b$  by

$$a = \frac{1}{3!} \left[ \frac{d^3 U(r)}{dr^3} \right]_{r=r_e}, \quad b = \frac{1}{4!} \left[ \frac{d^4 U(r)}{dr^4} \right]_{r=r_e}$$

$\left\{ \text{Since the minimum in } U(r) \text{ occurs at } r = r_e, \left[ \frac{dU(r)}{dr} \right]_{r=r_e} \equiv 0. \right\}$

In terms of the variable  $\xi$ , and the substitution  $rR(r) = S(\xi)$ , Eqs. (1) and (4) lead to

$$\frac{d^2 S(\xi)}{d\xi^2} + \frac{8\pi^2 \mu}{h^2} (W - U_J) S(\xi) \equiv 0 \quad (5)$$

If the series expansion (4) for  $U_J$  is limited to the first three terms, the wave equation (5) can be solved exactly to give for the energy levels the expression

$$W, \text{ ergs} = U(r_e) + \frac{h^2 J(J+1)}{8\pi^2 \mu r_e^2} + h\nu_e(v + \frac{1}{2}) \quad (6)$$

The first term simply fixes a reference point for measurement of energy for the molecule. The second is the quantum-mechanical expression appropriate for the rotational energy levels of a *rigid* two-particle system for fixed internuclear distance  $r_e$ . The third term, in which the vibrational quantum number  $v$  can have the values 0, 1, 2, 3, . . . , represents



the energy levels of a one-dimensional harmonic oscillator. Corresponding to this energy-level formula, the functions  $S(\xi)$  are identical in form with those for the one-dimensional harmonic oscillator.

The relation (6) provides a first approximation to the desired result, but to obtain an expression which can accurately characterize the energy-level system for a real molecule, the effect of the other terms in series (4) must be determined. On the assumption that these terms are reasonably small, so that the energy levels for the system will lie close to those given by the rigid-rotator harmonic-oscillator approximation, standard methods of perturbation theory may be employed to give the following result:

$$W_{v,J}, \text{ cm}^{-1} = \frac{1}{hc} W_{v,J}, \text{ ergs} = E(r_e) + \tilde{\nu}_e(v + \frac{1}{2}) + B_e J(J + 1) - x_e \tilde{\nu}_e(v + \frac{1}{2})^2 - \alpha_e(v + \frac{1}{2})J(J + 1) - D_e J^2(J + 1)^2 \quad (7)$$

where

$c$  = velocity of light

$$\tilde{\nu}_e = \nu_e/c$$

$$E(r_e) = \frac{U(r_e)}{hc} + \frac{3bh}{128\pi^4\mu^2c^3\tilde{\nu}_e^2} - \frac{7a^2h}{1024\pi^6\mu^3c^5\tilde{\nu}_e^4}$$

$$B_e = \frac{h}{8\pi^2c\mu r_e^2} \quad D_e = \frac{h^3}{128\pi^6\mu^3r_e^6c^3\tilde{\nu}_e^2} = \frac{4B_e^3}{\tilde{\nu}_e^2}$$

$$x_e = \frac{3}{2} \frac{h}{16\pi^4\mu^2c^3\tilde{\nu}_e^3} \left( \frac{5}{2} \frac{a^2}{4\pi^2\mu c^2\tilde{\nu}_e^2} - b \right)$$

$$\alpha_e = \frac{3h^2}{32\pi^4\mu^2r_e^4c^2\tilde{\nu}_e} \left( \frac{-2ar_e}{4\pi^2\mu c^2\tilde{\nu}_e^2} - 1 \right)$$

The term in  $x_e$  reflects the anharmonicity of the vibrational motion; that in  $\alpha_e$  is a vibration-rotation interaction term which may be associated with the change in the effective value of the moment of inertia of the molecule as the vibrational energy is increased. The quantity  $D_e$  is called the centrifugal-distortion coefficient, since it appears because of the tendency of the internuclear distance for the nonrigid molecule to increase as the rotational energy increases.

The expression (7) for the energy levels is not exact. In a higher approximation there would appear terms proportional to  $(v + \frac{1}{2})^3$ , etc., and further vibration-rotation interaction effects such as a dependency of the centrifugal-distortion coefficient on the vibrational quantum number. Such refinements are rarely justified by the accuracy of the spectroscopic data available.

Defining the rotational coefficient  $B_v$  corresponding to value  $v$  for the vibrational quantum number as

$$B_v = B_e - \alpha_e(v + \frac{1}{2}) \quad (8)$$

$$W_{v,J}, \text{ cm}^{-1} = \tilde{\nu}_e(v + \frac{1}{2}) - x_e \tilde{\nu}_e(v + \frac{1}{2})^2 + B_v J(J + 1) - D_e J^2(J + 1)^2 \quad (9)$$

where  $W_{v,J} = W_{v,J} - E(r_e)$

Consider the difference in energy of the states characterized by  $v = v''$ ,  $J = J''$  and  $v = v'$ ,  $J = J'$  respectively

$$\begin{aligned} W' &= (v' + \frac{1}{2})\tilde{\nu}_e - x_e\tilde{\nu}_e(v' + \frac{1}{2})^2 + B_{v'}J'(J' + 1) - D_eJ'^2(J' + 1)^2 \\ W'' &= (v'' + \frac{1}{2})\tilde{\nu}_e - x_e\tilde{\nu}_e(v'' + \frac{1}{2})^2 + B_{v''}J''(J'' + 1) - D_eJ''^2(J'' + 1)^2 \\ \Delta W &= W' - W'' = (v' - v'')\tilde{\nu}_e - x_e\tilde{\nu}_e(v' - v'')(v' + v'' + 1) \\ &\quad + B_{v'}J'(J' + 1) - B_{v''}J''(J'' + 1) \\ &\quad - D_e[J'^2(J' + 1)^2 - J''^2(J'' + 1)^2] \quad (10) \end{aligned}$$

A transition between these two states may be accomplished by absorption of a photon of wave number  $\tilde{\nu}$  such that  $\tilde{\nu} = \Delta W$ , *provided* that:

1. The molecule is heteronuclear, so that vibrational or rotational motion of the molecule creates an oscillating electric moment.

2. The rotational quantum number  $J$  changes so that  $J' = J'' \pm 1$ . There is no restriction on the change in the vibrational quantum number  $v$ . The principal near-infrared rotation-vibration absorption band occurs for the so-called fundamental transition, for which  $v'' = 0$  (ground vibrational state) and  $v' = 1$  (first excited vibrational state). The first overtone band ( $v'' = 0$ ,  $v' = 2$ ) and the second overtone band ( $v'' = 0$ ,  $v' = 3$ ), etc., are found to be progressively weaker.

For a given change in vibrational quantum number, the set of absorption frequencies corresponding to transitions in which the rotational quantum number  $J$  changes by  $+1$  constitutes the  $R$  branch of the rotation-vibration absorption band; the set for which  $\Delta J = -1$  constitutes the  $P$  branch. The absorption frequencies for the two branches may be summarized as follows:

$$\begin{aligned} R \text{ branch:} \quad & J' = J'' + 1 \quad J'' = 0, 1, 2, 3, \dots \\ \tilde{\nu}_R &= (v' - v'')\tilde{\nu}_e - x_e\tilde{\nu}_e[(v' - v'')(v' + v'' + 1)] + (B_{v'} + B_{v''})(J'' + 1) \\ &\quad + (B_{v'} - B_{v''})(J'' + 1)^2 - 4D_e(J'' + 1)^3 \quad (11) \end{aligned}$$

$$\begin{aligned} P \text{ branch:} \quad & J' = J'' - 1 \quad J'' = 1, 2, 3, \dots \\ \tilde{\nu}_P &= (v' - v'')\tilde{\nu}_e - x_e\tilde{\nu}_e[(v' - v'')(v' + v'' + 1)] - J''(B_{v'} + B_{v''}) \\ &\quad + J''^2(B_{v'} - B_{v''}) + 4D_eJ''^3 \quad (12) \end{aligned}$$

Because the rotational quantum number must change for an allowed transition, there is a discontinuity in the line spacing at the center of the band. For the harmonic-oscillator, rigid-rotator model, this so-called "zero gap" would be exactly twice the common line spacing in the  $P$  and  $R$  branches, which in turn is twice the common value (in this approximation) of the rotational coefficient  $B$  for the two vibrational states involved.

**Apparatus.** Spectrometer records with calibration data;\* precision rule.

**Procedure.** Specialized research spectrometers<sup>8,9</sup> permit the determination of the wavelengths of emission or absorption lines in atomic and molecular spectra with an accuracy measured in parts per million or better, at wavelengths from the ultraviolet to the infrared region of the spectrum. At the present time, however, even standard commercial instruments can provide results whose interpretation can be accomplished quantitatively only in terms of the energy-level scheme defined by Eq. (7).

TABLE 1. REFRACTIVE INDEX OF STANDARD AIR<sup>10</sup>  
(0.03 per cent CO<sub>2</sub>, 15°C, 1 standard atm)

	Air, A	$(n^{\circ} - 1) \times 10^6$	
		Observed <sup>10</sup>	Edlen formula
Hg	5,460.74	277.943	277.901
Ne	7,032.41	275.804	275.758
Hg	10,139.79	274.141	274.104
Hg	11,287.41	273.848	273.812
A	12,487.66	273.640	273.589
He	20,581.29	273.014	273.962

For each band for which a record is provided, the distances of the various lines from a selected reference mark are determined. The wavelengths of the lines are then computed by use of a calibration curve constructed by measurement of the distances from the same origin to the calibration marks provided on the chart. Separate tabulations are made for the *P* and *R* branches of line wavelength versus  $J''$ , the value of the rotational quantum number for the state in which the transition originates.

**Calculations.** The line wavelengths are corrected to wavelengths in vacuum by use of the relation

$$\lambda_{\text{vac}} = n\lambda_{\text{air}} \quad (13)$$

where  $n$  is the refractive index of air for the wavelength involved and the pertinent temperature and pressure; typical values of  $n$  are given in Table 1. The Edlen<sup>1</sup> dispersion formula for standard air (0.03 per cent

\* If spectrometer records of sufficient accuracy are not available a copy of a typical spectrum may be obtained at a nominal cost by writing to Professor Paul Bender, Department of Chemistry, University of Wisconsin, Madison 6, Wis.

CO<sub>2</sub>, 1 standard atm pressure) has been shown to hold quite accurately through the near-infrared region of the spectrum.

$$(n^\circ - 1) \times 10^8 = 6431.8 + \frac{2,949,810}{146 - \bar{\nu}_{\text{vac}}^2} + \frac{25,540}{41 - \bar{\nu}_{\text{vac}}^2} \quad (13a)$$

Any necessary correction to laboratory conditions of temperature and pressure may readily be made since the molar refraction of the medium is adequately constant for the range of conditions involved, and  $(n - 1)$  is quite small. Thus, to the required degree of approximation,

$$\frac{n^\circ - 1}{(n - 1)_{P,T}} = \frac{760}{P} \frac{T}{288.16} \frac{Z(P,T)}{Z^\circ} \quad (13b)$$

where  $Z(P, T)$  is the compressibility factor for air at the indicated pressure and temperature, and  $Z^\circ$  its value for the specified reference state. If the accuracy required in the value of  $(n - 1)$  is 0.1 per cent or less, the compressibility-factor ratio in Eq. (13b) can be set equal to unity; where higher accuracy is needed, the ratio may be calculated from the formula given by Schleuter and Peck.<sup>10</sup> Except for the most accurate work, the value of the refractive index may be considered to be constant over the wavelength region covered by one absorption band. For each line the vacuum wave number  $\bar{\nu}$  is then calculated as the reciprocal of the vacuum wavelength.

Now let  $R(J)$ ,  $P(J)$  represent, respectively, the wave numbers of the lines in the  $R$  and  $P$  branches which *originate* in the state characterized by  $J'' = J$ . Then from Eqs. (11) and (12) it follows that

$$\frac{1}{2}[R(J) + P(J + 1)] = (v' - v'')\bar{\nu}_e[1 - x_e(v' + v'' + 1)] + (B_{v'} - B_{v''})(J + 1)^2 \quad J = 0, 1, 2, \dots \quad (14)$$

$$R(J) - P(J) = 4B_{v'}(J + \frac{1}{2}) - 4D_e[(J + 1)^3 + J^3] \quad J = 1, 2, 3, \dots \quad (15)$$

$$R(J - 1) - P(J + 1) = 4B_{v''}(J + \frac{1}{2}) - 4D_e[(J + 1)^3 + J^3] \quad J = 1, 2, 3, \dots \quad (16)$$

Note that the difference  $[R(J) - P(J)]$  in Eq. (15) is selected because both lines then originate in transitions from identically the same lower state (i.e., same values for  $v''$ ,  $J''$ ), and hence the properties of the upper state can be determined without a knowledge of the coefficients for the lower state. Conversely, the transitions associated with the lines  $R(J - 1)$ ,  $P(J + 1)$  lead to the same *upper* state. For a given band the values for the band origin,  $(v' - v'')\bar{\nu}_e[1 - x_e(v' + v'' + 1)]$ , and  $B_{v'} - B_{v''}$  may be determined as the intercept and slope, respectively, of a plot of  $\frac{1}{2}[R(J) + P(J + 1)]$  against  $(J + 1)^2$ .

A graphical method based on Eqs. (15) and (16) may then be used for evaluation of  $B_v$ ,  $B_v''$ , and  $D_e$ . A plot of

$$\frac{R(J) - P(J)}{J + \frac{1}{2}} \quad \text{versus} \quad J^2 + J + 1$$

leads to values for  $B_v$  and  $D_e$ , and a similar plot based on Eq. (16) yields values for  $B_v''$  and  $D_e$ . The two values thus obtained for  $D_e$  should agree, and the difference ( $B_v - B_v''$ ) should be consistent with the result given by use of Eq. (14).

Analysis in this fashion of at least two bands for a molecule permits calculation, from the band origins, of the zero-order vibration frequency  $\tilde{\nu}_e$  and the anharmonicity factor  $x_e\tilde{\nu}_e$ . The values of  $B_e$  and  $x_e$  are obtained from a plot of the rotational coefficient  $B_v$  against  $v + \frac{1}{2}$ .

For the calculation of the equilibrium internuclear distance  $r_e$  the necessary atomic mass data may be taken from the tabulation provided by Moeller.<sup>5</sup> Accurate values must be used for the various physical constants required.

In cases where the isotope structure of the band is resolved, as for  $\text{HCl}^{35}$ ,  $\text{HCl}^{37}$ , it is possible to verify that the value of  $r_e$  is the same for the different isotopic species (within limits of experimental uncertainty) and that the zero-order vibrational frequencies satisfy the relation

$$\frac{\tilde{\nu}_{e,\text{HCl}^{37}}}{\tilde{\nu}_{e,\text{HCl}^{35}}} = \left( \frac{\mu_{\text{HCl}^{35}}}{\mu_{\text{HCl}^{37}}} \right)^{1/2} \quad (17)$$

Equation (17) is a necessary consequence of the fact that the electronic potential function  $U(r)$ , and hence  $[d^2U(r)/dr^2]_{r=r_e}$ , is the same for the two isotopic species.

**Practical Applications.** An accurate knowledge of the energy-level system for a molecule is essential in the calculation of thermodynamic properties by the methods of statistical thermodynamics.<sup>4,7</sup> The velocity of light may be calculated<sup>8</sup> from  $B_0$  values as given in terms of frequency by microwave spectroscopy and in  $\text{cm}^{-1}$  by infrared studies.

**Suggestions for Further Work.** A comparison may be made of the results obtained here with those given by the microwave spectrum. The energy-level expression (7) may be shown to be consistent with that derived by direct substitution of the Morse potential function<sup>6</sup> in the Schrödinger wave equation.

### References

1. Edlen, *J. Opt. Soc. Am.*, **43**, 339 (1953).
2. Herzberg, "Molecular Spectra and Molecular Structure," Vol. I, "Spectra of Diatomic Molecules," 2d ed., D. Van Nostrand Company, Inc., Princeton, N.J. (1950).
3. Landau and Lifschitz, "Quantum Mechanics," Addison-Wesley Publishing Company, Reading, Mass. (1958).

4. Mayer and Mayer, "Statistical Mechanics," John Wiley & Sons, Inc., New York (1940).
5. Moeller, "Inorganic Chemistry," John Wiley & Sons, Inc., New York (1952).
6. Pauling and Wilson, "Introduction to Quantum Mechanics," McGraw-Hill Book Company, Inc., New York (1935).
7. Pennington and Kobe, *J. Chem. Phys.*, **22**, 1442 (1954).
8. Plyler, Blaine, and Connor, *J. Opt. Soc. Am.*, **45**, 102 (1955).
9. Rank, Birtley, Eastman, Rao, and Wiggins, *J. Opt. Soc. Am.*, **50**, 1275 (1960).
10. Schleuter and Peck, *J. Opt. Soc. Am.*, **48**, 313 (1958).

#### B. NUCLEAR-MAGNETIC-RESONANCE SPECTROSCOPY

**Theory.**<sup>6,9,10,13</sup> The torque about the origin exerted on a particle, of mass  $m_i$  and position vector  $\mathbf{r}_i$ , due to the resultant  $\mathbf{F}_i$  of the external forces acting on it, is given by the relation

$$\boldsymbol{\tau}_i = \mathbf{r}_i \times \mathbf{F}_i \quad (1)$$

Since in vector form Newton's law of motion—force equals mass times acceleration—becomes

$$m_i \frac{d^2 \mathbf{r}_i}{dt^2} = \mathbf{F}_i \quad (2)$$

then 
$$\boldsymbol{\tau}_i = \mathbf{r}_i \times \mathbf{F}_i = m_i \mathbf{r}_i \times \frac{d^2 \mathbf{r}_i}{dt^2} \quad (3)$$

Because the vector product  $\mathbf{A} \times \mathbf{A}$  of a vector with itself is identically equal to zero,

$$m_i \mathbf{r}_i \times \frac{d^2 \mathbf{r}_i}{dt^2} = m_i \left( \mathbf{r}_i \times \frac{d^2 \mathbf{r}_i}{dt^2} + \frac{d\mathbf{r}_i}{dt} \times \frac{d\mathbf{r}_i}{dt} \right) = m_i \frac{d}{dt} \left( \mathbf{r}_i \times \frac{d\mathbf{r}_i}{dt} \right) \quad (4)$$

Since  $d\mathbf{r}_i/dt$  is equal to the linear velocity  $\mathbf{v}_i$  of the particle,

$$\boldsymbol{\tau}_i = \frac{d}{dt} (\mathbf{r}_i \times m_i \mathbf{v}_i) = \frac{d}{dt} (\mathbf{r}_i \times \mathbf{p}_i) \quad (5)$$

where  $\mathbf{p}_i$  is the linear momentum of the particle. For a system of particles,

$$\boldsymbol{\tau} = \sum_i \boldsymbol{\tau}_i = \frac{d}{dt} \left\{ \sum_i \mathbf{r}_i \times \mathbf{p}_i \right\} \quad (6)$$

The quantity  $\mathbf{r}_i \times \mathbf{p}_i$  is termed the *angular momentum* of particle  $i$ ; for a system of particles the angular momenta of the individual particles add vectorially to give the resultant angular momentum  $\mathbf{L}$  of the system.

The external torque  $\boldsymbol{\tau}$  thus determines the time rate of change of the angular momentum  $\mathbf{L}$ . If a system is put into motion in such a way as to give it a particular angular momentum, as long as no external torques act on it, the angular momentum must remain constant. The

angular momentum, then, is one of the "constants of the motion" of the system in classical dynamics.

In classical electromagnetic theory, the magnetic moment of a molecule as a system of charged particles is given by the expression

$$\mathbf{u} = \frac{1}{2c} \sum_i \epsilon_i \mathbf{r}_i \times \mathbf{v}_i \quad (7)$$

where  $\epsilon_i$  represents the charge of particle  $i$ , and  $c$  the velocity of light. The equivalent form

$$\mathbf{u} = \sum_i \frac{\epsilon_i}{2m_i c} \mathbf{r}_i \times \mathbf{p}_i = \sum_i \mathbf{u}_i \quad (8)$$

shows that the contribution per particle to the magnetic moment,  $\mathbf{u}_i$ , is proportional to the angular momentum of the particle. If a magnetic dipole of magnetic moment  $\mathbf{u}$  is placed in a magnetic field described by the field vector  $\mathbf{H}$ , the energy of the dipole in the field is given classically by

$$W = -\mathbf{u} \cdot \mathbf{H} \quad (9)$$

The angular momentum of a single particle about a particular origin can be resolved into components relative to a cartesian coordinate system centered on this origin. Letting  $\mathbf{i}$ ,  $\mathbf{j}$ ,  $\mathbf{k}$  be unit vectors in the  $x$ ,  $y$ ,  $z$  directions, respectively,

$$\mathbf{r}_i \times \mathbf{p}_i = \begin{vmatrix} \mathbf{i} & \mathbf{j} & \mathbf{k} \\ x & y & z \\ p_x & p_y & p_z \end{vmatrix} = L_x \mathbf{i} + L_y \mathbf{j} + L_z \mathbf{k} \quad (10)$$

where

$$\begin{aligned} L_x &= yp_z - zp_y \\ L_y &= zp_x - xp_z \\ L_z &= xp_y - yp_x \end{aligned} \quad (11)$$

The square of the magnitude of the angular momentum  $\mathbf{L}$  is given by

$$|L|^2 = \mathbf{L} \cdot \mathbf{L} = L_x^2 + L_y^2 + L_z^2 \quad (12)$$

In quantum theory, operators corresponding to these dynamical variables are formulated by replacing  $p_x$  by  $(h/2\pi i)(\partial/\partial x)$ , etc., to give

$$\begin{aligned} L_{x,\text{op}} &= \hat{L}_x = \frac{h}{2\pi i} \left( y \frac{\partial}{\partial z} - z \frac{\partial}{\partial y} \right) \\ L_{y,\text{op}} &= \hat{L}_y = \frac{h}{2\pi i} \left( z \frac{\partial}{\partial x} - x \frac{\partial}{\partial z} \right) \\ L_{z,\text{op}} &= \hat{L}_z = \frac{h}{2\pi i} \left( x \frac{\partial}{\partial y} - y \frac{\partial}{\partial x} \right) \\ L_{\text{op}}^2 &= \hat{L}^2 = (\hat{L}_x)(\hat{L}_x) + (\hat{L}_y)(\hat{L}_y) + (\hat{L}_z)(\hat{L}_z) \end{aligned} \quad (13)$$

$$L_{\text{op}}^2 = \hat{L}^2 = (\hat{L}_x)(\hat{L}_x) + (\hat{L}_y)(\hat{L}_y) + (\hat{L}_z)(\hat{L}_z) \quad (14)$$

Such an operator  $\hat{F}$  may be used for the prediction of the average value  $\bar{F}_n$  of the results of measurements of the dynamical variable  $F$  for the particular stationary energy state of the system described by the wave function  $\psi_n$ :

$$\bar{F}_n = \int_{\text{c.s.}} \psi_n^* (\hat{F} \psi_n) d\tau_q \quad (15)$$

The integration extends over the configuration space of the system. If the same value  $F_n$  is obtained every time the variable  $F$  is measured on the system when it is in the state  $\psi_n$ , then  $\bar{F}_n = F_n$ ; the state is then said to be an eigenstate of the variable  $F$ , and  $F_n$  is an eigenvalue of the corresponding operator  $F$  such that

$$\hat{F} \psi_n = F_n \psi_n \quad (16)$$

If two dynamical variables  $F, G$  are to have such well-defined values for a given state, it is necessary that the corresponding operators commute:

$$(\hat{F})(\hat{G}) = (\hat{G})(\hat{F}) \quad (17)$$

From the definitions given in Eqs. (13), it may be shown that  $\hat{L}^2$  commutes with any of  $\hat{L}_x, \hat{L}_y, \hat{L}_z$ , but the latter three do not commute with each other:

$$\begin{aligned} \hat{L}_x \hat{L}_y - \hat{L}_y \hat{L}_x &= \frac{i\hbar}{2\pi} \hat{L}_z \\ \hat{L}_y \hat{L}_z - \hat{L}_z \hat{L}_y &= \frac{i\hbar}{2\pi} \hat{L}_x \\ \hat{L}_z \hat{L}_x - \hat{L}_x \hat{L}_z &= \frac{i\hbar}{2\pi} \hat{L}_y \\ \hat{L}_i \hat{L}^2 - \hat{L}^2 \hat{L}_i &= 0 \quad i = x, y, z \end{aligned} \quad (18)$$

It is thus possible to determine experimentally for a particle the simultaneous values of the magnitude of the square of the total angular momentum and of its component along a particular direction in space, conventionally taken as the  $z$  direction.

In terms of ordinary spherical polar coordinates, with  $\hbar = (h/2\pi)$ ,

$$\begin{aligned} \hat{L}_z &= -i\hbar(\partial/\partial\varphi) \\ \hat{L}^2 &= -\hbar^2 \left[ \frac{1}{\sin\vartheta} \frac{\partial}{\partial\vartheta} \left( \sin\vartheta \frac{\partial}{\partial\vartheta} \right) + \frac{1}{\sin^2\vartheta} \frac{\partial^2}{\partial\varphi^2} \right] \end{aligned} \quad (19)$$

These expressions may be used together with the wave functions for the hydrogen atom obtained as solutions of the Schrödinger wave equa-



tion to give for the orbital angular momentum of the electron relative to the nucleus the results

$$L^2 = l(l + 1)\hbar^2 \quad l = 0, 1, \dots, (n - 1) \quad (20)$$

$$L_z = m\hbar \quad m = -l, -l + 1, \dots, l - 1, l \quad (21)$$

Here  $n$  represents as usual the principal quantum number which determines the energy associated with the relative motion of the electron and nucleus. The discrete set of values for  $L_z$  for a given value of  $L^2$  denotes a spatial quantization of the orbital angular momentum which becomes manifest when a special direction in space is created, as by application of a magnetic field.

Studies of the spectra of atoms and molecules show, however, that there also exists for electrons and nuclei a kind of quantized angular momentum which is different from orbital angular momentum. Postulation of this "spin angular momentum" is necessary to explain the doublet splitting in alkali-metal-atom spectra, the anomalous Zeeman effect in complex-atom spectra, the line-intensity variations observed in the pure rotational Raman spectra of homonuclear diatomic molecules and in the rotational fine structure of the infrared absorption bands of molecules such as  $\text{H}_2\text{O}$ , the existence of ortho- and para-hydrogen, etc. While the commutation relations given in Eqs. (18) arise from the classical concept of orbital angular momentum, it is possible to consider them as divorced from this origin and to postulate that they characterize the properties of angular momentum as a generalized concept. It may then be shown that the corresponding eigenvalues of the square of such angular momentum are given by

$$J^2 = j(j + 1)\hbar^2 \quad j = 0, \frac{1}{2}, 1, \frac{3}{2}, \dots \quad (22)$$

$$\text{while } J_z = m\hbar \quad m = -j, -j + 1, \dots, j - 1, j \quad (23)$$

For orbital angular momentum, integral  $j$  values apply. For the electron, the spin angular momentum corresponds to  $j = \frac{1}{2}$ . For an atomic nucleus, the nuclear spin angular momentum depends on the energy state of the nucleus. In ordinary chemistry, however, the nucleus remains in its ground nuclear-energy state, so it is customary to refer to the corresponding value as *the* nuclear spin quantum number for a particular nucleus. Values found include 0 for  $\text{C}^{12}$ ,  $\text{O}^{16}$ ;  $\frac{1}{2}$  for  $\text{H}^1$ ,  $\text{F}^{19}$ ; 1 for  $\text{H}^2(\text{D})$ ,  $\text{N}^{14}$ ;  $\frac{3}{2}$  for  $\text{B}^{11}$ ,  $\text{K}^{31}$ ; etc.

The proportionality between angular momentum and magnetic moment previously specified for the case of orbital angular momentum also extends to spin angular momentum. A nucleus which has a nonzero spin quantum number then possesses a magnetic moment which may be

written as the product of the spin angular momentum  $\mathbf{I}$  and the gyromagnetic ratio  $\gamma$ , a characteristic property of the nucleus concerned:

$$\mathbf{u} = \gamma \mathbf{I} \quad (24)$$

When the isolated nucleus is subjected to a magnetic field  $\mathbf{H}$ , the energy of the magnetic dipole in the field is given by

$$\mathcal{H} = -\mathbf{u} \cdot \mathbf{H} = -\gamma \mathbf{I} \cdot \mathbf{H} \quad (25)$$

If the direction of the magnetic field is taken to be the  $z$  direction,  $\mathbf{H} = H^\circ \mathbf{k}$ ,  $\mathbf{k}$  a unit vector in the  $+z$  direction, and

$$\mathcal{H} = -\gamma H^\circ I_z \quad \hat{\mathcal{H}} = -\gamma H^\circ \hat{I}_z \quad (26)$$

The energies  $W_n$  of the permitted levels for the system are then sought as the eigenvalues of the Hamiltonian operator  $\hat{\mathcal{H}}$ . The eigenvalues of  $\hat{I}_z$  are given by Eq. (23) as

$$I_z = m\hbar \quad m = -I, -I + 1, \dots, I - 1, I \quad (27)$$

where  $I$  represents the spin quantum number for the nucleus. This spatial quantization of the nuclear spin angular momentum creates a discrete set of energy levels for the nuclear magnet in the field, of energies given by

$$W_m = -m\hbar\gamma H^\circ \quad (28)$$

Further calculations show that a transition from a given level to the one just above it ( $\Delta m = -1$ ) may be achieved by absorption of energy from an electromagnetic field which is circularly polarized in a plane perpendicular to the direction of the magnetic field. The frequency of the radiation absorbed is determined by the relation

$$\Delta W = W_{m-1} - W_m = h\nu = \gamma\hbar H^\circ$$

or 
$$\nu = \frac{\gamma}{2\pi} H^\circ \quad (29)$$

Studies of such energy absorption constitute the field of nuclear-magnetic-resonance (NMR) spectroscopy.

For experimentally realizable magnetic field strengths, the absorption frequency  $\nu$  lies in the radiofrequency range. The gyromagnetic ratio for the proton,<sup>1</sup> for example, is equal to  $2.675 \times 10^4 \text{ sec}^{-1} \text{ gauss}^{-1}$ ; this corresponds to an absorption frequency of 60 megacycles ( $60 \times 10^6 \text{ sec}^{-1}$ ) for a 14,100-gauss field, the highest field strength routinely available with adequate homogeneity for high-resolution NMR work.

In ordinary optical-absorption spectroscopy, the energy levels are fixed

and the frequency of the radiation field must be adjusted to fit the energy per quantum to the energy-level spacing. The nuclear-magnetic-resonance spectrum may be scanned in this conventional way for a particular constant value of the magnetic field strength. In the NMR case, however, it is also possible to apply a radiofrequency field of fixed frequency and progressively change the magnetic field strength until the energy-level spacing has been matched to the energy per quantum of the radiofrequency field.

The important chemical applications arise from effects encountered when the nuclei studied are present in molecules. Electron circulation in the neighborhood of nucleus A in a molecule modifies the field that otherwise would be sensed by the nucleus. This effect is commonly a diamagnetic shielding effect and is quantitatively described by the "shielding constant"  $\sigma$  for the nucleus

$$H_A = H^\circ(1 - \sigma_A) \quad (30)$$

where  $H_A$  = field acting at nucleus A.

The value of the shielding constant is sensitive to the average electron density in the neighborhood of the nucleus. For protons the greatest difference in shielding constant is about  $1 \times 10^{-5}$ , so that all information of chemical interest in high-resolution proton NMR spectra is compressed into a frequency range of 1 part in 100,000 of the nominal absorption frequency for constant  $H^\circ$  (or of the nominal  $H^\circ$  for constant frequency). It is thus necessary to achieve a stability of the order of parts per billion in the control of the magnetic field strength and radiation field frequency to obtain the results now available in high-resolution NMR work.

Nuclei which have the same shielding constant are called *chemically equivalent*. Chemical equivalence necessarily characterizes nuclei in a symmetrically equivalent set, i.e., a set which is permuted by the symmetry operations for the molecule. It can also be produced by the averaging effect of sufficiently rapid intramolecular motion, as, for example, the equivalence of the protons in a methyl group due to the internal rotation about the carbon-carbon bond. In addition, sufficiently rapid exchange of a nucleus between two nonequivalent sites can result in a single resonance peak at an intermediate position, instead of the two separate peaks which would be obtained if the residence time were long enough in each of the two environments. In this connection, "long" means large compared with the reciprocal of the chemical shift (in cycles per second) between the two environments.

The chemical shift is a measure of the difference of line positions in a spectrum due to a difference in shielding constants for nuclei in different environments. For fixed frequency of the radiation field, the relative

chemical shift may be defined as

$$\delta = \frac{H_r - H}{H_r} \times 10^6 \quad (31)$$

where  $H$  = resonance field for signal specified

$H_r$  = resonance field for reference signal

For proton spectra, the reference signal commonly used is the single sharp peak from tetramethylsilane, the protons of which are very highly shielded. The definition given above then makes the chemical shift positive for protons in almost any other environment and of progressively greater magnitude as the shielding constant becomes smaller. The chemical shift may also be given in field units as

$$H_r - H = H_r \delta \times 10^{-6} \quad (32)$$

For practical purposes the nominal field strength  $H^0$  can be substituted for  $H_r$  on the right-hand side, since  $\delta \times 10^{-6}$  is so small.

The spacing of lines in an NMR spectrum is actually measured in frequency units by the so-called "side-band method." The magnetic field to which the sample is subjected is varied at an audiofrequency by passing an audiofrequency current through auxiliary coils whose axis coincides with the  $Z$  axis. As the amplitude of the small modulation field is increased, two new signals appear for every line otherwise present in the spectrum. These "side bands" are separated from their corresponding parent signal (from which the side-band energy is extracted) by the equivalent of the modulation frequency. Thus, if  $H$  is the field strength producing a given line for constant radiofrequency  $\nu_0$ , the upper side band will appear when the field has been increased to the value  $H_s > H$ , for which

$$\nu_0 + \nu_{au} = \frac{\gamma}{2\pi} H_s \quad (33)$$

where  $\nu_{au}$  is the modulation frequency. Alternatively, it is possible to obtain equivalent results by modulating the radiofrequency field instead of the magnetic field. The modulation must be restricted to a low level to avoid complications from higher side bands which correspond to the various integral multiples of the modulation frequency.

The actual determination of line spacings in a spectrum is made by adjusting the modulation frequency so as to superimpose on one line the side band from another, or by using the side-band technique to place calibration marks at intervals along the spectrum, the line spacings being determined by interpolation. The relative chemical shift can then be calculated as  $(\Delta\nu/\nu_0) 10^6$ . Typical chemical-shift results<sup>8</sup> for protons are summarized in Fig. 63. The ranges indicated are necessarily approxi-

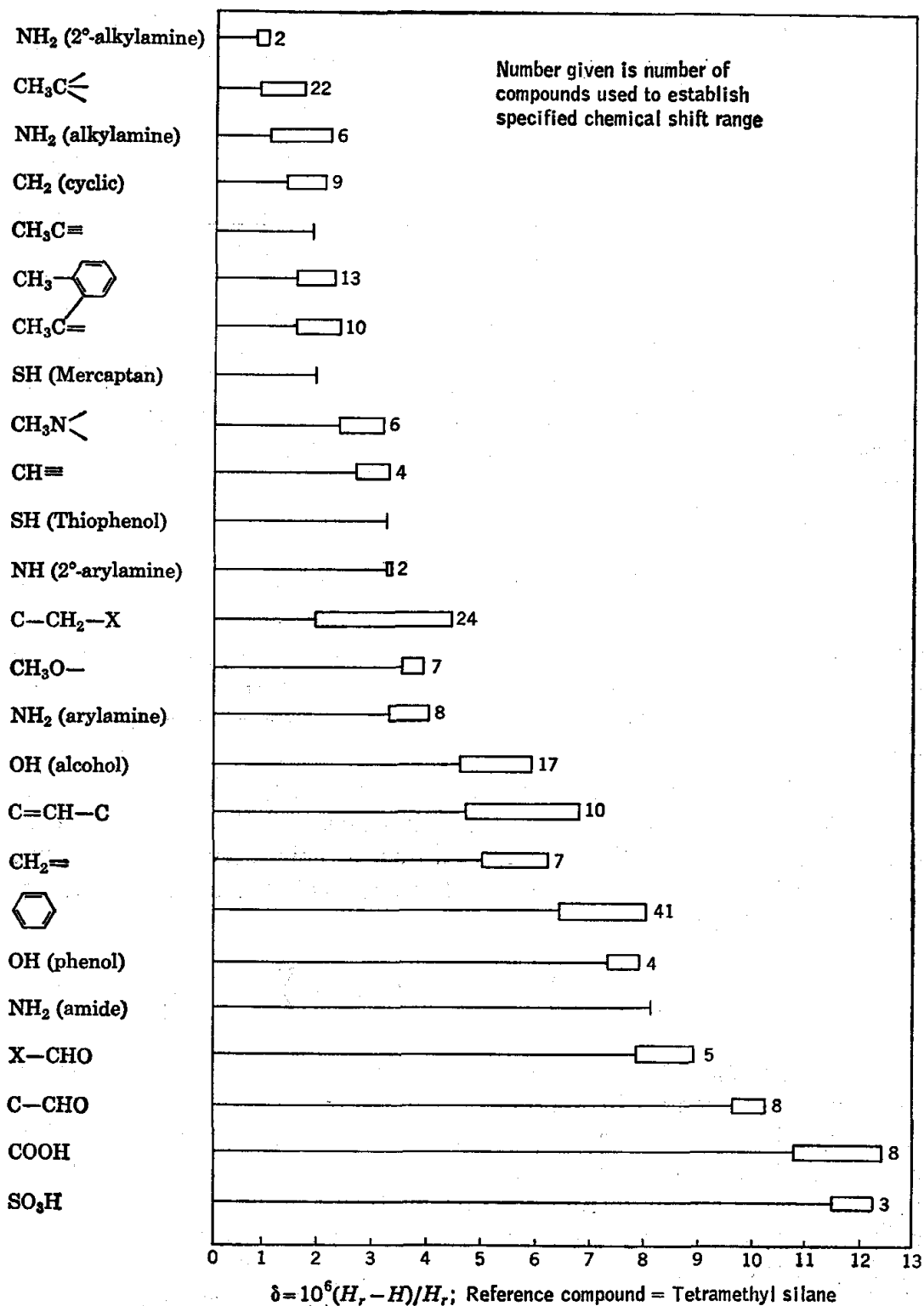


FIG. 63. Proton relative chemical-shift values for various structural environments. Results given are based on data of Meyer, Gutowsky, and Saika (Ref. 8) from measurements made primarily on pure-liquid samples.

mate; for best results the general results available in literature<sup>2,8,9,13</sup> must be supplemented by studies on compounds of known structure similar to those of interest.

The difference in shielding constants for nuclei in different electronic environments divides the high-resolution NMR spectrum into a sequence of groups of lines. It is advantageous to work at as high a magnetic field and corresponding radiofrequency as possible to minimize in so far as possible the overlapping of different groups in order to simplify the interpretation of the spectrum. The fine structure in a particular group arises from a phenomenon termed *spin-spin coupling*; the energy of a system of nuclei in a magnetic field depends not only on the magnetic field strength, but also on the relative orientations of the individual nuclear magnets. It has been found possible to account for the latter effect by the inclusion in the Hamiltonian function, representing the total energy of the system of nuclei in the field, of a remarkably simple field-independent term to obtain

$$\mathcal{H} = - \left\{ \sum_i \mathbf{u}_i \cdot \mathbf{H}_i + \sum_{i < j} \xi_{ij} \mathbf{u}_i \cdot \mathbf{u}_j \right\} \quad (34)$$


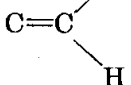
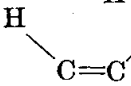
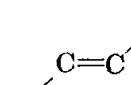
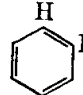
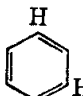
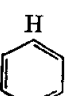
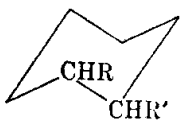
The first sum accounts for the interactions of the individual nuclear magnets with the field; the second, whose special form ensures that the interaction of each pair of nuclei is counted only once, accounts for the interactions between the nuclei. The constant factor  $\xi_{ij}$  measures the strength of the interaction of nucleus  $i$  with nucleus  $j$ . Explicitly recognizing the existence of the chemical-shift effect and the proportionality between nuclear magnetic moment and nuclear spin angular momentum, expressing  $I_z$  and  $\mathbf{I}_i$  in units of  $\hbar$ , and  $\mathcal{H}$  in units of cycles per second, Eq. (34) is converted to

$$\mathcal{H} = - \left\{ \sum_i \left( \frac{\gamma_i}{2\pi} \right) (1 - \sigma_i) H^0 (I_z)_i + \sum_{i < j} J_{ij} \mathbf{I}_i \cdot \mathbf{I}_j \right\} \quad (35)$$

The quantity  $J_{ij}$  is termed the *spin-coupling constant* for nuclei  $i$  and  $j$ . For protons, it ranges in magnitude from zero to about 30 cycles/sec. These spin interactions do not take place directly between the nuclei, but rather constitute an electron-coupled effect which is transmitted through the chemical-bond chain from one nucleus to the other. It is found that spin couplings are rarely transmitted effectively through more than a few chemical bonds. The magnitude of the coupling constant characterizing the interaction of two nuclei depends of course on the gyromagnetic ratios of the nuclei, and also on structural considerations such as the H—C—H angle for two protons bonded to the same carbon atom, or the dihedral angle between the two H—C—C planes for the interaction of protons

bonded to adjacent carbon atoms. The magnitudes of spin-coupling constants have been predicted with some success by quantum-mechanical methods,<sup>5,7</sup> supplementing the information obtained empirically through studies of molecules of known structure. In Table 1 are summarized

TABLE 1. COUPLING CONSTANTS FOR PROTON-PROTON INTERACTION<sup>9,12,13</sup>

Structural grouping	Configuration	<i>J</i> , cycles/sec
Ethyl	$\text{CH}_3\text{CH}_2\text{R}$ 	6-8
Olefinic	 gem	1-2
	 cis	8-12
	 trans	17-18
Benzene derivatives	 ortho	5-8
	 meta	1-3
	 para	1
Cyclohexane derivatives		
	axial-axial equatorial-equatorial or axial-equatorial	5-8 2-3

typical values<sup>9,12,13</sup> of coupling constants for proton interactions in organic molecules. The complication of the spectrum resulting from the spin interactions will commonly be helpful in the elucidation of the spectrum of a molecule from the observed NMR spectrum.

For two chemically nonequivalent nuclei A,B of a given kind, Eq. (35) becomes

$$\mathcal{H} = - \left\{ \left( \frac{\gamma}{2\pi} H^0 \right) [(1 - \sigma_A)(I_z)_A + (1 - \sigma_B)(I_z)_B] + J_{AB} \mathbf{I}_A \cdot \mathbf{I}_B \right\} \quad (36)$$

Since there are two orientations relative to the field possible for each nucleus, there are four discrete energy levels for the two-proton system. The energies of these levels are again sought as the eigenvalues of the quantum-mechanical operator corresponding to the specified Hamiltonian function. Because all three components of the spin angular momentum for each nucleus are involved in this Hamiltonian, the problem is more difficult than that earlier considered [Eq. (26)]. Standard quantum-mechanical procedures lead, however, to the following results for the case of spin  $\frac{1}{2}$ :

$$\begin{aligned} W_1 &= -\frac{1}{2}(\nu_A + \nu_B + \frac{1}{2}J_{AB}) \\ W_2 &= -\frac{1}{2}\{[(\nu_A - \nu_B)^2 + J_{AB}^2]^{\frac{1}{2}} - \frac{1}{2}J_{AB}\} \\ W_3 &= \frac{1}{2}\{[(\nu_A - \nu_B)^2 + J_{AB}^2]^{\frac{1}{2}} + \frac{1}{2}J_{AB}\} \\ W_4 &= \frac{1}{2}(\nu_A + \nu_B - \frac{1}{2}J_{AB}) \end{aligned} \quad (37)$$

Here  $\nu_A = (\gamma/2\pi)(1 - \sigma_A)H^\circ$ ; it represents the resonance frequency which would be found for nucleus A if there were no spin coupling to nucleus B. It is found that there are four allowed transitions between these levels:

$$\begin{aligned} \Delta W_{1 \rightarrow 3} &= W_3 - W_1 = \frac{1}{2}\{\nu_A + \nu_B + [(\nu_A - \nu_B)^2 + J_{AB}^2]^{\frac{1}{2}} + J_{AB}\} \\ \Delta W_{2 \rightarrow 4} &= W_4 - W_2 = \frac{1}{2}\{\nu_A + \nu_B + [(\nu_A - \nu_B)^2 + J_{AB}^2]^{\frac{1}{2}} - J_{AB}\} \\ \Delta W_{1 \rightarrow 2} &= W_2 - W_1 = \frac{1}{2}\{\nu_A + \nu_B - [(\nu_A - \nu_B)^2 + J_{AB}^2]^{\frac{1}{2}} + J_{AB}\} \\ \Delta W_{3 \rightarrow 4} &= W_4 - W_3 = \frac{1}{2}\{\nu_A + \nu_B - [(\nu_A - \nu_B)^2 + J_{AB}^2]^{\frac{1}{2}} - J_{AB}\} \end{aligned} \quad (38)$$

The relative intensities of the corresponding absorption lines are given by

$$\begin{aligned} I_{1 \rightarrow 3} &= I_{3 \rightarrow 4} = \frac{(1 - R)^2}{1 + R^2} \\ I_{1 \rightarrow 2} &= I_{2 \rightarrow 4} = \frac{(1 + R)^2}{1 + R^2} \\ R &= \frac{J_{AB}}{\nu_A - \nu_B + [(\nu_A - \nu_B)^2 + J_{AB}^2]^{\frac{1}{2}}} \end{aligned} \quad (39)$$

Since the energies above are expressed in cycles per second, the energy differences give directly the corresponding absorption frequencies for the system for the constant applied field  $H^\circ$ . It can be seen that for very weak coupling, the first two transitions can be associated with nucleus A, the other two with nucleus B, but for finite  $J_{AB}$ , all four characterize the two-nucleus system as a whole. The appearance of the spectrum depends only on the absolute value of the ratio  $J_{AB}/(\nu_A - \nu_B)$ , and it is not possible from the spectrum to determine either the sign of the coupling constant or which nucleus is more shielded, although chemical intuition



can often answer the latter question. Typical results for the two-spin system are shown in Fig. 64.

When the coupling is small compared with the chemical shift, the spectrum reduces to two doublets of individual spacing  $J_{AB}$ , with centers separated by the chemical shift ( $\nu_A - \nu_B$ ). This result corresponds to the use of first-order perturbation theory in the calculation of the energy levels, for which the interaction energy effectively reduces to  $J_{AB}(I_z)_A(I_z)_B$ .

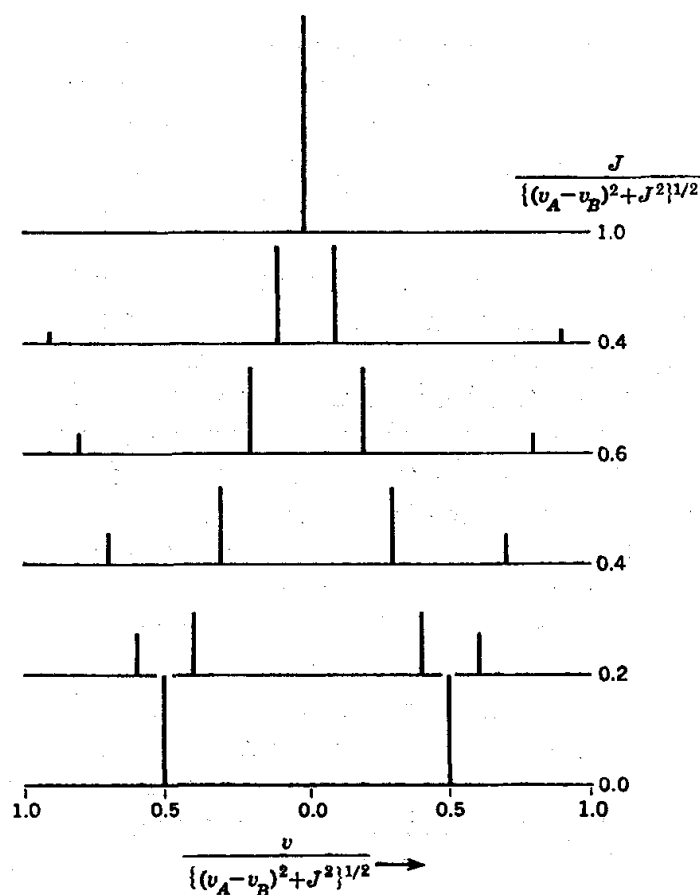


FIG. 64. Calculated spectra for two nonequivalent nuclei of spin  $\frac{1}{2}$ . The zero of the horizontal scale is located at the frequency  $\nu = \frac{1}{2}(\nu_A + \nu_B)$ .

To this degree of approximation, the coupling of nucleus B to nucleus A is equivalent to adding to the  $z$  component of the magnetic field acting on nucleus A the quantity  $m_B J_{AB}$ , where  $m_B$  is the quantum number describing the orientation of nucleus B relative to the field. For spin  $\frac{1}{2}$  there are two orientations possible, and because they differ in energy by so small an amount, their populations are practically equal. In the experimental spectrum which constitutes a study of a very large number of the two-spin systems considered, in half the cases nucleus A sees one orientation for B, in the remainder the other orientation for B, accounting for the splitting of the resonance of A into two lines of equal intensity and

separation equal to the coupling constant. The extension of this first-order prediction to more complex systems is considered below.

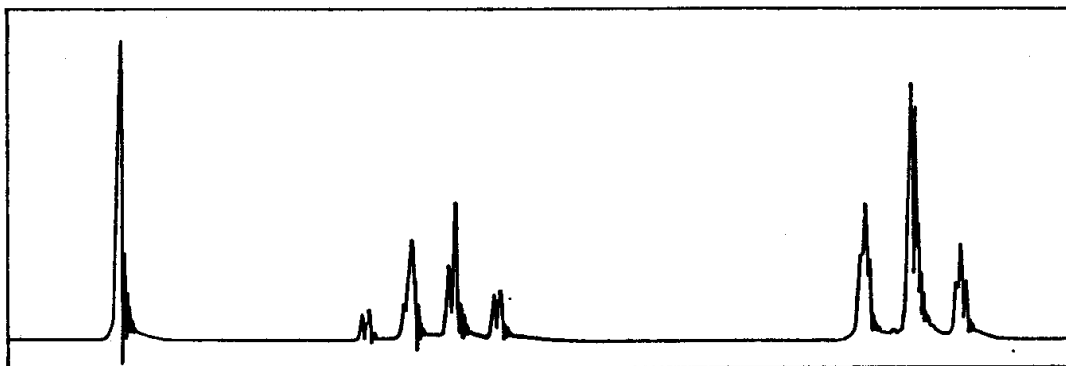
In the other extreme, where the chemical shift becomes small compared with the spin-coupling constant, the spectrum gives no indication of the existence of the coupling. In general, there will be no evidence in the spectrum of spin couplings between nuclei in a chemically equivalent set provided that the coupling to any nucleus outside the set is exactly the same for all nuclei in the set. If this special condition is satisfied, the set of nuclei is said to be magnetically equivalent as well as chemically equivalent. Such magnetic equivalence may be inherent in the symmetry of the molecule containing the nuclei, but can also result from the averaging effect of intramolecular motion. Thus the rotation of a methyl group about the carbon-carbon bond makes the three methyl protons magnetically as well as chemically equivalent.

The effect of the coupling of a nucleus B to a nucleus A can be observed only if nucleus B maintains a particular orientation relative to the field for a sufficiently long time. Exchange of nuclei between molecules or reorientation due to electric field gradients of a nucleus having an electric quadrupole moment can reduce the mean lifetime of a spin state to the point where an otherwise effective spin coupling disappears. For an appropriate intermediate range in lifetime, a marked broadening of the spin multiplet will occur, as is often observed in the spectra of molecules having spin coupling of protons to deuterium or nitrogen.

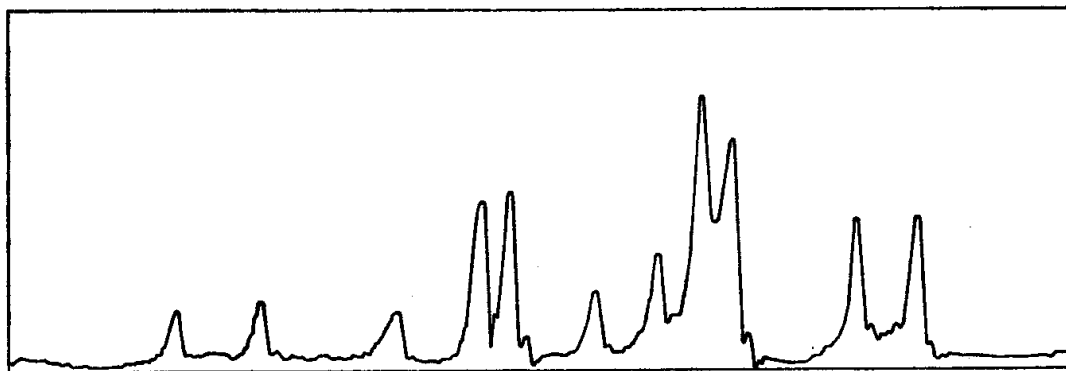
The foregoing principles provide a basis for the explanation of the structure of the spectrum of ethanol as shown in Fig. 65a. The sample studied contained a slight amount of acid to catalyze exchange of hydroxyl protons between molecules. The integrated intensities of the three groups of lines stand in the ratio of 1:2:3, confirming their assignment to the hydroxyl, methylene, and methyl protons, respectively. The appearance of the hydroxyl peak at the lowest applied field can be predicted on the basis of the relatively high electronegativity of oxygen, which produces a reduction of electron density in the neighborhood of the hydroxyl proton, and hence reduces its screening constant. The single hydroxyl peak results from the elimination of spin-coupling effects by the rapid exchange of hydroxyl protons between molecules.

The methylene and methyl line groups have approximately the quartet and triplet structures, respectively, that the first-order-perturbation prediction would suggest. The basic line spacing is seen to be essentially constant through the two multiplet groups, which are well separated in this spectrum, obtained with a spectrometer frequency of 60 Mc/sec. The two proton sets considered individually are chemically and magnetically equivalent because of the internal rotation about the carbon-carbon bonds in the molecule. The multiplet structure then results only

from interactions between the two sets. The first-order effect of the methylene protons on the methyl protons, as noted above, depends on the  $z$  component of the resultant spin angular momentum of the two methylene protons, each of which can have, with equal probability,  $m = +\frac{1}{2}$  or  $m = -\frac{1}{2}$ . The resultant value of  $I_z$  (in units of  $h/2\pi$ , of course) can then be  $+1$ ,  $0$ , or  $-1$ . The value  $0$  is twice as probable as either of the other two, since the resultant  $+1$  can arise only from  $(m_1 = +\frac{1}{2},$



(a)



(b)

FIG. 65. (a) High-resolution NMR spectrum of ethanol at 60 megacycles; (b) methylene-group spectrum of ethanol, 12-megacycle spectrometer frequency. (Courtesy Varian Associates, Instrument Division.)

$m_2 = +\frac{1}{2}$ ),  $-1$  from  $(m_1 = -\frac{1}{2}, m_2 = -\frac{1}{2})$ , while  $0$  can result from either  $(m_1 = +\frac{1}{2}, m_2 = -\frac{1}{2})$  or  $(m_1 = -\frac{1}{2}, m_2 = +\frac{1}{2})$ , where subscripts 1, 2 label the two methylene protons. It would then be expected that the single resonance line which would result from the chemically equivalent methyl protons in the absence of spin coupling would split into three lines, with the central component twice as intense as either of the other two. A similar line of reasoning will predict for the methylene resonance a splitting into four lines in a  $1:3:3:1$  intensity ratio.

These first-order arguments succeed reasonably well in this case because the spin-coupling constant is fairly small ( $J = 7.15$  cycles/sec) compared with the chemical shift of  $\Delta\nu = 147.4$  cycles/sec. The second-order corrections to the energies of the levels concerned are proportional to  $J^2/\Delta\nu$  and are not negligible even in the present case, as is obvious from the spectrum. If the spectrometer operating frequency is reduced to 12 megacycles, the methylene group spectrum as shown in Fig. 65b in no way resembles the first-order prediction. The second-order effects obviously constitute a complication which it is desirable to minimize, and this is a further reason for use of as high an operating frequency (and field) as possible, to increase the chemical shift between the interacting groups. Since the coupling constants are independent of the field, the result is a reduction of the second-order splittings.

In the high-resolution proton NMR spectrum, then, the positions of the line groups relative to the selected reference permit the identification of the various types of structural environments of the protons present. Determination of the integrated line intensities leads to a calculation of the relative numbers of protons in the several environments. Further structural information can be obtained from analysis of the fine structure due to spin-spin interaction, since a particular postulated structure will necessarily imply particular spin-coupling effects in the spectrum.

In order to obtain results characteristic of a given molecule, the experimental conditions must provide for the elimination of the effects of interactions between different molecules. For this reason high-resolution studies are made on liquids or solutions, where the reorientation of molecules due to random Brownian motion proceeds rapidly enough to average out the effects of all such interaction. A molecule in a liquid phase is present essentially in a cavity in a medium having magnetic properties which must be considered in a comparison of chemical shifts as measured, for example, on different pure liquids or on solutions in different solvents. Such comparisons are best made in terms of data obtained with solutions in a common solvent and for dilutions high enough so that solute-solute interactions are negligible. Solvents commonly used include  $\text{CCl}_4$ ,  $\text{CDCl}_3$ , and a variety of other deuterated species.

**Apparatus.** High-resolution NMR spectrum records† with calibration marks; precision scale.

**Procedure.** High-resolution NMR spectra are usually obtained by the crossed-coil nuclear induction method of Bloch described on page 523. The sample, as a dilute solution in a suitable solvent containing about

† If such records are not available, they may be obtained at a nominal cost by writing to Professor Paul Bender, Chemistry Department, University of Wisconsin, Madison 6, Wis.

1 per cent of tetramethyl silane or other reference substance as an internal standard, is sealed off in a 5-mm Pyrex tube. Care must be taken to eliminate oxygen from the solution because such paramagnetic material can cause undesirable line broadening. The spectrum is scanned by varying the magnetic field at a fixed radiofrequency. Reference marks for the determination of line spacings are produced by the side-band method described above. The amplitude of the radiofrequency field must be kept suitably low to avoid saturation effects; because the energy-level spacing here is very small, it is relatively easy to wipe out the difference in level population, and with it the possibility of observing an absorption spectrum, by pouring in too much energy at the appropriate frequency (p. 521).

To illustrate the features of NMR spectroscopy which are of primary interest in chemistry, a set of spectra is provided for study and interpretation. Each spectrum is marked with the empirical formula for the subject compound, the spectrometer operating frequency, and the identity of the nucleus studied. Several spectra for which the structure of the compound is completely specified are provided for preliminary practice.

**Data and Calculations.** From the side-band information provided, the chemical shifts are determined for the various line groups in a particular spectrum, and the number of protons associated with each group is estimated from the line areas and the empirical formula for the compound. From the chemical-shift results summarized in Fig. 63, each of the groups is identified. A structure is then postulated which is consistent with the spectrum and the empirical formula given. To any extent possible, spin-spin interaction effects should be accounted for. It should be noted that an arbitrary spectrum may be much more difficult to interpret than those supplied for introductory work.

It is instructive also to calculate the energy per quantum of a radiation field of frequency 60 megacycles and the ratio of the numbers of protons in the two spin states for a 14,000-gauss magnetic field.

**Practical Applications.** High-resolution NMR spectroscopy is the most important new tool for the qualitative study of molecular structure which has been introduced in the last several decades. Studies are not restricted to proton spectra, but may include fluorine, boron, phosphorus, sulfur, and carbon 13 as well. Other applications of NMR spectroscopy in general include studies of crystal structure<sup>1</sup> (notably the locations of protons, which may be difficult to establish by X-ray methods), rate processes,<sup>9</sup> etc.

**Suggestions for Further Work.** The results illustrated in Fig. 64 may be checked by calculations based on Eqs. (38) and (39). By reference to the literature,<sup>3,4,9</sup> a summary may be prepared describing applications of NMR spectroscopy other than high-resolution structure work, or the use of high-resolution spectra in the solution of difficult structural problems.

## References

1. Andrew, "Nuclear Magnetic Resonance," Cambridge University Press, Cambridge, Mass. (1955).
2. Chamberlain, *Anal. Chem.*, **31**, 56 (1959).
3. Gutowsky in Berl (ed.): "Physical Methods in Chemical Analysis," Vol. III, Academic Press, Inc., New York (1956).
4. Gutowsky in Weissberger (ed.): "Physical Methods of Organic Chemistry," 3d ed., Pt. IV, Interscience Publishers, Inc., New York (1960).
5. Gutowsky, Karplus, and Grant, *J. Chem. Phys.*, **31**, 1278 (1959).
6. Jackman, "Applications of Nuclear Magnetic Resonance Spectroscopy in Organic Chemistry," Pergamon Press, New York (1959).
7. Karplus, *J. Chem. Phys.*, **30**, 11 (1959).
8. Meyer, Gutowsky, and Saika, *J. Am. Chem. Soc.*, **75**, 4567 (1953).
9. Pople, Schneider, and Bernstein, "High Resolution Nuclear Magnetic Resonance," McGraw-Hill Book Company, Inc., New York (1959).
10. Reilly, *Anal. Chem.*, **30**, 839 (1958).
11. Roberts, "Nuclear Magnetic Resonance," McGraw-Hill Book Company, Inc., New York (1959).
12. Roberts, "Introduction to Spin-Spin Splittings in High Resolution Nuclear Magnetic Resonance Spectra," W. A. Benjamin Publishing Co., New York (1961).
13. Varian Associates Staff, "NMR and EPR Spectroscopy," Pergamon Press, New York (1960).

## C. STARK EFFECT IN THE ROTATIONAL SPECTRUM OF A MOLECULE

**Theory.**<sup>†</sup> The energy-level diagram for a polyatomic molecule is represented rather schematically in Fig. 66. We shall be concerned here with pure rotational transitions, i.e., transitions between different rotational levels of the same vibrational and electronic state. The application of an electrostatic field causes each rotational level of a molecule to split up into sublevels, each with slightly different energy (Fig. 67). As a result, a rotational absorption line is split into a group of closely spaced lines. This phenomenon is known as the molecular Stark effect. From an analysis of Stark-effect splittings, the permanent dipole moment (page 212) of a molecule can be found.

Although a molecule is a complex system of electrons and nuclei, we shall represent it by a simple model: a set of point masses, corresponding to the nuclei, held in a rigid arrangement by bonds of negligible mass. The fact that the actual molecule vibrates is taken into account only to the extent of recognizing that quantities which are functions of internuclear distances are, in effect, mean values for the given vibrational state and will therefore vary slightly from one vibrational state to another.<sup>‡</sup>

<sup>†</sup> A brief commentary on references suggested for various aspects of the theory outlined here appears at the end of this section, following the list of references.

<sup>‡</sup> The justification for this procedure and a discussion of higher-order terms which must be considered in a more detailed analysis of vibration-rotation spectra have been given by Wilson; the results are summarized in Reference 10.

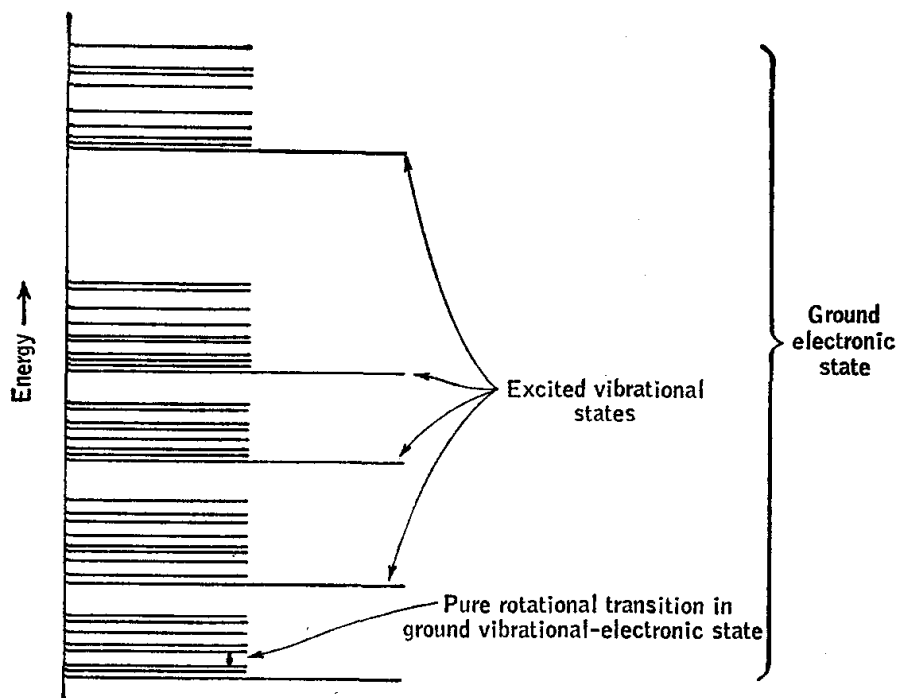


FIG. 66. A portion of the schematic energy-level diagram for the ground electronic state of a polyatomic molecule. A similar but not identical pattern of levels exists for the various stable excited electronic states.

Furthermore, the translation of the center of mass can be neglected in considering the rotational motion.

It is convenient to classify molecules into four categories, each of which exhibits certain characteristic rotational properties. Molecules in which all atoms lie on a single straight line are called linear. Nonlinear molecules are further classified according to the number  $n$  of axes of threefold or higher symmetry, as shown in Table 1. (The last column is given for later reference.) For a symmetric top, the unique axis of threefold or higher symmetry is called the *figure axis*.

Let the cartesian coordinate system  $x, y, z$  be fixed to the molecule with origin at the center of mass, considered to be at rest. The kinetic energy of rotation  $T_r$  of the molecule is

$$T_r = \frac{1}{2} \sum_i m_i v_i^2 \quad (1)$$

where  $v_i$  is the magnitude of the in-

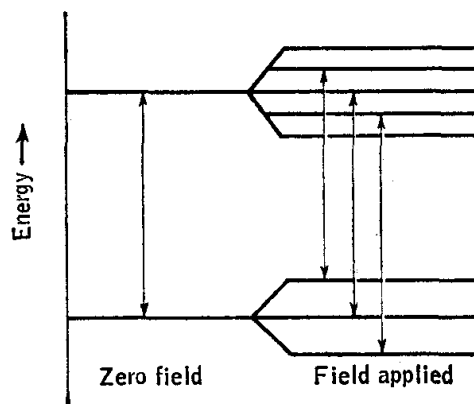


FIG. 67. Energy-level scheme for two rotational levels showing Stark splittings (exaggerated) produced by application of an electrostatic field.

stantaneous velocity of the  $i$ th nucleus and  $m_i$  is its mass. The vector representing the velocity of the  $i$ th nucleus is  $\mathbf{v}_i = (\boldsymbol{\omega} \times \mathbf{r}_i)$ , where  $\boldsymbol{\omega}$  is the angular velocity of rotation of the molecule, the same for all nuclei, and  $\mathbf{r}_i$  is the vector from the origin to the  $i$ th nucleus.<sup>4</sup> Through the substitution

$$v_i^2 = \mathbf{v}_i \cdot \mathbf{v}_i = (\omega_y z_i - \omega_z y_i)^2 + (\omega_z x_i - \omega_x z_i)^2 + (\omega_x y_i - \omega_y x_i)^2 \quad (2)$$

the kinetic energy of rotation may be expressed in terms of the components of  $\boldsymbol{\omega}$  along the axes  $x$ ,  $y$ , and  $z$ :

$$T_r = \frac{1}{2}I_{xx}\omega_x^2 + \frac{1}{2}I_{yy}\omega_y^2 + \frac{1}{2}I_{zz}\omega_z^2 - I_{xy}\omega_x\omega_y - I_{yz}\omega_y\omega_z - I_{zx}\omega_z\omega_x \quad (3)$$

where

$$\begin{aligned} I_{xx} &= \sum_i m_i(y_i^2 + z_i^2) & I_{xy} &= \sum_i m_i x_i y_i \\ I_{yy} &= \sum_i m_i(x_i^2 + z_i^2) & I_{yz} &= \sum_i m_i y_i z_i \\ I_{zz} &= \sum_i m_i(x_i^2 + y_i^2) & I_{zx} &= \sum_i m_i z_i x_i \end{aligned} \quad (4)$$

The coefficients  $I_{xx}$ ,  $I_{yy}$ ,  $I_{zz}$ , called *moments of inertia*, and  $I_{xy}$ ,  $I_{yz}$ ,  $I_{zx}$ , called *products of inertia*, depend on the structure of the molecule and on

TABLE 1. CLASSIFICATION OF MOLECULES ACCORDING TO THE NUMBER ( $n$ ) OF AXES OF THREEFOLD OR HIGHER SYMMETRY

Type	$n$	Examples	Relations among moments of inertia
Asymmetric top...	None	H <sub>2</sub> O, CH <sub>2</sub> Cl <sub>2</sub> , NOCl(bent)	$I_x \neq I_y \neq I_z$
Symmetric top....	One	CH <sub>3</sub> Cl, PF <sub>3</sub> , BrF <sub>5</sub> , BF <sub>3</sub>	$I_x = I_y \neq I_z$
Spherical top.....	More than one	CH <sub>4</sub>	$I_x = I_y = I_z$

the choice of coordinate system  $x$ ,  $y$ ,  $z$ . It is always possible to choose the orientation of the coordinate axes relative to the molecule in such a way that the products of inertia all vanish.<sup>8</sup> Axes chosen in this way are called *principal axes*, and the moments about these axes are referred to as *principal moments of inertia*. It is customary to use only a single subscript to denote a principal moment; thus the moment about  $x$  is written  $I_x$  if  $x$  is a principal axis. For a symmetric top, the identification of the principal-axis system is trivial because the figure axis and any axis perpendicular to it are principal axes.

The relations given in the last column of Table 1, though not immediately obvious, are necessary consequences of the symmetry properties specified in the second column.

The equations which govern the rotational motion take on their



simplest form when expressed in terms of angular-momentum variables.<sup>4</sup> The angular momentum  $\mathbf{P}$  of a rigid body is defined by

$$\mathbf{P} = \sum_i \mathbf{r}_i \times \mathbf{p}_i = \sum_i m_i \mathbf{r}_i \times \mathbf{v}_i \quad (5)$$

where  $\mathbf{p}_i = m_i \mathbf{v}_i$  is the linear momentum of the  $i$ th nucleus. In terms of components in the  $x, y, z$  system,

$$P_x = \sum_i m_i (y_i v_{zi} - z_i v_{yi}) \quad (6)$$

etc. With the use in Eq. (6) of expansions such as

$$v_{zi} = (\boldsymbol{\omega} \times \mathbf{r}_i)_z = \omega_x y_i - \omega_y x_i \quad (7)$$

it may be seen that *in the principal-axis system* the components of  $\mathbf{P}$  are simply related to the angular-velocity components:

$$\begin{aligned} P_x &= I_x \omega_x \\ P_y &= I_y \omega_y \\ P_z &= I_z \omega_z \end{aligned} \quad (8)$$

The kinetic energy, expressed in terms of the angular-momentum components *in this system*, becomes

$$T_r = \frac{P_x^2}{2I_x} + \frac{P_y^2}{2I_y} + \frac{P_z^2}{2I_z} \quad (9)$$

Consider now the case of a symmetric top with  $z$  the figure axis. Since  $I_x = I_y$ ,

$$\begin{aligned} T_r &= \frac{1}{2I_x} (P_x^2 + P_y^2) + \frac{1}{2I_z} P_z^2 \\ &= \frac{1}{2I_z} \mathbf{P}^2 + \frac{1}{2} \left( \frac{1}{I_z} - \frac{1}{I_x} \right) P_z^2 \end{aligned} \quad (10)$$

where

$$\mathbf{P}^2 = P_x^2 + P_y^2 + P_z^2 \quad (11)$$

A symmetric top is called *prolate* if  $I_z < I_x = I_y$ ; *oblate* if  $I_z > I_x = I_y$ . The sign of the second term in  $T_r$  differs for these two cases.

The classical motion, that is, the motion prescribed by Newton's laws, can be rather easily visualized for a symmetric top subject to no externally applied torques. The molecule rotates with a constant angular velocity  $\omega_z$  (and hence with a constant angular momentum  $P_z$ ) about the figure axis; at the same time, the figure axis precesses (i.e., describes a circular cone) with uniform angular velocity about the direction of the total angular-momentum vector  $\mathbf{P}$ , which is fixed in direction as well as mag-

nitude.<sup>5,8</sup> This motion is depicted in Fig. 68, where  $X, Y, Z$  is a space-fixed coordinate system. In this motion, the quantities

$$\mathbf{P}, P_z, P_x, P_y, P_z \quad (12)$$

remain constant. From Eq. (10),  $T_r$  also is constant. The values of these constants for any given case may be thought of as being determined by the initial conditions.

Since the spectroscopic transitions to be considered later consist of changes in energy of the molecule produced by the action of an electromagnetic field, it is instructive to examine briefly the classical theory of this effect. If an oscillating electric field  $E_z(t)$ , polarized along the space-

fixed  $Z$  axis, acts on the molecule, the latter is subjected to a torque<sup>4</sup>  $\tau$ ,

$$\tau = \mathbf{u} \times \mathbf{E}(t) \quad (13)$$

where  $\mathbf{u}$  is the permanent dipole moment of the molecule (page 212). For a symmetric top molecule,  $\mathbf{u}$  must lie in the direction of the  $z$  axis. Newton's equation of motion for the case of rotational motion of a rigid body is<sup>4</sup>

$$\frac{d\mathbf{P}}{dt} = \tau \quad (14)$$

where  $\tau$  is the torque due to external forces acting on the body. The

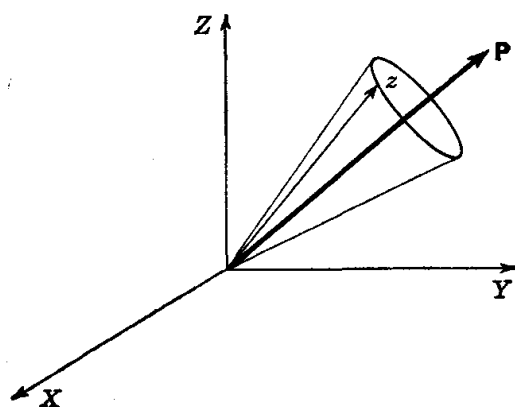


FIG. 68. Classical motion of a symmetric top. The figure axis  $z$  precesses about  $\mathbf{P}$ , which is constant in magnitude and in direction.

torque therefore causes  $T_r$  and several of the quantities of (12) to change. It is to be noted, however, that as  $\tau$  has no component in either the  $z$  or the  $Z$  direction, the components  $P_z$  and  $P_Z$  are not altered even with the field applied. The changes in  $T_r$  will be important only if the frequency of alternation of the field is close to that of some component of the rotational motion (classical resonance effect).

The quantum-mechanical treatment of the top begins with a recognition of the fact that the variables

$$\mathbf{P}^2, P_z, P_Z \quad (15)$$

can simultaneously have precisely specified values. As a manifestation of the uncertainty principle, the components  $P_z, P_y, P_x$ , and  $P_Y$  cannot also at the same time have precisely specified values. The eigenvalues of  $\mathbf{P}^2, P_z$ , and  $P_Z$  are, respectively,<sup>2,6,7</sup>

$$\mathbf{P}^2: J(J+1)\hbar^2 \quad \text{where } J = 0, 1, 2, 3, \dots \quad (16)$$

$$P_z: K\hbar \quad \text{where } K = 0, \pm 1, \pm 2, \dots, \pm J \quad (17)$$

$$P_Z: M\hbar \quad \text{where } M = 0, \pm 1, \pm 2, \dots, \pm J \quad (18)$$

where  $\hbar = h/2\pi$

$h$  = Planck's constant

States with precisely specified values of  $\mathbf{P}^2$ ,  $P_x$ , and  $P_z$  are therefore labeled by  $J$ ,  $K$ , and  $M$  and written symbolically as  $\Psi_{JKM}$ .

The *stationary states* of the symmetric top are states which satisfy the eigenvalue equation

$$\hat{\mathcal{H}}\Psi = W\Psi \quad (19)$$

where  $\hat{\mathcal{H}}$  is the Hamiltonian operator, which is derived from the classical expression for the energy [Eq. (10)] by replacing each quantity with the corresponding quantum-mechanical operator. The values of  $W$  satisfying (19) are the energy levels. It is clear that the states  $\Psi_{JKM}$  are eigenstates of  $\hat{\mathcal{H}}$ , and hence these are the stationary states for a symmetric top. The energy eigenvalues are immediately obtained from Eqs. (10), (16), (17), and (19) as

$$W = \frac{1}{2I_x} J(J+1)\hbar^2 + \frac{1}{2} \left( \frac{1}{I_z} - \frac{1}{I_x} \right) K^2 \hbar^2 \quad (20)$$

It should be noted that  $W$  does not depend on  $M$  or on the sign of  $K$ . The rotational energy is often written in the form

$$W = hBJ(J+1) + h(A-B)K^2$$

$$A = \frac{h}{8\pi^2 I_x} \quad B = \frac{h}{8\pi^2 I_z} \quad (21)$$

where  $A$  and  $B$  are called rotational constants, or, loosely, reciprocal moments. As defined in Eq. (21), they have dimensions of frequency.

If nonrigidity of the molecule is taken into account, the rotational-energy expression (9) must be augmented by the addition of terms involving higher powers of the angular momentum. The quantum-mechanical result for a symmetric top is<sup>3,5,9</sup>

$$W = hBJ(J+1) + h(A-B)K^2 - hD_K K^4 - hD_{JK} J(J+1)K^2 - hD_J J^2(J+1)^2 \quad (22)$$

where the coefficients  $D_K$ ,  $D_{JK}$ , and  $D_J$  are called centrifugal-distortion constants. The effects of these terms are roughly equivalent to a dependence of the effective rotational constants on  $J$  and  $K$ . It is not necessary to consider centrifugal distortion further in the present experiment, but Eq. (22) has been introduced here because it is often encountered in the literature.

If the molecule is subjected to an electromagnetic field of frequency  $\nu$ , transitions from one stationary state to another can occur with the absorption or emission of energy. The probability of occurrence of such a transition per unit time is a maximum if the frequency satisfies the Bohr

condition,

$$h\nu = W' - W'' \quad (23)$$

where  $W'$  = energy of upper state

$W''$  = energy of lower state

The probability of transition is proportional to  $\mu^2$ . Transitions which can be produced by an oscillating electric field along the  $Z$  direction acting on the dipole moment along the  $z$  direction are summarized by the selection rules

$$\Delta J = J' - J'' = 1 \quad (24)$$

$$\Delta K = K' - K'' = 0 \quad (25)$$

$$\Delta M = M' - M'' = 0 \quad (26)$$

Use of Eqs. (21) and (23) to (25) then leads to

$$\nu = B[J'(J' + 1) - J''(J'' + 1)] = 2BJ' \quad (27)$$

Typical values of  $B$  are in the range  $10^3$  to  $10^5$  Mc/sec, so the frequencies are in the microwave and far-infrared regions.

If a constant electrostatic field in the space-fixed  $Z$  direction is applied, the classical energy equation becomes

$$W_{\text{class}} = \frac{1}{2I_z} \mathbf{P}^2 + \frac{1}{2} \left( \frac{1}{I_z} - \frac{1}{I_x} \right) P_z^2 - \mu E_z \cos \theta \quad (28)$$

where  $\theta$  is the angle between the  $z$  and  $Z$  axes. The energy levels in the field are the eigenvalues of the quantum-mechanical Hamiltonian operator corresponding to Eq. (28); these eigenvalues may in principle be found as the roots of a determinant called the secular determinant for the given system. As the roots of the determinant derived from Eq. (28) cannot be found in closed form, advantage is taken of the fact that the last term is ordinarily sufficiently small so that an approximation method (perturbation theory) can be used with excellent results. The energy levels in the field are obtained in this way as a power series in the variable  $\mu E_z/hB$ ; since typical values for this ratio are much less than unity, the convergence is extremely good, and in fact it is rarely necessary to go beyond the second-order term. The result for the energy levels in the field, to the second order, is <sup>3,9</sup>

$$W = hBJ(J + 1) + h(A - B)K^2 - \frac{KM}{J(J + 1)} \mu E_z + W^{(2)} \quad (29)$$

with

$$W^{(2)} = -\frac{\mu^2 E_z^2}{6hB} \quad \text{for } J = 0$$

$$= \frac{\mu^2 E_z^2}{2hB} \left\{ \frac{[3K^2 - J(J + 1)][3M^2 - J(J + 1)]}{J^2(J + 1)^2(2J - 1)(2J + 3)} - \frac{M^2 K^2}{J^3(J + 1)^3} \right\}$$

for  $J > 0$

The third and fourth terms on the right side of Eq. (29) are, respectively, the linear and quadratic Stark-effect terms. The superscript on  $W^{(2)}$  denotes that this term is of second order in  $E_z$ .

Some discussion of this result may be helpful. To the extent that the second-order term  $W^{(2)}$  can be neglected, it is accurate to say that the stationary states are the same as in the absence of the field and that  $\mu \cos \theta$  in Eq. (28) can be replaced by its average value calculated for the unperturbed (zero-field) states  $\Psi_{JKM}$ . Classically, the time average of the precessing vector  $\mathbf{\mu}$  is equal to its projection along  $\mathbf{P}$ ; the projection of this component in turn along  $Z$  then gives the time average of  $\mu_z = \mu \cos \theta$  as

$$\langle \mu \cos \theta \rangle_{Av} = \mu \left[ \frac{K}{\sqrt{J(J+1)}} \right] \left[ \frac{M}{\sqrt{J(J+1)}} \right] = \mu \frac{KM}{J(J+1)} \quad (30)$$

since the cosines of the two angles of projection are  $P_z/P$  and  $P_z/P$ , respectively. This result offers some insight into the first-order term in Eq. (29). The second-order term is to be understood as follows. Application of the field results in a slight change in the stationary states, such that the average value of  $\mu \cos \theta$  is changed by a small increment proportional to  $E_z$ ; there results from this a change in energy proportional to  $E_z^2$ .

So long as the field is weak, the intensities of transitions produced by an oscillating field are the same as in the absence of the electrostatic field. With the electrostatic and oscillating fields both in the  $Z$  direction, the selection rules (24) to (26) still apply and the transition frequencies become

$$\nu = 2BJ' - \left[ \frac{K'M'}{J'(J'+1)} - \frac{K''M''}{J''(J''+1)} \right] \frac{\mu E_z}{h} + \dots \quad (31)$$

$$= 2BJ' + \left[ \frac{K'M'}{J'(J'^2-1)} \right] \frac{2\mu E_z}{h} + \dots \quad (32)$$

where only the first-order Stark-effect term has been given explicitly. In Eq. (32),  $\mu$  and  $E_z$  are in esu units, and  $\nu$  is in cycles per second. If, instead,  $\mu$  is expressed in Debye units and  $E_z$  in practical volts per centimeter, Eq. (32) is replaced by

$$\nu = 2BJ' + \frac{K'M'}{J'(J'^2-1)} (1.0070 \times 10^6) \mu E_z + \dots \quad (33)$$

with  $\nu$  still in cycles per second. The relative intensities of the different  $M$  components for given values of  $J$  and  $K$  are proportional to  $[(J')^2 - M'^2]$ .

It may be mentioned that for linear molecules, Eq. (29) may be used with  $K$  set equal to zero. For linear molecules, and for the  $K = 0$  states of symmetric tops, the Stark effect is therefore of second order in the field.

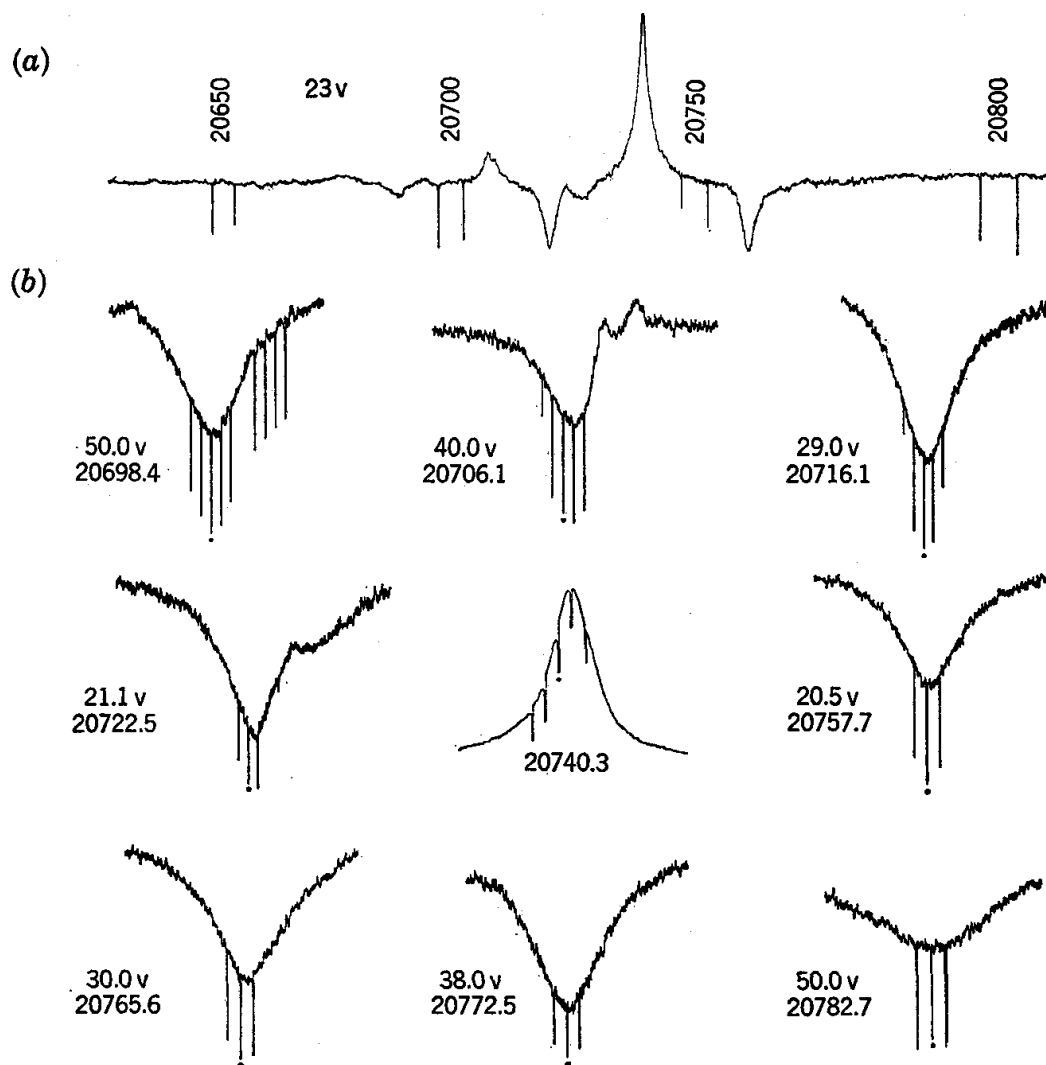


FIG. 69. (a) Microwave spectrum of  $\text{CH}_3\text{CF}_3$  near 20,700 Mc/sec, as displayed by a Stark-modulation type spectrograph (p. 530), at a modulation amplitude of 23 volts. Zero-field absorption lines produce upward deflections; Stark components produce downward deflections. The  $J = 0 \rightarrow 1$  transition for the ground vibrational state is near 20,740 Mc/sec, and the corresponding line from molecules in an excited torsional-vibrational state appears near 20,710 Mc/sec. Frequency marks (sharp spikes) are at 2.50 Mc/sec above and below the frequency values shown. (b) Expanded patterns of main line and its two Stark components at several voltages. The frequency values shown refer to the marks designated by dots. The interval between adjacent frequency marks is 0.50 Mc/sec for the Stark components and 0.20 Mc/sec for the main line. Frequency increases to the right (as in part a) in all cases. The frequency calibration marks are accurate to 0.02 Mc/sec. The average spacing between the electrode and the parallel walls of the waveguide (Fig. 147) is  $0.464 \pm 0.005$  cm. The voltages are accurate to  $\pm 0.1$  volt. (The sample and waveguide calibration data were kindly supplied by K. R. Lindfors.)

**Calculations.** The spectrum of a line of the symmetric-top molecule  $\text{CH}_3\text{CF}_3$  at several values of applied electrostatic field appears in Fig. 69. The value of  $J$  is confirmed from the qualitative appearance of the Stark pattern. The frequencies are measured and used for the determination of  $\mu$ . Values of rotational constant and moment of inertia are calculated from the frequency of the zero-field line.

**Suggestions for Further Work.** If the oscillating electric field is in the  $X$  direction, and hence perpendicular to the electrostatic field  $E_z$ , the selection rule on  $M$  becomes<sup>3,9</sup>

$$\Delta M = M' - M'' = \pm 1 \quad (34)$$

The student may calculate and plot the Stark pattern for the 20,740 Mc/sec line of  $\text{CH}_3\text{CF}_3$  for this case. The relative intensities for this case are proportional to<sup>3,9</sup>

$$(J' \pm M' - 1)(J' \pm M') \quad (35)$$

where the upper signs are for  $\Delta M = +1$  and the lower for  $\Delta M = -1$ .

### References

1. Brand and Speakman, "Molecular Structure," pp. 74-83, Edward Arnold & Co., London (1960).
2. Eyring, Walter, and Kimball, "Quantum Chemistry," pp. 39-47, John Wiley & Sons, Inc., New York (1944).
3. Gordy, Smith, and Trambarulo, "Microwave Spectroscopy," pp. 89-103, 154-159, John Wiley & Sons, Inc., New York (1953).
4. Halliday and Resnick, "Physics," Combined Ed., pp. 208, 213, 245-249, John Wiley & Sons, Inc., New York (1960).
5. Herzberg, "Infra-red and Raman Spectra of Polyatomic Molecules," D. Van Nostrand Company, Inc., Princeton, N.J. (1945).
6. Landau and Lifschitz, "Quantum Mechanics," Addison-Wesley Publishing Company, Reading, Mass. (1958).
7. Pauling and Wilson, "Introduction to Quantum Mechanics," McGraw-Hill Book Company, Inc., New York (1935).
8. Symon, "Mechanics," 2d ed., Addison-Wesley Publishing Company, Reading, Mass. (1960).
9. Townes and Schawlow, "Microwave Spectroscopy," pp. 48-82, 248-268, McGraw-Hill Book Company, Inc., New York (1955).
10. Wilson, Decius, and Cross, "Molecular Vibrations," pp. 11-14, 273-275, McGraw-Hill Book Company, Inc., New York (1955).

*Note:* Certain of the concepts of classical physics employed above are introduced by Halliday and Resnick<sup>4</sup> at an elementary level and with vector notation. Symon<sup>8</sup> gives an excellent classical treatment of the rotating top. The properties of angular momentum in quantum mechanics are developed by Eyring, Walter, and Kimball,<sup>2</sup> Landau and Lifschitz,<sup>6</sup> and, from a somewhat different viewpoint, by Pauling and Wilson.<sup>7</sup> Spectroscopic applications are discussed at an elementary level by Brand and Speakman<sup>1</sup> and at a more advanced level by Herzberg,<sup>5</sup> Gordy, Smith, and Trambarulo,<sup>3</sup> and Townes and Schawlow.<sup>9</sup> An excellent general reference on the separation of translational, rotational, and vibrational motions is Wilson, Decius, and Cross.<sup>10</sup>

## CHAPTER 12

# Diffraction

### 43. X-RAY DIFFRACTION OF CRYSTALS

This experiment illustrates the determination of the lattice type for cubic crystals and the calculation of the size and mass of the unit cell.

**Theory.** In the interpretation of the X-ray diffraction patterns of crystals, ideas of symmetry are of basic importance. A *symmetry operation* is a geometrical operation (such as a rotation about an axis or a reflection in a plane) such that an object assumes an aspect indistinguishable from its appearance before the operation. The individual symmetry operations are summarized in the following table. In the

Operation	Element	Symbols
Rotation.....	Axis	1, 2, 3, 4, 6
Reflection.....	Mirror plane	$m$
Inversion.....	Center of symmetry	$\bar{1}$
Rotation followed by inversion.....	Axis of rotatory inversion	$\bar{1}, \bar{2}, \bar{3}, \bar{4}, \bar{6}$

operation of inversion every point in the crystal is displaced in a straight line through a point, called the center of inversion, to a position an equal distance on the other side of the point. A twofold rotation-inversion about a given axis is equivalent to a reflection.

An *element of symmetry* is the line, point, or plane about which the operation is performed. For example, among the elements of symmetry of a cube are fourfold axes (which are perpendicular to the centers of faces), threefold axes (which pass through diagonally opposite corners), reflection planes, and a center of symmetry. For any object the symmetry elements must pass through a common point. Thus the symmetry operations leave one point unchanged.

A set comprising symmetry operations of an object constitutes a *point group*. Only axes of orders 1, 2, 3, 4, and 6 can occur in crystals; considering all compatible combinations of symmetry elements that pass through a common point, it then follows that there are only



32 for crystals point groups. A crystal can be classified according to symmetry by stating to which of these 32 point groups it belongs.

A *space lattice* is an array of points repeated indefinitely through space so that the environment of each point is identical. In 1848 Bravais showed that there are only 14 different ways of arranging points in a space lattice. Three of these are cubic space lattices: primitive, body-centered, and face-centered. If in any space lattice the distance from one point to another is measured, another point will be found at twice this distance in the same direction, a third at three times the distance, etc. A *unit cell* is defined by three of these unit displacements in three definite directions, all originating from the same point. There is an infinite number of ways in which a unit cell might be chosen, but it is advantageous to select a unit cell so that it has the smallest possible volume and the maximum symmetry of the lattice. In the primitive cubic unit cell there is a lattice point at each corner of the cube, in the body-centered unit cell there is an additional lattice point in the center of the unit cell, and in the face-centered unit cell there are six additional lattice points, one in the center of each face.

A crystal structure based on a lattice can be compared to a wallpaper pattern; the design of the wallpaper consists of a pattern or motif placed at each point of the two-dimensional lattice. In an analogous fashion the structure of a crystal consists of an atom or group of atoms as a motif situated about each lattice point. The lattice points themselves may be occupied by atoms as found in the crystal structures of many common metals, or they may serve as imaginary points about which a group of atoms is clustered. When the various symmetry operations are combined with the various space lattices, it is found that there are only 230 different possible combinations. These combinations are referred to as space groups, and each consists of a collection of symmetry elements, each with its own location in the unit cell defined. It is most helpful to know the space-group symmetry since the atoms, molecules, or ions in the unit cell must conform to give the configuration of the space group. As a result of symmetry, one needs only to specify the positions of a certain number of atoms in the cell; the positions of the other atoms are generated by the symmetry operations of the crystal. In this experiment we shall be concerned only with the space lattices of the cubic system.

*Scattering Theory.* X rays are scattered by the electrons of the atoms, and the superposition of waves scattered by the individual atoms results in diffraction, the intensity in any direction depending on whether the individual scattered waves are in phase. Hence the *intensities* of diffracted beams are determined by the *distribution of atoms* within the unit cell. One can think of X rays as being reflected from a given

family of planes as specified by Bragg's law: the *angles of reflection* of X rays are determined by the *geometry* of the lattice, that is, the size and shape of the unit cell.

In cubic crystals the interplanar spacing  $d_{hkl}$  of a family of planes with Miller indices  $hkl$  is given, from strictly geometrical considerations, by

$$d_{hkl} = \frac{a}{\sqrt{h^2 + k^2 + l^2}} \quad (1)$$

where  $a$  is the lattice constant, the length of the edge of the unit cell. The Miller indices of a given type of plane may be obtained by counting the number of planes crossed in moving one lattice spacing along the three axes of the crystal.

The angles  $\theta$  which the incident and diffracted beams make with the planes having Miller indices  $hkl$  depend upon the wavelength of the X rays and  $d_{hkl}$  according to Bragg's law,

$$\lambda = 2d_{hkl} \sin \theta \quad (2)$$

Equations (1) and (2) may be combined to obtain

$$\begin{aligned} \sin^2 \theta &= \frac{\lambda^2}{4a^2} (h^2 + k^2 + l^2) \\ &= \frac{\lambda^2 N}{4a^2} \end{aligned} \quad (3)$$

where  $N = h^2 + k^2 + l^2$ . The characteristic values of  $N$  possible for the various types of cubic crystals are summarized in Table 1. For primitive cubic crystals there is a repeating unit (ion, atom, molecule, or group of atoms) at each corner of the cubic unit cell. All lattice planes that can be drawn through the corners of the unit cells can lead to the reflection of X rays. As can be seen from Table 1,  $N = 7, 15, 23$  and certain larger values are missing; this is the distinguishing characteristic of the primitive cubic lattice. These values of  $N$  cannot be obtained as the sum of the squares of three integers.

For face-centered cubic crystals there is a repeating unit (ion, atom, molecule, or group of atoms) in the center of each face of the cubic unit cell, as well as at each corner. Consideration of the various types of reflecting planes shows that these extra lattice points lie on the planes for which the Miller indices are either all even or all odd: 111, 200, 220, 311, etc. Reflections are obtained from these planes, but reflections are not obtained from the planes for which the Miller indices are not all even or all odd, because for these cases there are lattice points between these planes which destroy the reflections by interference. Such systematic

TABLE 1. MILLER INDICES OF CUBIC CRYSTALS

N	Primitive	Face-centered	Body-centered
1	100		
2	110		110
3	111	111	
4	200	200	200
5	210		
6	211		211
7			
8	220	220	220
9	300, 221		
10	310		310
11	311	311	
12	222	222	222
13	320		
14	321		321
15			
16	400	400	400
17	410, 322		
18	411, 330		411, 330
19	331	331	
20	420	420	420
21	421		
22	332		332
23			
24	422	422	422
25	500, 430		
26	510, 431		510, 431
27	333, 511	333, 511	
28			
29	520, 432		
30	521		521
31			
32	440	440	440
33	441, 522		
34	530, 433		530, 433
35	531	531	
36	600, 442	600, 442	600, 442
37	610		
38	611		611
39			
40	620	620	620

TABLE 1. MILLER INDICES OF CUBIC CRYSTALS (*Continued*)

<i>N</i>	Primitive	Face-centered	Body-centered
41	621, 540, 443		
42	541		541
43	533	533	
44	622	622	622
45	630, 542		
46	631		631
47			
48	444	444	444
49	700, 632		
50	710, 543		710, 543
51	711, 511	711, 511	
52	640	640	640
53	720, 641		
54	721, 633, 552		721, 633, 552
55			
56	642	642	642
57	722, 544		
58	730		730
59	731, 553	731, 553	
60			
61	650, 643		
62	732, 651		732, 651

absences make it possible to determine the nature of the crystal lattice from X-ray diffraction.

For body-centered cubic crystals there is a repeating unit (ion, atom, molecule, or group of atoms) at the center of each unit cell, as well as at each corner. Inspection of the various types of reflecting planes shows that these extra lattice points lie on the planes for which the sum of the Miller indices ( $h + k + l$ ) is even: 110, 200, 211, 220, etc. The reflections from planes with  $h + k + l$  odd are destroyed by interference.

As a result of certain arrangements of atoms within the unit cell, certain reflections may be very weak. However, the correct structure can be obtained even when there are accidental absences of this sort.

The density  $\rho$  of a crystal is equal to the mass of a unit cell divided by the unit-cell volume. For a cubic crystal,

$$\rho = \frac{n(M/N_0)}{a^3} \quad (4)$$

where  $n$  is the number of units of molecular weight  $M$  in the unit cell. If a single atom or molecule is associated with each lattice point,  $n = 1$  for primitive cubic,  $n = 2$  for body-centered cubic, and  $n = 4$  for face-centered cubic.

In the powder method, originated by Hull and by Debye and Scherrer, a monochromatic X-ray beam is passed through a large number of fine crystals oriented in random directions. The arrangement of the film is shown in Fig. 70. Since crystals are oriented in all directions with respect to the incoming X-ray beam, all possible reflections are obtained. The rays reflected at a given angle form a cone.

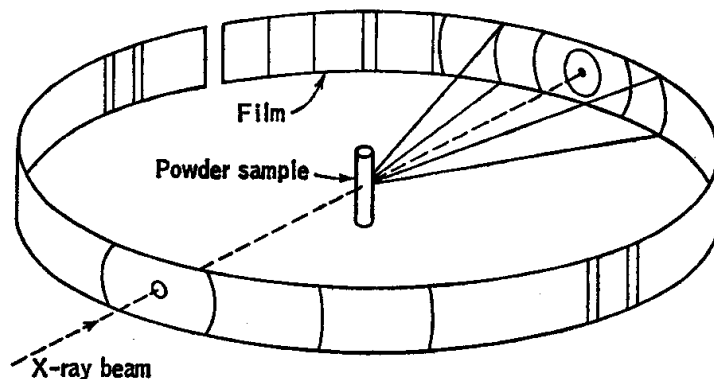


Fig. 70. X-ray powder camera.

There are a number of other experimental arrangements for studying X-ray diffraction. In the Laue method a single oriented crystal is irradiated with a collimated beam of polychromatic X rays. In other methods the crystal is rotated or rocked in a particular way during the exposure, and the film may also be moved. The interpretation of such experiments is more complicated than for powder patterns, but much more detailed information about the crystal structure may be obtained.

**Apparatus.** X-ray apparatus equipped with a powder camera; fine powders of cubic crystals, for example, KCl, NaCl, NaBr; X-ray film and supplies for developing it; accurate millimeter scale or microcomparator.

**Procedure.** It is important that the crystalline sample be pure, since small amounts of impurities will give rise to additional lines that may make the interpretation of the X-ray pattern difficult. If the crystals are not sufficiently fine, the sample is ground further with a mortar and pestle, so that the diffraction pattern will not contain large spots due to single crystals. The sample is either mounted in a thin-walled capillary or is attached to the outside of a thin glass rod, using a cement, as prescribed by the instructor.

The sample is mounted in the powder camera so that it is precisely

lined up with the collimator for the X-ray beam. The alignment of the sample is checked with the motor rotating the sample, as it will during the exposure. The specific instructions for using the particular X-ray powder camera employed should be followed in detail.

After the exposure the photographic film is developed, washed, and dried. Information about photography is to be found on page 503.

**Calculations.** The first step is to find the  $\theta$  values (definition page 290) for the observed reflections. The diffraction angles in degrees will be calculated from

$$2\theta = 180 \frac{X}{R}$$

where  $X$  = distance of a line from center of exit hole

$R$  = distance from center of entrance hole to center of exit hole

The distances  $X$  and  $R$  are lengths of arc measured along the film. The best procedure is to first tabulate the positions of the lines relative to an arbitrary reference point. This may be done by means of a steel scale which is laid along a line between the points where the X-ray beam would have passed through the film in entering the camera to the position where it would have passed through the film in leaving the camera. Note that the lines occur in pairs placed symmetrically about the exit hole. The positions of the holes are found by averaging the positions of several pairs of corresponding lines.

Next, the lattice type is to be identified by finding which column of  $N$  values (Table 1) is consistent with the values of  $\theta$  found. To do this, first tabulate values of  $\sin^2 \theta$ , since these should be proportional to  $N$  values. (Tables of  $\sin^2 \theta$  are available in certain handbooks.) The largest common factor of the values of  $\sin^2 \theta$  is found by subtracting each value from the next higher and examining the differences. The values of  $\sin^2 \theta$  are divided by this common factor to obtain the apparent  $N$  values, which are then compared with Table 1. These values should be sufficiently close to integers so that the corresponding integer can be recognized, provided that  $N$  is not too large. Impurities in the crystal-line sample will produce extra lines which cannot be accounted for in this way.

In order to obtain the lattice parameter  $a$  for the crystal,  $\lambda^2 N / 4 \sin^2 \theta$  is computed for a number of lines and  $a$  is calculated using Eq. (3).

The average wavelength of copper  $K\alpha$  radiation is 1.542 Å. Actually, this radiation consists of two lines,  $K\alpha_1$  and  $K\alpha_2$ . For low values of  $\theta$  these two lines are not resolved, but at large values of  $\theta$  they may be visible. When they are, the average position is taken.

Using the value of  $a$  obtained, the density of the crystal is calculated from Eq. (4). This value is compared with the literature value.

**Suggestions for Further Work.** Unknown powder samples may be identified by determining the  $d$  spacings of the three most intense lines and looking these distances up in the ASTM X-ray Diffraction Pattern Card Index. If there are several crystals which have nearly the same strong lines, these crystals may be distinguished from each other on the basis of further lines in the pattern.

The next level of complexity in powder patterns is encountered with tetragonal crystals. The procedure for analyzing such patterns is discussed in textbooks of X-ray diffraction.

Other types of X-ray diffraction experiments may be used. For example, Laue patterns may be taken of a single crystal which is oriented so that a beam of "white" X rays passes down various axes of the crystal.

### References

1. Azaroff and Buerger, "The Powder Method in X-ray Crystallography," McGraw-Hill Book Company, Inc., New York (1958).
2. Cullity, "Elements of X-ray Diffraction," Addison-Wesley Publishing Company, Reading, Mass. (1956).
3. Daniels and Alberty, "Physical Chemistry," John Wiley & Sons, Inc., New York (1961).
4. D'Eye and Wait, "X-ray Powder Photography," Butterworth & Co. (Publishers) Ltd., London (1960).
5. Klug and Alexander, "X-ray Diffraction Procedures," John Wiley & Sons, Inc., New York (1954).
6. Lipscomb *in* Weissberger (ed.): "The Technique of Organic Chemistry," Vol. I, Interscience Publishers, Inc., New York (1960).

## *Macromolecular Chemistry*

### 44. VISCOSITY OF HIGH-POLYMER SOLUTIONS

Viscosity determinations are very important in the study of high polymers. Using simple viscosity measurements, an average molecular weight of the polymer may be determined and certain qualitative conclusions may be made as to the general form of the macromolecules in solution.

**Theory.** Einstein<sup>2</sup> showed that the coefficient of viscosity  $\eta$  of a dilute suspension of small unsolvated rigid spheres is given by

$$\eta = \eta_0(1 + \frac{5}{2}\phi) \quad \text{or} \quad \frac{(\eta/\eta_0) - 1}{\phi} = \frac{\eta_{sp}}{\phi} = \frac{5}{2} \quad (1)$$

where  $\eta_0$  = coefficient of viscosity of solvent

$\eta/\eta_0$  = viscosity ratio

$\phi$  = total volume of spheres divided by that of the suspension

The quantity  $(\eta/\eta_0) - 1 \equiv \eta_{sp}$ , which occurs frequently in the theory of the viscosity of solutions, is called the specific viscosity. The ratio  $\eta_{sp}/c$  is called the viscosity number.

In the case of polymer solutions it is not possible to calculate the volume occupied by polymer in an unambiguous way, and so concentrations are generally expressed in terms of weight of polymer per unit volume (usually 100 ml). It is necessary to extrapolate  $\eta_{sp}/c$  to zero concentration since this ratio depends upon concentration. Plots of  $\eta_{sp}/c$  versus  $c$  are generally linear in the low-concentration range, and the extrapolated value  $[\eta]$  is named the limiting viscosity number or intrinsic viscosity.<sup>6</sup>

$$[\eta] = \lim_{c \rightarrow 0} \frac{\eta_{sp}}{c} = \lim_{c \rightarrow 0} \frac{1}{c} \ln \frac{\eta}{\eta_0} \quad (2)$$

where  $c$  is the number of grams of polymer in 100 ml of solution.† In

† Sometimes the concentration is expressed in grams solute per milliliter of solution. On this basis the new  $[\eta]$  is larger by a factor of 100 as compared with the customary one. Its unit is called the Staudinger.



order to show that  $\eta_{sp}/c$  and  $(1/c) \ln (\eta/\eta_0)$  extrapolate to the same limit at zero concentration, the logarithmic function may be expanded as an infinite series.

$$\ln \frac{\eta}{\eta_0} = \ln (1 + \eta_{sp}) = \eta_{sp} - \frac{\eta_{sp}^2}{2} + \dots \quad (3)$$

Since the second- and higher-order terms in  $\eta_{sp}$  become negligible compared with the first as concentration approaches zero, the functions given in Eq. (2) extrapolate to the same limit.

The following equation, often known by the names Mark-Houwink, expresses the relation between limiting viscosity number (or intrinsic viscosity) and molecular weight of the high polymer.

$$[\eta] = KM^a \quad (4)$$

The exponent  $a$  is a function of the geometry of the molecule in solution and varies from 0.5 for curled polymer molecules with a relatively small amount of permeation of solvent, the so-called random coils, to about 1.7 for rigidly extended molecules. The constants  $a$  and  $K$  depend upon the type of polymer, the solvent, and the temperature of the viscosity determinations; they are determined experimentally by measuring the intrinsic viscosities of polymers for which the molecular weight has been determined by an independent method, such as osmotic pressure, light scattering, or sedimentation equilibrium. The values of  $K$  and  $a$  listed in Table 1 have been determined for fractionated polymers.

TABLE 1. PARAMETERS FOR EQUATION (3)<sup>a</sup>

Polymer	Solvent	Temperature, °C	$K$	$a$
Cellulose acetate.....	Acetone	25	$1.49 \times 10^{-4}$	0.82
Polyisoprene.....	Toluene	25	$5.02 \times 10^{-4}$	0.67
Polystyrene.....	Toluene	25	$3.7 \times 10^{-4}$	0.62
GR-S copolymer.....	Toluene	30	$5.4 \times 10^{-4}$	0.66
Methyl methacrylate....	Benzene	25	$0.94 \times 10^{-4}$	0.76
Polyisobutylene.....	Toluene	20	$3.6 \times 10^{-4}$	0.64

<sup>a</sup> Goldberg, Hohenstein, and Mark, *J. Polymer Sci.*, **2**, 502 (1947).

In addition to yielding molecular weights, viscosity measurements give us some insight into the general form of polymer molecules in solution.<sup>1,4,7,8,10</sup> A long-chain molecule in solution takes on a somewhat kinked or curled shape, intermediate between a tightly rolled up mass and a rigid linear configuration. Presumably, all possible degrees of curling are represented, owing to the internal Brownian movement of the flexible chains. In a "good" solvent, i.e., one which shows a zero or negative heat of mixing with the polymer, the polymer molecule

is rather loosely extended, as represented in Fig. 71a, and the intrinsic viscosity is high. In a "poor" solvent, i.e., one in which the polymer dissolves with absorption of heat (positive heat of mixing), the segments of the polymer molecule attract each other in solution more strongly than they attract solvent molecules, and the result is that the molecule assumes a more compact shape as illustrated in Fig. 71b. Consequently,

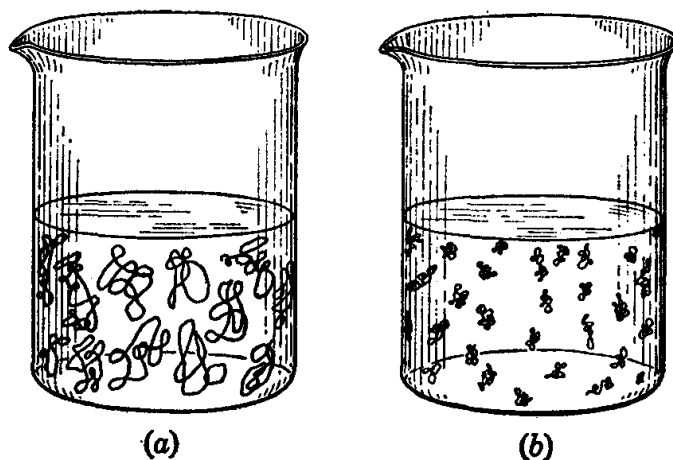


FIG. 71. Long-chain polymers in (a) a "good" solvent; (b) a "poor" solvent.

in a "poor" solvent the intrinsic viscosity will be lower than in a "good" solvent.

**Apparatus.** Ostwald viscometer; stop watch; pipettes; 25-ml volumetric flasks; polymer sample;† toluene; methanol.

**Procedure.** Solutions of the polystyrene sample of unknown molecular weight are prepared in a good solvent (toluene) and a poor solvent (a mixture of toluene and methanol). Since the polymer may dissolve rather slowly, warming in a water bath may be used to accelerate solution. When this is done, the solution should be cooled to 25° before adding solvent to bring the meniscus up to the mark on the volumetric flask. The following solutions are needed:

1. Five hundred milligrams of polystyrene is dissolved in toluene and diluted to exactly 25 ml in a volumetric flask.
2. One hundred milliliters of a solution containing 15 per cent methanol and 85 per cent toluene by volume is prepared. Again 500 mg of polystyrene is dissolved in this solvent and diluted to exactly 25 ml. The remaining solvent is required for dilutions and a flow-time determination.

After the viscometer has been thoroughly cleaned with cleaning solution, it is rinsed and dried by aspirating through it clean air from the

† Dow polystyrenes.

laboratory. It is important for the viscometer to be perfectly dry inside before organic solvents are added.

The flow time of the viscometer is determined for toluene and for the methanol-toluene solvent as described in Exp. 26. The flow time for the solution of polystyrene in toluene is determined. The sample is then diluted by a factor of 2, and the flow time determined. The accuracy of the dilutions may be improved by use of two calibrated pipettes, one calibrated for *withdrawal* of solution and the other for *delivery* of solvent. This dilution is repeated until the viscosity ratio of the polymer solution becomes so close to 1 that there is a large error in the specific viscosity. Since the densities of the dilute polymer solutions are not significantly different from that of the solvent, it is unnecessary for our present purpose to determine the densities.

The same procedure is now repeated with the solution of polystyrene in methanol-toluene, in this case diluting with the mixed solvent.

Since methanol is a nonsolvent for polystyrene, the addition of further quantities will cause precipitation of the polymer. The per cent methanol by volume required to cause the first turbidity is determined by titrating a few milliliters of the solution of polystyrene in toluene.

*Notice:* Before the viscometer is allowed to dry inside, it should be rinsed thoroughly with toluene so that a film of polymer will not be left in the capillary.

**Calculations.** The limiting viscosity number is obtained by plotting  $\eta_{sp}/c$  and  $(1/c) \ln (\eta/\eta_0)$  versus  $c$  (in grams polymer per 100 ml of solution) for the solution of polystyrene in toluene. The limiting viscosity number in methanol-toluene is determined by a similar graph. The advantage of the double extrapolation is that the intercept may be determined more precisely than by using only one straight line. Furthermore, there is a simple relationship between the slopes of the two lines which may be verified. For the dependence of viscosity number with concentration, Huggins has written

$$\eta_{sp} = [\eta]c + k_1[\eta]^2c^2 \quad (5)$$

Similarly,

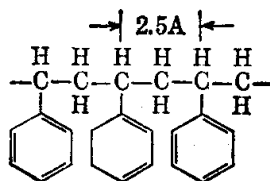
$$\ln \frac{\eta}{\eta_0} = [\eta]c - k_2[\eta]^2c^2 \quad (6)$$

To a good approximation it can be shown by application of Eq. (3) that  $k_1 + k_2 = 0.5$ .

Using the values of  $K$  and  $a$  given in Table 1, the molecular weight of the sample of polystyrene is calculated from its limiting viscosity number in toluene. It should be realized that this is an average molecular weight, some of the molecules being larger and some smaller; even

the more homogeneous of the so-called living polymers show some heterogeneity.<sup>9</sup>

An estimate as to the size of the average polystyrene molecule in the sample is obtained by calculating the volume of one molecule from the molecular weight, using 0.903 g/ml for the density of polystyrene. The radius of the molecule is calculated, assuming the molecule to be spherical. The length of the extended polymer molecule



is calculated, assuming the length per monomer unit is 2.5 Å. The actual shape of the polystyrene molecule in solution is intermediate between the spherical and stretched-out forms and depends upon the solvent and temperature.

**Practical Applications.** Determination of the molecular weight of the soluble organic high polymers such as polyisobutylene, polymethyl methacrylate, and polyvinyl chloride is important because the physical properties of these materials depend markedly on molecular weight.

**Suggestions for Further Work.** The general subject of the viscosity of polymer solutions has been well reviewed in the literature,<sup>3,7,8,10</sup> where suggestions for further work may be found.

Viscosity determinations at higher concentrations are used to show that the linear relation between  $\eta_{sp}/c$  and  $c$  does not hold at higher concentrations. Ordinary polystyrene may be separated into several fractions by precipitating part of it with methyl alcohol. The average molecular weight of each fraction is estimated by means of viscosity determinations.

For a given polymer,  $[\eta]$  may be determined for various concentrations of non-solvent and plotted against per cent nonsolvent.<sup>1</sup>

#### References

1. Alfrey, Bartovics, and Mark, *J. Am. Chem. Soc.*, **64**, 1557 (1942).
2. Einstein, *Ann. Physik*, **19**, 259 (1906); **34**, 591 (1911).
3. Ewart in Kraemer (ed.): "Advances in Colloid Science," Vol. II, Interscience Publishers, Inc., New York (1942).
4. Flory, "Principles of Polymer Chemistry," Cornell University Press, Ithaca, N.Y. (1953).
5. Goldberg, Hohenstein, and Mark, *J. Polymer Sci.*, **2**, 503 (1947).
6. Kraemer, *Ind. Eng. Chem.*, **30**, 1200 (1938).
7. Mark and Tobolsky, "Physical Chemistry of High Polymeric Systems," 2d ed., Interscience Publishers, Inc., New York (1950).
8. Onyon in Allen (ed.): "Techniques of Polymer Characterization," Academic Press, Inc., New York (1959).
9. Szwarc, Levy, and Milkovich, *J. Am. Chem. Soc.*, **78**, 2656 (1956).
10. Tompa, "Polymer Solutions," Academic Press, Inc., New York (1956).

#### 45. DETERMINATION OF THE OSMOTIC PRESSURE OF A SOLUTION OF HIGH POLYMER

The number-average molecular weight of a sample of polystyrene is calculated from the osmotic pressure of a solution of the polymer in methyl ethyl ketone.

**Theory.** Of the four colligative properties of solutions, boiling-point elevation, freezing-point lowering, vapor-pressure lowering, and osmotic pressure, only the last is useful in determining the molecular weights of solutes in the colloid size range—synthetic high polymers, proteins, and polysaccharides. For example, an aqueous solution containing 10 g liter<sup>-1</sup> of a solute of molecular weight 100,000 would have a boiling-point elevation of  $5 \times 10^{-5}$  deg, a freezing-point lowering of  $2 \times 10^{-4}$  deg, a vapor-pressure lowering of  $5 \times 10^{-5}$  mm Hg, but an osmotic pressure of 25 mm of water.

When a solution and the pure solvent are separated by a semipermeable membrane (that is, one which permits the passage of molecules of solvent from one side to another, but not molecules of solute), solvent molecules will pass through the membrane into the solution or in the opposite direction, depending upon the pressure difference across the membrane. The *osmotic pressure* is the excess pressure which must be applied to the solution to establish equilibrium. Since at equilibrium the fugacity of the solvent is the same in the solution phase as in the pure solvent phase, the relation of osmotic pressure to molecular weight may be derived thermodynamically.<sup>8</sup> The basic thermodynamic equation is

$$\pi = \frac{RT}{\bar{V}_1} \ln \frac{f_1^\circ}{f_1} \quad (1)$$

where  $\pi$  = osmotic pressure

$R$  = gas constant

$T$  = absolute temperature

$\bar{V}_1$  = partial molal volume of solvent

$f_1^\circ$  = fugacity of pure solvent at 1 atm pressure

$f_1$  = fugacity of solvent in solution at 1 atm pressure

If it is assumed that (a) fugacities may be replaced by vapor pressures, (b) Raoult's law applies to the solvent in dilute solutions of the polymer, and (c) the solutions are sufficiently dilute so that  $\bar{V}_1$  may be replaced in dilute solutions by the molar volume of the solvent, Eq. (1) leads to

$$\lim_{c \rightarrow 0} \frac{\pi}{c} = \frac{RT}{M} \quad (2)$$

where  $c$  = concentration (weight of polymer per unit volume of solution)

$M$  = molecular weight of polymer

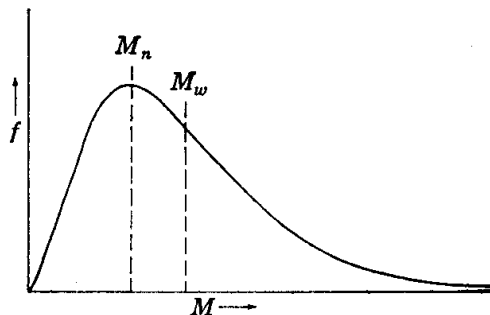


FIG. 72. Distribution of molecular weight for a high polymer. The values of  $M_n$  and  $M_w$  for this molecular-weight distribution are shown.

in a given range of width  $dM$  is proportional to the magnitude of  $dM$ . In the figure,  $f$  is plotted versus  $M$ .

When there is a distribution of molecular weights, several types of average molecular weights may be defined. The *number-average* molecular weight is defined by

$$M_n = \frac{\sum_i n_i M_i}{\sum_i n_i} \quad (3)$$

where  $n_i$  is the number of molecules of weight  $M_i$ . The *weight-average* molecular weight is defined by

$$M_w = \frac{\sum_i n_i M_i^2}{\sum_i n_i M_i} \quad (4)$$

Different experimental methods yield different types of average molecular weight. Since the osmotic pressure depends on the number of molecules per unit volume without regard to their size, Eq. (2) yields the *number-average molecular weight*. The viscosity method (Exp. 44) yields a molecular weight which is closely, but not exactly, related to  $M_w$ . The weight-average molecular weight must obviously be greater than the number-average molecular weight for a heterogeneous polymer. For a homogeneous polymer,  $M_n = M_w$ .

A general review of osmotic-pressure measurements has been written by Wagner and Moore.<sup>6</sup>

The osmometer to be used is of the Schultz-Wagner<sup>5</sup> type, which is illustrated in Fig. 73. It consists of a graduated capillary (0.75 to 1.0 mm inside diameter) attached to a short section of larger tubing

The limiting value of  $\pi/c$  is obtained by plotting  $\pi/c$  versus  $c$  and extrapolating linearly to  $c = 0$ .

The molecules in a sample of a synthetic high polymer do not all have the same weight. The molecular-weight distribution may be represented by a plot such as that shown in Fig. 72. The fraction of molecules having molecular weights in the interval  $M$  to  $M + dM$  is represented by  $f dM$ . The  $dM$  appears here because the fraction of molecules

(12 mm inside diameter) which has a ground lower surface against which the membrane is held by a brass clamp. The purpose of the lower plate is to hold the membrane tightly against the glass tubing and to support the membrane so that it will not bulge out and stretch during the experiment. The osmometer is filled with polymer solution by use of a syringe with a long stainless-steel needle. This method of filling the osmometer has the advantage that ground-glass joints and valves are avoided so that possibilities for leaks are reduced to a minimum.

Since the permeability of a membrane to various types of solvents may be very different, osmotic-pressure measurements may be made more rapidly with one solvent than with others. In the case of cellophane membranes, Browning and Ferry<sup>1</sup> showed that equilibrium is reached more rapidly with methyl ethyl ketone than with benzene or toluene.

**Apparatus.** Two Schultz-Wagner osmometers; polystyrene; methyl ethyl ketone; 5-ml syringe with long stainless-steel needle; volumetric flasks; cellophane membranes.

**Procedure.** Du Pont Cellophane 600 is soaked overnight in 30 per cent sodium hydroxide and washed a few minutes in progressively more dilute solutions of sodium hydroxide and then water. This treatment is necessary to increase the porosity of the membrane. The progressive dilutions of alkali are essential to avoid wrinkling of the membrane. The membranes are then washed in progressively more concentrated solutions of methyl ethyl ketone in water and may be stored in methyl ethyl ketone; hence it is unnecessary for each student to carry out the sodium hydroxide treatment.

A weighed sample of polystyrene is dissolved in methyl ethyl ketone, and the solution is diluted to the desired volume in a volumetric flask. A suggestion as to the concentration to use may be obtained from an instructor. Since 2 to 4 days is required for equilibration, two osmometers should be set up at one time. The osmotic pressures for at least two concentrations of the same polymer are measured.

In assembling the osmometer, it is important to keep the membrane moistened with methyl ethyl ketone, since the value of the sodium hydroxide treatment will be lost if the membrane is allowed to dry out.

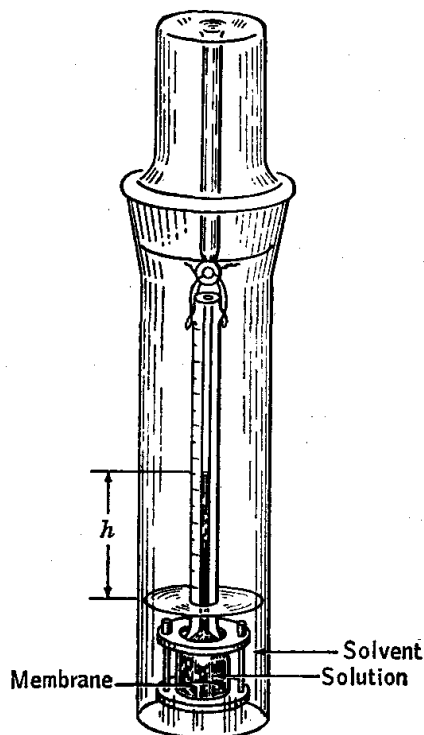


FIG. 73. Simple osmometer.

Two disks of a smooth hard filter paper are moistened with methyl ethyl ketone and placed on the bottom brass plate. The filter paper serves as a support for the membrane so that it cannot sag into the holes and facilitates a good seal between the membrane and the ground-glass surface of the osmometer bulb. The membrane is placed on the filter paper, and the glass osmometer tube is attached. The knurled nuts are tightened with the fingers. The polystyrene solution is placed in the osmometer by use of a syringe with a long stainless-steel needle, taking care to avoid trapping bubbles at any point. **Precaution:** The syringe and needle should be rinsed out with methyl ethyl ketone after being used to transfer the polymer solution so that no polystyrene residue will be left in them. Since methyl ethyl ketone is a solvent for many of the plastics used in fountain pens and pencils, carelessness may result in damage to them.

Enough methyl ethyl ketone is placed in the outer glass tube so that the meniscus comes to the lower part of the graduated capillary when the osmometer is hung in the tube.

The height of the liquid column in the capillary is set at a value several centimeters above, or below, that expected at equilibrium. If it is possible to use two osmometers for each solution, the height is set higher than the expected pressure in one and lower in the other. The osmometer is then suspended in methyl ethyl ketone so that the membrane is completely immersed.

The osmometers are placed in a well-regulated thermostat. After allowing some time for temperature equilibration, an initial reading is taken. Readings are then taken at intervals over a period of 2 or more days.

An unfractionated polymer sample contains molecules of a wide range of molecular weights, and some of the lowest-molecular-weight material may diffuse through the membrane. If there is appreciable leakage of low-molecular-weight material, a constant osmotic pressure will not be obtained. It is necessary to correct the observed meniscus height for the capillary rise of the solution. It is satisfactory to determine the capillary rise of the solvent and to assume, for the purpose of this experiment, that the capillary rise for the polymer solution will be the same as that determined for the solvent.

Data required for making another correction should also be obtained with the osmometer used. The need for this further correction arises since the equilibrium height in the capillary is, in general, different from the initial height. If the equilibrium height of the meniscus is greater than the initial height, solvent has passed into the polymer solution, and so the equilibrium polymer solution is more dilute than the original solution. In order to compute the equilibrium concentration it is necessary



to know the volume of the osmometer bulb and the radius of the capillary. The volume of the bulb may be determined with sufficient accuracy by measuring the volume of water required to fill it, and the radius of the capillary may be calculated from the capillary rise of methyl ethyl ketone (cf. Exp. 49). The surface tension of pure methyl ethyl ketone is 23.9 dynes  $\text{cm}^{-1}$  at 25°, and its density at 25° is 0.803  $\text{g cm}^{-3}$ .

**Calculations.** Plots of height  $h$  versus time are useful in determining the osmotic pressure. The osmotic pressure  $\pi$  in atmospheres may be calculated from the equilibrium height  $h$  from the equation

$$\pi = (h - h_c)\rho_s g \quad (5)$$

where  $h_c$  = capillary-rise correction

$\rho_s$  = density of high-polymer solution (assumed to be the same as for solvent)

If  $h$  is in cm,  $\rho_s$  in  $\text{g cm}^{-3}$ , and  $g$  in  $\text{cm sec}^{-2}$ ,  $\pi$  will be in dynes  $\text{cm}^{-2}$ . In order to obtain the pressure in atmospheres, this value is divided by  $1.013 \times 10^6$  dyne  $\text{cm}^{-2}$  atm $^{-1}$ .

The concentrations  $c$  in  $\text{g liter}^{-1}$  are calculated by correcting the initial concentrations as described above for the flow of solvent in or out. A plot of  $\pi/c$  versus  $c$  is extrapolated to zero concentration. Such plots are expected to be linear in the concentration range suggested. If the range of values of  $\pi/c$  is within the range of experimental error, the best horizontal line is drawn through the points. The number-average molecular weight is calculated from the extrapolated value of  $\pi/c$  by use of Eq. (2).

**Practical Applications.** Since the properties of a solid plastic or synthetic rubber will depend upon the molecular weight of the polymer, the measurement of osmotic pressure is widely used in industry. The viscosity method which is also used is illustrated in Exp. 44.

**Suggestions for Further Work.** The molecular weight of a sample of polystyrene may be determined in another solvent. Although the number-average molecular weight obtained from the intercept of a plot of  $\pi/c$  versus  $c$  should be the same, the slope may be quite different.<sup>2</sup> On the other hand, the slopes for a series of polystyrene samples of different molecular weight in a given solvent will be very nearly the same.

If the polymer sample contains low-molecular-weight material which leaks through the membrane, this material may be eliminated by precipitating about 75 per cent of the polymer by the addition of methyl alcohol to a solution in benzene. The lowest molecular-weight fraction will remain in the supernatant liquid. The precipitate may be dissolved in benzene and dried by vacuum sublimation of the benzene to obtain a porous preparation of polystyrene which can be readily redissolved.

The polymer sample may be fractionated into samples of different number-average molecular weight by dissolving it in a good solvent and partially precipitating it by the addition of a poor solvent, for example, methyl alcohol. The molecular weights of the polymer in the precipitate and in the solution phase may be shown to be different by osmotic-pressure measurements.

The osmotic pressure of gelatin or serum albumin in aqueous solution may be determined, and the number-average molecular weights calculated.<sup>4</sup> To reduce the Donnan effect, 0.2 M sodium chloride is used as solvent and the pH is adjusted to the isoelectric point of the protein. The Donnan effect is the contribution to the osmotic pressure due to the unequal distribution of the electrolyte ions across the membrane at equilibrium.

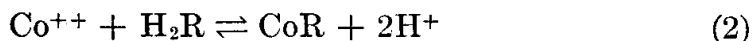
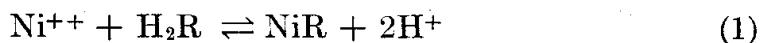
#### References

1. Browning and Ferry, *J. Chem. Phys.*, **17**, 1107 (1949).
2. Flory, *J. Am. Chem. Soc.*, **65**, 373 (1943).
3. Flory, "Principles of Polymer Chemistry," pp. 273-282, Cornell University Press, Ithaca, N.Y. (1953).
4. Scatchard, Batchelder, and Brown, *J. Am. Chem. Soc.*, **68**, 2320 (1946).
5. Wagner, *Ind. Eng. Chem., Anal. Ed.*, **16**, 520 (1944).
6. Wagner and Moore in Weissberger (ed.): "Technique of Organic Chemistry," 3d ed., Vol. I, Pt. I, Interscience Publishers, Inc., New York (1959).

#### 46. ION-EXCHANGE CHROMATOGRAPHY

The separation of cations by means of elution from a cation-exchange resin with a complexing reagent is illustrated. The relation of an idealized chromatographic experiment to the adsorption isotherm is discussed.

**Theory.** An ion-exchange resin is made up of insoluble macromolecules with ionizable groups attached. A cation-exchange resin has sulfonic, phenolic, or carboxylic groups, which provide negatively charged binding sites for cations. An anion-exchange resin has basic binding sites. If a cation-exchange resin is treated with acid, it is said to be in the hydrogen form because the negatively charged groups are neutralized by protons. If metal ions are added to the solutions, protons are displaced. For example, if  $\text{Ni}^{++}$  and  $\text{Co}^{++}$  ions are present, the following equilibria are established:



where R represents the part of the insoluble macromolecular ion that binds one divalent metal ion. Since these equilibria are reversible, the metal ions may be displaced by raising the acid concentration.

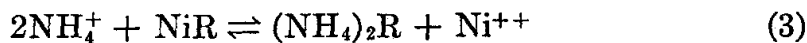
The affinity of the resin for a metal ion is affected by two factors, the radius of the hydrated ion and the valence of the ion. Thus two different metal ions will be held by the resin to different extents. A separation of the two ions might then be achieved by taking advantage of this difference in the affinity of the two ions for the resin.

If a bed of resin is arranged in column form and metal ions are adsorbed in the top layer, they may be washed through the column by a flow of solvent, the rate of transport of the ions being dependent upon their

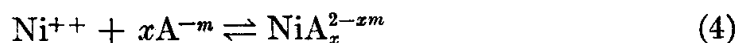
equilibrium concentration in the solution. As the equilibrium solution is washed down the column, the adsorbed ions at the upper edge of the band dissociate into solution and a certain portion of the ions carried to the layer of fresh resin becomes adsorbed by the resin.

The separation of different metal ions obtainable in this way may be enhanced by use of a complexing agent (such as citrate buffer or tartrate buffer) which complexes with metal ions and competes with the resin for the cations. The speed with which a given ion moves down the resin column is then dependent upon the affinity of the resin for the ion and the extent to which the ion is complexed by the complexing agent.

When a solution of ammonium citrate (of a pH at which nickel citrate complex ions are formed) is passed through a resin column on which nickel ion has been adsorbed at the top, the following reversible reaction is set up:



At the same time, the citrate anion of average charge  $-m$  (represented by  $\text{A}^{-m}$ ) reacts with the  $\text{Ni}^{++}$  ion as indicated by the reversible reaction



where  $x$  is the number of anions which complex with each nickel ion. The fraction of the total nickel found in each form, i.e., as  $\text{Ni}^{++}$ ,  $\text{NiR}$ , and  $\text{NiA}_x^{2-xm}$ , is determined by the equilibrium constants for reactions (3) and (4). A similar set of two reactions occurs for the  $\text{Co}^{++}$  ion. Now, if these two equilibrium constants for the nickel reactions are sufficiently different from those for the cobalt reactions, a separation may be achieved. By using a complexing agent, there are two equilibrium constants instead of one with which to work.

When ammonium citrate buffer is passed into the column, the  $\text{Ni}^{++}$  ion is complexed, thereby shifting the equilibrium of reaction (3) to the right. The nickel in solution moves down the column to a region of "fresh" resin  $(\text{NH}_4)_2\text{R}$ , where the  $\text{Ni}^{++}$  ion is readsorbed. Thus, as the solution passes down the column, the  $\text{Ni}^{++}$  is successively adsorbed and desorbed in a process similar to fractional distillation in which a substance is successively vaporized and condensed. The same process is going on with the  $\text{Co}^{++}$  ions. Thus the small differences in equilibrium constants are made use of many times, with the result that a better separation is achieved by column operation than in a batch experiment. When citrate buffers of higher pH are used, reaction (4) is displaced to the right and the metal ions are eluted more rapidly from the column.

For the case in which the adsorption isotherm is linear, as in the low-concentration range, the slope of the isotherm may be calculated from the velocity of the zone of adsorbed substance down the chromatographic

column. The slope of the adsorption isotherm  $K$  (distribution coefficient) is the ratio of the weight of solute adsorbed by 1 g of adsorbent to the equilibrium concentration in grams per milliliter of solution. Although the theory<sup>3,6</sup> of chromatographic separation is complicated, the relation between the position of the zone and the distribution coefficient is quite simple provided that the adsorbed solute is in equilibrium with dissolved solute at every step in the process.

$$K = \frac{V}{Fm}$$

where  $V$  = volume of elutant which has flowed into column, ml

$m$  = mass of adsorbent in column, grams

$F$  = fraction of length of column swept through by center of zone

**Apparatus.** Ion-exchange column filled with Dowex-50; citrate buffer (50 g citric acid monohydrate and 1 g phenol per liter of water adjusted to pH 3.30 to 3.40 with concentrated aqueous ammonia);  $\text{NiCl}_2$ ;  $\text{CoCl}_2$ ; two 25-ml graduates; spectrophotometer; spectrophotometer cells; lens tissue; long tube with bulb.

**Procedure.** The experimental arrangement for this experiment is illustrated in Fig. 74. If it is not certain that the resin has been completely freed of nickel and cobalt and washed with distilled water, the column is washed with about 300 ml of 2 N HCl, followed by about 300 ml of distilled water. Washing may be stopped when the effluent is basic to methyl orange (about pH 4.5).

Quantities of nickel and cobalt chlorides containing 200 mg of the metal are weighed out, mixed, and dissolved in a small quantity of distilled water (not over 20 ml). In order to save time, it is advisable to suck out the water above the resin bed by using a long glass tube and rubber bulb before pouring on the solution of the metals. The solution containing metal ions is poured on the top of the resin bed and allowed to flow into the column. If distilled water is then poured carefully into the tube above the resin bed, it will form a layer above the salt solution and there will be an adequate head to force the solution through the column. A siphon is connected to the column, and about 150 ml of distilled water is allowed to flow through it. If the washings are colorless, they are discarded.

The distilled water above the column is then withdrawn with the long glass tube and bulb, and citrate buffer is poured on the column. A large container of citrate buffer is connected by means of a siphon. The rate of elution is controlled by means of a pinch clamp so that the flow rate is 2.5 to 3.0 ml min<sup>-1</sup>. Twenty-five-milliliter samples of the effluent are collected until the first nickel appears, and from that point on, 10-ml samples are collected. For each fraction the volume and time are

recorded (the flow rate may be checked from these data), and a test tube full of the solution is corked for analysis.

Since the cobalt tends to tail out through a large volume, the last bit may be removed by washing the column with 2 N HCl and then with distilled water (at least 300 ml).

The solutions are analyzed directly with a spectrophotometer. It has been found convenient to analyze for cobalt at a wavelength of  $510\text{ m}\mu$  and nickel at  $650\text{ m}\mu$ . A small amount of nickel does not interfere with

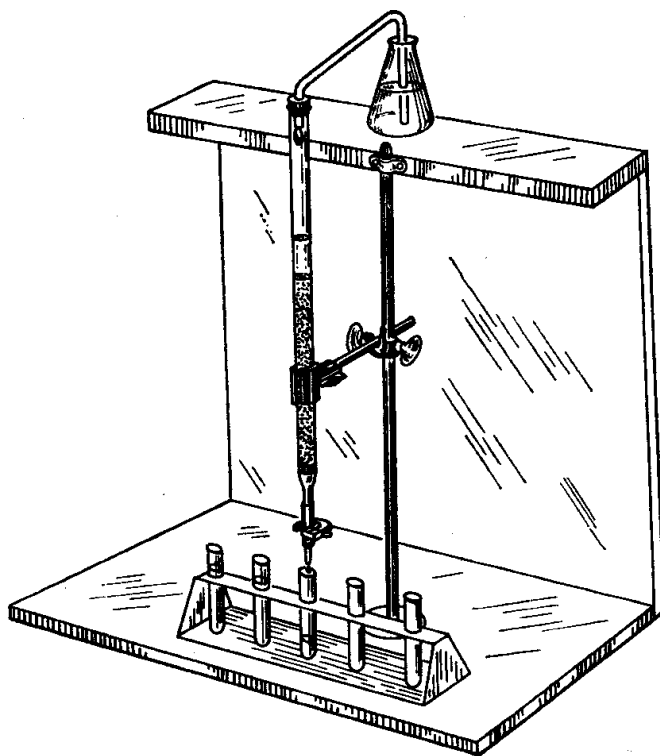


FIG. 74. Ion-exchange column.

the analysis for cobalt, and vice versa. The concentrations are read directly from plots of absorbancy  $[\log (I_0/I)]$  (Exp. 16) versus concentration of nickel or cobalt; these are provided in the laboratory or determined separately.

**Calculations.** The concentrations of nickel and cobalt in the various fractions are plotted versus volume of effluent. The quantities of nickel and cobalt recovered from the column are calculated from the concentrations and volumes of the fractions. The per cent recovery is computed.

**Practical Applications.** Chromatographic adsorption is finding many applications. It is widely used for qualitative analysis of organic compounds and for the separation of different compounds in a mixture of biological materials. It has been used even for the separation of isotopes.<sup>5</sup>

**Suggestions for Further Work.** The influence of pH, rate of elution, or ratio of weight of metal to weight of resin may be investigated.

A vertical tube packed with powdered sugar under the proper conditions may be used for separating by chromatographic adsorption the various plant pigments obtained by crushing leaves and treating them with petroleum ether.

#### References

1. Block, Durrum, and Zweig, "Paper Chromatography and Paper Electrophoresis," Academic Press, Inc., New York (1955).
2. Cassidy in Weissberger (ed.): "Technique of Organic Chemistry," 2d ed., Vol. X, Interscience Publishers, Inc., New York (1957).
3. Giddings, *J. Chem. Phys.*, **31**, 1462 (1959).
4. Nachod, "Ion Exchange: Theory and Application," Academic Press, Inc., New York (1949).
5. Roberts, Willeford, and Alberty, *J. Chem. Educ.*, **29**, 545 (1952).
6. Series of papers on the separation of rare earths and radio-isotopes by ion exchange, *J. Am. Chem. Soc.*, **69**, 2769-2881 (1947), especially Tompkins, Khyn, and Cohn, p. 2769.
7. Spedding, Powell, and Svec, *J. Am. Chem. Soc.*, **77**, 6125 (1955).
8. Tompkins, *J. Chem. Educ.*, **26**, 92 (1949).

#### 47. SEDIMENTATION RATE AND PARTICLE SIZE DISTRIBUTION

The measurement of the velocity of sedimentation of particles in the earth's gravitational field or a centrifugal field gives valuable information concerning their size. When the dispersed particles are so large that they exceed the limit of colloidal dimensions, and when the density of the particle relative to that of the suspension medium is sufficiently great, they settle out under the force of gravitation. By measuring rates of sedimentation, particle size and size-distribution determinations can be made with finely divided solids for which other sizing methods would be impractical or impossible.

**Theory.** The constant velocity with which a spherical particle falls in a liquid may be expressed with a relatively simple law. The force of friction resisting the fall of the particle is  $6\pi\eta r(dx/dt)$ , and the force of gravity acting on the particle is  $mg$ , or  $\frac{4}{3}\pi r^3(\rho_p - \rho)g$ . In these expressions  $\eta$  is the coefficient of viscosity of the liquid,  $r$  is the radius of the particle,  $dx/dt$  is the velocity of fall of the particle,  $\rho_p$  and  $\rho$  are the densities of the particle and of the suspension medium,  $m$  is the effective mass of a particle, and  $g$  is the acceleration due to the earth's gravitational field. The force of gravity and the force of friction are exactly opposed and equal when the system reaches a "steady state"; i.e., the particle falls with constant velocity, and

$$6\pi\eta r \frac{dx}{dt} = \frac{4}{3}\pi r^3(\rho_p - \rho)g$$

or

$$r = \sqrt{\frac{\frac{9}{2}\eta}{(\rho_p - \rho)g} \frac{dx}{dt}} \quad (1)$$

This equation is known in the literature as Stokes' law.

Thus, if the sedimentation rate of spherical particles is measured and the coefficient of viscosity of the liquid, the difference in density between the particle and the liquid, and the constant of the sedimentation field are known, the particle size can be calculated. For nonspherical particles an apparent radius can be calculated. This statement is true for sedimentation in the ultracentrifuge as well as for ordinary sedimentations, and a very large number of determinations of the size of particles has been made by using the formula of Stokes. If the particles are asymmetric in shape, the exact particle size cannot be obtained in this way, but there may be evaluated an "equivalent radius," or the radius of an imaginary spherical particle of the same substance with the same observed velocity of sedimentation. The particle must possess some appreciable degree of asymmetry before this factor makes a marked difference in sedimentation rates.

In actual particulate systems, heterogeneity of size is the rule rather than the exception. They have usually been prepared by grinding, milling, precipitation from solution, etc. Such systems may be characterized in two ways, either by an average size or weight or by a size frequency distribution or tabulation. If the sample contains a broad range of sizes, the values found for the average size by various methods may be greatly different. The methods which give number averages are strongly influenced by the particles of the smaller sizes which make less important contributions to the weight of the sample; in turn, these particles have relatively little effect on the weight-average values.<sup>3,5</sup> The size frequency distributions give more complete information. They may be integral or differential distributions.

Sedimentation methods are useful for the determination of the size distribution of particles with diameters below 50  $\mu$ . These methods which use gravitational force are applicable to particles as small as 1  $\mu$ , provided their density is sufficiently different compared with that of the suspension medium. There are accumulation methods and incremental methods. The one illustrated in this experiment is a cumulative manometric method which makes use of a graphical analysis of tangential intercepts to correct for the continually separating particles, thus to produce an integral distribution curve.

The differential distribution curves for materials which have been prepared by the methods indicated are generally skewed toward the larger sizes; thus the distribution is not described by the simple Gaussian function. Sometimes a logarithmic-number distribution function can be used, but in general the functions are quite involved and beyond the scope of this experiment.

**Apparatus.** Sedimentation-tube assembly; finely divided solid, such as precipitated lead sulfate or glass beads of diameter 1 to 20  $\mu$ ; gum arabic; stop watch.

**Procedure.** The apparatus (Fig. 75) consists of an inclined capillary, side tube *C*, containing the suspension medium, in this case water, connected to the main vessel *A*, at the sampling level. At equilibrium, the water column will have a height greater than that of the suspension in the large tube, since the suspension of the dense powder has a higher density than the pure suspension medium. As the suspended solid settles out below the sampling level, the density of the suspension becomes less and the levels in the two tubes approach the same value. It is the

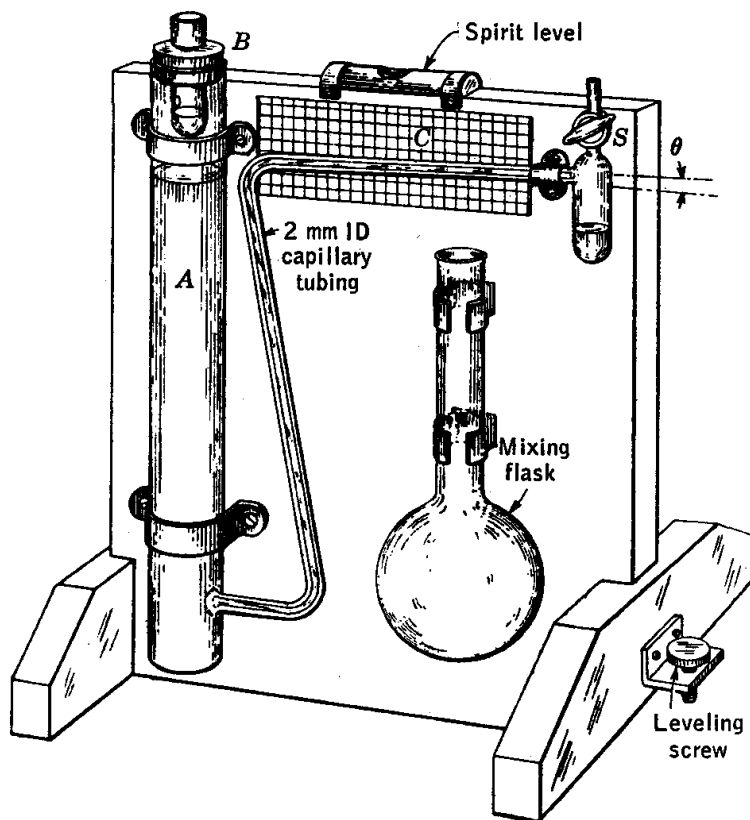


FIG. 75. Sedimentation-tube assembly.

measurement of the excess height in the inclined capillary tube as a function of time that provides a curve showing the variation of the mean density of the suspension between its surface and the sampling level.

The capillary sidearm is bent to a small angle to provide means to make a more accurate estimate of the difference in the levels in the two tubes. The apparatus is adjusted with the aid of the spirit level and the leveling screw to ensure accuracy of the sidearm angle.

Enough lead sulfate or glass beads are weighed out to make about 150 ml of a 3 per cent suspension. If lead sulfate is used, the powder is mixed with 2 or 3 ml of 5 per cent gum arabic solution and about 1 ml of 5 per cent lead nitrate solution. This mixture is rubbed well on a glass plate



with a spatula, the purpose being to break up the agglomerates of small particles. The paste is now transferred to the mixing flask and diluted with distilled water. The glass beads may be suspended directly in distilled water.

The sedimentation tube and its sidearm are cleaned thoroughly with hot cleaning solution and rinsed with distilled water. This preliminary treatment is of the utmost importance, since the slightest trace of foreign matter will cause sticking of the meniscus. With the stopcock open, the apparatus is filled with distilled water to such a height that the meniscus in the side tube rests near the lower end of the inclined part of the capillary. The top height in the large tube, *A*, is marked, and the distance between this mark and the sampling level is measured to give the height *h*. The water is then drawn up to a point on the scale near the further end of the inclined capillary tube. The stopcock is closed, and the large tube emptied. The suspension is now poured in to the top-height mark, and the suspension is stirred. After opening the stopcock, the level in the capillary is read at suitable intervals of time. At least 5 hr of settling should be allowed if lead sulfate is used, but the experiment can be completed in 3 hr with the glass-bead suspensions, and they are recommended. For other materials longer or shorter periods may be required, depending upon the system studied.

Distilled water placed in the reservoirs of *B* and below *S* serves to minimize errors due to evaporation in the sedimentation tube.

It is also necessary to measure the inside diameter of the tube for use in the calculations. The tangent of the angle  $\theta$  of inclination of the side tube is read from the graph-paper backing as ordinate divided by abscissa.

**Calculations.** The relationship between the weight of material  $M_t$ , which settles out in time *t*, and the horizontal displacement of the meniscus *x* is found in the following way:

$$a = \frac{D}{\rho} h - h = x \tan \theta \quad (2)$$

where *a* = difference in height of menisci in two tubes

*D* = mean density of suspension

$\rho$  = density of suspension medium, in this case, water

*h* = distance from sampling level to meniscus in large tube

*x* = length of base as determined from positions of meniscus

$\theta$  = angle capillary tube makes with horizontal

The weight of the material which settles past the sampling level is obtained from densities and volumes. Thus

$$D = \frac{V\rho - V_s\rho + M}{V}$$

where  $V$  = volume of suspension corresponding to height  $h$

$V_s$  = volume of medium displaced, i.e., volume of solid

$M$  = weight of solid phase in suspension above sampling level

Now, if  $\rho_s$  is the density of the solid,

$$D = \frac{\rho_s V \rho - M \rho + M \rho_s}{V \rho_s}$$

Substitution of this expression in Eq. (2) leads to the desired relationship, namely,

$$M = \frac{V \rho_s \rho \cdot x \cdot \tan \theta}{h(\rho_s - \rho)} = kx \quad (3)$$

The weight of material,  $M_t$ , which has settled below the sampling level in time  $t$  is simply the difference between the weight initially,  $M_0 = kx_0$ , and that at time  $t$ ,  $kx$ .

$$M_t = k(x_0 - x) \quad (4)$$

where  $x_0$  = initial horizontal position of meniscus ( $t = 0$ )

$x$  = horizontal position of meniscus at time  $t$

$k$  = proportionality constant, computed from Eq. (3), using data found in standard handbooks and certain apparatus constants

From Eq. (4) the weight  $M_t$  settled below the sidearm entrance may be calculated after any time. A sedimentation curve may then be constructed by plotting the weight settled against time. The time scale is then converted to particle size by the use of Stokes' law. Tangents are drawn on this plot at times corresponding to equal particle-size intervals. The difference between the intercepts of any two tangents on the ordinate corresponds to the percentage of material in the size interval at whose limits the tangents were drawn.

This can perhaps best be seen from the construction of a synthetic curve similar to the experimental one, except that only a few sizes of particles are allowed, thus giving rise to a plot of connected straight segments. If all particles in a sample were of exactly the same size, the sedimentation "curve" would look like one of the curves labeled from 1 to 5 in the lower part of Fig. 76. For example, in curve 3 the sediment collects at a uniform rate until time  $t_3$  is reached, when all the material  $M_3$  will have settled out and no further change in  $M$  with time occurs;  $t_3$  will thus be the time required for this particular size of particle to fall the distance  $h$  in the sedimentation tube. The equation for the curve is  $M = m_3 t$  for  $t < t_3$ , where  $m_3$  is the slope, and  $M = M_3$  for  $t > t_3$ .

If five sizes of particles are present together, the sedimentation curve will assume the form of the upper curve in the figure. Any point on this curve for a given time is obtained by summing corresponding points on all

the individual curves. It can be verified by inspection that the equation of straight-line segment A, for example, is

$$M = (m_3 + m_4 + m_5)t + M_1 + M_2 \quad t_2 < t < t_3$$

Now this particular segment is tangent to the sedimentation curve between  $t_2$  and  $t_3$ , and according to this equation the intercept on the weight axis is simply the total weight of material having sizes which have completely settled out at time  $t_2$ . The intercept of segment B is then

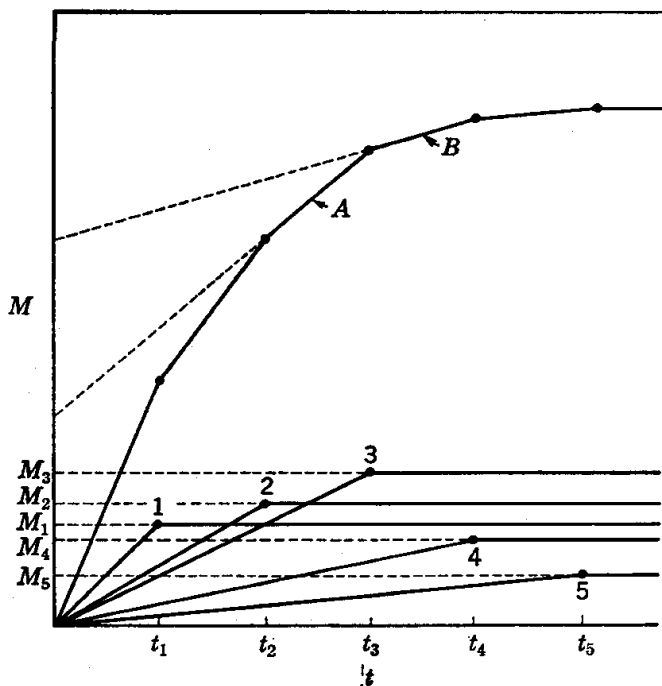


Fig. 76. Hypothetical mass-time curve.

$M_1 + M_2 + M_3$ , and the difference between the two intercepts is just  $M_3$ , which is the weight of material in size class 3 (i.e., between 2 and 4).

In practice, an infinite variety of sizes is present and a smooth curve is obtained. The above analysis can be readily extended to this case.

A plot of intercept differences for equal size intervals versus average radius is the particle size distribution curve which is desired.

**Practical Applications.** Knowledge of particle size and size distribution is finding important use in the cement, ceramic, ore-flotation, photographic-emulsion, and paint-pigment technologies. The rate of settling of precipitates is often important in analytical chemistry. Relationships between the size and the behavior of soils, the stability of pastes, etc., have been recognized for a long time.

**Suggestions for Further Work.** Sedimentation studies with typical soils, paint pigments, or cements may be carried out, and more complete mathematical analyses of the distribution curves may be attempted.

The weight of particles settling from a suspension may be determined directly by suspending a pan from one arm of a balance in the medium. When carefully done, this method is capable of considerable precision.<sup>6</sup>

At least in principle, the use of floats of known density might eliminate many of the practical difficulties of the sedimentation-tube method used in this experiment.<sup>1</sup> Presumably, problems encountered in the construction of suitable floats could be solved to provide a more accurate measure of the small density differences which are involved.

#### References

1. Dotts, *Ind. Eng. Chem., Anal. Ed.*, **18**, 326 (1946).
2. Goodhue and Smith, *Ind. Eng. Chem., Anal. Ed.*, **8**, 469 (1936).
3. Herdan and Smith, "Small Particle Statistics," Elsevier Press, Inc., Houston, Tex. (1953).
4. Kelly, *Ind. Eng. Chem.*, **16**, 928-930 (1924); "Colloid Symposium Monograph," Vol. 2, pp. 29-36 (1925).
5. Orr and Dalla Valle, "Fine Particle Measurement," The Macmillan Company, New York (1959).
6. Svedberg and Rinde, *J. Am. Chem. Soc.*, **45**, 943 (1923).
7. Wiegner, *Landwirtsch. Vers.-Sta.*, **91**, 41 (1918).

#### 48. THERMODYNAMIC ANALYSIS OF RUBBERLIKE ELASTICITY

From the temperature dependence of the force required to maintain stretched soft vulcanized rubber at a fixed elongation, the force can be separated into two contributions associated, respectively, with entropy and energy changes. From the shape of the force-elongation curve, the average molecular weight between cross-links in the vulcanization network is calculated.

**Theory.** When an elastic body is deformed at constant temperature by an external force, its free energy is increased by an amount equal to the work of deformation. Since  $\Delta G = \Delta H - T\Delta S$ , the work of isothermal deformation is in general due partly to a change in enthalpy and partly to a change in entropy. The two contributions can be separated by measuring the change in force required to maintain the body in a constant state of deformation when the temperature is varied. Soft rubberlike substances are of particular interest because for them the change in enthalpy is nearly zero.

For a pure substance the state of the body is determined as usual by temperature  $T$  and pressure  $P$  but now by tension  $f$  as well. By tension is meant the force tending to stretch the sample. The work done by the body as a result of a reversible change of length,  $dl$ , is  $-fdl$ , and

$$dG = VdP - SdT + fdl \quad (1)$$

Thus, at constant temperature and pressure,

$$f = \left( \frac{\partial G}{\partial l} \right)_{P,T} = \left( \frac{\partial H}{\partial l} \right)_{P,T} - T \left( \frac{\partial S}{\partial l} \right)_{P,T} \quad (2)$$

From Eq. (1), since the second-order cross-derivatives are equal,

$$-\left(\frac{\partial S}{\partial l}\right)_{P,T} = \left(\frac{\partial f}{\partial T}\right)_{P,l}$$

Therefore

$$f = \left(\frac{\partial H}{\partial l}\right)_{P,T} + T \left(\frac{\partial f}{\partial T}\right)_{P,l} = a + bT \quad (3)$$

The two terms on the right side of Eq. (3) may be regarded as the enthalpy and entropy contributions, respectively, to the force of stretching. The latter is obtained by measuring the change in force with temperature at constant stretched length, and the former is then obtained by difference, since  $f$  is also measured.

The molecular structure of soft vulcanized rubber is a network of flexible threadlike molecular strands which are in constant agitation because of their thermal energy. On stretching, these strands assume a partial alignment in the direction of stretch. Equation (3) shows that as the temperature of the rubber is increased, an increasing tension is required to maintain a given length, i.e., a given extent of molecular-strand alignment. As the temperature is increased, the thermal motion tending to produce randomness of arrangement becomes intensified.

The alignment represents diminished randomness and thus a decreased entropy. From statistical mechanics, the change in entropy with length is calculated to be

$$\left(\frac{\partial S}{\partial l}\right)_T = -\frac{\rho R A_0}{M_c} \left(\frac{l}{l_0} - \frac{l_0^2}{l^2}\right) \quad (4)$$

where  $\rho$  = density of rubber

$R$  = molar gas constant

$A_0$  = unstretched cross-section area of sample

$M_c$  = average molecular weight of a network strand

$l$  = stretched sample length

$l_0$  = unstretched length

By combining Eqs. (3) and (4) with the approximation that  $(\partial H/\partial l)_T$  is nearly zero, the value of  $M_c$  can be obtained, thus determining the degree of cross-linking in the network. A small correction associated with the thermal expansion of the rubber is here neglected.

It is to be noted that a certain amount of cross-linking is required for this kind of behavior. With either no cross-linking as in amorphous materials or an excessive amount as in hard rubber, this type of elasticity is nonexistent. There are a number of elastic polymers in which the energy is essentially independent of length, so any work done as a result of a change in length must be attributed to entropy change. A knowl-

edge of such behavior is helpful in the study of the physiology of muscle behavior.

**Apparatus.** Assembly with low-friction pulley for measuring the extension of a rubber sample under selected loads; thermostat for approximate control of temperature from near 0 to 50°C; pure-gum rubber band about 3 mm in thickness.

**Procedure.** The complete apparatus is shown in Fig. 77. A suitable length, about 15 cm, of pure-gum rubber band is blackened with India ink in such a way that narrow marks will appear at positions of about 3

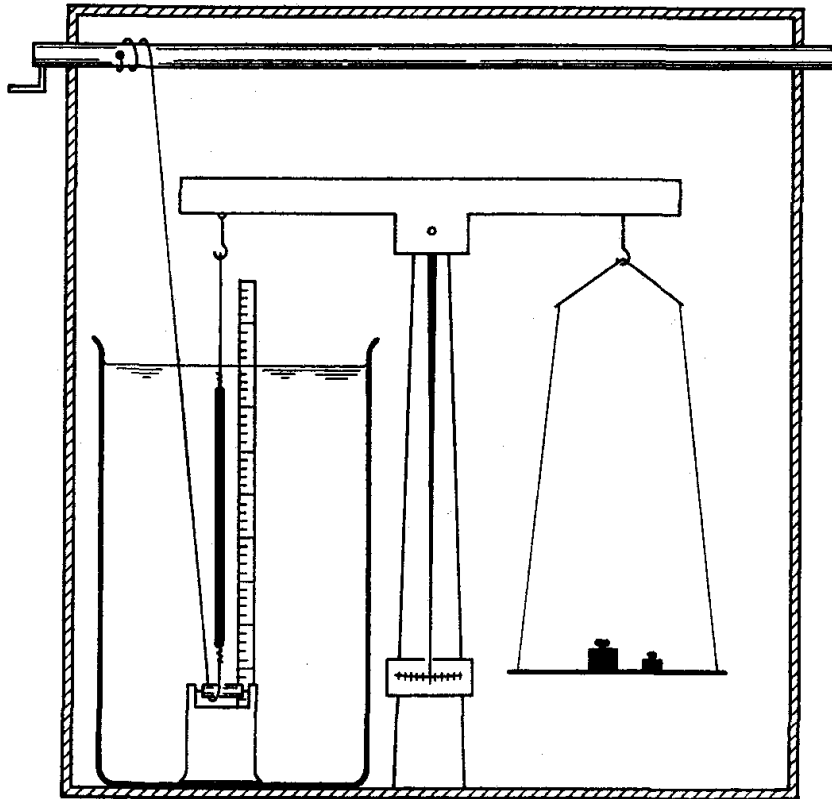


FIG. 77. Apparatus for the study of rubberlike elasticity.

and 6 cm from the upper end of the band when it is inserted in the apparatus. These marks are conveniently made by stretching the band and touching to it lightly a razor blade which has been dipped in the ink.

This upper end is attached to the counterweight portion of the balance, the band is passed over a pulley in the brass block at the bottom, and the other end is fixed to a nylon cord, which in turn is attached to the shaft mounted above the balance. This shaft, which can be rotated, provides the means to extend the rubber band. The glass jacket is then filled with water and the circulation of temperature-controlled water begun.

The thermostat is maintained at the lowest possible temperature which the cold water will provide. The nylon cord is tightened, and weights

are placed on the balance pan in such a manner as to bring the rubber band to the "just-taut" condition and to bring the balance pointer to zero. A period of about  $\frac{1}{2}$  hr is required for the achievement of thermal equilibrium. During this period the band may "relax" somewhat and imbibe a small amount of water. Records are made of the pan weight required to keep the band in this just-taut condition and the distance  $l_0$  between the reference marks on the band. This distance may be measured by means of a precision scale as shown in the figure or, better, with a cathetometer.

Without changing the temperature of the bath, the load is now increased to stretch the length to exactly double its initial value ( $l/l_0 = 2$ ) by adding more weights and again tightening the nylon cord. After the relaxation period both weight and distance are recorded when the balance pointer reads zero. Several readings are taken at slightly different values of  $l$  so that the weight corresponding precisely to  $l/l_0 = 2$  can be obtained by interpolation.

The temperature of the thermostat is now raised, and the net load corresponding to  $l/l_0 = 2$  is determined at approximately  $10^\circ$  intervals up to  $50^\circ\text{C}$ . The length  $l_0$  is assumed to be independent of temperature.

Finally, near room temperature, an isothermal load-elongation curve is determined by measuring the net loads corresponding to various elongations at approximately 10 per cent intervals up to 100 per cent. The unstretched cross-sectional area of the rubber band, required for subsequent computations, is obtained by weighing a dry piece of known length, assuming its density to be  $0.92\text{ g/cm}^3$ .

**Calculations.** The force at 100 per cent elongation is plotted against temperature, and, from the slope, values of  $T(\partial f/\partial T)_l$  and  $(\partial H/\partial l)_T$  are calculated at various temperatures by Eq. (3). These quantities should be expressed in dynes.

From the isothermal load-elongation data,  $f$  is plotted against  $l/l_0 - l_0^2/l^2$ . From the slope of this plot, together with Eqs. (3) and (4), the value of  $M_c$  is calculated. The gas constant must be expressed in  $\text{erg deg}^{-1}\text{ mole}^{-1}$  if  $f$  is in dynes. From  $M_c$ , the number of network strands per cubic centimeter may be obtained.

**Practical Applications.** Most of the uses to which natural and synthetic rubbers are put depend on the remarkable mechanical properties which have been here illustrated. The modulus of elasticity or stiffness depends on the degree of cross-linking as measured by the number of network strands per unit volume. The molecular structure of the rubber will determine the relative magnitudes of the entropy and enthalpy contributions to the retractive force, and hence the degree to which the force depends on temperature. In many applications, such as in automobile tires, the operating temperature may be considerably different from that of the surroundings.

**Suggestions for Further Work.** The measurements may be repeated for a different type of rubber, such as silicones, GR-S, or a heavily loaded stock such as is used

in tire casings. In the latter, the presence of a large proportion of finely divided carbon alters the mechanical properties. Data for force-temperature plots may be obtained at higher and lower elongations than 100 per cent. The thermodynamic analogies between stretching a "perfect" rubber [for which  $(\partial H/\partial l)_T = 0$ ] and compressing a perfect gas [for which  $(\partial H/\partial V)_T = 0$ ] may be explored by comparing equations in which  $f$  corresponds to pressure and  $l$  corresponds to volume.

#### References

1. Edsall and Wyman, "Biophysical Chemistry," Academic Press, Inc., Vol. 1, Chap. IV, New York (1958).
2. Flory, *Chem. Revs.*, **35**, 51 (1944).
3. Flory, "Principles of Polymer Chemistry," Chap. XI, Cornell University Press, Ithaca, N.Y. (1953).
4. Guth, *Publ., Am. Assoc. Advance Sci.*, **21**, 103 (1944).
5. Treloar, "The Physics of Rubber Elasticity," Oxford University Press, London (1949).
6. Wildschut, "Technological and Physical Investigations on Natural and Synthetic Rubbers," Elsevier Publishing Co., Inc., Houston, Tex. (1946).



## Surface Chemistry

### 49. SURFACE TENSION

Three different methods are used for determining surface tensions of liquids. The effect of temperature on surface tension is investigated.

**Theory.**<sup>1,2</sup> The molecules at the surface of a liquid are subject to the strong attractive forces of the interior molecules. A resultant force, whose direction is in a plane tangent to the surface at a particular point, acts to make the liquid surface as small as possible. The magnitude of this force acting perpendicular to a unit length of a line in the surface is called the *surface tension*  $\gamma$ . The surface, or interface, where the tension exists is between the liquid and its saturated vapor in air, usually at atmospheric pressure. A tension may also exist at the interface between immiscible liquids; this is commonly called the *interfacial tension*. The dimensions of surface tension are force per unit length and are commonly expressed in the cgs system as dynes per centimeter.

In order to illustrate the above definition of surface tension, we shall consider the principles involved in the three methods of measurement discussed in this experiment and shown in Fig. 78. Surface tension is a property of an interface. Usually it is measured by balancing it along a certain boundary line against an equal force which can be measured.

In the *capillary-rise* method, the liquid rises, because of its surface tension, in a capillary tube of small internal diameter immersed in it (provided that the liquid wets the tube). The circular boundary line is located at some point above the meniscus and has a length  $2\pi r$ , where  $r$  is the inside tube radius. The force which causes the liquid to rise in the tube is  $2\pi r\gamma \cos \theta$ , where  $\theta$  is the contact angle shown in Fig. 78a. At equilibrium the downward force  $mg$  due to gravity prevents the liquid from rising higher in the capillary. Here  $m$  is the mass of liquid in the capillary and  $g$  is the acceleration of gravity. For a liquid of density  $\rho$  rising to a height  $h$  in the capillary, this downward force is  $\pi r^2 h \rho g$ . At equilibrium this force is just balanced by the vertical force due to the surface tension,  $2\pi r\gamma \cos \theta$ . For water and most organic liquids this contact angle is practically zero; this means that the surface of the liquid

at the boundary is parallel with the wall of the capillary. Setting the two forces equal, we have, for zero contact angle,

$$\begin{aligned} 2\pi r\gamma &= \pi r^2 h \rho g \\ \gamma &= \frac{1}{2} h r \rho g \end{aligned} \quad (1)$$

In this derivation it has been assumed that the vapor does not have an appreciable density as compared with that of the liquid.

In the *ring* method, a platinum-iridium ring in the surface of the liquid is supported by a stirrup attached to the beam of a torsion balance. The ring is pulled upward from the liquid by turning the torsion wire, thus applying a force which is known from calibration of the instrument. For an idealized system, the force just necessary to break the liquid film is equal to  $4\pi R\gamma$ , where  $R$  is the mean radius of the ring. Doubling of

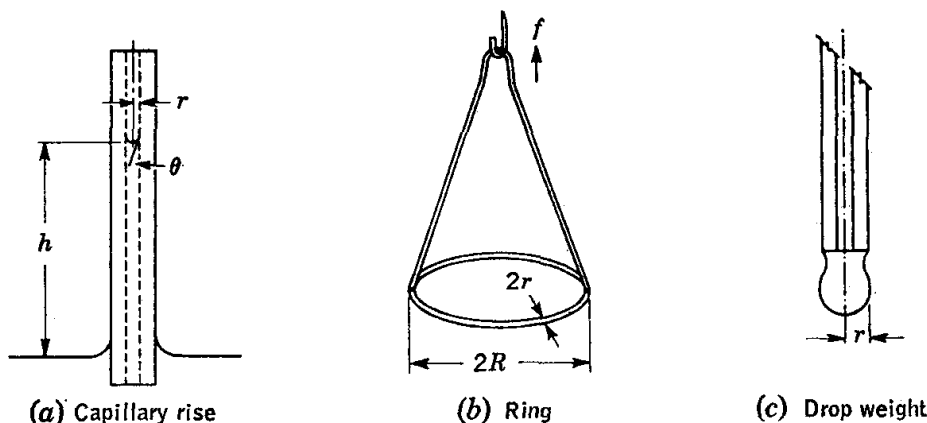


FIG. 78. Principles of three surface-tension methods.

the perimeter  $2\pi R$  arises from the fact that there are two boundary lines between liquid and wire, one on the outside and one on the inside of the ring. This treatment holds for liquids with zero contact angle, a condition usually met, and for an ideal situation where the ring holds up a thin cylindrical shell of liquid before the break occurs, a condition which is not met. Actually, the shape of the liquid held up influences the force necessary for breaking away. The shape is a function of  $R^3/V$  and  $R/r$ , where  $V$  is the volume of liquid held up and  $r$  is the radius of the wire. This volume  $V$  is computed from the force equation,  $f = mg = \rho Vg$ . The surface tension is thus given by the equation

$$\gamma = \frac{f}{4\pi R} F_r \quad (2)$$

where  $f$  = maximum force registered on torsion-balance scale

$F_r$  = correction factor due to shape of liquid held up and ring dimensions (values in Table 1)

TABLE 1. CORRECTION FACTORS FOR THE RING METHOD  
( $R/r = 40$ )

$R^3/V$	$F_r$	$R^3/V$	$F_r$
0.30	1.038	0.80	0.923
0.40	0.996	0.90	0.913
0.50	0.969	1.00	0.905
0.60	0.950	1.10	0.897
0.70	0.935	1.20	0.890

These factors have been determined experimentally by Harkins and Jordan.<sup>4</sup> Over extreme variations of  $R^3/V$  and  $R/r$ ,  $F_r$  varies between about 0.75 and 1.02. In ordinary cases it is close to 1.

In the *drop-weight* method, a drop forms at the end of a tube, and the boundary line is the outside perimeter of the tube,  $2\pi r$ . When the drop just detaches itself, the downward force on the drop,  $mg$ , is equal to the force acting upward,  $2\pi r\gamma$ . Actually, only a portion of a drop falls, and Harkins and Brown<sup>3</sup> propose the equation

$$m_i g = 2\pi r \gamma \quad (3)$$

where  $m_i$  is the mass of an "ideal" drop. An equation which is equivalent to Eq. (3) and more convenient to use is  $\gamma = (mg/r) F_d$ , where  $F_d$  is an empirically determined function of  $V/r^3$  and  $V$  is the actual volume of the drop.

Correction factors for the drop-weight calculations are given in Table 2. Values of  $V/r^3$  between 1 and 3 give the best results. For values of  $F_d$  outside the limits of Table 2, the tables of Harkins and Brown<sup>2,3,5</sup> are to be consulted.

TABLE 2. EXPERIMENTAL VALUES OF DROP-WEIGHT CORRECTIONS

$V/r^3$	$F_d$
2.995	0.261
2.637	0.262
2.341	0.264
2.093	0.265
1.706	0.266
1.424	0.265
1.211	0.264
1.124	0.263
1.048	0.262

Surface tension decreases as the temperature rises and is practically unaffected by changes in total area, pressure, or volume. The surface tension becomes zero at the critical point. The temperature coefficient of surface tension,  $d\gamma/dT$ , is of importance in the thermodynamic treat-

ment of surfaces. The total surface energy per unit area  $U_A$  of a film is given by the equation<sup>2</sup>

$$U_A = \gamma - T \frac{d\gamma}{dT} \quad (4)$$

where  $\gamma$  = work done on increasing surface by 1 cm<sup>2</sup>

= free surface energy

$-T(d\gamma/dT)$  = heat absorbed during the process

The negative of the temperature coefficient of surface tension,  $-(d\gamma/dT)$ , is the surface entropy  $S_A$  per unit area. Equation (4) is the two-dimensional analogue of the Gibbs-Helmholtz equation.

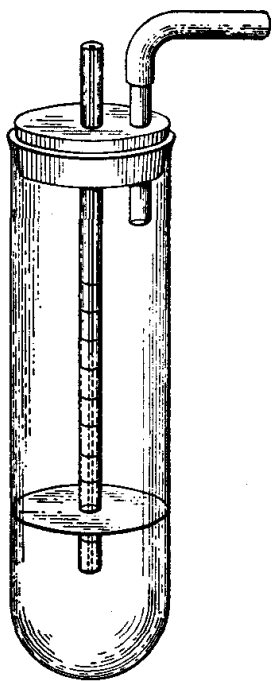


FIG. 79. Capillary-rise apparatus for measuring surface tension.

**Apparatus.** Assembly for surface-tension measurements by capillary-rise, ring, and drop-weight methods; organic liquid such as acetone or absolute ethyl alcohol.

**Procedure.** The three methods for measuring surface tension described above are to be compared by careful measurements on a single organic liquid. Acetone or absolute ethyl alcohol is suggested. Distilled water is used for calibration purposes.

The *capillary-rise* apparatus is shown in Fig. 79. The capillary tube of radius about 0.02 cm is provided with engraved millimeter graduations.† It is cleaned with *hot* cleaning solution and rinsed with distilled water and then with the liquid to be used. In case the liquid involved is immiscible with water, an intermediate rinsing with acetone is necessary. Air from pressure lines should not be blown through the capillary, since it is contaminated with oily substances. The test tube must be cleaned in the same manner.

The assembled apparatus is placed in a 25° thermostat, and pure liquid is poured into the test tube to a depth of several centimeters. The stopper is replaced; a clean dust-free rubber tube is fitted with a loose wad of cotton to keep out dirt and spray and is attached to the projecting tube as shown. After coming to the temperature of the thermostat, the liquid in the capillary is raised slightly by gently blowing into the rubber tube and allowed to fall back to its equilibrium level. Then it is

† Another convenient form of apparatus makes use of a U tube, with one arm a capillary of this radius and the other a tube of radius sufficiently large to give a flat meniscus. This rise in the capillary would then be measured with a cathetometer to give data of higher precision.

depressed by slight suction and again allowed to come to equilibrium. If the capillary is clean, the reading on the scale after equilibrium is attained should be the same after raising the level as after depressing it.

The difference in the level of the liquid in the capillary tube and in the test tube is read on the scale, the bottom of the meniscus being read in each case. A wide test tube gives a more nearly flat meniscus. Four or five measurements are made on the liquid, and the results are averaged.

The radius of the tube is obtained by observing the capillary rise with pure water, the surface tension of which is known to be 71.8 dynes/cm at 25°C. At least five observations are made. The average value of  $h$  is

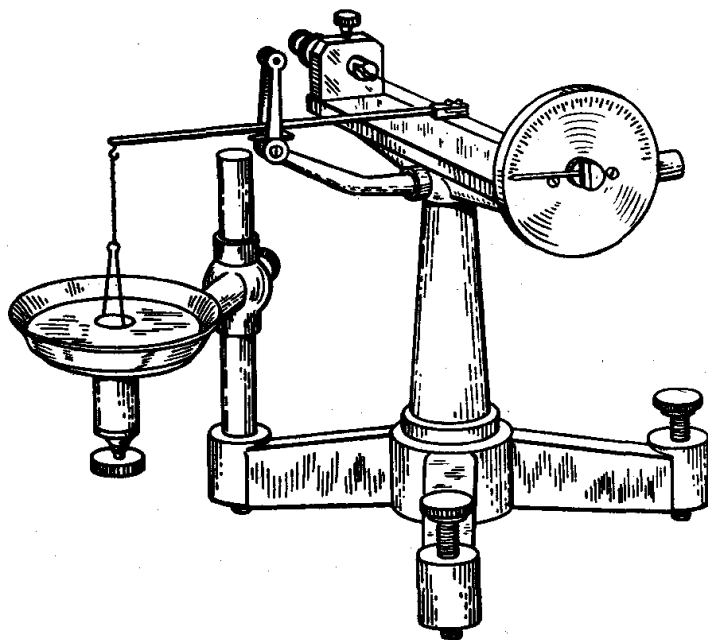


FIG. 80. DuNouy ring-pull apparatus for measuring surface tension.

obtained from the scale readings, and  $r$  is obtained by solving Eq. (1), using the known value of  $\gamma$ .

The surface tension of acetone is measured at 0°C by using an ice bath and at three other temperatures, 25, 35, and 50°, using thermostats if they are available. A hand-regulated bath may be used for less accurate work, with a thermometer immersed directly in the liquid.

The DuNouy tensiometer is illustrated in Fig. 80. It is a widely used example of the *ring method*.

The ring of platinum-iridium wire is cleaned with *hot* cleaning solution, thoroughly rinsed with warm distilled water, and dried by carefully touching with a clean filter paper or cloth and allowing to stand in the air. Occasionally, the ring may be heated momentarily in a bunsen flame if further cleaning is necessary. It must not be touched with the fingers,

and care should be used not to bend it. The apparatus is adjusted by hanging the ring in the hook and turning the knob at the right until the pointer is at zero. The setscrew at the back is then turned until the lever nearly touches the arm at the left. It must not actually touch, but the gap must be very small. The platform holding the small beaker (30 ml) with the liquid is now raised until the liquid just touches the ring. The knob at the right is then turned slowly and steadily until the ring is suddenly torn from the surface of the liquid. The guard above the lever is adjusted so that the ring cannot be thrown off the edge of the small beaker.

As the pointer is turned, the ring pulls away slightly from the small beaker before it breaks the film, and the beam is raised above the original horizontal position. To compensate for this effect, the platform is lowered gradually while the pointer is turned, so that the beam is at its horizontal position when the ring is pulled off. If this adjustment is not made, the readings will be too high.

Several readings are taken on the liquid, and the average is computed. The temperature is determined by immersing a thermometer in the liquid. Unfortunately, close temperature control is not convenient with this instrument.

After the determinations have been made, the instrument is calibrated over the range of scale readings involved. The ring is dried, a weighed square of paper is inserted, and a fractional gram weight is added. The pointer is turned until the lever just barely clears its support and lies in its standard horizontal position. The weight of paper and fractional gram weight divided by the scale reading and multiplied by 981 gives the value in dynes of one scale division. The procedure is repeated once or twice, using more weights.

A useful form of *drop-weight* apparatus is shown in Fig. 81. The end of the capillary is ground flat and polished. It must be free from chips in order to obtain reproducible results, and to this end a permanent guard tube surrounds it.

Before the performance of the experiment the bulb and capillary should be scrupulously cleaned with hot cleaning solution, followed by rinsings with distilled water and the liquid to be studied. After the apparatus has been conditioned and assembled, a dried weighing bottle is weighed and placed in the protecting bottle, which is then screwed into the cap. A very thin layer of stopcock grease applied to the ground joint of the weighing bottle will prevent loss by evaporation in subsequent weighings. A small air vent is provided in the cap to keep pressure from building up inside. The assembly is now introduced into the thermostat.

The liquid whose surface tension is to be measured is added through the side tube and capillary, and the liquid levels are adjusted until the time of formation of a drop is of the order of 5 min. The difference in liquid

liquid differs much from 25°, a correction to this temperature may be estimated from the temperature coefficient of surface tension.

The surface tensions determined by the three methods are compared with the literature values, and the percentage deviations are computed.

The surface tensions of acetone at the several temperatures are plotted as ordinates against temperature as abscissa. The slope of the line is determined, and the total surface energy computed [Eq. (4)] in ergs per square centimeter at some representative temperature.

**Practical Applications.** Surface tension is an important phenomenon in the study of macromolecular chemistry. It is an important factor in the concentration of ores by the flotation process. Surface-tension measurements find valuable applications in the biological sciences, particularly in bacteriology; the movement of the moisture of the soil and the passage of sap in plants are only two of the many agricultural phenomena that involve surface tension.

**Suggestions for Further Work.** Measurements are made so rapidly with the DuNouy apparatus that the surface tension of a large number of liquids and solutions may be determined. If a solute lowers the surface tension, it concentrates in the outer layers of the solution, but if it increases the surface tension of the solution, it is driven away from the surface. Surface tension, then, is never increased very much by the addition of a solute, but it may be decreased by a considerable amount. This theory may be checked by a number of determinations.

Another convenient apparatus to measure the change in surface tension when solute is added to a solvent or solution is the Wilhelmy balance.<sup>8</sup> It consists of a wetted plate, conveniently a microscope cover glass, which dips into the solution while hanging from the arm of a balance. The force on the plate corresponds to the surface tension of the liquid. Some of the data obtained with the DuNouy ring may be verified in this way.<sup>6,7</sup>

### References

1. Bikerman, "Surface Chemistry," 2d ed., Academic Press, Inc., New York (1958); "Foams," pp. 161-169, Reinhold Publishing Corporation, New York (1953).
2. Harkins and Alexander in Weissberger (ed.): "Technique of Organic Chemistry," 3d ed., Vol. I, Pt. I, Chap. 14, Interscience Publishers, Inc., New York (1959).
3. Harkins and Brown, *J. Am. Chem. Soc.*, **41**, 499 (1919).
4. Harkins and Jordan, *J. Am. Chem. Soc.*, **52**, 1751 (1930).
5. International Critical Tables, Vol. IV, p. 435, McGraw-Hill Book Company, Inc., New York (1928).
6. Kraemer, Williams, and Alberty in Taylor and Glasstone (eds.): "Treatise on Physical Chemistry," 3d ed., Vol. II, D. Van Nostrand Co., Inc., Princeton, N.J. (1951).
7. Mysels, "Introduction to Colloid Chemistry," Interscience Publishers, Inc., New York (1959).
8. Padday and Russell, *J. Colloid Sci.*, **15**, 503 (1960).

## 50. ADSORPTION FROM SOLUTION

Quantitative measurements of adsorption by an ion-exchange resin are made. The isothermal data are expressed by means of an equation, and the regeneration of the adsorbent is illustrated.

level to meet this requirement is ordinarily less than 1 cm. The apparatus may be tipped at first to get the liquid started in the capillary.

The first drop is allowed to form over this relatively long period of time in order to saturate the space within the container. After the detachment of this first drop, additional liquid is added to the side tube, or slight pressure is carefully applied to increase the drop rate. Care must be taken that each drop falls only under the influence of gravity. After the first drop, 30 sec should suffice for the formation of each of the others.

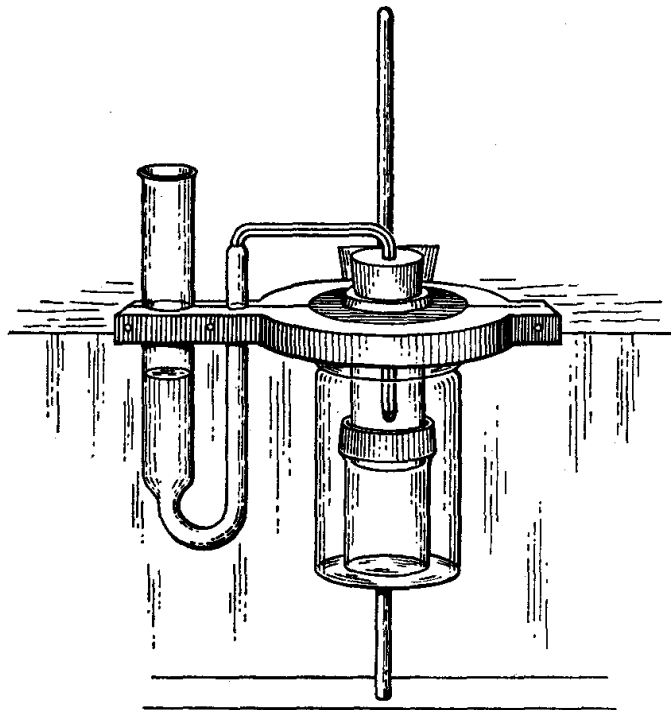


FIG. 81. Drop-weight apparatus for measuring surface tension.

A total of 20 to 25 drops should be adequate for the determination. The bottle is then weighed again.

If the radius of the capillary is not known, it may be measured with a comparator microscope.

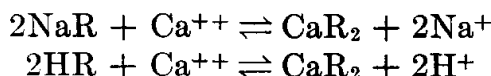
**Calculations.** The surface tension of the liquid as determined by the different methods is computed, using Eqs. (1) to (3). The density of the liquid may be found in tables.

The value of  $R/r$  for the ring of 4-cm perimeter usually supplied with the commercial-type student ring-method instrument may be taken as 40 unless a different value is specifically given. The volume of liquid held up,  $V$ , is calculated from the density and the reading on the dial scale, which can be converted to mass of liquid. Correction factors to be applied in Eq. (2) are given in Table 1 for  $R/r = 40$  and for different values of  $R^3/V$ . For other values of these parameters the work of Harkins and Jordan<sup>4</sup> must be consulted. If the temperature of the



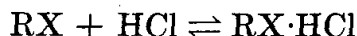
**Theory.** Solids have the property of holding molecules at their surfaces, and this property is quite marked in the case of porous and finely divided material. Various forces are involved, ranging from those which are definitely physical in nature to those which are referred to as chemical. Adsorption is frequently quite specific, so that one solute may be adsorbed selectively from a mixture. Such differences in adsorbability are required for the success of the several chromatographic processes.

In the case of so-called "exchange adsorbents," the adsorption is actually a chemical reaction in which an ion is liberated from the adsorbent as another is "adsorbed." The softening of water, using naturally occurring or synthetic zeolites, is an example of this phenomenon. An important advance in the field of exchange adsorbents was made by Adams and Holmes<sup>1</sup> in 1935 when they discovered that phenol-formaldehyde resins exhibited ion-exchange properties. The advantage of synthetic resins is that the exchange-adsorption properties may be varied at will by the selection of the reactants for the polymerization reaction.<sup>3,6-8</sup> For example, the condensation of polyhydric phenols with formaldehyde yields resins which adsorb calcium ions, liberating hydrogen ions or sodium ions.



where NaR represents the sodium salt of the cation-exchange resin, and HR represents the acid form. By treating the exhausted resin with an excess of  $\text{Na}^+$  or  $\text{H}^+$ , the reactions may be reversed, regenerating the resin.

Synthetic resins prepared by condensing aromatic amines with formaldehyde exhibit anion-exchange, or acid-adsorbent, properties as illustrated by the following equation:



where RX represents the anion-exchange resin. The capacity of a resin ranges from about 4 to 9 milliequiv of acid per gram of dry resin. In this case the regeneration is accomplished by treating the exhausted resin with a solution of sodium carbonate.



By passing water successively through columns of base-exchange (hydrogen form) and acid-binding resins, deionized water comparable in quality with distilled water may be obtained.

The amount of solute adsorbed by a given quantity of adsorbent increases with the concentration of the solution. In some cases the layer of adsorbed molecules is only one molecule deep, and further adsorption

ceases when the surface of the crystal lattice is covered. The equilibrium between the dissolved solute and the material adsorbed also depends upon the nature of the solvent and the temperature, the amount adsorbed increasing at lower temperatures. In many cases the equilibrium may be rapidly established; in any event one must ascertain that the system is at equilibrium for a satisfactory representation of the data.

The relation between the amount adsorbed and concentration in a limited concentration range may be represented by the adsorption isotherm of Freundlich,

$$\frac{x}{m} = kc^n \quad (1)$$

where  $x$  = weight of material, in grams, adsorbed by  $m$  grams of adsorbing material

$c$  = concentration in solution, g/liter

$n$  = constant ranging from 0.1 to 0.5

$k$  = another constant

Although  $k$  varies considerably with the temperature and nature of the adsorbent, the ratio of  $k$  values for two different adsorbents is constant for different solutions. By taking the logarithm of Eq. (1) we obtain

$$\log \frac{x}{m} = n \log c + \log k \quad (2)$$

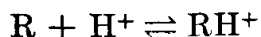
According to this equation a plot of  $\log x/m$  versus  $\log c$  is a straight line, and the constants may be evaluated from the slope  $n$  and the intercept  $\log k$ .

The adsorption equation of Langmuir is based upon a theoretical consideration of the process of adsorption. This equation may be written

$$\frac{x}{m} = \frac{\alpha c}{1 + \beta c} \quad \text{or} \quad \frac{c}{x/m} = \frac{1}{\alpha} + \frac{\beta}{\alpha} c \quad (3)$$

where  $\alpha$  and  $\beta$  are constants. For cases in which this equation represents the data,  $c/(x/m)$  may be plotted as a linear function of  $c$ , and the constants evaluated from the slope  $\beta/\alpha$  and intercept  $1/\alpha$ . The Langmuir equation differs from the Freundlich equation in that the adsorption approaches a finite limit as the concentration is increased.

The Langmuir equation is actually one description of the law of mass action, which may be seen in the following argument. Suppose we use the symbol  $R$  for the part of the resin which combines with a hydrogen ion according to the reaction



The constant for the association is  $K = c_{RH^+}/c_{H^+}c_R$ , or  $c_{RH^+} = Kc_{H^+}c_R$ .

The total active resin concentration is  $c_{R,t} = c_{RH^+} + c_R$ , so that

$$c_{RH^+} = Kc_{H^+}(c_{R,t} - c_{RH^+})$$

Thus

$$\frac{c_{RH^+}}{c_{R,t}} = \frac{Kc_{H^+}}{1 + Kc_{H^+}}$$

The ratio  $c_{RH^+}/c_{R,t}$  represents the number of moles of bound hydrogen per mole of resin combining sites, and the expression for it formally resembles the Langmuir function.

**Apparatus.** Twelve 250-ml Erlenmeyer flasks; two burettes; 1 N acetic acid; 0.1 N sodium hydroxide; anion-exchange resin† or, as an alternative, highly activated adsorbent charcoal; 100-ml volumetric flask; weighing bottle.

**Procedure.** The exchange resin consists of particles (approximately 20 to 50 mesh) which are kept in a regenerating solution of 8 per cent sodium carbonate when not in use. The carbonate solution is decanted, and the resin rinsed with three portions of distilled water, allowing the resin to settle before each decantation. The loss of finer particles during decantation is not serious.

The resin is now collected on a filter and pressed to remove excess moisture. Twelve samples of damp resin of approximately 2 g in weight are weighed to  $\pm 10$  mg. Two additional samples of the resin weighed at the same time are placed in the oven and dried at 110°C to constant weight. In the calculations, the adsorption  $x/m$  is calculated on the basis of the dry resin.

Acetic acid solutions of different concentrations are made by running out 1 N acetic acid from a burette and diluting to 100 ml with water; 50, 25, 10, 5, 2.5, and 1 ml are diluted with distilled water to 100 ml. Each solution is transferred to a 250-ml Erlenmeyer flask, and 2 g of wet exchange resin (or 1 g of adsorbent charcoal) is then added to each flask. The solutions are set up in duplicate. The solutions are agitated and allowed to stand overnight or longer. A thermostat is unnecessary if the room temperature is fairly constant.

After equilibrium has been reached and the resin has settled, a suitable volume (5 or 25 ml, depending on the concentration) is pipetted from the clear supernatant solution in each flask and titrated with 0.1 N sodium hydroxide. Whenever the titration volume falls below 25 ml, the base may be diluted by a known ratio, such as 1:1. Blank determinations should be made on all distilled water used for this purpose.

The experiment may be repeated with oxalic acid instead of acetic acid.

After the experiment has been completed, the resin is regenerated by the addition of 10 ml of 8 per cent by weight  $\text{Na}_2\text{CO}_3$  per gram of resin and returned to the stockroom.

† Amberlite IR-4B is satisfactory and is obtainable from chemical supply houses.

**Calculations.** The total weight of acetic acid in each solution is calculated from the data of the original solutions, and titration gives the weight remaining in 100 ml of the solution in equilibrium with adsorbent. The difference gives directly the weight of acetic acid adsorbed by the  $m$  grams of adsorbent.

The concentration of the solution in equilibrium with the adsorbed acetic acid is calculated from the sodium hydroxide titrations, and the values of  $x/m$  are plotted against these equilibrium concentrations.

The data are examined graphically with the object of learning which of Eqs. (1) and (3) better represents the behavior of the system studied.

**Practical Applications.** The adsorption isotherm or equivalent form is important in the quantitative expression of the adsorption process, and as such it finds use in some dyeing and in various purification operations. It is useful also to characterize the adsorption of gases. In the theories descriptive of chromatography, the Langmuir equation has been very useful in accounting for the shape of the band passing through the column, the explanation of "tailing," etc.<sup>11</sup>

Ion-exchange resins are important in softening water, recovering ions from solutions of low concentration, and separating the rare earths.<sup>10</sup>

**Suggestions for Further Work.** If the system is in equilibrium, the same results should be obtained whether approached from concentrated or from more dilute solutions. Equilibrium may be tested by repeating the adsorption experiments and then diluting the solution with water after it has stood with the adsorbent. Acetic acid should be released by the adsorbent, and the final values of  $x/m$  and  $c$  should still fall on the same curve.

Various other materials may be adsorbed—weak acids, or bases. Ammonium hydroxide is suitable if a cation-exchange resin is used.

The adsorption isotherm may be tested nicely with dyes adsorbed from solutions (not necessarily in water) on charcoal, silicic acid, certain fibers,<sup>9</sup> etc. The initial and final concentrations of dye in solution may be obtained with either colorimeter or spectrophotometer.

The adsorption experiments may be carried out at 0°C and at elevated temperatures.

The values of the constants  $k$  and  $n$  in Eq. (1) are compared for the different materials and temperatures.

### References

1. Adams and Holmes, *J. Soc. Chem. Ind. (London)*, **54**, 1–67 (1935).
2. Alexander, "Colloid Chemistry," Vol. I, Reinhold Publishing Corporation, New York (1926).
3. Edwards, Schwartz, and Boudreaux, *Ind. Eng. Chem.*, **32**, 1462 (1940).
4. Glasstone, "Textbook of Physical Chemistry," pp. 1194–1210, D. Van Nostrand Company, Inc., Princeton, N.J. (1946).
5. Morton, "Laboratory Techniques in Organic Chemistry," Chap. IX, McGraw-Hill Book Company, Inc., New York (1938).
6. Myers in Kraemer (ed.): "Advances in Colloid Science," Vol. II, Interscience Publishers, Inc., New York (1942).
7. Myers and Eastes, *Ind. Eng. Chem.*, **33**, 1203 (1941).
8. Myers, Eastes, and Myers, *Ind. Eng. Chem.*, **33**, 697 (1941).
9. Schroeder *et al.*, *Faraday Soc., Discussions*, **16**, 210 (1954).

10. Spedding *et al.*, *J. Am. Chem. Soc.*, **69**, 2777, 2786, 2812 (1947).
11. Giddings, *J. Chem. Phys.*, **31**, 1462 (1959).

## 51. ADSORPTION OF GASES

In this experiment the amounts of gas adsorbed at various pressures on activated charcoal or silica gel are determined by a volumetric method.

**Theory.** Adsorption is a process whereby gases or solutes are attracted and held to the surface of a solid. The material adsorbed is called the adsorbate, and the material on which it is adsorbed is called the adsorbent. Often the force of attraction is physical in nature, involving an interaction between dipoles or induced dipoles, but sometimes the force of attraction involves chemical bonds, as when oxygen is adsorbed on charcoal. In many cases the layer of adsorbed molecules is only one molecule deep, an atom of adsorbent at the surface being unable to extend its attractive force beyond the first molecule of adsorbate. Since the amount of gas which is adsorbed is proportional to the amount of surface exposed, the good adsorbents are those which have enormous surface areas, such as activated charcoal or silica gel, but adsorption of gases at low temperatures has been measured on clean glass surfaces, mercury surfaces, and metallic wires. Sometimes the large surface is produced by a cellular structure originally present in the plant, as in the case of charcoal.

If the adsorbent is porous on a submicroscopic scale, so-called capillary condensation may take place below the normal saturation pressure. This type of adsorption can be distinguished from the unimolecular-layer type of adsorption by heats of adsorption and by other criteria.

The experimental data for adsorption are plotted as "adsorption isotherms," in which the quantity of gas adsorbed (expressed as milliliters at 0° and 760 mm) per gram of adsorbing material is plotted against the equilibrium pressure.

In many cases of adsorption it is possible to relate the amount of adsorbed material to the equilibrium pressure, using the empirical equation of Freundlich,

$$V = kP^n \quad (1)$$

where  $V$  = number of milliliters of gas, corrected to 0° and 760 mm, adsorbed per gram of adsorbing material

$P$  = pressure

The constants  $k$  and  $n$  may be evaluated from the slope and intercept of the line obtained when  $\log V$  is plotted against  $\log P$ .

One of the most successful theoretical interpretations of gas adsorption is that of Langmuir,<sup>4,5</sup> who considered adsorption to distribute mole-

cules over the surface of the adsorbent in the form of a unimolecular layer. Consideration of the dynamic equilibrium between adsorbed and free molecules leads to the following relation:

$$\frac{P}{V} = \frac{P}{V_u} + \frac{1}{kV_u} \quad (2)$$

where  $P$  = gas pressure

$V$  = volume of gas (0°C, atm) adsorbed per gram of adsorbent

$V_u$  = volume of gas (0°C, atm) adsorbed per gram of adsorbent when unimolecular layer is complete

$k$  = constant characteristic of adsorbent-adsorbate pair

Thus, if  $P/V$  is plotted against  $P$ , a straight line will be obtained if the Langmuir equation (2) applies. The slope of the line is equal to  $1/V_u$ ; when the line is extrapolated to low pressures, as  $P \rightarrow 0$ ,  $P/V$  approaches the finite limit  $1/kV_u$ . The values of the constants in the Langmuir equation may also be obtained by plotting  $1/V$  versus  $1/P$ .

By postulating the building up of multimolecular adsorption layers on a surface, Brunauer, Emmett, and Teller<sup>1-3</sup> have extended the Langmuir derivation for unimolecular-layer adsorption to obtain an isotherm equation for the more complicated case. The extension is not without some empiricism, yet it is often useful. Thus, knowing the volume of gas required to form a complete unimolecular layer over the surface of the adsorbent, it is possible to compute the surface area of the adsorbent, if it is assumed that each molecule of the adsorbate occupies the volume that it would occupy if the density of the unimolecular film is the same as that of the liquid adsorbate at the same temperature.

A graph of adsorption data giving the pressure as a function of temperature for a specific volume of gas adsorbed is referred to as an isostere. Such graphs bear a close resemblance to graphs in which the vapor pressure is plotted against the temperature, and the heat of adsorption,  $q_{\text{isosteric}}$ , may be calculated in a manner similar to that used for calculating the heat of vaporization of a liquid using the following modification of the Clausius-Clapeyron equation:

$$\ln \frac{P_2}{P_1} = \frac{q_{\text{isosteric}}(T_2 - T_1)}{RT_1T_2} \quad (3)$$

where  $P_1$  = equilibrium pressure for a given amount of gas adsorbed at  $T_1$

$P_2$  = equilibrium pressure of same amount of gas adsorbed at  $T_2$

By calculating  $q_{\text{isosteric}}$  for different volumes of gas adsorbed, the variation of heat of adsorption with volume adsorbed may be found. A variation of heat of adsorption with the volume adsorbed indicates changes in the magnitude of the forces between the adsorbent and the adsorbate.

**Apparatus.** Apparatus as shown in Fig. 82, consisting of a mercury manometer, a mercury-filled gas burette, six stopcocks, and a ground-glass joint; vacuum pumps; tanks containing methyl chloride or other suitable gas; adsorbent charcoal or silica gel.

**Procedure.** The flexible Tygon connecting tube from the gas tank attached to *E* is flushed out by removing the ground-glass tube *J* and opening the stopcocks *E*, *D*, *C*, and *B*. Stopcock *E* is closed; the tube *J* is replaced; the leveling bulb of mercury is lowered as far as possible and

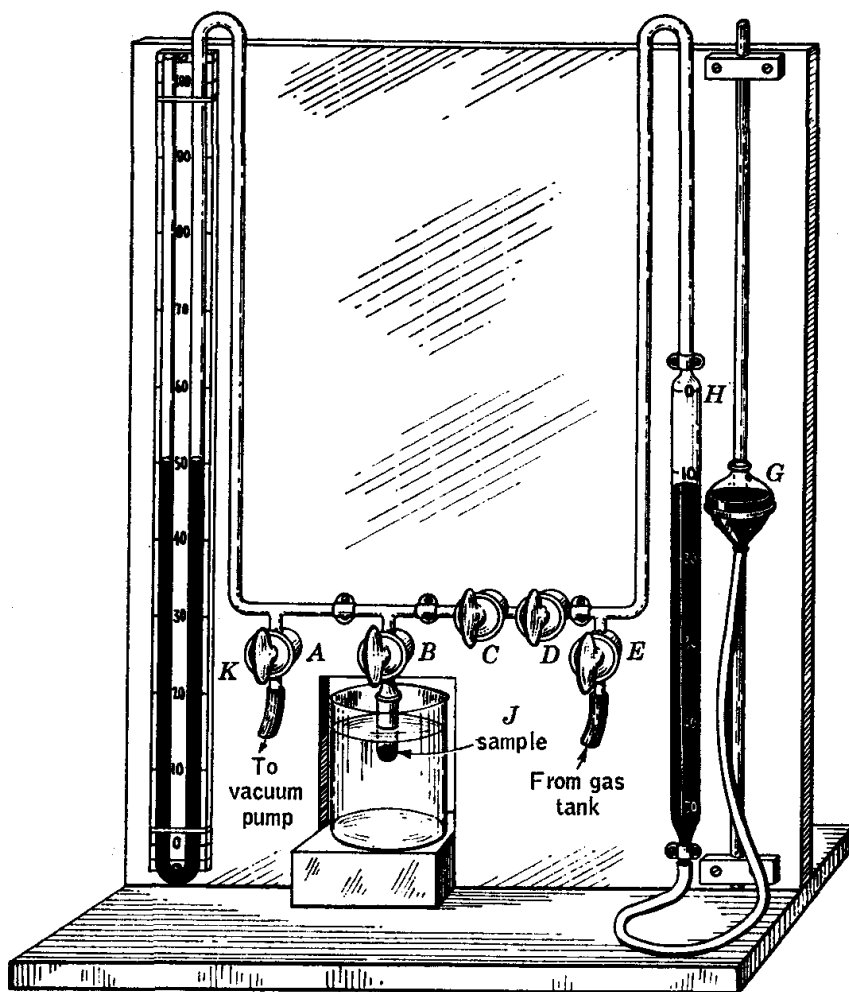


FIG. 82. Gas-adsorption apparatus.

the whole system is evacuated with a vacuum pump through stopcock *A*. Stopcock *D* is closed, and methyl chloride is admitted through *E* until the burette *H* is filled at atmospheric pressure. Stopcock *E* is then closed, and the leveling bulb *G* is adjusted carefully until the gas in the burette is at precisely atmospheric pressure. The volume of gas in the burette is then recorded.

The amount of gas which is adsorbed by the adsorbent is to be determined by measuring the volume of gas which must be admitted from the

burette in order to give a specified pressure. Part of the gas from the burette is adsorbed, but an additional part, known as the "dead volume," is needed for filling the apparatus up to the given pressure at which the adsorption measurement is made. The dead volume of the apparatus between the manometer *K* and the stopcock *D* is determined by finding the volume of gas admitted from the burette which is necessary to produce a given pressure in the absence of any adsorbing material in *J*.

The apparatus is first tested for leakage by observing the manometer. There should be no detectable change in the levels of the manometer *K* over a period of at least 5 min when the apparatus is evacuated. Then gas from the burette is admitted into the system through stopcocks *C* and *D* until the pressure in the apparatus is about 50 mm, and the exact manometer reading, burette readings, and temperature of the room are recorded. These data are used for calculating the dead volume of the gas under standard conditions. The dead volume is determined in a similar manner at pressure increments of about 100 mm. The burette is refilled when necessary by closing stopcock *D*, opening stopcock *E*, and lowering the leveling bulb *G*.

The volume of methyl chloride adsorbed by activated charcoal at a given pressure is determined by placing 0.080 to 0.100 g of the charcoal in the ground-glass tube *J*, inserting it at *B*, and placing a beaker of water at room temperature around it. Stopcocks *C* and *D* are closed, and the charcoal is outgassed for 5 min by evacuating through *A*. Methyl chloride is then admitted from the burette until the pressure is about 50 mm. The pressure will decrease as the gas becomes adsorbed on the charcoal, but after 5 min or so there is no tendency toward further change if the pressure is kept constant. The two stopcocks *C* and *D* with the intervening space of about 0.05 ml volume provide a convenient means for introducing gas into the system in small amounts so as to maintain the pressure constant. (A much longer time is required to reach equilibrium if a given quantity of gas is introduced and allowed to decrease in pressure until reaching an equilibrium.) When equilibrium has been reached and no more additions of gas are necessary to maintain the pressure, the volume of gas introduced from the burette is recorded.

This operation is repeated by using pressure increments of 30 to 50 mm up to about 250 mm and then using increments of about 100 mm up nearly to atmospheric pressure.

The adsorption measurements on charcoal are then repeated at 0° by using an ice bath in the beaker which surrounds the adsorbent.

**Calculations.** Part of the gas introduced from the burette is adsorbed on the charcoal, and part remains in the manometer and connecting tubes. The volume of gas adsorbed at a given equilibrium pressure is obtained by subtracting the dead-space volume in the apparatus from the



total volume of gas introduced from the burette. The dead volume in milliliters at a given pressure is obtained by interpolation on a line obtained by plotting the corrected dead volume against the pressure measured in the absence of any adsorbent. All these observed volumes are reduced by calculations to the volumes of gas at 0° and 760 mm. When several additions of gas have been made to the adsorbent, giving a specified equilibrium pressure, they are all added together to obtain the total volume. The volume  $V$  adsorbed per gram of charcoal is then determined by dividing the corrected volume by the weight of the adsorbent.

Three graphs are drawn to interpret the adsorption. In the first graph, the corrected volume of gas,  $V$ , adsorbed per gram of adsorbent is plotted vertically, and the equilibrium pressures are plotted horizontally.

In the second graph,  $\log V$  is plotted against  $\log P$  in accordance with the Freundlich equation (1), and the constants  $k$  and  $n$  are calculated for the equation  $V = kP^n$  as discussed on page 333.

In the third graph, the values of  $P/V$  are plotted against  $P$  to evaluate the constants  $k$  and  $V_u$  of the Langmuir equations (5) and (6), and the constant  $V_u$  is used for calculating the surface area of the adsorbent.

The volume of one molecule in the layer of adsorbate is calculated on the assumption that the molecule has the same volume as a molecule in the liquid state. The number of molecules in the unimolecular layer is calculated by dividing the volume  $V_u$  of adsorbate in the unimolecular layer by the volume of a mole of the gas, 22,400, and multiplying by the Avogadro number  $6.02 \times 10^{23}$ . Then the volume of a molecule of adsorbate is calculated by dividing the volume of a mole of the material in the liquid state (obtained from tables of liquid densities) by the Avogadro number. The surface area covered by a single molecule is equal to the two-thirds power of the volume of the molecule. The surface area of a gram of adsorbent is equal, then, to the number of molecules in the saturated unimolecular layer multiplied by the cross-sectional area of a molecule.

The isosteric heat of adsorption is computed by Eq. (3) for several different volumes of gas adsorbed, and these values are plotted against the volume adsorbed. This plot is then used to interpret qualitatively the forces which exist between the adsorbent material and the gas being adsorbed.

**Practical Applications.** The adsorption of gases is used for purification and recovery of vapors. Solvent vapors are adsorbed from a stream of gas by adsorption in activated charcoal or silica gel and then recovered in concentrated form by heating the adsorbent to drive out the adsorbed vapors.

The drying of air is carried out on a large scale by adsorbing the water vapor with silica gel. When the silica gel becomes saturated, it is reactivated by heating to about 150° to expel the water and prepare the adsorbent for another cycle of adsorption.

High vacuum is conveniently produced in a vessel by connecting to a tube containing an adsorbent at liquid-air temperatures.

The effective surface of powders and catalysts is determined by measuring the amount of gas adsorbed. The adsorption of nitrogen on material at the temperature of liquid air has been used in such determinations.

Measurements of the Brunauer, Emmett, and Teller<sup>2</sup> (BET) constants are carried out on a routine basis in some catalyst testing programs.

**Suggestions for Further Work.** The experiments and calculations may be repeated, using 0.5 g of silica gel instead of 0.1 g of activated charcoal. The silica gel should be activated by evacuating the system while gently heating the sample at  $J$  to about  $150^{\circ}$  with a bunsen flame.

Other gases and vapors may be used instead of the methyl chloride, e.g., ammonia, sulfur dioxide, or Freon, with suitable weights of adsorbents.

In general, the higher the boiling point of a liquid, the higher is the temperature at which the adsorption experiments should be carried out.

Different grades of silica gel and activated charcoal may be used for adsorption experiments.

The rate of adsorption may be studied by maintaining the pressure as nearly constant as possible and measuring the volume adsorbed at different times. The rate of adsorption at different temperatures may be studied.

#### References

1. Brunauer, "Physical Adsorption," Chaps. I-IV, p. 222, Princeton University Press, Princeton, N.J. (1945).
2. Brunauer, Emmett, and Teller, *J. Am. Chem. Soc.*, **60**, 310 (1938).
3. Emmett, *Ind. Eng. Chem.*, **29**, 639 (1945).
4. Kraemer, Williams, and Alberty in Taylor and Glasstone (eds.): "A Treatise on Physical Chemistry," 3d ed., Vol. II, Chap. V, D. Van Nostrand Company, Inc., Princeton, N.J. (1951).
5. Langmuir, *J. Am. Chem. Soc.*, **38**, 2267 (1916); **40**, 1361 (1918).

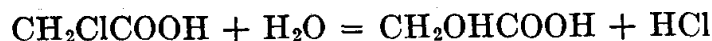
## CHAPTER 15

# *Photochemistry*

### 52. PHOTOHYDROLYSIS OF MONOCHLOROACETIC ACID

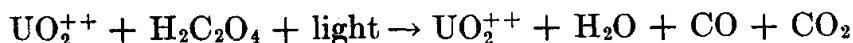
This experiment illustrates the use of an actinometer and the calculation of the quantum yield.

**Theory.** Monochloroacetic acid hydrolyzes according to the reaction



At room temperature the reaction rate is relatively small, but under irradiation by ultraviolet light, the reaction proceeds much more rapidly. Not every molecule that absorbs a photon undergoes reaction, since some molecules lose their excess energy before they react. The *quantum yield* for a photochemical reaction is defined as the number of molecules reacted per photon *absorbed*.

For determination of the number of photons absorbed, an actinometer is used. This consists of a solution of uranyl nitrate and oxalic acid. Oxalic acid alone in solution is nearly transparent to the radiation employed. With the addition of uranyl ions, the solution absorbance increases to a large value, and the reaction



takes place. It is to be noted that the uranyl ion, though essential to the process, is finally left unchanged. The amount of oxalic acid decomposed is readily found by titration. From the known quantum yield for this reaction and the amount reacted, the number of photons absorbed by the actinometer solution can be calculated.

The actinometer samples are so placed as to receive the same *incident* intensity as the monochloroacetic acid samples. In order to calculate the number of quanta *absorbed* by the monochloroacetic acid solution, it is necessary to know the relative absorbancies of the two solutions. With the concentrations and thicknesses used, the actinometer solution absorbs practically all the incident light for  $\lambda < 4360 \text{ \AA}$ . The monochloroacetic acid solution absorbs completely the light at 2537  $\text{\AA}$ , but not that of the longer wavelengths present in the radiation. The high-

voltage "cold" mercury lamp used emits radiation of which approximately 85 per cent has a wavelength of 2537 Å. It may therefore be assumed for the present experiment that the monochloroacetic acid solution absorbs 85 per cent of the incident light from these lamps, practically all of which is in the ultraviolet.

**Apparatus.** Germicidal mercury-vapor lamp available at electric-fixture stores; four small rectangular plastic dishes or small crystallizing dishes; 50-ml pipette; two burettes; 200 ml 0.2 M uranyl nitrate; 200 ml 0.02 M oxalic acid; 500 ml 0.025 N potassium permanganate; 200 ml 0.1 M monochloroacetic acid, freshly prepared; 100 ml 0.01 M mercuric nitrate and 10 per cent sodium nitroprusside or 200 ml 0.005 M silver nitrate; potentiometer; silver electrodes.

**Procedure.** The oxalic acid is weighed out accurately so that this solution may be used to standardize the potassium permanganate solution. An equal volume of the uranyl nitrate solution is mixed with the

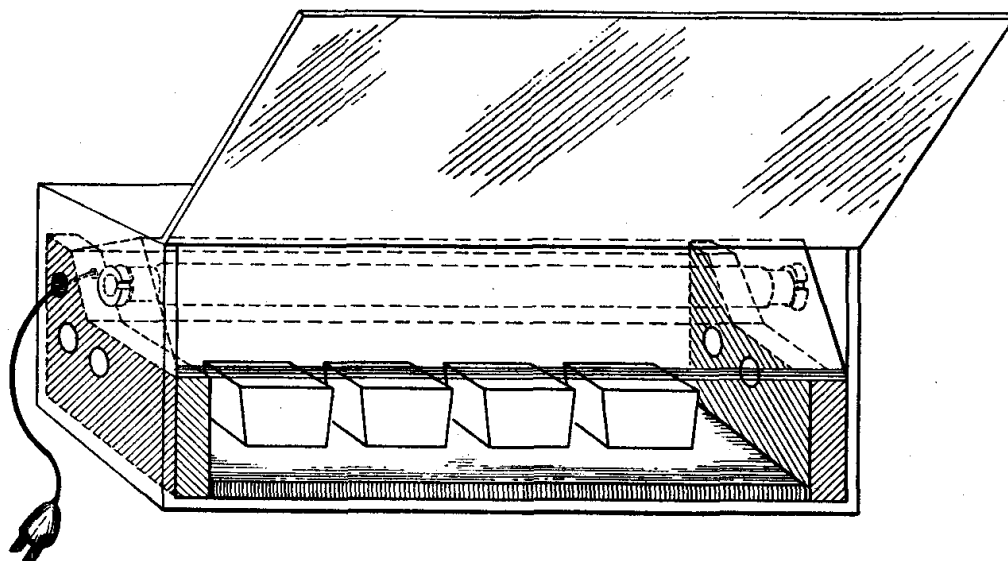


FIG. 83. Apparatus for photohydrolysis of monochloroacetic acid.

oxalic acid solution. The monochloroacetic acid need not be made up accurately because the determination of the chloride ion, produced by the ultraviolet light, is the only analytical measurement to be made.

The apparatus is shown in Fig. 83. Four rectangular polyethylene dishes, commercially available for household uses, are filled with 50 ml of solution and placed in line under two or more 8-watt germicidal ultraviolet lamps. These are mounted parallel in the top of a wooden box provided with a hanging hinged door in front to protect the eyes from the ultraviolet light. To prevent overheating, air at about  $15 \text{ ft}^3 \text{ min}^{-1}$  is drawn through the box past the lamps by an exhaust fan. *The radiation should not be viewed directly.*

Since the light intensity varies with position, the actinometer solution is placed in the first and third positions and the monochloroacetic acid solution in the second and fourth. The time of exposure is recorded. It should be long enough (over 2 hr) to give a satisfactory titration.

The uranyl oxalate is titrated with 0.02 N potassium permanganate after adding an excess of sulfuric acid (15 ml of 5 N  $\text{H}_2\text{SO}_4$  is sufficient for 50 ml of oxalate solution) and heating to about  $60^\circ\text{C}$ .

The two monochloroacetic acid solutions are titrated with 0.01 M mercuric nitrate. The titration follows the reaction  $\text{Hg}^{++} + 2\text{Cl}^- = \text{HgCl}_2$ ; the  $\text{HgCl}_2$  produced is soluble but undissociated. About 0.2 ml of 10 per cent sodium nitroprusside is added as indicator. The end point is recognized by the appearance of a faint, permanent turbidity due to the formation of a precipitate of mercuric nitroprusside. The amount of reaction is small, and the solutions are dilute, so that sharp end points cannot be expected. For this titration, it is helpful to use a darkened room and to arrange side lighting of the sample flask.

In a control experiment, the extent of any *dark reaction*, i.e., reaction taking place by a mechanism not involving absorption of light, is obtained by titration of unirradiated samples of the monochloroacetic acid solution.

The mercuric nitrate solution is standardized against a solution of HCl or NaCl of a known concentration similar to that of the  $\text{Cl}^-$  in the samples. A blank experiment is performed with nitroprusside in water alone.

Alternatively, the chloride ion may be titrated with 0.005 M  $\text{AgNO}_3$  and the titration followed potentiometrically. Two silver wire electrodes are used, one being placed in a 0.01 M  $\text{AgNO}_3$  solution; the latter is connected through a salt bridge of ammonium nitrate to a beaker containing the monochloroacetic acid solution, in which is immersed the second silver electrode. The voltage is plotted as a function of the volume of  $\text{AgNO}_3$  added. The voltage remains nearly constant until the chloride ion is nearly gone. Thereafter, it changes rapidly with further addition of silver nitrate. The end point may be taken as the point of greatest slope in the titration curve.

In a check experiment, the uranyl oxalate solution may be placed in the first and second positions, and the monochloroacetic acid, in the third and fourth.

**Calculations.** The number of photons absorbed by the actinometer is calculated from the permanganate titration data and the known quantum yield, 0.57 molecule per photon, for the actinometer reaction.<sup>2</sup> The number of photons absorbed by the two monochloroacetic acid samples is assumed to be 15 per cent less than the number absorbed by the actinometer solutions. The quantum yield for the monochloroacetic

acid samples is calculated on the basis of the amount reacted by a photochemical mechanism, and the result compared with literature values.

**Practical Applications.** The determination of quantum yield is an essential first step in seeking to understand the mechanism for the reaction. A great deal of effort has been devoted to the study of photochemical processes in nature such as photosynthesis. The quantum yield is an important factor in determining the potential efficiency of various proposed methods for conversion of solar energy into a form in which it can be stored for later utilization.

**Suggestions for Further Work.** A better method<sup>3</sup> for measuring the energy absorption consists in making a determination with a flat quartz dish containing a concentrated solution of monochloroacetic acid (which absorbs light of wavelength 2537 Å) placed over the uranyl oxalate dish. In a second experiment the upper quartz dish contains water. The titration *a* obtained for uranyl oxalate with the monochloroacetic acid filter gives a measure of the number of quanta of wavelength longer than 2537 Å, and the titration *b* with the water gives a measure of all the radiation absorbed by uranyl oxalate, together with a correction for losses of light from the filter due to reflection—amounting to about 4 per cent each at the air-quartz interface and at the air-solution interface. If the titration obtained in the absence of an upper filter solution is denoted by *c*, the corrected titration for light of 2537 Å alone is  $c - (c/b)a$ .

The bleaching of dyes such as methylene blue or malachite green may be followed colorimetrically, using as standards various concentrations of the unbleached dyes.

The photodecomposition of hydrogen peroxide may be followed by titration with potassium permanganate. This is a chain reaction subject to catalytic influences. Chain reactions give large quantum yields and do not require micro methods for chemical analysis.

The photobromination of cinnamic acid in carbon tetrachloride provides a good experiment.<sup>1</sup> The quantum yield shows that the reaction is a chain reaction. It increases when dissolved oxygen is removed by boiling under reduced pressure produced by a water aspirator. Equal portions of 0.005 M bromine in carbon tetrachloride and 0.01 M cinnamic acid in carbon tetrachloride are mixed and placed in the light. The bromine adds to the double bond when exposed to light, and the decrease in free bromine is determined by adding potassium iodide solution and titrating with standard sodium thiosulfate. The bromine removal may be determined also spectrophotometrically.

#### References

1. Bauer and Daniels, *J. Am. Chem. Soc.*, **56**, 387, 2014 (1934).
2. Leighton and Forbes, *J. Am. Chem. Soc.*, **52**, 3139 (1930).
3. Noyes and Leighton, "The Photochemistry of Gases," pp. 82-85, Reinhold Publishing Corporation, New York (1941).
4. Smith, Leighton, and Leighton, *J. Am. Chem. Soc.*, **61**, 2299 (1939).
5. Thomas, *J. Am. Chem. Soc.*, **62**, 1879 (1940).

## *Radioactive Isotopes and Tracers*

### 53. DETERMINATION OF RANGE AND ENERGY

This experiment provides experience in the use of the Geiger-Müller counter and scaling circuit for the characterization of radioactive materials. The range of  $\beta$  particles is determined.

**Theory.**<sup>2,4,8</sup> The  $\beta^-$  particles (electrons) which are emitted by radioactive nuclei originate in a nuclear transformation in which a neutron is changed into a proton and a  $\beta$  particle is released. The electrons emitted do not all have the same energy; there is a continuous distribution of energy among them, as is shown by Fig. 84. The maximum energy  $E_{\max}$  is characteristic of the nuclear transformation concerned. The complete distribution curve of Fig. 84 may be established experimentally by means of the electromagnetic  $\beta$ -ray spectrograph,<sup>4</sup> but the value of  $E_{\max}$  may be estimated by simpler measurements.

When high-velocity electrons enter a material medium, they undergo collisions with the electrons of the molecules or atoms they encounter; in these collisions they lose energy and are slowed down and eventually stopped. The distance that the electron can travel in the medium depends upon its initial energy and upon the electron density in the material and is called the range of the electron in the absorbing substance. The range will vary for different substances if expressed in terms of centimeters, but if it is expressed in terms of mass per square centimeter, it is almost independent of the identity of the absorbing material. This result follows from the fact that the number of electrons per unit mass is *nearly* the same for all atoms, so that there will be approximately the same number of electrons in equal masses of two different materials.

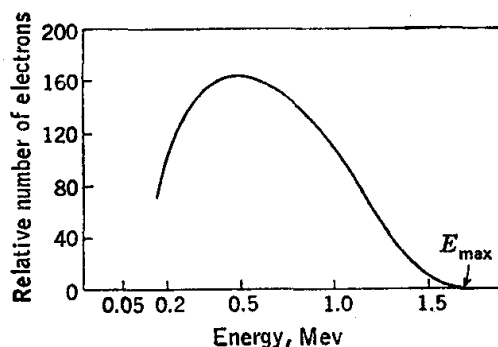


FIG. 84. Energy-distribution curve for  $\beta$  particles of  $P^{32}$ . (After Lyman.<sup>6</sup>)

The range of a  $\beta$  particle in an absorber will then depend on the initial energy of the particle, and the maximum range will be determined by the value of  $E_{\max}$ . From an experimentally determined value of the maximum range, the corresponding value of  $E_{\max}$  may be obtained by interpolation on a standard curve established by measurements with  $\beta$  particles for which the values of  $E_{\max}$  have been found by means of the magnetic spectrograph. The range determination is made by finding the thickness of a suitable absorbing material, such as aluminum, which is required to prevent the passage of any  $\beta$  particles from the source. The range is most easily determined by measuring the counts per minute obtained with various absorber thicknesses and estimating from a plot (of the logarithm of the number of counts per minute against absorber thickness) the absorber thickness through which  $\beta$  particles can no longer be detected above the background. This visual method is capable of high accuracy in cases where  $\gamma$  rays are not present or are present in such low intensity that their contribution to the counting rate is negligible.

A more generally applicable method has been suggested by Feather;<sup>3</sup> the absorption curve for a selected  $\beta$  emitter, for which the range is known, is used as a standard for the determination of the range for  $\beta$  radiation from another source. The primary reference standard for such work has been radium E (5d Bi<sup>210</sup>), but UX<sub>2</sub> (1.18 m Pa<sup>234</sup>) has also been recommended. For the  $\beta$  particles of UX<sub>2</sub>, the range has been found to be 1105 mg cm<sup>-2</sup>.

The detection and counting of the transmitted  $\beta$  particles is accomplished by means of the Geiger-Müller tube and a scaling circuit. The statistical considerations concerning the accuracy of counting-rate determinations are outlined in Chap. 18. Because of the random nature of the disintegration process, the number of  $\beta$  particles emitted per minute is not constant, but may be expressed in terms of a distribution curve giving the probability of a given number of counts versus the number of counts. The breadth of the distribution may be expressed by the standard deviation (page 395). A useful relation to remember is that the standard deviation in a total of  $n$  counts is approximately equal to the square root of  $n$ .

**Apparatus.** Geiger-Müller tube and mount; scaling circuit; impulse register; electric timer or stop watch; aluminum absorbers; radioactive substances such as phosphorus 32, UX<sub>2</sub> (Pa<sup>234</sup>) in equilibrium with uranium, etc.†

**Procedure.** The Geiger-Müller tube, shown in Fig. 85, the impulse register, and the electric timer are connected to the scaling unit. With all switches in the "off" position and the high-voltage control in the "low" position, the unit is connected to the 110-volt a-c line. The main

† Radioactive reference sources of many types may be purchased.



power switch is then turned on, and a warm-up period of 2 min allowed. The high-voltage switch can then be turned on, and when the applied potential has registered on the voltmeter, the counting switch is thrown on and a radioactive sample is placed under the tube on the top shelf. The first part of the experiment consists in the determination of the plateau (page 487) of the Geiger-Müller tube. The high-voltage control is now turned up *slowly*, until the starting potential for the particular tube in use is reached when counts will be recorded by the scaling unit as shown by the response of the neon interpolation bulbs.

The number of counts in a period of 2 min† is determined at this voltage; duplicate determinations are made. The counting switch is turned off, and the reset switch momentarily depressed to extinguish the interpolation lights and clear the scaling circuit. The reading of the impulse register is then recorded, the timer reset to zero, and the counting switch turned on for an accurately measured period of 2 min. At the end of the counting period the counting switch is turned off, and the counting time is recorded, together with the new reading of the impulse register and the number of counts recorded on the interpolation tubes.

The voltage applied to the Geiger-Müller tube is raised in successive steps of 25 volts, and the number of counts in a 2-min period is determined at each voltage until three successive counting rates agree within  $\pm 10$  per cent, showing that the plateau for the tube has been reached (Chap. 23). The operating voltage so found is employed in all subsequent counting work. *Under no circumstances should the posted maximum voltage for the counter tube be exceeded, since higher voltages will cause severe damage to this sensitive and expensive instrument.*

† If the activity of the sample is low, sufficient counting time should be allowed to give approximately 2000 counts.

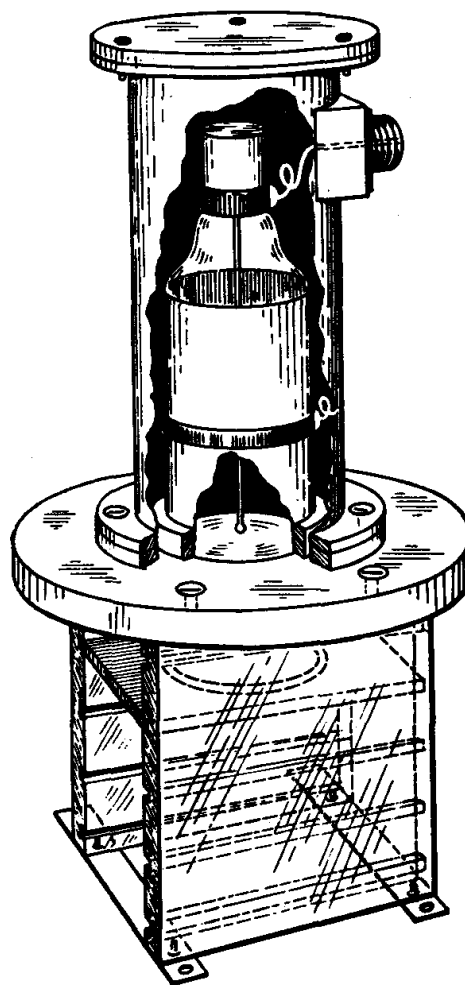


FIG. 85. Geiger-Müller tube and sample holder.

The number of counts in a 10-min period is next determined with no sample in the holder or near the Geiger-Müller tube. The counts registered, which are due to cosmic rays and stray radiation in the laboratory caused by natural radioactivity and contamination with radioactive materials, constitute the "background" of the counter, which contributes to the observed counting rate in any measurement. Radioactive materials, including radium-activated luminous watch dials, should be kept remote from the counter tube. (When maximum accuracy is required, as with weakly radioactive samples, heavy lead shields may be placed around the counting tube to reduce the background.)

A sample containing phosphorus 32 (or some other single  $\beta$  emitter) in sufficient quantity to give an initial counting rate of 5000 to 10,000 counts per minute is then placed on the second shelf of the mount, and the number of counts in a 2-min period is measured. The counting rate is then determined with a series of aluminum absorbers placed on the first (top) shelf; thicknesses of approximately 50, 100, 200, 400, 800, and 1200 mg cm<sup>-2</sup> are used singly and in combinations until an essentially constant counting rate is obtained, showing that all the  $\beta$  particles from the source are being absorbed. Longer counting periods will be necessary as the counting rate grows smaller; a minimum of 300 counts should be recorded in any period.

When this procedure is carried out for the  $\beta$  radiation from  ${}_{91}\text{Pa}^{234}$  as obtained from a standard sample of uranyl nitrate or, preferably, of  $\text{U}_3\text{O}_8$ , the sample must be covered by a thin aluminum foil of *known* thickness (about 30 mg cm<sup>-2</sup>) to cut out completely the soft  $\beta$  radiation and  $\alpha$  particles from the  ${}_{90}\text{Th}^{234}$  with which the  ${}_{91}\text{Pa}^{234}$  is in equilibrium.

To illustrate some of the complications which may be encountered in practical work, an absorption curve is then determined for a material which produces either a strong  $\gamma$ -ray contribution to the counting rate in addition to a  $\beta$  particle (as  $5.3\text{y Co}^{60}$ ) or two  $\beta$  particles of *different energies* (as Sr-Yt). Additional absorbers in the thin range may be required here.

Data are then taken to illustrate the random nature of the radioactive disintegration process. A sample of low activity is placed in the Geiger-Müller tube mount in the position where a counting rate of approximately 100 counts per minute is obtained. The number of counts in each of a series of 20 or more accurately measured 1-min counting periods is then recorded.

A proportional counter (page 489) or a scintillation counter (page 490) may be used rather than a Geiger counter. These two types of counters are useful for the determination of the energies of ionizing particles by measuring the size of the pulse produced. By use of a pulse-height analyzer, the number of particles in various energy ranges may be deter-

mined. Scintillation counters, which have solid or liquid absorbing materials, are especially useful for studying  $\gamma$  rays since the probability of the absorption of a  $\gamma$ -ray photon by the gas in the small volume of Geiger or proportional counter is quite small.

Instead of a scaling circuit and a mechanical counter to determine the number of particles absorbed in a given period of time, a rate meter may be used. In a rate meter a special circuit supplies constant increments of charge per pulse into the metering circuit at a pulse spacing depending on the input counting rate. Thus the counting rate is read directly on a meter. A rate meter may, for example, cover the range  $10^2$  to  $10^6$  counts per minute in several ranges.

**Calculations.** The number of counts per minute for each of the steps of the absorption-curve determinations is calculated. A plot is made of the logarithm of the number of counts per minute, background included, against the total absorber thickness in  $\text{mg cm}^{-2}$  for each of the materials studied. The total absorber thickness is the sum of contributions from all the materials between the sample and the sensitive volume of the Geiger-Müller tube. The thicknesses of the aluminum absorbers are known; the contribution of the air may be taken as  $1 \text{ mg cm}^{-2}$  per centimeter of path in air, and that of the window in the Geiger-Müller tube will be specified by the manufacturer. For a mica-window tube it will be approximately  $3.5 \text{ mg cm}^{-2}$ . Any covering placed over the sample, as in the case of  $_{91}\text{Pa}^{234}$ , must be taken into account. Some absorption takes place in the sample itself, but this effect is important only for low-energy particles.

The maximum range of the  $\beta$  particles is estimated visually from the plot for  $_{15}\text{P}^{32}$  or  $_{91}\text{Pa}^{234}$ , as indicated in Fig. 86, and the value of  $E_{\text{max}}$  is obtained by use of Fig. 87. For  $_{15}\text{P}^{32}$  the magnetic-spectrograph value of  $E_{\text{max}}$  is 1.69 million electron volts (Mev). The form of the absorption curve for the other material studied is interpreted qualitatively.

The numbers of counts observed in the series of approximately 1-min counting periods are corrected to the common basis of an exact 1-min counting time; for this calculation, a uniform counting rate in each period is assumed. The average number of counts is determined. The deviations of the individual numbers of counts per minute from the average value are then found and are plotted as in Fig. 103 on page 403.

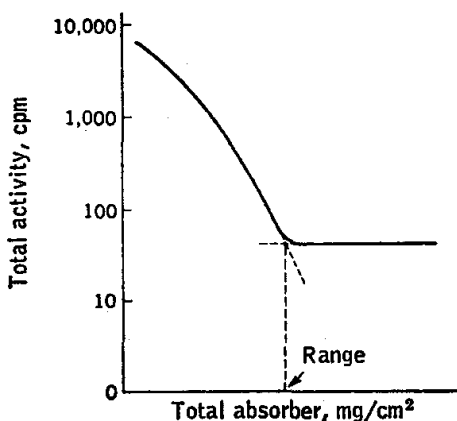


FIG. 86. Determination of the range of  $\beta$  particles.

**Practical Applications.** The absorption method is a very common and simple procedure for the determination of the energies of the radiations emitted by radioactive materials. Such information is useful in the identification of unknown radioisotopes as isolated, for example, from fission products.

**Suggestions for Further Work.** The effect of the supporting material on the counting rate obtained for a  $\beta$ -emitting sample may be investigated. A  $\beta$ -ray source, on a very thin plastic or mica sheet, is supported under the counter tube on an aluminum plate with a clearance hole cut through it under the sample, and the counting rate measured. Various metal sheets of differing thicknesses are then placed under the source, and their effects on the counting rate due to backscattering determined.

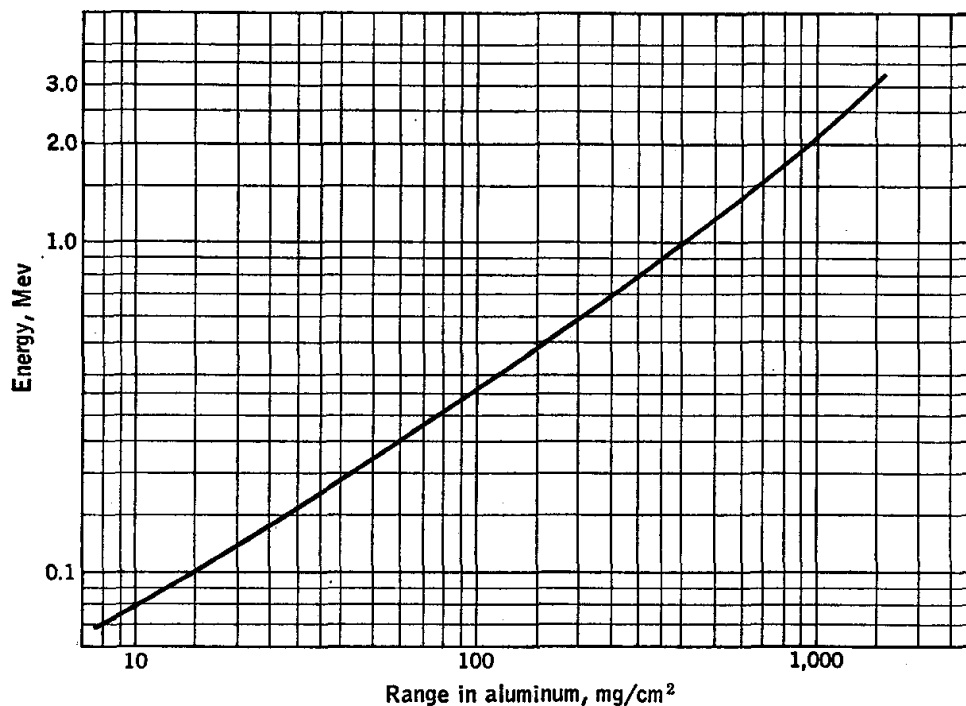


FIG. 87. Range-energy relation for  $\beta$  particles. [After Glendenin, *Nucleonics*, 2, 12 (1948).]

A range of thicknesses can conveniently be obtained in copper; comparison of results obtained with a particular thickness of metals of different atomic number is also pertinent. The effect of the energy of the beta radiation may also be checked, by use of a different emitter.

The counting rate obtained with a sample of fixed activity depends on the area over which the sample is distributed as well as the distance from the counting tube. These geometrical factors affecting counting efficiency may be studied.

A correction for the absorption of  $\beta$  particles within the sample itself is necessary when the sample is not negligibly thin. A self-absorption curve may be constructed by measuring the apparent beta activity observed with weighed samples of different thickness of the same material.  $\text{U}_3\text{O}_8$ , prepared by thermal decomposition of uranyl nitrate, is a readily prepared source for such work. The various samples should be of the same superficial area and at the same distance from the counter tube. An absorber of about  $30 \text{ mg cm}^{-2}$  should be placed above the emitter to block out radiation from the  ${}_{90}\text{Th}^{234}$  present. The sample thicknesses are best characterized in terms of  $\text{mg cm}^{-2}$ . Self-absorption is a particular problem with  $\beta$  emitters such as  $\text{C}^{14}$  and  $\text{S}^{35}$ , for which the maximum  $\beta$ -ray energy is low.

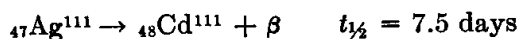
An interesting experiment on the statistics of radioactive measurement is described by Cook and Duncan.<sup>2</sup>

It is instructive to determine the half-life of an isotope with a half-life of the order of several minutes to an hour since the decay process can be followed through several half-lives during a single laboratory period. The purchase of isotopes with such short half-lives is obviously impractical. However, such a short-lived daughter may be separated from a long-lived parent. For example, 1.18-min  $\text{Pa}^{234}$  may be separated from uranium and its half-life determined.<sup>1,8</sup> Hayes and Butler<sup>5</sup> have described the details of a procedure for separating  $\text{Ba}^{137\text{m}}$  ( $t_{1/2} = 2.63$  min) from  $\text{Cs}^{137}$  ( $t_{1/2} = 30$  years) using an ion-exchange column.

The half-life of a short-lived isotope, such as phosphorus 32 or silver 111, may be determined. Phosphorus 32 decays with the emission of an electron with 1.69 Mev of energy to form a stable sulfur isotope.



Silver 111 decays with the emission of a 1-Mev  $\beta$  particle.



A sample of suitable size is prepared by evaporating a solution on a small watch glass, using an infrared heat lamp mounted a few inches above the sample. If too rapid heating is used, the sample will boil and spatter. The sample is mounted in a piece of cardboard and covered with cellophane fastened down with Scotch tape. The student's name and laboratory period are written on the card, which is filed near the counter. The activity of the covered sample is measured several times over a period of 2 weeks or more. The half-life is calculated from a plot of the log of the activity (corrected for background) versus time. If more than one isotope is present, the log plot will be a curve which may be resolved into two or more straight lines. Such a curve is analyzed by extrapolating the final linear section back to shorter times, subtracting the activity of this isotope from the earlier counting rates, and making a new plot of the data corrected in this way.

### References

1. Braunstein and Young, *J. Chem. Educ.*, **38**, 31 (1961).
2. Cook and Duncan, "Modern Radiochemical Practice," Oxford University Press, New York (1952).
3. Feather, *Proc. Cambridge Phil. Soc.*, **34**, 599 (1938).
4. Friedlander and Kennedy, "Nuclear and Radiochemistry," John Wiley & Sons, New York (1955).
5. Hayes and Butler, *J. Chem. Educ.*, **37**, 590 (1960).
6. Lyman, *Phys. Rev.*, **51**, 1 (1937).
7. Miller and Curtiss, *J. Research, Natl. Bur. Standards (U.S.)*, **38**, 359 (1947).
8. Overman and Clark, "Radioisotope Techniques," McGraw-Hill Book Company, Inc., New York (1960).
9. Whitehouse and Putnam, "Radioactive Isotopes," Oxford University Press, New York (1953).

### 54. THE SZILARD-CHALMERS PROCESS AND THE HALF-LIFE OF RADIOIODINE

In this experiment a radioisotope is prepared by the neutron bombardment process, and its half-life is determined. The concentration of

radioactive elements by the Szilard-Chalmers technique is illustrated. Experiments illustrate the rate of exchange between iodine molecules and iodide ions and the slow rate of exchange between iodine molecules and organic iodides.

**Theory.**<sup>1,2,10,11</sup> When a slow neutron is captured by a target nucleus, the resulting nucleus, which is one unit larger in mass, is produced initially in an excited energy state and often becomes stabilized through the emission of one or more  $\gamma$ -ray photons. This process is called the  $(n,\gamma)$  reaction, or radiative neutron capture. Sometimes an  $\alpha$  particle is emitted, giving an  $(n,\alpha)$  reaction. Because the law of conservation of momentum must be satisfied, the recoiling nucleus in the emission process has an abnormally large kinetic energy which is ordinarily very much greater than chemical-bond energies. The result is not only the rupture of the bond originally holding the atom involved in the molecule, but also the breaking of numerous other bonds in other molecules as the recoiling atom expends its excess energy. The atoms and molecular fragments so produced recombine in various ways, and the incorporation of radioactive atoms in appropriate chemical species sometimes permits their chemical concentration. This process of concentration, made possible by the chemical consequences of the nuclear transformation, is commonly called the Szilard-Chalmers process.<sup>9</sup>

When an alkyl iodide, such as ethyl iodide, is irradiated with slow neutrons, the  $(n,\gamma)$  reaction on  $I^{127}$  produces the radioactive isotope  $I^{128}$ . A large fraction of the radioiodine formed ends up in inorganic form, i.e., as molecular iodine,  $I^{127}I^{128}$  or  $HI^{128}$ , which may be separated from the organic medium by extraction with aqueous sodium hydroxide solution. The "organic yield," the fraction of radioiodine remaining in organic combination, has been found to depend on the structure and phase of the alkyl iodide irradiated and to be influenced also by the presence of added iodine.<sup>4</sup>

Radioactive  $I^{128}$  decays to stable  $Xe^{128}$  either directly with the emission of a  $\beta$  particle of 2.02-Mev maximum energy, or indirectly with the emission of a  $\beta$  particle of 1.59-Mev maximum energy, to form an  $Xe^{128}$  atom in an excited nuclear-energy state. The  $Xe^{128}$  immediately becomes stabilized by emission of a  $\gamma$ -ray photon of energy 0.43 Mev. (Note that  $1.59 + 0.43 = 2.02$ .)

The rate of disintegration of a radioisotope ( $-dN/dt$ ) is proportional to the number  $N$  of radioactive atoms present:

$$-\frac{dN}{dt} = \lambda N \quad (1)$$

Integrating from  $t = 0$ , when the number of atoms present is  $N_0$ , to

time  $t$ , when the number of atoms present is  $N$ ,

$$2.303 \log \frac{N}{N_0} = -\lambda t \quad (2)$$

or

$$N = N_0 e^{-\lambda t} \quad (3)$$

In characterizing a radioisotope, the half-life  $t_{1/2}$  is more commonly used than the rate constant  $\lambda$ . The half-life is the time required for the number of radioactive atoms to decrease to one-half the number originally present; by setting  $N_t/N_0$  equal to  $\frac{1}{2}$  in Eq. (2),

$$t_{1/2} = \frac{2.303 \log 2}{\lambda} = \frac{0.693}{\lambda} \quad (4)$$

If a neutron flux of  $\phi$  neutrons per second per square centimeter is incident upon a thin layer of material containing  $n$  nuclei per square centimeter, the number of neutron captures occurring per second per square centimeter is  $n\phi\sigma$ , where the proportionality factor  $\sigma$  is called the *cross section* for neutron capture. The cross section is commonly reported in terms of *barns* (1 barn =  $10^{-24}$  cm<sup>2</sup>), and its value depends on the energy of the incident neutron as well as the identity of the nucleus involved. For  $\text{I}^{127}$  the cross section  $\sigma$  is 6.85 barns for slow, thermal neutrons.

With a small neutron source centered in a flask containing an organic iodide the neutron flux is not constant throughout the medium. The number of radioiodine atoms produced per unit time, however, is constant at a value  $P$  determined by the neutron-capture cross section and the radial depth and iodine atom concentration of the medium. The net rate of increase of radioactive atoms is this rate of production minus the rate of disintegration,  $\lambda N$ , as given by Eq. (1):

$$\frac{dN}{dt} = P - \lambda N \quad (5)$$

Integration from  $t = 0$ ,  $N = 0$ , to a later time  $t$ , when the number of radioactive atoms is  $N$ , gives

$$N = \frac{P}{\lambda} (1 - e^{-\lambda t}) \quad (6)$$

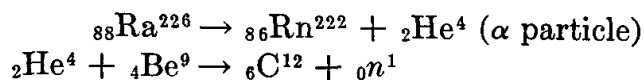
The number of disintegrations per second of the sample is equal to  $\lambda N$ :

$$\lambda N = P(1 - e^{-\lambda t}) \quad (7)$$

It is seen that  $P$  also represents the limiting activity and that the fraction of this limiting activity attained in time  $t$  is

$$\frac{\lambda N}{P} = (1 - e^{-\lambda t}) = 1 - \exp\left(\frac{-0.693t}{t_{1/2}}\right) \quad (8)$$

For laboratory use an adequate neutron flux can be obtained from a small radium-beryllium source:



Approximately  $10^7$  neutrons per second are produced per gram of radium; a typical laboratory source containing 10 mg radium thus provides  $10^5$  neutrons per second. The neutrons produced may have kinetic energies up to 13 Mev and must be slowed down to thermal energies. This is effected by elastic collisions with nuclei. Hydrogen-containing substances make good moderators since the transfer of energy from a neutron to a proton in an elastic collision is very efficient because of the similarity in mass. Thermal neutrons are neutrons which have been slowed down to energies of the magnitude of that of thermal agitation, about  $RT$  per mole. Such neutrons are not monoenergetic, but are characterized by a Maxwellian distribution of velocities; their *average* energy depends on the temperature of the medium in which they were slowed down.

**Apparatus.** Neutron source† and lead storage shield; remote-handling device; irradiation-flask assembly; irradiation-flask shield; 1-liter separatory funnel; 50-ml pipette; two 150-ml beakers; two 125-ml Erlenmeyer flasks; 25-ml graduate; special sintered-glass filter crucible or small Büchner funnel and filter paper; filter-flask assembly; bunsen burner and ring stand; counting tube, scaler, and timer; ethyl iodide; 0.5 N sodium hydroxide; nitric acid; 0.01 N silver nitrate solution; carbon tetrachloride; iodine.

**Procedure.**<sup>8</sup> About 850 ml of ethyl iodide is placed in a 1-liter Pyrex flask. Approximately 10 mg of iodine is weighed out and dissolved in the ethyl iodide to act both as a scavenger and as a carrier for the iodine released by the neutrons from chemical combination in the organic molecule, ethyl iodide. The neutron source is then removed from its lead protective housing *by the instructor*, using a remote-handling device,‡ and transferred to the irradiation flask of ethyl iodide as shown in Fig. 88. The irradiation is allowed to proceed for 1 hr.

The test-tube holder for the neutron source is of soft glass because Pyrex glass contains boron, which has a high capture cross section for neutrons and interferes with the absorption of neutrons by the iodine of the ethyl iodide.

† Such sources may be obtained from Atomic Energy of Canada, Limited, Commercial Products Division, P.O. Box 379, Ottawa, Canada, or the Oak Ridge National Laboratory, Oak Ridge, Tenn.

‡ Obtainable from suppliers of nuclear apparatus.



**Caution:** The source must always be kept at a safe distance from all personnel.† The radium-beryllium neutron source represents a radiation hazard;  $\gamma$  rays as well as neutrons are emitted. It should be stored in a lead housing and must be handled by means of a remote-control device. Lead shielding is also provided for the irradiation flask during the irradiation period. The  $I^{128}$  is not produced in hazardous amounts, so that the special precautions are required only with the operations involving the neutron source itself.

Because of the relatively short half-life of  $I^{128}$ , rapid processing of the irradiated material is essential. During the irradiation period preparations should be carefully made for the subsequent operations. By means of a pipette, 50 ml of 0.5 N sodium hydroxide is placed in a 1-liter separatory funnel supported on a ring stand. A 1 N nitric acid solution is prepared by dilution of concentrated acid. A quantity of this acid slightly in excess of that required to neutralize the 50 ml of the sodium hydroxide solution is placed in a 250-ml beaker. It is found by titration, using methyl orange indicator. In separate flasks are placed 15 ml of carbon tetrachloride and 25 ml of a 0.01 N solution of silver nitrate. The auxiliary equipment (filter flask, burner, etc.) is set up, and the counting equipment (Exp. 53) prepared for use at this time.

At the end of the 1-hr irradiation period the neutron source is removed by the instructor and returned to storage. The few atoms of newly produced radioactive  $I^{128}$  present as inorganic iodine or iodides are easily dissolved in a suitable immiscible aqueous solvent and removed from the large quantity of unchanged ethyl iodide, making use of the Szilard-Chalmers process. They undergo a chemical change as well as a nuclear change, which permits their chemical concentration. There is such a small amount of radioactive iodine that it could become lost in any chemical or physical operations. Accordingly, the carrier of ordinary iodine is added in sufficient quantity for handling, and the radioactive iodine mixes with all the inorganic iodine, and thus the loss of radioactive iodine in the subsequent operations is relatively small.

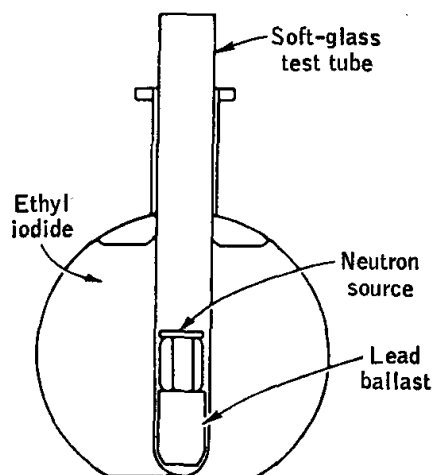


FIG. 88. Irradiation-flask assembly.

† Permissible radiation exposures are outlined in Handbook 59 of the National Bureau of Standards, available for 30 cents from the Superintendent of Documents, Washington 25, D.C. A survey meter should be used to check radiation levels.

The ethyl iodide with dissolved iodine is transferred to the separatory funnel containing the sodium hydroxide solution, and the mixture shaken vigorously. The rapid disappearance of the iodine color from the organic layer indicates the extraction of the iodine into the aqueous phase. The two phases are allowed to separate, and the heavier ethyl iodide layer is collected in the irradiation flask and saved. When the experiment has been completed, the ethyl iodide should be returned to the instructor since it can be used again.

The aqueous phase is then extracted in a separatory funnel with the carbon tetrachloride to remove any residual ethyl iodide. The carbon tetrachloride extract is withdrawn and discarded. The aqueous layer is then drained into the dilute nitric acid; the stirred solution is tested with methyl orange indicator to make sure it is slightly acid. The silver nitrate solution is added, and the mixture heated rapidly to boiling to coagulate the silver iodide formed. The precipitate is collected by use of a glass-filter crucible, the body of which has been cut off close to the sintered-glass disk to permit the precipitate to be mounted close to the window of the radiation counter tube. Alternatively, filter paper and a small Büchner funnel may be used. The precipitate is washed with distilled water, then with acetone, and air is drawn through to dry it. The crucible (or filter paper) is mounted on an aluminum or cardboard plate for counting. The number of counts obtained in 1-min counting periods is determined at 2-min intervals for a period of at least 50 min. The laboratory background count is also recorded. (The use of the counting equipment is described under Exp. 53.)

The preceding experiment could not be carried out if the molecular iodine containing the radioactive iodine exchanged iodine rapidly with the ethyl iodide. This exchange is very slow. The exchange between molecular iodine and iodide ion, however, is very rapid, as shown by the following experiment.

Ethyl iodide is irradiated as before, but no carrier iodine is added. The irradiation product mixture is extracted with a solution of 25 mg of potassium iodide in 50 ml of water. The ethyl iodide is returned to the instructor. The aqueous phase is extracted with carbon tetrachloride to remove any residual organic iodide. The resulting aqueous phase, which contains radioiodine as iodide ion, is shaken in the separatory funnel with 25 ml of carbon tetrachloride containing 10 mg of iodine. The carbon tetrachloride layer is separated, and the iodine removed from it by extraction with dilute sodium hydroxide. The basic solution obtained is acidified with dilute nitric acid, and silver nitrate solution added. The silver iodide precipitate is collected as before and tested for activity. The presence of radioiodine in this material is evidence of a rapid exchange of iodine between iodide ion and molecular iodine.

**Calculations.** A plot is made of the logarithm of the number of counts per minute from the radioiodine samples against the time of observation. The counting rate which is measured is proportional to the number of radioactive atoms which are present. Limits of uncertainty are calculated at the different points and indicated by marking a spread on the graph. An appreciable error for low activity results from the background. At high counting rates the "dead time" due to lag in recovery by the Geiger-Müller counter may cause an error. The rate constant for the disintegration of  $I^{128}$  is determined from the slope of the straight line considered to give the best representation of the experimental results. The half-life of the radioiodine is calculated and compared with the accepted value.

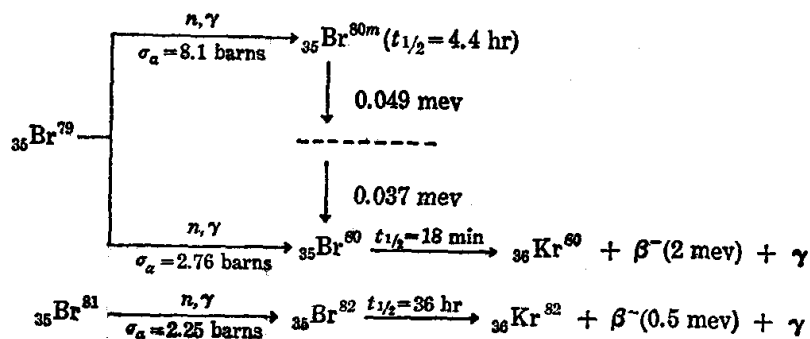
The fraction of the limiting activity obtained in the irradiation period used is calculated. It is shown that Eq. (8) is equivalent to the relation

$$\frac{\lambda N}{P} = 1 - \frac{1}{2^n} \quad (9)$$

where  $n$  is the length of the irradiation period in half-lives of the radioisotope formed.

**Practical Applications.** Neutron bombardment, particularly in the high neutron fluxes furnished by nuclear reactors, is the most important method for the production of radioisotopes.

**Suggestions for Further Work.**<sup>1,3</sup> The  $(n, \gamma)$  reaction on bromine may also be studied. The modes of production of the three radioactive species formed and their individual decay schemes may be represented as follows:



The  $\text{Br}^{80}$  and  $\text{Br}^{80m}$  constitute a pair of nuclear isomers; the latter is a relatively long lived metastable excited nuclear state of the former. The decay of  $\text{Br}^{80m}$  to  $\text{Br}^{80}$  is termed an *isomeric transition*. The 0.049-Mev transition occurs almost exclusively by the process of *internal conversion*, in which a direct transfer of energy from the nucleus to an adjacent orbital electron takes place, with the resultant ejection of a *conversion electron*. The 0.037-Mev transition occurs by conversion electron emission in about half of the events and by  $\gamma$ -ray emission in the other half.

Ethylene dibromide is irradiated for at least 4 hr, and preferably overnight, with the neutron source. The irradiated mixture is extracted with a solution of about 25 mg of potassium bromide in 50 ml of distilled water. (A small amount of a reduc-

ing agent such as sodium sulfite may be helpful also.) The aqueous layer is separated and acidified to methyl orange indicator with nitric acid, and silver bromide precipitated by addition of silver nitrate solution. The precipitate is collected as described previously for silver iodide, and the number of counts per minute from the radio-bromine sample determined at 2-min intervals for the first half hour and at longer intervals thereafter. An absorber of thickness about  $100 \text{ mg cm}^{-2}$  is placed between the sample and the counting tube to absorb the relatively weak  $\beta$  emission from the  $\text{Br}^{82}$  present. A total counting period of 4 hr or more is recommended. The counting rate initially decreases rapidly as the  $\text{Br}^{80}$  present disintegrates. Ultimately the rate of decay of  $\text{Br}^{80}$  becomes equal to its rate of production from  $\text{Br}^{80m}$ ; the activity thereafter decays with a half-life of 4.4 hr. It should be noted that the counts registered here are due to the  $\beta$ -ray emission from the daughter  $\text{Br}^{80}$  in equilibrium with the  $\text{Br}^{80m}$ , since the counting efficiency for the accompanying  $\gamma$  rays is negligible relative to that for the  $\beta$  particles. The  $\gamma$  rays are so penetrating that only a few are counted.

A plot is made of the logarithm of the number of counts per minute from the radio-bromine sample versus the time of observation. A straight line is drawn through the points corresponding to the later observations, and the half-life of  $\text{Br}^{80m}$  is calculated from its slope. Data for a corresponding plot for the 18-min activity can be obtained by subtracting from the total numbers of counts per minute at the early times of observation the contributions of the 4.4-hr activity evaluated from the extrapolation of the straight line referred to above.

After the irradiated ethylene dibromide has stood for about 2 hr following the first extraction, a second extraction may be made. The activity thus isolated will decay with a half-life of 18 min. It arises from  $\text{Br}^{80}$  released from organic combination by bond rupture accompanying the isomeric transition from  $\text{Br}^{80m}$  by the internal conversion process.

Radiomanganese,  $\text{Mn}^{56}$ , whose half-life is 2.6 hr, may be isolated by the Szilard-Chalmers process by irradiation of concentrated aqueous potassium permanganate solution.<sup>1,5</sup> The efficiency of the separation depends on the pH of the solution and becomes low when the pH is high.<sup>5</sup>

The nonequivalence of the two sulfur atoms in the thiosulfate ion may be demonstrated<sup>6</sup> by the use of radiosulfur obtained from the U.S. Atomic Energy Commission. The maximum  $\beta$ -ray energy for  $\text{S}^{35}$  is low, 0.165 Mev, so that a counting tube with a very thin mica window must be used.

### References

1. Cook and Duncan, "Modern Radiochemical Practice," Oxford University Press, New York (1952).
2. Friedlander and Kennedy, "Nuclear and Radiochemistry," John Wiley & Sons, Inc., New York (1955).
3. Hamill, Williams, and Schuler, *J. Chem. Educ.*, **26**, 310 (1949).
4. Levey and Willard, *J. Am. Chem. Soc.*, **74**, 6161 (1952).
5. Libby, *J. Am. Chem. Soc.*, **62**, 1930 (1940).
6. McCool and Hentz, *J. Chem. Educ.*, **32**, 329 (1955).
7. Overman and Clark, "Radioisotope Techniques," McGraw-Hill Book Company, Inc., New York (1960).
8. Schuler, Williams, and Hamill, *J. Chem. Educ.*, **26**, 667 (1949).
9. Szilard and Chalmers, *Nature*, **134**, 462 (1934).
10. Willard, *Ann. Rev. Nuclear Sci.*, **3**, 193 (1953).
11. Williams, Hamill, and Schuler, *J. Chem. Educ.*, **26**, 210 (1949).

## 55. EXCHANGE REACTIONS WITH DEUTERIUM OXIDE

By the use of concentrated deuterium oxide it is possible to determine the number of hydrogen atoms in a hydrogen-containing compound which may be exchanged with hydrogen atoms of water. A dry sample of the compound is dissolved in heavy water, and then the heavy water is sublimed out of the sample by use of a vacuum pump and dry-ice trap. The increase in weight of the compound is due to the substitution of deuterium for hydrogen. Some hydrogen atoms exchange so rapidly that it has not been possible to determine rates, while hydrogen atoms in other positions may exchange very slowly.

**Theory.** Although the chemical reactions of isotopes are nearly identical, there are very minor differences which show up most prominently in the elements of low atomic weight, and especially in hydrogen. If a mixture of water containing equal parts of the light isotope H and the heavy isotope D is electrolyzed, it is found that H is liberated by electrolysis about five times as fast as D. Other methods, such as exchange reactions and highly efficient fractional distillation on a large scale, are used also to produce an enrichment in deuterium oxide.

**Apparatus.** Water containing a known percentage of  $D_2O$ ;† analytical balance; 15-ml weighing bottle; vacuum pump (0.3  $\mu$ ); drying trap (Fig. 89); Dewar flask; dry ice; hot plate; ammonium sulfate; trichloroethylene.

**Procedure.** Ammonium sulfate is satisfactory for this experiment because it is nonvolatile and 6 per cent of its mass is due to hydrogen. A convenient amount of ammonium sulfate to use is 0.7 g. The ammonium sulfate is dried by placing it in a weighing bottle in an apparatus such as that illustrated in Fig. 89. The apparatus is evacuated by use of a mechanical vacuum pump. A trap surrounded by dry ice in trichloroethylene is placed between the drying chamber and the pump so that moisture does not get into the oil of the vacuum pump or oil vapor into the sample. The Dewar flask is about one-third filled with liquid, and then crushed dry ice is added (slowly at first). The ammonium sulfate may be dried more quickly if the drying chamber is immersed in a beaker of boiling water.

After the ammonium sulfate has been dried, it is weighed, about 1 g of heavy water is placed on the sample, and the weighing bottle and contents reweighed. The supply of heavy water should be kept stoppered so that  $D_2O$  will not exchange with  $H_2O$  in the air. The sample must be completely dissolved in the heavy water (by heating if necessary) so that the entire sample has an opportunity to exchange. It is necessary to

† Heavy water containing 99.8 per cent  $D_2O$  or higher may be purchased from the Stuart Oxygen Company of San Francisco.

evaporate the  $D_2O$  out of contact with room air so that exchange with ordinary  $H_2O$  will not occur. To avoid bubbling, the water is sublimed from the frozen solution. To avoid losses, a small wad of glass wool is weighed and is placed in the top of the weighing bottle before the solution is frozen in the dry ice-trichloroethylene freezing mixture.

The weighing bottle containing frozen solution is placed in the drying apparatus and evacuated. The evaporation of  $D_2O$  molecules may not be sufficiently rapid to keep the solution frozen. It is essential that the

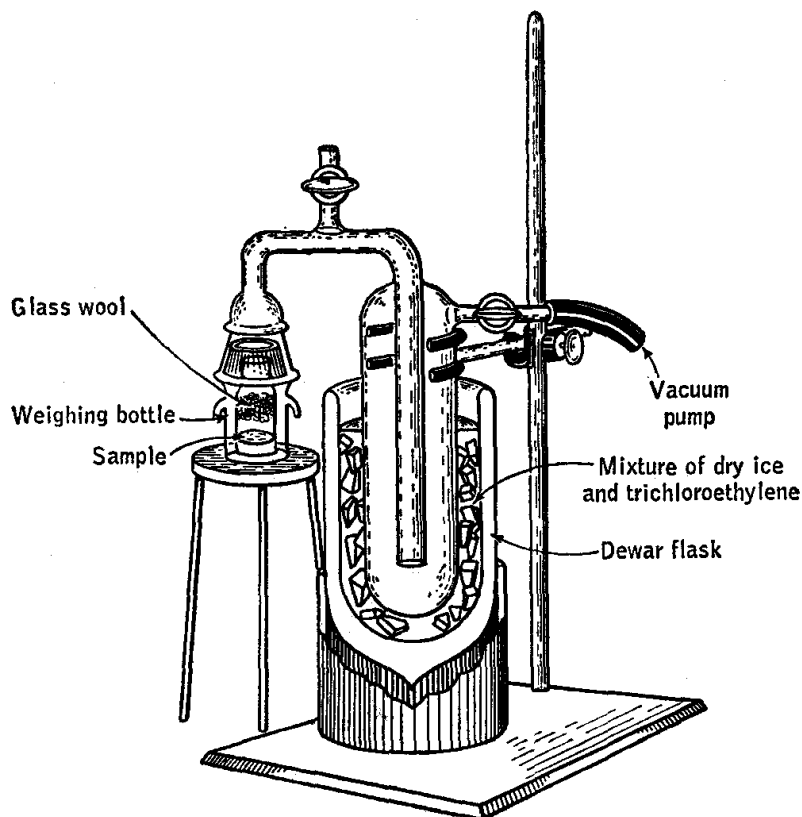


FIG. 89. Apparatus for evaporating water.

sample not be allowed to become so warm that bumping occurs, as some of the sample will be lost in this way. However, if the chamber containing the weighing bottle is kept immersed in ice water, the sample will generally remain sufficiently cold. When the liquid content has been reduced to the point that there is no longer danger of bubbling, the ice bath is replaced by a beaker of room-temperature water, and finally by a beaker of boiling water. By raising the temperature in this way, the drying time is considerably reduced.

The dried salt is weighed and then placed in the drying apparatus for another hour at  $100^\circ$  and reweighed to be sure constant weight has been reached.

If a vacuum pump is not available, the experiment may be carried out by passing air dried with Ascarite or other desiccant over the sample. If air is drawn through the sample chamber by use of a water aspirator, a second drying tube should be used to prevent diffusion of ordinary water vapor into the sample chamber.

**Calculations.** It is desired to determine how many of the hydrogens in the ammonium sulfate molecule can exchange with deuterium in the solvent water. Only certain types of hydrogen atoms in organic compounds do exchange with the hydrogen atoms in water. If the ammonium sulfate were in equilibrium with pure deuterium oxide, all the readily dissociable hydrogens would be replaced by deuterium. However, the deuterium oxide becomes diluted with ordinary water by the exchange with hydrogen from the ammonium sulfate. Since the ammonium sulfate and heavy water are in equilibrium, the mole fraction of replaceable hydrogens which are replaced by deuterium will be equal to the mole fraction of the deuterium oxide in the water which is in equilibrium with ammonium sulfate.

The mole fraction of  $D_2O$  in the water at equilibrium is calculated from the original weight  $w$  of heavy water taken, the weight fraction  $f$  of  $D_2O$  in the original deuterium oxide, and the gain in weight of the ammonium sulfate,  $g_2 - g_1$ . The total number of moles of water is

$$\frac{fw}{20} + \frac{(1-f)w}{18} \quad (1)$$

This is the number of moles of water added originally, and it is also the total number after exchange, because there is no change in the total number of molecules of  $D_2O$  and  $H_2O$ , merely a change in the relative proportions of each. The decrease in the number of moles of  $D_2O$  as a result of exchange with the ammonium sulfate, leaving deuterium in the ammonium sulfate instead of hydrogen and forming  $H_2O$ , is  $(g_2 - g_1)/2$ , where the factor 2 enters because there are 2 atoms of hydrogen per molecule of water and a difference in atomic weights of D and H of 1. Thus the mole fraction of  $D_2O$  at equilibrium is

$$X_{D_2O} = \frac{(fw/20) - (g_2 - g_1)/2}{(fw/20) + (1-f)w/18} \quad (2)$$

The gain in weight per mole of ammonium sulfate would be  $AX_{D_2O}$ , where  $A$  is the number of gram atoms of hydrogen involved in the exchange equilibrium per gram molecule of ammonium sulfate.

The gram-molecular weight of ammonium sulfate is designated by  $M$ . If  $g_1$  is the initial dry weight of the ammonium sulfate and  $g_2$  is the weight

after exchange, the gain in weight for  $g_1/M$  moles of ammonium sulfate is

$$g_2 - g_1 = AX_{D_2O} \frac{g_1}{M} \quad (3)$$

Solving for  $A$ ,

$$A = \frac{(g_2 - g_1)M}{g_1 X_{D_2O}} \quad (4)$$

**Practical Applications.** The interest in isotopic hydrogen lies chiefly in the fact that hydrogen atoms can be labeled by their greater weight and followed through various chemical reactions and physical processes. From the final distribution of the heavy and light atoms, much information can be obtained concerning the nature of the process. The applications in biology have been particularly important.

**Suggestions for Further Work.** Other exchange reactions may be studied, such as acetone with water,<sup>2</sup> carbohydrates with water,<sup>3</sup> or urea with water.

The concentration of deuterium in  $D_2O$ - $H_2O$  mixtures can be determined by surface tension or by the thermal conductivity<sup>6</sup> of  $H_2$  and  $D_2$ .

The main application of this method is to nonvolatile substances of high solubility in water which have a reasonably large percentage change in mass when D is substituted for H. Several organic compounds of interest for this type of work are malonic acid, succinic acid, and malic acid. The hydrogens of  $-COOH$  and  $-OH$  are expected to exchange very rapidly with the solvent. According to the literature, the  $\alpha$ -hydrogens of malonic acid are 100 per cent exchanged in 760 hr at  $50^\circ$ . The  $\alpha$ -hydrogens in sodium malate are 100 per cent exchanged in 5 hr at  $100^\circ$ . There is no exchange of  $\alpha$ -hydrogens of succinic acid in 160 hr at  $100^\circ$ .

#### References

1. Bonhoeffer, *Trans. Faraday Soc.*, **34**, 252 (1938).
2. Halford, Anderson, and Bates, *J. Am. Chem. Soc.*, **56**, 491 (1934).
3. Hamill and Freudenberg, *J. Am. Chem. Soc.*, **57**, 1427 (1935).
4. Kimball, "Bibliography of Research on Heavy Hydrogen Compounds," McGraw-Hill Book Company, Inc., New York (1949).
5. Kirshenbaum, Murphy, and Urey, "Physical Properties and Analysis of Heavy Water," McGraw-Hill Book Company, Inc., New York (1951).
6. Selwood and Taylor, *J. Am. Chem. Soc.*, **56**, 998 (1934).
7. Urey and Teal, *Revs. Modern Phys.*, **7**, 34 (1935).



## *General Experimental Techniques*

### 56. GLASSBLOWING

This experiment offers the opportunity for learning simple techniques used in constructing glass apparatus. Practice is obtained in performing some basic operations in glassblowing.

**Theory.** Pyrex glass is almost universally used for bench-blown glassware and will be used in this experiment. The disadvantage of the higher softening point of Pyrex is more than compensated for by its lower coefficient of thermal expansion and high strength. The following characteristics of Pyrex and soft glass are of importance to the glassblower:

Characteristic	Pyrex (No. 774)	Soft glass
Softening point.....	820°C	626°C
Strain point.....	510°C	389°C
Annealing point.....	560°C	425°C
Linear coefficient of expansion.....	$32 \times 10^{-7}$	$90 \times 10^{-7}$

Pyrex glass requires an oxygen-air-gas or oxygen-gas flame. When Pyrex is heated above the strain point, harmful strains may be introduced unless the piece is reheated and then cooled slowly and uniformly. Annealing is best done in a furnace which may be heated to 580 to 585°C, but in the laboratory a small piece of glass apparatus may be annealed in a flame. The glass is heated in a soft bushy flame until it is uniformly softened. The working temperature is slowly decreased by manipulating the glass in the cooler parts of the flame and by lowering the flame temperature until a layer of soot has been deposited from the smoky flame which is finally used.

A more detailed description of glassblowing than can be given here is to be found in several excellent books listed at the end of the experiment.

**Apparatus.** Burner; hand torch; oxygen tank; Pyrex glass tubing 10 to 12 mm outside diameter; file or glass knife; 4-mm Pyrex cane (rod); corks; forceps; rubber tubing; didymium eyeglasses.

**Procedure.** Practice is obtained in drawing "points" and making bends, straight seals, and T seals. It is essential that all tubing used for glassblowing be clean and dry.

Small tubes and rods are easily cut by making a single file scratch with a sharp file, placing the two thumbs toward each other on either side of the scratch but on the other side of the tubing, and breaking with a combined bending and pulling force. It will be found helpful to moisten the scratch before the break is attempted.

In the case of large tubes, a small point of heated glass is touched against one end of the file scratch, and a crack is produced under the file scratch which extends for a short distance beyond. The crack may be extended if necessary by touching the heated glass point to the tube just beyond the end of the crack.

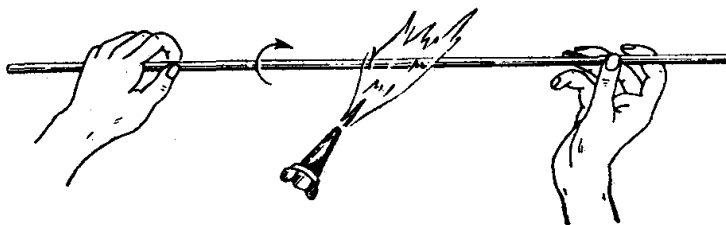


FIG. 90. Glassblowing: rotating the tube.

The tube may be cracked more neatly and more quickly by wrapping nichrome or other heating wire around the tube over the file scratch. The wire is heated red hot with an electric current, using a suitable resistance in series.

The proper procedure for lighting a burner is to ignite the gas first, then turn on the air, and lastly turn on the oxygen. The optimum temperature for the flame depends upon the size of the piece being worked and the ability of the operator. A more skillful operator may use a higher temperature, which makes possible faster working. The hottest part of a flame is at the tip of the inner cone. Didymium glasses should be worn to protect the eyes from the sodium light produced by the vaporization of sodium from the glass.

The first operation to be learned is uniform rotation of the glass (Fig. 90). A suitable length of tubing 10 to 12 mm outside diameter is selected as a convenient size for practice in this and subsequent operations. The tubing is held by the last three fingers of the left hand, which act as a bearing; the thumb and forefinger are used to rotate the glass. The right hand supports the other end of the tubing. (Left-handed persons may reverse the order given.) Here again, the thumb and forefinger are used to rotate the tube while the other fingers are used mainly for support. The palm of the left hand is downward, while that of the right hand is

upward. These positions permit the glassblower to blow into the right-hand end of the tubing, which should be the shorter end. Rotation is in such a direction that the top of the tubing moves away from the glassblower. The right- and left-hand movements are synchronized to prevent twisting of the tubing. The tube is held in a straight line, and bending, pushing, or pulling the glass is avoided except when required for a specific purpose. The student will find that a considerable amount of practice will be required.

The importance of mastering this rotation technique cannot be too strongly emphasized; it is essential for obtaining uniform wall thickness

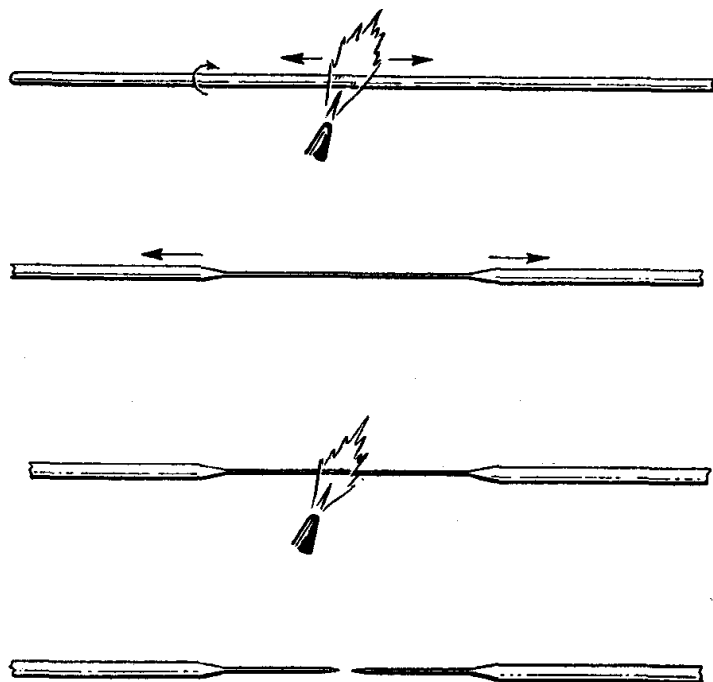


FIG. 91. Glassblowing: pulling a point.

and symmetrical shapes. The student should practice this operation until he gets the "feel" before any glassblowing is tried.

The next operation is pulling a "point" (Fig. 91). This is an elongation on the end of a tube formed by pulling the tube to a small diameter. Points form convenient handles for holding short pieces of tubing and provide a means for closing the tube and for cutting the glass with the flame. To pull a point, the tube is rotated in the flame so as to heat a length of about  $\frac{1}{2}$  in. When the glass is pliable, it is removed from the flame, and while still rotating, it is pulled slowly to a length of 8 or 9 in. The drawn-out portion is melted apart at the center, thus closing both points. If the points do not have the same axis as the tube, it will be necessary to heat at the shoulders, where they join the tube to straighten

them. The position of the point with respect to the tube is a test of the student's mastery of the rotation technique.

The straight seal is tried next (Fig. 92). One end of the tube to be held in the left hand is stoppered, the tube in the right hand being left open for blowing. The ends of the tubes which are to be sealed together are heated in the flame, with rotation, until softened. The two ends are then pushed together carefully on the same axis, and as soon as the contact is effected, the joint is pulled slightly. The joint is now rotated in

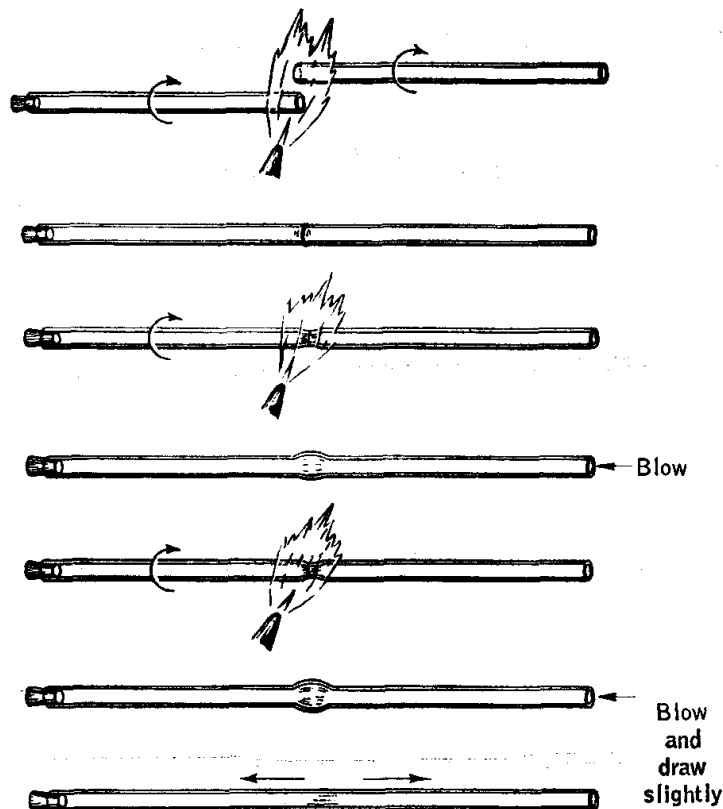


FIG. 92. Glassblowing: the straight seal.

the flame until the diameter of the tubing is somewhat decreased and the wall thickness is increased at the point of juncture. While it is still being rotated, the tube is removed from the flame and the joint is blown to a somewhat greater size than the original tubes. The tubing should not be pulled at this point, since this will decrease the wall thickness at the seal. The tubing is now reheated at the enlarged portion until its diameter is decreased; it is then removed from the flame and blown to a slight bulge. Before the tube has cooled appreciably, the joint is pulled sufficiently to reduce the diameter to that of the tube. Note that the tubing is continuously rotated in all these operations. If the rotation technique has been mastered, seals which are all but indistinguishable from the

remainder of the tubing can be made very quickly. If two pieces of tubing of different diameter are to be joined, the larger is first drawn down and cut off to give an end of the same diameter and wall thickness as the smaller tube.

The T seal (Fig. 93) presents a different problem, since the tubing cannot be rotated easily except by using a special glassblower's clamp. One end of a tube is closed by a cork, and with a sharp flame a spot on the side

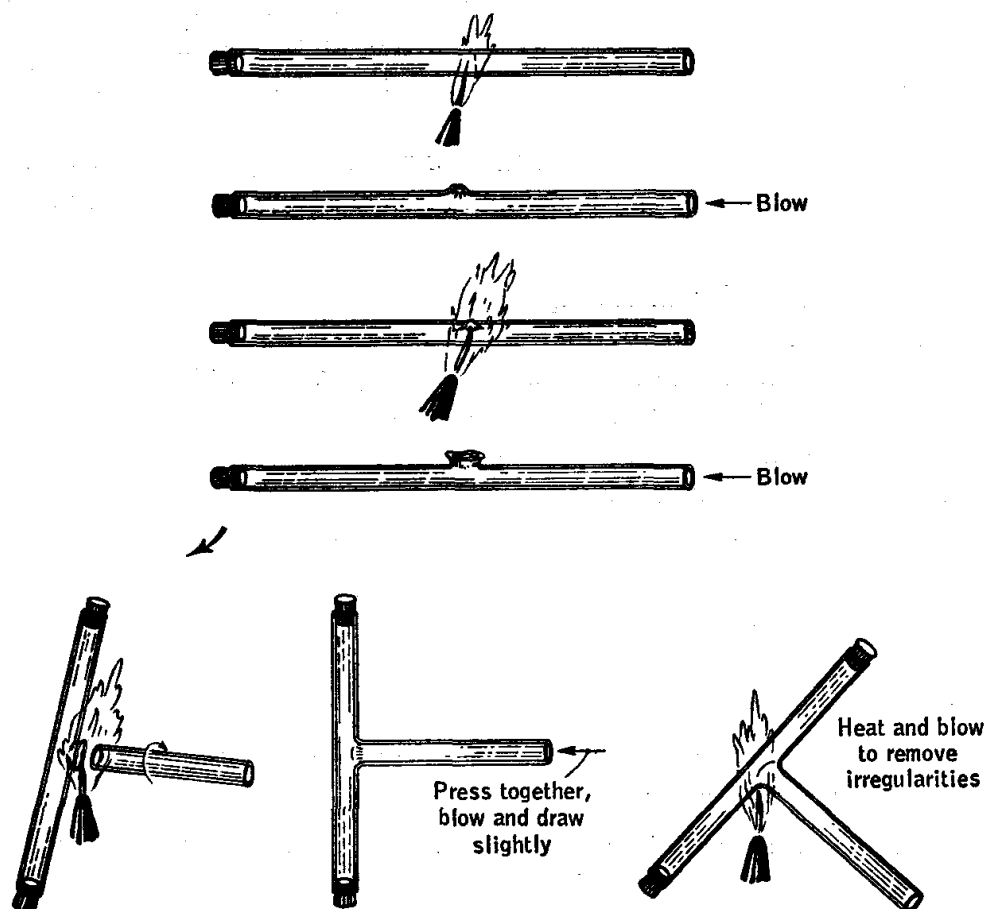


FIG. 93. Glassblowing: the T seal.

of the tube is heated. The heated spot is blown to form a bulge, which is then reheated and blown to a small bulb having thin walls. This bulb is broken, and the excess glass chips removed by scraping with wire gauze. The size of the hole thus formed should be about the same size as or slightly smaller than the tube which is to be attached. The other end of the tube with the side hole is now sealed with another cork. The side opening and the end of the tube to be sealed are heated until soft, removed from the flame, and brought quickly together and given a slight pull as soon as contact has been made. The joint is blown slightly to expand it and to remove any irregularities. If the glass was sufficiently softened

when joined, this procedure results in a good seal; however, should it not appear uniform, small parts can be heated with a sharp flame and then blown to proper size. The entire seal is reheated to remove stresses and to adjust the angle between the tubes.

A bend may be made after the tubing has been heated until it is pliable and it has been removed from the fire. In order to obtain a smooth uniform bend, one end of the tube is closed with a cork, and as soon as the bend is completed, the open end of the tube is blown into with sufficient pressure to eliminate any irregularities in the bend. In order to prevent sagging of a bend, the ends of the tube are bent upward with the heated portion downward.

Practice should be continued on each of the techniques described above until at least one satisfactory specimen of each of the following types has been produced:

1. Straight seal, 10 mm tubing
2. Straight seal, 7 mm tubing
3. T, 10 mm tubing, two ends sealed off, open end polished
4. T, 7 mm tubing, two ends sealed off, open end polished
5. Straight seal, 10 to 7 mm tubing, large end sealed, open end polished
6. 135° bend, 10 mm tubing
7. 90° bend, 7 mm tubing.

Items 4 and 5 are tested for pinholes. The test is made by attaching the unit to a vacuum system, which is then pumped down to a vacuum of the order of 0.1 mm Hg, and exploring the tip with a Tesla coil (page 380) held  $\frac{1}{2}$  to  $\frac{1}{4}$  in. from the surface.

The completed items should be assembled together for inspection and approval by the instructor.

**Suggestions for Further Work.** As soon as the student has acquired reasonable proficiency in the above operations, he may proceed to more difficult operations such as joining capillary tubing or small-diameter tubing and making ring seals and closed circuits of tubing. Further directions will be found in the reference books. Flaring the end of the tubing and blowing small bulbs are also good exercises.

Metal-to-glass seals are required in certain types of work. Platinum wire can be sealed into soft glass and also in Pyrex if the diameter is small; these seals, however, are not recommended for vacuum work. Tungsten in small diameters can be sealed directly into Pyrex, and larger diameters can be sealed if an intermediate grading glass is used. Special alloys have been tailored to order for sealing to low-expansion glasses like Pyrex. One or more grading glasses are usually required for the Pyrex-to-metal seal. Kovar† and Fernico‡ are examples and can be obtained in the form of tubing, wire, and various fabricated shapes, either alone or already sealed to glass. The latter is the preferred way to obtain these materials, since the sealing operation is an

† Manufactured by Stupakoff Ceramic and Manufacturing Co., Latrobe, Pa.

‡ Manufactured by General Electric Co., Schenectady, N.Y.

art which requires considerable practice. Copper can be sealed into either soft glass or Pyrex by the Housekeeper<sup>4</sup> method, which requires that the copper be very thin where it is sealed to the glass.

### References

1. Frary, Taylor, and Edwards, "Laboratory Glass Blowing," 2d ed., McGraw-Hill Book Company, Inc., New York (1928).
2. Heldman, "Techniques of Glass Manipulation in Scientific Research," Prentice-Hall, Inc., Englewood Cliffs, N.J. (1946).
3. "Laboratory Glass Blowing with Pyrex Brand Glasses," Corning Glass Works, Corning, N.Y. (1952).
4. Strong, "Procedures in Experimental Physics," Chap. I, Prentice-Hall, Inc., Englewood Cliffs, N.J. (1939).
5. Wright, "Manual of Laboratory Glass-blowing," Chemical Publishing Co., Brooklyn, N.Y. (1943).

## 57. HIGH VACUUM

This experiment illustrates some of the elements of importance in the production and measurement of low pressure.

**Theory.** In vacuum technology, pressures are usually expressed in *microns* of mercury. The cgs unit of pressure, 1 dyne cm<sup>-2</sup>, is called the *microbar*. The relations between these units can be summarized as follows:

$$1 \text{ micron} = 1 \mu = 10^{-3} \text{ mm Hg} = 10^{-6} \text{ m Hg} = 1.3332 \mu\text{bar}$$

The volume unit used commonly is the liter. Quantity of gas, at a particular temperature, is conveniently expressed as liter-microns, or the equivalent in other pressure and volume units.

The speed  $S$  of a pumping system which is removing gas from a vessel of fixed volume  $V$  may be defined† by the relation

$$S = - \frac{dv}{dt} = - \frac{V}{P} \frac{dP}{dt} \quad (1)$$

where  $dv$  = volume of gas, measured at temperature and pressure  $P$  of vessel, removed in time  $dt$

$dP$  = corresponding change in pressure

The pumping speed can be regarded as a *conductance*, since it has the dimensions of volume of gas removed per unit time, and is customarily expressed in liters per second.

The speed of the pumping system determines the time required to reduce the pressure in the volume  $V$  from one specified level to another.

† A more realistic definition takes into account the finite low-pressure limit the pumping system can reach,  $P_s$ , and gives  $S(P - P_s) = -VdP/dt$ . If it is assumed that  $P_s$  is negligibly small compared with  $P$ , Eq. (1) follows directly.

This problem is considered in detail by Dushman,<sup>2</sup> but for the case where  $S$  is constant over the range from the initial pressure  $P_1$  to the final pressure  $P_2$ , integration of Eq. (1) gives for the required pumping time

$$t_2 - t_1 = \frac{V}{S} \ln \frac{P_1}{P_2} \quad (2)$$

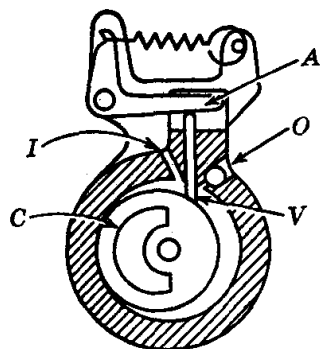


FIG. 94. Principle of operation of typical rotary oil pump.

#### VACUUM PUMPS

In laboratory practice two types of vacuum pumps are commonly employed, mechanical and diffusion pumps. The principle of operation of a typical rotary oil pump is indicated in Fig. 94. The vane  $V$  is kept in close contact with the eccentric cylinder  $C$  by the spring-loaded rocker arm  $A$ . As the cylinder rotates in the oil-filled chamber, air is drawn in at the inlet tube  $I$  and driven around to the outlet at  $O$ . The vane  $V$  and the close fit of the eccentric rotor with the stator produce an efficient pumping action. The entire pump unit is oil-immersed; the ball check shown at  $O$  prevents backflow of oil when the rotor is stopped. Ordinarily, two such units, with rotors on a common shaft, are connected in

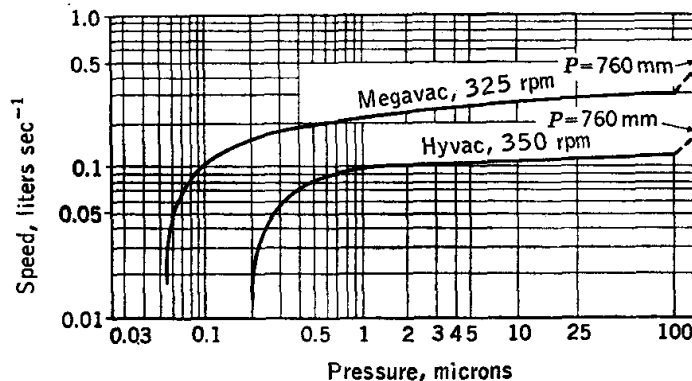


FIG. 95. Performance curves for typical rotary oil pumps.

series to form a single compound pump. The pumping speed of such a rotary oil pump depends on its size, but in any case drops off rapidly as the micron range is approached. Performance curves for typical laboratory pumps are shown in Fig. 95.

For efficient pumping at low pressures the diffusion pump is employed. A typical mercury-vapor pump is illustrated in Fig. 96. The pressure in the pump and system is first reduced by means of a rotary oil pump, the *forepump*, connected to the outlet  $O$ . A high-velocity stream of mercury vapor generated in the boiler by electrical heating is then driven through the nozzle  $N$ . Air molecules diffuse through the inlet tube  $I$  into the



vapor stream and are driven downward by collisions with mercury atoms. The latter, because of their relatively high mass, are only slightly deflected and proceed to the water-cooled wall, where they are condensed and returned to the boiler. The gas molecules are driven down to the outlet, where they are removed by the forepump. Very high pumping speeds and low ultimate pressures can be obtained by this pump. The pressure maintained by the forepump must be below a critical value, determined by the diffusion-pump design and the power input to the boiler, if the diffusion pump is to work. This necessary forepressure may be increased by the use of multistage diffusion pumps.

Mercury as the working fluid has the disadvantage that its vapor pressure at room temperature is relatively high, about  $1 \mu$ , so that an efficient cold trap must be used between a mercury-vapor pump and a system in which mercury cannot be tolerated. High-molecular-weight organic pumping fluids, such as butyl sebacate, are commonly used instead of mercury, since they have vapor pressures at room temperature which are negligible for practically all purposes. They are, however, subject to cracking if overheated and must be heated only under vacuum because of susceptibility to air oxidation. The use of silicone pumping fluids offers a solution to these particular problems.

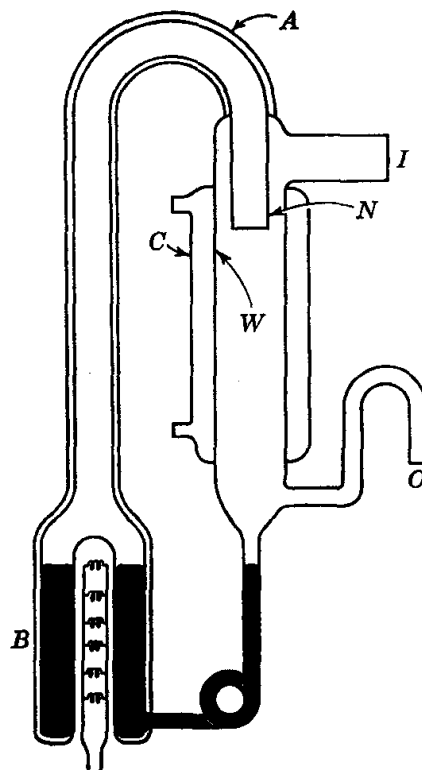


FIG. 96. Typical mercury-vapor diffusion pump.

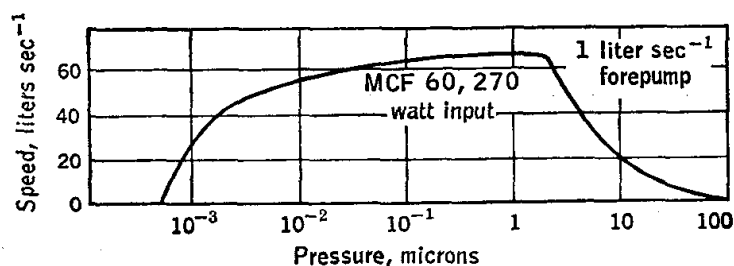


FIG. 97. Performance curve for a small three-stage diffusion pump, Type MCF 60, Consolidated Vacuum Corp.

Modern oil diffusion pumps can produce pressures below  $10^{-6}$  mm Hg at room temperature without cold traps, and pumping speeds as high as 20,000 liters  $\text{sec}^{-1}$  at  $10^{-4}$  mm Hg are available with large-scale commercial units. In Fig. 97 is given a performance curve for the small

three-stage commercial pump illustrated in Fig. 98. On the low-pressure side the measured pumping speed drops to zero at a pressure fixed by the vapor pressure of the pumping fluid; the actual pumping speed for *air* remains high at this same pressure, as may be shown by the use of a pressure gauge with a liquid-air trap.

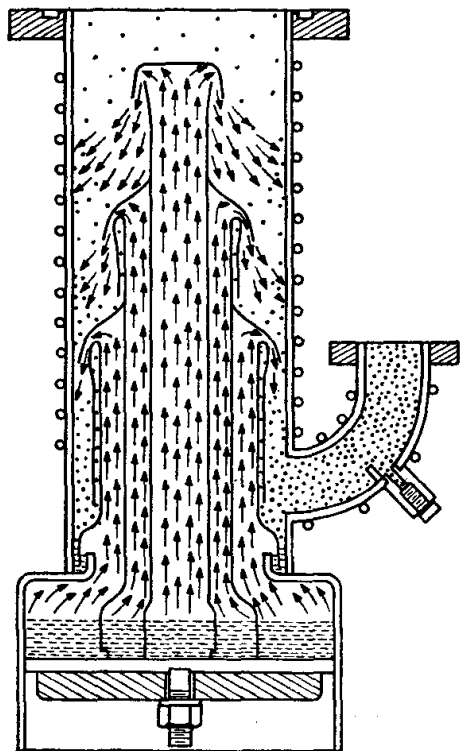


FIG. 98. Three-stage oil diffusion pump, Type MCF, Consolidated Vacuum Corp.

A diffusion pump can remove vapors (water, organic liquids) which would condense into the oil of the forepump and seriously impair its performance. Where such a possibility exists, the forepump should be protected by a suitable trap. Drying towers filled with solid desiccants, etc., are of limited utility when it is desired to conserve the speed of the pump. Liquid-cooled traps can provide very efficient performance. For routine forepump protection, cooling with solid carbon dioxide is in general adequate; a mixture of solid carbon dioxide and *trichloroethylene* is used. Trichloroethylene is now readily available commercially, and should always be used, instead of the inflammable acetone which was commonly used in the past. It should be remembered that the vapor pressure of ice at the temperature of solid carbon dioxide is about  $0.1 \mu$ .

Liquid air is a very effective trap refrigerant but involves an explosion hazard if organic materials are brought into contact with it, through breakage of a glass trap, for example. The problem is intensified by the fractionation that takes place on evaporation of the liquid air, which leaves the residual liquid progressively richer in oxygen. Liquid-air traps are preferably made of metal, or else a metal jacket should be used around a glass trap so that the latter does not come in direct contact with the liquid air.

Liquid nitrogen has marked advantages over liquid air as a refrigerant because of its chemical inertness. It may be prepared by fractionation of liquid air; if only a moderate quantity is required, it may be produced by expansion of tank nitrogen through a throttle valve after precooling by passage through a copper tubing coil immersed in liquid air.

Of increasing importance is the use of gettering and ion pumping to attain high vacuum.<sup>4</sup> No coolant traps or baffles are required, nor are

there present any of the organic vapors or other volatile materials common to the earlier pumps. The lowest pressure obtainable is about  $10^{-7}$  mm Hg.

#### CONDUCTANCE OF A PUMPING SYSTEM

The speed of the pumping system depends not only on the intrinsic speed of the pump proper,  $S_0$ , but also on the conductance of the connection between the pump and the vessel to be evacuated. For the connecting tube this conductance  $F$  relates the quantity  $Q$  of gas transferred per unit time to the pressure drop  $\Delta P$  across the tube:

$$Q = F\Delta P \quad (3)$$

In vacuum work the experimental conditions are in general such that turbulent flow of gas through the connecting tubes is not encountered. At the higher pressures of interest Poiseuille's law of viscous flow applies:

$$n = \frac{\pi}{256\eta} \frac{d^4}{l} \frac{P_2^2 - P_1^2}{RT} \quad (4)$$

where  $n$  = number of moles of gas (assumed to obey ideal-gas law) which flow per second through a cylindrical tube

$d$  = diameter of tube, cm

$l$  = length of tube, cm

$P_2, P_1$  = inlet and outlet pressures,  $\mu$ bars (i.e., dynes  $\text{cm}^{-2}$ )

$\eta$  = coefficient of viscosity of gas, poises, at  $T^\circ\text{K}$

Since  $nRT$  can be set equal to  $PV$ , the quantity of gas  $Q$  in microbar cubic centimeters transferred per second can be written

$$Q = \frac{\pi d^4}{256\eta l} (P_2^2 - P_1^2) = \frac{\pi d^4}{128\eta l} \frac{P_2 + P_1}{2} (P_2 - P_1) \quad (5)$$

As  $(P_2 + P_1)/2$  is the average pressure in the tube in microbars,  $\bar{P}_{\mu\text{bar}}$ , Eq. (3) shows that the conductance  $F_v$  of the tube in the viscous-flow region is given by

$$F_v = \frac{\pi d^4}{128\eta l} \bar{P}_{\mu\text{bar}} \text{ cm}^3 \text{ sec}^{-1} \quad (6)$$

At very low pressures a different relation obtains because the mechanism of flow changes. As the pressure is reduced, the mean free path of the molecules increases; for air at  $25^\circ\text{C}$ , the mean free path  $\lambda$  in centimeters is given by  $\lambda = 5.09/P_\mu$ , where  $P_\mu$  is the pressure in microns. When the mean free path becomes larger than the diameter of the tube through which the gas is moving, collisions between molecules become of negligible importance compared with collisions of the molecules with the

tube walls. The gas is then referred to as a "Knudsen gas," because of the contributions made by the physicist Knudsen to the kinetic theory of gases for such conditions. Each molecule then moves in essential independence of the others. The wall, to an incident molecule, is an extremely rough surface. It is hence legitimate to assume that the direction in which a molecule will bounce off the wall will be independent of the angle of incidence calculated on the assumption of a perfectly smooth surface. The resulting transfer of gas down the tube, termed *molecular flow* by Knudsen, can then be treated by statistical methods to give the following result for the conductance  $F_m$  for a cylindrical tube of diameter  $d$  centimeters and length  $l$  centimeters:

$$F_m = \frac{1}{3} \sqrt{\frac{\pi}{2}} \frac{1}{\sqrt{\rho_1}} \frac{d^3}{l} \text{ cm}^3 \text{ sec}^{-1} \quad (7)$$

Here  $\rho_1$  is the gas density in grams per cubic centimeter at a pressure of 1  $\mu$ bar. It should be noted that in the molecular-flow region the conductance is independent of pressure.

At intermediate pressures the flow is partly viscous and partly molecular. The general expression given by Knudsen must be used for this range:

$$F = F_v + F_m Z = F_v + F_m \left( \frac{1 + \frac{d \sqrt{\rho_1}}{\eta} \bar{P}_{\mu\text{bar}}}{1 + \frac{2.47d \sqrt{\rho_1}}{2\eta} \bar{P}_{\mu\text{bar}}} \right) \text{ cm}^3 \text{ sec}^{-1} \quad (8)$$

For air at 25°C, with the average pressure expressed in microns,  $d$  and  $l$  in centimeters, and  $F$  in liters per second,

$$F = 0.177 \frac{d^4}{l} \bar{P}_\mu + 12.2 \frac{d^3}{l} Z \quad (9)$$

$$Z = \frac{1 + 0.246 \bar{P}_\mu d}{1 + 0.304 \bar{P}_\mu d} \quad (10)$$

The factor  $Z$  varies between 0.81 at high pressures and 1 at low pressures. As pointed out by Hecker,<sup>3</sup> if  $\bar{P}_\mu d$  is greater than 1000, the flow is over 95 per cent viscous, while for  $\bar{P}_\mu d$  less than 2, it is over 95 per cent molecular. An alternative criterion for molecular flow given by Knudsen states that the flow is over 95 per cent molecular if  $d/\lambda$  is less than 0.4. The molecular-flow range is of primary concern in high-vacuum work, but conductance calculations for the intermediate pressure range are often required in the design of connecting lines between diffusion pumps and forepumps (see below).

The quantity of gas moved per second through two tubes in series is the same for each tube. If the conductances of the tubes are  $F_1$  and  $F_2$ ,  $F$  that of the series combination,  $P_3 - P_2$  the pressure drop across the first tube and  $P_2 - P_1$  that across the second,

$$Q = F_1(P_3 - P_2) = F_2(P_2 - P_1) = F(P_3 - P_1) \quad (11)$$

so that

$$\frac{1}{F} = \frac{1}{F_1} + \frac{1}{F_2} \quad (12)$$

This result may also be obtained by thinking of the conductance as the reciprocal of a resistance to flow. The additivity of resistances in series again leads to Eq. (12).

Bends and elbows in a tube of constant diameter and axial length have relatively little effect on the conductance at low pressures. As the mean free path becomes large compared with the diameter of the tube, however, molecules experience a difficulty getting into the tube from an adjacent region of relatively larger cross section. This difficulty may be characterized quantitatively by a conductance for the tube *entrance*, which for a circular aperture of diameter  $d$  can be written approximately as

$$F_0 = \frac{1}{4} \sqrt{\frac{\pi}{2}} \frac{d^2}{\sqrt{\rho_1}} \quad (13)$$

For molecular flow the resultant conductance for a tube plus the entrance is obtained by combining the relations of Eqs. (7) and (13) in accordance with Eq. (12). The result for air at 25°C is

$$F = \frac{9.17d^2}{1 + \frac{3}{4}l/d} \text{ liters sec}^{-1} \quad (14)$$

Consider a composite pumping system of speed  $S$  consisting of a pump of speed  $S_0$  in series with a connecting tube of conductance  $F$ . The rate  $Q$  at which this system removes gas from a vessel where the pressure is  $P$  must be equal to  $SP$ , from the definition of pumping speed. Similarly,  $Q = S_0P_0$ , where  $P_0$  is the pressure at the pump entrance proper. Also, since the same gas is driven through the conductance  $F$  by the pressure drop  $(P - P_0)$ ,  $Q = F(P - P_0)$ . Hence

$$Q = SP = S_0P_0 = F(P - P_0) \quad (15)$$

and

$$\frac{1}{S} = \frac{1}{S_0} + \frac{1}{F} \quad (16)$$

This relation is of basic importance in vacuum technique. It must be

utilized in the design of high-vacuum systems to obtain efficient use of the pump employed.

#### MEASUREMENT OF SPEED OF VACUUM PUMPS

A number of methods are available for the measurement of the speed of vacuum pumps. The procedure suggested by Howard<sup>5</sup> is convenient for pumps of moderate speed. The apparatus used is shown in Fig. 99. The capillary tube and the 1-mm-bore stopcock *C*, whose plug is grooved

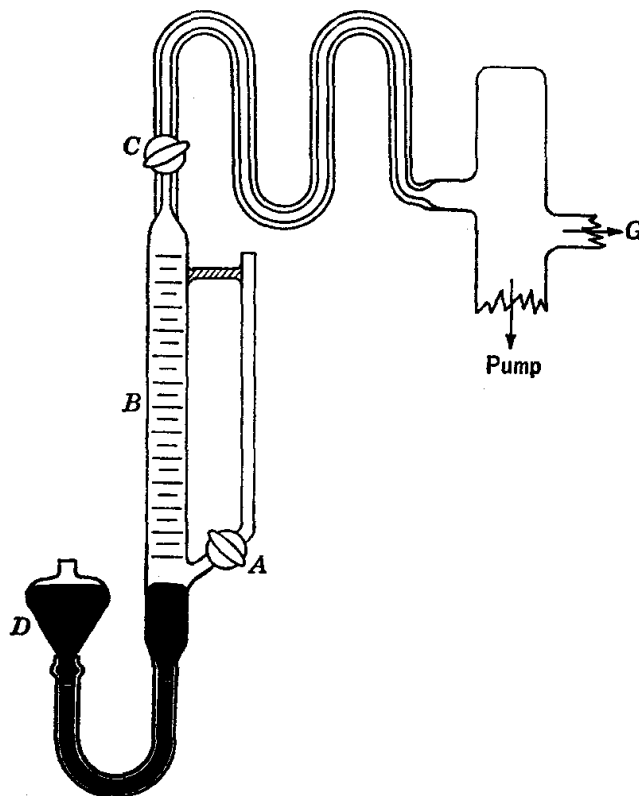


FIG. 99. Apparatus for Howard's method for the measurement of the speed of a pump.

slightly at the edge of the hole to facilitate adjustment of the leak rate, permit a slow leakage of air from the 50-ml gas burette *B*. Initially the stopcock *C* is closed and the pump set in operation. The mercury leveling tube *D* is lowered so that stopcock *A* can be opened to the atmosphere. Stopcock *C* is then opened carefully until the pressure maintained by the pump, as measured by a McLeod gauge connected at *G*, is approximately equal to the pressure for which the pumping speed is to be determined. The pressure in the system is checked periodically, and when it has become constant, the mercury level in the burette is raised slowly past the stopcock *A*, which is then closed. The position of the mercury level in the burette, the time, and the barometric pressure are recorded. The

leveling bulb is progressively raised as required to keep the pressure in the burette constant as gas is removed by the pump. When an appropriate volume of air has been pumped out, stopcock *C* is closed and the time and burette reading are recorded. The pumping speed is calculated by multiplying the volume of air removed per second by the ratio of the burette pressure to the pump working pressure.

In another useful method the gas removed by the pump is delivered by a flow tube whose conductance can be calculated; the experimental arrangement is shown in Fig. 100.

The bulbs *B*, *B'* should be of about 1-liter volume. The appropriate dimensions for the flow tube *T* depend on the kind of pump under test,<sup>1</sup> but for the smaller laboratory diffusion pumps a tube of 1 cm diameter and 50 cm length can be used for the low-pressure range. Initially the capillary leak (a sensitive high-vacuum needle valve should be used) is closed and the pump started. The leak is then opened gradually until the pressure *P*<sub>1</sub> has reached the level for which the speed is desired. When

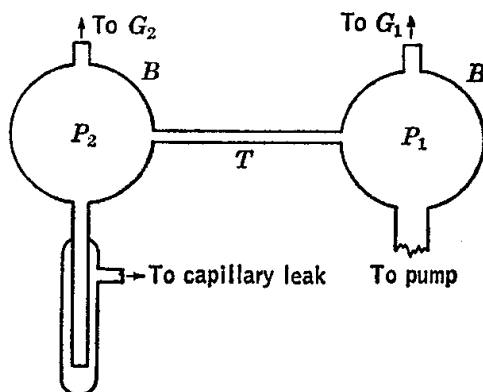


FIG. 100. Apparatus for flow-tube method for pumping-speed determination.

the pressures *P*<sub>2</sub> and *P*<sub>1</sub> have become constant (as measured by the vacuum gauges *G*<sub>2</sub> and *G*<sub>1</sub>), the rate of flow of gas through the tube can be evaluated by use of the calculated conductance *F* of the flow tube.

$$Q = F(P_2 - P_1) \quad (17)$$

The pump speed is then given by  $Q/P_1$ , provided the pump is connected directly to *B'*. Otherwise the conductance of the connecting tube must be taken into account [cf. Eq. (16)].

#### VACUUM GAUGES

The McLeod gauge, one design of which is shown in Fig. 101, is a basic instrument for low-pressure measurements. A large volume of gas, *V*, at the unknown pressure *p*, is compressed to a small volume *v*, and the corresponding pressure *P* is measured; *p* is then calculated from the relation  $p = Pv/V$ , which holds quite accurately for the low pressures involved. In use, the high-vacuum stopcock *C* is gradually opened, and as the pressure in the gauge is reduced, the two-way stopcock *T* is opened carefully to the auxiliary vacuum line to keep the mercury from rising appreci-

ably in the connecting tube. To make a pressure measurement the control stopcock *T* is opened *slightly* to the atmosphere (a capillary leak here may be used to prevent an undesirable rush of air into the vessel) to produce a slow rise of mercury into the gauge. When the rising mercury reaches the cutoff *D*, the gas in the gauge bulb *B* is trapped at the pressure

to be determined. For highest sensitivity in the pressure measurements, this gas is compressed until the mercury meniscus in the reference capillary *R* has reached the level of the top of the gauge capillary *W*. The difference of *h* millimeters in the levels of the mercury in the two capillaries represents the final pressure of the compressed gas. The reference capillary is made of the same tubing as the gauge capillary in order to eliminate the effect of the capillary depression.

Previous calibration measurements give the total volume *V* of the bulb *B*, and the volume per millimeter length, *v*<sub>0</sub>, of the capillary *W*. The gas volume at the unknown pressure *p* is *V*, while at the final pressure *h* millimeters of mercury it is *v*<sub>0</sub>*h*, so that

$$p = \frac{v_0 h}{V} h = \frac{v_0}{V} h^2 \text{ mm Hg} \quad (18)$$

The volumes *V* and *v*<sub>0</sub> must be expressed in the same units. The various levels *h* corresponding to initial gas pressures of 10<sup>-6</sup>, 10<sup>-3</sup>, and intermediate values, in millimeters of mercury, are calculated, and the gauge calibration scale is

constructed. This scale is termed the quadratic scale, or the logarithmic scale.

A different method of operation can be used to extend the range of the gauge to higher pressures than can be measured on the quadratic scale. The gas in the bulb *B* is compressed until the meniscus in the bulb has reached the reference mark *S* in the lower capillary section. The final volume of the gas is then always equal to the volume *V*<sub>1</sub> of the section above *S*. The final pressure is read as the height *h'* millimeters above the

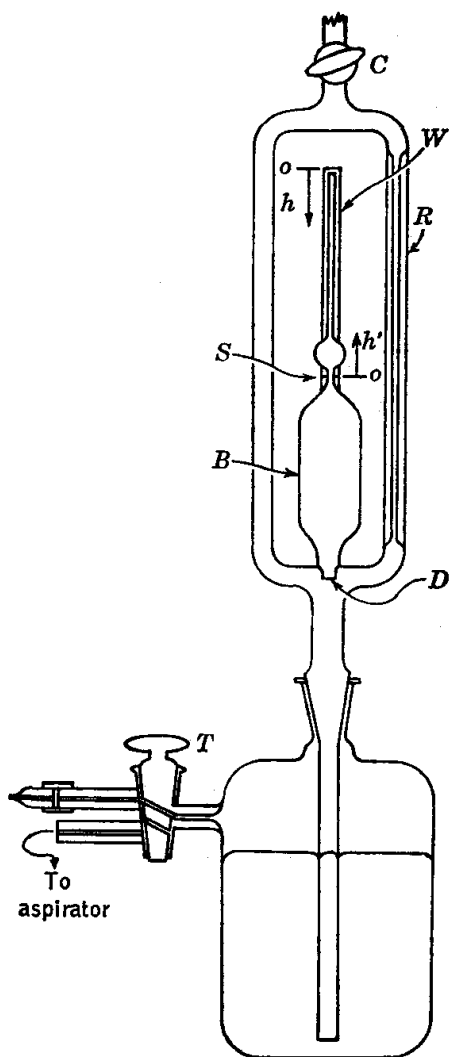


FIG. 101. McLeod gauge.



level  $S$  of the mercury meniscus in the reference capillary  $R$ . Then

$$p = \frac{V_f}{V} h' \text{ mm Hg} \quad (19)$$

This method thus yields a linear scale. A typical laboratory McLeod gauge will have a range of  $10^{-1}$  to  $10^{-6}$  mm on the quadratic scale and of  $10^{-1}$  to 2 mm on the linear scale.

After the pressure reading has been made, the stopcock  $T$  is opened to the vacuum line and the mercury drawn out of the gauge. When the gauge pressure is raised to the atmospheric level, the reservoir pressure must be increased at the same rate. The care required in this process is one of the main disadvantages of this particular design. In another version the gauge bulb is connected to a tube at least 760 mm long, connected to a mercury well provided with a plunger with a threaded top. When the plunger is forced down and the threads engaged, the mercury rises in the gauge. The threaded section facilitates the fine adjustment of the mercury level. The tube and well can be made of metal to provide a very rugged construction.

Small McLeod gauges are available in which a flexible or rotating connection to the system permits the whole gauge to be tipped or rotated as required to force mercury into the gauge bulb.

The sensitivity of the McLeod gauge is governed by the ratio  $v_0/V$ . It is not practical to make  $V$  larger than 500 ml, because of the weight of such a large volume of mercury. Similarly, the capillary diameter should not be less than 0.5 mm because of the tendency of mercury to stick in small capillaries. The mercury used must be quite pure, and the gauge itself carefully cleaned before filling. An efficient cold trap is required when a McLeod gauge is used with a system from which mercury must be excluded. This gauge cannot be degassed, nor can it be used to measure the pressure of a vapor which condenses to a liquid when compressed into the gauge capillary.

The basic importance of the McLeod gauge is that it is an *absolute* pressure gauge, because the calibration scale can be calculated directly from the measured physical characteristics of the instrument. As such it can be used as a reference standard† for the calibration of other types of gauges commonly employed in vacuum work.

At low pressures, the thermal conductivity of a gas becomes directly proportional to the pressure when the distance between the hot and cold surfaces becomes smaller than the mean free path. This property is exploited in the *thermocouple gauge* and the *Pirani gauge*. In the thermo-

† The Knudsen radiometer gauge, discussed in detail by Dushman,<sup>2</sup> is also an absolute gauge, but is much more difficult to construct and use.

couple gauge a constant current is passed through a resistance wire, to the center of which a thermocouple is attached. The temperature of the wire changes as the pressure changes because of the variation of the thermal conductivity of the gas, and this change is indicated by a microammeter connected in series with the thermocouple. The thermocouple gauge is rugged and relatively inexpensive and has a useful range extending from about 1 to 500  $\mu$ . In the Pirani gauge the resistance wire is connected as one arm of a Wheatstone bridge; the extent of the bridge unbalance, as registered by a microammeter connected as the bridge detector, indicates the pressure in the gauge. A second resistance filament, identical with the first but sealed off in a tube under high vacuum, is used in the opposite arm of the bridge to compensate for room-temperature changes, etc., to obtain better gauge performance. The useful range of a typical commercial Pirani gauge extends from 1 to 500  $\mu$ . The Pirani gauge is subject to erratic zero shift, and its calibration must be checked regularly. A separate calibration is required for every different gas for both of these thermal conductivity gauges.

For measurements of very low pressures *ionization* gauges are employed. The electrode arrangement in the conventional type is similar to that of the triode illustrated in Fig. 164, except that a filamentary cathode and more rugged grid construction are used. Electrons emitted from the heated cathode are accelerated toward the concentric helical grid, which is maintained *positive* with respect to the cathode by a suitable power supply. In collisions between these electrons and gas molecules present, ionization of molecules takes place. The positive ions so produced are attracted to the cylindrical plate, which is made *negative* with respect to the cathode. The resulting current in the plate-cathode circuit is proportional to the pressure of the gas in the gauge provided the electron current from cathode to grid is held constant. The plate current may be measured directly with a microammeter in the less sensitive instruments, but for low-pressure work the potential drop caused by the flow of the current through a series resistance is measured after amplification. The gauge sensitivity is only slightly dependent on the plate potential provided the latter is at least  $-10$  volts relative to the cathode.

This particular electrode arrangement, i.e., plate negative and grid positive, is utilized to provide increased sensitivity. The grid has a relatively small area, so most of the electrons accelerated toward it pass through the helix and continue on toward the plate. As they approach the negative plate they are repelled and move back toward and through the grid. This process continues and increases considerably the average distance traveled in the gauge by the electrons before they are captured by the grid. The lengthened path means an increased number of ionizing collisions with gas molecules, and hence increased gauge sensitivity.

The standard ionization gauge can measure gas pressures as low as  $10^{-8}$  mm Hg. The upper pressure limit is about  $5 \mu$ ; it is not possible to operate this gauge at higher pressures without harming it. Commonly, a thermocouple or Pirani gauge is used to show when the pressure is low enough to permit the operation of the ionization gauge.

A second type of ionization gauge is the Phillips gauge. In this unit a high-voltage ( $\sim 2000$  volts) discharge is created between a cold cathode and a ring-shaped anode. The resulting current depends on the gas pressure and is measured directly by a microammeter in the grounded side of the high-voltage supply. Small permanent magnets are suitably arranged in the gauge to cause the electrons to move to the anode in spiral paths to obtain increased sensitivity. The Phillips gauge has a range from about  $10^{-2}$  to  $25 \mu$ . It is a rugged instrument and remains unharmed when subjected to atmospheric pressure. The discharge aids in the removal of adsorbed surface gases within the gauge, making it unnecessary to degas this gauge for low-pressure measurements. The response of all ionization gauges depends on the nature of the gas present, so separate calibrations are required for different gases. It should be emphasized also that in the use of any vacuum gauge to determine the pressure in a system, particularly if that pressure is not constant, the possible effect of the conductance of the connection to the gauge must be considered.

The general ranges of applicability for the several vacuum gauges are summarized in Table 1.

TABLE 1. RANGES OF VACUUM GAUGES IN MILLIMETERS OF MERCURY

Mercury manometer.....	1-1000
Butyl phthalate manometer.....	0.01-10
Pirani gauge.....	$10^{-4}$ -0.5
Thermocouple gauge.....	$10^{-3}$ -0.5
McLeod gauge.....	$10^{-6}$ -2
Phillips gauge.....	$10^{-5}$ - $10^{-2}$
Knudsen gauge.....	$10^{-6}$ - $10^{-2}$
Ionization gauge.....	$10^{-8}$ - $10^{-3}$

One of the basic problems in the attainment of very low pressures is the "outgassing" of surfaces, particularly of metals, as the pressure is reduced, due to the release of adsorbed gases or vapors. The best method for elimination of this interference is a "degassing" procedure in which the system is heated to drive off these materials. Adsorbed water comes off at about  $200^{\circ}\text{C}$ , and other gases, mainly carbon monoxide, at higher temperatures. Obviously, the whole system must be degassed at once for efficient performance, and no materials containing volatile components, such as vacuum waxes, Glyptal, rubber, brass (zinc volatilizes easily), etc., can be present. Without degassing, the best vacuum that

can be expected is about  $1 \times 10^{-6}$  mm, and protracted pumping may be required to do this well. For good results vacuum gauges, such as ionization gauges, must be degassed. Ordinarily, provision is made in the gauge-control unit for degassing by electrical heating of the gauge elements.

In any vacuum system, connections between the various sections present a problem. In metal systems, flange joints with Neoprene gaskets are often used; for a demountable joint in a section which must be degassed, copper gaskets can be employed. Great convenience can be obtained by use of O-Ring gaskets† with appropriately machined flanges; with these units, connections between metal sections, or between metal and glass sections, are easily made, as are effective seals on rotating or sliding rods or tubes which enter the system. For glass systems and moderately high vacua, standard taper joints can be used with vacuum wax or a good grade of vacuum grease. Stopcocks used should be of the specially processed high-vacuum type and of a suitably large bore for the particular application.

#### LEAK DETECTION

The detection and elimination of leaks is an inevitable step in the setting up of a vacuum system. All leaks must obviously be located, and very small ones may be extremely difficult to find. A complication in the latter case is the so-called "virtual leaks," which actually are due to the continuous evolution of gas inside the system. If it is possible to build up an excess air pressure within the system, leaks may be found by painting the outside in the suspected areas with a soap solution. In glass sections moderate leaks may be found with a Tesla coil; the high-frequency discharge will jump to a pinhole or crack in the glass, illuminating it brightly. Precautions must be taken to avoid puncturing thin-walled areas by use of too violent a discharge. Neither of these first two methods is useful for small leaks.

Because their response depends upon the nature of the gas present as well as its pressure, the thermal conductivity and ionization gauges can be used in leak hunting in appropriate pressure ranges. When the area including the leak is sprayed with acetone, for example, the acetone is drawn into the system and causes a change in the reading of the gauge. The Pirani gauge is considered more sensitive than the thermocouple gauge for this work. The ionization gauge can be used when the leaks are small enough so that an appropriately low pressure can be maintained in the system.

† O-Ring gaskets are available from Linear, Inc., Philadelphia. The manufacturer's recommendations on their use should be followed in detail.

Special leak-detecting units are available commercially. The halogen-sensitive type utilizes the increase in the emission of positive ions (presumably originating from alkali metal impurities) from hot platinum which occurs when halogen-containing molecules strike the electrode surface; carbon tetrachloride, chloroform, or Freon 1-1 is commonly used with this gauge. Extremely high sensitivity is obtained in the helium-leak detector by use of the mass spectrometer principle to obtain a specific response to helium. Leaks are located by virtue of the response when a stream of helium is played over the outside of the system.

The detailed treatment of problems and procedures in vacuum technique given by Dushman<sup>2</sup> is the basic reference in this field. Other general treatments include those of Jnanananda,<sup>6</sup> Reimann,<sup>7</sup> Yarwood,<sup>11</sup> and Hecker.<sup>3</sup> A series of papers on applications of engineering interest and presented at a symposium on high vacuum have been published together.<sup>10</sup> Modern vacuum pumping systems and equipment are also described in a paper by Sullivan.<sup>9</sup>

**Apparatus.** Rotary oil pump(s); mercury diffusion pump; oil diffusion pump; Howard pumping-speed apparatus; flow-tube pumping-speed apparatus; McLeod gauge(s); Tesla coil; thermocouple gauge, Pirani gauge, ionization gauge, and control units; acetone.

**Procedure. Part A.** The pumping speed for a rotary oil pump at a pressure near atmospheric is determined by the flow-tube technique. In this case a flow tube 1 m long and of 3 mm internal diameter is suitable; one end is open to the atmosphere, the other is connected to a short section of larger-diameter tubing which leads directly to the pump. A differential manometer is used to measure the pressure drop across the flow tube. One side of this manometer is connected through a stopcock to the low-pressure side of the flow tube; the other is open to the atmosphere. With the stopcock closed, the pump is started. The stopcock is then opened slowly, and when the pressure drop indicated by the manometer has become constant, its value is recorded, together with the barometric pressure and the dimensions of the flow tube. It is convenient to use an oil as the manometer fluid; its density will be specified by the instructor.

**Part B.** The rotary pump is then connected as the forepump for a mercury diffusion pump. The latter is connected to a manifold to which a McLeod gauge and a Howard pumping-speed assembly are attached. The stopcocks leading to these two units are closed, and the forepump is started. After a few minutes the stopcock connecting the McLeod gauge is opened, and a pressure measurement is made with the McLeod gauge, as described above. The pressure is rechecked until it has dropped below 100  $\mu$ . The water line to the diffusion-pump condenser jacket is then

turned on, and power applied to the pump heater. As the pump goes into operation, the pressure in the system will drop rapidly, and the McLeod gauge is used to measure the resulting low pressure, which should soon reach  $10^{-2} \mu$ . The capillary leak of the Howard apparatus is then opened slowly until a pressure of about  $1 \mu$  is found with the McLeod gauge. The pumping speed of the diffusion pump is then determined at this pressure as described under Theory. Finally, the mercury is drawn down out of the gauge, and the gauge stopcock *C* is closed. The diffusion-pump heater is turned off, then the forepump, and the system slowly opened to the atmosphere by means of a stopcock connected to the forepump line. The gauge is then returned to atmospheric pressure also. After the diffusion-pump boiler has cooled, the condenser water supply is shut off.

*Part C.* The calibration of a McLeod gauge is undertaken next. A gauge-bulb assembly will be supplied by the instructor, together with a piece of the tubing used for the gauge capillary. The clean and dry gauge bulb is weighed empty. It is then filled completely with water to the cutoff at *D* (Fig. 101) and reweighed. A hypodermic syringe with a long needle will facilitate the filling of the capillary. The temperature of the water is recorded. The bulb is emptied with the help of an aspirator, placed in a drying oven, and reevacuated, with the aspirator, while warm, to assist in drying it. A thread of mercury is drawn into the capillary tube supplied, and its length is measured. The mercury is emptied into a tared weighing bottle, and its weight determined.

*Part D.* Measurements are made with an oil diffusion pump attached to a flow-tube apparatus like that shown in Fig. 100. It is convenient to use two thermocouple gauges, one to measure the forepressure, and the other on the high-vacuum side of the diffusion pump to indicate when it is safe to turn on the ionization gauge connected at *G*<sub>1</sub>. The gauge *G*<sub>2</sub> may be a Pirani gauge or a Phillips gauge.

All stopcocks connected to the system are closed, the forepump is turned on, and several minutes allowed for the pressure in the system to be reduced below the millimeter level. The thermocouple forepressure gauge is turned on, and when the pressure has dropped below  $200 \mu$ , the diffusion-pump heater can be connected. For an air-cooled pump the air supply is turned on, or the water in the case of a water-cooled pump; the manufacturer's operating instructions for the particular pump used should be carefully followed.

While the system pressure is being reduced, the Pirani or Phillips gauge is put into operation. When the pressure has dropped below  $1 \mu$ , the ionization gauge may be turned on. A pressure of the order of  $10^{-2} \mu$  should be reached after the diffusion pump has been in operation for some time. The speed of the latter is then determined for a pressure of about

0.2  $\mu$ , following the procedure described in the Theory section. The capillary leak connected to bulb *B* (Fig. 100) is slowly opened until the pressure  $P_1$  has reached the desired level. The pump is then allowed to operate until the pressures  $P_2$  and  $P_1$  become constant; their values are recorded, together with the dimensions given for the flow tube. The capillary leak must be opened very carefully for the protection of the ionization gauge. It is possible to dispense with the leak by connecting bulb *B* to the forepump, but the high-vacuum needle valve provides greater versatility.

*Part E.* The ionization gauge is turned off, and leak detection is illustrated by use of a tube with a pinhole leak in it connected through a high-vacuum stopcock to bulb *B*. This stopcock is now opened slowly, and the Tesla coil turned on and the discharge played over the tube surface to locate the leak. The readings of the various gauges still in operation are noted. The area around the pinhole is then sprayed with acetone, and the effect on the gauge response noted.

The diffusion-pump heater and the vacuum gauges are turned off. After the pump fluid has cooled, the forepump is stopped and the system pressure raised to 1 atm. This is conveniently done by opening a stopcock connected to the forepump line.

**Calculations.** *Part A.* The pressure drop across the flow tube used with the rotary oil pump is converted to millimeters of mercury, and the mean pressure in the tube and the pressure at the pump are calculated. The tube conductance in liters per second is calculated by use of Eq. (6), which for air at 25°C may be written as

$$F_v = 0.177 \frac{d^4}{l} \bar{P}_\mu \quad (20)$$

where  $\bar{P}_\mu$  is the mean pressure in microns, and  $d$  and  $l$  are in centimeters. The quantity of gas  $Q$  delivered per second to the pump by the flow tube is calculated by use of Eq. (17). Division of  $Q$  by the pressure at the pump gives the pumping speed.

*Part B.* The determination of pumping speed by the Howard method has been described in the Theory section.

*Part C.* The volume  $V$  of the McLeod gauge bulb is calculated from the weight of water it holds and the density of the water (page 613). The volume per millimeter length,  $v_0$ , of the gauge capillary is calculated from the weight of the mercury thread, its length, and the density of the mercury. A calibration scale for the gauge bulb is drawn for pressure in decade steps from  $10^{-6}$  to  $10^{-2}$  mm Hg, in accordance with Eq. (18).

*Part D.* The conductance of the flow tube used with the oil diffusion pump is calculated by use of the molecular-flow formula, Eq. (14).

The speed of the pump is then calculated as described for the other flow-tube experiment. For this pumping speed there is calculated the diameter for a 20-cm connecting tube necessary to give a conductance which would not reduce the pump speed by more than 10 per cent.

**Practical Applications.** High-vacuum techniques, fundamental in many research fields in natural science, are finding many practical industrial applications, such as in vacuum furnaces in metallurgy, the application of surface coatings by the vacuum evaporation process, freeze-drying of various materials, vacuum distillation of high-molecular-weight compounds, etc., as well as the more familiar examples of light bulbs, electron tubes, and Dewar flasks.

**Suggestions for Further Work.** The volume of the McLeod gauge capillary above the reference mark *S* (Fig. 101) may be determined, and a linear calibration drawn up. The formula for the conductance of an orifice, Eq. (13), may be derived from the relation  $n_s = \frac{1}{4}n \sqrt{8kT/m\pi}$  for the number of molecules striking a surface per square centimeter per second; *n* represents the number of molecules per cubic centimeter of gas, *m* is the mass per molecule, *k* the Boltzmann constant, and *T* the absolute temperature. The effect on the speed of a diffusion pump of variation in the heater-power dissipation or the forepressure may be studied. The conductance formula of Eq. (9) may be checked with tubes of various diameters and lengths. The vacuum evaporation of aluminum may be attempted; directions are given by Strong.<sup>8</sup>

### References

1. Backhurst and Kaye, *Phil. Mag.*, **47**, 918 (1924).
2. Dushman, "Vacuum Technique," John Wiley & Sons, Inc., New York (1949).
3. Hecker in Weissberger (ed.): "Technique of Organic Chemistry," 2d ed., Vol. IV, Pt. II, Chap. 6, "Distillation," Interscience Publishers, Inc., New York (1951).
4. Herb, Davis, Divatia, and Saxon, *Phys. Rev.*, **89**, 897 (1953); Davis and Divatia, *Rev. Sci. Instr.*, **25**, 1193 (1954).
5. Howard, *Rev. Sci. Instr.*, **6**, 327 (1935).
6. Jnanananda, "High Vacua," D. Van Nostrand Company, Inc., Princeton, N.J. (1947).
7. Reimann, "Vacuum Technique," Chapman & Hall, Ltd., London (1952).
8. Strong, "Procedures in Experimental Physics," Prentice-Hall, Inc., Englewood Cliffs, N.J. (1939).
9. Sullivan, *Rev. Sci. Instr.*, **19**, 1 (1948).
10. Various contributors, Symposium on High Vacuum, *Ind. Eng. Chem.*, **40**, 778-847 (1948).
11. Yarwood, "High Vacuum Technique," 2d ed., John Wiley & Sons, Inc., New York (1945).

## 58. ELECTRONICS

The properties of several types of electronic circuits are illustrated, and experience is provided with the application of the oscilloscope and other test instruments.

**Theory.** Chapter 27 includes an introduction to the principles of operation of the circuits considered here.



**Apparatus.** Experimental chassis and components for the construction of circuits of Figs. 102, 165, and 188; oscilloscope;† vacuum-tube voltmeter;‡ power supply (0 to 250 volts d-c, 6.3 volts a-c outputs);‡ tube manual; soldering iron or gun; needle nose pliers; diagonal cutter; hookup wire; screwdriver with insulated handle.

**Procedure.** Three of the circuits discussed in Chap. 27 are to be wired up and studied quantitatively. For this purpose units will be furnished with the heavier components mounted on a metal plate or plywood board, which serves as experimental chassis.

The schematic symbols and color-code conventions for electronic components are given in the Appendix. Tube-socket terminals (pins) are numbered clockwise as viewed from *below*, starting at the key or gap. The manufacturer's tube manual gives the pin numbers for the various electrodes. Any unused transformer leads should be doubled back and taped carefully, or otherwise insulated, to avoid accidental short circuits. All circuit wiring should be carefully rechecked *before* the power switch is turned on. Circuit changes should be made *only* when the power is off. Safety precautions in electronics work are emphasized on page 608.

The principles of operation of the auxiliary equipment, especially the oscilloscope and vacuum-tube voltmeter, should be studied in advance. In practice, the ground terminal of the oscilloscope should be connected to the ground of the circuit under study and an *insulated* test prod employed to pick up the voltage whose waveform is to be viewed.

**Part A.** The d-c power supply of Fig. 188 (page 589) is constructed, with:

$L = 15$  henrys, rated at 50 ma d-c current

$C = 10\ \mu\text{f}$ , 450 volts d-c (VDC) voltage rating

$R_b = 10,000$  ohms, 25 watts, fixed power resistor

$T =$  power transformer, 470 volts center-tapped (VCT) at 40 ma;  
5.0 VCT at 2.0 amp; 6.3 VCT at 2.0 amp

The experimental chassis is furnished with these units and the tube socket already mounted and the various component leads connected to binding posts‡ or barrier-type terminal strips. Interconnections are conveniently made by means of leads‡ consisting of lengths of test prod wire with insulated banana plugs or spade lugs, as appropriate, attached at the ends. Banana plugs and binding posts of the best quality should be used to ensure that secure connections are made. The power cord for connection to the 115-volt 60-cycle line is fused and is terminated at an outlet box which is fastened to the experimental chassis to provide a switch-

† Constructed easily and at relatively low cost from commercially available kits, such as those manufactured by the Heath Company, Benton Harbor, Mich.

‡ Superior Electric Co. Series DF30 five-way binding posts and Pomona (Peco) stack-up test leads, B series, are very satisfactory in this application.

controlled power outlet. A good ground connection, at least to the power-line conduit, is also provided.

When the connections have been made and carefully checked, the power is switched on and the d-c voltage measured at points *A*, *B*, and *C* with a vacuum-tube voltmeter. Next, the a-c voltage waveforms at points *A*, *B*, and *C* are observed with the oscilloscope. This a-c ripple voltage is shown to be primarily of 120-cycle frequency by comparison of its waveform with that of a 60-cycle signal obtained from the 6.3-volt filament winding of the power transformer; the center tap of this winding should be grounded.

The effectiveness of the filtering action may be illustrated by comparing the a-c ripple voltages at points *A*, *B*, and *C* as measured with a vacuum-tube voltmeter. The accuracy of this measurement is limited because as a rule a vacuum-tube voltmeter nominally calibrated to indicate root-mean-square (rms) voltage indicates this correctly only for a sinusoidal waveform.

When the power has been turned off, the filter condensers should be shorted by means of a screwdriver with an *insulated handle* to ensure their complete discharge.

*Part B.* Characteristic curves are determined for the 6C4 triode with the circuit shown in Fig. 165 (page 562). An experimental chassis similar to that used in Part A is provided for this experiment. The grid bias is set successively at even voltages from 0 to  $-20$  volts, relative to the cathode, as measured by the vacuum-tube voltmeter. For each grid bias value the plate voltage is increased from zero until a response is noted on the plate milliammeter. The plate current is then determined at 20-volt intervals in plate voltage until the plate dissipation (plate current times plate voltage) approaches 3.5 watts, the maximum rating for this tube.

*Part C.* The properties of the basic triode amplifier circuit of Fig. 171 are to be studied from the point of view of the equivalent circuit, Fig. 170. In particular, the gain is to be measured as a function of load resistance to illustrate the theoretical relationship (page 566)

$$A = \frac{e_p}{e_g} = -\mu \frac{R_L}{r_p + R_L} \quad (1)$$

where  $A$  = gain of triode stage

$e_p$  = a-c component of plate voltage (relative to cathode)

$e_g$  = a-c component of grid voltage (relative to cathode)

$R_L$  = load resistance

$r_p$  = plate resistance of triode, at given operating point

$\mu$  = amplification factor of triode, at given operating point

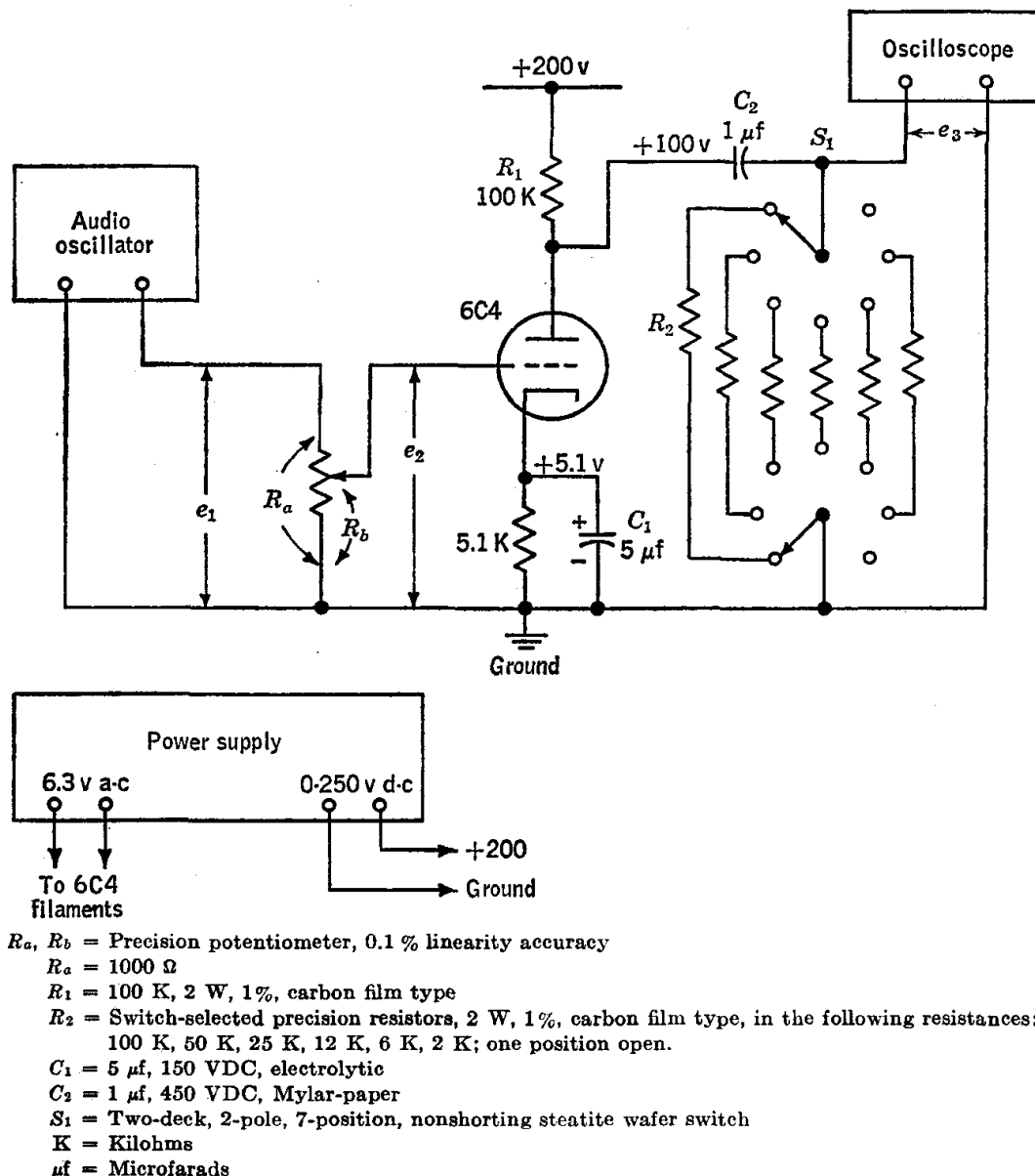


FIG. 102. Experimental arrangement for study of triode amplifier circuit. The numerical voltages given are nominal d-c values, while  $e_1$ ,  $e_2$ , and  $e_3$  represent a-c components. Tables of electronic symbols and abbreviations are given in the Appendix.

The full definitions of  $r_p$  and  $\mu$  are given on page 565. Since the cathode resistor is bypassed with capacitor  $C_1$ , the cathode is held practically at a-c ground potential. The load resistance  $R_L = R_1 R_2 / (R_1 + R_2)$  is the resistance equivalent to that in the actual a-c circuit between triode plate and ground.

The experimental arrangement is shown in Fig. 102. The precision potentiometer, tube socket, switch assembly with precision resistors, and

a terminal board (solder type) are supplied already mounted on a sturdy aluminum plate. The latter is supported in a horizontal position and held secure by two wooden blocks, in such a fashion that the tube itself is below the plate and all terminals are on top for easy access.† The remaining components of the triode circuit are soldered into place by the student. To minimize damage to the tube-socket pins from repeated soldering, each pin is connected to a terminal of the terminal board, so that all connections to the rest of the circuit can be made at the terminal board.

Individuals who have not had previous experience in the soldering of electronic circuits should learn the proper technique from an instructor. Failure of circuits constructed by inexperienced persons is often attributable to poorly soldered connections. It is a good idea to place a check mark near the corresponding symbol in the diagram when a component is wired into place, as an aid to avoiding mistakes.

The precision potentiometer has three terminals, one at each end and one connected to a variable tap. The end-to-end resistance is  $R_a$ ; the resistance between the variable tap and ground is  $R_b$ . The potentiometer should be connected into the circuit in such a way that the scale reading *increases* as the variable tap moves *away* from the grounded terminal; the scale readings will then be proportional to  $R_b$ . Commercially available precision potentiometers usually bear labels showing the internal connections.

Lastly, the leads to the audio generator,‡ oscilloscope, and power supply are connected to the triode circuit, but these units are not turned on until the entire assembly has been checked again to see that the connections and part sizes are correct and that each junction has been properly soldered.

When the assembly has been completed and checked, the power supply is turned on; the filament power is supplied to the triode first, and then, after about 30 sec, the plate voltage is applied. The latter should initially be set at a low value, and then gradually increased to 200 volts.

The d-c voltages to be expected at the plate and cathode are indicated on the schematic. As a preliminary test, these voltages should be

† An alternative type of experimental chassis which is satisfactory for this work can be constructed easily from chassis kits or punched insulating boards, both available from Vector Electronics, Glendale, Calif.

‡ If an audio generator is not available, a suitable input voltage may be derived from the 6.3-volt filament supply. A voltage of proper amplitude (about 1 volt rms) may be obtained by connecting one side of the 6.3-volt supply (or the center tap) to the experimental circuit ground, and inserting a 5.1 K (or 2.7 K) resistor between the ungrounded 6.3-volt lead and the top of  $R_a$ . In this case, however,  $C_1$  should be increased to 25  $\mu\text{f}$ ,  $C_2$  to 2  $\mu\text{f}$ , and the lowest value of  $R_2$  omitted.

checked with a vacuum-tube voltmeter; variations of the order of 10 per cent from the values shown are to be expected. If an abnormal discrepancy is found, the tube should be tested or replaced and the wiring checked again. If the difficulty persists, the instructor should be consulted. When proper voltages have been obtained, the measured values are recorded and used to calculate the tube current, the d-c plate-to-cathode voltage, and the plate dissipation, all of which should be within the maximum ratings specified for this tube type in the tube manual.

The amplifying action of the circuit is studied qualitatively by displaying the input- and output-voltage waveforms successively on the oscilloscope; these are the a-c components labeled on the schematic as  $e_2$  and  $e_3$ , respectively. While the output voltage is being observed, the input-voltage amplitude is increased gradually from a very low value to illustrate the result of overdriving the tube.

Next, the gain of the circuit is measured as a function of  $R_2$ . In the procedure to be described, the precision potentiometer serves to provide a variable and accurately known attenuation (voltage loss) which is adjusted to compensate exactly for the gain of the amplifier, so that  $e_1$  equals  $e_3$ . The oscilloscope is used only as an indicating device for matching the amplitudes of these two voltages.

The oscilloscope is connected initially to display  $e_1$ . The audio generator is set at a nominal frequency of 1000 cycles/sec and at an amplitude somewhat below the level at which appreciable distortion in the amplifier will occur; a value of about 3 volts peak to peak (p-p) is satisfactory. The oscilloscope gain or vertical amplifier control is adjusted carefully until the peak-to-peak deflection has an arbitrary, conveniently reproducible value. The oscilloscope gain is then left unchanged until the measurements have been completed.

The oscilloscope is next connected to the output to indicate the amplitude of  $e_3$ . With the switch for selecting  $R_2$  set at the open position, the precision potentiometer is adjusted to make the amplitude of  $e_3$  the same as that of  $e_1$ . Actually, the condition achieved is

$$e_3 = -e_1 \quad (2)$$

but the fact that  $e_3$  is inverted relative to  $e_1$  will not be observed unless the oscilloscope sweep is synchronized directly with the audio generator. The gain of the amplifier itself is now

$$A = \frac{e_3}{e_2} = -\frac{e_1}{e_2} = -\frac{R_a}{R_b} \quad (3)$$

so that  $A$  can be calculated from the known ratio  $R_a/R_b$ .

A series of measurements is made in which  $R_2$  is set successively at the available values; for each value of  $R_2$ , the precision potentiometer is adjusted to match  $e_3$  with  $e_1$  and the values of  $R_b$  and  $R_2$  are recorded.

When the experimental work has been completed, the components and leads which were soldered into place by the student are removed and the experimental chassis restored to its original condition.

**Calculations.** The observed ripple-reduction factors for the  $LC$  filter sections used with the full-wave rectifier are compared with the values predicted by the equation

$$\alpha = \frac{\text{alternating voltage at output of section}}{\text{alternating voltage at input of section}} = \frac{1}{(2\pi f)^2 LC - 1} \quad (4)$$

which applies to each of the two  $LC$  sections. For the full-wave rectifier the frequency  $f$  is to be taken as 120 cycles. The higher ripple frequencies present (higher multiples of 60 cycles) will be attenuated more than the 120-cycle component.

The characteristic curves for the triode are plotted as plate current versus plate voltage for the various grid-bias levels.

The measured values of  $A$  are plotted versus  $R_L$  to illustrate the general character of their relationship. For the purpose of testing the form of Eq. (1) more critically and deriving the values of the tube parameters  $\mu$  and  $r_p$  for the operating point used, a graph of  $1/A$  versus  $1/R_L$  is drawn; this procedure is based on a rearranged form of Eq. (1).

**Practical Applications.** The circuits studied are so widely used in research apparatus that a thorough grasp of the principles involved will prove invaluable in almost any sort of physical-chemical experimental work. The concept of the equivalent circuit for a triode is very useful for design purposes and can be quite helpful as a means to understanding the behavior of triodes under a wide variety of circumstances.

**Suggestions for Further Work.** With the circuit of Part C, the effect of the cathode bypass capacitor on the gain is easily and strikingly demonstrated. With  $R_2$  set at any convenient value, the peak-to-peak amplitude at the grid is adjusted for about 1 volt, as measured on the oscilloscope, and the output amplitude is noted. The cathode capacitor  $C_1$  is then removed, and the amplitude at the output is again noted. The equivalent circuit of Fig. 172 (page 568) covers this case.

With the addition of a suitable feedback circuit, the amplifier of Fig. 102 becomes an audio oscillator (page 598).

It is instructive to examine the variation of gain of the triode circuit with frequency. The frequencies at which the gain drops off can be estimated theoretically with reasonable accuracy with the aid of the equivalent circuit with bypass, coupling, stray, and tube electrode capacitances included (page 568).

Other circuits given in Chap. 27, such as the triode relay circuit of Fig. 191 or 192 or the constant-current circuit of Fig. 190, may be constructed and tested.

### References

Pertinent references are given in Chap. 27.

**PART II**

***Apparatus and Methods***

## *Treatment of Experimental Data*<sup>1</sup>

### ERRORS OF MEASUREMENT

Errors in experimental measurements may be divided into two classes: (a) *systematic errors* and (b) *random errors*. It is possible to correct for errors of the first type, and they are therefore frequently designated as *corrigible*, or *determinate*, errors, to distinguish them from the random errors which are encountered in all measurements and are beyond the control of the observer. Many systematic errors may be eliminated by the application of familiar corrections. For example, in accurate weighings calibrated weights are used and a buoyancy correction (Chap. 21) is applied if the density of the substance being weighed is appreciably different from that of the weights. In the determination of atmospheric pressure using a mercury barometer, corrections must be applied to allow for the difference between the thermal expansion of mercury and the brass scale (page 611). This is required because one atmosphere pressure as defined is equal to the pressure exerted by a column of mercury 760 mm in height in an evacuated glass tube at a temperature of 0°C at sea level and at a latitude of 45°. In very precise work it is necessary, in addition, to correct for the capillary depression of the mercury and for the difference between the acceleration of gravity where the barometer is being used and the defined acceleration at 45° latitude. In calculating the pressure of a gas inside an inverted burette filled with water, it is necessary to subtract the pressure due to water vapor (see Appendix).

In other cases where the theory has not been as well developed, it is necessary to determine corrections experimentally. For example, in the drop-weight method for the determination of surface tension (Exp. 49), corrections which have been determined by using substances of known surface tension are applied. The correction factor to be applied is a function only of  $V/r^3$ , where  $r$  is the outer radius of the tube and  $V$  is the

<sup>1</sup> Crumpler and Yoe, "Chemical Computations and Errors," John Wiley & Sons, Inc., New York (1940); Worthing and Geffner, "Treatment of Experimental Data," John Wiley & Sons, Inc., New York (1943); Fisher, "Statistical Methods for Research Workers," Oliver & Boyd, Ltd., Edinburgh (1932).



volume of the drop, and therefore does not depend upon the nature of the liquid studied. Such corrections are referred to as empirical corrections.

Systematic errors do not manifest themselves by fluctuations in measurements and cannot be eliminated by merely repeating the measurements, since the same error is involved in each measurement. These errors are therefore especially serious and insidious and can be avoided only by careful calibrations and consideration of all possible corrections. Sometimes systematic errors are indicated by a drift in consecutively measured values or by the change in the measured value resulting from a change in experimental technique.

The second class of errors, *random errors*, or *accidental errors*, is indicated by fluctuations in successive measurements. These random variations are due to small errors beyond the control of the observer. For example, if a barometer is read several times in succession, the values read from the vernier will be found to fluctuate about a mean value. Strictly speaking, we can never measure the true value of any quantity, but only an approximation to it. The purpose of the statistical treatment of experimental data is to determine the most probable value of a measured quantity and to estimate its reliability.

The error of a measurement is the difference between the observed value and the true value of the quantity. If the error is small compared with the magnitude of the measured quantity, the measurement is said to be *accurate*. The statement of the accuracy of a result, therefore, implies that the true value is known. Since the true value is generally unknown, the mean of the series of determinations is used, and the differences between the observed values and the mean are referred to as *residuals*. If the residuals are small compared with the magnitude of the measured quantity, the measurement is said to be *precise*. A precise measurement is not necessarily an accurate measurement, but an accurate measurement must be a precise measurement. Small random errors occur more frequently than large ones, and for many experimental measurements the error distribution may be adequately represented by the Gaussian function, or "error function,"

$$y(r) = \frac{h}{\sqrt{\pi}} e^{-h^2 r^2} \quad (1)$$

where  $y(r)dr$  gives the probability of finding a residual in the range from  $r$  to  $r+dr$ . If the precision constant  $h$  has a large value, the probability decreases rapidly from its maximum at  $r = 0$  to very small values, so that the probability of making large errors is small. If  $h$  is small, the probability curve falls off very slowly and larger errors occur more frequently. It may be shown that if the set of residuals of a series of measurements of a quantity  $x$  follows Eq. (1), the arithmetic mean  $x_m$  is the

best approximation to the true value of the quantity measured, to which the arithmetic mean converges as the number of observations increases indefinitely. For a set of  $n$  measurements, sufficiently large in number and all made with equal care, the precision index for a single measurement of a quantity  $x$  is given in terms of the *standard deviation*  $\sigma_x$  or the *probable error*  $P_x$ ,

$$\sigma_x = \left( \frac{\sum_{i=1}^n r_i^2}{n} \right)^{1/2} \quad P_x = 0.6745\sigma_x$$

To allow for the fact that the residual  $r_i = x_i - x_m$  is calculated relative to the arithmetic mean of a finite set of measurements rather than the true value of the quantity, it is customary to replace the above formulas by the relations

$$\sigma_x = \left( \frac{\sum_{i=1}^n r_i^2}{n-1} \right)^{1/2} \quad P_x = 0.6745 \left( \frac{\sum_{i=1}^n r_i^2}{n-1} \right)^{1/2} \quad (2)$$

The probable error  $P_x$  so calculated for a single observation is to be interpreted in the following way. Given a value  $x_m$  and the corresponding value of  $P_x$ , if additional measurements of  $x$  are made under conditions corresponding to those of the first set, then there is a 50 per cent probability that an additional measured value will fall in the range

$$x_m - P_x \text{ to } x_m + P_x$$

A random error has less than a 1 per cent chance of being larger than four times the probable error  $P_x$  of a single observation.

For the series of measurements as a whole there may be reported the *standard deviation of the mean*  $\sigma_{\bar{x}}$  or the *probable error of the mean*  $P_{\bar{x}}$ .

$$\sigma_{\bar{x}} = \left[ \frac{\sum_{i=1}^n r_i^2}{n(n-1)} \right]^{1/2} \quad P_{\bar{x}} = 0.6745\sigma_{\bar{x}} \quad (3)$$

The probable error of the mean defines the range about  $x_m$  within which would fall 50 per cent of further values of this quantity obtained through additional *sets* of measurements equivalent to the first.

Statistical methods of interpretation of experimental data can be of the greatest importance if properly applied with full understanding of their implications and the underlying assumptions which determine their limitations. When the number of observations is small, the preceding formulas must be modified in any case. Further, for the conditions of much experimental work, there is no certainty that the normal error

distribution defined by Eq. (1) is valid. The various observations in a set often are not made under equivalent circumstances, as, for example, because of improvement of the operator's technique through practice. Under such conditions it is appropriate to use the arithmetic mean to represent the result of the measurement and to characterize its reliability in terms of the average of the residuals (the average deviation from the mean):

$$x = x_m \pm \frac{1}{n} \sum_{i=1}^n |r_i| \quad (4)$$

Here  $|r_i|$  represents the absolute value of  $r_i$ .

*Example.* Atmospheric pressure is measured with a Fortin-type barometer, with which the lower mercury level is set at a reference ivory point and the position of the upper level measured relative to the instrument scale. In four successive determinations results were obtained as follows:

$i$	$h_i$ , scale units	$r_i = h_i - h_m$	$ r_i $
1	737.27	-0.03	0.03
2	737.32	+0.02	0.02
3	737.36	+0.06	0.06
4	737.25	-0.05	0.05
<hr/>			
$h_m = \frac{1}{4} \sum_{i=1}^4 h_i$		$\sum_{i=1}^4  r_i  = 0.16$	
$= 737.30$		$\frac{1}{4} \sum_{i=1}^4  r_i  = 0.04$	

Then  $h = 737.30 \pm 0.04$  scale units.

To reduce this result to units of standard millimeters of mercury, corrections must be applied as described on page 393.

**Estimation of Experimental Errors.** In order to determine the precision of a measurement, it is necessary to repeat the measurement a number of times in order to find how much the values scatter about the mean. In many cases, however—and this is particularly true for experiments in the physical-chemistry laboratory, where time is limited—it is necessary to *estimate* the precision of a measurement. No fixed values can be given for the precisions of various types of measurements because the precision depends upon the apparatus, the conditions under which it

is used, and the carefulness of the operator. Therefore it is necessary to develop an awareness of various sources of error in order to make reliable estimates.

In the measurement of weight in the laboratory, the precision may vary over a wide range. An ordinary analytical balance may be used to obtain weights to  $\pm 0.1$  mg, but the precision will depend upon the sensitivity of the balance and the way in which it is used, as well as the quality of the weights. Large objects may be weighed on a trip balance with a precision of  $\pm 0.1$  g.

In the measurement of volume the precision will depend upon whether volumetric flasks, pipettes, or burettes are used and on the size of the volume to be measured. The National Bureau of Standards tolerances for volumetric equipment are given in textbooks on quantitative analysis. In brief, a 25-ml volumetric flask (to contain) should be reliable to 0.03 ml, or 0.12 per cent, and a liter volumetric flask to 0.5 ml, or 0.05 per cent. A 10-ml transfer pipette should be reliable to 0.01 ml, or 0.1 per cent, and a 2-ml pipette to 0.006 ml, or 0.3 per cent. Of course, the accuracy of a volume required to reach an end point in a titration depends upon the sharpness of the end point as well as the accuracy of the burette.

In the measurement of pressure an ordinary laboratory barometer can be read to  $\pm 0.2$  mm, and the pressure should be accurate within this uncertainty after the necessary corrections have been made (see Appendix). On the other hand, the pressure obtained with a simple mercury manometer without a special reading device will be uncertain by about  $\pm 1$  mm.

The uncertainty in a measurement of temperature will be quite different if the temperature is measured with a good mercury-in-glass thermometer near room temperature or by use of a thermocouple at a high temperature. In calculating the percentage error in the temperature it must be remembered that it is the uncertainty of the value which is used in the calculation that is significant. Thus an uncertainty of  $1^\circ$  at  $25^\circ$  would not cause a 4 per cent error in a calculation of molecular weight from the ideal-gas law, but a 0.3 per cent error. In other types of experiments it is the change in temperature that is significant, rather than the absolute temperature, and so it is important to estimate the precision with which this difference can be measured.

In other cases, a scale can be read to a greater precision than is warranted by other factors in the experimental arrangement. For example, if a low-sensitivity galvanometer is employed for detection of the null point in a potentiometric circuit, it may be observed that the potentiometer slide-wire can be adjusted several divisions before a detectable movement of the galvanometer occurs. In this case, the precision is determined by the galvanometer rather than the graduated slide-wire.

**Influence of Experimental Errors on the Final Result.** A final physical-chemical result is usually obtained by combining the results of different kinds of measurements. The accuracy of any final result is influenced by the accuracy of the measurements of the several quantities involved. If it happens that one of the quantities involved is subject to a much greater error than the others, it will have the preponderant effect in determining the accuracy of the final result. For example, in the determination of molecular weight from the elevation of the boiling point (Exp. 11), the solvent and solute can be weighed more accurately than the boiling-point elevation can be determined. If, however, the relative errors in the various measured quantities are of the same order of magnitude, the errors introduced by all the measured quantities must be considered. In trying to improve the accuracy of a given experimental determination it is important to emphasize improvement of the least accurate measurement.

The result  $u$ , calculated from a set of experimentally determined quantities  $x, y, z, \dots$ , constitutes a function dependent on the values assumed for these quantities as independent variables. Corresponding to differential changes  $dx, dy, dz, \dots$  in the independent variables, the differential change in the result  $u$  is given by the conventional expression for the exact differential of a function of several independent variables. Restricting the treatment to a basis of three independent variables (the extension to a larger number is obvious),

$$du = \left(\frac{\partial u}{\partial x}\right)_{y,z} dx + \left(\frac{\partial u}{\partial y}\right)_{x,z} dy + \left(\frac{\partial u}{\partial z}\right)_{x,y} dz \quad (5)$$

The partial derivatives are derived from the relation by means of which  $u$  itself is calculated. Equation (5) provides a simple basis for estimation of the possible range of uncertainty which must be assigned to the value calculated for  $u$  as a consequence of the acknowledged uncertainties in the experimental data. In this procedure it is assumed that the accuracy of the measurements is reasonably good (of the order of a few per cent or better), so that to an adequate degree of approximation Eq. (5) may be replaced by

$$\Delta u \approx \left(\frac{\partial u}{\partial x}\right)_{y,z} \Delta x + \left(\frac{\partial u}{\partial y}\right)_{x,z} \Delta y + \left(\frac{\partial u}{\partial z}\right)_{x,y} \Delta z \quad (6)$$

Here  $\Delta u$  approximates the finite change  $u(x + \Delta x, y + \Delta y, z + \Delta z) - u(x, y, z)$  in the calculated value of  $u$ , which results from the changes  $\Delta x, \Delta y, \Delta z$  in the independent variables away from the values  $x, y, z$ , for which  $u$  and the partial derivatives are evaluated.

In the present application, the variations in  $x, y, z$  correspond to the uncertainties in the experimental data, which are known with respect to

*estimated magnitude* but not with respect to sign. It is thus possible to calculate with confidence only the magnitude of each term appearing on the right-hand side of Eq. (6); the sum of these quantities then gives the extreme value for the absolute magnitude of the change in the derived quantity  $u$  which is consistent with specified uncertainties in  $x$ ,  $y$ ,  $z$ . Thus, for

$$\begin{aligned}
 x &= x_m \pm \Delta x \\
 y &= y_m \pm \Delta y \\
 z &= z_m \pm \Delta z \\
 u &= u_m \pm |\Delta u| = u(x_m, y_m, z_m) \pm |\Delta u| \\
 |\Delta u| &= \left| \left[ \left( \frac{\partial u}{\partial x} \right)_{y,z} \right]_{\substack{x=x_m \\ y=y_m \\ z=z_m}} \right| |\Delta x| + \left| \left[ \left( \frac{\partial u}{\partial y} \right)_{x,z} \right]_{\substack{x=x_m \\ y=y_m \\ z=z_m}} \right| |\Delta y| \\
 &\quad + \left| \left[ \left( \frac{\partial u}{\partial z} \right)_{y,x} \right]_{\substack{x=x_m \\ y=y_m \\ z=z_m}} \right| |\Delta z| \quad (7)
 \end{aligned}$$

It must be emphasized that, if the ranges of uncertainty in the experimentally measured quantities are not properly estimated, the above calculation loses its practical significance, and that in any case the possible effects of systematic errors are not included.

*Example.* The molar refraction for a fluid is defined by the relation

$$\mathcal{R} = \frac{n^2 - 1}{n^2 + 2} \frac{M}{\rho} \quad (8)$$

where  $M$  = molecular weight

$n$  = refractive index

$\rho$  = density of fluid

For 25°C, one standard atmosphere pressure, the following results are specified for liquid benzene, for which the molecular weight may be considered as 78.114 g/mole with negligible error.

$$\begin{aligned}
 \rho &= 0.8737 \pm 0.0002 \text{ g/ml} \\
 n &= 1.4979 \pm 0.0003
 \end{aligned}$$

Then  $\mathcal{R} = 26.20$  ml/mole.

From Eq. (8),

$$\begin{aligned}
 \left( \frac{\partial \mathcal{R}}{\partial n} \right)_\rho &= \frac{M}{\rho} \left[ \frac{2n}{n^2 + 2} - \frac{2n(n^2 - 1)}{(n^2 + 2)^2} \right] = \frac{M}{\rho} \left[ \frac{6n}{(n^2 + 2)^2} \right] \\
 &= \mathcal{R} \left[ \frac{6n}{(n^2 - 1)(n^2 + 2)} \right]
 \end{aligned}$$

$$\left(\frac{\partial \mathcal{R}}{\partial \rho}\right)_n = \frac{n^2 - 1}{n^2 + 2} \left(\frac{-M}{\rho^2}\right) = -\frac{\mathcal{R}}{\rho}$$

$$d\mathcal{R} = \mathcal{R} \left[ \frac{6n}{(n^2 - 1)(n^2 + 2)} \right] dn - \frac{\mathcal{R}}{\rho} d\rho$$

$$|\Delta \mathcal{R}| = (26.20) \left[ \frac{(6)(1.4979)}{\{(1.4979)^2 - 1\} \{(1.4979)^2 + 2\}} \right] (0.0003) \\ + \frac{26.20}{0.8737} (0.0002)$$

$$= 0.013 + 0.006 = 0.019$$

$$\mathcal{R} = 26.20 \pm 0.02 \text{ ml/mole}$$

In an alternative approach which is often convenient, recognizing that  $d \ln f = df/f$ , one can write

$$d \ln \mathcal{R} = d \ln (n^2 - 1) - d \ln (n^2 + 2) - d \ln \rho$$

$$\frac{d\mathcal{R}}{\mathcal{R}} = \frac{d(n^2 - 1)}{n^2 - 1} - \frac{d(n^2 + 2)}{n^2 + 2} - \frac{d\rho}{\rho} \\ = \left( \frac{2n}{n^2 - 1} - \frac{2n}{n^2 + 2} \right) dn - \frac{d\rho}{\rho}$$

or, as above,

$$d\mathcal{R} = \mathcal{R} \left[ \frac{6n}{(n^2 - 1)(n^2 + 2)} \right] dn - \mathcal{R} \frac{d\rho}{\rho}$$

**Addition and Subtraction.** For  $u = x \pm y$ ,

$$\Delta u = \Delta x \pm \Delta y$$

and

$$|\Delta u| = |\Delta x| + |\Delta y| \quad (9)$$

Thus the possible absolute uncertainty in a sum or difference is equal to the sum of the absolute values of the uncertainties in the measured quantities.

**Multiplication or Division.** For

$$u = x^{\pm n} y^{\pm m}$$

where  $n, m$  are positive numbers,

$$\ln u = \pm n \ln x \pm m \ln y$$

$$\frac{du}{u} = \pm n \frac{dx}{x} \pm m \frac{dy}{y}$$

$$\left| \frac{\Delta u}{u} \right| = n \left| \frac{\Delta x}{x} \right| + m \left| \frac{\Delta y}{y} \right| \quad (10)$$

Then, as the uncertainty in  $x$  becomes relatively small, the percentage uncertainty in  $x^2$  approaches twice the percentage uncertainty in  $x$ , while the percentage uncertainty in  $\sqrt{x}$  becomes one-half that in  $x$  itself.

**Propagation of Probable Errors.** If circumstances justify the calculation of the probable error for the two independent variables  $x, y$  from which the function  $u$  is calculated, the probable error in  $u$  may be computed as follows. For the present purpose it is the values of the arithmetic means  $x_m, y_m$  and the associated probable errors  $P_x, P_y$  that are important, not the particular numbers of observations in the sets which led to these values. Then it is possible without loss of generality to assume that there are equal numbers of observations in the two sets, so that the experimental results can be considered to consist of  $n$  pairs of values  $(x_i, y_i)$  of the variables.

Now define  $\Delta u_i$  by the relation

$$\Delta u_i = u(x_i, y_i) - u(x_m, y_m) = u(x_m + \Delta x_i, y_m + \Delta y_i) - u(x_m, y_m) \quad (11)$$

and let

$$u'_x(x, y) = \left( \frac{\partial u}{\partial x} \right)_y \quad u'_y = \left( \frac{\partial u}{\partial y} \right)_x$$

Then, from Eq. (6),

$$\begin{aligned} \Delta u_i &= u'_x(x_m, y_m) \Delta x_i + u'_y(x_m, y_m) \Delta y_i \\ (\Delta u_i)^2 &= [u'_x(x_m, y_m)]^2 (\Delta x_i)^2 + [u'_y(x_m, y_m)]^2 (\Delta y_i)^2 \\ &\quad + 2[u'_x(x_m, y_m)u'_y(x_m, y_m)] \Delta x_i \Delta y_i \end{aligned} \quad (12)$$

For the Gaussian error distribution assumed here, an error of given magnitude has equal probability of being positive or negative, and hence if Eq. (12) is summed over all pairs  $i$ , the cross-product terms can be expected to cancel out to an extent determined by the common number  $n$  of observations in the two sets. Such a cancellation leaves, for large  $n$ ,

$$\sum_{i=1}^n (\Delta u_i)^2 = [u'_x(x_m, y_m)]^2 (\Delta x_i)^2 + [u'_y(x_m, y_m)]^2 (\Delta y_i)^2 \quad (13)$$

Multiplying through by  $(0.6745)^2/[n(n-1)]$ , and defining the probable error in  $\bar{u}$  by

$$P_{\bar{u}} = 0.6745 \left[ \frac{\sum_i \Delta u_i^2}{n(n-1)} \right]^{1/2} \quad (14)$$

$$P_{\bar{u}}^2 = [u'_x(x_m, y_m)]^2 P_x^2 + [u'_y(x_m, y_m)]^2 P_y^2 \quad (15)$$

$$P_{\bar{u}} = \{[u'_x(x_m, y_m)]^2 P_x^2 + [u'_y(x_m, y_m)]^2 P_y^2\}^{1/2} \quad (16)$$

The extension to more than two independent variables is straightforward.

For the sum or difference of two variables,  $u = x \pm y$ ,

$$P_{\bar{u}} = \sqrt{P_x^2 + P_y^2} \quad (17)$$



which is less than the sum of the probable errors of the mean of the two variables. Similarly, for the quotient  $u = x/y$ ,

$$P_u = \frac{x_m}{y_m} \sqrt{\frac{P_x^2}{x_m^2} + \frac{P_y^2}{y_m^2}} \quad (18)$$

**Random Errors.** The determination of the average emission rate of a radioactive sample offers an example of random errors which are subject to mathematical treatment. The actual rate of emission of ionizing radiation is continually fluctuating because of the random nature of the disintegration process, so that the number of counts recorded by a Geiger-

TABLE 1. NUMBER OF COUNTS OBTAINED IN 120 SEC USING A  
GEIGER-MÜLLER COUNTER  
(Average count = 537)

Trial	Count	Deviation from average	Trial	Count	Deviation from average
1	552	+15	26	534	- 3
2	510	-27	27	521	-16
3	542	+ 5	28	539	+ 2
4	559	+22	29	508	-29
5	547	+10	30	519	-18
6	569	+32	31	532	- 5
7	513	-24	32	528	- 9
8	524	-13	33	590	+67
9	544	+ 7	34	540	+ 3
10	546	+ 9	35	517	-20
11	581	+44	36	504	-33
12	516	-21	37	538	+ 1
13	519	-18	38	525	-12
14	567	+30	39	533	- 4
15	530	+ 7	40	578	+41
16	551	+14	41	562	+25
17	514	-23	42	525	-12
18	586	+49	43	526	-11
19	540	+ 3	44	521	-16
20	551	+14	45	556	+19
21	524	-13	46	551	+14
22	544	+ 7	47	523	-14
23	531	- 6	48	549	+12
24	519	-18	49	583	+46
25	534	- 3	50	534	- 3

Müller counter during equal time intervals with the same radioactive sample will be randomly distributed about an average value. This is illustrated in Table 1, which gives the number of counts obtained in successive intervals of 120 sec for a sample of uranyl nitrate. For reasons to be mentioned later, the mean value is generally taken as the most probable value for the quantity being measured. In this case, the average number is 537 counts, and the deviations of the individual values from the average are given in column 3. These deviations may be referred to as

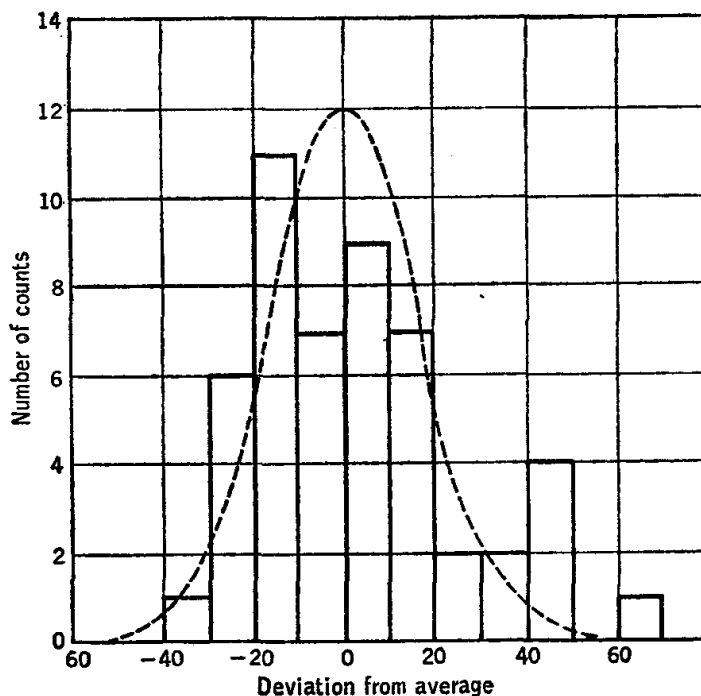


FIG. 103. Frequency of errors in the determination of radioactivity, using a Geiger-Müller counter.

residuals or errors. It is seen that 25 of the values are larger than the average and 25 are smaller, and it may be noted that values which depart widely from the mean occur less frequently than those for which the deviation is small.

The frequency of errors of a given magnitude is given by the graph in Fig. 103, in which the number of deviations having values between 0 and 9, 10 and 19, 20 and 29, etc., is plotted versus the deviation. Such a graph is referred to as a frequency-distribution curve. If a much larger number of measurements was made, the distribution would approach that represented by the dashed curve, which is the result that would theoretically be obtained from an infinite number of trials. (The scale of the ordinate is arbitrary.)

In the case of radioactive counting, the probability of a given count may be calculated from Poisson's equation,<sup>1</sup> but in many other cases it is not possible to predict in advance the exact distribution law followed. For the great majority of experimental measurements, however, the error distribution may be adequately represented by the Gaussian function, or "error function," which is given by Eq. (1).

Equation (1) is referred to as a *normalized* distribution function, since the coefficient is such that the probability of  $x$  lying between  $x = -\infty$  and  $x = +\infty$  is unity. For large numbers of counts, the frequency distribution may be adequately represented by the Gaussian function, and the dashed line in Fig. 103 represents the probability distribution which would be obtained for an infinitely great number of trials. The probable percentage error in a given determination of radioactivity depends upon the total number of counts and may be predicted<sup>2</sup> from a consideration of the laws of probability. Table 2 gives the probable percentage error and the

TABLE 2. THE ERROR OF COUNTING DETERMINATIONS

Total counts	Probable error, %	Nine-tenths error, %
100	7.8	16
1,000	2.2	5.1
10,000	0.7	1.6
100,000	0.23	0.5

nine-tenths error for various total numbers of counts. The probable error is the error which is exceeded 50 times in 100 trials, and the nine-tenths error is the error which is exceeded 10 times in 100 trials, on the average.

### SIGNIFICANT FIGURES

The accuracy of a measurement should be indicated by the number of significant figures used in recording its magnitude, and care must be exercised that too many significant figures are not used.

In calculations performed by longhand multiplication or a calculating machine, more figures are obtained than are significant, and the final result must be rounded off in accordance with the experimental uncertainty. Most of the multiplications and divisions required for work in the physical-chemistry laboratory may be made with a slide rule. The significant figures of a number include all the certain digits and the first (and first only) doubtful digit of that number. If no statement of accu-

<sup>1</sup> Rasetti, "Elements of Nuclear Physics," pp. 32-35, Prentice-Hall, Inc., Englewood Cliffs, N.J. (1936).

<sup>2</sup> Strong, "Procedures in Experimental Physics," p. 298, Prentice-Hall, Inc., Englewood Cliffs, N.J. (1939).

racy accompanies an experimental result, it is assumed that the last digit may be uncertain by 2 or 3. Thus, if the experimentally determined molecular weight of carbon dioxide is given as 44.0, it would indicate that the most probable value for the molecular weight lies between about 43.7 and 44.3. If the experimental value is given as 44.00, it would indicate that the most probable value for the molecular weight lies between 43.97 and 44.03. The statement of an experimental result is incomplete unless the uncertainty in the value is indicated.

The digit 0 requires special consideration, since zeros to the left of the decimal point are not necessarily significant in regard to accuracy. For example, a volume of water measured in a 2-liter graduate might be recorded as 1800 ml. Since such graduates are graduated every 20 ml, the last zero is not significant, and this fact could be indicated by writing the result as  $1.80 \times 10^3$  ml. Zeros preceding the numbers in a decimal fraction are not significant. Thus, in the number 0.0000053, there are only two significant figures. In the case of very large or very small numbers it is convenient to use exponential notation, and so the preceding number could be written  $5.3 \times 10^{-6}$ .

## REPRESENTATION OF DATA

There are three principal methods by which experimental data may be represented: tables, graphs, and equations.

**Tabular Representation.** Tables may be divided into three classes: qualitative, statistical, and functional tables. A *statistical* table, as its name implies, is one which lists statistical facts. Thus a table in the World Almanac which lists countries with a series of columns for population, area, national income, and the like, is a statistical table, as is Table 1 of Exp. 12. Such tables are fairly common in scientific work, but for the purposes of physical chemistry the functional table is of primary importance.

In the *functional* table, corresponding values of an independent variable  $x$  and a dependent variable  $y$  are listed side by side. As in all tables, every functional table should have a title which is clear and complete, yet brief, and each column of the table should have a heading giving the name and the unit of the quantity listed. The choice of the independent variable is to some extent arbitrary, but it should be a simple one, such as time, temperature, distance, etc. One should usually choose rounded values of the independent variable in order of increasing values, with successive values differing by a constant amount. The dependent variable is preferably given in terms of smoothed data. Numerical items are arranged so that the decimal points are vertically aligned in each column. The rules governing significant figures should be observed.

There are several ways of obtaining smoothed data, the most common one being to plot the primary data, draw a representative smooth curve, and read information directly from the curve at desired points. The equation of the curve may also be found (page 409), and data may be computed from the equation at any desired value of the independent variable.

These principles are illustrated in Table 3. Data represented are from a student's determination of the vapor pressure of acetone as a function of the temperature. In column 1 are listed data read directly from the

TABLE 3. THE VAPOR PRESSURE OF ACETONE AS A FUNCTION OF TEMPERATURE ILLUSTRATING DIFFERENT MEANS OF SMOOTHING DATA

$t, ^\circ\text{C}$	(1) $P, \text{ cm Hg}$ From curve, Fig. 104a	(2) $P, \text{ cm Hg}$ From straight line, Fig. 104b	(3) $P, \text{ cm Hg}$ From Eq. (19) with $m = -1.662 \times 10^3,$ $b = 6.929$
5	8.91	9.02	8.98
10	11.39	11.6	11.47
15	14.50	14.1	14.49
20	18.17	18.2	18.16
25	22.53	22.8	22.67
30	28.00	28.0	27.98
35	34.57	34.3	34.28
40	42.09	42.0	41.82
45	50.76	50.9	50.64
50	61.07	61.5	61.09
55	72.30	73.8	73.40

curve of  $P$  versus  $T$  (Fig. 104a). The graph as originally prepared was of large scale and permitted readings to four significant figures. In column 2 are data obtained from the straight-line graph of Fig. 104b, which is plotted from the same experimental data. The scale of this graph did not permit reading beyond three significant figures. In column 3 are data computed from the equation

$$\log P = m \left( \frac{1}{T} \right) + b \quad (19)$$

where the constants have been evaluated by the method of least squares (page 413).

Actually, none of these methods yields smoothed data of the highest possible quality in this particular case, for the following reasons:

1. *From  $P$  versus  $T$  Curve.* Although the curve drawn for  $P$  as a function of  $T$  is the best approximation to the correct functional form, the

decision as to how the curve should fit the points will be in slight error if the estimation is done purely by eye.

2. *From Eq. (19) with Constants Determined by Least Squares.* This would be the last word in data smoothing if  $\log P$  versus  $1/T$  were actually a straight line. The best line through the points does, however, have a slight curvature. If the precision of the data was not quite so good, it is unlikely that the curvature could be assigned with certainty.

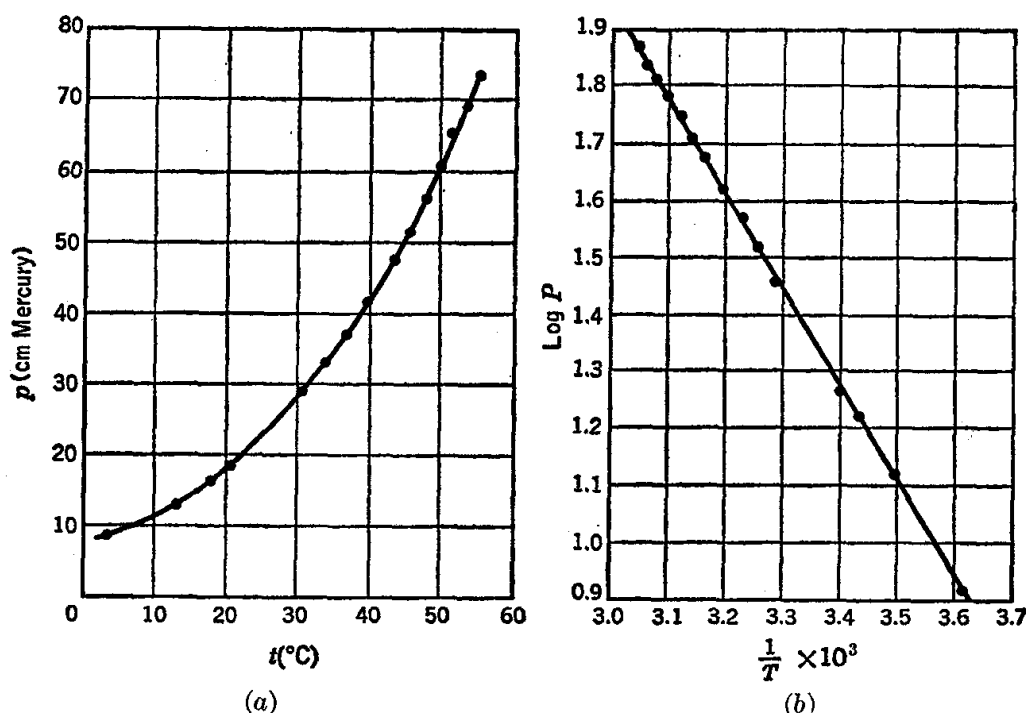


FIG. 104. (a) The vapor pressure of acetone as a function of temperature; (b) a plot of  $\log P$  versus  $1/T$  for acetone.

If a three-constant equation of the form

$$\log P = m \left( \frac{1}{T} \right) + a \log T + b$$

or better,  $\log P = [A/(T + C)] + B$ , were used in place of Eq. (19), the least-squares method, or even an approximate method, for evaluating the constants would yield smoothed data of very high quality. However, the labor of computation would be increased greatly.

3. *Directly from the Straight Line of Fig. 104b.* This is the usual procedure, yet it involves the errors encountered in both the other methods.

Other topics concerned with functional tables, including several methods of smoothing data by arbitrary numerical procedures, and the problems of interpolation and extrapolation are treated fully by Worthing and Geffner.<sup>1</sup>

<sup>1</sup> *Op. cit.*

**Representation of Data by Graphs.** Graphs have many advantages which favor their use in representing data. One of the most important of these advantages is that a graph may reveal maxima, minima, inflection points, or other significant features in data which might be overlooked in a tabular or formula representation. Furthermore, direct differentiation may be performed by drawing tangents to a curve, and integration may be accomplished by determining the area under a curve; in many cases these operations would otherwise be tedious or impractical.

The steps to be followed in preparing a satisfactory graph have been extensively treated and illustrated with numerous examples by Worthing and Geffner.<sup>1</sup> We shall summarize here only some of the more important points.

1. *Choosing the Graph Paper.* Ordinary rectangular coordinate paper is satisfactory for a large majority of purposes. Semilogarithmic paper is convenient when one of the coordinates is to be the logarithm of an observed variable (Exp. 6). If both coordinates are to be logarithms of variables, log-log paper may be used (Exp. 50). Where an unknown functional relation is involved, these types of paper are sometimes used because it is found by trial and error that they yield a closer approximation to a straight line than does rectangular coordinate paper. Another special-purpose paper which has triangular coordinates is used in Exp. 20.

It is practically always worth the extra expense to obtain high-quality paper made by a reputable manufacturer. Translucent paper is available for tracing or blueprinting. If the graph is to be reproduced in print, it is well to remember that blue coordinate lines will not show up; main coordinate lines may be traced over with India ink for satisfactory reproduction.

2. *Choosing the Coordinate Scales.* Five rules are listed by Worthing and Geffner. They are not altogether inflexible, and in case of doubt common sense should prevail.

Rule 1. The scale for the independent variable should be plotted along the  $X$  axis (abscissa).

Rule 2. The scales should be so chosen that the coordinates of any point on the plot may be determined quickly and easily.

Rule 3. The scales should be numbered so that the resultant curve is as extensive as the sheet permits, provided that the uncertainties of measurement are not made thereby to correspond to more than one or two of the smallest divisions.

Rule 4. Other things being equal, the variables should be chosen to give a resultant plot which approaches as nearly as practicable to a straight line.

<sup>1</sup> *Op. cit.*

Rule 5. Scales should be chosen such that the curve will, to the extent possible, have a geometrical slope approximating unity.

3. *Labeling the Coordinate Scales.* Main coordinate lines (or alternate ones) are labeled with the values they represent. The name of the quantity represented is given along each axis, together with the units in which it is measured.

4. *Plotting the Data.* Each point should be surrounded by a suitable symbol, such as a circle. If at all practicable, it is customary to have the size of the symbol correspond approximately to the precision of the determination.

It frequently happens that several curves are to be plotted on the same sheet of graph paper. This is the customary manner in which a third variable is treated on a two-dimensional graph. When this is done, a different type of symbol should be used for each set of data.

One should not carry the above considerations to the extreme. It is possible to have such a hodgepodge of points and curves that fundamental relations are obscured.

5. *Fitting a Curve to the Plotted Points.* If sufficient points are available and the functional relation between the two variables is well defined, a smooth curve is drawn through the points. These conditions prevail in practically all physical-chemical work. French curves, splines, or other devices should be used for maximum smoothness, unless a straight line is being graphed. Generally speaking, inflections or discontinuities will be absent; however, if such irregularities are greater than the experimental error, one must not ignore them. An inflection in the cooling curve of a molten alloy (Exp. 19) indicates the freezing point.

The curve should pass as close as reasonably possible to all the plotted points, though it need not pass through any single one. There is a natural tendency to overestimate the importance of the end points; often these are the least accurate points on the graph.

6. *Preparing a Descriptive Caption.* This should include a more or less complete description of what the graph is intended to show. The caption is usually included in an open region directly on the graph paper unless it is to be reproduced for printing. If the data have been taken from the work of another, the source should be acknowledged.

**Representation of Data by Equations.** In order to obtain the maximum usefulness from a set of experimental data, it is frequently desirable to express the data by a mathematical equation. An advantage of this method is that data are represented in a compact fashion and in a form which is convenient for differentiation, integration, or interpolation. Frequently the form of the relationship between the dependent and independent variable is known, and it is desired to determine the values of the coefficients in the equation, since these coefficients corre-



spond to physical quantities. Common examples of such equations follow.

Vapor-pressure equation:

$$\log P = \frac{-\Delta H}{2.303R} \frac{1}{T} + \text{constant} \quad (\text{Exp. 6})$$

Beer-Lambert law:

$$\log \frac{I}{I_0} = -acb \quad (\text{Exp. 16})$$

First-order reaction-rate equation:

$$\log c = \frac{-kt}{2.303} + \text{constant} \quad (\text{Exp. 22})$$

Langmuir adsorption equation:

$$\frac{c}{x/m} = \frac{1}{\alpha} + \frac{\beta}{\alpha} c \quad (\text{Exp. 50})$$

Radioactive decay law:

$$\log \frac{N_t}{N_0} = -0.3010 \frac{t}{t_{1/2}} \quad (\text{Exp. 54})$$

In many cases the form of the relation between the independent and dependent variables is unknown and must be determined. This may be done by plotting the data and comparing the shape with that for known functions.<sup>1</sup> Frequently the functional relationship is such that a straight-line graph may be obtained by changing the variables. For example, in the case of the Langmuir adsorption equation, a plot of amount adsorbed,  $x/m$ , versus concentration  $c$  is a curved line, while a plot of  $c/(x/m)$  versus  $c$  yields a straight line. When the data or some function of the data can be plotted as a straight line, the constants can be determined simply from the slope and intercept. In many cases where a straight line is not obtained it is best to use a power series of the type

$$y = a + bx + cx^2 + dx^3 + \dots$$

with as many empirical constants as necessary to represent the data to within the experimental uncertainty.

Three methods for the evaluation of the constants in a linear equation will be discussed. In order of increasing degree of objectivity, these methods are (1) graphical method, (2) method of averages, (3) method of least squares.

<sup>1</sup> Graphs of a wide variety of functions are given in Worthing and Geffner, *op. cit.*, p. 57.

1. *Graphical Method.* This method is especially useful for the determination of the constants in a linear equation. If a given equation is not linear with respect to the variable, it may frequently be arranged in a linear form by making a simple substitution. For example, in the case of the vapor-pressure equation given above, the linear equation

$$y = mx + b$$

is obtained by substituting  $\log P = y$ ,  $1/T = x$ ,  $m = -\Delta H/2.303R$ , and  $b = \text{constant}$ . Thus, when  $\log P$  is plotted versus  $1/T$ , a straight line is obtained if this equation is correct. A plot of student data for the vapor pressure of acetone determined by the Ramsay-Young method is shown in Fig. 104b. The best straight line is drawn "through" these points with a transparent straightedge. The slope  $m$  of the line is calculated from the coordinates  $x_1, y_1$  and  $x_2, y_2$  of two points on the line:

$$m = \frac{y_2 - y_1}{x_2 - x_1}$$

These points are not selected from the original data and are taken as far apart as possible. The constant  $b$  is equal to the intercept on the  $Y$  axis for  $x = 0$ . In this case, it is more convenient to calculate  $b$  from the slope  $m$  and the coordinates of one of the points on the line:

$$b = y_1 - mx_1$$

The values of  $m$  and  $b$  calculated graphically from Fig. 104b are

$$\begin{aligned} m &= -1.662 \times 10^3 \text{ deg} \\ b &= 6.929 \end{aligned}$$

2. *Method of Averages.* The constants in a linear equation may be calculated from only two pairs of values for the variables. In general, more than two pairs of values are available, and different values for the constants will be obtained when different experimental points are used in the calculation. One method for determining the constants by using all the experimental data is the method of averages. This method is based on the assumption that the correct values of the constants  $m$  and  $b$  are those which make the sum of the residuals equal zero. The residuals  $v_i$  are the differences between the values of  $y$  calculated from the empirical equation and the experimentally determined values  $y_i$ . In the case we are discussing, the residuals are

$$v_i = mx_i + b - y_i \quad (20)$$

This assumption gives only one condition on the constants, and so it is further assumed that if there are  $r$  constants, the residuals may be divided into  $r$  groups and  $\Sigma v_i = 0$  for each group. The groups are chosen

to contain nearly the same number of experimental values, but it should be noted that different methods of choosing the groups will lead to different values for the constants. If the number of residuals in a group is  $k$ , the summation of Eq. (20) yields

$$\sum_1^k v_i = m \sum_1^k x_i + kb - \sum_1^k y_i = 0$$

If the data in Table 4 are divided into two groups, 1 to 7 and 8 to 15, the two equations are

$$23.715m + 7b - 9.089 = 0$$

$$24.886m + 8b - 14.061 = 0$$

The values of  $m$  and  $b$  calculated from these simultaneous equations are

$$m = -1.6571 \times 10^3 \text{ deg}$$

$$b = 6.9125$$

The values of the residuals calculated from Eq. (20) by using these constants and the values obtained experimentally are given in Table 4 to indicate the precision with which the data are represented.

TABLE 4. APPLICATION OF A LINEAR EQUATION TO EXPERIMENTAL DATA

	$\frac{1}{T} \times 10^3$ $= x \times 10^3$	$\log P$ $= y$	$x^2 \times 10^6$	$xy \times 10^3$	Residuals $(mx_i + b - y_i) \times 10^3$		
					Graphical method	Method of averages	Method of least squares
1	3.614	0.920	13.06100	3.324880	+5	+4	+2
2	3.493	1.121	12.20105	3.915653	+5	+3	+2
3	3.434	1.221	11.79236	4.192914	+3	+1	0
4	3.405	1.271	11.59402	4.327755	+1	-1	-2
5	3.288	1.463	10.80944	4.810344	+4	+1	0
6	3.255	1.522	10.59502	4.954110	-1	-3	-4
7	3.226	1.571	10.40708	5.068046	-1	-4	-4
8	3.194	1.623	10.20164	5.183862	0	-3	-3
9	3.160	1.679	9.98560	5.305640	0	-3	-3
10	3.140	1.711	9.85960	5.372540	+1	-2	-1
11	3.117	1.749	9.71569	5.451633	+2	-2	-1
12	3.095	1.783	9.56902	5.518385	+4	+1	+1
13	3.076	1.814	9.46178	5.579864	+5	+1	+2
14	3.060	1.838	9.36360	5.624280	+7	+4	+4
15	3.044	1.864	9.26594	5.674016	+8	+4	+4
$\Sigma$	48.601	23.150	157.89433	74.303922			

3. *Method of Least Squares.* The methods already described give different values of the constants, depending upon the judgment of the investigator. The method of least squares has the advantage of giving a unique set of values for the constants, and the values of  $y$  calculated by using the constants determined by this method are the most probable values of the observations, it being assumed that the residuals follow the Gaussian law of error. The principle of least squares asserts that the best representative curve is that for which the sum of the squares of the residuals  $v_i$  is a minimum. In the case of the equation which we have been discussing, this sum is

$$\begin{aligned} S &= \sum_{i=1}^n (x_i m + b - y_i)^2 \\ &= m^2 \sum_{i=1}^n x_i^2 + 2bm \sum_{i=1}^n x_i - 2m \sum_{i=1}^n x_i y_i + nb^2 - 2b \sum_{i=1}^n y_i + \sum_{i=1}^n y_i^2 \end{aligned}$$

The necessary conditions for a minimum are

$$\begin{aligned} \frac{\partial S}{\partial m} &= 0 = 2m \sum_{i=1}^n x_i^2 + 2b \sum_{i=1}^n x_i - 2 \sum_{i=1}^n y_i x_i \\ \frac{\partial S}{\partial b} &= 0 = 2m \sum_{i=1}^n x_i + 2b(n) - 2 \sum_{i=1}^n y_i \end{aligned}$$

These two equations may be solved simultaneously for  $m$  and  $b$  to yield

$$\begin{aligned} m &= \frac{(n)\sum y_i x_i - \sum x_i \sum y_i}{(n)\sum x_i^2 - (\sum x_i)^2} \\ b &= \frac{\sum x_i^2 \sum y_i - \sum x_i \sum x_i y_i}{(n)\sum x_i^2 - (\sum x_i)^2} \end{aligned}$$

where the summations are to be carried out from 1 to  $n$ . Thus, in order to compute the constants by this method, it is necessary to calculate  $\sum x_i$ ,  $\sum y_i$ ,  $\sum x_i^2$ , and  $\sum x_i y_i$  as shown in Table 4. The calculations are carried out with more figures than the number of significant figures in the experimental data because the experimental values are assumed to be exact for purposes of the calculation.

The values of  $m$  and  $b$  obtained are

$$\begin{aligned} m &= -1.6601 \times 10^3 \text{ deg} \\ b &= 6.9221 \end{aligned}$$

and the values of the residuals are given in the last column of Table 4 for comparison with those obtained by the other methods. Calculations by the least-squares method are time-consuming and are therefore carried out only for reliable data.

The student is referred to books on mathematics for the application of this method to equations with three or more variables.<sup>1</sup>

### ERROR PROBLEMS

1. The molecular weight  $M$  of an ideal gas may be calculated from the gas law

$$PV = \frac{g}{M} RT$$

where  $P$  = pressure, atm

$V$  = volume, liters

$g$  = weight, g

$T$  = absolute temperature

$R$  = gas constant, 0.08206 liter-atm deg<sup>-1</sup> mole<sup>-1</sup>

In an experiment with CH<sub>4</sub>, a student obtains the following values and estimates the indicated maximum errors:

$$P = 735 \pm 1 \text{ mm}$$

$$V = 210 \pm 2 \text{ ml}$$

$$g = 137 \pm 2 \text{ mg}$$

$$T = 25 \pm 1^\circ\text{C}$$

Calculate the molecular weight and the range of uncertainty corresponding to these data, assuming CH<sub>4</sub> follows the ideal-gas law exactly.

2. The relationship between the intensity  $I$  of light transmitted through a solution, the incident intensity  $I_0$ , the length  $b$  in centimeters of the absorbing path, and the concentration of the solution  $c$  in moles per liter is known as the Beer-Lambert law and may be written

$$\log \frac{I_0}{I} = acb$$

where  $a$  is the absorbancy index.

A solution of a dye containing  $5.00 \times 10^{-4}$  mole liter<sup>-1</sup> transmits 8 per cent of light of a certain wavelength through a 1-cm cell. The uncertainty in the reading is  $\pm 1$  per cent in transmission. The sample is diluted *accurately* by a factor of 2, and the measurement repeated. The following data are obtained in this way:

$c \times 10^4$	Transmission, %
5.000	$8 \pm 1$
2.500	$27 \pm 1$
1.250	$53 \pm 1$
0.625	$73 \pm 1$

<sup>1</sup> Sokolnikoff and Sokolnikoff, "Higher Mathematics for Engineers and Physicists," 2d ed., McGraw-Hill Book Company, Inc., New York (1941).

Calculate a value of  $a$  and its range of uncertainty from the data given for each solution.

3. A student determines the heat capacity of a calorimeter bomb by burning benzoic acid, which has a heat of combustion of  $6315.0 \pm 0.5 \text{ cal g}^{-1}$ . The pellet of benzoic acid weighed  $0.5478 \pm 0.0003 \text{ g}$ . Also,  $0.020 \pm 0.001 \text{ g}$  of wire with a heat of combustion of  $1600 \pm 1 \text{ cal g}^{-1}$  is burned. The calorimeter contained  $1875 \pm 2 \text{ g}$  of water of specific heat  $0.9990 \pm 0.0005 \text{ cal g}^{-1}$ . The measured temperature rise was  $1.57 \pm 0.01^\circ\text{C}$ . Calculate the heat capacity  $x$  of the bomb by using the following equation:

$$x = \frac{6315G + 1600g}{t} - 0.999W$$

where  $G$  = grams of benzoic acid

$g$  = grams of wire

$t$  = observed temperature rise

$W$  = grams of water in calorimeter

What is the range of uncertainty in the heat capacity of the bomb due to the errors in the various measurements?

4. The relative viscosity  $\eta_1/\eta_2$  of a liquid may be calculated from the time  $t_1$  required for a given volume to flow through the capillary of a viscometer using

$$\frac{\eta_1}{\eta_2} = \frac{\rho_1 t_1}{\rho_2 t_2}$$

where  $t_2$  = flow time for reference liquid (water)

$\rho_1, \rho_2$  = densities for liquid and water, respectively

If at  $25^\circ$ ,  $\rho_2 = 0.99707 \pm 0.00005 \text{ g cm}^{-3}$  and  $t_2 = 45.1 \pm 0.4 \text{ sec}$ , calculate  $\eta_1/\eta_2$  and the range of uncertainty in this value for a liquid for which  $\rho_1 = 0.897 \pm 0.003$  and  $t_1 = 36.4 \pm 0.4 \text{ sec}$ .

5. The molecular weight  $M$  of a solute may be calculated from the elevation of the boiling point,  $\theta$ , for a solution containing  $g$  grams of solute in  $G$  grams of solvent using the equation

$$M = \frac{1000K_b g}{G\theta}$$

where  $K_b$  is a constant characteristic of the solvent. The assumptions made in the derivation of this relation (page 73) are sources of systematic error.

In an experiment in which the molecular weight of naphthalene in benzene is to be determined, it is found that the reading of the Beckmann thermometer for boiling benzene is  $2.975 \pm 0.005^\circ$ , and for a solution containing  $1.054 \pm 0.001 \text{ g}$  of naphthalene in  $87.0 \pm 0.1 \text{ g}$  of benzene, the reading is  $3.210 \pm 0.005^\circ$ . This type of thermometer is used only

in determining temperature differences. If the value of  $K_b$  is given as 2.530, calculate  $M$  and the range of uncertainty introduced by these estimated experimental errors.

6. The rotational constant  $B_0$  (cf. page 257) for the ground vibrational state of carbon monoxide has been found to be  $(57,635.965 \pm 0.005) \times 10^6$  cycles/sec by microwave-absorption studies, where the instrument calibration is made on a basis of frequency. A value of

$$B_0 = 1.922521 \pm 0.000035 \text{ cm}^{-1}$$

has been found by analysis of the rotation-vibration absorption band in the near-infrared region of the spectrum, where the calibration is made in terms of wavelength by interferometric methods. Calculate from these results a value for the velocity of light, and specify the range of uncertainty imposed by the data given.

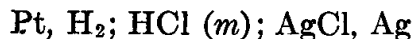
7. The vacuum wavelength for a particular Raman line is measured as  $4529.3 \pm 0.2 \text{ \AA}$ . The excitation line used was the blue mercury line of wavelength  $4358.35 \text{ \AA}$ . Calculate the vacuum wave number  $\tilde{\nu} = 1/\lambda_{\text{vac}}$  for each line, and the "Raman shift" ( $\tilde{\nu}_{4358} - \tilde{\nu}_{4529}$ ), together with the pertinent range of uncertainty in this difference.

8. The apparent molar volume (cf. page 89) for a solute in a binary solution system at a given temperature and pressure is defined as

$$\phi_V = \frac{1}{m} \left\{ \frac{1000 + mM_2}{\rho} - \frac{1000}{\rho_1} \right\}$$

For an aqueous solution of potassium hydroxide (molecular weight  $M_2 = 56.108$ ), determine the accuracy required in the molality  $m$  of the solute and the difference in density ( $\rho - \rho_1$ ) of the solution and the pure solvent if the acknowledged range of uncertainty in the value of  $\phi_V$  is not to exceed 0.01 ml for  $m = 0.01$ .

9. The electromotive force of the cell



is given by the relation

$$E = E^\circ - \frac{RT}{F} \ln \frac{(\gamma_{\pm} m)^2}{P_{\text{H}_2}^{1/2}}$$

where  $\gamma_{\pm}$  = mean ionic activity coefficient for HCl

$m$  = molality of solute

$P_{\text{H}_2}$  = partial pressure of hydrogen gas at the hydrogen electrode, standard atm

= (barometric pressure  $P_{\text{bar}}$ ) - (vapor pressure of electrolyte solution)

For  $T = 298.15 \pm 0.01^\circ\text{K}$ , calculate the value of  $\gamma_{\pm}$  and the range of uncertainty corresponding to the following data:

$$\begin{aligned} E &= 0.27227 \pm 0.00003 \text{ volt} & m &= 0.5000 \pm 0.0003 \\ E^\circ &= 0.22239 \pm 0.00005 \text{ volt} & P_{\text{bar}} &= 740.00 \pm 0.05 \text{ standard mm Hg} \\ \text{Vapor pressure of solution} &= 23.34 \pm 0.03 \text{ standard mm Hg} \end{aligned}$$

10. The refractive index  $n$  of "standard air" (0.03 per cent  $\text{CO}_2$ ,  $15^\circ\text{C}$ , 1 standard atm pressure) is given as  $1.00027794 \pm (3 \times 10^{-8})$  for a wavelength of 5460 Å (green light). The molar refraction  $\mathcal{R}$  for this wavelength,

$$\mathcal{R} = \frac{n^2 - 1}{n^2 + 2} V \quad (1)$$

where  $V$  is the molar volume, may be treated as constant for small variations in temperature and pressure.

a. Identify the assumptions made in the derivation of the formula

$$\frac{(n - 1)_{288.15^\circ\text{K}, 1 \text{ std atm}}}{(n - 1)_{T^\circ\text{K}, P \text{ std atm}}} = \frac{T}{288.15} \frac{1}{P} \quad (2)$$

b. Calculate the value of  $n - 1$  for a temperature of  $25.00 \pm 0.03^\circ\text{C}$  and pressure of  $740.00 \pm 0.05$  standard mm Hg and determine the effect on this value of the uncertainties in the data given and of the assumptions made in the derivation of Eq. (2).

For air, the compressibility factor  $Z$  ( $V = ZRT/P$ ) may be taken as  $0.99958 \pm 0.00001$  at  $15^\circ\text{C}$ , 1 standard atm pressure, and as  $0.99969 \pm 0.00001$  at  $25^\circ\text{C}$ , 740 standard mm pressure.



## *Opticochemical Measurements*

Many types of analyses may be made by optical methods. These methods have the advantage that they are rapid and sensitive and leave the sample unchanged. Also, the optical tools are popular as instruments of physical chemistry in the determination of the structure, size, and shape of both ordinary and large molecules in solution or of colloidal particles in suspension.

### REFRACTOMETRY

**Refractometers Measuring Critical Angle.** The basic principles of operation and the construction of the Abbe and immersion refractometers have been described in a number of places.<sup>1</sup> The compensator (or Amici prism), which makes possible the use of white light in the Abbe and immersion refractometers, consists of two direct-vision prisms in the telescope barrel which can be rotated in opposite directions. The direct-vision prisms are made to give dispersion, with a minimum of deviation, by cementing a dense prism of flint glass between two prisms of crown glass. If the first direct-vision prism spreads out the light into a spectrum, and if the second prism is set at the same angle, the dispersion is doubled. However, if the prism is rotated through 180°, the second prism will subject the dispersed beam to an opposite dispersion, thus reproducing white light. The refractometer prism and the liquid produce dispersion, the amount varying with the refractive index of the liquid. The extent to which the prisms of the compensator must be rotated in order to offset the dispersion of the refractometer and liquid to produce white light must be determined each time by trial. The reading on the compensator drum is a measure of the dispersion of the liquid.

The Abbe refractometer is checked by placing against the upper prism a plate glass of known refractive index supplied with the instrument. The two surfaces are held together with a drop of liquid having a higher

<sup>1</sup> Bauer, Fajans, and Lewin *in* Weissberger (ed.): "Physical Methods of Organic Chemistry," 3d ed., Vol. I, Pt. II, Interscience Publishers, Inc., New York (1960).

index of refraction, for example,  $\alpha$ -bromonaphthalene. If the refractometer does not give the proper reading, it is adjusted by means of the small screw at the back of the telescope. The immersion refractometer is checked with distilled water. If the shadow edge does not fall at 15.0 for 17.5°C or at 13.25 for 25°C, adjustment is made by means of a screw inside the micrometer drum.

The Pulfrich refractometer is perhaps the oldest and the most accurate instrument of this kind. It requires a sodium or mercury lamp or other source of monochromatic light because it does not have a compensating Amici prism. The horizontal beam of monochromatic light goes through a cup of liquid cemented to the top of the prism and is refracted through an angle which is measured directly by rotating the eyepiece until it picks up the colored line of light, directly coincident with the point of intersection of the cross hairs. The angle of refraction is read directly in degrees on a circular scale, using a vernier and lens.

The zero setting of the instrument is obtained by holding a small light at arm's length in front of the small square window near the eyepiece and turning the graduated circular scale until the image of the cross hairs reflected from the face of the main prism coincides with the cross hairs themselves. This window has a right-angled prism which directs a light beam on to the prism surface, from which it is reflected back into the eyepiece. The zero setting is subtracted from the reading of the angle of refraction.

The refractive index  $n_\lambda$  at each wavelength  $\lambda$  is calculated by means of the formula

$$n_\lambda = \sqrt{N_\lambda^2 - \sin^2 i}$$

where  $N_\lambda$  = refractive index of glass prism against air for wavelength of light used

$\sin i$  = sine of angle of emergence  $i$  measured on circular scale

The values of  $N_\lambda$  are furnished with the Pulfrich instrument, usually for the blue (4358 Å), green (5460 Å), and yellow (5780 Å) lines of the mercury arc.

The cup of the Pulfrich refractometer is cemented to the prism. For organic liquids, fish glue may be used. Still better is a concentrated gelatin solution containing potassium dichromate, which is exposed to bright sunlight after setting in place. When aqueous solutions are used, the glass cup must be attached with Canada balsam or other waterproof cement. A smaller metal cup with circulating thermostated water is set into the cup of liquid.

The Pulfrich and the immersion refractometers may be provided with interchangeable prisms which extend the range to different refractive indices. The immersion refractometer is provided with a small metal

cap with a glass bottom which fits over the prism and permits measurements to be made with small amounts of liquid.

The refractive index of liquids changes considerably with temperature, and temperature control to 0.1 or 0.2° is necessary. The refractive index of glass against air changes also, but to a considerably smaller extent. For example, in the Pulfrich refractometer, the refractive index of the prism is given for 20° and an increase of 3° gives an increase in the refractive-index calculations of about 1 in the fifth decimal place. This temperature correction for the glass may be neglected in ordinary work at room temperature.

**Differential Instruments.** One of the ways in which the concentration of a solution may be analyzed, or the refractive-index increment for the solute determined, is by means of a differential refractometer. There are a number of varieties of instrument, but in all of them their refracting surfaces represent the equivalent of two adjacent prisms, one with solvent and the other with (dilute) solution. With solvent in both prisms there is zero deflection of an image, but with solvent of refractive index  $n_0$  in one and solution of refractive index  $n$  in the other, the displacement of the image is nearly proportional to  $n - n_0$ . There are many advantages of the differential method, especially that of very high accuracy. Temperature control is maintained by enclosing the cells in a jacket through which water can be pumped from a thermostat.

Differential refractometers are especially important instruments to the macromolecular chemist. In connection with the estimation of molecular weights from the data on light scattering, a knowledge of the refractive-index increment in dilute solutions is required. The construction and alignment of differential refractometers have been described by Debye,<sup>1</sup> Brice and Speiser,<sup>2</sup> and Svensson.<sup>3</sup>

**Schlieren Techniques.** To observe the changes in boundary position and breadth which take place in electrophoresis, diffusion, velocity sedimentation, and chromatography experiments, optical methods are indispensable. Some time ago the light-absorption method was developed to a high degree of precision by Svedberg and associates<sup>4</sup> to give concentration as a function of distance in an optical cell; it is now again a useful procedure.

When there is no convenient absorption band, the refraction methods, which give not concentration, but concentration gradient (more strictly refractive-index gradient), as a function of distance in the cell, are

<sup>1</sup> *J. Appl. Phys.*, 17, 392 (1946).

<sup>2</sup> *J. Opt. Sci. Am.*, 36, 364 (1946).

<sup>3</sup> *Anal. Chem.*, 25, 913 (1953).

<sup>4</sup> Svedberg and Rinde, *J. Am. Chem. Soc.*, 46, 2677 (1924); Tiselius and Gross, *Kolloid-Z.*, 66, 11 (1934).

effective. The classical one is the scale method of Lamm, which is quite accurate but somewhat tedious in use. There have come into use other refractive methods, based upon the schlieren effect, the methods having been devised by Wiener, Svensson, Philpot, and Longsworth.<sup>1</sup> They depend upon the formation of shadows on the image of a cell by the interference of convergent rays which, in passing through a boundary between solvent and solution, have been deviated by the inhomogeneous layers of liquid. The cylindrical-lens schlieren optical system is illustrated in Fig. 105. This method makes use of the bending light by the refractive-index gradient between two solutions of different composition, and hence of different refractive index, and of the fact that the angular deflection of the light is directly proportional to the magnitude of the gradient. An

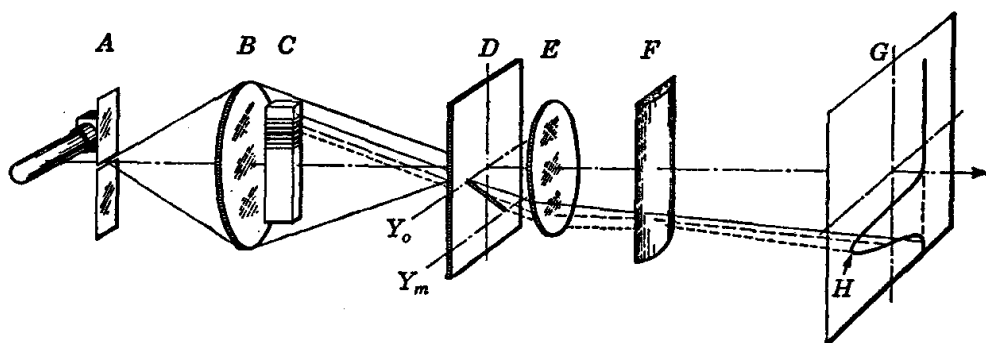


FIG. 105. Schlieren optical system for observing and photographing refractive-index gradients.

image of the horizontal illuminated slit *A* is focused by means of a large lens (schlieren lens) *B* on a diagonal slit in the focal plane *D* of the schlieren lens. The cylindrical lens *F* with its axis vertical is focused on the inclined slit and on the photographic plate *G*. The camera lens *E* focuses the cell *C* on the photographic plate. The presence of the cylindrical lens does not alter the vertical coordinates of a point in the photograph of the cell, but in conjunction with the diagonal slit will displace the ray of light horizontally across the optical axis if it has been bent downward by a refractive-index gradient. This lateral displacement is directly proportional to the refractive-index gradient in the cell at the level at which the light ray passed through, so that the photograph obtained is a plot of refractive-index gradient versus vertical height in the cell.

If the liquid in the cell is homogeneous, all the light passing through it is concentrated in the normal slit image of  $Y_0$  and is focused on the photo-

<sup>1</sup> Wiener, *Ann. Physik*, **49**, 105 (1893); Svensson, *Kolloid-Z.*, **87**, 181 (1939); Philpot, *Nature*, **141**, 283 (1938); Longsworth, *J. Am. Chem. Soc.*, **61**, 529 (1939); *Ind. Eng. Chem., Anal. Ed.*, **18**, 219 (1946).

graphic plate by the camera lens to form the vertical base line of the pattern. With a boundary between two solutions of different refractive index in the cell, the light through the layer having the maximum gradient is deflected to  $Y_m$ . These rays pass through the inclined slit to the right of the optical axis (when we look toward the light source) and are therefore passed to the left by the cylindrical lens to form the peak of the pattern at  $H$ . Other rays through regions in which the refractive-index gradients are less intersect the diagonal slit at positions between the normal slit image and  $Y_m$  and form points in the refractive-index-gradient plot in the photographic plate. The plot of refractive index versus vertical height in the cell may be obtained by integration of the refractive-index-gradient curve.

**Interferometric Methods.** Still more accurate optical systems for the study of moving and diffusing boundaries depend upon several interference phenomena. The rigorous quantitative use of the Gouy interference effect<sup>1</sup> in the study of diffusion was the pioneering effort in this direction. Now Rayleigh integral fringe optical systems are being developed and used in diffusion and in sedimentation analysis.<sup>2</sup> They give the refractive index along the linear (vertical) or radial cell dimension.<sup>3</sup> The assembly of Longworth<sup>4</sup> is very useful.

## LIGHT SCATTERING

A number of light-scattering phenomena have been studied, for example, turbidimetry, nephelometry, Tyndall effects, dissymmetry of depolarization, etc. One of the effects in which the physical chemist is currently interested is the scattering from dilute solutions of macromolecules, mathematical analyses and expressions for solute molecular weight being obtained by treating the scattering as resulting from statistical fluctuations in the density of the solvent and in the concentration of the solute, which produce momentary variations in dielectric constant and therefore in refractive index.

Some light is scattered even by a pure liquid because it is inhomogeneous on a microscopic scale. The scattering by a solution is correspondingly greater because of local differences in refractive index due to

<sup>1</sup> Kegeles and Gosting, *J. Am. Chem. Soc.*, **69**, 2516 (1947); Coulson, Cox, Ogston, and Philpot, *Proc. Roy. Soc. (London)*, **A192**, 382 (1948); Gosting and Onsager, *J. Am. Chem. Soc.*, **74**, 6066 (1952); Creeth, *J. Am. Chem. Soc.*, **77**, 6428 (1955).

<sup>2</sup> Longworth, *Rev. Sci. Instr.*, **21**, 524 (1950); *Anal. Chem.*, **23**, 346 (1951); Creeth and Gosting, *J. Phys. Chem.*, **62**, 58 (1958); Creeth, *ibid.*, **62**, 66 (1958); Schachman, "Ultracentrifugation in Biochemistry," Academic Press, Inc., New York (1959).

<sup>3</sup> Philpot and Cook, *Research (London)*, **1**, 234 (1948); Svensson, *Acta Chem. Scand.*, **3**, 1170 (1949); **4**, 399, 1329 (1950); **5**, 72, 1301, 1410 (1951).

<sup>4</sup> *J. Am. Chem. Soc.*, **74**, 4155 (1952).

fluctuations in concentration of solute. The study of the intensity of light scattered by a solution of a high polymer (or protein) may be used to determine the molecular weight and shape of these molecules.<sup>1</sup> In the case of molecules having dimensions comparable with the wavelength of light or greater, measurements of light scattered at several angles are required; thus the apparatus is arranged so that the photomultiplier

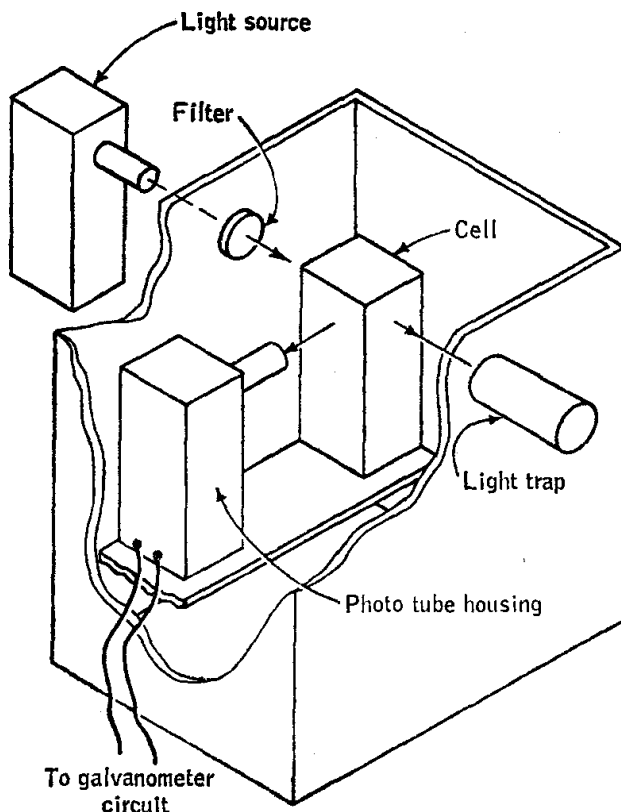


FIG. 106. Light-scattering apparatus.

detector may be placed at several angles.<sup>2</sup> The principle of operation of the apparatus is illustrated by Fig. 106.

To use the equations, two optical measurements are required: a quantitative comparison of the two intensities of the scattered and incident beams, and the determination of the specific-refractive-index increment of the solution. The measurement of the intensity of light scattered by a dilute solution is carried out in an apparatus (Fig. 106) which consists of a light source, a collimation system for the incident

<sup>1</sup> Debye, *J. Phys. Colloid Chem.*, **51**, 18 (1947); Zimm, *J. Chem. Phys.*, **16**, 1099 (1948); Bender, *J. Chem. Educ.*, **29**, 15 (1952).

<sup>2</sup> Stein and Doty, *J. Am. Chem. Soc.*, **68**, 159 (1946); Debye, *J. Applied Phys.*, **17**, 392 (1946).

beam, a cell to hold the solution, a collimation system for the scattered light, a photomultiplier, and a measuring device for the impulse. The photomultiplier is so mounted that it may be moved in an arc around the solution cell in order that the quantity called the *Rayleigh ratio* may be determined at several angles. Some form of permanent working standard is used to check variations in the performance of the apparatus; molecular weights are given in reference to that of some standard substance.

Specific refractive index increment data are obtained by using a differential refractometer.

Light scattering as applied to the study of large molecules has been reviewed by Stacey<sup>1</sup> and by Oster.<sup>2</sup>

### MICROSCOPY

**Light Microscope.** The resolving power (R.P.) of the common microscope is a measure of its capacity to reproduce minute details of the structure of the object in the image. It is directly proportional to a quantity called the numerical aperture (N.A.) and inversely proportional to the wavelength  $\lambda$  of the light employed; thus

$$\text{R.P.} = \frac{\text{N.A.}}{\lambda}$$

This formula is valid only for central illumination; if sufficiently oblique illumination is used, the resolving power may be almost doubled. The resolving power also increases with an increase in the refractive index of the medium intervening between the front lens of the objective and the cover glass over the specimen. Thus, by using water-immersion and oil-immersion lenses, the resolving power can be further increased.

Eyepieces equipped with a measuring scale are known as micrometer eyepieces. The scale may be calibrated in absolute units by means of a stage micrometer, which is viewed in the same manner as any object would be. The scale must be calibrated for each objective used. The filar micrometer is almost indispensable for measurements of small lengths.

Binocular microscopes are advantageous from several points of view; they give a correct stereoscopic image, they prevent fatigue in prolonged studies, and with a properly constructed camera, very satisfactory stereophotomicrographs can be made.

<sup>1</sup> Stacey, "Light Scattering in Physical Chemistry," Academic Press, Inc., New York (1956).

<sup>2</sup> Oster, *Chem. Revs.*, 43, 319 (1948); in Weissberger (ed.), *op. cit.*, Vol. I, Pt. III.

Phase-contact microscopy began with Zernicke.<sup>1</sup> It enhances the contrast of the image which is observed, making possible an observation of sections too thin or too transparent for the conventional techniques. It is also valuable in the microscopic determination of refractive index.

Microscopes for use in the chemical laboratory should be provided with polarizing and analyzing Nicol prisms. Very important information is often secured by examinations of substances in polarized light. Special microscopes known as chemical microscopes are available, having such prisms and other useful accessories.

**Electron Microscope.** The limiting factor in the resolution of small objects by the optical microscope is the wavelength of the light. The details of material under examination cannot be seen if they are smaller than the wavelength of the light used in the observation. A beam of monoenergetic electrons can exhibit interference effects characteristic of a wave motion with a wavelength  $\lambda$  of

$$\lambda = \frac{300hc}{Ee}$$

where  $E$  = accelerating potential, volts

$e$  = electron charge, esu

$h$  = Planck's constant

$c$  = velocity of light

It is readily calculated that a beam of electrons can have a wavelength of a fraction of an angstrom unit, as against 4000 to 8000 Å for the wavelength of visible light. Moreover, the electron beam can be bent by an electrostatic or an electromagnetic field so that it can be focused by simple adjustment of current and voltage. These principles have been applied in the design electron microscopes,<sup>2</sup> and many excellent pictures have been taken with them. Bacteria, fine powders such as carbon black, fibers, and many things of biological interest have been examined with enormously greater magnification than was previously possible, and new details of structure have been revealed.

The principle of the electron microscope is shown in Fig. 107. Electrons are emitted from a hot filament, accelerated by fields of 30,000 to 100,000 volts, and focused with magnetic fields as indicated. The object is placed on a thin nitrocellulose film, which is fairly transparent to the beam and shows no structure of its own. The electrons pass through and are focused on a fluorescent plate, where the image is viewed by eye. The

<sup>1</sup> In Bouwers: "Achievements in Optics," Elsevier Press, Inc., New York (1946). Cf. also Bennett, Jupnik, Osterberg, and Richards, *Trans. Am. Microscop. Soc.*, **65**, 99 (1946); "Phase Microscopy," John Wiley & Sons, Inc., New York (1951).

<sup>2</sup> Hall, "Introduction to Electron Microscopy," McGraw-Hill Book Company, Inc., New York (1953); Hamm in Weissberger (ed.), *op. cit.* p. 1561, Vol. I, Pt. II.



electrons are scattered by the denser parts of the object, but the transparent parts of the object show up more brightly. A photographic plate is then substituted for the fluorescent screen, and a short exposure gives a satisfactory picture. The monograph of Hall and the chapter by Hamm are but two sources of much information about the physical principles involved in the design of electron microscopes and the ways in which they are applied in the construction of the instrument.

The details in an electron-microscope picture sometimes may be brought out more clearly by producing "shadows" of the more prominent parts of an object. Vapors of a heavy element such as uranium may be

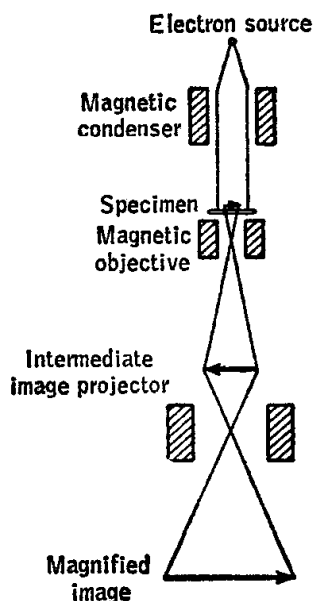


FIG. 107. Principle of the electron microscope.

directed across the object in an evacuated space, or the object may be embedded in a thin layer of an inorganic gel consisting of a compound of a heavy element. The less dense or thinner parts of the object then transmit the electron beam more readily, thus producing the shadows and revealing finer details of the structure.

### POLARIMETRY

The development first of carbohydrate chemistry and now protein chemistry and steroid chemistry is associated with polarimetry. When ordinary, unpolarized light passes through a Nicol prism at the proper angle to the optic axis, only the plane-polarized extraordinary ray is transmitted. Now, if this emergent ray is caused to fall upon another Nicol, the ray will pass through if it has parallel orientation. If the second prism is rotated through  $90^\circ$ , the plane-polarized light is extin-

guished and the Nicols are said to be "crossed." Such Nicols with light source, sample tube, and eyepiece form the basic elements of the polarimeter.

On passage through optically anisotropic liquids or solutions, a change in the direction of vibration of the linearly polarized light may be produced. Pasteur's principle that a compound will be optically active if its structure cannot be brought into coincidence with its mirror image is quite general; the presence of an asymmetric carbon atom is not required. This principle will be met whenever the three-dimensional molecule has neither a plane of symmetry nor a center of symmetry. Another case of optical activity, now of special interest, is the molecular dissymmetry due to the presence of a helical structure, producing an optical activity which is superimposed upon that due to the asymmetric carbon atoms in polypeptides and proteins.

The various types of available instruments and underlying principles have been described in detail by Heller.<sup>1</sup> The subject of the dispersion of optical rotation has been considered by Djerassi<sup>2</sup> and by Klyne and Parker.<sup>3</sup>

<sup>1</sup> In Weissberger (ed.), *op. cit.*, Vol. I, Pt. III (1960).

<sup>2</sup> "Optical Rotatory Dispersion," McGraw-Hill Book Company, Inc., New York (1960).

<sup>3</sup> In Weissberger (ed.), *op. cit.*, Vol. I, Pt. III (1960).

## *Thermal Measurements*

### THERMOMETRY<sup>1</sup>

**The International Temperature Scale.** Although the constant-volume hydrogen thermometer is the standard on which the centigrade and absolute scales are based, such a thermometer is inconvenient to use except as an ultimate standard. The international temperature scale is defined by several fixed points (Table 1), and means for interpolating between the fixed points are provided.

**TABLE 1. FIXED POINTS OF THE INTERNATIONAL TEMPERATURE SCALE**  
[All at 1 atm pressure (760 mm Hg)]

Substance	Designation	Temperature, °C
Oxygen.....	Boiling point	-182.97
Water (air-saturated).....	Freezing point	0.000
Water.....	Boiling point	100.000
Sulfur.....	Boiling point	444.60
Antimony.....	Freezing point	630.50
Silver.....	Freezing point	960.5
Gold.....	Freezing point	1063

From the ice point to 660° the international centigrade temperature is computed from the resistance  $R_t$  of a standard platinum resistance thermometer by means of the equation

$$R_t = R_0(1 + At + Bt^2) \quad (1)$$

The constants  $R_0$ ,  $A$ , and  $B$  are determined by calibration at the ice, steam, and sulfur points. From -190° to the ice point a platinum

<sup>1</sup> A standard reference book on this subject is "Temperature: Its Measurement and Control in Science and Industry," Reinhold Publishing Corporation, New York (1941). It includes 125 papers presented at a symposium. See also Griffiths, "Methods of Measuring Temperature," Charles Griffin & Co., Ltd., London (1947); Sturtevant in Weissberger (ed.): "Technique of Organic Chemistry," 3d ed. Vol. I, Pt. I, Chap. 6, Interscience Publishers, Inc., New York (1959).

resistance thermometer is also used, with a modified interpolation formula:

$$R_t = R_0[1 + At + Bt^2 + C(t - 100)t^3] \quad (2)$$

$R_0$ ,  $A$ , and  $B$  are the same as before, and  $C$  is determined by measurement at the oxygen point.

From 660 to 1063° the temperature is computed from the electromotive force  $E$  of a standard platinum versus platinum-rhodium thermocouple by means of the equation

$$E = a + bt + ct^2 \quad (3)$$

where  $a$ ,  $b$ , and  $c$  are obtained from measurements at the antimony point, silver point, and gold point.

Above the gold point an optical method, based on the Wien formula for blackbody radiation, is used.

The international temperature scale assures laboratories throughout the world of an accurate and readily reproducible basis of temperature measurement. It should be pointed out, however, that the relationship between absolute centigrade and international scales is subject to such changes as are occasioned by production of new materials of higher purity or more refined experimental techniques in gas thermometry.

**Mercury Thermometers.** The mercury thermometer is the simplest and most widely used instrument for measuring temperature. Mercury is particularly suitable because it has a very uniform coefficient of expansion, it does not wet glass, it is easily purified, and the thermometer is easily read. At atmospheric pressure it remains liquid from  $-40$  to  $+357^\circ\text{C}$ .

Thermometers of various grades and ranges are available, including (a) 0 to 100, 250, and  $360^\circ$ , graduated in degrees for general purposes; (b) sets of thermometers from  $-40$  to  $+400^\circ$ , each having a range of  $50^\circ$  and graduated to  $0.1^\circ$ ; (c) 18 to  $28^\circ$ , graduated to  $0.01^\circ$ , or 17 to  $31^\circ$ , graduated to  $0.02^\circ$ , for calorimetric work; (d)  $-5.0$  to  $+0.5^\circ$ , graduated to  $0.01^\circ$  for freezing-point lowering; (e) Beckmann-type thermometers with adjustable range, graduated to  $0.01^\circ$ ; (f) high-temperature thermometers, in which special combustion glasses or quartz are used with nitrogen or argon under pressure to extend the upper temperature limit as high as  $750^\circ\text{C}$ .

The graduations should extend a little beyond the nominal limits, and a high-grade thermometer of any range should have an ice point for standardization if actual temperatures are to be measured. If only differences in temperature are required, the ice point is not necessary.

*Reading.* Exposed stem, parallax, and sticking mercury constitute three important sources of error in the reading of thermometers.

Thermometers are usually calibrated for total immersion of the mercury, and a correction is necessary when part of the stem is exposed. The thermometer will read too low if the air surrounding the stem is colder than the bath in which the bulb is immersed, and too high if the air is warmer. A second thermometer is placed near the exposed stem, and the stem correction  $S$  is given by the formula

$$S = 0.00016n(t' - t)$$

where  $n$  = length of exposed mercury column in terms of scale degrees

$t'$  = temperature of bath

$t$  = average temperature of emergent stem

The factor 0.00016 is suitable for the glass used in most thermometers.

It should be emphasized that stem corrections are not accurate, and for very high or very low temperatures a considerable error may be introduced. It is better to avoid the exposed stem by improving the experimental conditions.

Parallax may cause an erroneous reading, depending upon the extent to which the eye is below or above the level of the top of the mercury thread. It may be eliminated completely by reading the thermometer from a distance with a cathetometer (telescope and cross hair), and it may be reduced considerably by carefully regulating the position of the eye. Special thermometer lenses sliding along the stem are helpful.

A thermometer should be read whenever possible with a rising thread rather than a falling thread, and in either case it is necessary in accurate work to tap the thermometer gently before reading, to prevent sticking.

*Standardization.* In the simplest method, the thermometer is compared with a standard thermometer, for which purpose a thermometer certified by the National Bureau of Standards is useful. The two thermometers are set side by side in a thermostat, vapor bath, or large, well-stirred body of liquid. The National Bureau of Standards thermometer is immersed nearly to the top of the thread, and the other thermometer is immersed to the depth at which it is to be used. The true temperature as given by the standard thermometer is obtained by adding or subtracting the correction indicated on the National Bureau of Standards certificate, after correction for a possible change in the ice point.

The ice point is always taken before a standardization, and it should check with the ice point given on the certificate, if the corrections as given in the certificate are to apply. In case the ice point does not check, a constant adjustment of all the corrections is necessary.

In taking the ice point of a thermometer, it is necessary to have the ice very finely divided and intimately distributed throughout the whole bath. A large layer of water is not allowed to accumulate, and the spaces

between the pieces of ice must be filled with water, not air. For ordinary work, finely shaved, close-packed ice in distilled water makes a satisfactory ice bath. For precision work, the recommendations of White<sup>1</sup> should be followed.

Fixed boiling points, freezing points, or transition temperatures of pure materials are also used for standardizing thermometers (Table 1). Calibration against a platinum resistance thermometer certified by the National Bureau of Standards is the best method.

The standardization of a mercury-in-glass thermometer should be rechecked frequently at one point, usually the ice point. Slow permanent changes in the glass result in changes in the volume of the bulb. Furthermore, temporary changes in the bulb volume are likely to result from heating; the bulb may not regain its original volume for several days.

**Beckmann Thermometer.** A Beckmann thermometer is shown in Fig. 108. This instrument reads directly to  $0.01^\circ$  and can be estimated to  $0.001^\circ$ . Its range is only  $5$  or  $6^\circ$ , but it can be set for any temperature by adjusting the mercury in the reservoir at the top of the scale. The thermometer is warmed until sufficient mercury has been driven over into the reservoir, and it is then given a sharp tap with the hand to break the thread at the entrance to the reservoir.



FIG. 108. Beckmann thermometer.

The thread is broken when the temperature is a little above the desired temperature, because a certain amount of cooling is necessary to bring the mercury back on the scale.

**Other Liquid Thermometers.** If thallium is added to mercury to give an 8.5 per cent solution, the amalgam can be cooled to  $-60^\circ$  before freezing. Liquid pentane can be used down to liquid-air temperatures, and toluene can be used to  $-100^\circ$ , which is below the temperature of carbon dioxide "dry ice."

**Bimetallic Thermometers.** In this type of thermometer the temperature is indicated on a dial by a pointer actuated by the differential expansion of a bimetallic strip. These thermometers are usually accurate to only about 1 per cent, but they are rugged and useful where high accuracy is not important.

**Gas Thermometers.** Gas thermometers are inconvenient to use for any purpose other than ultimate standardization. For such

<sup>1</sup> *J. Am. Chem. Soc.*, 46, 2418 (1924).

purposes the experimental arrangement and the calculations are quite complex.<sup>1</sup>

**Resistance Thermometers.** The electrical resistance of a wire increases in a regular manner as the temperature rises, and since the resistance of a wire can be measured with great precision, this measurement offers an accurate method for determining temperatures.

Platinum wire is commonly used because of its chemical inertness and its high resistance. It must be of the highest grade, carefully purified, and annealed by heating to redness with an electric current. It is annealed again at a lower temperature after winding.

The wire is wound on mica supports in such a way that the metal is subjected to as slight a strain as possible when the thermometer is heated

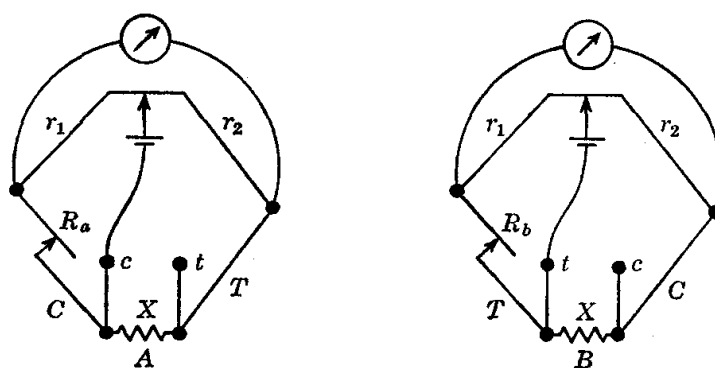


FIG. 109. Circuit diagram illustrating resistance measurements of a four-lead thermometer.

or cooled. Usually the coil is enclosed in a sealed glass or quartz tube; when it is desired to minimize the lag of the thermometer, the coil is enclosed in a flattened metal case. Platinum resistance thermometers are usually manufactured with a resistance of 25.5 or 2.55 ohms at  $0^\circ$ . The resistance then changes by about 0.1 or 0.01 ohm  $\text{deg}^{-1}$ , respectively.

In accurate resistance thermometry, it is essential that the resistance from which the temperature is computed be that of the thermometer element itself and contain no contribution from the leads. This is accomplished by using a four-lead thermometer and a suitable bridge, in which the lead resistance is effectively eliminated by a switching arrangement. In Fig. 109,  $r_1$  and  $r_2$  are equal ratio arms,  $C$ ,  $c$ ,  $T$ , and  $t$  are the four leads,  $X$  is the thermometer resistance, and  $R_a$  and  $R_b$  are the resistances required to balance the bridge in the two arrangements. It is evident that  $R_a + C = X + T$  and  $R_b + T = X + C$ . Hence,  $X = (R_a + R_b)/2$ .

<sup>1</sup> For example, the following papers in "Temperature: Its Measurement and Control in Science and Industry," Reinhold Publishing Corp., New York (1941): Keyes, p. 45; Roebuck and Murell, p. 60; Cragoe, p. 89.

If temperatures are to be determined to a precision of  $\pm 0.001^\circ$ , it is necessary to employ a carefully calibrated bridge in which the resistance of the contacts between decades has been eliminated.<sup>1</sup>

For computing temperatures from observed resistances, the equation

$$t = \frac{100(R_t - R_0)}{R_{100} - R_0} + \delta \left( \frac{t}{100} - 1 \right) \frac{t}{100} \quad (4)$$

is more convenient than Eq. (1). The constants  $R_0$ ,  $R_{100} - R_0$  (the "fundamental interval"), and  $\delta$  are determined by calibration at the ice, steam, and sulfur points. This calibration is performed by the National Bureau of Standards for a reasonable charge. The value of  $t$  is calculated from  $R$  by successive approximations, a process which is not difficult because of the relatively small value of  $\delta$ . Convenient tables for converting platinum-resistance values to degrees centigrade have been published.<sup>2</sup>

A carefully constructed and standardized platinum resistance thermometer is preeminent in the field of thermometry for its reliability in both accuracy and precision over long periods of time. Other resistance thermometers can be made of nickel, copper,<sup>3</sup> Hytemco,<sup>4</sup> and other metals and alloys in cases where extreme accuracy is subordinate to economy and ease of construction.

The resistance of a thermometer may also be determined by comparing with a potentiometer the potential drop across the thermometer with that across a standard resistor in series with the resistance thermometer, while a small current is flowing.

Resistance thermometers can also be made of semiconductors in which the resistance *decreases* very sharply as the temperature increases. Such thermometers are called "thermistors." They permit the use of a less accurate bridge for temperature measurement and are suitable for small temperature *differences*.

**Thermocouples.**<sup>5</sup> In a closed circuit of dissimilar metals, a current is generated when the junctions are at different temperatures. A simple

<sup>1</sup> For a discussion of this point and other factors in precision resistance thermometry, see Mueller in "Temperature: Its Measurement and Control in Science and Industry," Reinhold Publishing Corp., New York (1941), and "Resistance Thermometers," Leeds and Northrup Co., Philadelphia.

<sup>2</sup> Werner and Frazer, *Rev. Sci. Instr.*, **23**, 163 (1952).

<sup>3</sup> Maier, *J. Phys. Chem.*, **34**, 2860 (1930).

<sup>4</sup> An alloy with an exceptionally high temperature coefficient of resistance, manufactured by the Driver-Harris Co., Harrison, N.J.

<sup>5</sup> For a comprehensive discussion, see Roeser in "Temperature: Its Measurement and Control in Science and Industry," p. 180; Roeser and Lonberger, "Methods and Testing Thermocouples and Thermocouple Material," *Natl. Bur. Standards (U.S.), Circ.*, **590**, (1958).



thermocouple is shown in Fig. 110, together with a multiple-junction assembly which is called a *thermel*. The heavy line represents one metal, and the lighter line represents the other.

In Fig. 110 the use of the thermocouple in determining the freezing curves of alloys is illustrated. The potentiometer shown is a commercial instrument of moderate precision made expressly for use with thermocouples, with a low voltage range, up to 0.1 volt.

The common types of thermocouples and their important characteristics are illustrated in Table 2. Extended tables of electromotive force

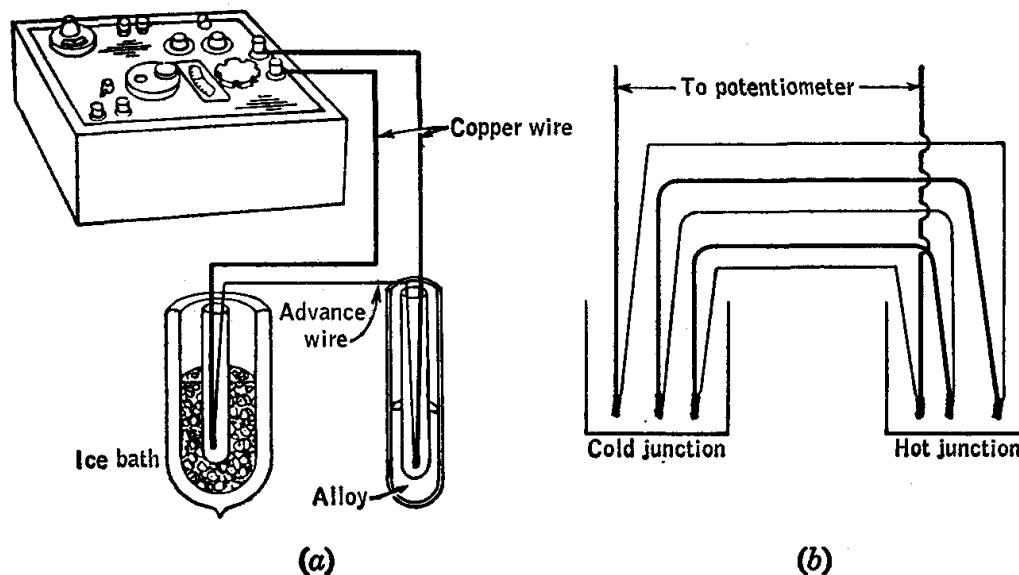


FIG. 110. (a) Use of the thermocouple in alloy-cooling-curve studies; (b) a three-junction thermel.

as a function of temperature for the different types are found in many of the standard handbooks and in a circular published by the U.S. National Bureau of Standards.<sup>1</sup>

Copper and constantan may be soldered together by using rosin or other noncorrosive flux, but the other metals are welded together in an oxy-gas flame or in an electric arc. The two wires are twisted together for a short distance, held in an insulated clamp, and connected to one pole of the electric circuit (110 volts). An insulated carbon rod is connected through a suitable resistance (15 ohms) to the other electrode. The rod is touched to the end of the thermocouple and pulled away slightly, giving an electric arc. As soon as the two wires are welded together, the electrode is pulled farther away to stop the arc.

For room temperature, insulation of cloth or enamel is sufficient; for high temperatures, wire can be obtained with Fiberglas insulation, or

<sup>1</sup> Corruccini and Shenker, *J. Research, Natl. Bur. Standards (U.S.)*, **50**, 229 (1953); *Research Paper 2415; Natl. Bur. Standards (U.S.), Circ.*, **561**, (1955).

TABLE 2. TYPES OF THERMOCOUPLES

Type	Usual temperature range, °C	Maximum temperature, °C (for short periods)	Millivolts per degree at room temperature
Copper-constantan <sup>a</sup> .....	-190 to 300	600	0.0428
Iron-constantan <sup>a</sup> .....	-190 to 760	1000	0.0540
Chromel-P-alumel <sup>b</sup> .....	-190 to 1100	1350	0.0410
Platinum to platinum—10 per cent rhodium.....	0 to 1450	1700	0.0064

<sup>a</sup> Constantan is a general name given to a group of copper-nickel alloys. It can be obtained under the trade name Advance from the Driver-Harris Co., Harrison, N.J., or from pyrometer manufacturers.

<sup>b</sup> Chromel-P and alumel are high-nickel alloys obtainable from the Hoskins Manufacturing Co., Detroit, or from pyrometer manufacturers.

separate sleeving of the latter can be obtained. Porcelain tubes are also widely used. It is essential to protect the wires carefully from corrosion; in furnaces, long gas-tight tubes of glass, porcelain, or quartz are used. For work with solutions at room temperatures, the thermocouple is usually encased in a thin glass tube, frequently filled with oil to give better thermal contact. When several junctions are used, the exposed junctions come at higher and higher levels in the encasing tube to prevent short-circuiting of the uninsulated tips of the thermocouples.

For precision work, the wire must be carefully selected and tested. Full particulars for making and using these thermoelectric thermometers are available.<sup>1</sup> They can be made sensitive to 0.00001°.

A thermoelectric thermometer is used either with a potentiometer or with a millivoltmeter or galvanometer. The former is necessary in precision work, but the latter is so much more convenient that it is frequently used in industrial work. In the latter case, the current rather than the electromotive force is measured, and an error is introduced because the change in current with temperature is due not only to the thermocouple electromotive force but also to the change in resistance of the wires. To minimize this error, large wires are used, so that the changeable resistance of the thermocouple is small in comparison with the fixed resistance of the galvanometer. Galvanometer or millivoltmeter scales may be calibrated directly in terms of degrees. The resistance of the thermocouple should be about equal to the critical-damping resistance of the galvanometer.

<sup>1</sup> Adams, *J. Am. Chem. Soc.*, **37**, 481 (1915); International Critical Tables, Vol. I, p. 57, McGraw-Hill Book Company, Inc., New York (1926).

Thermocouples are used extensively in many industrial operations. Recording potentiometers are commonly employed where a permanent record of temperature at all times is desired. Instruments are available which will record as many as 24 temperatures as a function of time on a single strip of paper.

For accurate work the potentiometer is specially designed to avoid spurious thermal electromotive forces or leakage. Reversing switches are particularly useful in this work. The White potentiometer,<sup>1</sup> Wenner potentiometer,<sup>1</sup> and microvolt potentiometer<sup>2</sup> are specially designed for use with thermocouples.

The cold junction is usually set into cracked ice in a vacuum-jacketed bottle as shown in Fig. 110, but in crude work at high temperatures it is sometimes left at room temperature. A fluctuation in the temperature of the cold end is, of course, just as effective as a fluctuation in the furnace; the meter reading depends on the difference in temperature between the two junctions.

Thermocouples are calibrated with fixed temperatures, of which the most common are freezing mercury,  $-38.87^{\circ}\text{C}$ ; melting ice,  $0^{\circ}$ ; boiling water,  $100^{\circ}$  (with barometer correction); the transition temperature of sodium sulfate,  $32.38^{\circ}$ ; boiling sulfur,  $444.6^{\circ}$ ; freezing tin,  $231.9^{\circ}$ ; freezing cadmium,  $320.9^{\circ}$ ; freezing lead,  $327.3^{\circ}$ ; freezing zinc,  $419.5^{\circ}$ ; freezing silver,  $960.8^{\circ}$ ; freezing gold,  $1063.0^{\circ}$ ; freezing palladium,  $1552^{\circ}$ ; and freezing platinum,  $1768^{\circ}$ . The National Bureau of Standards calibrates thermocouples, determines the thermal electromotive forces of thermocouple materials, and supplies a few metals with certified freezing points.

**Optical Pyrometers.**<sup>3</sup> The operation of optical pyrometers depends on the fact that the radiation emitted by a hot body is a function of the temperature. They are very easy to use and are popular in industrial control operations. They are about the only instruments that can be used for the measurement of very high temperatures. They are not suitable for temperatures below  $500$  or  $600^{\circ}$ , because the radiation is not sufficiently intense.

Several types are available, but the disappearing-filament type shown in Fig. 111 is one of the simplest and most practical.

The furnace, crucible, or other hot object is viewed through the telescope. An electric-light bulb with a carbon filament is placed in the optical system so that the observer sees the filament across the field. A variable resistance changes the current through the lamp. The wire appears bright on a darker field when the wire is hotter than the hot

<sup>1</sup> Leeds and Northrup Company, Philadelphia.

<sup>2</sup> Rubicon Company, Philadelphia.

<sup>3</sup> Optical and Radiation Pyrometry in "Temperature: Its Measurement and Control in Science and Industry," pp. 1115ff, Reinhold Publishing Corp., New York (1941).

object, and it appears dark on a light field when it is colder. When the two temperatures are exactly the same, the filament seems to disappear and the whole field becomes uniform. A red screen is used, and for very high temperatures the brightness of the radiation from the furnace is reduced with a thicker screen. The current required to make the filament disappear is noted on the milliammeter, and the corresponding temperature is obtained by reference to a table supplied by the manufacturers for use with the lamp.

The table is prepared by calibrating the lamp at known temperatures, reading the milliammeter when the rheostat is so adjusted as to make the filament disappear. A few readings are sufficient, the rest being obtained

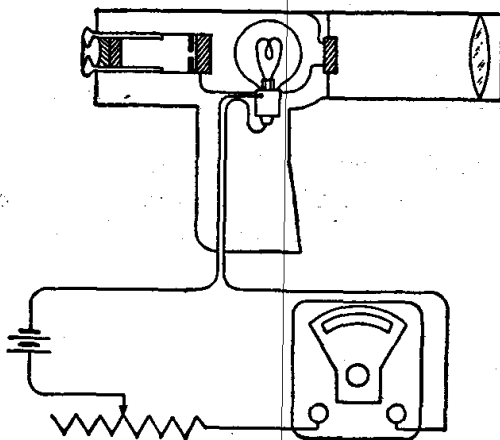


FIG. 111. Radiation pyrometer of the disappearing-filament type.

by interpolation. The temperature of the furnace may be determined with a thermocouple or resistance thermometer. The melting points of antimony, silver, and gold may be used for calibration temperatures.

The furnace should be nearly closed and viewed through a small opening so as to give true blackbody radiation. If an open strip of metal is viewed, the calculated temperature may be considerably too low. Empirical corrections for radiation from the surface of exposed platinum and various other metals have been worked out.

## CALORIMETRY

Calorimetric measurements, several examples of which are treated in Exps. 3 to 5, form an important part of experimental physical chemistry. A comprehensive survey of this field has been given by Sturtevant.<sup>1</sup> The specific details of the equipment and procedures employed in accurate work depend upon the particular type of measurement being made.

<sup>1</sup> In Weissberger (ed.): "Technique of Organic Chemistry," 3d ed., Vol. I, Pt. I, Chap. 10, Interscience Publishers, Inc., New York (1959).

Representative references on typical calorimetric problems include the following: heats of combustion (general;<sup>1</sup> liquids;<sup>2</sup> gases<sup>3</sup>); heat capacities of solutions;<sup>4</sup> heats of dilution;<sup>5</sup> heats of hydrogenation;<sup>6</sup> heat capacity of liquids;<sup>7</sup> heats of vaporization;<sup>8</sup> heat capacity of gases;<sup>9</sup> ice calorimeter;<sup>10</sup> low-temperature heat capacity, heat of fusion, etc.<sup>11</sup>

<sup>1</sup> Coops *et al.*, *Rec. trav. chim.*, **66**, 113–176 (1947) (in English); Dickinson, *Natl. Bur. Standards (U.S.)*, *Bull.* **11**, 189 (1915); Jessup and Green, *J. Research, Natl. Bur. Standards (U.S.)*, **13**, 469 (1934).

<sup>2</sup> Prosen and Rossini, *J. Research, Natl. Bur. Standards (U.S.)*, **27**, 289 (1941).

<sup>3</sup> Prosen, Maron, and Rossini, *J. Research, Natl. Bur. Standards (U.S.)*, **42**, 269 (1949).

<sup>4</sup> Gucker, Ayres, and Rubin, *J. Am. Chem. Soc.*, **58**, 2118 (1936).

<sup>5</sup> Gucker, Pickard, and Planck, *J. Am. Chem. Soc.*, **61**, 459 (1939); Sturtevant, *J. Phys. Chem.*, **45**, 127 (1941).

<sup>6</sup> Kistiakowsky, Romeyn, Ruhoff, Smith, and Vaughan, *J. Am. Chem. Soc.*, **57**, 65 (1935).

<sup>7</sup> Osborne and Ginnings, *J. Research, Natl. Bur. Standards (U.S.)*, **39**, 453 (1947).

<sup>8</sup> *Ibid.*; Waddington, Todd, and Huffman, *J. Am. Chem. Soc.*, **69**, 22 (1947).

<sup>9</sup> Masi and Petkof, *J. Research, Natl. Bur. Standards (U.S.)*, **48**, 179 (1952); Waddington, Todd, and Huffman, *loc. cit.*

<sup>10</sup> Ginnings and Corruccini, *J. Research, Natl. Bur. Standards (U.S.)*, **38**, 583 (1947).

<sup>11</sup> Aston and Eidenoff, *J. Am. Chem. Soc.*, **61**, 1533 (1939); Huffman, *Chem. Revs.*, **40**, 1 (1947); Ruehrwein and Huffman, *J. Am. Chem. Soc.*, **65**, 1620 (1943); Waddington, Todd, and Huffman, *loc. cit.*

## *Physical Properties of Fluids*

### PHYSICAL PROPERTIES OF GASES

**Volume by Displacement.** A measured quantity of gas may be introduced into a system by displacing it with a measured quantity of liquid, in a flask provided with a two-holed rubber stopper. In an alternative method, the gas may be drawn over by running out a measured volume of liquid. The gas must be insoluble in the liquid. Mercury is the best liquid for most purposes, but it is too heavy for large volumes, and water, oil, nitrobenzene, and sulfuric acid have been used. Some of these liquids have a negligible vapor pressure, but a correction is necessary in the case of water. The temperature of the incoming liquid must be the same as that of the vessel.

Large volumes of gas are measured conveniently with commercial gas meters, in which cups or vanes rotate in a closed chamber containing a liquid at the bottom. The number of revolutions is recorded on one or more circular scales. The meters are calibrated with known volumes of gas.

**Flowmeters.** The rate of flow of a gas is conveniently measured with a flowmeter, as illustrated in Fig. 112.

The difference in pressure on the two sides of a capillary tube, as indicated by the manometer, is a measure of the rate of flow of gas through the flowmeter. The flowmeter is calibrated at several different rates of flow, and a smooth curve is drawn showing the rate of flow as a function of the difference in levels (Fig. 113).

A convenient flowmeter is available which is made entirely of Pyrex

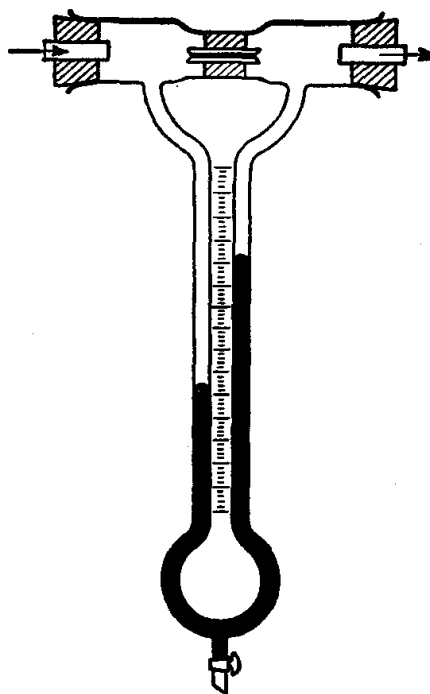


FIG. 112. Flowmeter.

glass. A graduated tube is mounted vertically in a larger concentric tube, and the displacement of the liquid due to the passage of gas is read directly on the tube. The rate of flow

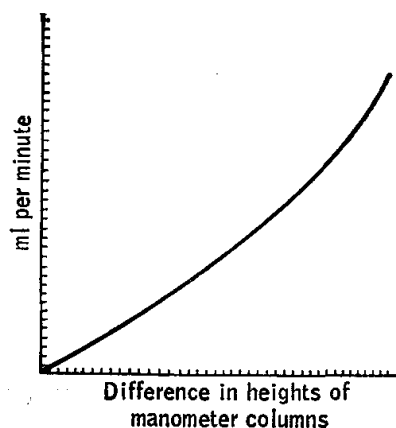


FIG. 113. Calibration curve for flowmeter.

is nearly a straight-line function of the scale reading, and the rate of flow corresponding to any reading of the scale may be interpolated with accuracy. The factors involved in the theory and use of the flowmeter have been discussed by Benton.<sup>1</sup>

In calibrating a flowmeter, air or other gas is passed through the flowmeter by a displacement method, while the liquid used in the manometer is maintained continuously at a constant setting. The time taken for a given volume to pass through is determined accurately with a

stop watch. Capillary tubes of different bores may be used for different velocity ranges.

Another type of flowmeter is finding use in the measurement of the flow of both gases and liquids. A vertical tube provided with a linear scale has a larger internal diameter at the top than at the bottom. When gas rushes upward through this tube, it carries a small float upward. The greater the flow of gas or liquid, the higher the float rises, but at the greater rates of flow, the area of the annular ring between the float and the containing tube becomes larger. These factors are so balanced that the height of the float is a linear function of the rate of flow. The Flow-rator,<sup>2</sup> or Rotameter,<sup>3</sup> diagramed in Fig. 114, is a convenient meter of this type. Laboratory kits with a set of interchangeable metering tubes and floats of different sizes are available with capacities from 0.06 to 220 ml of liquid water per minute. The meters can be used for fluids other than water and air, with the help of standard corrections, depending on the density of the fluid and the float and on viscosity and pressure.<sup>2</sup>

**Manometers.** The mercury manometer is the instrument most commonly used for the measurement of pressure in the laboratory. It may be used for absolute measurements by evacuation of the space over the liquid level in one arm, or for determination of the differential pressure between two levels. The range of pressure covered usually extends from a few centimeters to several meters of mercury for a single manometer; multiple manometers<sup>4</sup> connected in a cascade arrangement have been

<sup>1</sup> *Ind. Eng. Chem.*, 11, 623 (1919).

<sup>2</sup> Fischer and Porter Co., Hatboro, Pa.

<sup>3</sup> Brooks Rotameter Co., Lansdale, Pa.

<sup>4</sup> Roebuck and Ibser, *Rev. Sci. Instr.*, 25, 46 (1954).

used for very accurate absolute-pressure measurements at as high as 200 atms.

An initially good vacuum over the mercury surface in the closed end of a mercury manometer can be obtained only by careful outgassing of the glass walls before the tube is filled, followed by vacuum distillation of mercury into the manometer while the tube is still fairly hot, i.e., over 100°C. The vacuum inevitably deteriorates with age, however, because of motion of gas along the interface between the tube wall and the mercury, and further outgassing of the tube wall due to electric-discharge effects associated with the motion of the mercury due to changes in applied pressure. For best results it is desirable to evacuate the "closed end" continuously by means of a diffusion pump.

Because of the large surface tension of mercury, relatively large internal diameter tubes (about 20 mm) are required to give menisci adequately flat to permit accurate measurements and to minimize the uncertainty due to unequal surface-tension effects at the two menisci. It is often assumed that a common tube diameter for the two arms will provide a cancellation of such surface-tension effects. This is true only as a rough approximation, since variations in the conditions at the interface can result in a wide variation in the capillary depression for a given tube diameter. When the highest accuracy is required, the individual meniscus heights must be measured and the appropriate corrections applied; correction tables which facilitate this process are available.<sup>1,2</sup>

The accuracy of measurement of the difference in height of the two mercury levels is determined not only by the intrinsic accuracy of the scale used, but also by the method by which the readings are obtained. The best procedure is to use a scale, located in the (vertical) plane of the manometer, which is read by means of a cathetometer telescope from a distance of several feet. This procedure is preferable to basing measurements on the cathetometer scale itself, which introduces the difficulty of assuring that the telescope axis is accurately horizontal.

In either case, the measured height difference  $h_t$  is obtained in terms of

<sup>1</sup> Gould and Vickers, *J. Sci. Instr.*, 29, 85 (1952).

<sup>2</sup> Mercury Barometers and Manometers, *Natl. Bur. Standards (U.S.), Monograph 8* (1960).

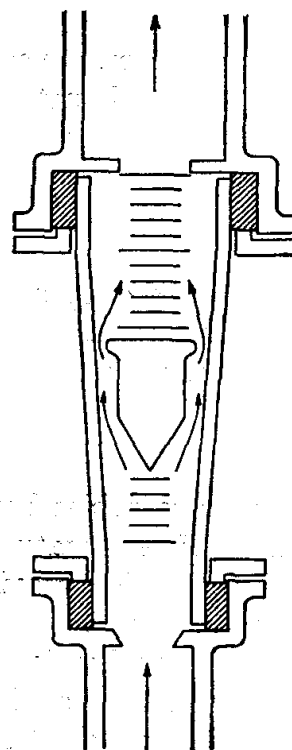


FIG. 114. Rotameter, or Flowrator, for measuring the rate of flow of gases or liquids.



scale readings at the ambient temperature  $t$ . Since the scale can read correctly only at its calibration temperature  $t_c$ , the true height difference must be calculated from a knowledge of the linear coefficient of expansion,  $s$ , of the scale material:

$$h = h_i[1 + s(t - t_c)]$$

Application of the scale and capillary corrections gives the pressure in terms of millimeters of mercury at the manometer temperature. In terms of standard millimeters of mercury,

$$P = \frac{\rho}{\rho_s} \frac{g}{g_s} h$$

Here  $\rho$  and  $g$  represent the density of mercury and acceleration of gravity for the local manometer conditions, while the standard values of these quantities are

$$\begin{aligned}\rho_s &= 13.5951 \text{ g/cm}^3 \\ g_s &= 980.665 \text{ cm/sec}^2\end{aligned}$$

Extensive tables have been formulated to facilitate correction for the effect of temperature on mercury density and the scale material.<sup>1</sup> The correction for gravity is normally less important, but is essential in accurate work.

A comprehensive discussion of mercury barometers and manometers has been made available by the National Bureau of Standards.<sup>1</sup>

Other manometric fluids than mercury can be used, of course. The essential properties include a known density, sufficiently low viscosity and vapor pressure, inertness toward the gas whose pressure is being measured, and an adequately low solvent power for the gas. The manometer readings can be expressed in terms of standard millimeters of mercury from a knowledge of the densities of the two fluids.

**Bourdon Gauge.**<sup>2</sup> The active element in a Bourdon gauge is a hollow tube of elliptical cross section bent into a circular or spiral form. Higher pressure inside the tube than outside causes a deflection of the end of the tube due to its tendency to straighten out. As shown in Fig. 115a, this motion of the tube end is coupled mechanically to the dial pointer of the gauge. Modern Bourdon gauges are stable, rugged, and reliable and are available in corrosion-resistant metals for use with reactive fluids. Accuracy as high as one-tenth of one per cent of full scale and sensitivity several times as good as this can be obtained. Ranges as low as 0.1 to 20 mm Hg and as high as 0 to 50,000 psi are available.

<sup>1</sup> Mercury Barometers and Manometers, *Natl. Bur. Standards (U.S.), Monograph 8* (1960).

<sup>2</sup> *Instruments and Control Systems*, 34, 1057 (1961).

**Deadweight Gauge.**<sup>1</sup> The principle of the deadweight is illustrated in Fig. 115b. The pressure measurement is made in terms of a balance of force at the bottom of the piston *A*, which has been carefully lapped to a close sliding fit in cylinder *B*, from which it is separated by a very thin film of oil. The upward force exerted on the piston is given by the pressure acting there times the effective area of the piston. The downward force, in addition to that due to atmospheric pressure, is calculated as mass times acceleration, where the mass includes that of the piston,

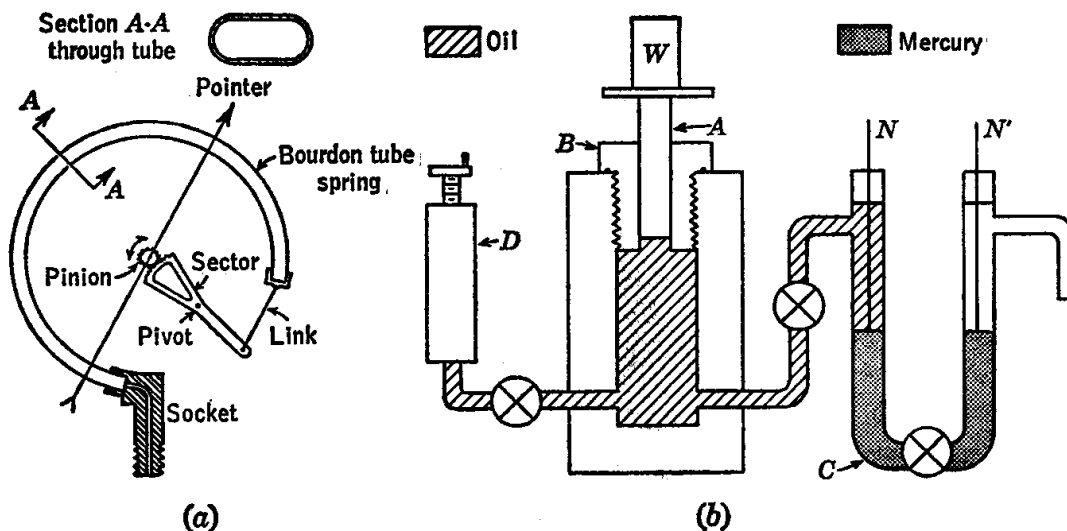


FIG. 115. (a) Principle of the Bourdon gauge; (b) deadweight gauge assembly: *A*, piston; *B*, cylinder; *C*, steel U tube; *D*, oil injector; *N, N'*, indicator contact needles.

the weight pan, and the weights *W* required to achieve the balance condition, and the acceleration is the local acceleration of gravity.

The effective area of the piston is determined by an effective diameter which is very nearly equal to the mean diameter for the piston and cylinder. On this basis the deadweight gauge can be used as an absolute instrument. More commonly, the effective piston area is determined experimentally by a gauge calibration against a known pressure. For this purpose the vapor pressure of liquid carbon dioxide at the ice point is used, measured very accurately by several workers.<sup>2</sup>

To prevent sticking of the piston in the cylinder, the piston may be oscillated<sup>3</sup> back and forth by a yoke driven by an eccentric. The yoke acts on a lever arm fastened to the piston; during part of each cycle the

<sup>1</sup> Keyes, *Proc. Am. Acad. Arts Sci.*, **68**, 505 (1933); Meyers and Jessup, *J. Research, Natl. Bur. Standards (U.S.)*, **6**, 1061 (1931).

<sup>2</sup> Bridgman, *J. Am. Chem. Soc.*, **49**, 1174 (1927); Roebuck and Cram, *Rev. Sci. Instr.*, **8**, 215 (1937).

<sup>3</sup> Mercury Barometers and Manometers, *Natl. Bur. Standards (U.S.)*, Monograph 8 (1960).

lever arm is not in contact with the yoke and the piston floats freely in the cylinder. Alternatively, the piston may be rotated continuously in the cylinder.<sup>1</sup>

An unbalance in pressure will result in either a rise or fall of the piston, and this change in its position may be used as a balance indicator for work of moderate accuracy. Where maximum accuracy is required, the detection system may be based on the change in the volume below the piston resulting from its motion. Any such change will cause a displacement of the mercury in the steel U tube *C*, and thus provide a positive electrical connection between one of the insulated detector pins *N*, *N'* and the steel tube, which may complete a relay actuating circuit. The mercury trap also serves to isolate the oil in the deadweight gauge from the medium whose pressure is to be measured.

The range of a deadweight gauge is determined by the nominal piston diameter, which usually is from  $\frac{1}{2}$  to  $\frac{1}{8}$  in. For accurate results the pressure range extends from about 2 atm to over 500 atm. The accuracy attained can be as high as 1 or 2 parts in 10,000, and the precision several times as good as that. Naturally, these figures refer to the pressure as measured at the gauge piston; for an arbitrary external system,

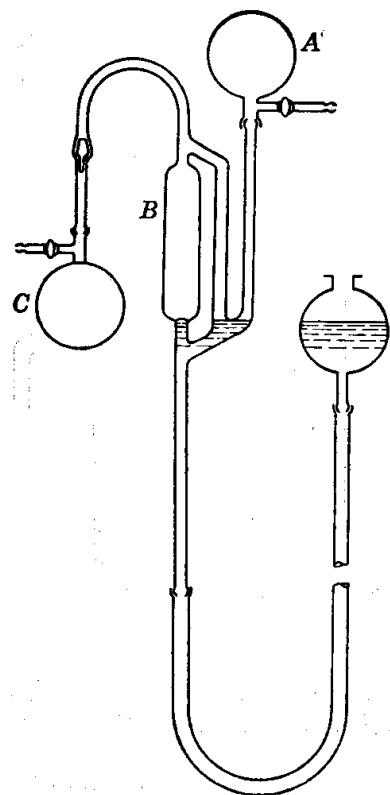


FIG. 116. Toepler pump.

all hydrostatic head contributions to the pressure between the system and the reference level at the bottom of the piston must be properly evaluated.

**Pumps.** Several types of vacuum pumps and certain vacuum techniques are described in Exp. 57.

The Toepler pump is used for transferring gas from one vessel to another under reduced pressure. It operates by alternately raising and lowering a mercury level as shown in Fig. 116. Each time the mercury level is lowered, the gas from *A* expands into *B*, and each time it is raised, the gas is forced from *B* into *C* or out into the room. The height of the mercury tube must be greater than the barometer height, or the mercury level may be raised by applying compressed air to the top of the mercury in the reservoir, thus permitting the reservoir to be just below the pump.

<sup>1</sup> Keyes, *Proc. Am. Acad. Arts Sci.*, **68**, 505 (1933); Meyers and Jessup, *J. Research, Natl. Bur. Standards (U.S.)*, **6**, 1061 (1931).

## DETERMINATION OF THE BOILING POINT<sup>1</sup>

The boiling point of a liquid is a characteristic property which is often useful for purposes of identification and for the determination of purity. The boiling point is usually taken as the temperature established on the bulb of a thermometer on which a thin layer of the condensed liquid coexists with the vapor. Boiling liquids are generally superheated by the heating device used, and any boiling liquid is superheated because it boils under the pressure at the surface plus the hydrostatic pressure at the level in the liquid at which the temperature is measured. Special ebulliometers are required for the measurement of the boiling temperature of a liquid or of a solution. In the case of a pure liquid, the true boiling and condensation temperatures are equal.

If certain precautions are observed, the boiling point of a pure liquid may be determined in an ordinary distilling flask. The thermometer should be short, so that the whole column of mercury is surrounded by the vapor, or else a rather unsatisfactory stem correction is necessary (page 430). The thermometer bulb should be near the outlet tube so that it registers the temperature of the exit vapors. The boiling should not be so violent as to cause spray to reach the thermometer bulb or so rapid as to build up a pressure in the flask appreciably greater than atmospheric pressure. To avoid splashing, the flask should not be over half full.

One of the greatest sources of error comes from overheating the neck of the flask and heating the thermometer bulb by radiation. A large gas flame is particularly bad in this respect. A small gas flame without wire gauze or sand bath is better. It is a good plan to heat the distilling flask in a beaker of hot water (or oil, at higher temperatures) to a temperature only slightly above the boiling point of the liquid, as determined with an ordinary thermometer in the water bath. A thin-walled cylindrical tube placed in the vapor between the thermometer and the flask is sometimes used to minimize radiation.

Overheating may be minimized by using an electrical heating mantle covered with glass cloth or by using a heating coil immersed in the boiling liquid. The vapor rises from the electrically heated liquid and passes over into a side tube, completely enveloping the thermometer, which is suspended on a platinum wire attached to a glass hook on the stopper. A trap at the bottom may be used to return the liquid to the boiling flask. If the thermometer is completely within the vapor, a proper thermometer reading is ensured. Both stoppers may be made of glass if corks or rubber stoppers must be avoided.

<sup>1</sup> This subject has been reviewed by Swietoslawski and Anderson *in* Weissberger (ed.): "Technique of Organic Chemistry," 3d ed., Vol. I, Pt. I, Chap. 8, Interscience Publishers, Inc., New York (1959).

This design gives good circulation of the liquid and allows the heating to be carried on until only a small volume of liquid remains. The heating coil of bare platinum wire is sealed through long glass tubes which pass down through the stopper of the flask. Copper wires leading to the source of current are welded to the platinum wires before the latter are sealed in glass.

**Superheating.** The liquid should boil smoothly and steadily, but in some cases there is a tendency for the liquid to become heated above its boiling point. Superheating may be greatly reduced by any means of trapping small air bubbles in the liquid. Small chips of unglazed porcelain with air enclosed in the pores, or pieces of platinum or platinized platinum, are effective. The smoothest boiling is obtained with the internal electrical heating coil described above.

Distilling flasks covered with sintered glass powder are effective in preventing bumping.<sup>1</sup> Some of the same glass of which the flask is made is ground in a mortar and moved around inside while the flask is heated in a blast lamp to its softening temperature. Again, the surface may be coated with silica by evaporating a dilute solution of sodium silicate, heating to dull-red heat, cooling, and treating with dilute hydrochloric acid and rinsing.<sup>2</sup>

Bumping is particularly apt to be troublesome under reduced pressure, and it may be advisable to have a small stream of air bubbling through the liquid. A tube is inserted in the stopper, with its lower end drawn out into a capillary extending into the liquid. Its upper end is closed by a rubber tube and an adjustable pinchcock to control the rate of bubbling.

If only a small amount of liquid is available, the boiling point may be determined by the method of Smith and Menzies.<sup>3</sup> The liquid is placed in an inverted bulb and fastened to the bulb of a thermometer and immersed in a bath of water or other transparent liquid which is immiscible with the liquid being studied. The temperature is raised gradually, and when the boiling point is reached, a stream of bubbles issues from the bulb.

**Ebulliometers.** An ebulliometer is a special apparatus for the measurement of the boiling temperature of a liquid or of a solution. With a differential ebulliometer, the boiling and condensation temperatures may be measured simultaneously. This apparatus may also be used for the determination of the degree of purity of liquid substances, of the molecular weight of a nonvolatile solute, or of the pressure coefficient of the boiling point.

<sup>1</sup> Morton, *Ind. Eng. Chem., Anal. Ed.*, 6, 384 (1934).

<sup>2</sup> Swietoslawski, *J. Chem. Educ.*, 5, 469 (1928).

<sup>3</sup> *J. Am. Chem. Soc.*, 32, 879 (1910).

Another differential boiling-point apparatus is described by Menzies and Wright.<sup>1</sup> A narrow graduated tube is closed at one end and bent up to give a U tube, with the closed arm about 2 cm long and the other about 12 cm long. It is partly filled with water or other liquid, sealed off at the ends, and placed vertically in a flask. There is thus an air pocket in the short arm and another one at the top of the long arm. A vapor pump pours the boiling solution over the pocket in the lower arm, whereas the pocket at the top of the long arm is surrounded only by vapor. Measured changes in the level of the enclosed liquid enable one to calculate the differences in vapor pressure of this liquid, and from the differences in vapor pressure, the corresponding differences in temperature can be calculated. This temperature difference then is equal to the difference in temperature between the solution boiling in the flask and its vapor. At 35° a difference in level of 1 mm of water corresponds to 0.0313°, and at 100° it corresponds to 0.0026°.

## MEASUREMENT OF VAPOR PRESSURE

The measurement of vapor pressure is closely related to the measurement of boiling point, so that it is difficult to make a distinction between these two types of measurements. If the boiling point is determined at a series of pressures, the vapor-pressure-temperature relation is obtained. This is the essence of the so-called dynamic method, which is especially important. Three other general methods, some of which may be adapted as differential methods, will be described briefly.

**Dynamic Method.** The construction of apparatus used at the National Bureau of Standards is described by Willingham and coworkers.<sup>2</sup> This apparatus consists of an electrically heated boiler, a vapor space with a vertical reentrant tube containing a platinum resistance thermometer, and a condenser. The pressure is controlled by an automatic device actuated by electrical contacts sealed through the barometer tube.

Special apparatus has been designed for the study of binary solutions.<sup>3</sup>

**Static Method.** In the simplest method the liquid is contained in a bulb connected with a mercury manometer and a vacuum pump. The greatest source of error lies in the presence of air or other permanent gases which have been dissolved by the liquid or trapped by the mercury.

<sup>1</sup> *J. Am. Chem. Soc.*, **43**, 2314 (1921).

<sup>2</sup> Willingham, Taylor, Pignocco, and Rossini, *J. Research, Natl. Bur. Standards (U.S.)*, **35**, 219 (1945).

<sup>3</sup> Scatchard, Raymond, and Gilman, *J. Am. Chem. Soc.*, **60**, 1275 (1938); Scatchard and Raymond, *J. Am. Chem. Soc.*, **60**, 1278 (1938); Scatchard, Wood, and Mochel, *J. Am. Chem. Soc.*, **61**, 2306 (1939); *ibid.*, **62**, 712 (1940); Othmer and Josefowitz, *Anal. Chem.*, **39**, 1175 (1947); Othmer and Morley, *Ind. Eng. Chem.*, **38**, 751 (1946); Thomson in Weissberger (ed.), *op. cit.*, Vol. I, Pt. I, Chap. 9 (1959).

Enough liquid is evaporated with the pump to sweep out all the gases. The evacuation is repeated until further evacuation gives no lowering of the vapor pressure. The whole apparatus should be thermostated. The method has been used by many investigators.

The isotenoscope of Menzies<sup>1</sup> is useful for the determination of vapor pressure of a liquid or a solution.

Differential static methods have been developed by Frazer and Lovelace<sup>2</sup> and by Menzies.<sup>3</sup>

**Gas-saturation Method (Transpiration Method).** In this method a measured volume of air or other inert gas is saturated by passing it through the liquid at a definite temperature. The quantity of liquid vaporized is obtained from the loss in weight of the liquid, or by removal of the vapor from the gas stream in weighed absorbing tubes. Assuming Dalton's law of partial pressures and the ideal-gas law, the partial pressure of the vapor,  $P$ , is calculated by the formula

$$P = \frac{g}{MV} RT$$

where  $R$  = gas constant

$T$  = absolute temperature

$V$  = total volume of gas (including air and vapor) containing  $g$  grams of vapor of molecular weight  $M$

When  $V$  is expressed in liters and  $P$  in atmospheres,  $R$  is expressed in liter-atm deg<sup>-1</sup> mole<sup>-1</sup>. In case the vapor pressure is very low, it can be neglected in comparison with the atmospheric pressure in calculating the volume of the gas.

If a gas is passed first through pure solvent and then through a solution, the vapor pressure of the solution can be calculated from the vapor pressure of pure solvent, the total pressure at each saturator, and the gain in weight of each absorber, thus eliminating the need of measuring the volume of the gas.

Premature condensation must be avoided if the vapor is to be absorbed and weighed, and at higher temperatures the saturator, absorption tubes, and connecting tubes are all immersed in the thermostat. It is essential to saturate completely the air or other gas with the vapor of the liquid; but, on the other hand, there must be no stoppage in the apparatus which might build up a changing or an unknown hydrostatic pressure. If the air is passed through the saturator so slowly that a still slower rate gives no greater vapor pressure, it may be concluded that the air is completely saturated. The air-saturation method has been used in precision

<sup>1</sup> Smith and Menzies, *J. Am. Chem. Soc.*, **32**, 1412 (1910).

<sup>2</sup> Frazer, Lovelace, et al., *J. Am. Chem. Soc.*, **45**, 2930 (1923).

<sup>3</sup> *J. Am. Chem. Soc.*, **33**, 1615 (1911).

researches by Washburn<sup>1</sup> for the determination of vapor pressures of aqueous solutions and has been further developed by additional workers.<sup>2</sup> When both components of a solution are volatile, it is necessary to have a suitable means for analyzing the condensed vapor. A physical method such as refractometry or a chemical method such as titration may be used.

**Isopiestic Method.** This method is used in studies on solutions of nonvolatile solutes. Vessels containing solutions of two different solutes are placed side by side in a closed container. A net transfer of solvent from the solution of higher vapor pressure to the solution of lower vapor pressure proceeds until equilibrium is attained. The fugacity of the solvent (and hence the vapor pressure of each solution, since the solute is nonvolatile) is then the same for each solution. The solutions are analyzed, and if the vapor pressure of one of the solutions is known from other absolute measurements, the vapor pressure of the other has been determined.

It is important that the vessels be in good thermal contact. This is ordinarily achieved by using metal cups which fit snugly into holes bored in a large copper block. This block fits into a stainless-steel vessel with a cover and a lead gasket, so that the whole system can be evacuated and rotated in a large thermostat kept constant nearly to 0.001°. After 24 hr, the little cups are covered and weighed. They are replaced in the vessel, the covers removed, and the determinations repeated again after 24 hr or until there is no further change in weight.

Robinson and Sinclair<sup>3</sup> compared the activities of water in solutions of inorganic halides with those in solutions of potassium chloride at different concentrations. Scatchard, Hamer, and Wood<sup>4</sup> determined the activities of water in solutions of potassium chloride, sulfuric acid, sucrose, urea, and glycerol as compared with solutions of sodium chloride. The results are very accurate and permit a check on the several different methods that have been used for the determination of the activity of water in solution.

## FRACTIONAL DISTILLATION<sup>5</sup>

The separation of two liquids by distillation and the determination of the number of theoretical plates for laboratory fractionating columns

<sup>1</sup> Washburn and Heuse, *J. Am. Chem. Soc.*, **37**, 309 (1915).

<sup>2</sup> Pearce and Snow, *J. Phys. Chem.*, **31**, 231 (1927); Pearce and Eckstrom, *J. Am. Chem. Soc.*, **59**, 2689 (1937); Bechtold and Newton, *J. Am. Chem. Soc.*, **62**, 1390 (1940).

<sup>3</sup> *J. Am. Chem. Soc.*, **56**, 1830 (1934).

<sup>4</sup> *J. Am. Chem. Soc.*, **60**, 3061 (1938).

<sup>5</sup> For further material the following references are recommended: Robinson and Gilliland, "Elements of Fractional Distillation," 4th ed., McGraw-Hill Book Com-



have been described in Exp. 9. In addition to the number of theoretical plates, there are a number of factors, such as feed rate and operating holdup, to be considered in selecting or designing fractionating columns. The feed rate of the column is defined as the rate of entry of vapor into the bottom of the column, and, depending upon the design of the column, a certain feed rate may not be exceeded without flooding the packing. It is desirable to use as high a feed rate as possible so that a given distillation may be accomplished in the shortest possible time. The operating holdup of a column is the quantity of vapor and liquid in the column under operating conditions. It is desirable that the column have a small holdup so that a minimum amount of liquid is held in the column at any time. It may be shown<sup>1</sup> that the sharpness of separation obtainable in a batch distillation is approximately a linear function of the ratio of charge to holdup. Thus decreasing the holdup relative to the charge enables a sharper separation to be obtained with the same number of theoretical plates and the same total distillation time. Actually, high feed rate and small holdup are not easily obtained in the same column and must be balanced against each other.

A number of different types of fractionating columns have been devised in an effort to improve the contact between the liquid and the ascending vapor. The ideal packing offers uniformly distributed interstices, a large surface for contact, and enough free space for a desirable feed rate. Too large packing has a small area for contact and a tendency to channel, while too small packing allows insufficient feed rate. If the ratio of column diameter to diameter of the individual packing units is greater than 8:1 and the ratio of column height to column diameter is greater than 15:1, the tendency to channel will be slight.

A fractionating column is most efficient when its operation is adiabatic throughout its length. An insulating jacket, a vacuum jacket, or an electrically heated jacket may be used. If an electrically heated jacket is used, it is important to keep the column somewhat hotter at the bottom than at the top.

Two types of still heads may be used to control the reflux ratio: (a) liquid-dividing heads and (b) vapor-dividing heads. Vapor-dividing heads have the advantage that the reflux ratio may be controlled more

---

pany, Inc., New York (1950); Morton, "Laboratory Techniques in Organic Chemistry," Chap. IV, McGraw-Hill Book Company, Inc., New York (1938); Carney, "Laboratory Fractional Distillation," The Macmillan Company, New York (1949); Ward, Review of the Literature on the Construction, Testing, and Operation of Laboratory Fractionating Columns, *U.S. Bur. Mines, Tech. Paper*, 600 (1939); Glasebrook and Williams in Weissberger (ed.), *op. cit.*, Vol. IV (1951).

<sup>1</sup> Rose, Welshans, and Long, *Ind. Eng. Chem.*, 32, 673 (1940).

precisely. Automatic devices may be used with both types to control reflux ratios conveniently.

**High-vacuum Distillation.** With the development of efficient vacuum pumps (see Exp. 57), high-vacuum distillation of material of low volatility has become a common commercial and laboratory operation. This method has the advantage that high-molecular-weight organic molecules, such as vitamins, sterols, and synthetic polymers, which cannot be distilled at their normal boiling points without decomposition, may be distilled unharmed. Hickman<sup>1</sup> and others have developed new tools and special techniques for such distillations. When vacuum distillations are carried out with the usual flask-condenser-receiver-vacuum-pump apparatus, it is found that reducing the pressure in the receiver below about 5 mm Hg produces little increase in the rate of distillation or lowering of the temperature of the distillation. This is because of the resistance to the flow of the vapor exerted by the neck and sidearm of the distillation flask. In order to avoid this difficulty and to increase the amount of vapor which actually reaches the condenser, the condenser must be placed quite close to the surface where evaporation is taking place. If the distance of transfer is comparable with the mean free path of the vapor molecules, the process is known as *molecular* distillation.

There are important differences in principle between ordinary distillation and molecular distillation. In ordinary distillation, molecules from the vapor reenter the surface and tend to produce equilibrium between liquid and vapor phase. Under these conditions the quantities of the various constituents distilling are proportional to their partial pressures. In molecular distillation, on the other hand, molecules do not reenter the liquid phase and there is no equilibrium between liquid and vapor. The separation achieved depends only upon the differences in rates of evaporation of the various components.

The differences in the ordinary and molecular distillation processes lead to important differences in apparatus design. In molecular distillation it is clear that there is no generation of vapor bubbles below the surface because the vapor would have to exert a pressure of the order of a millimeter of mercury, while at the temperature of the distillation, the vapor pressure is actually less than 0.001 mm. It is important, therefore, for the liquid film to be thin and the surface constantly changed. This has been achieved by the falling-film still, in which a thin film of liquid flows down over the heater, and by the centrifugal still, in which a thin film of solution is spun out over the surface of a shallow conical evaporator which is rotated at a high speed. Another reason for using a very thin film is to reduce thermal decomposition by subjecting the sensitive organic compounds to a high temperature for only a very short time. In a centrif-

<sup>1</sup> *Chem. Revs.*, **34**, 51 (1944); *Am. Scientist*, **33**, 205 (1945).

ugal still, the liquid is heated for less than a tenth of a second. Thus thermal decomposition is greatly reduced by carrying out the distillation at a low pressure and by allowing only short exposure to the elevated temperature.

The measurement of the temperature of the vapor is not practical in short-path distillation, but information can be gained by distilling a number of known substances at different temperatures and plotting a curve of material condensed against temperature. In this way the relative temperature at which an unknown material comes over can be determined by reference to some known material.<sup>1</sup> These separations may be made very conveniently with a series of pilot dyes<sup>2</sup> of different volatilities which condense to give a colored deposit.

### DENSITY<sup>3</sup>

Densities of liquids are most frequently expressed in grams per milliliter. Since the milliliter is defined as one one-thousandth of the volume of 1 kg of pure, ordinary water at its temperature of maximum density (3.98°C), the density in grams per milliliter is numerically equal to the ratio of the absolute density of the liquid at  $t^{\circ}\text{C}$  to the absolute density of water at 3.98° and is frequently represented by  $\rho_4^t$ .

The densities of liquids may be determined by measurement of the weight of liquid occupying a known volume (pycnometric methods) and by buoyancy methods based on Archimedes' principle.

**Pycnometers.** Pycnometers are vessels with capillary necks in which a definite volume of liquid is weighed. The volume is determined by weighing the vessel filled with water at a definite temperature. A table giving the density of water as a function of temperature is given in the Appendix. Two types of pycnometers are illustrated by Fig. 23.

In order to obtain fifth-place accuracy in density determinations, a number of precautions must be observed. The weights should be checked against each other to obtain their relative values. It is not necessary to compare the set with a certified standard mass. One of the largest errors is often due to the adsorption of an uncertain amount of moisture by the glass, and it is necessary to wipe the pycnometer with a damp cloth and allow it to stand in the balance case for several minutes

<sup>1</sup> Embree, *Ind. Eng. Chem.*, **29**, 975 (1937).

<sup>2</sup> Hickman, *Ind. Eng. Chem.*, **29**, 968, 1107 (1937).

<sup>3</sup> Discussions of experimental methods for the determination of density are to be found in Bauer and Levin in Weissberger (ed.), *op. cit.*, 3d ed., Vol. I, Pt. I, Chap. 4 (1959); Reilly and Rae, "Physico-chemical Methods," 5th ed., Vol. 1, pp. 577-608, 609-628, D. Van Nostrand Company, Inc., Princeton, N.J. (1953).

before weighing. A similar pycnometer of approximately the same volume may be used to advantage as a counterpoise.

In order to obtain the true weight of the liquid in the pycnometer, it is necessary to correct for the buoyancy of the air. The volume occupied by the glass of the pycnometer can be left out of the calculation if the tare has very nearly the same weight and density. The true (vacuum-corrected) weight  $W_0$  is calculated from the equation

$$W_0 = W \left( 1 + \frac{\rho_{\text{air}}}{\rho_s} - \frac{\rho_{\text{air}}}{8.5} \right)$$

where  $W$  = apparent weight given by brass weights

$\rho_{\text{air}}$  = density of air

$\rho_s$  = density of substance being weighed

In the present case,  $\rho_s$  is the density of the liquid in the pycnometer. For fifth-place accuracy the density of the weights may be assumed to be 8.5 g/ml even when the small-denomination weights are made of material of different density. The density of the air may usually be taken to be 0.0012 g/ml, but for accurate work the variation of the density of air due to changes in room temperature, barometric pressure, and relative humidity must be considered. If the temperature ( $t^\circ\text{C}$ ), barometric pressure ( $P$  millimeters of mercury), and the relative humidity ( $H$ , in per cent) are measured at the time of the weighing, the density of air may be calculated from the equation

$$\rho_{\text{air}} = \frac{0.001293 - P - k}{1 + 0.00367t} \frac{1}{760}$$

where  $k = 0.0038HP_{\text{H}_2\text{O}}^t$

$P_{\text{H}_2\text{O}}^t$  = vapor pressure of water, mm Hg at  $t^\circ\text{C}$

For determining the density of a solid, a pycnometer with a wide mouth that will admit the solid is necessary. The ordinary type is a small bottle with a ground-glass stopper through which is bored a fine capillary.

The bottle is filled with water, and the stopper is inserted firmly, after which it is placed in a thermostat. The excess liquid is wiped off, and the pycnometer is dried and weighed. The pycnometer is weighed empty and again with the solid. After filling with water (plus the solid) it is weighed again, and all the data are then available for calculating the weight and volume of the solid and its density. In case the solid is soluble in water, some other inert liquid is used, and the density of the liquid is determined also.

The greatest source of error in determining the density of a solid is the adsorption of air by the solid. For this reason, the pycnometer containing the solid and some liquid is set in a larger bottle, which is connected to a vacuum pump, and evacuated until all air bubbles have ceased rising from the solid; then the pycnometer is filled completely.

**Buoyancy Methods.** The Westphal balance is more accurate than the floating graduated hydrometer. It depends on the principle of Archimedes, according to which the buoyant effect is directly proportional to the weight of the liquid displaced. The sinker is suspended in pure water, with the unit weight in position, and a threaded counterpoise is turned until the pointer reads zero on the scale. The sinker is then dried and suspended in the liquid whose density is to be measured. The smaller weights are set at the proper places on the scale so as to restore the point of balance. Some balances are constructed with three riders,

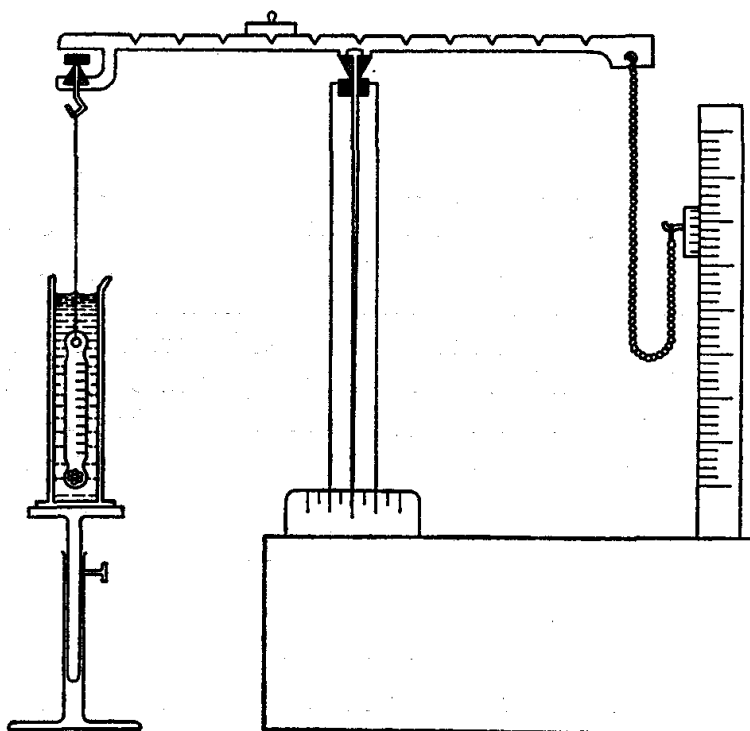


FIG. 117. Chainomatic balance for determining the density of liquids.

corresponding to 0.1, 0.01, and 0.001, and the scale is divided into 10 equal parts. The position on the scale gives the numerical value for each rider; e.g., if the 0.1 rider is at 9, the 0.01 at 8, and the 0.001 at 7, the specific gravity is 0.987.

The temperature is read directly on a thermometer which is enclosed in the sinker. A very fine platinum wire is used for suspending the sinker; the surface-tension effect on this wire is negligible for ordinary work, but for accurate work it may prove to be a source of error. The wire should be immersed to the same depth for each measurement.

The same principle of weighing a sinker which is suspended in a liquid is used in the chainomatic balance, shown in Fig. 117. With this more

elaborate instrument, densities may be determined quickly with an accuracy of 1 part in 10,000. The value of the instrument is increased by the introduction of an electrical heating coil and switch, to maintain the liquid at a definite temperature.

**Floating Equilibrium.** The objection to the wire projecting through the surface of the liquid in the case of the Westphal balance can be eliminated by having the plummet so carefully adjusted that it neither sinks nor rises in the liquid.

Lamb and Lee<sup>1</sup> obtained accurate results by placing a piece of iron in the float and measuring the strength of the electromagnetic field necessary to keep the bulb in floating equilibrium. A more recent design for such apparatus has been described by MacInnes *et al.*<sup>2</sup>

Gilfillan<sup>3</sup> adjusted the hydrostatic pressure on the liquid with a mercury column until equilibrium of the bulb was obtained. He calibrated the apparatus with dilute potassium chloride solutions of known densities.

The density of solids can be determined in a somewhat similar way by mixing two liquids of different density until the solid neither rises nor sinks. The system must be evacuated to remove air from the solid. A heavy liquid like methylene iodide is mixed with a light liquid like benzene, and the density of the final mixture is determined with a pycnometer. The density of the liquid is the same as the density of the solid with which it is in floating equilibrium.

This method has been used by Hutchinson and Johnston<sup>4</sup> for the accurate determination of the density of lithium fluoride. The necessary precautions have been described, and the determinations were sufficiently accurate to follow the concentration of lithium isotopes<sup>5</sup> by electrolysis.

**Falling Drop.** The falling-drop method of Barbour and Hamilton<sup>6</sup> is especially useful when only small quantities of solution are available. This method is sufficiently sensitive to be useful for determining the concentration of deuterium oxide in water. The method consists in measuring the velocity of fall of a drop of water through a nonmiscible liquid of known density, usually *o*-fluorotoluene.<sup>7</sup> The density of a water drop may be calculated to 1 to 2 parts per million by using Stokes' law.

<sup>1</sup> *J. Am. Chem. Soc.*, **35**, 1666 (1913); cf. also Jones and Hall, *ibid.*, **59**, 258 (1937).

<sup>2</sup> MacInnes, Dayhoff, and Ray, *Rev. Sci. Instr.*, **22**, 642 (1951); cf. also MacInnes and Dayhoff, *J. Am. Chem. Soc.*, **75**, 5219 (1953).

<sup>3</sup> *J. Am. Chem. Soc.*, **56**, 406 (1934).

<sup>4</sup> *J. Am. Chem. Soc.*, **62**, 3165 (1940).

<sup>5</sup> Johnson and Hutchinson, *J. Chem. Phys.*, **8**, 869 (1940).

<sup>6</sup> *Am. J. Physiol.*, **69**, 654 (1924); *J. Biol. Chem.*, **69**, 625 (1926).

<sup>7</sup> Keston, Rittenberg, and Schoenheimer, *J. Biol. Chem.*, **122**, 227 (1937).

VISCOMETRY<sup>1</sup>

The Ostwald viscometer (Exp. 26) has been improved by Bingham.<sup>2</sup> The liquid is forced through a capillary with compressed air maintained at constant pressure. There are marks at the top and bottom of the bulb, and the time required for the liquid to flow first up and then down is recorded. Kaaschow<sup>3</sup> gives a detailed discussion of the design and testing of Ostwald-type viscometers.

The use of automatic timing for the transit of the meniscus of the liquid in the capillary tube, by means of a photoelectric cell, has been developed to a high degree of perfection by Jones and Talley<sup>4</sup> and by Riley and Seymour.<sup>5</sup> Details of the necessary assembly have been given by these investigators in articles in which they also analyze sources of error in the use of viscometers.

The rotation-cylinder, or Couette-type, viscometer, in which is measured the torque that is required to rotate a cylinder at a given rate of speed in the solution, has certain advantages over the capillary-tube type. A source of error in a capillary-tube type of viscometer arises from the fact that the shearing stress exerted on the liquid is not uniform but varies with the distance from the center of the capillary. This effect is not important if the viscosity of the liquid is independent of the shearing stress (Newtonian liquid), but in the case of non-Newtonian liquids, the viscosity obtained is an average value which depends on the dimensions of the instrument and the relation between viscosity and shearing stress. In the rotating-cylinder viscometer, this difficulty may be avoided.

One of the simplest methods for determining viscosity depends upon the determination of the velocity of a sphere falling through the liquid when it has reached a uniform velocity. This is based on Stokes' law relating the viscosity of the liquid to the frictional force which acts on a moving sphere. It is necessary to apply corrections for the influence on the velocity of the wall of the tube to avoid end effects. For a small sphere of radius  $r$  falling axially through a viscous liquid in a cylindrical tube, the complete expression is given on page 152. In meas-

<sup>1</sup> The general subject of viscometry is discussed by Hatchek, "The Viscosity of Liquids," George Bell & Sons, Ltd., London (1928); Barr, "Viscometry," Oxford University Press, New York (1931); Philippoff, "Viscosität der Kolloide," Steinkopff, Dresden and Leipzig (1942); Blair, "A Survey of General and Applied Rheology," Pitman Publishing Corporation, New York (1944); Swindells, Ullman, and Mark in Weissberger (ed.), *op. cit.*, 3d ed., Vol I, Pt. I, Chap. 12 (1959).

<sup>2</sup> "Fluidity and Plasticity," p. 76, McGraw-Hill Book Company, Inc., New York (1922).

<sup>3</sup> *Ind. Eng. Chem., Anal. Ed.*, 10, 35 (1938).

<sup>4</sup> *Physics*, 4, 215 (1933); *J. Am. Chem. Soc.*, 55, 624 (1933).

<sup>5</sup> *Ind. Eng. Chem., Anal. Ed.*, 18, 387 (1946).

urements with spheres of equal radius in tubes of the same dimensions

$$\eta = K(\rho - \rho_0)t$$

The tube constant  $K$  may be evaluated experimentally by measuring the time of fall through a liquid whose density and viscosity are known or may be calculated from Eq. (22) on page 152. In determining relative viscosities, the tube constant cancels:

$$\frac{\eta}{\eta_s} = \frac{(\rho - \rho_0) t}{(\rho - \rho_s) t_s}$$

The subscript  $s$  refers to the standard liquid. The sphere is discharged slowly into the tube, a few centimeters below the surface, through a glass tube slightly larger than the sphere; 1.5 mm is a suitable diameter for the sphere, and 20 cm is a satisfactory height for fall. The vessel should have a diameter at least ten times that of the sphere. A steel ball such as those used in ball bearings makes an excellent ball for the experiment.

The determination of absolute viscosities is rather difficult. It requires careful measurements of the apparatus, including the length and radius of the capillary, and some rather uncertain corrections. Further details concerning absolute measurements are given by Thorpe and Rodger<sup>1</sup> and by Bingham, Schlesinger, and Coleman.<sup>2</sup>

Viscosity has been studied at very high pressures.<sup>3</sup>

## SURFACE TENSION<sup>4</sup>

When the surface tension of a liquid is to be determined (Exp. 49), one should choose the particular method which will give the best results with the least effort. The realms of utility for three methods are outlined as follows:

### 1. *Single liquids*

- a. *Capillary rise*: For highest accuracy, but not rapid.
- b. *Ring method*: Very fast and reasonably accurate if suitable apparatus is available. Can be used for interfacial tension.
- c. *Drop weight*: Best general method for both surface and interfacial tensions if both accuracy and speed are considered. Can be used with very small quantities of liquid.

<sup>1</sup> *Phil. Trans.*, A185, 397 (1894).

<sup>2</sup> *J. Am. Chem. Soc.*, 38, 27 (1916); Hyde, *Proc. Roy. Soc. (London)*, A97, 240 (1920).

<sup>3</sup> Bridgman, "The Physics of High Pressures," George Bell & Sons, Ltd., London (1931).

<sup>4</sup> The measurement of surface tension has been reviewed by Harkins and Alexander in Weissberger (ed.), *op. cit.*, 3d ed., Vol. I, Pt. I Chap. 14 (1959); Adam, "Physics and Chemistry of Surfaces," Oxford University Press, New York (1942); Reilly and Rae, *op. cit.*, pp. 629-659.



2. *Solutions*

- a. *Drop weight*: Best method for surface and interfacial tension if long time effects are not involved.
- b. *Ring method*: Excellent for surface tension, even if time effects are involved.
- c. *Drop shape*: Excellent for the study of time effects.

## DIFFUSION

An important transport process is that of molecular diffusion in solution, with any difference in concentration being reduced by a spontaneous transfer of matter. It is caused by the Brownian motion of the dissolved molecules.

The flow of matter is defined as the amount of material which in unit time passes through a unit area of plane perpendicular to the direction of flow. It is the product of a concentration and a velocity. Thus, if the concentration is expressed in moles per cubic centimeter and the distance of displacement is given in centimeters, then the flow  $J$  is measured in moles  $\text{cm}^{-2} \text{sec}^{-1}$ .

The diffusion coefficient  $D$  is defined by two laws of Fick.<sup>1</sup> They are, for a two-component system,

$$J = -D \frac{\partial c}{\partial x} \quad (1)$$

$$\frac{\partial c}{\partial t} = \frac{\partial}{\partial x} \left( D \frac{\partial c}{\partial x} \right) \quad (2)$$

The coefficient which is defined by these equations is often referred to as a constant. This is only approximately true, and the study of the variation of  $D$  with concentration gives useful information. Equation (2) may be derived from Eq. (1) by introduction of a statement of the conservation of mass.

The diffusion of molecules in liquid media has been the subject of a number of reviews.<sup>2</sup> There are several types of experiment.

**Free Diffusion.** In this method, which is based on the second law of Fick, an initially sharp boundary is formed between the solution and the solvent with the more dense phase in the bottom of the diffusion cell. The cell should be tall enough so that the composition at the bottom and at the top of the column remains unchanged during the period of observation. The gradual blurring of the boundary may be followed by a number of methods. In early work, samples of solution were taken from various levels in the cell and their concentrations used to calculate the

<sup>1</sup> *Pogg. Ann.*, **94**, 59 (1855).

<sup>2</sup> Williams and Cady, *Chem. Revs.*, **14**, 171 (1934); Neurath, *Chem. Revs.*, **30**, 257 (1942); Harned, *Chem. Revs.*, **40**, 462 (1947); Geddes in Weissberger (ed.), *op. cit.*, Vol. I, Pt. I, pp. 551-619; Gosting, *Adv. Protein Chem.*, **11**, 429 (1956).

diffusion coefficient. In some cases, it is possible to determine the concentration at every level in the diffusion cell by means of quantitative light-absorption measurements. The most generally applicable and accurate methods for the determination of the diffusion coefficient are optical methods which depend upon the fact that light is deflected upon passing through a refractive-index gradient such as that established in a diffusion column. In the Lamm<sup>1</sup> scale method, the displacements of lines in the photograph of a linear scale placed behind the diffusion cell are measured with a microcomparator. The schlieren method, in which a plot of refractive-index gradient versus position in the cell is obtained directly, is described in Chap. 19. The diffusion coefficient may be calculated from the shape of the curve by several methods.

Interference methods developed by Kegeles and Gosting,<sup>2</sup> Longworth,<sup>3</sup> and Coulson *et al.*<sup>4</sup> yield more accurate diffusion coefficients than any of the above methods.

A number of cells have been designed for the purpose of forming a sharp initial boundary between solution and solvent.<sup>5</sup>

**Restricted Diffusion.** Harned<sup>6</sup> has used a conductivity method for the determination of concentration changes of salts in a diffusion cell. In this method, the difference in the conductances of the solution as measured between pairs of electrodes at the bottom and at the top of the cell is utilized in the calculation of the diffusion coefficient. This method is limited to the study of electrolytes, and an experimental precision of 0.1 per cent may be obtained at concentrations less than 0.01 N.

**Steady-state Diffusion.** In this method the first law of Fick serves as the means for the computation of the result. Diffusion takes place through a region in which the concentration gradient is independent of time. An example of this method is the porous-plate method of Northrop and Anson.<sup>7</sup> One form of the diffusion cell consists of a bell-shaped glass vessel, closed at the narrow top end by a stopcock and at the wide-bottom end by a sealed-in sintered-glass disk. The cell is filled with a solution and is immersed in a beaker of water just touching its surface. Various sizes have been used, from 10 to 200 ml capacity. Diffusion is allowed to proceed until the concentrations in the pores of the sintered-glass disk are those for a "steady state," which generally requires several

<sup>1</sup> *Arkiv Kemi., Mineral. Geol.*, **17B**, No. 13 (1943).

<sup>2</sup> *J. Am. Chem. Soc.*, **69**, 2516 (1947); Gosting, Hanson, Kegeles, and Morris, *Rev. Sci. Instr.*, **20**, 209 (1949).

<sup>3</sup> *J. Am. Chem. Soc.*, **74**, 4155 (1952); **75**, 5705 (1953).

<sup>4</sup> Coulson, Cox, Ogston, and Philpot, *Proc. Roy. Soc. (London)*, **A192**, 382 (1948).

<sup>5</sup> Loughborough and Stamm, *J. Phys. Chem.*, **40**, 1113 (1936); Claesson, *Nature*, **158**, 834 (1946).

<sup>6</sup> *Loc. cit.*

<sup>7</sup> *J. Gen. Physiol.*, **12**, 543 (1929); Clack, *Proc. Phys. Soc. (London)*, **36**, 313 (1924).

hours. When steady-state concentrations have been attained, the cell is placed in contact with a fresh sample of solvent, and diffusion is allowed to proceed for a suitable length of time. From concentrations determined after various times in aliquots of solution and solvent, the diffusion coefficient may be calculated. It is necessary to calibrate the cell by an experiment with a substance of known diffusion coefficient. The advantage of this method is that it is useful for determining the diffusion coefficients of radioisotopes or biologically active substances in dilutions so low that optical methods cannot be used. In such experiments very careful control of temperature is required to prevent thermal convection.<sup>1</sup>

Micro methods for use with colored materials have been developed by Fürth<sup>2</sup> and Nistler.<sup>3</sup>

#### OSMOTIC PRESSURE<sup>4</sup>

Osmotic-pressure determinations may be divided into two classes according to the molecular weight of the solute. If the membrane is permeable only to solvent molecules, the so-called "total osmotic pressure" is obtained. In the case of solutions which contain solutes of both low and very high molecular weight, the total osmotic pressure would be due to both classes of solute molecules. However, if the osmotic-pressure determination is carried out with a membrane permeable to both solvent molecules and low-molecular-weight solute molecules, the osmotic pressure measured is due only to the large molecules and is referred to as "colloid osmotic pressure."

In the case of solutes of molecular weight less than 10,000, the great difficulties encountered in the preparation of membranes impermeable to solute molecules preclude the general use of the osmometric method. In the apparatus of Frazer and Myrick,<sup>5</sup> a porous clay cup contains an electrolytically deposited membrane of copper ferrocyanide which allows the passage of solvent but not of the low-molecular-weight solute. This clay cup, containing the solvent, is surrounded by a strong bronze cylinder containing the solution and the connection to the manometer. To measure the pressure, an electrical-resistance gauge or a water interferometer may be used in place of the customary mercury manometer. With this apparatus Frazer and his coworkers have measured osmotic pressures up to 273 atm.

<sup>1</sup> Mouquin and Cathcart, *J. Am. Chem. Soc.*, **57**, 1791 (1935).

<sup>2</sup> *Kolloid-Z.*, **41**, 300 (1927).

<sup>3</sup> *Kolloidchem. Beih.*, **28**, 296 (1929).

<sup>4</sup> A general review of this subject is given by Wagner and Moore in Weissberger (ed.), *op. cit.*, 3d ed., Vol. I, Pt. I, Chap. 15 (1959).

<sup>5</sup> *J. Am. Chem. Soc.*, **38**, 1907 (1916); Frazer and Lotz, *J. Am. Chem. Soc.*, **43**, 2501 (1921).

Osmotic pressure may be successfully used to determine the molecular weights of macromolecules, such as high polymers, proteins, and polysaccharides. A simple calculation will show that an osmotic pressure of 1 mm of water corresponds to a freezing-point depression of roughly  $0.0001^{\circ}\text{C}$ . Such a freezing-point depression might be caused by a minute trace of salt in a protein solution, while the salt would not significantly affect the osmotic pressure of the isoelectric protein measured with a membrane permeable to small ions and water molecules.

Osmotic-pressure measurements may be carried out by dynamic or static methods. In the dynamic method,<sup>1</sup> the rate of movement of the

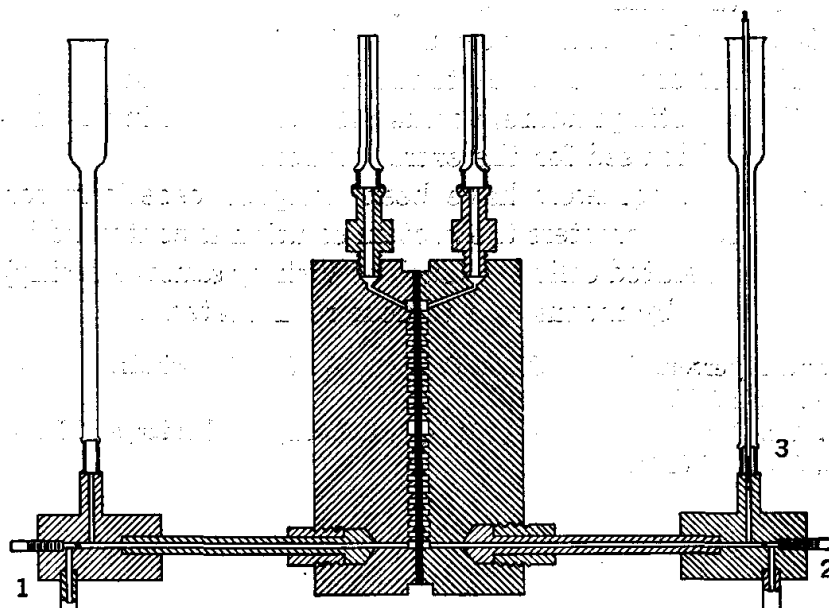


Fig. 118. Static osmometer.

meniscus in the capillary tube is measured at a number of heights and used to obtain the equilibrium height, whereas in the static method, the equilibrium height is determined directly. The construction of a standard type of static osmometer for high-polymer work is illustrated in Fig. 118.<sup>2</sup> The cell consists of two stainless-steel plates clamped together, with the membrane between the plates. The faces of the two plates are machined with a set of concentric cuts 2 mm wide and 2 mm deep. The solution is placed in one half-cell, and the solvent in the other, and the membrane simultaneously acts as a gasket. With valves 1 and 2 closed and valve stem 3 removed, solution is poured into the left-hand tube, while solvent is simultaneously poured into the right one, so that the

<sup>1</sup> Montanna and Jilk, *J. Phys. Chem.*, **45**, 1374 (1941).

<sup>2</sup> Fuoss and Mead, *J. Phys. Chem.*, **47**, 59 (1943); Flory, *J. Am. Chem. Soc.*, **65**, 374 (1943).

liquid level rises at about the same rate on both sides of the membrane. Valve 3 is then inserted and closed, and valve 1 is opened to drop the meniscus in the solution standpipe to its desired position. The left meniscus is maintained at constant height, while the rate of approach of the right meniscus to its equilibrium position is determined from both the high-pressure and low-pressure sides. Smaller glass osmometers<sup>1</sup> are also widely used.

Semipermeable membranes for use with polymer solutions are generally prepared by treating cellophane with 3 per cent sodium hydroxide or by denitrating collodion (cellulose nitrate), using ammonium polysulfide.

Because of the nonideality of polymer solutions, it is necessary to extrapolate osmotic-pressure measurements at several concentrations to infinite dilution in order to calculate the molecular weight. A plot of  $\pi/c$ , where  $\pi$  is the osmotic pressure, versus  $c$  is quite linear in the low-concentration range and is used for the extrapolation.

A number of osmometers have been designed especially for protein work.<sup>2</sup> In these osmometers the protein solution is contained in a bag of collodion or regenerated cellulose (such as Visking sausage casing) and the pressure measured by means of a toluene manometer.

<sup>1</sup> Zimm and Myerson, *J. Am. Chem. Soc.*, **68**, 911 (1946); Schulz, *Z. physik. Chem.*, **A176**, 317 (1936); *ibid.*, **B52**, 1 (1942).

<sup>2</sup> Bull, *J. Am. Chem. Soc.*, **68**, 742 (1946); Scatchard, Batchelder, and Brown, *J. Am. Chem. Soc.*, **68**, 2320 (1946).

## *Electrical Measurements*

A wide variety of electrical measurements are met with in physical chemistry. These include observations of the electromotive forces of electrochemical cells, uses of thermocouples and thermopiles, measurements of resistance in the determination of electrolytic conductance and of temperature, measurement of quantity of electricity in the determination of transference numbers and ionic mobilities and of electrical energy in calorimetry, and determinations of dielectric constant.

The absolute electrical units are based upon the fundamental mechanical units of mass, length, and time by the use of accepted principles of electromagnetism. These units are maintained, as were the international units used before 1948, by groups of standard resistors and of standard cells. The international ohm and volt are slightly larger than the corresponding absolute units. The conversion factors for adjusting values of standards in this country are as follows:<sup>1</sup>

1 int ohm	=	1.000495 abs ohms
1 int volt	=	1.00033 abs volts
1 int amp	=	0.999835 abs amp
1 int coulomb	=	0.999835 abs coulomb
1 int henry	=	1.000495 abs henrys
1 int farad	=	0.999505 abs farad
1 int watt	=	1.000165 abs watts
1 int joule	=	1.000165 abs joules

### **GALVANOMETERS**

In these days of automatic recording instruments for voltage (potentiometers), resistance, capacitance, and frequency, the electronic circuits have made galvanometers less common items of the physical-chemistry laboratory as compared with a decade ago. However, galvanometers are still useful in many assemblies for electrical measurements; furthermore,

<sup>1</sup> *Natl. Bur. Standards (U.S.), Circ., C459 (1947).*

ammeters and voltmeters are essentially portable galvanometers of low sensitivity, so they warrant some description.

The D'Arsonval galvanometer consists of a rectangular coil of wire suspended from a fine wire in the field of a permanent magnet. The bottom part of the coil is made steady by a loosely coiled metallic spring, which also serves as a lead. The current in the moving coil flows perpendicular to the lines of magnetic force, producing a torque on the coil. The coil turns until the restoring moment due to the twist in the spring is just equal to the torque due to the current. The motion of the coil is observed and magnified by means of a beam of light reflected from a small mirror mounted on the coil. A wide variety of galvanometers is available to provide the sensitivity, period, and ruggedness desired. The current sensitivity of a galvanometer is defined as the current in microamperes required in the galvanometer coil to produce a standard deflection, usually 1 mm on a scale placed perpendicular to the reflected light beam at a distance of 1 m. Sometimes the sensitivity is expressed in microvolts, which is the electromotive force which produces the standard deflection when it is introduced into the series circuit consisting of the galvanometer and its external critical-damping resistance. The microvolt sensitivity is therefore the product of the microampere sensitivity and the sum of the galvanometer resistance and its external critical-damping resistance. The sensitivity of a galvanometer is less frequently given in terms of the ballistic sensitivity, which is the quantity of electricity which must be discharged through a galvanometer in a time which is short compared with its free period to produce the standard deflection.

The period of a galvanometer is the time in seconds required for one complete undamped oscillation of the galvanometer. In most galvanometer applications, a period as short as possible, consistent with other necessary requirements, is desired. Short periodicity conserves the time of the observer and makes possible precision of measurement of fluctuating phenomena that would otherwise be unobtainable. For other measurements, such as ballistic measurements, long periods are desirable to facilitate reading.

For most applications it is desirable to damp a galvanometer so that the final reading is obtained without oscillation. A critically damped galvanometer reaches its final reading without oscillation and in the shortest possible time. It is customary to take the period of a critically damped galvanometer as equal to its undamped period, for although the critically damped period is theoretically infinite, practically, a critically damped deflection is within about 1.5 per cent of its final position in the undamped periodic time. If the resistance of the external circuit is too small, the galvanometer will be overdamped; that is, the coil will rotate too slowly. In this case, more resistance is added in series. If the resistance of the external circuit is too great, the galvanometer will be

underdamped, and critical damping is achieved by reducing the resistance in parallel.

For the most satisfactory operation of a galvanometer, one should select an instrument whose external critical-damping resistance is slightly lower than the resistance presented to the galvanometer by the circuit with which it is to be employed. An ordinary laboratory has use for low-resistance galvanometers (20 to 100 ohms) for thermopile work and calorimetry and for high-resistance galvanometers (over 1000 ohms) for measurements of electromotive force. In an a-c galvanometer, sensitivity

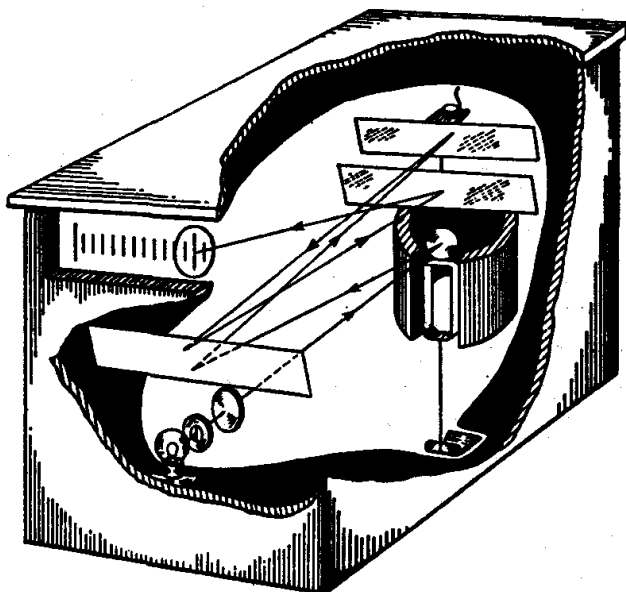


FIG. 119. Portable galvanometer using multiple reflections.

and period are important, but critical-damping resistance as such is of less significance because proper damping also depends on capacitance and inductance.

Portable box-type galvanometers are taut-suspension moving-coil instruments with built-in lamps and scales, as illustrated in Fig. 119. The light beam traverses the case five times after reflection from the moving mirror, thus considerably increasing the sensitivity. Such galvanometers are commonly available with sensitivities down to  $2.5 \mu\text{volts mm}^{-1}$  and  $0.005 \mu\text{amp mm}^{-1}$ .

For greater sensitivity, galvanometers with more delicate suspensions must be used. These galvanometers must be carefully leveled and mounted on vibrationless supports.<sup>1</sup> The beam of light from a small lamp is focused on a scale at 1 m distance, by means of a focusing mirror or a long-focus lens attached to the glass window of the galvanometer.

<sup>1</sup> The design of vibrationless supports has been discussed by Strong, "Procedures in Experimental Physics," pp. 328, 590, Prentice-Hall, Inc., Englewood Cliffs, N.J. (1939).



High-sensitivity galvanometers are commonly available with sensitivities down to  $0.1 \mu\text{volt mm}^{-1}$  or  $0.0001 \mu\text{amp mm}^{-1}$ .

If a sensitivity much greater than  $10^{-8}$  amp or  $10^{-7}$  volt  $\text{mm}^{-1}$  is required with a low critical-damping resistance, it is necessary to use a special type of galvanometer or some type of amplification. Very small direct currents, as from thermopiles, may be amplified by vacuum-tube circuits if the current is subjected to mechanical interruption. Such methods are especially useful in infrared spectroscopy and have been reviewed by Williams.<sup>1</sup>

Another type of amplified galvanometer is the photoelectric galvanometer, which consists of a taut-suspension galvanometer and a double-cathode photocell in a balanced-bridge circuit. In the null position, the galvanometer light beam illuminates both photocell cathodes equally, under which condition the photocell constitutes a balanced bridge with zero potential difference across the photocell cathodes. Displacement of the light beam produces a signal in the photocell circuit whose magnitude and polarity are determined by the magnitude and polarity of the electromotive force applied to the galvanometer terminals. This method has been useful in amplifying thermopile currents.<sup>2</sup>

Ammeters for registering current are of very low resistance and are connected in series in the circuit. Voltmeters, for measuring the potential between two points in a circuit, on the other hand, are connected in parallel with the circuit, and their resistance must be so high that only a small fraction of the current flows through them. For example, if a meter with which the full-scale deflection is obtained with 1 milliamp is to be used as a 10-volt voltmeter, a series resistance  $S$  must be added. If the resistance of the meter is  $R$ ,  $R + S = 10/0.001$ , and the resistance to be placed in series so that the meter will show a full-scale deflection for 10 volts is  $(10/0.001) - R$ . Similarly, the series resistance required to use the milliammeter as a 100-volt voltmeter is  $(100/0.001) - R$ . High-grade commercial ammeters and voltmeters are guaranteed to be correctly graduated to as close as  $\frac{1}{4}$  per cent of the full-scale reading, but cheaper instruments are generally accurate only to about 2 per cent of the full-scale reading, irrespective of the actual reading.

### MEASUREMENT OF ELECTROMOTIVE FORCE<sup>3</sup>

**Potentiometers.** The principle of the potentiometer has been discussed in Exp. 31. Since the galvanometer acts only as a null-point

<sup>1</sup> *Rev. Sci. Instr.*, **19**, 135 (1948).

<sup>2</sup> Gershinowitz and Wilson, *J. Chem. Phys.*, **6**, 197 (1938); Mortimer, Blodgett, and Daniels, *J. Am. Chem. Soc.*, **69**, 822 (1947).

<sup>3</sup> Tanford and Wawzonek in Weissberger (ed.): "Physical Methods in Organic Chemistry," 3d ed., Vol. 1, Pt. IV, Interscience Publishers, Inc., New York (1960).

indicator, the accuracy of measurement depends only on the accuracy of the standard-cell voltage and the accuracy of the resistance coils, provided that the galvanometer is sufficiently sensitive and the resistance of the circuit is not too great. The resistance coils can be manufactured with exceedingly high precision, so the accuracy of the method depends principally on the constancy of the standard-cell voltage. Potentiometers for research purposes are designed in such a way that it is possible to check the potentiometer against the standard cell without disturbing the setting of the resistances in the measuring circuit. This is illustrated in Fig. 120. Fixed connections for the standard cell span a definite portion of the

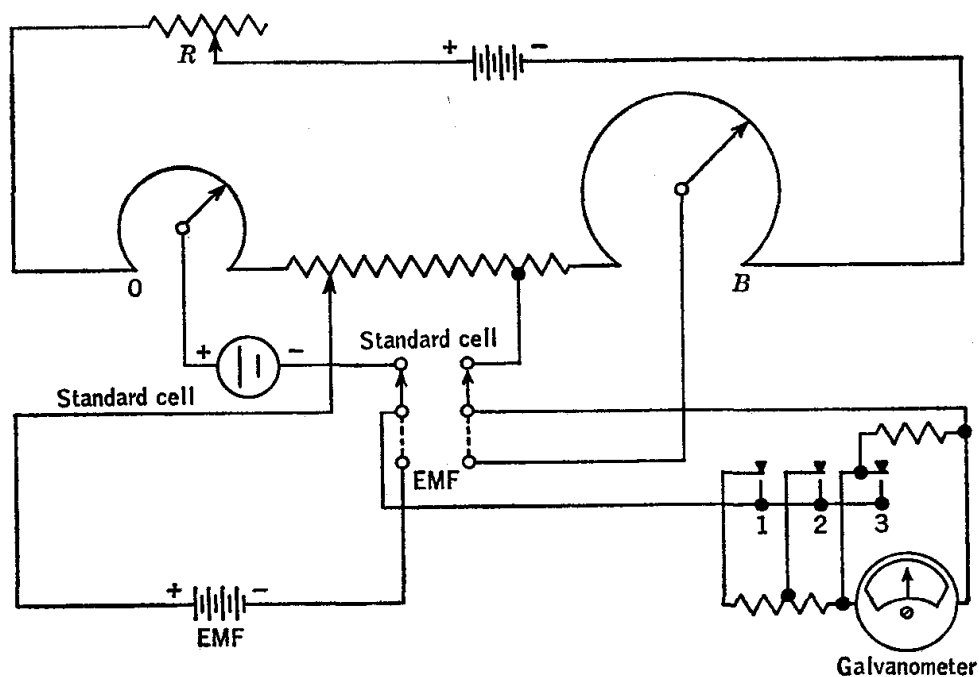


FIG. 120. Potentiometer circuit.

circuit  $OB$ , across which the fall in potential is adjusted to be equal to the voltage of the standard cell by varying  $R$ . By means of a double-pole double-throw switch, either the standard cell or the unknown electromotive force can be put in the circuit through the galvanometer. In making the first trial balance, the galvanometer keys 1 and 2 are used to include a high resistance in the galvanometer circuit and prevent a large current from flowing through the standard cell. When the potential drop of the potentiometer and the electromotive force of the unknown cell or standard are nearly balanced, key 3 is pressed to obtain maximum galvanometer sensitivity. When the total resistance of the unknown cell is comparatively small, such as 100 ohms, a potential difference of, say, 0.0001 volt between the potential drop in the slide-wire and the electromotive force of the unknown cell can cause sufficient current to

flow through the galvanometer to produce a deflection. However, if the resistance of the unknown cell is, say, 5 megohms, the current through the circuit due to 0.0001 volt is only  $0.0001/(5 \times 10^6)$ , or  $2 \times 10^{-11}$  amp, which is too small to turn the coil of an ordinary galvanometer. In such a case, it is necessary to use an electrometer or vacuum-tube voltmeter.

Special potentiometers have been designed for thermocouple work. These include the Wenner potentiometer<sup>1</sup> and the White potentiometer. Double potentiometers of the White type are particularly useful in calorimetry where it is desired to measure, practically simultaneously, two temperatures which are appreciably different, without resetting dials.

**Recording Potentiometers.** There are now available recording potentiometers which perform the operations of balancing against an applied potential automatically and of standardizing themselves by balancing against the standard cell or Zener diode at regular intervals. The automatic balancing mechanism replaces the galvanometer in the usual potentiometer circuit. This electronic device consists of an amplifier which drives a motor whose direction and speed depend upon the polarity and voltage of the unbalance. The motor moves the contact on the potentiometer slide-wire, and the attached pen makes a trace on the moving chart. The basic circuitry for such instruments has been described by Witherspoon.<sup>2</sup>

Here again "damping" is required in the potentiometer recorder, it being generally achieved by a resistance-capacitance damping circuit in the input to the amplifier in the instrument. The theory of damping in such systems is described in several places.<sup>3</sup>

The precision of recording potentiometers at any point on the chart is about 0.3 per cent of the full-scale voltage. Since so many measurements may be reduced to a measurement of voltage, recording potentiometers can be used in a wide variety of applications. They can be fitted with mercury switches or microswitches which can operate heaters or motors at certain potentials.

More specific information as to the potential required for a full-scale displacement, the time required for the pen to move across the full scale to a new balance point, the rate at which the paper moves under the pen of the instrument, etc., may be obtained from the manufacturers.

**Standard Cells.** The electromotive force of the Weston cell in the new absolute system is 1.0186 volts at 20°. This cell is set up in an air-tight H-shaped vessel, with platinum wires sealed through the bottoms for connection with the electrodes, as shown in Fig. 121. The positive

<sup>1</sup> Behr, *Rev. Sci. Instr.*, 3, 109 (1932).

<sup>2</sup> *Instruments*, 25, 900 (1952).

<sup>3</sup> Tustin (ed.): "Automatic and Manual Control," pp. 249ff., Butterworth & Co. (Publishers) Ltd., London (1952).

electrode consists of pure mercury, which is covered by a thick paste of mercurous sulfate and a small quantity of cadmium sulfate. The negative electrode is a cadmium amalgam containing 12.5 per cent of cadmium. On the top of the solidified amalgam and the mercurous sulfate paste are placed some rather large and clear cadmium sulfate crystals; then the cell is filled with a saturated solution of cadmium sulfate. The ends of the tubes are closed, allowing sufficient air space for thermal expansion. The materials must be thoroughly purified. The temperature coefficient of the cell is small, so that the electromotive force may be given with accuracy sufficient for most purposes by the expression

$$E_t = E_{20} - 0.0000406(t - 20)$$

In actual laboratory measurements the unsaturated cadmium cell is more commonly used than the Weston cell. This cell contains a solution of cadmium sulfate saturated at 4° and has the advantage that the temperature coefficient ( $0.00001 \text{ volt deg}^{-1}$ ) is less than for the saturated cell. The voltage of the unsaturated cadmium cell varies between 1.01856 and 1.01910 int volts.

The following precautions should be taken in using standard cells. (a) The cell should not be exposed to temperatures below 4°C nor above 40°C. (b) Abrupt changes of temperature should be avoided because they may produce temporary variations of several hundredths of 1 per cent in the electromotive force. (c) All parts of the cell should be at the same temperature. (d) Current in excess of 0.0001 amp should never pass through the cell. (e) The electromotive force of the cell should be redetermined at intervals of a year or two.

**Reference Electrodes.** The cells whose electromotive forces are to be determined may be considered to be made up of two electrodes, one an indicator and the other a reference electrode. The calomel electrodes and the silver-silver chloride electrode are the most commonly used reference electrodes.

There are three types of calomel electrodes in common use, depending upon the concentration of the potassium chloride solution used: 0.1 N, N, or saturated. The electromotive forces at 25° of the three calomel electrodes are as follows:<sup>1</sup>

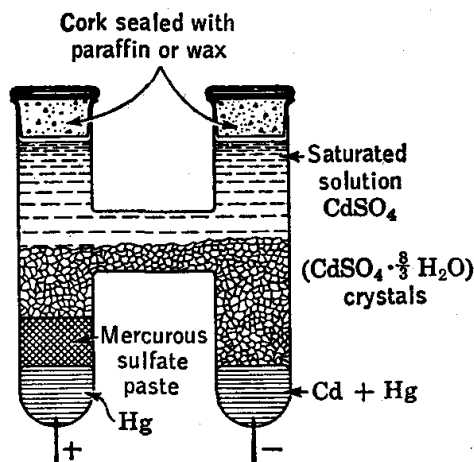


FIG. 121. Weston normal cell.

<sup>1</sup> Hamer, *Trans. Electrochem. Soc.*, 72, 45 (1937).

Hg, Hg <sub>2</sub> Cl <sub>2</sub> (s); KCl (0.1 N)	$E = 0.3356$
Hg, Hg <sub>2</sub> Cl <sub>2</sub> (s); KCl (1.0 N)	$E = 0.2802$
Hg, Hg <sub>2</sub> Cl <sub>2</sub> (s); KCl (sat)	$E = 0.2444$

Commercially available saturated calomel cells such as that illustrated in Fig. 47 are especially convenient for work in the physical-chemistry laboratory.

For the silver-silver chloride electrode the electromotive force at 25°C is given by the statement

Ag(s), AgCl(s); KCl (0.1N)	$E = 0.2880$
----------------------------	--------------

The calomel electrode may be prepared as follows. The electrode consists of a test tube with a sidearm bent down at right angles and fitted with a ground-glass plug which serves as a salt bridge, the current being carried by the thin liquid film between the wall of the tube and the plug. It is preferable to have the tube made of Pyrex and the plug of soft glass. If the plug is cooled before insertion into the tube, it will become firmly fixed upon subsequent warming to room temperature. This type of junction has a high resistance and requires the use of a high-resistance galvanometer (approximately 1000 ohms) in the potentiometer circuit. A junction of this type should be kept immersed in potassium chloride solution when not in use so that the liquid film will not dry out. An alternative method of reducing diffusion at the junction involves constricting the end of the bridge arm to a tip which contains solidified agar. This connecting bridge has a much lower resistance than the type with a ground-glass joint. Better still is a simple connecting salt bridge with sintered glass at the ends.<sup>1</sup>

The glass vessels are cleaned and rinsed thoroughly, using distilled water for the latter operation. The calomel paste is made by grinding calomel in a mortar with purified mercury and potassium chloride solution of the concentrations indicated above (depending on the type of electrode to be used). A few milliliters of redistilled mercury is placed in the tube and is covered with calomel paste to a depth of approximately 1 cm. The tube and the bridge are then filled with potassium chloride solution of the desired concentration, and an electrode consisting of a platinum wire fused to a copper wire, which is sealed in a glass tube mounted in a stopper, is placed in the pool of mercury.

In all precise electromotive-force work, oxygen must be carefully excluded from the cell. This may be done by bubbling purified nitrogen through the solutions in the cell for a period of time. Tank nitrogen is readily freed from small amounts of oxygen by passing over heated copper turnings. The effluent nitrogen is bubbled first through a sample

<sup>1</sup> Laitinen, *Ind. Eng. Chem., Anal. Ed.*, 13, 393 (1941).

of the solution in a presaturator and then into the solutions in order to avoid excessive evaporation from the latter. Another type of purification system is described by van Brunt.<sup>1</sup>

## MEASUREMENT OF ELECTROLYTIC CONDUCTANCE<sup>2</sup>

**Alternating-current Wheatstone Bridge.** The measurement of electrolytic conductance using the Wheatstone bridge has been described in Exp. 27. Alternating current must be used to prevent electrical polarization of the electrodes, and this introduces a number of problems not present in d-c bridge measurements. A simple Wheatstone bridge for measurements of resistance with direct current is illustrated in Fig. 37 (page 161). Resistance  $R_3$  is adjusted to bring points  $A$  and  $B$  to the same potential, as indicated by the absence of a galvanometer deflection when the tap switch is closed. If a d-c source is used, only pure resistances are involved, and when  $A$  and  $B$  are at the same potential,

$$\frac{R_1}{R_2} = \frac{R_3}{R_4}$$

If an alternating source of current is used, it is necessary to balance the reactances in the circuit as well as the resistances. In the a-c bridge circuit illustrated in Fig. 122 the conductance cell presents an admittance which includes a capacitative term as well as a conductance term, because there is an accumulation of charge on each plate as well as a flow of charge through the cell when a potential difference exists between the terminals. The cell is therefore electrically equivalent to a resistance  $R_2$  in parallel with a capacitance  $C_2$ . The balance condition for alternating current can be satisfied only by introducing at least one other reactive element. Capacitor  $C_1$  is added for this purpose. For a null output, the resistors and  $C_1$  must be adjusted to make the a-c potential at points  $B$  and  $D$  equal in respect to both phase and amplitude. These dual conditions are met when the equations

$$\frac{R_1}{R_2} = \frac{R_3}{R_4} = \frac{C_2}{C_1}$$

are satisfied.

In practice, adjusting  $R_1$ ,  $R_3$ ,  $R_4$ , and  $C_2$  leads to a minimum in bridge output but not to a perfect null. The reason is, if  $D$  and  $B$  are not at ground potential, current flows through the detector or earphones to

<sup>1</sup> van Brunt, *J. Am. Chem. Soc.*, **36**, 1448 (1914).

<sup>2</sup> Robinson and Stokes, "Electrolyte Solutions," 2d ed., p. 87, Academic Press, Inc., New York (1959); Shedlovsky in Weissberger (ed.), *loc. cit.*

the ground via distributed capacity. In precise measurements, it is necessary to provide means for adjusting points  $D$  and  $B$  to ground potential. The most common circuit for this purpose is referred to as a Wagner earthing device. As illustrated in Fig. 122, this device consists of adjustable resistances ( $R_5$  and  $R_6$ ) and capacitances ( $C_3$  and  $C_4$ ) between  $A$  and ground and between  $C$  and ground. After adjusting the bridge to the minimum signal of the detector or earphones, the switch  $S_1$  is closed to the grounded position, and the resistances and capacitances of the Wagner earthing device are adjusted to the minimum signal of the

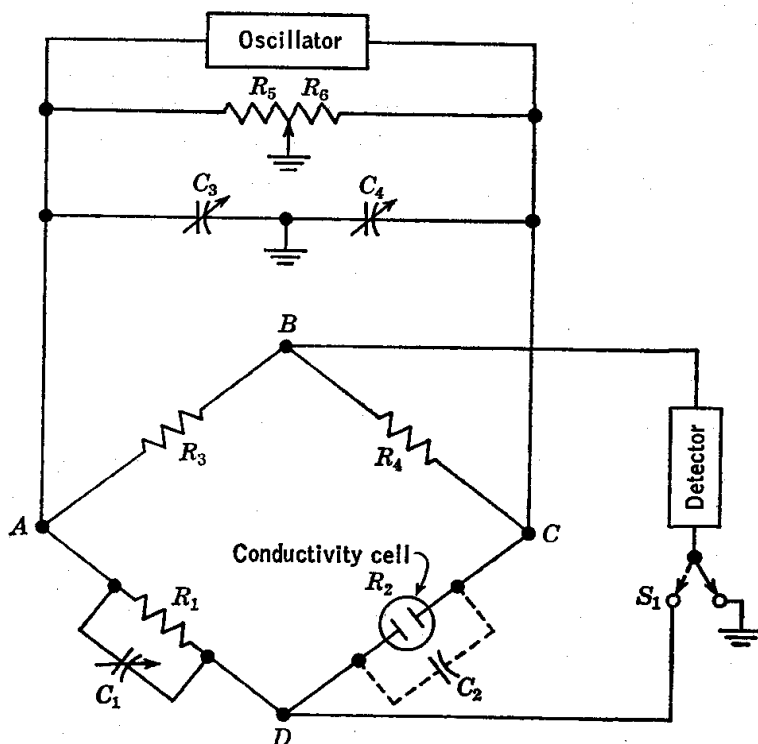


FIG. 122. Alternating-current bridge circuit.

detector. In this way, point  $B$  is brought to ground potential. It should be noted that since alternating current is used, the potentials of  $C$  and  $A$  vary sinusoidally with time, one being above ground potential while the other is below ground potential. Finally, the main-bridge balance is readjusted, with the detector in the original position.

The source of power is usually a vacuum-tube oscillator such as that described on page 601. Such an oscillator may be designed to give a pure-sine-wave current so that the current in one direction exactly offsets that in the other. At audiofrequencies a telephone headset may be used as a detector, but to attain the best results, an amplifier must be used, since the bridge current should be maintained at a low value in order to

avoid heating effects in the conductivity cell. This is achieved by limiting the voltage input from the oscillator.

Edelson and Fuoss<sup>1</sup> have given the specifications for the construction of a portable audiofrequency conductance bridge. They discuss the use of an oscilloscope for obtaining the balance points.<sup>1,2</sup> This method is more sensitive and indicates the resistance and capacitance balance separately.

The theory and design of a-c bridges for measuring the conductance of electrolytic solutions have been discussed by Jones and Josephs<sup>3</sup> and by Shedlovsky.<sup>4</sup>

The construction of bridges for high-precision work (accuracy of 0.02 per cent or better) has been discussed by Dike<sup>5</sup> and Luder.<sup>6</sup>

The resistance coils of the Wheatstone bridge must be wound non-inductively; i.e., the wire is doubled back in the middle, and the two parts of the wire with current going in opposite directions are side by side. Coils can be constructed in this way so that the difference between d-c and 20,000-cycle a-c resistances is less than 0.01 per cent.

Electrolytic conductance may also be measured with direct current using nonpolarizable electrodes.<sup>7</sup> This method is capable of quite precise results, but it is applicable only to those electrolytes for which nonpolarizable electrodes are available.

**Conductivity Cells.** A number of forms of conductivity cells are shown in Fig. 123. The cells are usually constructed of highly insoluble glass, such as Jena 16III or Pyrex, or of quartz. The platinum electrodes should be heavy and well anchored, so that the cell constant will not change when the cell is used frequently. The conductivity cell for a given measurement should be chosen with an appropriate cell constant, so that the resistance will not fall far below 1000 ohms, where excessive polarization difficulties are encountered with the usual apparatus, or above 10,000 to 30,000 ohms, where errors due to insulation leakage are encountered. For solutions of low conductance, the electrodes should be large and close together. For solutions of high conductance, the electrodes should be smaller and farther apart. Jones and Bollinger<sup>8</sup> have shown that in many cells which have been commonly used, the filling tubes are relatively close to the electrode leads, so that disturbing parasitic currents can flow

<sup>1</sup> *J. Chem. Educ.*, **27**, 610 (1950).

<sup>2</sup> Jones, Mysels, and Juda, *J. Am. Chem. Soc.*, **62**, 2919 (1940).

<sup>3</sup> *J. Am. Chem. Soc.*, **50**, 1049 (1928).

<sup>4</sup> *J. Am. Chem. Soc.*, **52**, 1793 (1930).

<sup>5</sup> *Rev. Sci. Instr.*, **2**, 379 (1931).

<sup>6</sup> *J. Am. Chem. Soc.*, **62**, 89 (1940).

<sup>7</sup> Andrews and Martin, *J. Am. Chem. Soc.*, **60**, 871 (1938); Schiff and Gordon, *J. Chem. Phys.*, **16**, 336 (1948).

<sup>8</sup> *J. Am. Chem. Soc.*, **53**, 411 (1931).



through capacitance-resistance paths, and these can produce variations in cell constant with resistance. The cell designed by Jones and Bollinger is shown in Fig. 123a. The Roseveare cell (Fig. 123b), with the corners of the thin platinum plates welded in the glass, is easy to make. In measuring the conductivity of solutions which show any tendency to foam, it is desirable to use a cell with conical electrodes (Fig. 123c), through which the electrolyte is flowed into the cell. The flask-type cell

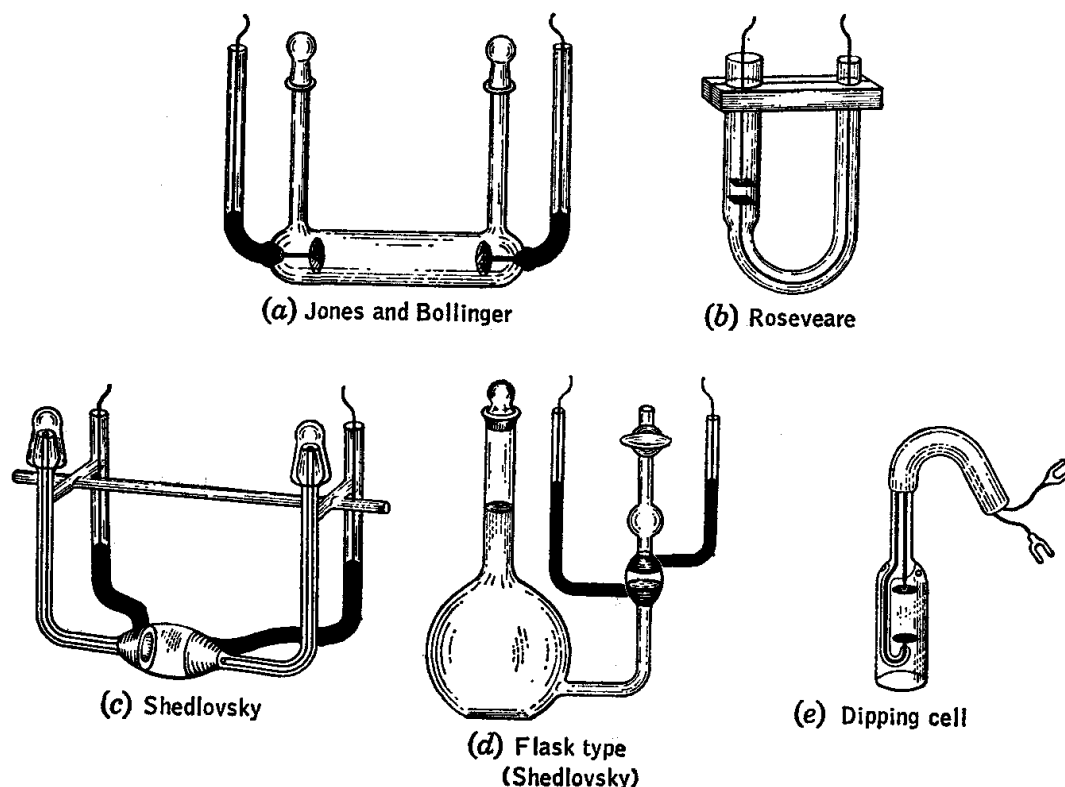


FIG. 123. Conductivity cells.

shown in Fig. 123d is useful for preparing and measuring the conductivities of very dilute solutions without risk of contamination from atmospheric or other impurities.<sup>1</sup> The dipping-type cell (Fig. 123e) is not suitable for precise measurements, but is often convenient for practical measurements. A Freas-type conductivity cell is illustrated in Fig. 38.

Polarization may be practically eliminated by using a pure-sine-wave alternating current of moderate frequency and by coating the electrodes with platinum black. The electrodes can be platinized by immersing them in a solution containing 3 g of platinic chloride and 0.02 g of lead acetate in 100 ml of water and connecting them to two dry cells connected in series. The current is regulated by means of a rheostat, so that only a small amount of gas is evolved. After the electrodes are coated with

<sup>1</sup> Shedlovsky, *J. Am. Chem. Soc.*, 54, 1411 (1932).

platinum black, they are removed from the solution and thoroughly washed with distilled water. Any traces of chlorine adsorbed from the plating solution may be removed by continuing the electrolysis, with the same connections, in a dilute solution of sulfuric acid. In precise measurements of electrical conductance, it is especially important to test for the possibility of polarization.<sup>1</sup> Polarization has the effect of increasing the measured resistance and, in general, is less important at higher frequencies.

A cell with platinized electrodes should always be filled with distilled water when stored.

For work in very dilute solutions the platinized surface must be dispensed with because it is so difficult to rinse out the last traces of electrolyte from it. Bright platinum electrodes are used, but since some polarization results, it is necessary to make measurements at several frequencies and to extrapolate the values to infinite frequency.

**Conductance of Potassium Chloride Solutions.** In a very careful and exacting research, Jones and Bradshaw<sup>2</sup> have redetermined the electrical conductance of standard potassium chloride solutions for use in the calibration of conductance cells. The results of the work are summarized in Table 1. The values given in this table do not include the conductance due to water, which must be added and should be less than  $\kappa_{H_2O} = 10^{-6} \text{ ohm}^{-1} \text{ cm}^{-1}$  in work with dilute solutions. The potassium chloride should be fused in an atmosphere of nitrogen to drive out water, and in the case of salts which are deliquescent, it is necessary to use a Richards bottling apparatus<sup>3</sup> to avoid exposure to air.

TABLE 1. SPECIFIC CONDUCTANCE OF STANDARD POTASSIUM CHLORIDE SOLUTIONS

Grams of potassium chloride per 1000 g of solution in vacuum	Specific conductance, $\text{ohms}^{-1} \text{ cm}^{-1}$		
	0°C	18°C	25°C
71.1352	0.06517 <sub>6</sub> <sup>a</sup>	0.09783 <sub>8</sub>	0.11134 <sub>2</sub>
7.41913	0.007137 <sub>9</sub>	0.011166 <sub>7</sub>	0.012856 <sub>0</sub>
0.745263	0.0007736 <sub>4</sub>	0.0012205 <sub>2</sub>	0.0014087 <sub>7</sub>

<sup>a</sup> The lowering of the last figure indicates that this figure is uncertain.

**Conductance Water.** In all conductance measurements made in aqueous solution it is necessary to have very pure water. Distillation in a seasoned glass vessel and condenser with ground-glass joints or with a block-tin condenser can give water with a specific conductance of about

<sup>1</sup> Jones and Bollinger, *J. Am. Chem. Soc.*, **57**, 280 (1935).

<sup>2</sup> *J. Am. Chem. Soc.*, **55**, 1780 (1933).

<sup>3</sup> Richards and Parker, *Proc. Am. Acad. Arts. Sci.*, **32**, 59 (1896).

$1 \times 10^{-6} \text{ ohm}^{-1} \text{ cm}^{-1}$  if a little potassium permanganate is added to the flask. If such a distillation is carried out in air, the water is saturated with the carbon dioxide of the air (0.04 per cent). Some of the dissolved carbon dioxide can be removed to give a higher resistance by bubbling carbon dioxide-free air through the water.

It is interesting to note that Kohlrausch and Heydweiller<sup>1</sup> reported the preparation of purified water with a specific conductance at 18° of only  $0.043 \times 10^{-6} \text{ ohm}^{-1} \text{ cm}^{-1}$ .

Conductance water for laboratory use may be prepared on a large scale by redistilling distilled water and condensing in a block-tin condenser. By condensing the water at relatively high temperatures, the absorption of carbon dioxide is reduced.

### MEASUREMENT OF CURRENT AND QUANTITY OF ELECTRICITY

The most direct method for the measurement of quantity of electricity involves the use of a coulometer, as, for example, a silver coulometer, in which silver is plated on a platinum crucible from a silver nitrate solution. Other coulometers have been used in which iodine is liberated from a potassium iodide solution and titrated with standard sodium thiosulfate solution, copper is deposited from an acidified copper sulfate solution, or water is decomposed and the volume of gas evolved is measured.

The most accurate and convenient method for the determination of a steady current is to measure the potential drop across a standard resistance through which the current flows, as illustrated earlier on page 26. The current is calculated by Ohm's law. When accurate resistors are required in the laboratory, calibrated resistors of the National Bureau of Standards type<sup>2</sup> should be used. These resistors are constructed of selected manganin wire and are immersed in oil. The limit of error is 0.01 per cent for wattage dissipation up to 0.1 watt and 0.04 per cent up to 1.0 watt. Since the limit of error on a good standard resistance is 0.01 per cent and the potential may be determined versus a standard cell for which the electromotive force is known to 0.01 per cent, the current may be calculated with considerable accuracy. For accurate measurements of current in transference or electrical-heating experiments, it is desirable to have rather constant current. This may be accomplished by means of a mechanical<sup>3</sup> or an electronic<sup>4</sup> current regulator.

<sup>1</sup> Kohlrausch and Holborn, "Leitvermögen der Elektrolyte," 2d ed., Teubner Verlagsgesellschaft, Leipzig (1916).

<sup>2</sup> Rosa, *J. Research, Natl. Bur. Standards (U.S.)*, **4**, 121 (1912).

<sup>3</sup> Longworth and MacInnes, *J. Opt. Soc. Am.*, **19**, 50 (1929).

<sup>4</sup> Le Roy and Gordon, *J. Chem. Phys.*, **6**, 398 (1938); Bender and Lewis, *J. Chem. Educ.*, **24**, 454 (1947).

MEASUREMENT OF ELECTRICAL ENERGY IN CALORIMETRY<sup>1</sup>

Calorimetric data are generally given in units of electrical energy. The unit is the absolute joule, the product of absolute volts, absolute amperes, and time in seconds. The 15°-calorie is 4.1840 abs joules.<sup>2</sup> With the voltage  $E$  in absolute units, the resistance  $R$  in absolute ohms, and the time in seconds, the energy dissipated is  $E^2t/R$  absolute joules, or  $E^2t/4.1840R$  defined calories. The resistance of the heater may be measured with a Wheatstone bridge, or it may be computed from the

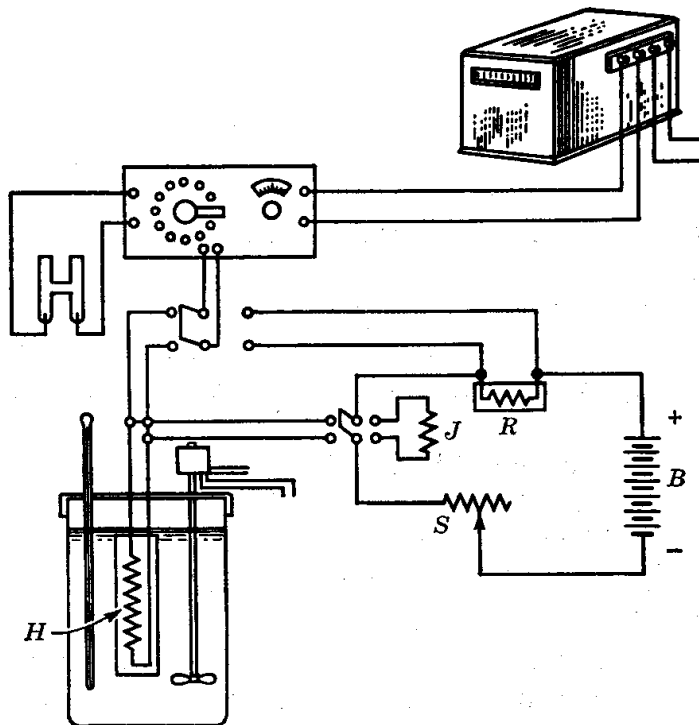


FIG. 124. Measurement of electrical energy in calorimetry.

voltage drop across the heater, and the current determined by measuring the voltage drop across a standard resistor connected in series with the resistor. Current and voltage drop are maintained at a constant value during the performance of an experiment. A basic wiring diagram is shown in Fig. 124.

The heating coil  $H$  is of manganin or other wire having a low temperature coefficient of resistance. It may be wound on mica, insulated between two mica sheets, and encased in a silver or copper sheath or made by winding resistance wire on a threaded tube of anodized aluminum.

<sup>1</sup> Sturtevant in Weissberger (ed.), *op. cit.*, Vol. I, Pt. I.

<sup>2</sup> Stimson, *Am. J. Phys.*, 23, 614 (1955).

The current is supplied by steady storage batteries  $B$  in good condition or preferably by an electronically regulated supply. The standard resistance  $R$  consists of uncovered manganin or constantan wire or other alloy having a negligible temperature coefficient of resistance. It is immersed in oil to keep the temperature nearly constant, and it should be proved that the current used in the experiment does not raise the temperature of the wire sufficiently to change its resistance. Any excessive heating effect may be reduced by using wire of larger diameter and greater length. The resistance of  $R$  should be chosen so that the potential drop across it may be conveniently measured with the potentiometer.

The potentiometer is used to measure the potential drop across the heater or across the standard resistance. It is not permissible to use a voltmeter, because the voltmeter itself carries some current and acts as a shunt around the resistance which is being measured. A voltmeter may be used, however, in a compensation method, if it is used with a galvanometer.

The upper double-pole double-throw switch connects the potentiometer either to the heating coil or to the standard resistance. It must be of good quality, with good contacts and no electrical leakage across the base.

The current is kept constant by continuous adjustment of the rheostats. It is important to have the contacts of the rheostat in good condition. They should be rubbed with emery paper frequently and coated with a thin film of petroleum jelly. Two rheostats are convenient, one for coarse adjustments and one for fine adjustments.

If plenty of batteries are available, it is well to use a large number and bring the current down with a high resistance. In this way, any slight change in the resistance of the circuit has a slight effect on the current. The circuit is closed by throwing the upper double-pole double-throw switch to the left. Before starting a determination, the lower switch is thrown to the right for several minutes so that the current will flow through a resistance  $J$  which is approximately equal to the resistance of the heating coil. In this way the battery reaches a steady condition before the experiment is started. If the switch is thrown immediately to the left from the position of open circuit, the battery voltage drops rather rapidly at first and renders difficult the control of the current at a constant amperage. The calculation is simplified and the accuracy is increased if the current is kept constant throughout the experiment.

The time of passage of the current is determined with a stop watch or an electric clock or timer. If the time, as measured with a stop watch, is the least accurate factor, a chronometer may be used, or the time may be increased by decreasing the rate of heating. Stop watches used for such

work should be checked frequently, since they are likely to get out of order.

For precision work an equipotential shield is provided to eliminate stray currents. All the instruments are set on a piece of sheet metal, which is grounded, and under every insulator is placed a grounded metal shield.

### MEASUREMENT OF TRANSFERENCE NUMBERS AND IONIC MOBILITIES<sup>1</sup>

The moving-boundary method<sup>2</sup> for the determination of transference numbers and ionic mobilities has largely replaced the earlier Hittorf

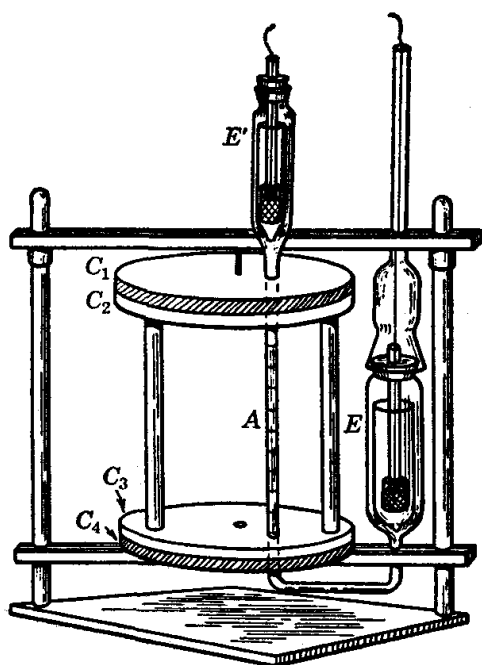


FIG. 125. Moving-boundary apparatus.

method. This has happened because the velocity of a moving boundary may be measured considerably more accurately (to  $\pm 0.02$  per cent) than the change in concentration of an ion in an electrode chamber of the Hittorf apparatus. The moving-boundary method also has the advantage that it may be applied to mixtures of ions, particularly proteins. In the moving-boundary apparatus used in Exp. 28, the anode was made of metallic cadmium, so that the solution following the moving boundary was cadmium chloride. In general, it is desirable to be able to use other salts as following electrolyte, and so there is the problem of forming an initially sharp boundary between the leading electrolyte and the following electrolyte. This is best achieved by the shearing mechanism invented by MacInnes and Brighton.<sup>3</sup> The construction of the modern apparatus is shown in Fig. 125. Heavy glass plates  $C_1$ ,  $C_2$ ,  $C_3$ , and  $C_4$  are ground so that  $C_1$  and  $C_2$ , and  $C_3$  and  $C_4$ , fit well together and rotate on each other. The moving-boundary tube  $A$  is mounted in  $C_2$  and  $C_3$ . The silver-silver chloride electrodes  $E'$  and  $E$  are attached to  $C_1$  and  $C_4$ . Electrode chambers are required to prevent products of the electrode reaction from

<sup>1</sup> Robinson and Stokes, *op. cit.*, pp. 43, 102; Spiro in Weissberger (ed.), *op. cit.*, Vol. I, Pt. IV.

<sup>2</sup> MacInnes and Longworth, *Chem. Revs.*, 11, 171 (1932).

<sup>3</sup> *J. Am. Chem. Soc.*, 47, 994 (1925).

reaching the moving-boundary cell. If the boundary is to be a rising boundary, it is formed at  $C_3$ - $C_4$  as follows. Electrode vessel  $E$  and the tube connecting it to  $C_4$  are filled with the indicator electrolyte; the glass plates  $C_1$  and  $C_2$  are clamped firmly together, and  $C_3$  is rotated with respect to  $C_4$  so that initially the tube  $A$  does not connect to electrode  $E$ . Tube  $A$  and  $E'$  are then filled with the leading electrolyte. Electrode  $E'$  is shut to the atmosphere, and  $A$  is rotated into juxtaposition with the hole in  $C_4$ , connecting  $E$ . Upon application of the current, the sharp boundary formed by this method moves up tube  $A$ . The time required for the boundary to move between graduations on  $A$  is determined. Since it is not practical to use coulometers for the measurement of current, it is desirable to hold the current constant by one of the devices mentioned on page 592 and to use a potentiometer and an accurately known resistance to measure the current.

It is necessary to apply a correction for the volume change due to the electrode reaction and to the migration of ions into and out of the region between the moving boundary and the closed electrode.<sup>1</sup>

If neither the indicator nor the leading electrolyte contains colored ions, it is necessary to locate the boundary by the difference in refractive index of the two solutions. In the case of sharp boundaries, this may be done by focusing a lens on the boundary while placing an illuminated slit behind and somewhat below the boundary. If the refractive-index gradients are not sharp, as in the case of moving protein boundaries, more complicated optical methods must be used for the determination of boundary velocity. One such method is the schlieren optical system, which is described in Chap. 19.

## MEASUREMENT OF DIELECTRIC CONSTANT

Some methods for the measurement of dielectric constant are more suitable for use in dipole-moment determinations, while others are preferred where dielectric loss is involved. Restricting the description to the former, we may classify them as heterodyne-beat methods, resonance methods, and bridge methods. The first two have been discussed to a certain extent in connection with Exps. 36 and 37. An interesting modification of resonance method has been described by Wyman<sup>2</sup> for use when the solutions under investigation have an appreciable electrical conductance.

The bridges for measurement of the dielectric constants of solutions are normally made up of two resistance arms and two capacity arms.

<sup>1</sup> Longworth, *J. Am. Chem. Soc.*, **65**, 1755 (1943); Longworth and MacInnes, *J. Am. Chem. Soc.*, **62**, 705 (1940).

<sup>2</sup> *Phys. Rev.*, **35**, 623 (1930).

By a symmetrical construction of the bridge elements, the inductance is kept to a minimum amount. One of the advantages of the bridge is that if the solution or material being studied has some slight conductance, allowances for it can be made in balancing the bridge and a loss factor determined.

The steady current flowing in a d-c circuit depends upon the magnitude of the applied potential and the resistance of the circuit. In the case of alternating current, the equilibrium current is limited by the circuit impedance  $Z$ , which depends not only on the circuit resistance  $R$ , but also on the reactance  $X$ , which arises from the capacitance and inductance in the circuit. The reactance, and hence the impedance, is a function of the frequency of the current. The phase relationships between the currents

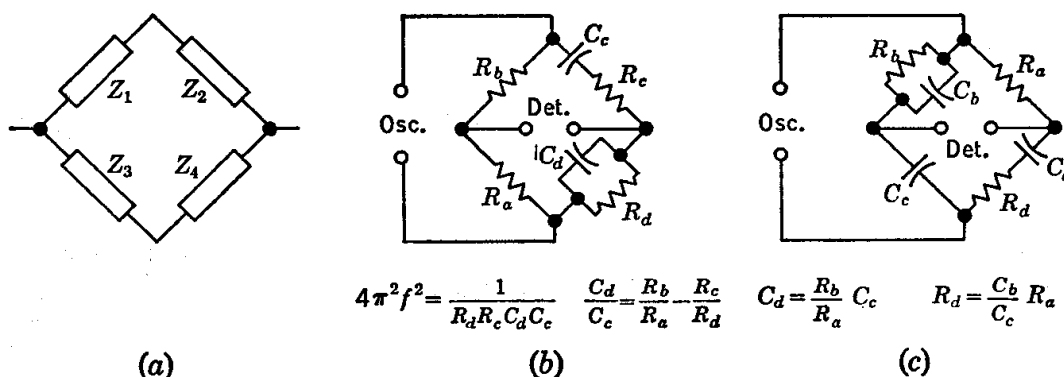


FIG. 126. (a) Generalized representation of impedance bridge; (b) Wien impedance bridge; (c) Schering impedance bridge.

and voltages in the various branches of an a-c circuit depend also upon the reactances of the components involved.

The impedance bridge is a four-terminal network of the type shown in Fig. 126a in which the arms are impedances, which will, in general, consist of some combination of resistance, capacitance, and inductance. The familiar Wheatstone bridge is a particular type of impedance bridge where all four arms are pure resistances; in a-c bridge operation this represents a limiting condition only, as indicated below. Two common forms of impedance bridge are shown in Figs. 126b and c, together with a statement of the conditions which are satisfied at bridge balance, i.e., zero voltage across the detector. These conditions are obtained from the requirements that the voltages appearing at the two points across which the detector is connected (measured relative to some common reference point) must be equal both in magnitude and in phase when the bridge is balanced. The frequency of the applied voltage may or may not enter explicitly into the balance equations.



Capacitance measurements with the impedance bridge are usually made by the substitution method. In the parallel-substitution method, a standard capacitor is connected in the bridge circuit in parallel with the unknown capacitor, and the bridge is balanced. The unknown capacitor is then removed, and the bridge again balanced by resetting the standard capacitor. The change in capacitance of the standard required to reestablish balance is then equal to the capacitance of the unknown plus any changes in lead capacitances or other stray-capacitance effects which may have been involved. The series-substitution method may also be employed. Because of these lead capacities, etc., it is desirable where possible to use a variable-capacitance cell for the measurement of dielectric constants, as described under Exps. 36 and 37, since high accuracy is thereby achieved.

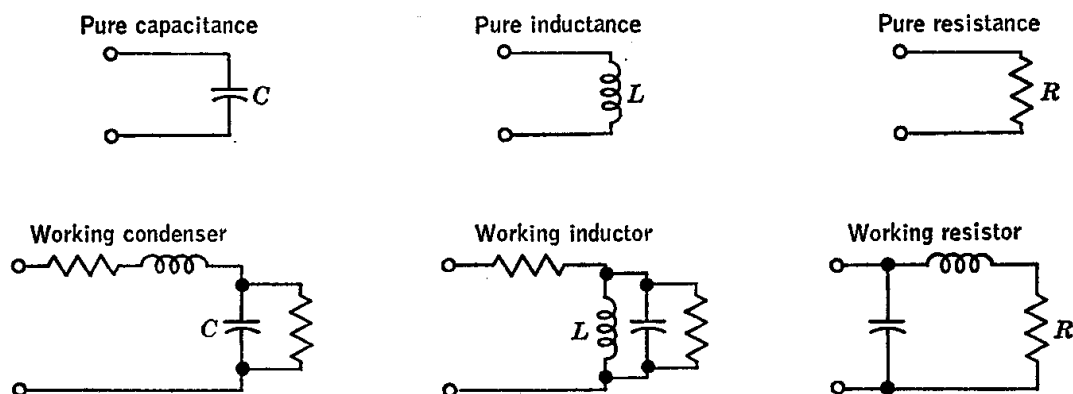


FIG. 127. Schematic representation of working circuit elements.

It is customary to think of resistances, capacitances, and inductances as separately realizable entities. In actual practice, however, it is impossible to construct a pure resistance, capacitance, or inductance. Any circuit element is an impedance in which one contribution may predominate but in which all three appear. As the operating frequency increases, this fact becomes more and more important. In Fig. 127 are given the schematic representations of capacitance, inductance, and resistance, showing to a first approximation how each of these circuit elements behaves in an a-c circuit.

Careful attention to proper shielding and grounding of the bridge is required in order to prevent the environment, including the operator, from influencing the performance of the bridge. Successful work, particularly at high frequencies, requires a sound understanding of the theory of a-c bridge circuits, which is treated comprehensively by Hague<sup>1</sup>

<sup>1</sup> "Alternating Current Bridge Methods," 5th ed., Sir Isaac Pitman & Sons, Ltd., London (1945).

and by Hartshorn,<sup>1</sup> and a good background of practical experience in the field.

The power source for the bridge must have adequate frequency stability and power output. At audiofrequencies the resistance-capacitance-coupled oscillator mentioned above is a versatile and reliable unit. At radiofrequencies, crystal-controlled oscillators or stable variable-frequency oscillators of several types are available. Suitable power sources in practically any frequency range are available from commercial manufacturers.

**Measurements at Very High Frequencies.** At frequencies in excess of  $10^8$  cycles the difficulties encountered in working with the traditional circuits become very great. There is the frequency range  $10^8$  to  $3 \times 10^9$  cycles/sec, in which the measuring techniques are still rather unsatisfactory, and there is the microwave region,  $3 \times 10^9$  to  $6 \times 10^{10}$  cycles/sec, that portion of the frequency spectrum in which the free-space wavelength corresponding to the frequency of oscillation is comparable in magnitude with that of the laboratory equipment. A large variety of satisfactory equipment has now been developed for use at the microwave frequencies, and the precautions which are required in order to obtain accurate measurements have been set down. These methods of measurement of dielectric constant are classed as being resonator methods or transmission methods; both depend on the transmission properties of a dielectric-filled waveguide or coaxial line. (A resonator can be considered as a length of waveguide short-circuited at both ends.) The technique and equipment employed in such work have been described in a number of places, including text and reference works.<sup>2</sup>

<sup>1</sup> "Radio-frequency Measurements by Bridge and Resonance Methods," John Wiley & Sons, Inc., New York (1941).

<sup>2</sup> Roberts and von Hippel, *J. Appl. Phys.*, **17**, 610 (1946); Collie, Hasted, and Ritson, *Proc. Phys. Soc. (London)*, **60**, 71 (1948); Barlow and Cullen, "Microwave Measurements," Constable & Co., Ltd., London (1950); Montgomery (ed.), "Technique of Microwave Measurements," Radiation Laboratory Series, Vol. 11, McGraw-Hill Book Company, Inc., New York (1948).

## *Nuclear and Radiation Chemistry*<sup>1</sup>

### AVAILABILITY OF ISOTOPES

For the 102 elements which are now known, over 600 isotopes are known.<sup>2</sup> Isotopes of an element have different mass numbers (i.e., total number of neutrons and protons in the nucleus) but the same atomic number (i.e., number of protons in the nucleus). The nuclei of most of these isotopes are unstable and decay with the emission of  $\alpha$  particles,  $\beta$  particles,  $\gamma$  rays, or positrons, which can be detected with instruments discussed in this chapter. The relative concentrations of stable isotopes may be determined by mass spectrometry, spectroscopy, nuclear magnetic resonance, and other methods to be mentioned.

Research involving isotopes has been greatly accelerated by the increased availability of radioisotopes and stable isotopes from the U.S. Atomic Energy Commission, the Atomic Energy Commission of Canada, and similar agencies of other nations. A number of radioisotopes which do not occur naturally have been made available in large quantities by the operation of uranium nuclear reactors which produce neutrons in high concentrations. A great variety is available at nominal prices in quantities of fractions of a millicurie to several curies. (A curie

<sup>1</sup> General references include the following: Calvin, Heidelberger, Reid, Tolbert, and Yankwich, "Isotopic Carbon," John Wiley & Sons, Inc., New York (1959); Glasstone, "Sourcebook on Atomic Energy," D. Van Nostrand Co., Inc., Princeton, N.J. (1950); Friedlander and Kennedy, "Nuclear and Radiochemistry," John Wiley & Sons, Inc., New York (1955); Hollaender (ed.), "Radiation Biology," Vol. 1, McGraw-Hill Book Company, Inc., New York (1954); Wahl and Bonner, "Radioactivity Applied to Chemistry," John Wiley & Sons, Inc., New York (1951); Overman and Clark, "Radioisotope Techniques," McGraw-Hill Book Company, Inc., New York (1960); Price, "Nuclear Radiation Detection," McGraw-Hill Book Company, Inc., New York (1958); Washtell, "Radiation Counters and Detectors," Philosophical Library, Inc., New York (1960).

<sup>2</sup> Tabulated information on various nuclei is available in *Nuclear Data, Nat. Bur. Standards (U.S.), Circ., 499* (1950). Various Supplements have been issued, and now nuclear-data sheets may be obtained on subscription from the National Academy of Science-National Research Council, Washington, D.C. In these sheets new data from the literature are "cumulated" with old data.

is the quantity of a radioisotope that supplies  $3.7 \times 10^{10}$  disintegrations per second.) Catalogues, price lists, and application blanks can be obtained from the U.S. Atomic Energy Commission, Isotopes Division, Oak Ridge, Tenn. A prospective purchaser of isotopes must state that he is equipped to handle them, that his monitoring instruments are properly calibrated, that he will take adequate precautions in the handling of waste materials, and that he will accept legal responsibility for any damage from radioactivity.

Many organic and inorganic compounds which have been synthesized with radioactive elements for use in tracer experiments are commercially available.

Radioisotopes may be formed by  $(n,\alpha)$ ,  $(n,p)$ , and  $(n,\gamma)$  reactions in uranium nuclear reactors in which neutrons are absorbed and  $\alpha$  particles, protons, or  $\gamma$  rays are emitted. Production of these isotopes involves the insertion of an element, often in the form of a chemical compound, contained in a small aluminum container, into the nuclear reactor for a few days or months. Important examples of isotopes made in this way are  $C^{14}$ ,  $I^{131}$ ,  $P^{32}$ ,  $Br^{82}$ , and  $Fe^{59}$ .

Isotopes may be obtained also by separation from other fission products produced in a nuclear reactor.

Stable isotopes including  $H^2$ ,  $B^{10}$ ,  $O^{18}$ ,  $Hg^{198}$ ,  $C^{13}$ ,  $N^{15}$ , and a number of metals in concentrated form are available.

Deuterium oxide is produced on a large scale by use of exchange reactions carried out with solid catalysts in a column operation for the first stages of separation. In the later stages of purification fractional distillation and electrolysis are used. Nitrogen 15 is concentrated by the passage of ammonia gas upward through a packed tower, down which a stream of ammonium chloride solution is passing.<sup>1</sup>

The isotopes of a number of metals have been separated electromagnetically (that is, by use of large mass spectrometers designed for the purpose) and are available from the U.S. Atomic Energy Commission on a loan basis.

## ANALYSIS FOR STABLE ISOTOPES

**Mass Spectrometry.**<sup>2</sup> In a mass spectrometer ions in the gas phase are accelerated by an electric field and passed through a magnetic field to separate the ions according to their mass-to-charge ratio. A gas to be studied is ionized by bombarding it with electrons which have been accelerated by a potential difference of 50 to 100 volts. Solids may be

<sup>1</sup> Thode and Urey, *J. Chem. Phys.*, 7, 34 (1939); Hutchison, Stewart, and Urey, *J. Chem. Phys.*, 8, 532 (1940).

<sup>2</sup> Robertson, "Mass Spectrometry," John Wiley & Sons, Inc., New York (1954).

used if they are first vaporized with a hot filament. The type of mass spectrometer designed by Nier<sup>1</sup> is illustrated in Fig. 128. The glass tube, containing an ion source at one end and an ion collector at the other, is evacuated with a diffusion pump. It must be heated before it is used in order to drive out traces of adsorbed water and gases. The ions to be studied are accelerated by a potential of from 800 to 1000 volts, and the ion paths are bent by the field of an electromagnet (about 3500 gauss). The ion current at the collector is amplified and recorded automatically.

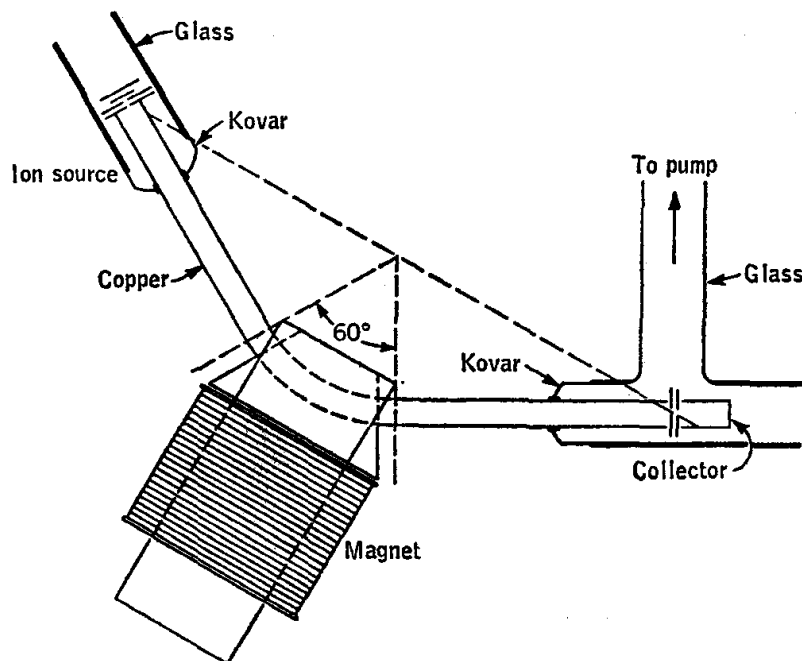


FIG. 128. Nier mass spectrometer.

Mass spectrometers are finding extensive use for the analysis of organic mixtures as well as isotope ratios.

#### ANALYSIS FOR RADIOACTIVE ISOTOPES

**Ionization Chambers.** In an ionization chamber a low voltage is applied across two electrodes, usually a wire at a positive potential and a coaxial cylinder at a negative potential. If a source of radiation is brought into the vicinity of the ionization chamber, ions are produced in the gas in the chamber, and these ions are attracted to the electrodes. As the potential difference between the wire and the cylinder is increased, the current increases because more gaseous ions are drawn to the electrodes before they have a chance to recombine. Eventually a saturation

<sup>1</sup> *Rev. Sci. Instr.*, **11**, 212 (1940).

current is reached because all the electrons and gas ions produced by the radiation are drawn to the electrodes. This plateau, or "saturation," region is shown by  $BC$  and  $B'C'$  in Fig. 129. The saturation current produced by  $\alpha$  particles is greater than that produced by the same number of  $\beta$  particles of approximately the same energy. Because of their greater

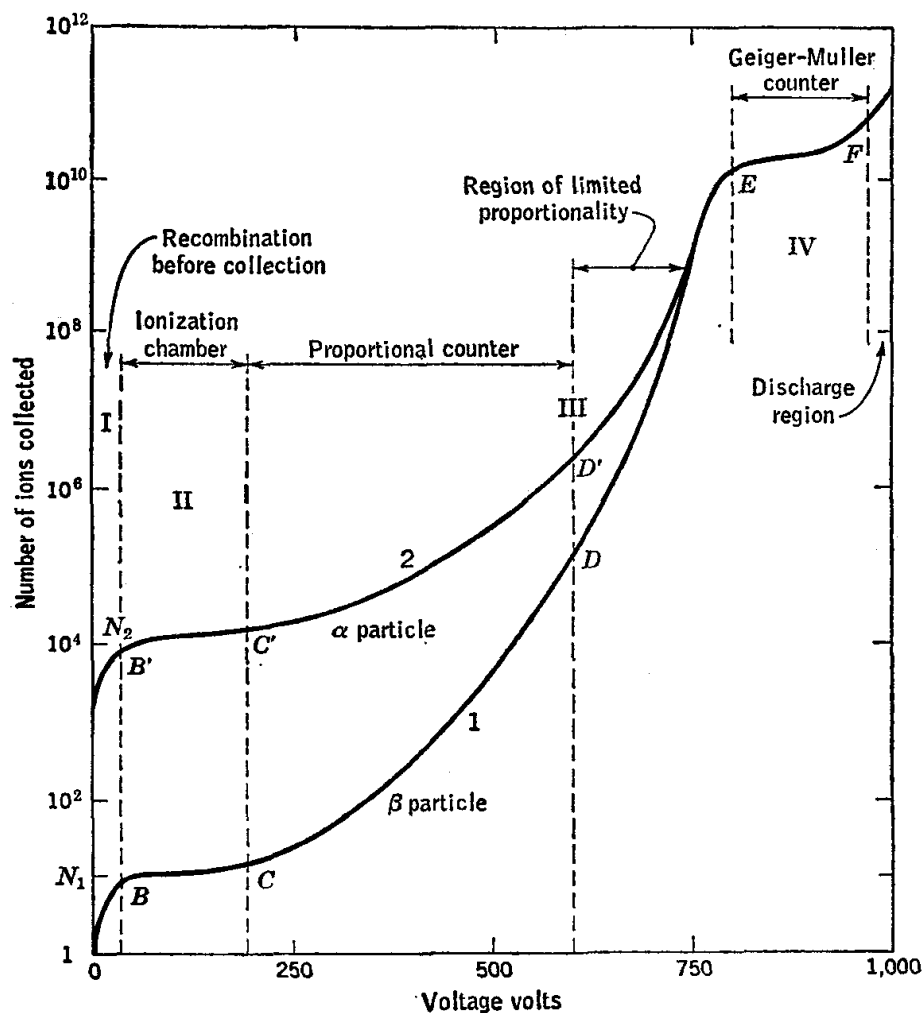


FIG. 129. Curves of pulse height versus applied voltage to illustrate ionization, proportional, and Geiger-Müller regions of operation. Adapted from Montgomery and Montgomery [*J. Franklin Inst.*, **231**, 447 (1941)] by Overman and Clark, in "Radioisotope Techniques," p. 27, McGraw-Hill Book Co., Inc., New York (1960).

range,  $\beta$  particles may not expend all their energy within the chamber, but may pass on through, while the  $\alpha$  particles all come to rest in the chamber.

The current produced in an ionization chamber is typically of the order of  $10^{-17}$  amp. Such small currents may be measured using electrometer tubes or a vibrating-reed electrometer. In this latter device a metallic reed is driven at a fixed frequency, such as 400 cycles/sec, and

an alternating current is obtained from the ionization current. This signal is amplified by an a-c amplifier.

Ionization chambers are especially useful for  $\alpha$  particles which produce a large specific ionization. Since the range of  $\alpha$  particles is low, the sample is usually placed inside the chamber.

The Lauritsen quartz-fiber electroscop shown in Fig. 130 is an example of an integrating type of ionization chamber. The sensitive element is a metallized quartz fiber (about  $3 \times 10^{-4}$  cm in diameter) mounted parallel to a metal repelling post. At the free end of the quartz fiber a short quartz segment is attached at right angles, and it is this segment which is observed with the microscope, as illustrated in Fig. 130. The quartz fiber and repelling post are charged to a potential of several hundred volts

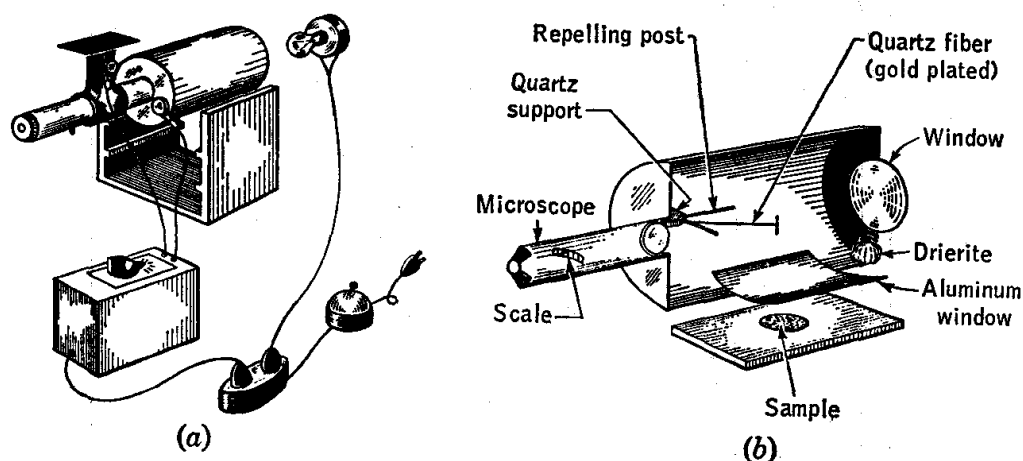


FIG. 130. (a) Lauritsen electroscop; (b) quartz fiber in electroscop.

with a small rectifier or friction charger. The ionization current is determined as the rate of loss of charge from the electroscop measured by the rate of movement of the quartz fiber over a scale. It is characteristic of this type of electroscop that the rate of movement of the fiber is not the same in all parts of the scale. For this reason the rate of movement of the fiber is determined at different positions on the scale, using a sample of constant radioactivity. A plot of the rate of movement of the fiber versus position on the scale will be nearly horizontal in one region, and quantitative measurements of radioactivity are limited to this plateau. A thin aluminum window having a weight of about  $5 \text{ mg cm}^{-2}$  allows a large fraction of the  $\beta$  particles to enter the electroscop chamber. A thin plastic window is required for work with low-energy  $\beta$  and high-energy  $\alpha$  rays. It has been found that reproducibility is increased by keeping the inside of the electroscop dry by inclusion of a small bag of Drierite and by discharging the electroscop two or three times, by means of a fairly strong sample, before use.

The sensitivity of a Lauritsen electroscope is such that 1 millicurie of radium at a distance of 1 m produces a movement of 2 to 5 scale divisions per minute. The background due to cosmic rays and low levels of natural radioactivity in the laboratory is approximately 3 scale divisions per hour. The electroscope is in general about one-tenth as sensitive as a Geiger-Müller counter, but when weak  $\beta$  emitters are counted inside the electroscope, the sensitivity is about the same as that of a Geiger-Müller counter.

**Proportional Counters.** As the voltage between a positive wire and the negative coaxial cylinder is increased above that required to collect all the ions produced by radiation, the current again increases, as shown in Fig. 129. The primary ions are accelerated sufficiently in the field of the center electrode so that they produce secondary ionization by their interaction with gas molecules. The electrons must be accelerated sufficiently between collisions so that their kinetic energy becomes greater than the ionization potential of the gas. The increase in current is approximately proportional to the applied voltage, and so the region  $CD$  or  $C'D'$  is called the proportional region. As seen from the figure, the amplification achieved in a proportional counter is of the order of  $10^3$  or  $10^4$ . In this region the number of ions collected for an  $\alpha$  particle and a  $\beta$  particle remains different, as in the ionization-chamber region. In a proportional counter the discharge due to a single ionizing particle is localized to a small portion of the tube. The discharge stops when all the electrons produced are swept to the collector. Very high counting rates may be used compared with Geiger-Müller counters. Windowless proportional counters in which methane or other counting gas flows continuously through the tube are widely used for determining alpha and weak beta activities.

The voltage required for a proportional counter ranges from several hundred to several thousand volts, depending upon the pressure and ionization potential of the gas used and the geometry of the counter. A very stable high-voltage supply is required for a proportional counter since the number of ions collected per ionizing particle depends markedly upon the voltage. As the voltage is raised above the proportional region, the strict proportionality between voltage and amount of charge collected is lost as shown by Fig. 129.

**Geiger-Müller Counters.** In the Geiger-Müller region  $EF$ , the electric field strength in the vicinity of the positively charged wire in the center of the coaxial conducting tube becomes so high that the ionization becomes a chain reaction, and an "avalanche" of ions is produced by each particle of radiation. In this region an  $\alpha$  particle and a  $\beta$  particle give rise to the same number of ions collected at the electrode. Therefore Geiger-Müller counters cannot be used to distinguish between radiations



of different energies. In contrast to the proportional region, the discharge covers the entire length of the central wire. There is a danger that multiple pulses may arise from the radiation emitted by the ions as they collect electrons from the wall in becoming neutral atoms again.

This is prevented by adding an organic quenching gas which dissociates in absorbing the de-excitation radiation. This type of Geiger-Müller tube eventually wears out because the quenching gas is used up. As seen in Fig. 129, the gas amplification factor is of the order of  $10^6$  to  $10^9$ .

One of the problems with Geiger-Müller counters is that, although the collection time for electrons is of the order of a microsecond, the collection time for positive ions is of the order of several hundred microseconds. During this time the tube is inoperative, and an ionizing particle coming in this dead time will not be counted. A correction for such coincidence losses may be made<sup>1</sup> if the resolving time of the tube and electronic circuit is known. Much faster disintegration rates may be measured with proportional counters because their resolving times are in the range 0.01 to 0.01  $\mu\text{sec}$ .

Since Geiger-Müller counters must have windows, it is difficult to count very weak  $\beta$  rays. Gamma rays cannot be counted very successfully because their probability of being absorbed in the counter gas, often argon, is low.

**Scintillation Counters.**<sup>2</sup> When ionizing radiation is absorbed by matter, electrons are ejected from atoms and molecules, and light may be emitted as electrons return to the vacated energy levels. This radiation

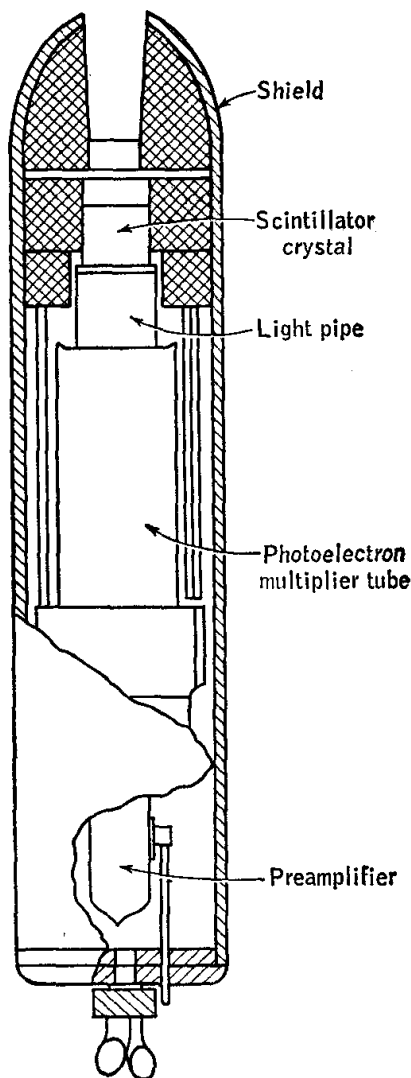


FIG. 131. Schematic diagram of probe type of scintillation detector.

may be detected with a photomultiplier tube as illustrated in Fig. 131. In the absorption of a  $\gamma$  ray, a quantum of energy is transferred to an electron as kinetic energy. This energetic electron loses its excess energy in a series of interactions with atoms and molecules. Thus a

<sup>1</sup> Overman and Clarke, *op. cit.*, p. 55.

<sup>2</sup> Birks, "Scintillation Counters," McGraw-Hill Book Company, Inc., New York (1953).

single  $\gamma$ -ray photon gives rise to many photons, and the amount of light produced is proportional to the energy of the radiation. Scintillation counters are widely used for  $\gamma$  rays because they have a high sensitivity. Gas-filled counters have a low sensitivity for  $\gamma$  rays since the probability that a  $\gamma$  ray will be absorbed in a small volume of gas is low. The use of pulse-height analyzers with scintillation detectors makes possible the separate determination of  $\gamma$  rays of different energy in the same sample.

Certain organic or inorganic solids or organic liquids emit light when irradiated and may therefore be used in scintillation counters. Sodium iodide with a trace of thallium as an excitant is widely used for high-efficiency  $\gamma$ -ray detection because of its high density, high light output, and high transparency. Since NaI is hygroscopic, the crystal is encased in a water-tight metallic shell. For beta counting, anthracene and stilbene crystals are often used. For the detection of weak beta radiation, the sample to be measured may be dissolved in a liquid-scintillator solution. The scintillator, such as *p*-terphenyl, may be dissolved in a solvent, such as benzene or toluene. When  $C^{14}$  and  $H^3$  are counted in this way, the pulses from the low-energy beta radiation are so small that they may be in the range of the random noise from the photomultiplier tube. This thermal noise is reduced by cooling the photomultiplier tube.

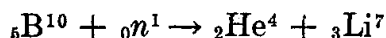
The decay period for NaI (activated by Tl) is  $3 \times 10^{-7}$  sec, and the decay periods for the organic phosphors which are used are 10 to 100 times shorter. Thus if the associated electronic equipment does not introduce appreciable delay, high counting rates may be handled without significant coincidence losses.

A scintillation counter may be used in conjunction with a pulse-height analyzer to determine the energy spectrum of  $\gamma$  rays. In a single-channel analyzer only those pulses falling in a certain voltage range are counted. In more complex instruments there are a number of channels, so that pulses in different energy ranges may be counted simultaneously. In addition to the sharp peak in the plot of number of particles versus energy which is due to the ejection of a photoelectron by the  $\gamma$  ray, there is also Compton scattering of the  $\gamma$ -ray photons. The Compton scattering results in a broad region of pulse heights at lower energies.

**Solid-state Detectors.** Various crystals have been used for the detection of radiation by coating opposite faces with electrodes and measuring the conductivity by use of special circuits. Since the crystals are insulators, no appreciable current flows in the absence of ionizing radiation. When ionizing radiation is absorbed by the crystal, electrons are raised to the conduction band and positive holes are left in the valence band. Under the influence of an applied electric field, the electrons and holes drift through the crystal, and the current is measured in the external circuit. These detectors have the advantage of (a) high stopping power,

so that high-energy particles may be detected with small detectors, (b) proportionality between absorbed particle energy and pulse height, and (c) fast rise times so that high counting rates may be used.

**Neutron Counters.** Neutrons may be detected by use of the  $(n, \alpha)$  reaction



The  $\alpha$  particle and lithium nucleus have a total kinetic energy of 2.78 Mev and produce ionization which may be detected by use of an ionization chamber, proportional counter, or scintillation detector. The  $\text{B}^{10}$  is available in its isotopic form and may be placed in the detector as  $\text{BF}_3$  or as a thin coating of boron on the inside of the counter chamber.

Neutrons may also be detected by the determination of the proton,  $\gamma$  ray, or fission products produced in  $(n, p)$ ,  $(n, \gamma)$ , and  $(n, \text{fission})$  reactions. Since the probabilities of different reactions depend in different ways upon the neutron energies, different reactions are useful for determining fast and slow neutrons. Neutrons may also be detected by the radioactivity of fission products in a counter containing uranium. The fissionable material is usually incorporated into the chamber in the form of a thin film or a multiple-plate construction. In such counters use is made of the kinetic energy of the fission products or of their resulting radioactivity.

**Miscellaneous Methods.** When a particle passes through matter at a velocity which is greater than the speed of light in the medium, the particle is decelerated and radiation is emitted. The first detailed study of the visible light emitted was made by Cerenkov. The Cerenkov radiation is analogous to the bow wave of a ship which is moving faster than the velocity of surface waves, or to the shock wave produced by an object moving through air at a supersonic velocity. The radiation may be detected by use of photomultiplier tubes. For the detection of single particles, special techniques are required, since the intensity is low. For example, only 250 photons of visible light is produced per centimeter of path by an electron traveling through Lucite at nearly the speed of light.

Ionizing radiation produces latent images in photographic plates. When the plate is developed, grains of silver appear along the tracks of particles.<sup>1</sup> By study of these paths and the records of various types of collisions, nuclear physicists obtain detailed information about mass, charge, and energy of the particles. Special nuclear emulsions have been developed for this type of work, since ordinary emulsions are not suitable.

<sup>1</sup>Yogada, "Radioactive Measurements with Nuclear Emulsions," John Wiley & Sons, Inc., New York (1949).

The general blackening of a photographic plate may be used to measure the integrated intensity of radiation, as in a film badge for radiation safety. The location of radioactivity in a sample may be determined by laying the sample on a photographic plate in the dark (radioautography). For example, the location of radioactive compounds on a filter-paper chromatogram or the location of radioactive phosphorus in a leaf may be determined. If the intensity of radiation is weak, long times may be used.

Ionizing particles may also be detected by use of cloud chambers and bubble chambers. In a bubble chamber the pressure on a liquid is suddenly reduced to a value below the vapor pressure. Under these circumstances ionizing radiation produces nuclei for the formation of bubbles, and these small bubbles are photographed. Bubble chambers containing liquid hydrogen are especially useful for studying the particles produced with high-energy accelerators.

## RADIATION CHEMISTRY

Convenient sources of high intensities of gamma radiation are available for the study of the chemical changes which occur when  $\gamma$  rays are absorbed by matter. Radioactive  $\text{Co}^{60}$  is available, from the Oak Ridge National Laboratory or from Atomic Energy of Canada Limited, in the form of slugs of cobalt metal with activities up to about 50 curies. These sources require special housings to make them safe and convenient to use.<sup>1</sup> Unseparated fission products from nuclear reactors may also be used as high-intensity-radiation sources. The fission products are simply used in the form of spent fuel elements.<sup>2</sup>

**Radiation Safety.**<sup>3</sup> The safe handling of radioactive material and the proper disposal or storage of waste are required in any laboratory investigations using radioactive isotopes.<sup>4</sup> Many excellent instruments are now on the market for monitoring laboratories and personnel. Photographic film badges, pocket meters, and portable instruments for detecting and measuring  $\alpha$ ,  $\beta$ , and  $\gamma$  rays are available.

<sup>1</sup> Firestone and Daniels, *Rev. Sci. Instr.*, **24**, 904 (1953); Schwarz and Allen, *Nucleonics*, **12**, 58 (1954); Eastwood, *Nucleonics*, **13**, 52 (1955).

<sup>2</sup> Loeding, Petkus, Yasui, and Rodger, *Nucleonics*, **12**, 14 (1954).

<sup>3</sup> Claus, "Radiation Biology and Medicine," Addison-Wesley Publishing Company, Reading, Mass. (1958).

<sup>4</sup> "Safe Handling of Radioactive Isotopes," Natl. Bur. Standards (U.S.), Handbook 42; "Maximum Permissible Amounts of Radioactive Isotopes in the Human Body and Maximum Permissible Concentrations in Air and Water," Natl. Bur. Standards (U.S.), Handbook 52; "Permissible Dose from External Sources of Ionizing Radiation," Natl. Bur. Standards (U.S.), Handbook 59.

In general, it may be stated that for laboratory work, the exposure of the body to 0.1 roentgen per week is the maximum dosage which is permitted. However, the detailed specification<sup>1</sup> of exposure limits is complicated and depends upon the type of radiation, the part of the body exposed, the possibility of getting the material in the body, etc.

<sup>1</sup> "Standards for Protection against Radiation," U.S. Atomic Energy Commission, 1958.

## *Purification of Materials*

In many experiments, the factor which limits the accuracy of the results is the purity of the materials used rather than the refinement of the measurements. For example, nothing is gained by determining the refractive index of a liquid to five decimal places if it contains an impurity in amount sufficient to alter the refractive index in the third decimal place.

The need for chemicals of both high purity and established purity is great, and it extends to all branches of sciences. The U.S. National Bureau of Standards has been active in this field, and it now supplies some materials of high purity and provides other services such as standards of purity and descriptions of methods of purification. It is hoped that these services will be expanded. Many of the chemical companies supply chemicals of specified purity, and a committee of the American Chemical Society establishes standards of purity. The Johnson-Mathey Co. specializes in inorganic chemicals of high purity as determined spectroscopically. Some pure hydrocarbons are available from the Phillips Petroleum Company as "research grade" products whose purity has been established by the freezing-point method.

The degree of purity required depends on the material to be investigated, the use which is to be made of it, and the nature of the impurities. The different classes of chemical substances include (a) elements, including selected isotopes; (b) organic compounds, including hydrocarbons and derivatives such as alcohols, amines, and biologically important materials such as carbohydrates and proteins; (c) inorganic materials, including halides, oxides, acids, salts; semiconductors and phosphors; and (d) single crystals.

The level of attainable purity varies greatly. For example, 90 per cent purity is sufficient for some types of experiments, but 99.999 is required for some metals and organic substances and "nine nines" for certain components in semiconductors.

There are many techniques for purifying materials, including the following:

Absorption	Fractional distillation
Adsorption	Gas-liquid chromatography
Countercurrent distribution	Precipitation
Crystallization	Sedimentation
Distillation	Single-crystal growth
Electrolysis	Sublimation
Electrophoresis	Zone melting
Extraction	

The following are some of the means which can be used as criteria of purity and sometimes as quantitative measures of the amounts of impurities:

Absorption spectra	Magnetic properties
Bioassays	Neutron activation
Boiling points	Radioactivity
Electrical conductance	Refractive index
Emission spectra	Stoichiometry
Freezing points	Viscosity
Heats of reaction and phase change	X-ray spectra
Infrared absorption	

**Methods.** Considerable technical knowledge and laboratory skill are required for the proper purification of materials for precision measurements. A knowledge of the origin of the starting material is important, since it will suggest the identity of the probable impurities and thus influence the procedure adopted. For example, benzene from petroleum sources invariably contains thiophene and other sulfur compounds. Since these contaminants are more rapidly sulfonated than benzene, they can be removed by shaking the benzene repeatedly with small portions of concentrated sulfuric acid. Another example is provided by commercial "absolute" alcohol, which usually contains traces of benzene introduced in the removal of water from the alcohol by an azeotropic-distillation step (see below).

Purification procedures in general involve both chemical and physical processes. The chemical steps are specifically characteristic of the compounds involved. The physical procedures utilized will be selected most often from among the following processes.

*Crystallization.* One of the best methods of purification available is a series of fractional-crystallization steps. The impurities present must not form solid solutions with the compound being purified. When materials with low freezing points are treated, precautions must be taken to protect them from condensing atmospheric moisture.

*Fractional Distillation.* This is probably the most common procedure used for the purification of liquids. A very efficient distillation column

is required when the boiling points of the impurities are close to that of the major constituent. Azeotropic solutions, because of their constant boiling points at constant pressure, have often been mistaken for pure components. It should be recognized that fractional distillation is routinely and unimaginatively used in many cases when a better result could be obtained by fractional crystallization or other methods.

*Azeotropic Distillation.* Here advantage is taken of the formation of an azeotropic mixture involving an impurity to facilitate purification by fractional distillation. In the production of commercial absolute alcohol, benzene is added to the 95 per cent azeotrope of ethanol and water obtained by ordinary distillation. A ternary azeotrope of water, ethanol, and benzene can then be fractionated out to remove the water present. Further distillation removes the benzene in a binary azeotrope with ethanol and leaves essentially anhydrous ethanol contaminated with traces of benzene.

*Adsorption.* The selectivity shown in adsorption processes (illustrated in Exp. 46) can result in remarkably effective separations which are extremely difficult to obtain by other methods. A recent advance has been the development of vapor-phase chromatography.<sup>1</sup> Vapor-phase chromatography is similar to partition chromatography, the moving liquid phase being replaced by a gas phase. A column, which is usually heated, is filled with a packing such as diatomaceous earth moistened with a nonvolatile oil. A flow of helium gas is used to force the sample to be analyzed through the column. The rates at which various components of a mixture travel the length of the column depend upon the distribution of that substance between the condensed solution and gas phase.

*Drying.* It will commonly be found that the adequate elimination of water from a sample constitutes one of the most difficult problems in the whole purification process. The method of drying employed is determined primarily by the chemical properties of the material. If the product is not used immediately, care must be taken to prevent its recontamination by absorption of atmospheric moisture. Because of its low molecular weight, polar character, and chemical reactivity, relatively small amounts of water can be very troublesome. Heating at elevated temperatures until further heating gives no decrease in weight is often used for drying solids. Frequently a liquid can be freed from water by shaking with a drying agent such as anhydrous calcium chloride or phosphorus pentoxide. Both solids and liquids are often dried by keep-

<sup>1</sup> James and Martin, *Biochem. J.*, **50**, 679 (1952); Ray, *J. Appl. Chem.*, **4**, 21 (1954); Patton, Lewis, and Kaye, *Anal. Chem.*, **27**, 170 (1955); see also *Chem. Eng. News*, **34**, 1692 (1956).



ing them in a desiccator, for long periods of time, over sulfuric acid or other drying agent.

**Zone Refining.**<sup>1</sup> The requirements for very high purity of solids used in transistors and similar electronic instruments have led to the perfection of purification by zone melting. A long tube of the frozen solid is melted at one end by a narrow, movable electrical heating unit which melts the material in a narrow disc. The heating coil is moved slowly along the tube, and the melted zone which contains the impurities also moves along the tube, collecting more impurities as it goes. In this way the impurities are displaced to one end. The process is repeated several times.

**Criteria of Purity.** One of the best criteria available for organic compounds is the constancy of the freezing point or melting point throughout the phase transition.<sup>2</sup> If a liquid is impure, the impurities will become concentrated in the liquid phase as the solid separates out; the freezing point thus is gradually lowered. If the liquid phase can be treated as an ideal solution, an assumption of adequate validity in many cases, and if no solid solutions are formed, the amount of impurity can be calculated with fair accuracy from the shape of the freezing or melting curve. Since high sensitivity is required in the temperature measurements, a platinum resistance thermometer or multiple-junction thermocouple is used.

Comparison of the normal boiling point, refractive index, etc., with the accepted values for the compound concerned is often used to estimate its purity. A valuable reference tabulation of physical constants of organic compounds has been prepared by Timmermans.<sup>3</sup> Unfortunately, the reference data available are often of inadequate accuracy; the objective evaluation of purity furnished by the freezing-point method is hence much to be preferred in critical cases.

It is important to know the identity as well as the mole fraction of impurity present, in order to judge its effect on the measurements to be made. In addition, direct determination of the important contaminants may be possible through standard analytical procedures.

Spectrographic and polarographic analyses are used for testing for traces of impurities, and standard colorimetric and precipitation tests are available also. Infrared-absorption spectra are widely used.

<sup>1</sup> Pfann, "Zone Melting," John Wiley & Sons, Inc., New York (1958).

<sup>2</sup> White, *J. Phys. Chem.*, **23**, 393 (1920); Skau, *J. Phys. Chem.*, **37**, 609 (1933); Glasgow, Streiff, and Rossini, *J. Research, Natl. Bur. Standards (U.S.)*, **35**, 355 (1945); Sturtevant in Weissberger (ed.): "Physical Methods of Organic Chemistry," 3d ed., Vol. I, Pt. I, Chap. 10 (1959).

<sup>3</sup> "Physico-chemical Constants of Pure Organic Compounds," Elsevier Press, Inc., Houston, Tex. (1950).

**Water.** Ordinary distilled water is sufficiently pure for most work in physical chemistry, but for some applications, such as conductance measurements, it is necessary to use specially redistilled water.

Steam is generated from a dilute alkaline permanganate solution in a quartz or heavily tinned copper boiler and is partially condensed in a quartz or block-tin condenser. The escaping steam carries off gases evolved by the boiling liquid and prevents exposure of the condensate to the laboratory air. The condensate is collected in a quartz or tinned copper reservoir under air which has been treated to remove carbon dioxide, ammonia, etc. Polyethylene bottles can also be used for storage of water to prevent its contamination by impurities dissolved from glass bottles.

**Mercury.** It is assumed that reasonably pure mercury is available as starting material. A preliminary treatment is first necessary to remove oxidizable contaminants such as zinc, lead, etc. A pinhole is made at the apex of a dry-filter-paper cone placed in a dry funnel. Mercury is poured into the filter and collected in a glass filter flask of such a size that a layer 1 or 2 in. deep results. A 10 per cent solution of nitric acid, to which some mercurous nitrate has been added, is poured over the mercury to a depth of several inches. Into the neck of the flask is fitted a rubber stopper through which proceeds a glass tube drawn down to a diameter of about 1 mm at the lower end, which should extend well under the surface of the mercury. The sidearm of the flask is connected to a water aspirator, and a slow stream of air bubbled through the mercury for several days. A filter should be placed in the air line to prevent drawing dust from the laboratory into the mercury.

The mercury is then washed with distilled water and dried. It should again be run through a pinhole in a filter to eliminate surface scum, and is then transferred to a still and distilled under vacuum. A satisfactory still design is shown in Fig. 132; an automatic still of this type has been described by Cannon.<sup>1</sup> It is preferable to check the purity of the product by spectrographic analysis, since several distillations may be required to achieve the desired result. The danger of mercury poisoning should be kept in mind in any processing of mercury.

**Benzene.** Reagent-grade benzene is treated with concentrated sulfuric acid until it gives a negative test for thiophene with isatin. It is then washed repeatedly with water and dried first with calcium chloride and then with sodium. Fractional distillation results first in the elimination of residual water as the binary azeotrope; the product can then be collected. If extreme purity is required, slow fractional crystallization may be employed, as described by Schwab and Wichers.<sup>2</sup>

<sup>1</sup> *J. Research, Natl. Bur. Standards (U.S.)*, **25**, 747 (1940).

<sup>2</sup> *J. Chem. Educ.*, **28**, 272 (1951).

**Hydrocarbons.** A large number of hydrocarbons have been purified, and their physical properties studied, as part of the work of Research Project 44 of the American Petroleum Institute. The methods employed have been described in a series of publications.<sup>1</sup>

**Sodium Chloride.** Since sodium chloride has a small temperature coefficient of solubility, it cannot be easily purified by crystallization. A saturated solution of sodium chloride is treated with HCl gas to throw out pure salt. The gas is introduced through an inverted funnel, because a small tube is soon plugged up with the crystals. Rubber connections

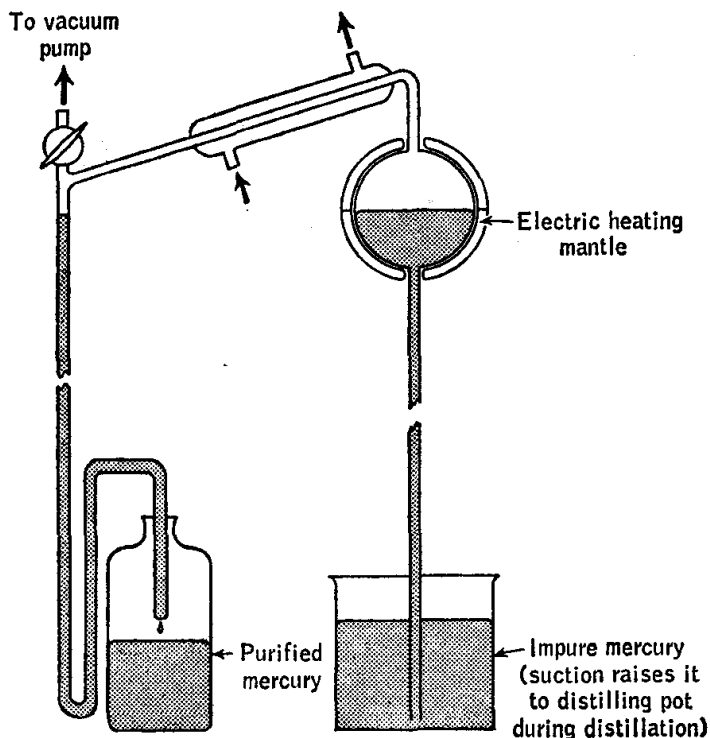


FIG. 132. Mercury still.

are attacked by hydrochloric acid, so the connections and the generating bottle are of glass with Tygon-tubing connections. The gas is generated by adding concentrated hydrochloric acid, drop by drop, to concentrated sulfuric acid, while shaking to avoid the formation of two layers, which might lead to an explosion.

The precipitated sodium chloride is packed into a funnel, rinsed with a minimum amount of water, and fused in a platinum dish at red heat.

**Sodium Hydroxide.** For most titrations with alkali, it is necessary to have the alkali free from carbonate to obtain a sharp end point. High-grade commercial sodium hydroxide may be obtained which

<sup>1</sup> *J. Research, Natl. Bur. Standards (U.S.)*, **35**, 355-373 (1945); **37**, 141-145 (1946); **38**, 53 (1947); **39**, 321 (1947); **41**, 323 (1948); *Chem. Eng. News*, **25**, 730 (1948).

ordinarily needs no further purification. Sodium hydroxide solution free from carbonate is readily prepared from a saturated stock solution. The carbonate is thrown out as an insoluble precipitate by the high concentration of sodium hydroxide which exists in a saturated solution. The clear supernatant solution is drawn off with a siphon and diluted with carbon dioxide-free water to the desired concentration, at room temperature. The saturated solution is about 15 M, and it is kept in a bottle, the inside of which has been covered with paraffin.

Methods for the purification of other substances may be found in the literature.

Recommendations concerning the purification of many organic liquids are given in "Organic Solvents."<sup>1</sup> Archibald<sup>2</sup> describes methods for the preparation of pure inorganic compounds, and Farkas and Melville<sup>3</sup> have specified methods for the preparation, purification, and analysis of a number of gases.

<sup>1</sup> Riddick and Toops, rev. 2d ed. of Weissberger and Proskauer's, "Organic Solvents," in Weissberger (ed.): "Technique of Organic Chemistry," Vol. VII, Interscience Publishers, Inc., New York (1955).

<sup>2</sup> "The Preparation of Pure Inorganic Substances," John Wiley & Sons, Inc., New York (1932).

<sup>3</sup> "Experimental Methods in Gas Reactions," Macmillan & Co., Ltd., London (1939).

## CHAPTER 25

# *Photochemistry*<sup>1</sup>

The first practical requirement in photochemical research is a source of light having sufficient intensity to produce a measurable reaction in a reasonable length of time. For quantitative research it is necessary to use nearly monochromatic light and to know the intensity of the light. Perhaps the greatest difficulty in photochemical technique lies in the fact that any means of restricting the light to a narrow range of wavelengths reduces its intensity and makes the measurement of the chemical change difficult.

### SOURCES OF LIGHT

**Tungsten Filament.** For reactions with visible light, a 200- to 1000-watt tungsten-filament lamp is often satisfactory. If the voltage tends to fluctuate seriously, the intensity of the lamp may be maintained uniform with special transformers or electronically controlled circuits. Ribbon-filament lamps are preferred if the light is to be focused on a cell or monochromator.

For high intensities, a 70-volt lamp may be operated on a 110-volt circuit. The life of the lamp is only about 4 hr under these conditions, but the lamps are not expensive. They are sold with photographic supplies under the name "photoflood lamps."

**Mercury Arc.** The mercury-vapor arc in quartz is the most convenient and powerful source of light for photochemical reactions, but there are only a few lines in its spectrum and it is without effect on those reactions which require intermediate wavelengths. As shown in a later section, however, the small number of lines is advantageous in procuring monochromatic light.

<sup>1</sup> General references include the following: Masson, Boekelheide, and Noyes in Weissberger (ed.), 2d ed: "Technique of Organic Chemistry," Vol. II, Interscience Publishers, Inc., New York (1956); Buttolph in Hollaender (ed.): "Radiation Biology," Vol. II, Chap. 2, McGraw-Hill Book Company, Inc., New York (1955); Scott and Sinsheimer, *ibid.*, Vol. II, Chap. 4; Withrow and Withrow, *ibid.*, Vol. III, Chap. 3 (1956).

The spectrum of the mercury arc is shown in Fig. 133. The widths of the lines in the diagram are proportional to the intensities.

Several types of mercury arcs are commercially available. Some intense lamps are operated at several amperes on direct current. As the lamp heats, the vapor pressure of the mercury increases, and the resistance of the lamp increases so that it is necessary to decrease the external resistance through operation of a rheostat. An ammeter is included in the circuit. After several minutes, the lamp reaches a steady condition. Care must be taken to connect the positive and the negative terminals correctly as labeled and to prevent, with suitable resistance, the passage

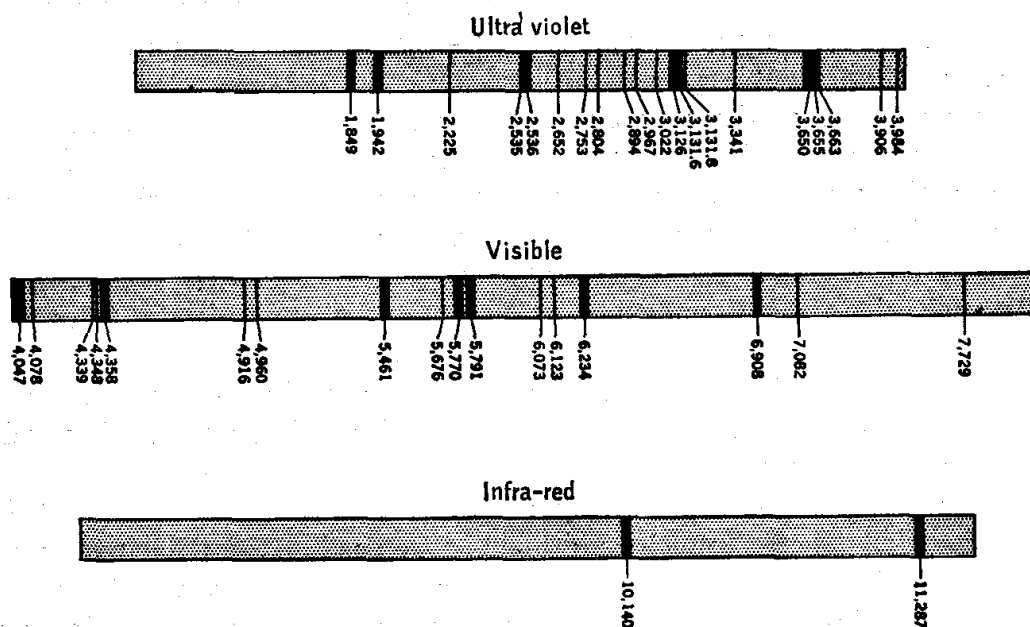


FIG. 133. Spectrum of the mercury arc. Numbers denote wavelengths in angstroms.

of too large a current. *Always* in working with ultraviolet light it is important to protect the eyes with tight-fitting, effective glasses (welding glasses). Albumins in the eye may be coagulated by ultraviolet light, and the effect is cumulative and irreversible.

Several lamps are available which operate at higher voltages on alternating current with a transformer and high reactance. The small lamps of the General Electric Type AH-4 or AH-5 are inexpensive and convenient when a very intense light is not needed. They require an inexpensive transformer.

Intense light for illuminating monochromator slits or small cells may be obtained with water-cooled capillary lamps, in which the light is concentrated in a small region. The AH-6 lamp of the General Electric Company is a very intense water-cooled lamp which operates on alternating current.

"Cold" quartz lamps operating on alternating current at about 6000 volts give about 85 per cent of all the light at the 2537 Å line. They are commercially available, and a low-energy lamp is marketed as a "germicidal lamp."

**Other Arcs.** Light of high intensity can be obtained with an arc passing between two carbon electrodes arranged to move in a sliding frame as they are used up. The control may be effected automatically with a clock mechanism. The light is not steady, and frequent renewals are necessary, but the intensity of the blue and long ultraviolet is high. The spectrum contains many bands and a continuous background. Special-cored carbons may be purchased,<sup>1</sup> containing one or more salts (such as iron, strontium, nickel, and rare-earth metals), which enrich the spectrum in different regions.

The spectrum of the iron arc contains a great many lines, and the intensity in any one is not great. It is rich in the ultraviolet, and it is perhaps the most convenient source of light for reaching the regions between the mercury lines. The iron arc does not waste away as fast as the carbon arc. It is usually operated with both electrodes vertical, the upper one (of smaller diameter) being negative. A small piece of titanium steel or tungsten, floating on the top of the lower electrode, serves to keep the arc centered. The brown fumes of the iron oxide are objectionable, and the evolution of heat may cause difficulties. The iron arc is much used in spectroscopy.

The sodium Lab-arc operating on 110 volts alternating current is recommended when monochromatic light is needed for polarimetry or other optical measurements. The light is too weak, however, for most photochemical reactions. The lamp contains a little neon, which ionizes readily and starts the lamp. Full intensity is not reached until the arc has been operating for several minutes. The neon introduces extra lines in the spectrum, but they are weak in comparison with the sodium lines. For most work they constitute no objection, but if necessary they may be removed with the help of optical filters. A cadmium-mercury lamp is available which gives a bright red line in addition to the mercury lines. It is useful with red optical filters for work in photosynthesis.

Copper, aluminum, and other metals may also be used as rods to give electric arcs.

The radiation emitted by the hydrogen arc<sup>2</sup> is nearly continuous throughout the ultraviolet when the arc is designed so that the atoms recombine rapidly to give molecular hydrogen. It is valuable for obtaining absorption spectra in the ultraviolet below the range of the

<sup>1</sup> National Therapeutic Arc Carbons, National Carbon Company, Cleveland.

<sup>2</sup> Noyes and Leighton, "The Photochemistry of Gases," p. 28, Reinhold Publishing Corporation, New York (1941); Munch, *J. Am. Chem. Soc.*, 57, 1863 (1935).

tungsten lamp. It is used also for photochemical reactions in the ultraviolet.

## TECHNIQUES FOR PRODUCING ATOMS AND RADICALS

Photochemically activated molecules may produce atoms, free radicals, or other activated intermediates, which are important in understanding the mechanism and kinetics of the reaction.

Flash photolysis<sup>1</sup> is a significant development in which photochemical reactions are carried out with light of great intensity, caused by the momentary discharge of electricity accumulated in large condensers. These intermittent flashes between electrodes are focused onto the reacting system, and they are sufficiently intense, for example, to dissociate chlorine gas  $\text{Cl}_2$  into colorless Cl atoms. The rate of recombination of the atoms is measured with photoelectric cells which record the amount of light transmitted through the mixture of chlorine molecules and atoms. The same technique is used for studying the photodecomposition of organic molecules and the recombination rate of free radicals and atoms.

Molecules may be rendered highly reactive not only by the absorption of light but by a sudden input of energy in the form of shock waves.<sup>2</sup> A gas or a mixture of gases is placed under extremely high pressures on one side of a diaphragm. When the pressure is increased still further, the diaphragm ruptures and the gas moves into the low-pressure chamber with great velocity, the molecules having kinetic energy equivalent to that which they would have at very high temperatures. Gaseous bromine molecules are broken down into bromine atoms, for example, and the new products and their rate of recombination are recorded by light absorption, using a photomultiplier and oscilloscope.

New information is being obtained concerning free radicals and energy-rich intermediates which are produced by the absorption of light or by exposure to radioactivity. Again, these "hot" radicals can be made by a nuclear transformation which releases enormous energies within a molecule that contains a disintegrating atom. A "hot" atom or "hot" radical is one which has been produced with energy much in excess of the average energy of the surrounding molecules and has not yet come into thermal equilibrium with them. These hot atoms are responsible for interesting phenomena, which throw light on the mechanisms of some reactions. An excellent review is given by Willard.<sup>3</sup>

<sup>1</sup> Christie, Norrish, and Porter, *Proc. Roy. Soc. (London)*, **A216**, 152 (1952).

<sup>2</sup> Carrington and Davidson, *J. Phys. Chem.*, **57**, 418 (1953).

<sup>3</sup> Radiation Chemistry and Hot Atom Chemistry, *Ann. Rev. Phys. Chem.*, **6** (1955).



Important progress in the study of free radicals and hot free radicals is being made by freezing them in solid materials, such as a frozen solvent, and measuring the light absorption of these immobilized units.

### OPTICAL FILTERS

**Glass Filters.** Filters are the cheapest and most convenient means of restricting the radiation to a narrow range of frequencies. With them it is possible to isolate many of the mercury lines for photochemical investigations. Although the filters absorb a considerable amount of the desired light, they absorb much more of the light in other parts of the spectrum. The filters are ground to a given thickness and polished in standard sizes, 2 in. square and larger. Many of the glasses have sharp

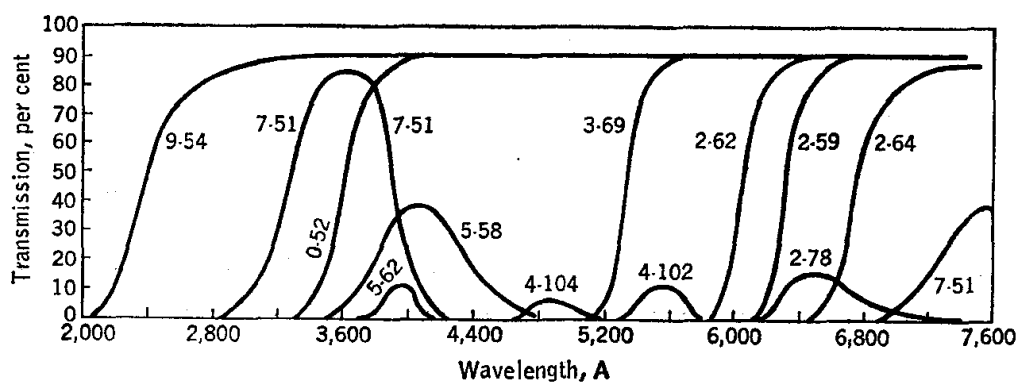


FIG. 134. Typical Corning glass filters.

cutoffs, the shorter wavelengths at the left of the curve being absorbed. Other filters have narrow transmission bands with almost no transmission at longer and shorter wavelengths.

About eighty different optical filters are described with transmission curves at different wavelengths, together with the code numbers, by the Corning Glass Works.<sup>1</sup> They include blue, blue-green, green, yellow, and red filters and filters which transmit ultraviolet light and infrared light, with and without transmission of the visible light.

Transmission data for a few typical filters are shown in Fig. 134.

The lines of the mercury arc can be isolated by using combinations of filters shown in Table 1, to give the color-code specifications listed.

**Solutions.** Several solutions and pure liquids have been used for isolating regions of the spectrum.

A molar solution of cupric chloride in a glass cell 1 cm thick transmits most of the light between 4000 and 6000 Å and absorbs the remaining light. Addition of calcium chloride cuts off more of the violet light, and with sufficient calcium chloride the solution can be made to absorb all light of wavelength shorter than 4800 Å.

<sup>1</sup> "Glass Color Filters," Corning Glass Works, Corning, N.Y. (1960).

TABLE 1. CORNING GLASS FILTERS FOR THE LINES OF THE MERCURY ARC

Wavelength, Å	Color	Color specification number
3650	Ultraviolet	7-83
4050	Violet	5-62
4360-4360	Blue	5-74
5460-5500	Green	4-102
5780-5800	Yellow	3-110

A concentrated solution of iodine in carbon disulfide is opaque to visible light but transmits a considerable amount of infrared light.

Most of the filters transmit some infrared light. Glass and water absorb the longer infrared but allow a considerable portion of light in the neighborhood of  $1\mu$  to pass through. A nearly saturated solution of copper sulfate, 2.5 or, preferably, 5 cm thick, has been used for absorbing the infrared. Such a solution absorbs large amounts of the visible light, too. Glasses which absorb much of the near infrared as well as the long infrared are now commercially available.

A set of solutions which act as filters for several lines of the mercury lamp has been assembled by Bowen.<sup>1</sup>

**Gelatin Filters.** A large collection of gelatin filters containing organic dyes is available.<sup>2</sup> They are used extensively in photography.

**Interference Filters.** Commercial interference filters<sup>3</sup> consist of thin evaporated layers of dielectric material between semitransparent metallic films on glass. A narrow range of wavelengths is transmitted, all others being reflected. Filters with a wide variety of transmission peaks (every 50 to 100 Å) are available, and a few of these are illustrated in Fig. 135. These interference filters offer a convenient means of transmitting light in narrow-wavelength regions, from 3400

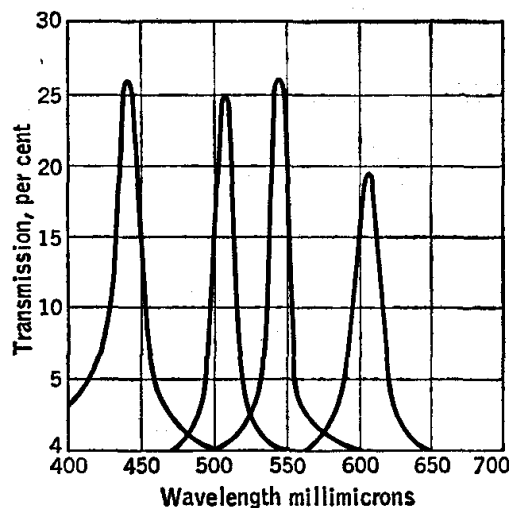


FIG. 135. Spectral transmission of four interference filters.

<sup>1</sup> *J. Chem. Soc.*, **76**, (1935).

<sup>2</sup> Kodak Wratten Filters, Eastman Kodak Co., Rochester, N.Y. (1960).

<sup>3</sup> Farrand Optical Co., Inc., New York; Baird Associates, Inc., Cambridge, Mass.; Bausch and Lomb Co., Rochester, N.Y.

to 10,000 Å, and are usually superior to the glass filters. Multilayer interference filters are prepared by evaporating up to 15 alternating layers of high- and low-refractive-index materials and mounting them between clear glass plates. Seventy per cent transmission is possible with a half-band width of 70 Å.

### MONOCHROMATORS

In general, the undesired wavelengths can be refracted to one side with a prism more effectively than they can be absorbed in a filter. A spectrometer system (Exp. 16) which is arranged to supply radiation of a narrow range of frequencies is called a *monochromator*.

If a continuous light source is used, there may be some overlapping of adjacent regions, and for this reason a discontinuous spectrum, such as that of the mercury arc, is particularly advantageous for use with the monochromator. The low intensity of monochromators can be offset in part by long exposures, by using larger prisms and lenses, and by using capillary arcs of greater intensity. A double monochromator gives radiation of high purity.

### THERMOPILES

A thermopile is made of a number of couples of unlike metals arranged in series with blackened-metal receivers attached to the junctions. The hot junctions are placed in the path of the light, and the cold junctions at one side in the shadow. Radiations of all wavelengths are absorbed by the black receivers and converted into heat so that the temperature of one set of junctions is increased.

The elements are chosen so as to give a maximum thermoelectric effect, and electrical conductance with a minimum of heat conductance between the two junctions. The material should be as thin as possible, to minimize the heat capacity, without being too fragile. Bismuth-silver thermopiles are often used, but copper-constantan and platinum-tellurium elements are satisfactory. Detailed instructions for constructing thermopiles are given by Cartwright and Strong.<sup>1</sup> The theory and practice of thermopile construction have been discussed critically by Leighton and Leighton.<sup>2</sup>

The ordinary linear thermopile is smaller than the reaction cell behind which it is placed, and it is necessary to move the thermopile over the

<sup>1</sup> "Procedures in Experimental Physics," Prentice-Hall, Inc., Englewood Cliffs, N.J. (1939).

<sup>2</sup> *J. Phys. Chem.*, **36**, 1882 (1932).

whole area of the transmitted beam in order to obtain an average value. Large-area thermopiles which do their own integrating are convenient for photochemical investigations. The thermocouples, thoroughly insulated with glyptal lacquer, are attached with de Khotinsky cement to the back of a blackened receiver of sheet silver, 10 by 40 mm in area and 0.02 mm in thickness. The cold junctions are attached in a similar manner to another silver sheet of the same size and heat capacity located at the side of the entering light beam. Twenty or more thermocouples of copper and constantan (Advance) wire are connected in series. The number is chosen so as to give the critical damping resistance for the galvanometer. The junctions are soldered with pure tin, using rosin for a flux and removing all excess tin. The thermocouples and receiver are attached to a bakelite frame, which is then set into a rectangular block of aluminum or other metal. Radiation strikes the blackened receiver through a quartz window.

The thermopile is connected directly to the galvanometer, and the deflection is proportional to the current through the galvanometer, which, in turn, is proportional to the voltage generated by the difference in temperature of the junctions. The temperature difference is proportional to the energy of radiation falling on the receivers. The radiation receiver is covered with lampblack, together with a little platinum black to increase the heat conductance. The mixture is suspended in methanol containing a trace of shellac, applied to the receiver, and allowed to evaporate. The black surface is practically nonselective, converting radiation of all wavelengths directly into heat. This is the advantage over photoelectric cells, which are much more sensitive than thermopiles but which respond only in restricted regions of the spectrum.

The thermopile should have a resistance equal to the critical-damping resistance of the galvanometer, so that a quick return to the zero reading is obtained. The galvanometer scale is arranged to slide back and forth so that it may be conveniently set at zero before each thermopile reading in order to avoid any error due to drift. The drift is caused by thermal inequalities in the thermopile circuit produced by unequal or fluctuating room temperature or by air currents. Evacuation not only improves the constancy of the zero point, but it may increase the sensitivity several fold.

**Calibration.** The deflection of the thermopile-galvanometer system is sufficient for comparative results, but for investigations connecting the quantity of chemical reaction with the energy absorbed (molecules per erg or per quantum), deflections are converted into absolute units. The quantity of radiation falling on the thermopile is obtained in ergs per second or in watts by calibration with a carbon-filament lamp standard-

ized at the National Bureau of Standards.<sup>1</sup> The apparatus is shown in Fig. 136. The standard lamp  $L$  is connected to storage batteries or other steady source of direct current, and the rheostat  $R$  is adjusted until the ammeter  $M$  gives an exact reading corresponding to one of the values given in the calibration table accompanying the lamp (for example, 0.4 amp). A black screen  $A$ , 1 m square, is set 100 cm back of the lamp, and another one,  $B$ , having a square hole 25 cm on a side, is set 25 cm in front of the lamp, with the opening directly in front of it. The thermopile slit is mounted exactly 200 cm from the tip of the lamp. The lamp is rotated so that the two lines etched on either side of the globe are in line with the thermopile, giving the same conditions as used in the standardization. The room must be dark and free from objects that may reflect

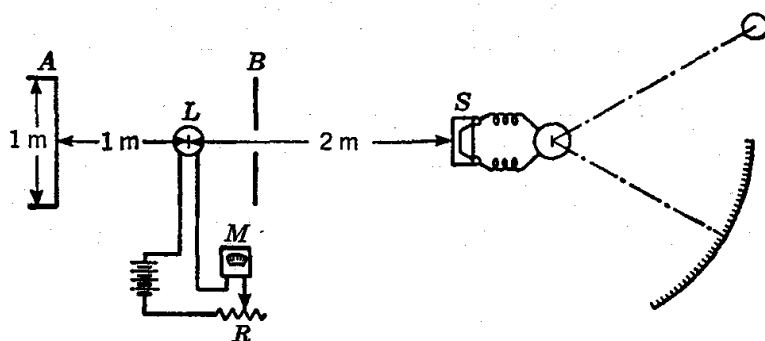


FIG. 136. Arrangement for calibration of a thermopile.

light on the thermopile  $S$ , and the operator must remain at a considerable distance.

The slit is narrower than the thermopile receivers, and its area must be accurately determined. If there are horizontal gaps between the receivers, a correction for the area must be made. The effective area is multiplied by the radiation in watts per square millimeter as given on the calibration sheet.

Windows on the thermopile are necessary to prevent fluctuations in output due to temperature changes and air drafts. Glass windows are unsatisfactory if the thermopile is to be calibrated in absolute units, because glass absorbs some of the infrared radiation emitted by the carbon-filament lamp. Polished quartz windows are preferred for this purpose, and a correction is made by finding the small percentage decrease in deflection caused by interposing a second quartz plate in front of the pile. The same procedure can be used for glass windows also, but the correction is larger. Thin, transparent plastic windows may be used.

<sup>1</sup> These lamps may be purchased at a nominal cost from the National Bureau of Standards. The calibration is described by Coblentz, *Natl. Bur. Standards (U.S.), Bull.*, 11, 87 (1915).

The total radiation  $E$  may be calculated from

$$E = \frac{g}{s} atr$$

where  $s$  = galvanometer deflection with standard lamp

$g$  = galvanometer deflection with monochromator

$r$  = radiation from standard lamp, ergs sec<sup>-1</sup> mm<sup>-2</sup>, under conditions specified by National Bureau of Standards

$a$  = area of slit

$t$  = time of radiation

## BOLOMETERS

The bolometer is essentially a sensitive Wheatstone bridge, with two arms consisting of strips of thin platinum foil placed side by side. One of the strips is blackened, and when it is exposed to radiation, its resistance is raised and a deflection of the galvanometer is produced. The increase in resistance of the foil is proportional to the rise in temperature, which in turn is proportional to the incident energy. The bolometer is capable of great accuracy.

A bolometer of extreme sensitivity has been described by Milton.<sup>1</sup> The sensitive element is a strip of columbium nitride kept at the temperature of boiling hydrogen, at which point the compound undergoes a transition to the superconducting state. The change in resistance is enormous for a minute amount of radiant energy falling on the element.

## PHOTOELECTRIC CELLS

When light of short wavelengths strikes the surface of potassium or other alkali metals (or their hydrides), electrons are emitted, and they conduct current in a photoelectric cell across the evacuated space of the enclosing glass vessel to a positive wire. The deflection of the galvanometer is proportional to the intensity of light when a d-c potential of 90 to 180 volts is applied. The spectral sensitivity of photoelectric cells is dependent on the particular alkali metal used, the metals of higher atomic weights being more sensitive for longer wavelengths.

Photoelectric cells and amplifiers for laboratory work are discussed by Strong.<sup>2</sup>

Although the photoelectric cell is selective in its response to radiation,

<sup>1</sup> *Chem. Revs.*, **39**, 419 (1946).

<sup>2</sup> *Op. cit.*

it can nevertheless be used in some photochemical work. The fact that it does not respond to the longer wavelengths is advantageous in certain cases. For example, if a filter is available to cut off light of wavelength shorter than that of the specified region, and the photocell does not respond to light of longer wavelengths, the photocell may give an accurate measure of the light absorbed in the photochemical reaction. The photoelectric cell and galvanometer circuit may be calibrated against a sensitive thermopile, using monochromatic light, to which the photoelectric cell is sensitive. The thermopile in turn is calibrated with white light from a carbon lamp as described on page 509.

Photomultiplier tubes are recommended for the quantitative measurement of light of very low intensity. A photomultiplier tube, which is comparatively inexpensive, contains nine electrodes placed at suitable angles in series, within the evacuated tube, with a 100-volt potential between each pair. The first electrode is coated with cesium or other material which ejects electrons when light falls on it. The photoelectrons are drawn at a 100-volt potential to a second electrode which is positively charged, and each electron, when it hits, ejects several more. Each of these in turn is drawn to the third electrode, which is 100 volts more positive than the second, and when they strike, additional electrons are released. This cascading effect is continued with each additional electrode, so that it is possible to detect and measure extremely small amounts of light. Photomultiplier tubes are finding important use in the studies of feeble fluorescence and luminescence.

Barrier-layer cells, or photovoltaic cells, are available for measuring the intensity of light. At the contact between two layers of different lattices of a semiconductor, there may be impurities which produce a negative and a positive layer, giving an  $n$ - $p$  junction. The light liberates electrons which reach an electrode and flow around a circuit and neutralize the positive vacancies, or "holes," in the crystal, which were produced when the electrons were liberated. The flow of electrons produces an electric current which can be measured or used for power. A copper-copper oxide surface, for example, generates a small voltage when struck by light. The reading of this voltage on a sensitive voltmeter is proportional to the intensity of light. This type of instrument is widely used for exposure meters in photography. The measurement of voltage without amplification provides a simple means of measuring the light intensity, but the barrier-layer cells are less sensitive than photocells, they have a much larger time lag, and they are subject to fatigue and some deterioration.

Several types of  $n$ - $p$ -junction photovoltaic cells are available, the most common of which is the silicon solar "battery." A single crystal of silicon is treated with pentavalent and trivalent impurities in such a way as to produce positive and negative layers, with which it is possible to

convert sunlight into electricity with over 10 per cent efficiency.<sup>1</sup> These silicon photovoltaic cells<sup>2</sup> respond to all the visible light and some of the near infrared. They are useful for measuring light intensities. Near-infrared light may be detected and measured with a variety of detectors which have been developed to a point where they are now very sensitive.<sup>3</sup>

## REACTION CELLS

Flasks or open dishes may be used for qualitative work. In precision work, the cell has front and back plates of polished quartz or glass, and the cell is placed between the exit slit of the monochromator and the thermopile.

Quartz is transparent throughout the whole visible and ultraviolet range down to 2000 Å. Pyrex in 2 mm thickness will transmit 10 per cent at 3000 Å, whereas Corex will transmit 20 per cent at wavelengths as low as 2750 Å. Vycor glass contains 96 per cent silica and is fairly transparent as low as 2500 Å. All these glasses are transparent throughout the longer ultraviolet, visible, and short infrared. Window glass is suitable for visible light.

Glass cells of various sizes and shapes for holding filter solutions or chemically reacting systems may be purchased, or they may be constructed by fusing a Pyrex tube around a closely fitting circular window cut from a polished plate of Pyrex with a revolving brass tube and emery powder. For some reactions, the cells may be made with polished-glass plates cemented to the ends of a glass tube with Tygon cement or other cement which is inert toward the solution used. When requirements for optical precision are not too great, the photoreaction cells may be made conveniently from Lucite or other plastic material, sawed out to the right size and held together tightly with brass screws and a little cement. It is usually desirable to arrange the cell so that it is almost completely filled by the light beam.

Corrections for the light reflected at an interface are necessary in accurate work. The light should strike the windows at right angles, but even under these conditions, about 4 per cent of the light is reflected at each glass-air or quartz-air surface. The light reflected at a glass-water or quartz-water surface is practically negligible. The fraction of light reflected at right angles is given by Fresnel's formula

$$\frac{I_r}{I_i} = \left( \frac{\mu - 1}{\mu + 1} \right)^2$$

<sup>1</sup> Chapin, Fuller, and Pearson, *J. Appl. Phys.*, **25**, 676 (1954).

<sup>2</sup> Hoffman Electric Co., Evanston, Ill.

<sup>3</sup> Moss, *Modern Infrared Detectors*, in Thompson (ed.): "Advances in Spectroscopy," Vol. I, Interscience Press, New York (1959).



where  $I_r$ ,  $I_i$  = intensity of reflected and incident light, respectively  
 $\mu$  = ratio of refractive indices of two media

The light entering the inside of the empty cell is greater than that registered on the thermopile receivers, by an amount that depends on the number of quartz-air (or glass-air) surfaces through which the light passes. Sometimes the light reflected from the thermopile window passes back through the cell. The corrections are usually small, and they vary with the particular arrangement of cells and thermostat windows. Usually the corrections can be made to cancel out in gas reactions by placing an empty cell in the path of the light when a zero reading is made. The difference in energies registered on the thermopile gives the energy absorbed. In the case of solutions, the amount of light absorbed is obtained by subtracting the galvanometer reading with solution in the cell from the reading with pure solvent in the cell. It is a great convenience to have two cells exactly alike, either one of which may be slid into the path of the light.

#### PHOTOGRAPHY<sup>1</sup>

Photography is indispensable for much laboratory work in physical chemistry. It is discussed in the experiments on spectroscopy (40) and Raman effect (41).

When sensitized grains of silver halide in the gelatin are exposed to light, they are activated in such a way that they are more easily reduced to silver by a suitable mild reducing agent. The action of light produces the *latent image*. Nuclei are produced in the silver halide crystals by the light, and when the plate is immersed in a solution of the proper reducing activity (proper reduction potential in the electromotive-force series), each grain containing a nucleus is reduced to silver. This process is called *development*, and the reducing solution is called a *developer*. The silver halide grains that do not contain nuclei are reduced only after a much longer period of development. The production of nuclei for the latent image depends upon the presence of imperfections in the crystal produced by impurities or strains formed during the nucleation and crystallization. The light energy produces electrons and positive holes

<sup>1</sup> Arenson, *J. Chem. Educ.*, **18**, 122 (1941); "Elementary Photographic Chemistry," Eastman Kodak Co., Rochester, N.Y.; Evans, Hedges, and Mitchell, *Theory of Photographic Sensitivity*, *J. Photographic Sci.*, **3**, 1-11 (1955); James and Higgins, "Fundamentals of Photographic Theory," John Wiley & Sons, Inc., New York (1948); Mack and Martin, "The Photographic Process," McGraw-Hill Book Company, Inc., New York (1939); Mees, "The Theory of the Photographic Process," The Macmillan Company, New York (1942); Neblette, "Photography: Its Principles and Practice," 5th ed., D. Van Nostrand Company, Inc., Princeton, N.J. (1955).

which are trapped at imperfections in the crystal, giving mobile silver and halogen atoms which start reaction with the developer. A diffusion of the silver and halogen atoms to the surface of the grain is involved.

After development, the plate is *fixed*. In this process the unreduced grains of silver halide are dissolved in sodium thiosulfate ("hypo"), leaving behind the grains which had light-induced nuclei and which were accordingly reduced by development to give black grains of silver. The parts of the plate that received the brightest light when the plate was exposed become the darkest when the plate is developed and fixed, and the finished plate is called a *negative*.

After fixation is complete, the plate is thoroughly washed and dried.

The amount of change produced on the plate by the action of the light is, of course, dependent upon the amount of light energy acting. Obviously, the same amount of light can be admitted through the lens by using a small aperture and long exposure, or a large aperture and short exposure. Better definition and greater depth of focus are obtained by the use of a small aperture.

In a perfect negative, i.e., one which has silver deposits in the various areas proportional in amount to the intensities of light reflected from the corresponding areas of the objects being photographed, the densities of the deposit are proportional to the logarithm of the corresponding exposure. If a series of identical plates are given exposures increasing in geometrical progression (so that their logarithms increase in arithmetical progression), and all plates are subjected to exactly the same process of development, a curve is obtained that shows the density of the developed photographic silver image as a function of the logarithm of the exposure, known as the *characteristic curve* of the film or plate. It has the general form shown in Fig. 137.

If the exposures are such as to bring the photographic plate into the region of the straight line, II, excellent results will be obtained. Good results may often be obtained, however, when the exposure is somewhat less, in the curved part, I, because the failure to give direct proportionality between density and exposure is partly compensated for in the printing of the positive.

The use of an exposure meter is recommended, with proper attention to the exposure index of the particular type of film or plate used. These

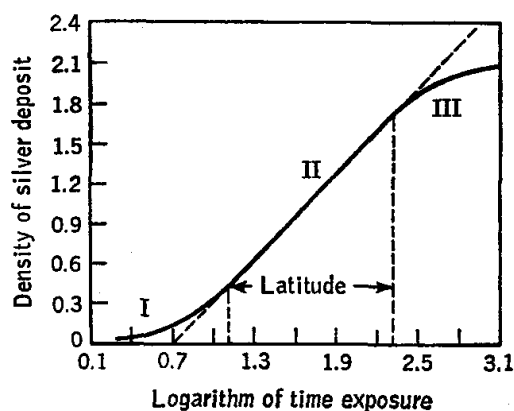


FIG. 137. Characteristic curve for the exposure of a photographic plate.

indices are supplied by the manufacturer and recorded on the box containing the films.

Emulsions with large grains (silver halide crystals) are faster. They are not suitable for enlargements or lantern slides, and for these a finer-grained, slower emulsion is used. For photographing laboratory material and apparatus and line drawings, high contrast is necessary. Process plates are suitable. For spectrographic work, panchromatic plates sensitive to all wavelengths of visible light are necessary.

In taking photographs, the camera is focused and then the loaded plateholder is inserted in the back of the camera, without changing the position of the camera. The shutter is closed, the diaphragm is adjusted to the desired opening, and the slide is pulled out of the plateholder. In the  $f$  system, the diaphragm opening represented by  $f/16$  means that the diameter of the opening is one-sixteenth of the focal length of the lens. With the setting of  $f/16$  and a process plate, an exposure of about 10 sec or less is appropriate, but the exact exposure is obtained from the exposure meter. After exposure, the slide is immediately replaced. It is a convention that the black side of the handle on the slide is always placed outward after the plate has been exposed.

Three trays containing developer, water, and fixing bath are placed near the red lamp in the darkroom. At 20°C, the image appears in 15 to 20 sec, but development should be continued until the details in the shadows are brought out, usually requiring about 3 min. Control of temperature is very important, as a few degrees of change greatly influence the action of the developer. The proper point at which development should be stopped must be learned by experience. The plate is then rinsed to remove alkali and placed in the fixing bath for about 20 min, or at least 5 min after all the halide (white) is apparently removed from the plate. After fixing, the plate is washed for at least half an hour in running water, placed on a rack, and allowed to dry. Upon completion of washing, the surface of the wet plate should be swabbed off (lightly) with wet absorbent cotton before drying. This removes any possible sediment that may have collected on the gelatin surface.

Ready-mixed developers may be purchased, or the developer may be prepared from the formula which accompanies the plate or film.

A suitable formula for process plates or contrast plates or films is prepared by mixing the two following solutions A and B.

Solution A		Solution B	
Water.....	100 ml	Water.....	100 ml
Hydroquinone.....	2.5 g	NaOH.....	4.0 g
Na <sub>2</sub> SO <sub>3</sub> .....	2.5 g		
KBr.....	2.5 g		

The following solutions are recommended for fixing plates or prints:

Solution A		Solution B	
Water.....	500 ml	Glacial acetic acid.....	10 g
"Hypo" ( $\text{Na}_2\text{S}_2\text{O}_3 \cdot 5\text{H}_2\text{O}$ , crude)....	125 g	Powdered alum.....	10.5 g
		$\text{Na}_2\text{CO}_3$ .....	10.5 g
		Water.....	75 ml

The water of solution A may be heated to dissolve the "hypo" quickly, but it must be cooled before solution B is added.

The reagents are added in the order given, and when they are fully dissolved, the hardening solution B is poured into the thiosulfate, or "hypo," solution A slowly, with stirring. The "hypo" must be *fully* dissolved before adding the hardener; otherwise sulfur will be deposited.

A simple photographic emulsion of silver halide and gelatin is usefully sensitive only to the blue, violet, and near ultraviolet. The short-wavelength limit is set by absorption of the gelatin; sensitivity falls rapidly below 2500 Å and is negligible below 1900 Å. The long-wavelength limit is set by the absorption of the silver halide and varies from about 4300 Å for pure silver chloride to 5200 Å for silver bromiodide.

In order to photograph radiation of wavelength less than 2000 Å, it is necessary to use emulsions very low in gelatin or to sensitize an ordinary emulsion with a fluorescent coating. The low-gelatin emulsions are called Schumann plates. Improvements of the Schumann plate are made by Ilford, Ltd., and sold as Q plates.

Ordinary emulsions may be sensitized to the short ultraviolet by coating with a material which, when exposed to ultraviolet, fluoresces with emission of radiation, to which the emulsion is sensitive. This method is convenient and gives good sensitivity, but the resolving power is lowered by spreading of the image. The ethyl ester of dihydrocollidinedicarboxylic acid is suitable for the short-ultraviolet sensitization. It may be obtained from the Eastman Kodak Co. as "ultraviolet sensitizing solution, No. 3177," or the Kodak plates may be purchased with the proper fluorescent coatings.

Sensitization to wavelengths longer than those absorbed by the silver halide is produced by adding to the emulsion special dyes (optical sensitizers) which are absorbed on the silver halide and sensitize it to the light absorbed by the dyed grains. The chemistry of the dyes and the mechanism of their action are described by Mees<sup>1</sup> and James and Higgins.<sup>2</sup>

Dyes of many chemical types may act as long-wavelength sensitizers, but the most important classes are the cyanines and merocyanines.

<sup>1</sup> *Op. cit.*, Chaps. 23-25.

<sup>2</sup> *Op. cit.*, Chap. 14.

Photographic plates and films sensitive to the green (orthochromatic), to the whole visible spectrum (panchromatic), and to the infrared out to 9000 Å and farther are available.<sup>1</sup>

Applications of photography to specific problems are described in a number of books.<sup>2</sup>

<sup>1</sup> Kodak Photographic Films and Plates for Scientific and Technical Use," 8th ed. (1960), and "Photographic Materials for Spectrum Analysis," Eastman Kodak Co., Rochester, N.Y.

<sup>2</sup> Shillaber, "Photomicrography in Theory and Practice," John Wiley & Sons, Inc., New York (1944); "Photomicrography," 14th ed., Eastman Kodak Co., Rochester, N.Y. (1944); Clark, "Photography by Infrared," 2d ed., John Wiley & Sons, Inc., New York (1946); Scott, "Photographic Evidence," Vernon Law Book Co., Kansas City, Mo. (1942); Longmore, "Medical Photography," Focal Press, London (1944); Tupholm, "Photography in Engineering," Faber & Faber, Ltd., London (1945); Mathews and Crabtree, Photography as a Recording Medium for Scientific Work, *J. Chem. Educ.*, 4, 9 (1927); "Infrared and Ultraviolet Photography," Eastman Kodak Co., Rochester, N.Y. (1959).

## CHAPTER 26

# Spectroscopy

Spectroscopy is the study of the interaction of matter with an electromagnetic field as a function of the frequency of the field. This interaction manifests itself in a number of processes, the most familiar being absorption, emission, scattering, and reflection of the electromagnetic energy.

Modern spectroscopic work covers a very wide range of frequencies, as illustrated in Fig. 138. The breakdown shown in the upper strip is an

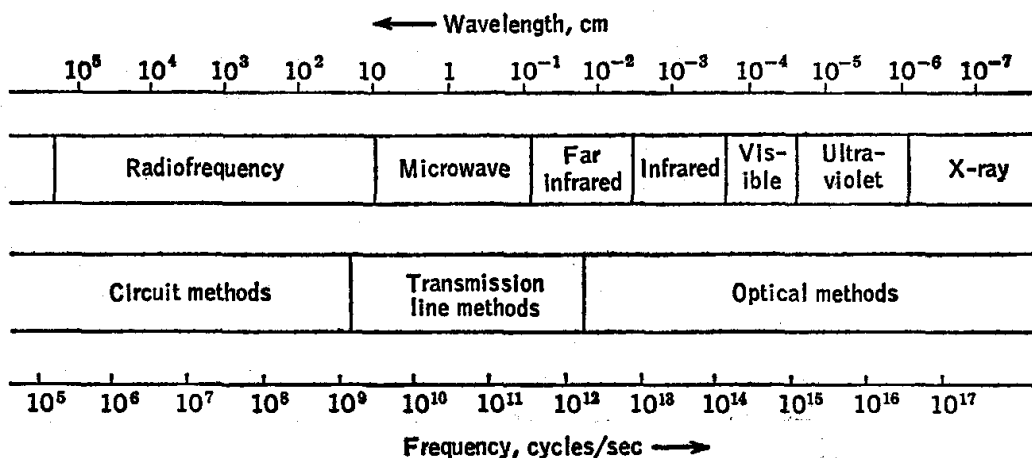


FIG. 138. Regions of the electromagnetic spectrum of chief spectroscopic interest and methods usually applicable for system dimensions of the order of magnitude of a centimeter.

experimental one: the devices used to generate, transmit, and detect the electromagnetic fields, and to measure the frequency or wavelength, vary from one region of the electromagnetic spectrum to another. It is helpful to bear in mind also a classification of techniques into three broad categories, namely, (1) circuit methods, (2) transmission-line methods, and (3) optical methods. The second strip in Fig. 138 indicates the approximate range of utility of each of these methods for the typical case in which the fields of interest occupy a region in the apparatus of the order of a few millimeters or centimeters in size. More generally, the

range of applicability of each technique could be indicated thus:

Circuit methods	$\lambda \gg l$
Transmission-line methods	$\lambda \approx l$
Optical methods	$\lambda \ll l$

where  $\lambda$  = wavelength

$l$  = an average dimension of the region which the fields of interest occupy

This chapter is intended to serve as an introduction to principles of experimental spectroscopy rather than as a survey of techniques. The following sections will be devoted to a discussion of several well-designed research spectrometers, representing circuit, transmission-line, and optical types. The particular examples chosen will serve to illustrate basic design principles which are widely used in modern spectroscopic instruments.

At this point, it is appropriate to introduce several concepts which are encountered so often that it seems desirable to mention them before turning to the discussion of specific spectrometers.

**Resolution.** In general, the function of a spectrometer is to measure the absorption coefficient or emission intensity as a function of frequency. Spectral lines as displayed by a spectrometer always appear to be spread over a finite frequency range, called the line width. In some cases this width represents an intrinsic property of the sample, the spectrometer output then being a true plot of absorption coefficient or emission intensity versus frequency. In other cases, the observed width may be ascribed either partly or entirely to instrumental effects. Resolution is measured by the observed line width, or, more or less equivalently, by the minimum separation for which two partially overlapping lines can still be recognized as being distinct.

**Sensitivity.** In general, the ability of a properly designed spectrometer to detect weak spectroscopic lines is limited ultimately by noise from statistical fluctuations of one sort or another. Usually, though not always, the offending noise is that generated in the device employed to detect the radiation. The true measure of sensitivity for a spectrometer is the signal-to-noise ratio obtainable for a given absorption coefficient, or equivalently, the minimum detectable absorption coefficient (corresponding to a signal-to-noise ratio of unity).

**Bandwidth and Response Time.** Since the noise power in electronic or mechanical systems is proportional to the bandwidth  $B$  (page 580), it is advantageous to reduce  $B$  in order to improve the signal-to-noise ratio. However, the response time  $\tau$  of the system (page 558) is inversely related to the bandwidth: regardless of the design of the system,

it does not appear to be feasible to reduce the product  $B\tau$  much below an optimum value,

$$B\tau \cong 0.2 \quad (1)$$

Thus, even if no other considerations enter, the use of very narrow bandwidths is often inconvenient because of the resulting slow response of the indicating device. A simple example is afforded by a highly damped galvanometer, which is good for averaging out fluctuations due to noise, but also is slow in responding to changes in the current being measured.

Another specific illustration of this principle may be informative. Suppose a spectrometer is to scan a range of 300 Mc/sec with a bandwidth of 0.1 cycle/sec and that the lines to be detected have a width of about 1 Mc/sec. If the spectrometer detector is of the phase-sensitive type (page 606) with output filtered by a simple low-pass  $RC$  filter, the effective noise bandwidth for the system may be shown to be  $B = 1/8RC$ . Thus the filter time constant<sup>1</sup> required to achieve the specified bandwidth is  $\tau_0 = RC = 1.2$  sec. A time of the order of  $10\tau_0$  should be allowed for passing through a line. The maximum permissible scanning rate is then 1 Mc/sec per 12 sec, so that about an hour is required for scanning this range. Even slower scanning rates would have to be used if accurate reproduction of line shapes were required.

**Saturation Effect.**<sup>2</sup> When radiation of the proper frequency to produce transitions between two quantum states  $m$  and  $n$  of a substance is present, both absorption and stimulated emission take place. The net rate of absorption is proportional to  $N_m - N_n$ , where  $N_m$  is the population of the lower state and  $N_n$  that of the upper state. In a system at thermal equilibrium, collisions (or some other form of interaction between molecules) maintain an excess population in the lower state, so that  $N_m - N_n$  has a definite value, dependent on the temperature of the system. A phenomenon known as the saturation effect occurs in spectroscopic experiments when the incident radiation intensity is sufficiently great that molecules are being raised from the lower into the upper state of the transition at such a rate that the collision processes are unable to maintain the normal population difference between the two states. Saturation is a common occurrence in radiofrequency and microwave spectroscopy and often sets an upper limit to the usable source power. Saturation rarely occurs in the optical region, where the available power density is usually relatively low.

<sup>1</sup> The time constant  $\tau_0 = RC$  is the time required for the output of the filter to reach 63 per cent of the final value after application of a step function. The 10 to 90 per cent response time  $\tau$  for a simple  $RC$  filter equals  $2.2\tau_0$ .

<sup>2</sup> Saturation is discussed in the references on microwave and radiofrequency spectroscopy cited at the end of this chapter.



**Absorption and Dispersion.** The two phenomena of absorption and dispersion are intimately related, although they produce quite distinct effects in a spectrometer system. Consider first the optical case. As a beam of radiation passes through a substance, a gradual decrease in intensity along the path results if energy is being taken up from the beam by the sample. This process is absorption. Another effect of the sample is to cause the wavelength to be different from that for radiation of the same frequency in vacuum. With this change in wavelength are associated the various phenomena of refraction. It is quite characteristic for

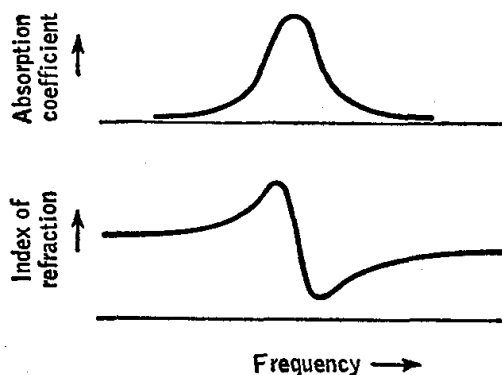


FIG. 139. Illustration of the typical relationship between absorption and dispersion.

rapid changes in refractive index with frequency to occur in the neighborhood of absorption lines (Fig. 139). This is the phenomenon of dispersion.

The same molecular processes which produce optical absorption and dispersion are manifested somewhat differently in the case of a substance which has been coupled closely to an electric circuit by being placed either between the plates of a capacitor or within a closely wound coil. In the circuit case, absorption

of energy by the sample has an effect equivalent to the introduction of resistance into the circuit, while dispersion effectively causes a change in the apparent value of capacitance or inductance, as the case may be.

The existence of a close relationship between absorption and dispersion is expected for both classical and quantum-mechanical systems.<sup>1</sup> A classical system exhibits this sort of behavior at frequencies close to its natural resonance frequencies; a quantum-mechanical system does so at frequencies which can produce transitions between stationary states of the system.

## RADIOFREQUENCY SPECTROMETER

Two radiofrequency spectrometers designed for investigation of nuclear magnetic resonances will be described. One illustrates the crossed-coils method of Bloch, Hansen, and Packard,<sup>2</sup> while the other

<sup>1</sup> Böttcher, "Theory of Electric Polarisation," pp. 240-253, Elsevier Press, Inc., Houston, Tex. (1952). (Classical theory.) Karplus and Schwinger, *Phys. Rev.*, **73**, 1020 (1948). (Quantum-mechanical theory pertinent to microwave and radiofrequency cases.)

<sup>2</sup> Bloch, Hansen, and Packard, *Phys. Rev.*, **69**, 127 (1946); **70**, 474 (1946).

employs a regenerative oscillator, utilizing a principle first introduced in this application by Roberts.<sup>1</sup>

The phenomenon to be detected by these instruments will first be briefly described. Let the sample, which may be solid, liquid, or gaseous, be contained in a glass vial and placed in a constant magnetic field  $H_z = H_0$ , taken to be in the  $z$  direction. Nuclei of spin  $\frac{1}{2}$  or greater in this sample exist in quantized energy levels which correspond to various allowed orientations of the nuclear-spin vectors relative to the  $z$  direction. Spectroscopic transitions occur when the sample is subjected to a sinusoidally varying magnetic field, the frequency  $\nu$  of which satisfies the condition

$$h\nu = \frac{\gamma}{2\pi} H_0 \quad (2)$$

where  $h$  = Planck's constant

$\gamma$  = gyromagnetic ratio, a constant characteristic of the given type of nucleus

Magnets providing fields of the required uniformity and stability are available for the kilogauss range. This places the frequencies for many common nuclei in the radiofrequency (rf) region.

To observe these transitions, the rf field of proper frequency is produced by impressing a voltage across a coil wound around the sample vial. This rf field is linearly polarized along the coil axis, here taken as the  $y$  axis. When a field at the resonance frequency, given by Eq. (2), is applied in this fashion, the total resultant magnetization vector<sup>2</sup> for the macroscopic sample, which otherwise would be polarized along the  $z$  direction, becomes tilted slightly and precesses about the  $z$  axis at the frequency of the rf field. The magnetization may therefore be resolved into components, a constant component along the  $z$  direction and a component of fixed magnitude rotating in the  $xy$  plane. This rotating component, which exists only when the sample is stimulated at a frequency close to resonance, will induce a voltage in any coil with its axis in the  $xy$  plane. In the crossed-coils method, a second coil ( $x$  coil) is placed with its axis perpendicular to the axis of the  $y$  coil, so that the voltage directly coupled from the  $y$  coil into the  $x$  coil in the absence of the sample resonance effect is minimized. The sample resonance is then detected by observing the very weak voltage which is induced in the  $x$  coil by the rotating sample magnetization. In single-coil methods, the reaction of the sample on the  $y$  coil itself is observed as a very slight change in its

<sup>1</sup> *Rev. Sci. Instr.*, **18**, 845 (1947).

<sup>2</sup> The magnetization vector is defined as the resultant magnetic-dipole-moment vector of the sample (or in this case, the part arising from the nuclear moments) per unit volume. This quantity is quite analogous to the electric polarization defined on page 213.

impedance, this change being detected from the effect on the circuit of which it is a part.

A block diagram of the crossed-coils apparatus of the type originally used by Bloch, Hansen, and Packard<sup>1</sup> appears in Fig. 140. A signal generator supplies rf power to the  $y$  coil. The receiver (tunable rf amplifier and detector) is tuned to the frequency of the signal generator. A sawtooth voltage synchronized with the oscilloscope horizontal sweep

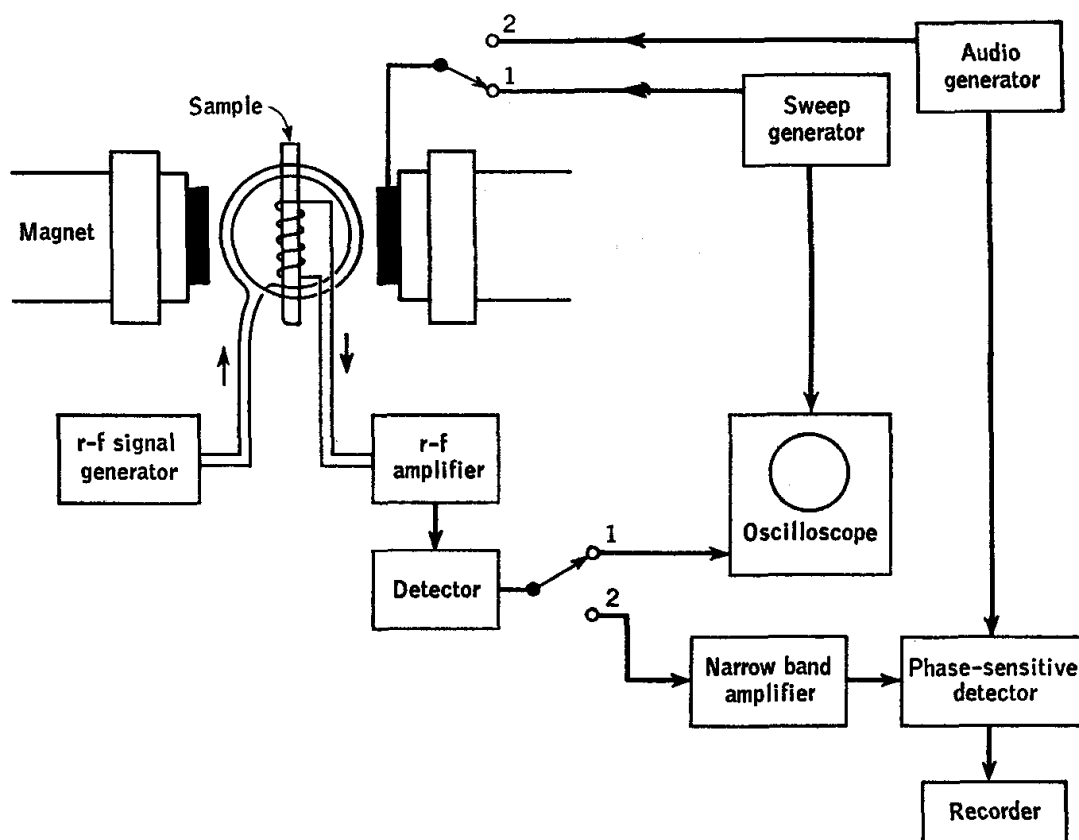


FIG. 140. Block diagram of a nuclear-magnetic-resonance spectrometer similar to that of Bloch, Hansen, and Packard. The apparatus used by Bloembergen, Purcell, and Pound differs from this mainly in that a radiofrequency bridge is employed instead of the crossed-coils arrangement.

is fed to the field modulation coils to produce a repetitive sweep in  $H_z$ . The receiver output is observed on the oscilloscope, effectively as a function of  $H_z$ .

A communications receiver can be used in this apparatus, though it is necessary for good sensitivity to precede it with a low-noise rf preamplifier, since the noise which limits sensitivity is generally that produced in the first stage of amplification of the voltage from the  $x$  coil. To permit the use of slow rates of sweep, the output for the oscilloscope is taken

<sup>1</sup> *Loc. cit.*

from the second detector of the receiver, since the gain of the audio amplifier in the receiver drops off rapidly below the audio range.

Since it is not practicable to achieve perfect geometry in the construction and alignment of the coils, the signal from a sample resonance would be swamped by rf leakage directly from the  $y$  coil to the  $x$  coil unless arrangements were made to balance this out. A satisfactory means of doing so is provided by two suitably oriented metallic paddles, or one-turn coils, which can be rotated to modify the coupling between the  $y$  and  $x$  coils. These are adjusted alternately until the leakage voltage is minimized.

In order to obtain a line shape corresponding to sample absorption, rather than a mixture of absorption and dispersion, it is necessary to detect that component of the voltage in the  $x$  coil which has the same phase as the voltage at the  $y$  coil. Although this objective can be achieved by the use of an rf phase-sensitive detector, the same result was accomplished in the earlier spectrometers by introducing a reference rf voltage of suitably adjusted phase into the receiver. Provided this voltage is larger than the signal from any sample resonance, it has the effect of converting an ordinary peak-following detector into a phase-sensitive detector. The inherent limitation in this scheme is that any fluctuations in this reference signal, whether they arise from variations in signal-generator output or from changes in gain of the receiver, can cause troublesome drift in the detector output.

To obtain better sensitivity it is essential to employ a narrow bandwidth and slower rates of sweep than are feasible in the presence of this drift. One very good method of obtaining narrower bandwidths with good base-line stability is the field-modulation method.<sup>1</sup> In this scheme, which corresponds to position 2 of the switches in Fig. 140, the sawtooth sweep is not used. An audio generator supplies a current to the modulation coils to produce a sinusoidal term in  $H_z$ . The sample absorption line, if plotted against frequency (Fig. 141a), would now appear to wobble back and forth along the frequency axis, since the frequency of the peak is, from Eq. (2), proportional to  $H_z$ . The amplitude of the deviation of  $H_z$  is set at a value a little below the expected sample line width (expressed in field units). The output of the receiver when the frequency is close to that of a sample resonance is now an audio voltage at the modulation frequency. This voltage is detected by a phase-sensitive detector with reference derived from the modulation oscillator. The output is displayed by a chart-type recorder, while the average value of  $H_z$  is changed at a slow and constant rate. The deflection, for small modulation amplitude, is proportional to the derivative of the true line shape (Fig. 141b). As an alternative to modulation of the field, an

<sup>1</sup> Bloembergen, Purcell, and Pound, *Phys. Rev.*, **73**, 679 (1948).

equivalent effect can be produced by frequency-modulating the rf oscillator of the signal generator.

The modulation frequency must be kept lower than the line width if distortion of the line shape is to be avoided. However, the effect of flicker noise from the amplifier is minimized by using modulation frequencies as high as is feasible within this restriction. Typically, modulation frequencies in the range 25 to 400 cycles/sec are used. This modulation method is used in modern research instruments designed for the study of relatively wide, weak resonances, as are commonly found in solids.

In the design of spectrometers for the observation of the relatively narrow resonances (often below 1 cycle/sec) characteristic of liquids,

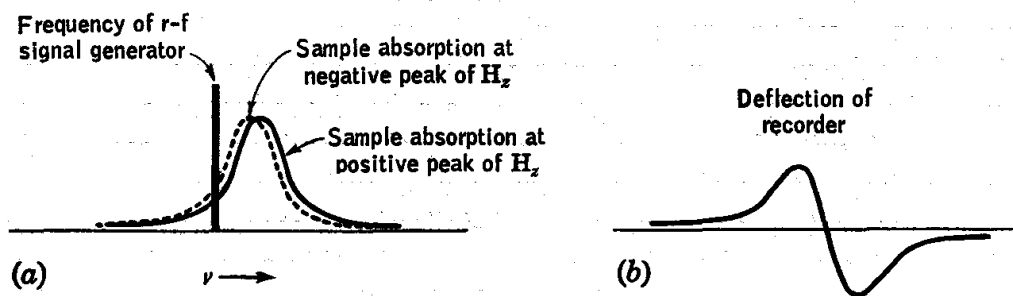


FIG. 141. (a) Illustration of the shift in an absorption line produced by modulation of  $H_z$ ; (b) resulting output of a phase-sensitive detector as plotted by a chart-type recorder while the average value of  $H_z$  is slowly increased, for the case of weak modulation amplitude.

emphasis has been placed on developing techniques for producing magnetic fields of very high stability and homogeneity. An example of a high-resolution spectrometer is illustrated in Fig. 142. The magnetic field is stabilized to within about 1 part in  $10^8$  at 14,000 gauss by a circuit which senses changes in the field and corrects for these by driving an appropriate current through a pair of coils mounted on the magnet pole caps and also, at the same time, acting through the regulator circuit of the power supply for the main field coils of the electromagnet. Careful temperature control of the magnet is essential to maintaining good stability. From time to time the magnet current is carried through an empirically determined cycling procedure to restore good homogeneity.

Crystal-controlled oscillator circuits are employed in the rf generator unit, since stability of the spectrometer frequency is as important as that of the magnetic field. The frequencies given in the diagram are those for the 60 Mc/sec generator, which is used for the detection of proton resonances at about 14,000 gauss.

Since line widths of the order of 1 cycle/sec are obtained, clearly the audio-modulation method of detection described above is not appropriate

and a different approach is used for the achievement of narrow bandwidths. In principle, a suitably narrow bandwidth and good absorption-line shape could be obtained by use of a sharply tuned amplifier at 60 Mc/sec, followed by a phase-sensitive detector (page 606) at this frequency. At the present state of the art, however, these functions can be performed more satisfactorily by heterodyning (page 557) to 5 Mc/sec

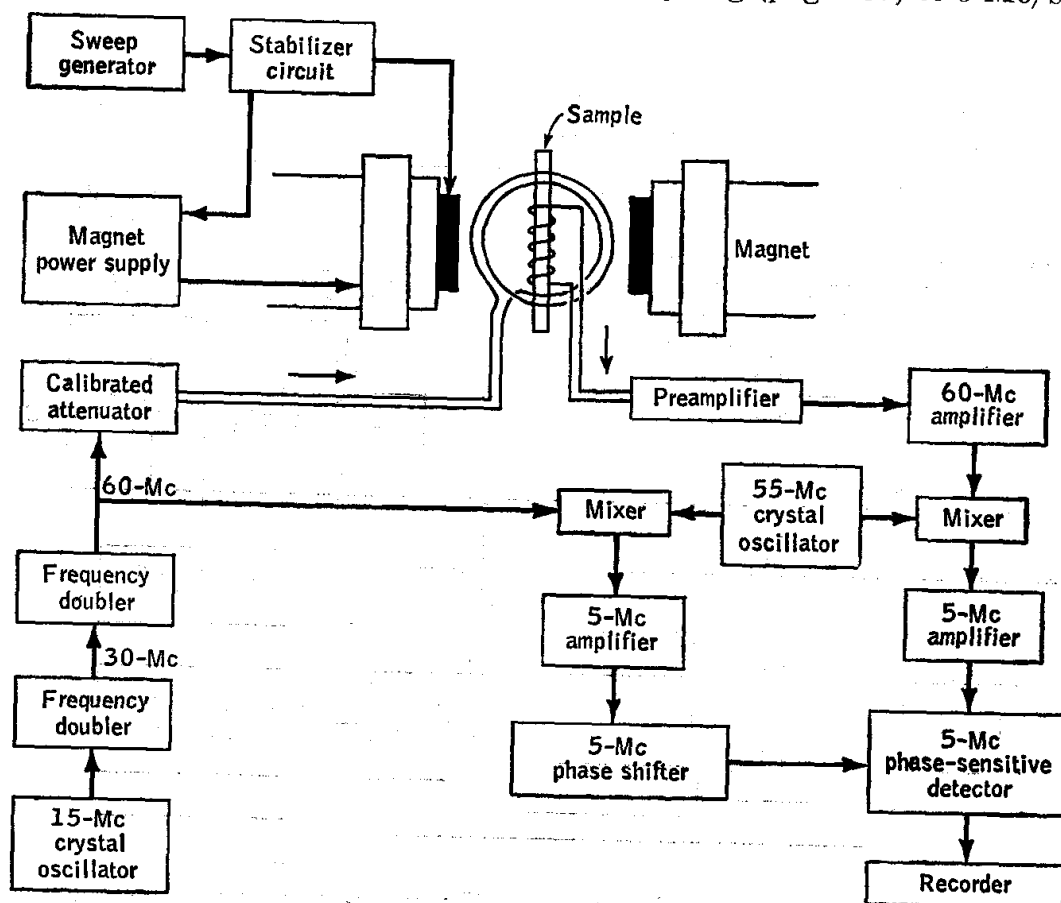


FIG. 142. Block diagram of high-resolution nuclear-magnetic-resonance spectrometer. (Principal features of Varian Associates Model V-4311.)

and employing a tuned amplifier and phase-sensitive detector at this frequency. The detector output, after filtering, is presented on a chart recorder.

Although the noise bandwidth is really determined by the phase-sensitive-detector output circuit, the bandwidth of the rf amplifier itself has to be kept reasonably narrow in order to permit a large gain to be obtained without the noise level becoming so high as to swamp the final stages.

The regenerative oscillator spectrometer of Pound and Knight,<sup>1</sup>

<sup>1</sup> *Rev. Sci. Instr.*, **21**, 219 (1950); Watkins and Pound, *Phys. Rev.*, **82**, 343 (1951); Pound, *Progr. in Nuclear Phys.*, **2**, 21 (1952).

illustrated in Fig. 143, is particularly well suited to those studies for which it is necessary to be able to change the spectrometer frequency easily, or even to search continuously over a wide frequency range. The range covered is 1 to 40 Mc/sec. The sample is placed in the coil of the tank circuit of the oscillator. To search for resonances, the oscillator is

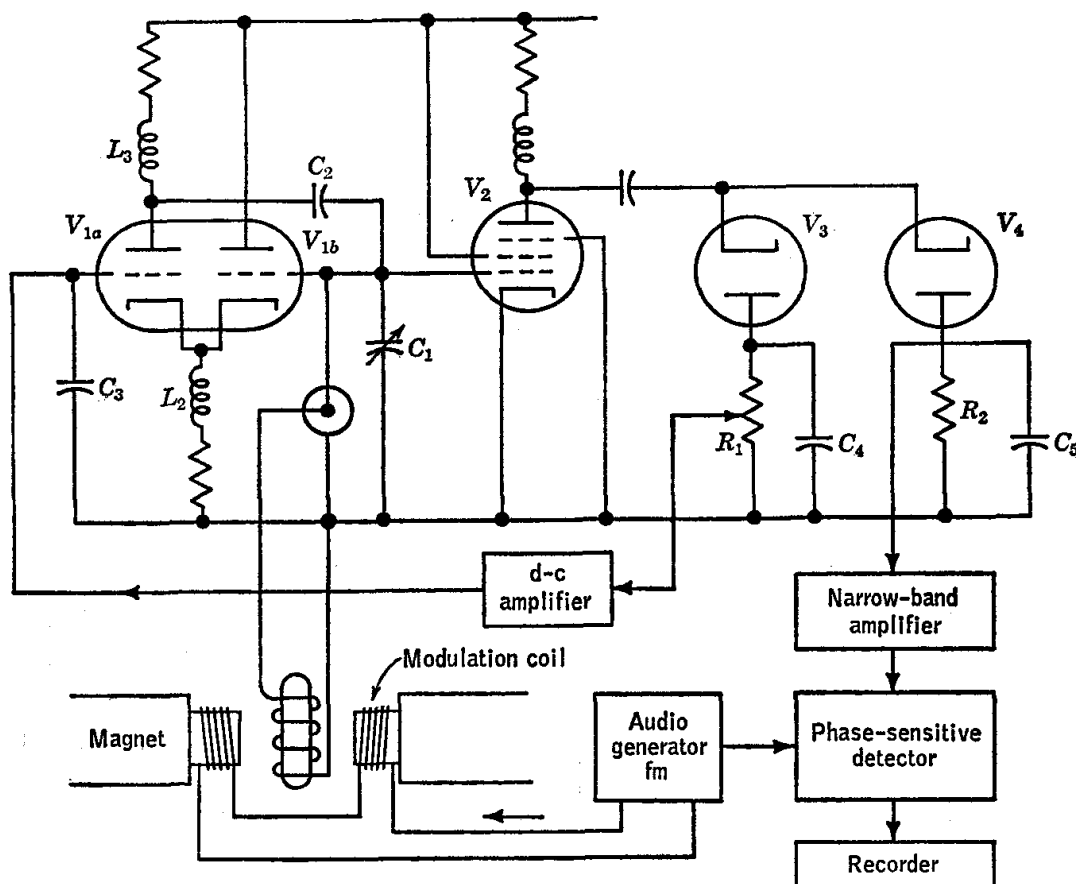


FIG. 143. Simplified diagram of Pound-Knight-Watkins radiofrequency spectrometer. The oscillator is of the cathode-coupled type. Oscillations in the resonant circuit (p. 550) consisting of  $C_1$  and the sample coil are sustained through amplification by  $V_1$  and feedback of power through  $C_2$ . Pentode stage  $V_2$  is a radiofrequency amplifier. The amplitude of the oscillations is held approximately constant through the action of diode detector circuit  $V_3$ ,  $R_1$ ,  $C_4$  (page 573), which determines the bias of  $V_{1a}$ . Modulation of the radiofrequency voltage produced by sample absorption (as in Fig. 141) is detected by  $V_4$  to yield a signal at the modulation frequency. This in turn is amplified and detected to produce a deflection of the recorder pen.

tuned by means of a synchronous motor which drives the rotor of the variable capacitor  $C_1$  of the tank circuit. When a resonance frequency of the sample is encountered, the absorption of energy by the sample causes a decrease in the  $Q$  of the tank circuit, and as a result the amplitude of oscillation is very slightly reduced. Audio modulation of either the field or the spectrometer frequency is used so that good sensitivity can be

obtained by a narrow-band amplifier, phase-sensitive detector, and chart-recorder system. This type of spectrometer has been widely employed for the study of resonances in solids. A similar spectrometer is available commercially.<sup>1</sup>

### MICROWAVE SPECTROMETER

Some of the special characteristics and design principles of a microwave spectrometer of the transmission-line type will be considered here. The purpose of the spectrometer to be described is to display the pure rotational spectra in gaseous samples with sufficient resolution for general

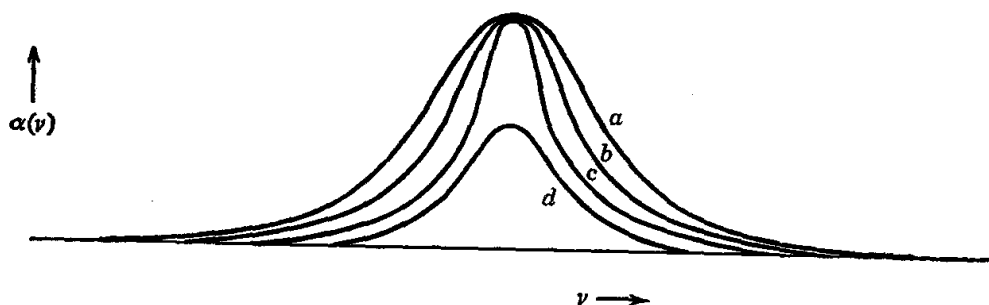


FIG. 144. Microwave absorption line, plotted against frequency  $\nu$ , for a series of different pressures, with pressure decreasing in the sequence  $a, b, c, d$ . Curves  $a, b, c$  illustrate the narrowing of the collision-broadened line which accompanies a decrease in pressure; curve  $d$  shows the decrease in peak value which eventually occurs when the pressure becomes so low that saturation is observed at the given microwave power level. Saturation can be avoided by reducing the power level, but the sensitivity becomes poorer at very low power levels.

molecular structural studies. For such work it is desirable to have an instrument which (a) covers a wide frequency range, corresponding to a substantial portion of the microwave region, (b) is capable of detecting lines with absorption coefficients<sup>2</sup> of the order of  $10^{-6}$  to  $10^{-9}$   $\text{cm}^{-1}$ , and (c) displays these lines with a width of the order of 1 Mc/sec or less.

The peak value of the absorption coefficient varies from one line to another and also depends on the temperature and pressure of the sample. As a rule, the width of the lines is due to collision broadening. The width from this source is, from a simple kinetic-theory calculation, proportional to the pressure (Fig. 144). For the width to be kept below

<sup>1</sup> Nuclear Magnetic Corporation, Norwalk, Conn.

<sup>2</sup> The absorption coefficient  $\alpha$  is defined by  $P = P_0 e^{-\alpha l}$  where  $P_0$  is the microwave power entering a transmission line as a traveling wave, and  $P$  is the power passing a cross section at a distance  $l$  farther along the line. In an empty waveguide, the power absorption is due to ohmic losses associated with wall currents; if the waveguide is filled with a gaseous sample which has an absorption line at the given microwave frequency, a very slight increment is added to  $\alpha$ . It is this increment which the spectrometer must detect.



1 Mc/sec, the sample pressure must ordinarily be of the order of  $10^{-2}$  mm or less. At such low pressures, the microwave power must be held to a reasonably low level, usually below 1 milliwatt, if saturation effects are to be avoided.

As an example of a spectrometer which very satisfactorily meets these requirements, we shall describe a Stark-effect modulation spectrometer. The Stark effect (page 278) is the splitting and shifting of spectral lines which occurs when the sample is subjected to an electrostatic field (Fig. 145). The introduction of the principle of Stark-effect modulation by Hughes and Wilson<sup>1</sup> provided an elegant and effective means of increasing sensitivity. Figure 146 is a block diagram of a spectrometer of the Hughes-Wilson type. Most research instruments now in use represent elaborations of this basic scheme.

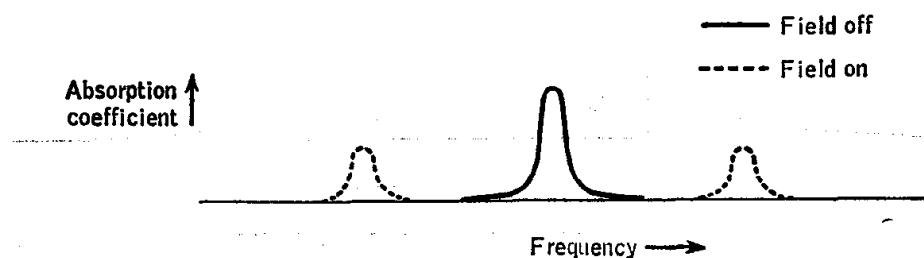


FIG. 145. Absorption line of a sample in the absence of an electrostatic field and with the field applied. The "field on" pattern is merely illustrative since the Stark patterns vary from one line to another.

The absorption cell consists of a length, perhaps 10 ft, of waveguide closed off at both ends by vacuum-tight mica windows. The sample is introduced into the cell from a vacuum manifold, through a few small holes so located in the waveguide wall as to cause the least interference with the propagation of the microwave fields. To permit the application of an electrostatic field, a strip of brass, supported and insulated by two grooved Teflon tapes, is placed inside the sample cell (Fig. 147). This Stark electrode is located in a plane which is perpendicular to the electric component of the microwave field and so does not seriously affect its transmission.

The source of microwave power is a klystron oscillator. A klystron is a special type of vacuum tube in which the electron beam interacts with a tunable cavity, resonant at the microwave frequency, in such a way as to sustain oscillations. Since the frequency of oscillation depends on the cavity dimensions, the oscillator is tuned by mechanically changing the size of the cavity. Small changes in frequency are made by shifting the

<sup>1</sup> *Phys. Rev.*, **71**, 562 (1947); McAfee, Hughes, and Wilson, *Rev. Sci. Instr.*, **20**, 821 (1949).

voltage supplied to one of the klystron electrodes. The klystron is well suited to spectroscopic use because it has reasonably good frequency stability and can be tuned relatively easily over a wide frequency range, often of the order of 1.5 to 1. In the future, klystrons may be displaced

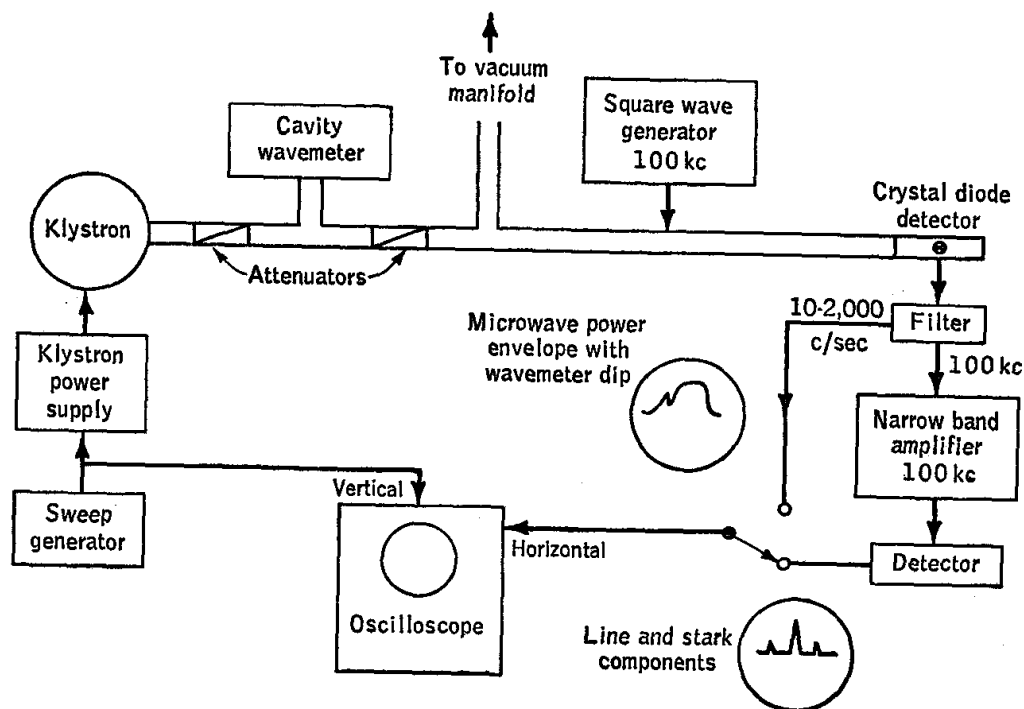


FIG. 146. Block diagram of Stark-modulation microwave spectrograph of the Hughes-Wilson type. Typical frequency range is 10 to 14,000 Mc/sec.

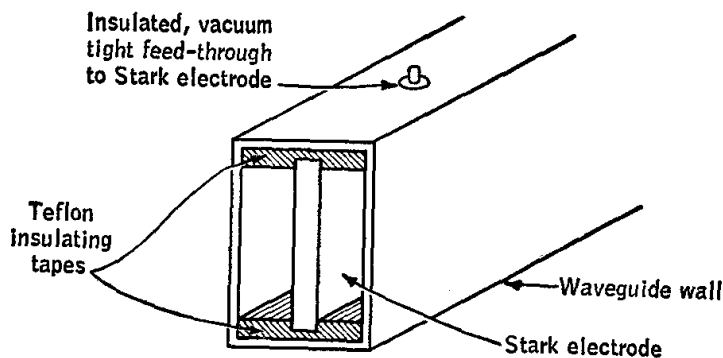


FIG. 147. Details of Stark-cell construction.

in this application by traveling-wave-tube oscillators, which cover even wider ranges.

The cavity wavemeter, which is used for approximate<sup>1</sup> measurement of the microwave frequency, consists of a cylindrically shaped cavity,

<sup>1</sup> Cavity wavemeters presently available commercially offer an accuracy of the order of 0.1 per cent and a precision of 0.01 per cent.

coupled to the main waveguide through a small hole. The cavity length is determined by the position of a micrometer-driven piston. A sharp dip in the power transmitted past the cavity hole occurs when the frequency is such that a cavity resonance is excited.

After going through the absorption cell, the microwave radiation is detected by a special microwave diode, consisting of a small semiconductor crystal mounted in a coaxial cartridge suitable for admitting power at microwave frequencies. The crystal diode rectifies the microwave currents and produces an output d-c current, the magnitude of which depends upon the amount of incident microwave power (page 571).

A sawtooth voltage sweep is introduced at one of the klystron electrodes to produce a corresponding sweep in the microwave frequency, over a range of perhaps 50 Mc/sec. The same sweep voltage is applied also to the horizontal deflection channel of the oscilloscope. The shape of the microwave power envelope arriving at the crystal is somewhat irregular because of the variation in oscillator output and in the microwave-system transmission characteristics over the course of a sweep. The crystal detector output follows this envelope. This can be displayed on the oscilloscope when desired. The wavemeter, when suitably tuned, produces a visible dip in this pattern. If there were a sample absorption line within the region swept, however, it would not be seen against this relatively uneven background unless it were an unusually strong line.

A zero-based square-wave voltage is applied between the Stark electrode and the waveguide. The frequency  $f_m$  of the modulating field produced in this way is relatively low, so that one may think of it as an electrostatic field which is alternately being switched on and off. As the klystron frequency goes through the frequency of a line, the microwave voltage at the crystal is modulated at the frequency of the Stark field; this happens because the sample absorbs at one frequency while the field is off and at different frequencies when the field is on. As a result, at those times during the sweep when the klystron is going through the frequency of a sample absorption line, there exists in the crystal output an a-c component, at the frequency  $f_m$ , which is due to sample absorption. A filter broadly tuned to this frequency passes this component on to the narrow-band amplifier. There is a signal at the point along the sweep where the sample absorbs when the field is off, and other smaller signals at points where the sample absorbs when the field is on. The latter are called *Stark components*; their position along the sweep changes when the amplitude of the Stark modulation voltage is changed. The a-c voltages due to sample absorption at the filter are very minute and are actually buried in noise voltages often thousands of times larger.

The narrow-band amplifier is tuned to the modulation frequency and selectively amplifies the a-c voltage from the absorption line, but not the

slow variations in microwave power level. It also discriminates against noise generated in the crystal, except for noise voltage components whose frequencies are within the passband of the amplifier. The detector output follows the envelope of the a-c voltage from the amplifier.

The limitation on sensitivity with this spectrometer is in most instances the noise generated within the crystal. As this is random noise, the noise power at the output of the narrow-band amplifier is proportional to the bandwidth, while the signal power is independent of the bandwidth. Therefore the signal-to-noise ratio improves as the bandwidth is narrowed. The bandwidth of the amplifier must be left broad enough, however, to accommodate drift in the modulation frequency or in the amplifier components which determine the amplifier tuning, for deterioration of signal will obviously occur if the modulation frequency is not well within the amplifier passband. Typically, the bandwidth is of the order of a few per cent of  $f_m$ .

In addition to Johnson noise (page 578), excess noise is produced in the crystal when d-c current flows (as it does whenever the crystal detects microwave power). This excess noise is referred to as semiconductor noise. The semiconductor noise power per unit bandwidth in the vicinity of a frequency  $f$  varies roughly as  $1/f$  in the audio- and radio-frequency regions. In the present case, the noise of concern is that within the passband of the amplifier tuned to frequency  $f_m$ . The modulation frequency is chosen high enough to achieve a significant reduction in crystal noise below that present at the low audiofrequencies. However, if  $f_m$  becomes comparable with the line width (expressed in frequency units), the modulation causes the lines to appear broadened. Thus the choice of modulation frequency involves a compromise between sensitivity and resolution. The modulation frequency is usually chosen in the range 50 to 100 kc/sec. In many cases, a communications receiver which extends into this range is used as narrow-band amplifier and detector.<sup>1</sup>

When it is desired to employ narrower bandwidths than are readily achievable with the arrangement of Fig. 146, the simple detector can be replaced by a phase-sensitive detector and chart recorder.<sup>2</sup> With this arrangement, somewhat lower modulation frequencies are sometimes used, down to about 5 kc/sec.

Figure 148 is a block diagram of a typical microwave frequency standard used for accurate frequency measurements. The 5-Mc/sec crystal-controlled oscillator provides a stable reference which is monitored against standard frequency transmissions of Station WWV. Various harmonics of this frequency are generated by the multiplier stages, and these, when fed into the microwave crystal, produce a lattice

<sup>1</sup> Model HRO-60, National Company, Malden, Mass.

<sup>2</sup> McAfee, Hughes, and Wilson, *loc. cit.*

of accurately known frequencies at intervals of 30 Mc/sec in the microwave band of interest. A sample of the klystron oscillator power enters the same crystal and mixes with power from the standard. The receiver is used to detect a beat note (usually the one of lowest frequency) between the klystron and one of the reference harmonics. The output of the receiver is displayed on the oscilloscope along with the output of the spectrometer detection system. When the klystron is swept, the beat note passes so rapidly through the passband of the receiver that only a sharp pip appears on the oscilloscope. Suppose, for example, that with

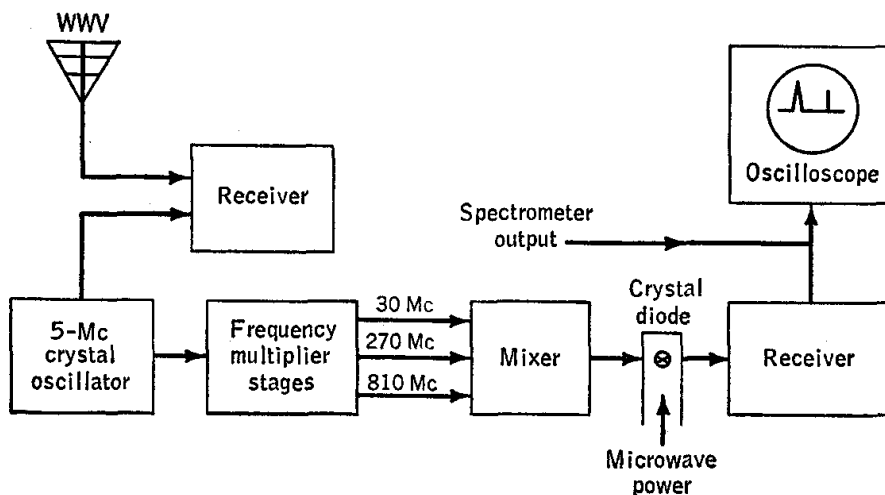


FIG. 148. Block diagram of microwave frequency-measuring equipment.

the receiver tuned to a frequency  $f_r$ , a beat mark is produced at the instant at which the klystron passes through the frequency of an absorption line. Then the frequency of the line is  $30n \pm f_r$  Mc/sec, where  $n$  is an integer. The value of  $n$  is determined with the aid of a cavity wavemeter, and the choice of sign made by noting the direction in which the position of the beat mark changes when the receiver frequency is increased. The accuracy of a system such as this is inherently of the order of a few kilocycles per second, so that the accuracy of frequency measurement is practically always limited only by the breadth of the lines.

Stark modulation spectrometers are commonly used over the frequency range 10,000 to 40,000 Mc/sec. At higher frequencies, the construction of the Stark cell presents difficulties as smaller waveguide sizes are used.

## INFRARED SPECTROMETER

To introduce some of the principles encountered in the design of an optical spectrometer, we shall discuss the Baird Associates<sup>1</sup> infrared

<sup>1</sup> Baird Associates, Cambridge, Mass.

spectrophotometer as modified by Evans for high-resolution work. This is one of several examples recently reported<sup>1</sup> in which commercial infrared instruments have been modified by the introduction of gratings to permit the study of the rotational structure of rotation-vibration bands of simple gaseous molecules. The range of this particular instrument is 2 to 12  $\mu$ .

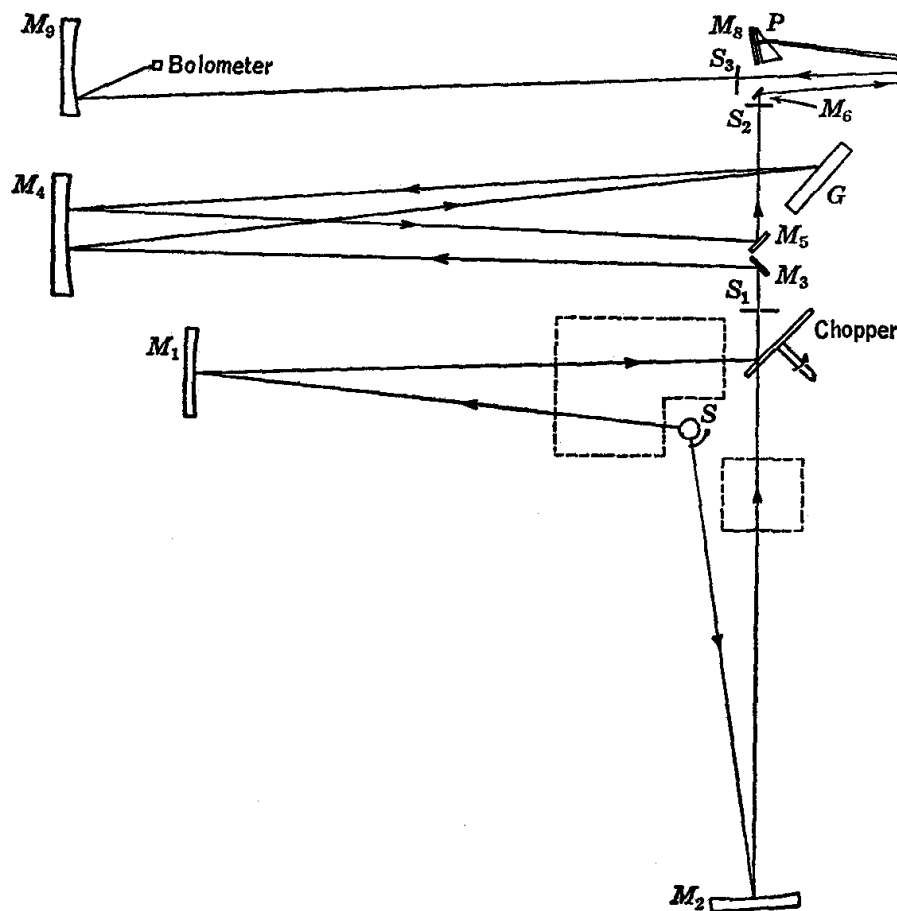


FIG. 149. Optical system of Baird Associates double beam infrared spectrophotometer as modified by Evans for high-resolution work.

A diagram of the optical system appears in Fig. 149. The radiation source  $S$  is a silicon carbide rod (Globar) which is heated electrically to approximately 1100°C. The wavelength distribution of the emitted radiation is nearly that of a blackbody at the same temperature. Because the performance of the spectrometer is limited by the energy available from the source, the source is kept at as high a temperature as is feasible.

The source is enclosed in a water-cooled housing, which has two apertures through which beams of infrared radiation emerge. These beams are focused by the concave mirrors  $M_1$  and  $M_2$  onto slit  $S_1$ .

<sup>1</sup> Cole, *J. Opt. Soc. Am.*, **44**, 741 (1954); Lord and McCubbin, *J. Opt. Soc. Am.*, **45**, 441 (1955); Evans (private communication).

En route from the mirrors to the slit, the beams pass through two wells (dotted), one of which contains the sample cell and the other, the reference cell. Immediately in front of the slit is a semicircular mirror which is rotated at 10 revolutions per second. This half-mirror sends the sample and reference beams alternately through the entrance slit  $S_1$ . Near the source is the *comb*, which intercepts a part of the reference beam and thereby functions as a variable attenuator. The position of the comb is controlled by a mechanism described below.

The portion of the instrument in the optical path between  $S_1$  and  $S_3$  functions as a bandpass filter which selects radiation of a narrow range of wavelengths, which is then focused on the detector by  $M_9$ . Slit  $S_1$  is in the focal plane of mirrors  $M_1$  and  $M_2$  and also in that of  $M_4$ . The divergent rays which pass through a single point in the aperture of  $S_1$  are directed by plane mirror  $M_3$  toward the concave spherical mirror  $M_4$  and are then collimated by  $M_4$  into a beam of parallel rays which go on to the diffraction grating  $G$ . The cross-sectional area of this bundle of rays is determined by the size of  $M_4$ , which is made large enough to utilize the full area of the grating. The grating is a carefully ruled film of aluminum on glass. Radiation is reflected from the grating in various directions, according to wavelength. The diffracted rays which reach  $M_4$  are subsequently brought to a focus in the plane of the exit slit  $S_2$ . The wavelength which falls at the midpoint of  $S_2$  is given by

$$\lambda = \frac{2d}{N} \sin \vartheta \cos (\delta/2) \quad (3)$$

where  $N$  = an integer, the *order* of the grating reflection

$d$  = spacing of rulings of the grating

$\delta$  = angle between the incident beam at the grating and the diffracted beam of wavelength  $\lambda$

$\vartheta$  = angle between the face normal of the grating and the bisector of  $\delta$

The angles in Eq. (3) are illustrated in Fig. 150. Numerical values for the instrument described here are

$$\delta = 4^\circ$$

$$d = 0.00667 \text{ mm}$$

$$\lambda = (13.33/N) \sin \vartheta, \text{ microns}$$

The spectrum is scanned by rotating the grating to change  $\vartheta$ , and hence the wavelength emerging from the center of  $S_2$ .

We have thus far considered only the radiation emitted from a single point in  $S_1$  which reaches a single point in  $S_2$ . To achieve adequate sensitivity it is necessary of course to employ slit apertures of appreciable size. Rays emerging from different points in  $S_1$  travel in slightly dif-

ferent directions in the collimated beam; similarly, the exit slit  $S_2$  accepts rays reflected from the grating in a small range of angles. Therefore the radiation which eventually leaves through  $S_2$  corresponds not to a single value of  $\vartheta$ , but to a small range of angles,  $\Delta\vartheta$ . This range, called the angular slit width, is determined by the widths of  $S_1$  and  $S_2$ . Through Eq. (3),  $\Delta\vartheta$  determines the range of wavelengths  $\Delta\lambda$  which actually reaches the detector.

For the present spectrometer, operated in the first order with a typical setting  $\vartheta \cong 30^\circ$ , the slits are usually adjusted to give a resolution  $\Delta\lambda$  of about  $0.5 \text{ cm}^{-1}$  at  $1500 \text{ cm}^{-1}$ .

The optical path between  $S_2$  and  $S_3$  consists of a small prism monochromator—comprising plane mirror  $M_6$ , spherical collimating mirror  $M_7$ ,

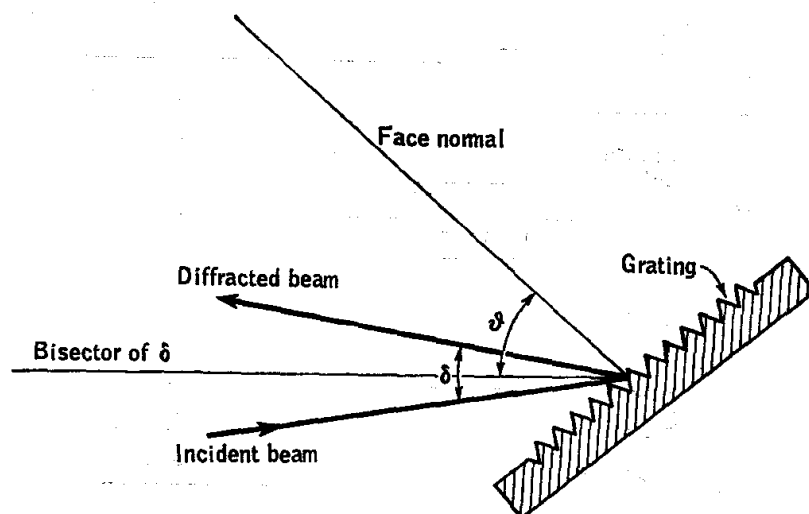


FIG. 150. Illustration of angles appearing in the grating equation (3).

sodium chloride prism  $P$ , and Littrow mirror  $M_8$ —which serves only to reject all diffraction orders other than the one desired. For example, if the grating monochromator is set for  $1500 \text{ cm}^{-1}$  at  $N = 1$ , then radiation at  $3000 \text{ cm}^{-1}$ ,  $4500 \text{ cm}^{-1}$ , . . . , also passes through  $S_2$ . The desired order is selected by rotating the prism-mirror assembly ( $P$  and  $M_8$ ) to direct the radiation of this order onto the slit  $S_3$ .

The rays from  $S_3$  are focused onto the bolometer detector by  $M_9$ . The bolometer is a thin strip of platinum, about  $0.2 \times 2 \text{ mm}$ , coated with platinum black to absorb the infrared radiation. The bolometer forms one arm of a balanced d-c Wheatstone bridge (Fig. 151). The effect of incident radiation is to alter the temperature, and hence the resistance, of the bolometer and thereby to produce an unbalance in the bridge. To minimize effects of convection currents and to improve sensitivity, the bolometer is mounted in an evacuated housing with a KBr window through which the radiation enters.



Unless the beams which come from the sample and reference paths are of equal intensity, the bolometer is subjected to radiation intensity which is modulated at 10 cycles/sec, and a 10-cycle/sec voltage appears at the output of the bridge. This voltage is amplified and then detected by a phase-sensitive detector. The phase of the 10-cycle/sec voltage, and hence the sign of the detector output, depend upon which of the two beams has the greater intensity. The output of the detector controls a motor which moves the comb until the 10-cycle/sec signal output from

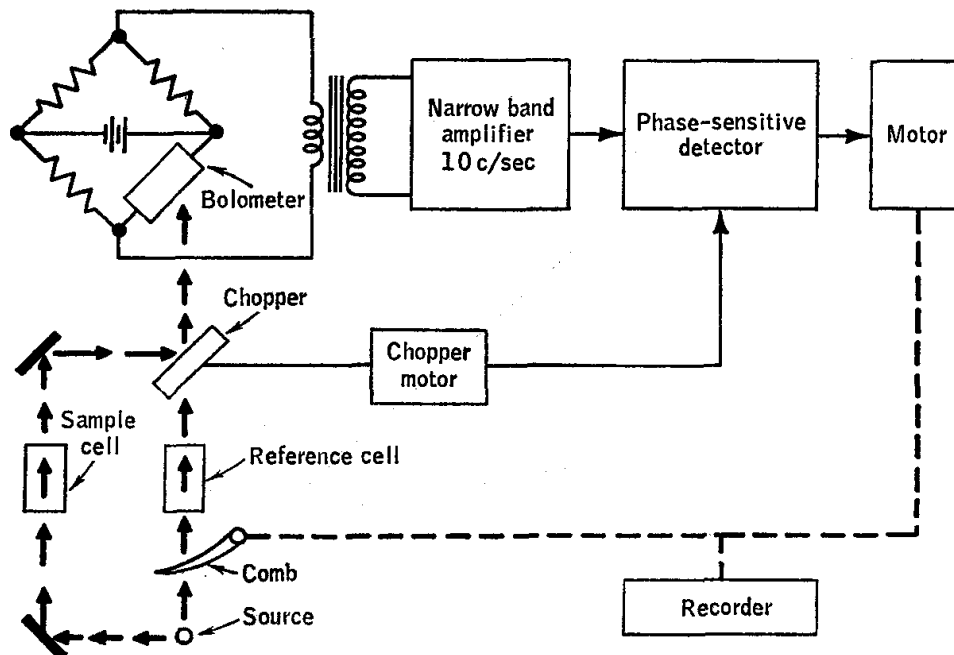


FIG. 151. Block diagram of electronic system of Baird Associates double beam infrared recording spectrophotometer. A few parts of the optical system (Fig. 149) have been included to clarify the function of the electronic system.

the bolometer bridge is reduced to zero. The pen of a chart recorder is coupled mechanically with the comb. As the spectrum is scanned by slow rotation of the grating, the changes in transmission of the sample are indicated by changes in position of the comb, and hence of the pen, which occur as the servomechanism operates to keep the beams matched. Thus the recorder traces the per cent transmission as a function of wavelength.

It is instructive to examine the way in which various features of the design of the optical system and detection system affect the sensitivity and resolution of the spectrometer.<sup>1</sup> To do this, we shall assume that the

<sup>1</sup> The discussion of sensitivity and resolution given here is based in part on an equation derived by Strong, *J. Opt. Soc. Am.*, **39**, 360 (1949). See also Jacquinot, *J. Opt. Soc. Am.*, **44**, 761 (1954); Lord and McCubbin, *loc. cit.*

resolution is determined by the optical system and that the sensitivity is limited by the noise generated in the detection system.

The response of the bolometer is of the form

$$e = S\Delta P \quad (4)$$

where  $e$  is the unloaded output-voltage change produced by a change  $\Delta P$  in power level incident on the bolometer, with the current through the bolometer held constant. The parameter  $S$  depends on the design of the bolometer and on the conditions under which it is operated.

If the bolometer is placed in a bridge with the resistances of the other three arms equal to that of the bolometer (matched condition), the output voltage of the unloaded bridge† is  $\frac{1}{2}S\Delta P$ . For the case of a beam chopped at 10 cycles/sec, this is the peak-to-peak value of a square wave. The effective signal voltage is the sinusoidal component of this at 10 cycles/sec, as only this component is amplified by the narrow-band amplifier. The rms value  $e_s$  of this component is (pages 544 and 555)

$$e_s = \frac{\sqrt{2}}{\pi} \left(\frac{1}{2}S\Delta P\right) = \frac{1}{\sqrt{2}\pi} S\Delta P$$

The rms noise voltage output of the bridge at open circuit, within the effective bandwidth  $B$  of the amplifier-detector system, is (page 580)

$$e_n = (4kTRB)^{1/2} \quad (5)$$

where  $k$  = Boltzmann constant

$T$  = absolute temperature of detector

$R$  = output resistance of bridge

For the matched bridge,  $R$  is equal to the bolometer resistance. The noise figure (page 579) of the bolometer and amplifier system,  $F$ , is unity if the only noise detected is Johnson noise from the bolometer and bridge and is larger than unity if excess noise is generated in the bolometer or bridge or is added in the amplification process. In practice, a noise figure close to unity is achieved in this case. The signal-to-noise ratio at the output of the detection system is

$$\frac{e_s}{e_n} = \frac{S\Delta P}{2\pi(2FkTRB)^{1/2}} \quad (6)$$

To calculate  $\Delta P$ , let us suppose that the sample absorbs a fraction  $\gamma$  of the incident power. Then  $\Delta P = \gamma P$ , where  $P$  is the radiant energy reaching the bolometer per unit time. The power  $P$  in watts is given by

$$P = B_\lambda A \frac{h}{f} (\Delta\nu) \mathfrak{J}(\Delta\lambda) \quad (7)$$

† Several applications of Thévenin's theorem (page 552) are made in this derivation.

where  $B_\lambda$  = brightness of source, watts/cm<sup>2</sup>-steradian per cm wavelength range, at given wavelength

$A$  = cross-sectional area, cm<sup>2</sup>, of collimated beam

$h$  = height of monochromator slits  $S_1, S_2$ , cm

$f$  = focal length of collimating mirror  $M_4$ , cm

$\Delta\vartheta$  = angular slit width, radians = slit width divided by  $f$

$\mathfrak{J}$  = transmission fraction of optical system of spectrometer

$\Delta\lambda$  = wavelength range passed by monochromator

Hence the signal-to-noise ratio is

$$\frac{e_s}{e_n} = \frac{S\gamma}{2\pi(2FkTRB)^{1/2}} B_\lambda A \frac{h}{f} (\Delta\vartheta)\mathfrak{J}(\Delta\lambda) \quad (8)$$

The resolution  $\Delta\lambda$ , assumed to be determined by the grating dispersion  $d\vartheta/d\lambda$ , is given by

$$\Delta\lambda = (\Delta\vartheta) \left( \frac{d\vartheta}{d\lambda} \right)^{-1} \quad (9)$$

It is apparent that increasing the slit width increases the sensitivity but impairs the resolution.

A useful figure of merit for a spectrometer of this type under the assumptions specified above is

$$\frac{e_s/e_n}{\gamma(\Delta\lambda)^2} = \frac{S}{2\pi(2FkTRB)^{1/2}} \left[ B_\lambda A \frac{h}{f} \mathfrak{J} \left( \frac{d\vartheta}{d\lambda} \right) \right] \quad (10)$$

which is obtained by substituting Eq. (9) in (8) and keeping only the purely instrumental parameters on the right-hand side. This equation shows very clearly the nature of the compromise which must be made between sensitivity and resolution.

As a rule, the goal of the designer is to make the right side of Eq. (10) large. The factors in front of the square brackets are determined by the detecting system. The quantity  $S/(FR)^{1/2}$  is a figure of merit for the bolometer-bridge-amplifier system and should be made as large as is possible with available detectors. To obtain a high figure of merit, the bolometer is made with a small sensitive area, and then  $M_4$  is so designed as to form an image of  $S_2$  which approximately matches the size of the bolometer. The bandwidth  $B$  is chosen to be as narrow as possible, consistent with a tolerable response time. Within the brackets,  $B_\lambda$  is determined by the source temperature, which is limited by the materials of construction of the source; the remaining factors are determined by the optical system. The practical upper limit to  $A$  is usually the area of the grating because this is the most expensive optical element in the system, and its cost rises rapidly with its area. Hence it is made as large as practical and the system designed to utilize it fully. With proper choice

of cell window material and use of a suitably blazed grating for the wavelength range of interest, the factor 3 can be made satisfactorily close to unity. The grating dispersion  $d\theta/d\lambda$  is limited largely by the technical problems associated with the ruling of precision gratings. Practical difficulties of a geometrical nature make it difficult to increase  $h/f$  beyond a certain point.

If the cross-sectional area of the collimated beam is to be large enough to fill the area of the grating, the solid angle  $\Omega$  formed by the rays entering the monochromator through  $S_1$  must not be too small. But  $\Omega$  equals the solid angle subtended at  $S_1$  by  $M_1$  and  $M_2$ . The areas and focal lengths of  $M_1$  and  $M_2$  must be chosen accordingly. Similarly, if all the light emerging from  $S_2$  (in the desired grating order) is to reach the detector, then the solid angles subtended by  $M_7$  at  $S_2$  and by  $M_9$  at  $S_3$  must not be made too small.

### General References

#### NUCLEAR MAGNETIC RESONANCE

- Andrew, "Nuclear Magnetic Resonance," Cambridge University Press, Cambridge, Mass. (1956).  
 Pople, Schneider, and Bernstein, "High Resolution Nuclear Magnetic Resonance," McGraw-Hill Book Company, Inc., New York (1959).  
 Ramsey, "Molecular Beams," Oxford University Press, London (1956).

#### MICROWAVE

- Gordy, Smith, and Trambarulo, "Microwave Spectroscopy," John Wiley & Sons, Inc., New York (1953).  
 Ingraham, "Spectroscopy at Radio and Microwave Frequencies," Butterworth & Co. (Publishers), Ltd., London (1955).  
 Strandberg, "Microwave Spectroscopy," Methuen & Co., Ltd., London (1954).  
 Townes and Schawlow, "Microwave Spectroscopy," McGraw-Hill Book Company, Inc., New York (1955).

#### INFRARED

- Moss, "Modern Infra-red Detectors," *Advances in Spectroscopy*, 1, 175 (1959).  
 Smith, Jones, and Chasmar, "Detection and Measurement of Infra-red Radiation," Oxford University Press, London (1957).  
 Strong, "Concepts of Classical Optics," W. H. Freeman and Company, San Francisco (1958).

#### PERIODICALS AND REVIEW JOURNALS

- Advances in Spectroscopy*  
*Annual Reviews of Physical Chemistry*  
*Canadian Journal of Physics*  
*Journal of Chemical Physics*  
*Journal of Molecular Spectroscopy*  
*Journal of the Optical Society of America*

## CHAPTER 27

# *Electronics*

The object of this chapter is to provide an introduction to certain principles of electronics, at a sufficiently quantitative level to be of practical use to the physical chemist who seeks to understand the capabilities and limitations of electronic circuits well enough to use them intelligently. The coverage is selective rather than broad, with the aim of going deeply enough to enable the reader to utilize the more detailed reference material available in the literature.

A few texts<sup>1</sup> and handbooks,<sup>2</sup> of the many available, are listed below. In general, the handbooks contain concise summaries of principles, along with design equations and other technical information of considerable value, but include a minimum amount of explanatory material. Current developments in the field are reported in a number of periodicals such as *Electronics*, the *Journal of the Instrument Society of America*, and the *Review of Scientific Instruments*. Attention should also be called to the technical literature issued by manufacturers of electronic components and equipment; in this rapidly changing field, this material often represents a valuable source of information covering principles as well as design data.

<sup>1</sup> Terman, "Electronic and Radio Engineering," 4th ed., McGraw-Hill Book Company, Inc., New York (1955). Valley and Wallman (eds.), "Vacuum Tube Amplifiers," Radiation Laboratory Series, Vol. 18, McGraw-Hill Book Company, Inc., New York (1948). Fich and Potter, "Theory of A-C Circuits," Prentice-Hall, Inc., Englewood Cliffs, N.J. (1958). Muller, Garman, and Droz, "Experimental Electronics," Prentice-Hall, Inc., Englewood Cliffs, N.J. (1945). Elmore and Sands, "Electronics: Experimental Techniques," McGraw-Hill Book Company, Inc., New York (1949). Goldman, "Frequency Analysis, Modulation, and Noise," McGraw-Hill Book Company, Inc., New York (1948). Cannon (ed.), "Electronics for Spectroscopists," Interscience Publishers, Inc., New York (1960). Hague, "Alternating Current Bridge Methods," 5th ed., Sir Isaac Pitman & Sons, Ltd., London (1945).

<sup>2</sup> Landee, Davis, and Albrecht, "Electronic Designers' Handbook," McGraw-Hill Book Company, Inc., New York (1957). Terman, "Radio Engineers' Handbook," McGraw-Hill Book Company, Inc., New York (1943).

## ALTERNATING-CURRENT CIRCUIT THEORY

This section contains a résumé of certain principles of a-c circuit theory. While it is not necessary to have a thorough knowledge of this subject in order to assimilate the material in subsequent sections, a good understanding of these principles can be a valuable aid to the physical chemist who uses electronic techniques.

**Basic Circuit Elements.** The three basic elements of a-c networks are the resistor, the capacitor, and the inductor. Each of these is a two-terminal device which can be characterized by a single parameter,  $R$ ,  $C$ , or  $L$ . A resistor is a device for which the value of current  $I$  (entering one terminal and leaving the other) at a given instant depends only on the voltage or potential difference  $E$  existing at that instant between the two terminals. The resistance  $R$  is defined by

$$R = \frac{E}{I} \quad (1)$$

A capacitor is a device capable of storing or accumulating charge, so that the charge  $Q$  which at a given instant has accumulated on one plate depends only on the voltage  $E$  existing between the two terminals at that instant. A charge of equal magnitude and opposite sign exists on the other plate. The capacitance  $C$  is defined by

$$C = \frac{Q}{E} \quad (2)$$

An inductor is a device which generates a well-localized magnetic field when a current passes through it, such that the magnetic flux  $\Phi$  linking the inductor at a given instant depends only on the current through it at that instant. The inductance  $L$  is defined by

$$L = \frac{\Phi}{I} \quad (3)$$

Any real physical device, a coil of wire, for example, shows all three of these properties to some degree, but it is possible to construct devices for which one or the other of these properties is so dominant over the other two as to make the idealization a useful one. Thus a coil of wire of high resistance may be primarily resistive, while a coil of very low resistance wire may be primarily inductive, at the frequency at which it is intended to be used.

While the defining equations (2) and (3) are of course of fundamental importance, one is often more interested in the relationship between instantaneous current and voltage for each of these devices. The three

relations are

$$E = RI \quad (4)$$

$$\frac{dE}{dt} = \frac{1}{C} I \quad (5)$$

$$E = L \frac{dI}{dt} \quad (6)$$

Equation (4) follows directly from (1); Eq. (5), from (2), since  $I$  equals  $dQ/dt$ ; and Eq. (6), from (3), since  $E$  equals  $d\Phi/dt$ .

**Properties of Sinusoidal Waveforms.** Of all the forms of time dependence encountered for voltages and currents in electronic circuits, the sine-wave, or sinusoidal, form is of preeminent importance:

$$A(t) = A_0 \cos(2\pi ft + \varphi) \quad (7)$$

where  $A(t)$  = instantaneous value of current or voltage at time  $t$

$f$  = frequency, cycles/sec

$\varphi$  = phase angle, deg or radians

$A_0$  = amplitude or peak value

As an alternative to the amplitude or peak value, two other measures are commonly used,

$2A_0$  = peak-to-peak value

$A_{rms}$  = root-mean-square value

with  $A_{rms}$  defined by

$$A_{rms} = \left\{ \frac{1}{t_0} \int_0^{t_0} [A(t)]^2 dt \right\}^{1/2} \quad (8)$$

whence

$$A_{rms} = \frac{1}{\sqrt{2}} A_0 = 0.707 A_0 \quad (9)$$

where  $t_0$  = period of one cycle =  $1/f$ .

As a matter of notational convenience,  $A(t)$  is often written

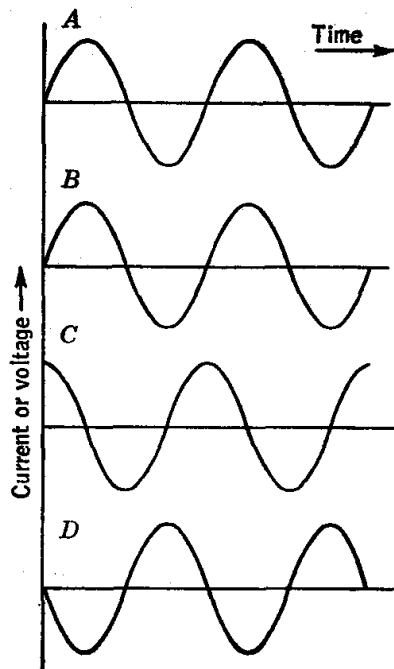
$$A(t) = A_0 \cos(\omega t + \varphi) \quad (10)$$

where  $\omega = 2\pi f$  = circular frequency, in radians per second.

Several of the possible phase relationships which can exist between two sinusoidal waveforms are illustrated in Fig. 152. Two

FIG. 152. Phase relationships for sinusoidal waveforms.

sinusoids are said to be *in phase* if they pass through corresponding points of their respective cycles at the same instant, as, for example,  $A$  and  $B$  of Fig. 152. Waveforms  $A$  and  $C$  are said to be  $90^\circ$  *out of phase*, while  $A$



and  $D$  are  $180^\circ$  out of phase. Waveform  $D$  is said to *lead*  $C$  by  $90^\circ$ , while  $B$  *lags*  $C$  by  $90^\circ$ .

It is useful to remember that an arbitrary sinusoidal wave, such as  $A(t)$  of Eq. (7), can be resolved into a pure sine and a pure cosine term of the same frequency  $f$ :

$$A_0 \cos(2\pi ft + \varphi) = (A_0 \cos \varphi) \cos 2\pi ft - (A_0 \sin \varphi) \sin 2\pi ft \quad (11)$$

Often it is necessary to find the waveform  $B(t)$  which results when two sinusoidal waveforms  $A'(t)$  and  $A''(t)$  of the same frequency are added:

$$B(t) = A'(t) + A''(t) \quad (12)$$

$$\text{where } A'(t) = A'_0 \cos(\omega t + \varphi') \quad (13)$$

$$A''(t) = A''_0 \cos(\omega t + \varphi'') \quad (14)$$

One could imagine plotting the two waveforms and adding the instantaneous values point by point, but this is awkward as a quantitative

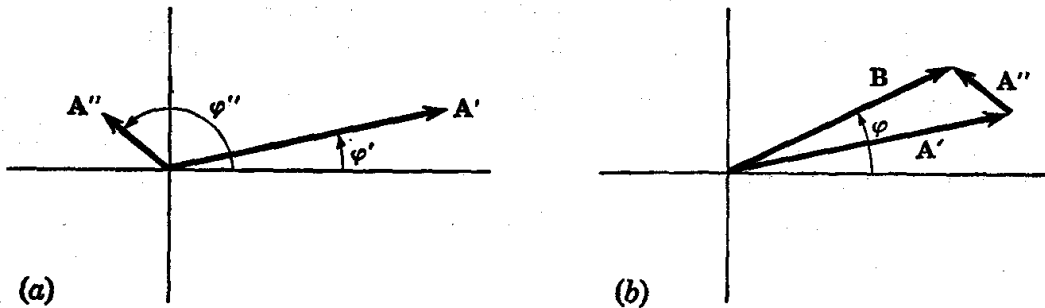


FIG. 153. Vector diagrams illustrating (a) vectors representing sinusoids  $A'(t)$  and  $A''(t)$  at  $t = 0$  and (b) addition of two sinusoids to form a resultant.

procedure, and not even particularly helpful as a way of visualizing the resultant. Two efficient methods of obtaining the sum will be described below, but it is worth noting that both are really based on Eq. (11). The waveforms  $A'(t)$  and  $A''(t)$  can each be resolved into sine and cosine terms; then the sine terms can be added directly, and similarly for the cosine terms. There is a clear analogy here with the composition of two vectors to form a resultant, an analogy which is of considerable help in understanding a-c circuit problems.

**Method A: Vector Diagrams.** The waveforms  $A'(t)$  and  $A''(t)$  can each be considered to be generated by rotation of a vector<sup>1</sup> of constant length in a plane. Thus let two vectors  $A'$  and  $A''$  be arranged as in Fig. 153a at  $t = 0$ . If these rotate counterclockwise with circular frequency  $\omega$ , the components along the horizontal axis generate, respectively,  $A'(t)$  and

<sup>1</sup> To avoid the connotation of geometrical significance which sometimes is attached to the term *vector*, the rotating vector which generates a sinusoidal waveform is called in many electrical-engineering texts a *phasor*, or *sinor*.



$A''(t)$ . Obviously, the vector sum  $\mathbf{B}$  formed in the usual way from  $\mathbf{A}'$  and  $\mathbf{A}''$  similarly generates  $B(t) = A'(t) + A''(t)$ . The amplitude and phase angle of  $B(t)$  are thus obtained readily, as shown in Fig. 153b. The amplitudes of the sine and cosine components of  $B(t)$  can also easily be found from this diagram as the projections at  $t = 0$  of the vector sum along the vertical and horizontal axes, respectively.

*Method B: Complex Algebra.* When it is desired to perform a calculation analytically rather than graphically, the vector diagrams obviously provide the basis for setting up the necessary equations, and this procedure is often followed. A more powerful analytical method, however, is available with the use of complex algebra. The rules for manipulation of complex quantities and the procedure for graphing them are summarized in the Appendix.

With each of the vectors of Fig. 153 we can associate a complex number, as follows:

Component along horizontal axis  $\longleftrightarrow$  real part

Component along vertical axis  $\longleftrightarrow$  imaginary part

In other words, we regard the diagram of Fig. 153 as existing in a complex plane and associate with each vector  $\mathbf{A}'$ ,  $\mathbf{A}''$ , . . . , the complex number corresponding to its terminus. Since there is a one-to-one correspondence between these vectors and complex numbers, the same symbol can be used for both. We get, for  $t = 0$ ,

$$\mathbf{A}' = A'_0 e^{i\varphi'} = A'_0 \cos \varphi' + iA'_0 \sin \varphi' \quad (15)$$

$$\mathbf{A}'' = A''_0 e^{i\varphi''} = A''_0 \cos \varphi'' + iA''_0 \sin \varphi'' \quad (16)$$

etc. The addition of two vectors then corresponds analytically to the addition of two complex numbers.

One advantage of complex notation is that the time dependence of rotating vectors can be represented in a very compact fashion. For example, the rotating vectors  $\mathbf{A}'(t)$  and  $\mathbf{A}''(t)$  are represented by the complex numbers

$$\mathbf{A}'(t) = A'_0 e^{i(\omega t + \varphi')} \quad (17)$$

$$\mathbf{A}''(t) = A''_0 e^{i(\omega t + \varphi'')} \quad (18)$$

Thus the sinusoidal waveforms  $A'(t)$  and  $A''(t)$  of Eqs. (13) and (14) can be thought of as the *horizontal components* of two rotating vectors or, equally well, as the *real parts* of two complex numbers.

These methods become particularly helpful in visualizing the addition of two sinusoidal waveforms of different frequency. Suppose, for example, one wishes to add the waveforms

$$C'(t) = C'_0 \cos \omega' t \quad (19)$$

$$C''(t) = C''_0 \cos \omega'' t \quad (20)$$

The corresponding vectors  $\mathbf{C}'(t)$  and  $\mathbf{C}''(t)$  rotate at different frequencies. The horizontal component of the resultant is not a simple sinusoidal waveform. For example, for  $\omega' \cong \omega''$ , the resultant could be described approximately as a sinusoidal waveform with slowly changing amplitude (phenomenon of beating).

**Impedance.** If the current

$$I_0 \cos(\omega t + \phi) \quad (21)$$

is passed through a resistor, capacitor, or inductor, the *steady-state* voltage  $E(t)$  developed across the device is, from Eqs. (4) to (6):

$$\text{For the resistor:} \quad E_R(t) = RI_0 \cos(\omega t + \phi) \quad (22)$$

$$\text{For the capacitor:} \quad E_C(t) = \frac{1}{\omega C} I_0 \sin(\omega t + \phi) \quad (23)$$

$$\text{For the inductor:} \quad E_L(t) = -(\omega L)I_0 \sin(\omega t + \phi) \quad (24)$$

These results are illustrated by the vector diagram of Fig. 154. The

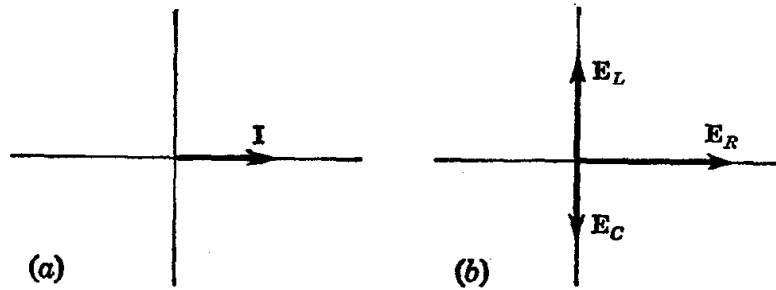


FIG. 154. Vector diagrams representing (a) assumed current and (b) resulting voltages for resistor, capacitor, and inductor. The vectors are shown for  $t = 0$ . They rotate counterclockwise with circular frequency  $\omega$ . The actual currents and voltages are the components along the horizontal axes.

corresponding equations in complex form are obtained by writing the expression for the current,

$$\mathbf{I}(t) = I_0 e^{i(\omega t + \phi)} \quad (25)$$

and relating the complex voltages to  $\mathbf{I}(t)$  through the use of Eqs. (4) to (6); the results are

$$\mathbf{E}_R(t) = R\mathbf{I}(t) \quad (26)$$

$$\mathbf{E}_C(t) = \frac{1}{i\omega C} \mathbf{I}(t) \quad (27)$$

$$\mathbf{E}_L(t) = (i\omega L)\mathbf{I}(t) \quad (28)$$

The reader may verify that Eqs. (26) to (28) are consistent with the vector diagrams of Fig. 154. These equations may be thought of as

providing a generalization of Ohm's law to the case of sinusoidal voltages and currents in a-c circuits. The great utility of the complex notation can now be appreciated. The relationship between current and voltage takes on a particularly simple and easily remembered form. Furthermore, the equations in complex form are immediately related to the vector diagrams, an important aid to visualization.

Equations (26) to (28) all have the form

$$\mathbf{E}(t) = Z\mathbf{I}(t) \quad (29)$$


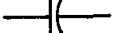
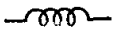
where  $Z$  is a complex number. The quantity  $Z$  which relates  $\mathbf{E}(t)$  and  $\mathbf{I}(t)$  in this way is called the *impedance*. The reciprocal of  $Z$  is a complex number  $Y = Z^{-1}$ , called the *admittance*, in terms of which Eq. (29) becomes

$$\mathbf{I}(t) = Y\mathbf{E}(t) \quad (30)$$

Admittance and impedance then represent extensions of the concepts of conductance and resistance, respectively. Table 1 gives the admittances and impedances of the basic circuit elements.

An element of a circuit is said to be *linear* if its impedance  $Z$  is independent of the amplitude of the current through it and of the voltage across it.

TABLE 1. ADMITTANCES AND IMPEDANCES OF THE BASIC CIRCUIT ELEMENTS

Element	Parameter	Symbol	Impedance	Admittance
Resistor.....	$R$		$R$	$1/R$
Capacitor.....	$C$		$1/i\omega C$	$i\omega C$
Inductor.....	$L$		$i\omega L$	$1/i\omega L$

**Impedance of a Network.** If a specified sinusoidal current  $I(t)$  passes into a network at one terminal and out at another, some definite steady-state voltage  $E(t)$  will exist between these terminals. The impedance  $Z$  which relates  $I(t)$  and  $E(t)$  through Eq. (29) is called the impedance of the network between these terminals.

If two elements with impedances  $Z_1$  and  $Z_2$  are connected in *series*, the equivalent impedance  $Z_S$  for the combination is

$$Z_S = Z_1 + Z_2 \quad (\text{series case}) \quad (31)$$

If two elements with admittances  $Y_1$  and  $Y_2$  are connected in *parallel*, the equivalent admittance  $Y_P$  for the combination is

$$Y_P = Y_1 + Y_2 \quad (\text{parallel case}) \quad (32)$$

For networks which can be written in a plane diagram without cross-overs, reduction to a single equivalent impedance is always possible by successive application of Eqs. (31) and (32), together with the general relation  $Z = Y^{-1}$ . For networks not amenable to this approach, the more general methods of mesh and nodal analysis are particularly useful.<sup>1</sup>

For any given frequency, complex impedances (or admittances) may be plotted in a complex plane and added like vectors. Figure 155 illustrates this *graphical* method of addition for the case of a resistor and capacitor.

The *magnitude*  $Z_0$  of an impedance  $Z$  is defined as the magnitude of the complex number  $Z$  and may be visualized as the length of the vector

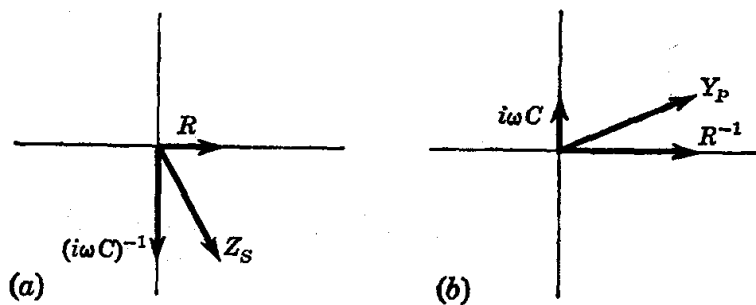


FIG. 155. Vector diagrams illustrating (a) the impedance of a series combination of  $R$  and  $C$  and (b) the admittance of a parallel combination of  $R$  and  $C$ .

from the origin to the point  $Z$  in a complex plane. If the current and voltage amplitudes are  $I_0$  and  $V_0$ , respectively, it is easily shown that these are related by

$$E_0 = Z_0 I_0 \quad (33)$$

It may be noted that the rms values are similarly related:



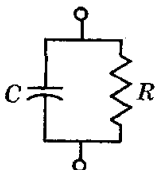

$$E_{\text{rms}} = Z_0 I_{\text{rms}} \quad (34)$$

The *algebraic* procedure for finding the impedance of a network can best be mastered by working out a few examples. Several are given in Table 2. It is instructive to examine the frequency dependence of  $Z$  and of  $Z_0$  for each of these networks.

Two physically different networks which have the same impedance are called *equivalent networks*. The equivalence may exist only at a single frequency or may hold over a wide range of frequencies. Examples will be encountered below.

<sup>1</sup> These methods are treated, for example, in Fich and Potter, *op. cit.*, and Landee *et al.*, *op. cit.*

TABLE 2. IMPEDANCES OF SEVERAL NETWORKS

Network	$Z$	$Z_0$
	$R - i\left(\frac{1}{\omega C}\right)$	$\left[R^2 + \frac{1}{\omega^2 C^2}\right]^{1/2}$
	$R + i\omega L$	$[R^2 + \omega^2 L^2]^{1/2}$
	$\left[\frac{1}{R} + i\omega C\right]^{-1}$	$\left[\frac{R^2}{1 + \omega^2 R^2 C^2}\right]^{1/2}$
	$R + i\left(\omega L - \frac{1}{\omega C}\right)$	$\left[R^2 + \left(\omega L - \frac{1}{\omega C}\right)^2\right]^{1/2}$

**Parallel Resonant Circuit.** A very common and important network, the parallel resonant circuit is shown in Fig. 156a. The resistance  $R$  shown is usually not present in the actual circuit as a separate component, but represents the effective resistance of the coil. The quality factor  $Q$  of the coil is defined by

$$Q = \frac{\omega L}{R} \quad (35)$$

A coil is said to possess a high  $Q$  if  $Q \gg 1$ . Both  $Q$  and  $R$  depend on frequency, but may often be considered constant over narrow ranges of frequency.

The impedance  $Z$  and its magnitude  $Z_0$  may be obtained by a straight-

forward calculation; the results are, for  $Q \gg 1$ ,

$$Y = \frac{1}{R + i\omega L} + i\omega C \quad (36)$$

$$Z \cong \omega L Q \frac{1}{1 + iQu} \quad (37)$$

where

$$u = \omega^2 LC - 1 = \frac{\omega^2 - \omega_0^2}{\omega_0^2} \quad (38)$$

$$\omega_0 = \frac{1}{(LC)^{1/2}} \quad (39)$$

The function  $Z_0(\omega)$  is plotted in Fig. 156b. It has a peak at  $\omega = \omega_0$  and

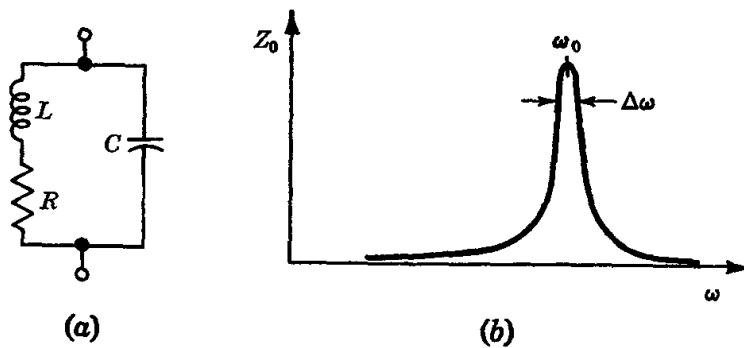


FIG. 156. (a) Parallel resonant circuit; (b) graph of  $Z_0$  against frequency for parallel resonant circuit.

is sharply resonant for  $Q \gg 1$ . The *bandwidth*  $\Delta\omega$  is defined as the separation between the two points at which  $Z_0 = Z_{\max}/\sqrt{2}$ . From Eq. (37) this is seen to depend on  $Q$ :

$$\frac{\Delta\omega}{\omega_0} = \frac{1}{Q} \quad (40)$$

For the high- $Q$  case,  $Z_0$  can be written, when  $\omega + \omega_0 \cong 2\omega_0$ , as

$$Z_0 \cong \omega L Q \left( \frac{1}{1 + 4[(\omega - \omega_0)/\Delta\omega]^2} \right)^{1/2} \quad (41)$$

which shows clearly how the decrease of  $Z_0$  from its peak value depends on the magnitude of  $\omega - \omega_0$  relative to the bandwidth  $\Delta\omega$ . A useful result to remember is that the impedance at resonance for the high- $Q$  case is  $\omega L Q$ .

If a voltage is to be injected in series with the coil of Fig. 156a, this same network can usefully be treated as a *series LRC* circuit. The analysis for this case is presented in Exp. 37 (page 227).

**Active Circuit Elements.** The circuit elements considered thus far are capable of dissipating or storing electromagnetic energy but not of

generating it. On the other hand, there are circuit elements, such as batteries or vacuum tubes, which act as sources of electromagnetic energy within a network. Such elements are called *active* elements.

An important property of an active element is its *internal impedance*. A simple illustration of this concept is provided by a battery. The voltage measured at the terminals falls below the open-circuit value when current is drawn. To a certain degree of approximation, an actual battery, then, is equivalent to a constant-voltage d-c generator (of zero

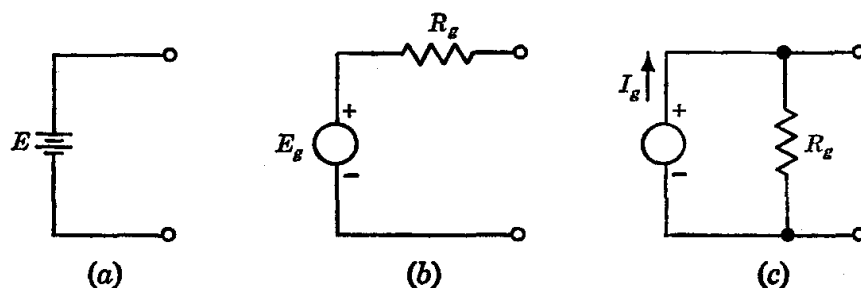


FIG. 157. Equivalent generators. (a) Actual circuit; (b) equivalent constant-voltage generator with series resistance; (c) equivalent constant-current generator with parallel conductance.

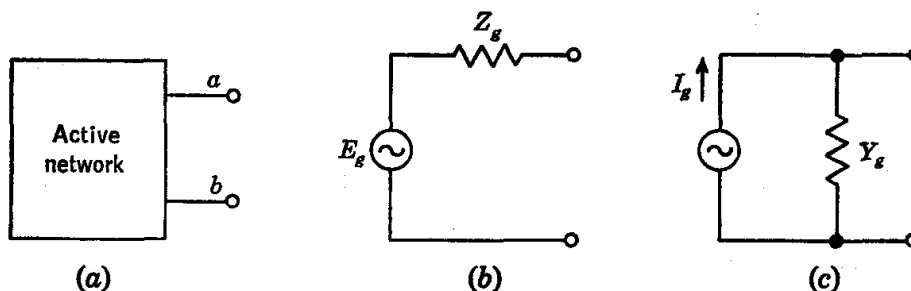


FIG. 158. (a) Active network; (b) equivalent network, by Thévenin's theorem; (c) equivalent network, by Norton's theorem.

impedance) acting in series with a fictitious resistance  $R_g$ , called the internal impedance of the battery. An entirely equivalent representation is that of a constant-current generator (of infinite impedance) acting in parallel with a conductance  $G_g = R_g^{-1}$ . These are represented in Fig. 157. The circuits (b) and (c) are equivalent to  $a$  in the sense that for any load impedance connected across the terminals, the current through the load and the voltage across it are the same for the two fictitious circuits as for the actual circuit (a).

**Thévenin's Theorem.** Suppose one has a network (Fig. 158a) which contains one or more active elements and which delivers power to a load of impedance  $Z_L$  connected across two terminals  $a$  and  $b$  of the network. For the purpose of calculating the current through (or voltage across)

the load, the active network can be replaced by an equivalent network (Fig. 158b), consisting of an idealized voltage generator  $E_o$  acting in series with an internal impedance  $Z_o$ , where  $E_o$  is the voltage produced between the output terminals  $a$  and  $b$  when the load is removed, and  $Z_o$  is the impedance measured between output terminals with load removed and with the active elements of the network replaced by their internal impedances. This is Thévenin's theorem. Stated briefly,

$E_o$  = open-circuit voltage of the active network

$Z_o$  = output impedance of the active network

An alternative equivalent circuit (Fig. 158c) for the active network is given by Norton's theorem. The idealized constant-current generator  $I_o$  here acts in parallel with an admittance  $Y_o$ , where  $I_o$  is the current which would pass from terminal  $a$  to  $b$  through a load of zero impedance (short-circuit current), and  $Y_o = Z_o^{-1}$  is the output admittance of the active network.

**Impedance Matching.** If a variable resistive load  $R_L$  is placed across the terminals of the battery of Fig. 157a, the power  $P$  delivered to the load is

$$P = I_L^2 R_L = \left( \frac{E_o}{R_o + R_L} \right)^2 R_L \quad (42)$$

where  $I_L$  is the current through the load. It is easily shown that  $P$  is a maximum for  $R_L = R_o$ .

More generally, if a device of fixed output impedance  $Z_1$  delivers power to a second device of input impedance  $Z_2$ , it can be shown that the power delivered to the second device is a maximum for the condition

$$Z_1 = Z_2^* \quad (43)$$

where  $Z_2^*$  is the complex conjugate of  $Z_2$ . The impedances are said to be *matched* when Eq. (43) holds.

**Magnetic Coupling.** Figure 159a shows two circuits which are coupled only through the magnetic flux common to the two coils. A change in current through coil 1 results in a changing magnetic flux which induces a voltage in coil 2. The mutual inductance  $M$  is given by

$$M = k \sqrt{L_1 L_2} \quad (44)$$

where  $L_1$  and  $L_2$  are the inductances of the separate coils, and  $k$  is the coefficient of coupling, which has its maximum value, unity, if all the flux generated by a current in one coil links the other coil. For the purpose of calculating current through the load  $Z$ , the network of Fig. 159b is equivalent to that of Fig. 159a.

Two limiting cases will be considered further. For sufficiently *loose*



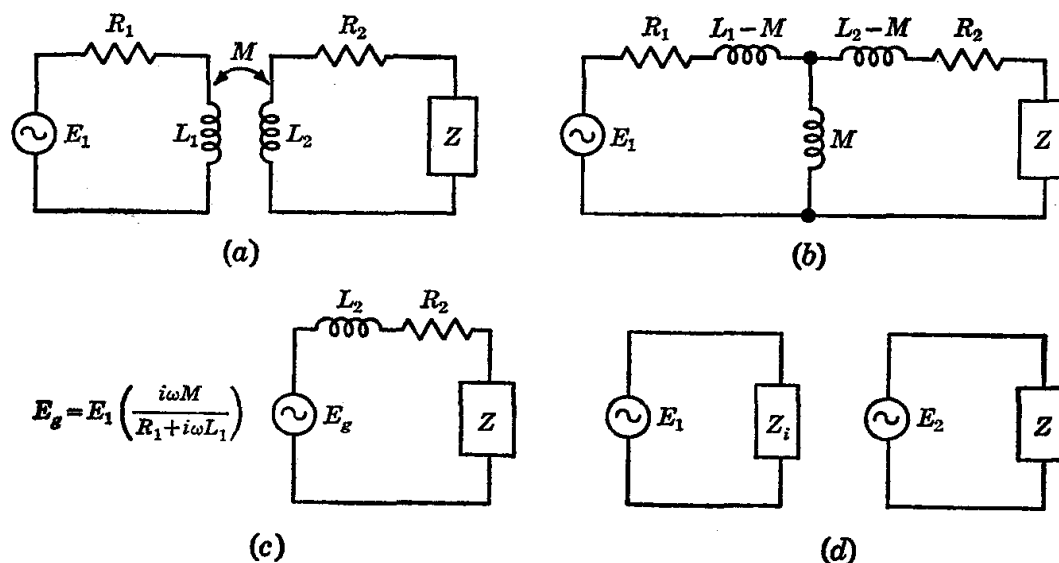


FIG. 159. (a) Magnetically coupled circuit; (b) equivalent circuit; (c) equivalent circuit for sufficiently loose coupling; (d) equivalent circuit for close coupling, under approximations specified by Eqs. (46) to (48).

coupling, i.e., such that

$$\omega M \ll |i\omega(L_2 - M) + R_2 + Z| \quad (45)$$

the equivalent secondary circuit reduces to that of Fig. 159c.

For very *close* coupling, that is,  $k \cong 1$ , and under the additional assumptions,

$$R_1 \ll \omega L_1 \quad (46)$$

$$R_2 \ll \omega L_2 \quad (47)$$

$$Z \ll \omega L_2 \quad (48)$$

the equivalent circuit reduces to Fig. 159d and the more familiar equations for transformer coupling are obtained:

$$\frac{E_2}{E_1} = \frac{N_2}{N_1} \quad (49)$$

$$Z_i = \left(\frac{N_1}{N_2}\right)^2 Z \quad (50)$$

where  $N_1$  = number of turns in primary winding

$N_2$  = number of turns in secondary winding

The point to be especially noticed is that the impedance effectively presented to the voltage source  $E_1$  is the so-called *reflected* impedance  $Z_i$ , rather than the actual load impedance  $Z$ . Thus a closely coupled transformer of proper design [consistent with Eqs. (46) to (48)] can be used to match the impedance of a given load to the impedance of a given voltage

generator. This is an efficient and useful arrangement because, to the extent that the above conditions can be met, the match is independent of frequency and is achieved with negligible loss of power.

**Response to Nonsinusoidal Excitation.** Since the concept of impedance is defined only for sinusoidal waveforms, the above methods of analysis are not directly applicable when nonsinusoidal functions are encountered. Three avenues of approach which are used in treating nonsinusoidal cases will be mentioned here:

1. Equations (4) to (6) are still applicable and for relatively simple networks often yield the required information quite readily. Thus, for

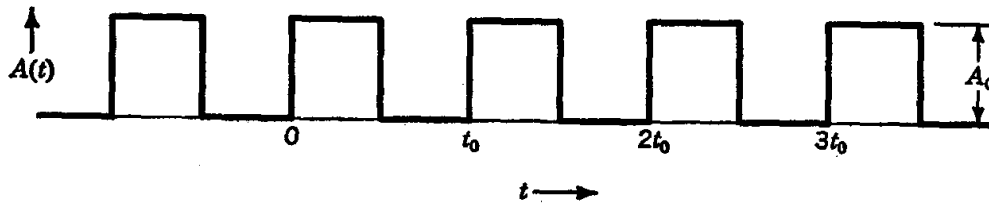


Fig. 160. Zero-based square wave, of period  $t_0$  and peak amplitude  $A_0$ .

example, application of a step function of voltage to a resistor and capacitor in series leads to the familiar exponential growth of the voltage across the capacitor and the exponential decay of the voltage across the resistor.

2. The methods of Fourier series analysis are applicable if the waveform is periodic. Thus, for example, the zero-based square wave  $A(t)$  of Fig. 160 can be expanded in the series<sup>1</sup>

$$A(t) = \frac{1}{2}A_0 + \frac{2}{\pi}A_0 \left( \sin \omega_0 t + \frac{1}{3} \sin 3\omega_0 t + \frac{1}{5} \sin 5\omega_0 t + \cdots \right) \quad (51)$$

where  $\omega_0 = \text{fundamental frequency} = 2\pi/t_0$ . The impedance of the circuit being known as a function of frequency, one can apply the methods for sinusoidal waveforms separately to each term.

The method of Fourier analysis is also very helpful in a qualitative way. Thus, for example, if a complex voltage waveform is applied to a series  $RC$  circuit, one can immediately see that Fourier components at frequencies  $f \ll 1/2\pi RC$  will appear principally across the capacitor, while components at frequencies  $f \gg 1/2\pi RC$  will appear principally across the resistor. Thus a degree of separation of the Fourier components of the input voltage according to frequency is achieved with this circuit.

3. The method of Fourier integral analysis<sup>1</sup> and the closely related

<sup>1</sup> A particularly good introduction to the use of Fourier analysis in a-c circuit theory is given by Goldman, *op. cit.*

method of the Laplace transform<sup>1</sup> represent very efficient tools for analyzing the response of a circuit to a wide variety of waveforms, both periodic and nonperiodic.

**Amplitude Modulation and Detection.** An amplitude-modulated wave may be visualized as a sinusoid with amplitude a function of time. The simplest example is that of pure-sine-wave modulation, shown in Fig. 161a.

The waveform

$$A(t) = A_0(1 + m \cos \omega_m t) \cos \omega t \quad (52)$$

is produced when the carrier  $A_0 \cos \omega t$  is modulated at frequency  $\omega_m$ . The

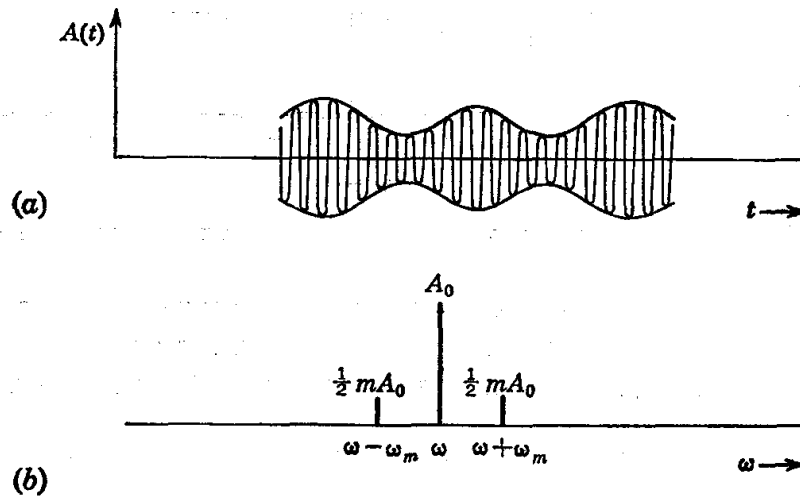


FIG. 161. (a) Amplitude-modulated waveform; (b) frequency spectrum of waveform bearing pure-sinusoidal modulation at a single modulation frequency  $\omega_m$ .

coefficient  $m$  is the *degree of modulation*,  $\omega_m$  is the *modulation frequency*, and  $\cos \omega_m t$  is the *modulation waveform*.

With the use of familiar trigonometric identities,  $A(t)$  may be written in the alternative form

$$A(t) = A_0 \cos \omega t + \frac{1}{2} m A_0 \cos (\omega + \omega_m) t + \frac{1}{2} m A_0 \cos (\omega - \omega_m) t \quad (53)$$

i.e., as a superposition of three pure sinusoids, a carrier and two *sidebands*. Equation (53) is really an illustration of the Fourier theorem. The frequency spectrum of  $A(t)$  is shown in Fig. 161b. It is important to note that  $A(t)$  does not contain a component at the modulation frequency  $\omega_m$ .

For the general case  $A(t) = A_0[1 + m(t)] \cos \omega t$  with a more complicated modulation waveform  $m(t)$ , additional sideband pairs appear. For example, if  $m(t)$  is a square wave, then a pair of sidebands is produced for each term in Eq. (51) beyond the first.

<sup>1</sup> An elementary introduction to the use of Laplace transforms for the analysis of network response is given by Fich and Potter, *op. cit.*

Given a modulated waveform, the process of extracting the waveform which corresponds to the envelope (or a reasonable approximation thereof) is called *detection*. A practical detector circuit is described on page 573.

**Frequency Modulation.** A frequency-modulated waveform is produced if the frequency of a sinusoidal waveform is made to vary with time. For modulation by a pure sinusoid, the instantaneous frequency is

$$\omega = \omega_c + (\Delta\omega) \cos \omega_m t$$

where  $\omega_c$  = carrier frequency

$\omega$  = instantaneous frequency of frequency-modulated waveform

$\Delta\omega$  = peak frequency deviation

$\omega_m$  = modulation frequency

The expression for the frequency-modulated waveform for this case is

$$A(t) = A_0 \cos \left( \omega_c t + \frac{\Delta\omega}{\omega_m} \sin \omega_m t + \phi \right) \quad (54)$$

where  $\phi$  is the phase angle. Equation (54) has the form  $A_0 \cos \theta(t)$  with  $d\theta/dt$  equal to  $\omega$ . The analysis of  $A(t)$  into Fourier components leads to a frequency spectrum which consists of sideband pairs at  $(\omega_c \pm \omega_m)$ ,  $(\omega_c \pm 2\omega_m)$ ,  $(\omega_c \pm 3\omega_m)$ , . . . , as contrasted with a single pair for the corresponding amplitude-modulation case. Another difference between the two types of modulation is in the phase relationships which exist among the sidebands.

**Mixing.** The operation of combining two or more waveforms in a nonlinear impedance in order to generate sum and difference frequencies is known as *mixing* or *heterodyning*.

As a simple example, suppose the two voltages

$$E_1 = E_{01} \cos \omega_1 t \quad (55)$$

$$E_2 = E_{02} \cos \omega_2 t \quad (56)$$

are applied in series to a diode (see pages 572–573) for which the current-voltage characteristic is represented well enough by the relation

$$I = aE + bE^2 \quad (57)$$

between instantaneous voltage and current. If the substitution

$$E = E_1 + E_2$$

is made in Eq. (57), the resulting current includes, among others, the term

$$bE_{01}E_{02}[\cos(\omega_1 + \omega_2)t + \cos(\omega_1 - \omega_2)t] \quad (58)$$

as the reader may easily show. If this current is made to flow through a resistor, the resulting voltage includes components at the sum and difference frequencies. (There are also components at  $\omega_1$ ,  $\omega_2$ ,  $2\omega_1$ , and  $2\omega_2$ .) It is especially to be noticed that the sum and difference frequency terms disappear if  $b$  vanishes. It is for this reason that a nonlinear impedance was specified; merely combining  $E_1$  and  $E_2$  in a linear network, however complicated, will not yield any output except at the original frequencies.

**Harmonic Generation.** If a pure sinusoidal voltage of frequency  $\omega_1$  is applied to a nonlinear impedance, the resulting current contains components at  $\omega_1$ ,  $2\omega_1$ ,  $3\omega_1$ , . . . . The process is similar to mixing, the higher harmonics being generated by higher-order terms in the current-voltage characteristic. Practically, this result is achieved by making the amplitude of the driving signal large.

Probably the most common use of harmonic generation is in frequency measurement. Given an oscillator which supplies an accurately known frequency, one may employ harmonic-generating circuits to produce a whole series of higher frequencies of comparable accuracy. The frequency of an unknown signal can then be compared with the nearest of these harmonics by mixing the two voltages and measuring the difference frequency.

**Bandwidth and Response Time.** The frequency-response characteristics of an amplifier<sup>1</sup> can be specified by giving the voltage amplitude gain  $G(f)$  for a sinusoidal waveform as a function of frequency.

The *half-power bandwidth*  $\mathcal{B}$  is defined by

$$\mathcal{B} = f_2 - f_1 \quad (59)$$

where  $f_1$  and  $f_2$  are the frequencies at which the power gain has dropped to half its peak value, or  $G(f)$  to 0.707 times its peak value. The half-power bandwidth is illustrated in Fig. 162a for a low-pass amplifier and in Fig. 162b for a bandpass amplifier. It is usually easy to determine  $\mathcal{B}$  experimentally.

If a step function of voltage (which might be the leading edge of a pulse) is applied at the input of a low-pass amplifier, the resulting output voltage does not reach its final value instantaneously, but rather approaches it monotonically or with one or more crossings of the final value. If the output does go beyond the final value momentarily, the maximum amount by which the final value is exceeded is called the *overshoot*. For a *low-pass* amplifier with little or no overshoot, the rise time  $\tau$ , defined as the time required for the output resulting from a step-

<sup>1</sup> The statements in this section actually apply to any linear network with two input terminals and two output terminals. The most common applications are to filters and amplifiers.

function input to rise from 10 to 90 per cent of its final value, is related approximately to the bandwidth by<sup>1</sup>

$$\tau B \cong 0.35 \quad (60)$$

Similarly, if an a-c voltage is suddenly applied at the input to a *band-pass* amplifier having little or no overshoot, the rise time, 10 to 90 per cent,

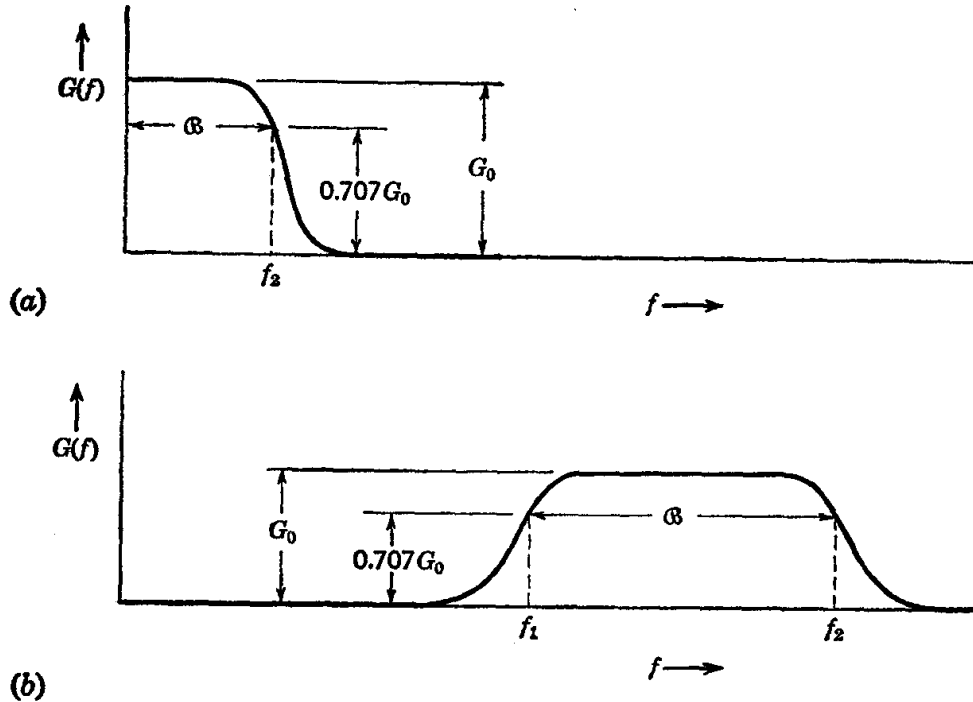


FIG. 162. Frequency-response characteristics and half-power bandwidths for (a) low-pass amplifier and (b) bandpass amplifier. The function  $G(f)$  is the voltage or current gain.

of the envelope of the resulting output a-c voltage approximately satisfies the relation<sup>2</sup>

$$\tau B \cong 0.7 \quad (61)$$

In general, then, since the response time varies inversely with the bandwidth, an amplifier of wide bandwidth must be employed if fast response is required.

## VACUUM TUBES

A vacuum tube consists of a number of electrodes mounted in an envelope of glass or metal, which is usually highly evacuated but which, for specific applications, may contain a suitable gas at low pressure.

<sup>1</sup> Walker and Wallman in Valley and Wallman (eds.), *op. cit.*, Chap. 2.

<sup>2</sup> Wallman in Valley and Wallman (eds.), *op. cit.*, Chap. 7.

One electrode, the *cathode*, supplies the electrons required for the operation of the tube. In the high-vacuum tubes and in most gas-filled tubes, the electrons are produced by thermionic emission. The cloud of electrons produced around the heated cathode is termed the *space charge*. The cathode may be of the filamentary type, i.e., a wire heated by the passage of an electric current, or of the indirectly heated type, in which the electron-emitting material is placed on the outside surface of a sleeve which is heated by a separate filament placed within it.

The other electrodes serve to collect the electrons passing through the tube or to control their flow. Most of the collecting is done by one electrode in particular, called the *plate*. The control electrodes are usually referred to as *grids*.

**The Diode and Rectification.** The diode contains two electrodes, a cathode and a plate. If the plate is maintained at a potential positive

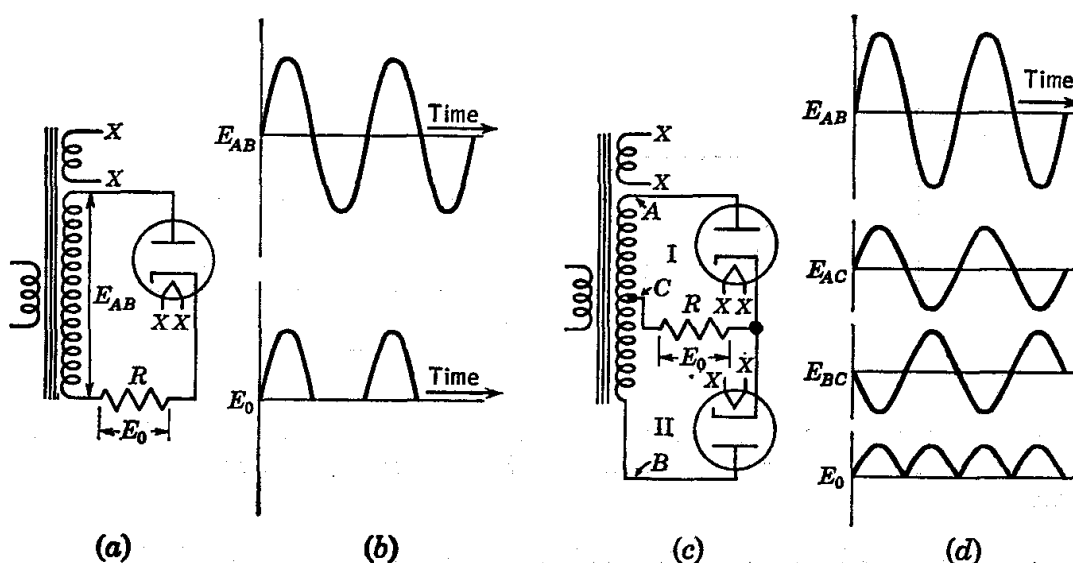


FIG. 163. Diode rectification and voltage waveforms. (a), (b) Half-wave-rectifier circuit; (c), (d) full-wave-rectifier circuit.

with respect to the cathode, electrons will be drawn to it from the space charge, where the electron density will be maintained by emission of electrons from the hot cathode. When the plate is negative with respect to the cathode, no electrons will be attracted to it. The diode thus provides a means of controlling the direction of flow of an electric current.

This property is applied in the conversion of alternating current to direct current, a process called rectification. The basic circuit employed is shown in Fig. 163a. Let an alternating voltage  $E_{AB}$  be impressed across the input terminals. During one half-cycle of the applied voltage, the plate will be positive with respect to the cathode, and current will flow through the tube and through the series load resistor  $R$ , producing a

potential drop  $E_0$  which will vary during this half-cycle as shown in Fig. 163b. During the other half of the cycle, the plate is negative with respect to the cathode; no current flows through the tube, and the potential drop  $E_0$  across the load resistor  $R$  is zero. This circuit is called a half-wave rectifier circuit. The maximum value of  $E_0$  is less than the crest value of  $E_{AB}$  because of the potential drop between the cathode and plate.

Both halves of the a-c wave are utilized in the full-wave rectifier circuit of Fig. 163c. During the half-cycle of the applied voltage in which point  $A$  is positive and  $B$  negative with respect to  $C$ , only diode I will conduct, producing a current through  $R$ , the load resistor. During the next half-cycle,  $B$  will be positive and  $A$  negative with respect to  $C$  and only diode II will conduct, producing a current which flows through  $R$  in the same direction as that of the previous half-cycle. The output voltage  $E_0$  across the load resistor then takes the form shown in Fig. 163d. The filtering of this pulsating voltage to obtain a steady d-c potential is discussed below.

**The Triode and Amplification.** The most important applications of vacuum tubes result from the control of the magnitude of the tube current which is made possible by the introduction of additional electrodes. The triode contains, in addition to a cathode and a plate, a third electrode called the *control grid* (or merely *grid*), which ordinarily consists of a wire helix surrounding the cathode and extending its full length, as shown in Fig. 164.

A triode is generally operated with a positive potential  $E_p$  applied to the plate and a much smaller negative potential  $E_c$  applied to the grid, both potentials being defined conventionally relative to the cathode. The current collected by the plate is denoted by  $I_p$ . Figure 165 shows a triode in a simple experimental circuit with variable potentials applied for the study of the relationship of plate current to plate and grid potentials. With the grid negative as shown, the current to the grid is negligible in many applications.<sup>1</sup>

<sup>1</sup> A small grid current may result from the flow of positive ions produced from residual gas in the tube and from the small fraction of the electrons in the space charge which have sufficient kinetic energy to reach the grid despite its negative potential. This current may be a serious source of noise in very sensitive amplifier circuits. There is also an a-c grid current due to interelectrode capacitance effects when an a-c voltage is applied to the grid.

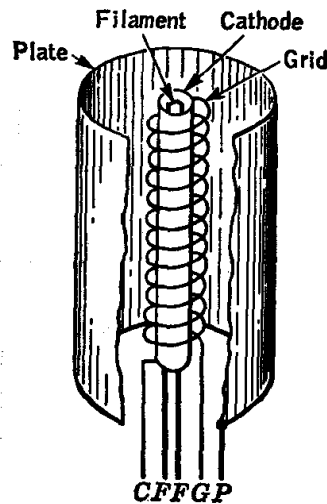


FIG. 164. Electrode arrangement of triode.



The plate current depends on both plate and grid potentials, the latter having the greater influence because it is so much closer to the cathode and space charge. Thus the grid acts somewhat as a valve which controls the flow of electrons to the plate. The dependence of  $I_p$  on the plate and grid potentials is given quantitatively by *characteristic curves*, such as those of Fig. 166.

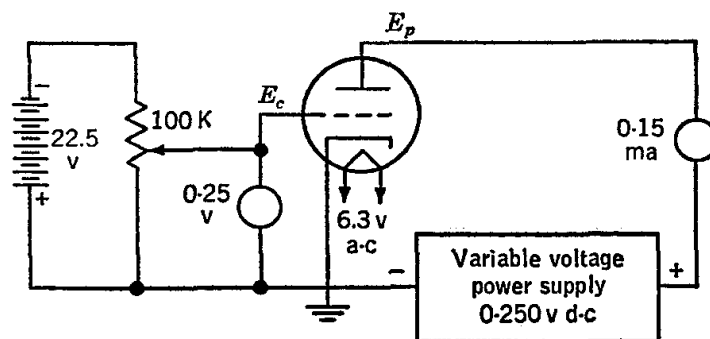


FIG. 165. Circuit for the determination of characteristic curves for a triode.

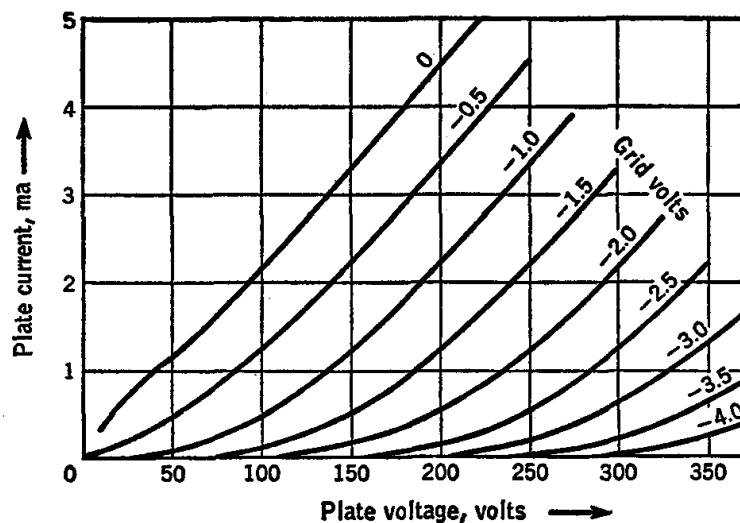


FIG. 166. Characteristics for 12AX7 triode.  $I_p$  versus  $E_p$  at constant  $E_c$ .

Amplification is made possible by connecting a suitable load impedance, such as a resistance, in series with the plate of the tube, as shown in Fig. 167. The time-dependent *signal voltage* to be amplified,  $e_s$ , is applied to the grid in series with the fixed *bias voltage*  $E_{cc}$ . The latter is ordinarily made large enough in relation to  $e_s$  so that the grid is at all times negative with respect to the cathode. The plate current  $I_p$ , which varies in response to changes in grid potential, is required to flow through the load resistance  $R_L$ , across which is produced a potential drop that changes whenever the plate current changes. By choosing the resistance of  $R_L$

to be suitably large, the variation in  $E_p$  can be made much greater than the variation in  $e_s$  which causes it.

The performance of the tube in amplification can be predicted quantitatively by a graphical procedure based on curves such as those of Fig. 166, or by an analytical "equivalent-circuit" method. The graphical procedure is particularly useful when the signals involved are relatively large. For low-amplitude signals, the equivalent-circuit method is superior. Both are outlined below.

In either case, the first step is to locate the *operating point* of the tube, i.e., the point on the plate-characteristics graph which corresponds to the condition of the tube in the given circuit when no signal voltage is present. The procedure for finding the operating point is illustrated in Fig. 168. The *load line*, dashed, gives the plate voltage of the tube as a function of

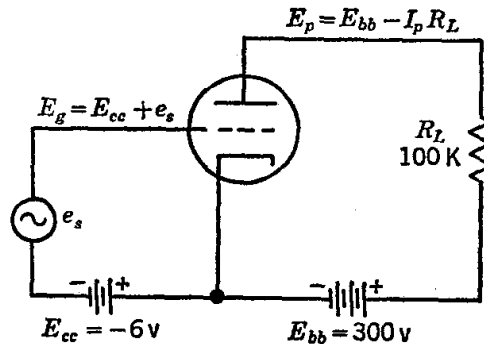


FIG. 167. Circuit diagram for single triode-amplifier stage.

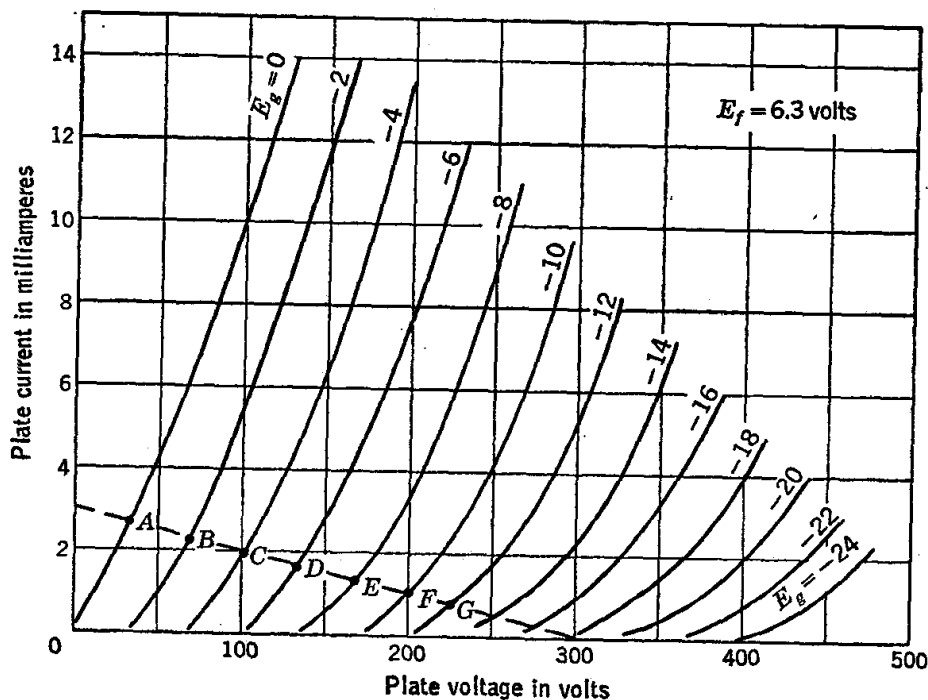


FIG. 168. Characteristics of a triode with load line, shown dashed, for  $R_L = 100$  kilohms,  $E_{bb} = 300$  volts.

the plate current for the given circuit. This line, which has the equation  $E_p = E_{bb} - I_p R_L$ , is constructed by drawing the straight line between the points ( $I_p = 0$ ,  $E_p = E_{bb}$ ) and ( $E_p = 0$ ,  $I_p = E_{bb}/R_L$ ). The operating

point may then be found as that point on the load line which corresponds to the actual bias. For the circuit in Fig. 167, the bias is  $-6.0$  volts and the operating point is  $D$ . The plate current is then about  $1.7$  ma, and the plate voltage about  $130$  volts.

**Graphical Analysis of Triode Amplifier.** When an a-c signal voltage  $e_s$  is added in series with the fixed bias voltage in the circuit of Fig. 167, the grid voltage varies above and below  $-6$  volts. The behavior of the circuit is then described by a point on the graph of Fig. 168 which moves back and forth along the load line in the vicinity of point  $D$ . The relationship of the output waveform to the input is best seen with the aid

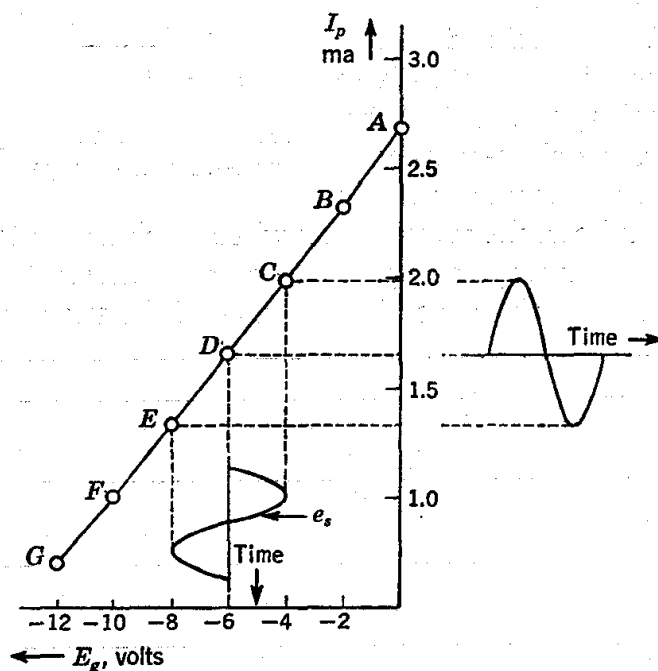


FIG. 169. Dynamic transfer characteristic for the triode of Fig. 168 with 100-kilohm plate load resistor.

of a *dynamic transfer characteristic*, shown in Fig. 169. The latter is plotted point by point with data read from the load line of the preceding figure. (Corresponding points on the two graphs are labeled with the same letters.) The graph of Fig. 169 shows directly the plate-current waveform which results for a given grid signal. The output voltage is  $I_p R_L$ . If the waveform of the output voltage is to be the same as that of the input voltage, i.e., if distortionless amplification is to be obtained, the dynamic transfer characteristic must be a straight line. In the case at hand, the change in grid voltage from  $-8$  to  $-4$  volts produces a change in the voltage across  $R_L$  of  $65$  volts, a sixteenfold voltage amplification.

**Dynamic Characteristics of Triodes.** Consider the effect on  $I_p$  of making small arbitrary changes in the values of  $E_g$  and  $E_p$ . Since  $I_p$  is

determined by  $E_g$  and  $E_p$ , a small increment  $dI_p$  is given by

$$dI_p = \left( \frac{\partial I_p}{\partial E_p} \right)_{E_g} dE_p + \left( \frac{\partial I_p}{\partial E_g} \right)_{E_p} dE_g \quad (62)$$

The dynamic plate resistance and transconductance are parameters of the tube defined by

$$\begin{aligned} r_p &= \text{plate resistance} = \left( \frac{\partial E_p}{\partial I_p} \right)_{E_g} \\ g_m &= \text{transconductance} = \left( \frac{\partial I_p}{\partial E_g} \right)_{E_p} \end{aligned} \quad (63)$$

In terms of  $r_p$  and  $g_m$ , the expression for  $dI_p$  is

$$dI_p = \left( \frac{1}{r_p} \right) dE_p + g_m dE_g \quad (64)$$

The relative effectiveness of grid and plate in bringing about changes in tube current is represented by a third parameter,

$$\mu = \text{amplification factor} = - \left( \frac{\partial E_p}{\partial E_g} \right)_{I_p} \quad (65)$$

The relationship of  $\mu$  to  $r_p$  and  $g_m$  may be seen by imposing small changes on  $E_p$  and  $E_g$ , such as to make  $dI_p = 0$ , and evaluating the right-hand side of Eq. (65) with the aid of Eq. (64). The result is

$$\mu = g_m r_p \quad (66)$$

The instantaneous values of plate voltage, grid voltage, and plate current may be written

$$\begin{aligned} E_g &= E_{og} + e_g \\ E_p &= E_{op} + e_p \\ I_p &= I_{op} + i_p \end{aligned} \quad (67)$$

where  $E_{og}$ ,  $E_{op}$ ,  $I_{op}$  are the quiescent values corresponding to the given operating point, and  $e_g$ ,  $e_p$ ,  $i_p$  are time-dependent terms present when an a-c input voltage is applied. Provided the time-dependent terms are of small amplitude, so that Eq. (64) holds, the relationship among them is

$$i_p = \left( \frac{1}{r_p} \right) e_p + \left( \frac{\mu}{r_p} \right) e_g \quad (68)$$

**Gain of a Triode Amplifier.** With the circuit of Fig. 167, we have  $e_i = e_g$  and  $e_o = e_p$ , where  $e_i$  and  $e_o$  are the a-c components of the input and output voltages, respectively.

The *amplification*, or *gain*,  $A$  is defined by

$$A = \frac{e_o}{e_i} \quad (69)$$

Since the output a-c voltage arises from the changing plate current through  $R_L$ ,

$$e_p = -i_p R_L = -\frac{R_L}{r_p} e_p - \frac{\mu R_L}{r_p} e_g \quad (70)$$

$$= -\mu e_g \frac{R_L}{r_p + R_L} \quad (71)$$

$$A = \frac{e_p}{e_g} = -\mu \frac{R_L}{r_p + R_L} \quad (72)$$

The negative result for  $e_p/e_g$  corresponds to the fact that an increase in  $E_g$  results in an increase in  $I_p$ , which in turn causes  $E_p$  to decrease. It may be noted that the magnitude of  $A$  cannot exceed  $\mu$ .

**Equivalent Circuit.** Examination of Eq. (71) shows that  $e_p$  is equal

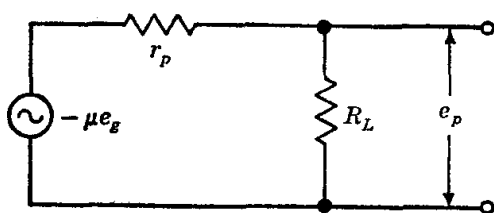


FIG. 170. Equivalent circuit for triode amplifier.

to the voltage which would be produced across the load resistance  $R_L$  by a hypothetical voltage generator which produced a voltage equal to  $-\mu e_g$  and which acted in series with a resistance  $r_p$ , as in Fig. 170; that is, the voltage  $-\mu e_g$  is divided in series between  $r_p$  and  $R_L$ . Thus, within the validity of the gain equation above, the circuit of Fig. 170 is the equivalent for alternating current of the output circuit of the triode amplifier.

The equivalent circuit is found to be of considerable utility in analyzing the performance of triode-amplifier circuits under a variety of conditions. For example, the effect on the gain of changing  $R_L$  is easily remembered from Fig. 170. For  $R_L \gg r_p$ , the gain is approximately  $\mu$ ; for  $R_L \ll r_p$ , the gain is approximately  $g_m R_L$ . For fixed input amplitude, the maximum *voltage* output is obtained for  $R_L \gg r_p$ , the maximum *current* through the load for  $R_L \ll r_p$ , and the maximum *power* dissipated in the load for  $R_L = r_p$ .

**Practical Triode-amplifier Circuit.** A practical triode-amplifier circuit suitable for the audiofrequency range is shown in Fig. 171. If this is compared with the simpler circuit of Fig. 167, several added features may be noted. Bias is obtained by the use of a cathode resistor  $R_k$ . For the case discussed above, the operating point for  $-6$  volts bias would be obtained by making  $R_k$  equal to  $6/(1.7 \times 10^{-3}) = 3500$  ohms.

The capacitor  $C_k$ , which is chosen to have a low impedance to alternating current at the frequencies to be amplified, serves to hold the cathode at a-c ground potential. If the bypass capacitor  $C_k$  were omitted, the periodic variation in plate current produced by  $e_i$  would cause also a periodic variation in the potential of the cathode relative to ground, such that the net a-c voltage at the true input to the tube, namely, between grid and cathode, would be less than  $e_i$ . This effect, termed *cathode degeneration*, is largely eliminated by the bypass capacitor, so that the cathode potential remains constant relative to ground, and the full a-c voltage  $e_i$  appears between grid and cathode.

The other important added feature in Fig. 171 is the output coupling network, comprising  $R_2$  and  $C_c$ . The coupling capacitor  $C_c$  blocks direct

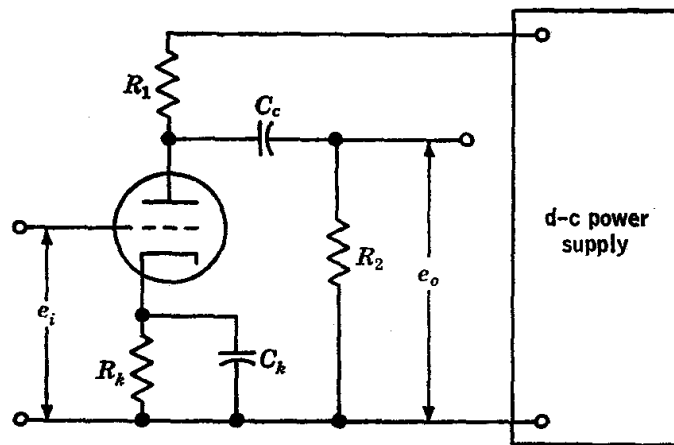


FIG. 171. Practical triode-amplifier circuit.

current but is chosen to have a low impedance to alternating current in the frequency range to be amplified. The purpose of the output coupling circuit is to eliminate the large d-c component of the potential at the plate while passing a-c signal voltages with negligible loss.

Observe that with the coupling circuit present, as in Fig. 171, resistors  $R_1$  and  $R_2$  are effectively in parallel in the a-c circuit. Thus, in Eq. (72) and in the equivalent circuit of Fig. 170, the effective load resistance  $R_L$  to be used is given by

$$R_L = \frac{R_1 R_2}{R_1 + R_2} \quad (73)$$

Equation (72) and the equivalent circuit of Fig. 170 describe the actual behavior of the amplifier circuit of Fig. 171 very satisfactorily over a considerable frequency range, but at very low or very high frequencies the gain drops off. To understand this behavior, the more complete

equivalent circuit of Fig. 172 should be considered. Here the cathode bias and coupling capacitors are shown explicitly, and it can be seen that at sufficiently low frequencies the impedance of  $C_k$  and  $C_c$  will become appreciable and account for a decrease in gain. Also shown explicitly are the interelectrode capacitances and stray capacitances, which account for the reduction in gain at high frequencies.

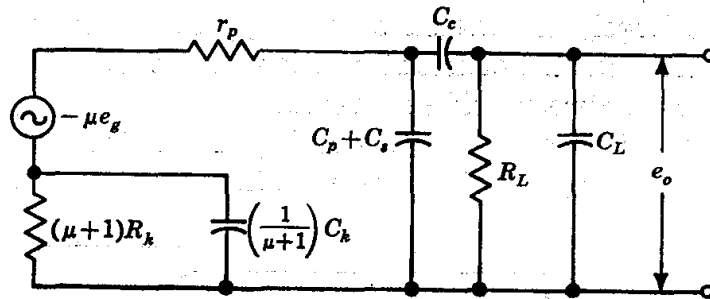


FIG. 172. More complete equivalent circuit of triode amplifier.  $C_p$  = triode output capacitance;  $C_s$  = stray wiring capacitance;  $C_L$  = capacitance of load.

**The Pentode.** In addition to causing loss of gain at high frequencies, the interelectrode capacitances of triodes can also lead to instability at high frequencies because of the resulting interaction between plate and grid circuits. This interaction is very materially reduced by the introduction of additional electrodes in the pentode, or five-electrode tube.

The two additional electrodes of the pentode are grids which are placed between the control grid and the plate. The one nearer the control grid, called the *screen grid*, is maintained at a constant potential positive with respect to the cathode and acts as an electrostatic shield, which may reduce the plate-to-grid capacitance to a value as low as  $0.005 \mu\mu\text{f}$ . Because of the shielding action of the screen grid, the plate voltage has relatively little effect, except at low plate voltages, in determining the plate current, which is principally controlled by the control grid and screen grid potentials. The screen grid also acts as a collector of electrons, but because its effective area is much smaller than that of the plate, this screen grid current is small compared with the plate current under normal operating conditions.

The fifth electrode, the *suppressor grid*, is located between the screen grid and the plate. It is generally operated at cathode potential, and its function is to create a potential distribution between the screen grid and the plate which will cause electrons emitted from the plate (*secondary emission*) to return to the plate.

Characteristic curves for a typical pentode are shown in Fig. 173. A simple experimental circuit for determining these curves is given in Fig. 174.

Pentodes typically have much higher values of  $\mu$  and of  $r_p$  than have

triodes. With a single pentode-amplifier stage, much higher gain can usually be achieved than with a single triode stage. However, for many applications this advantage is more than offset by the even higher gain and added design flexibility offered by twin triodes (two electrically

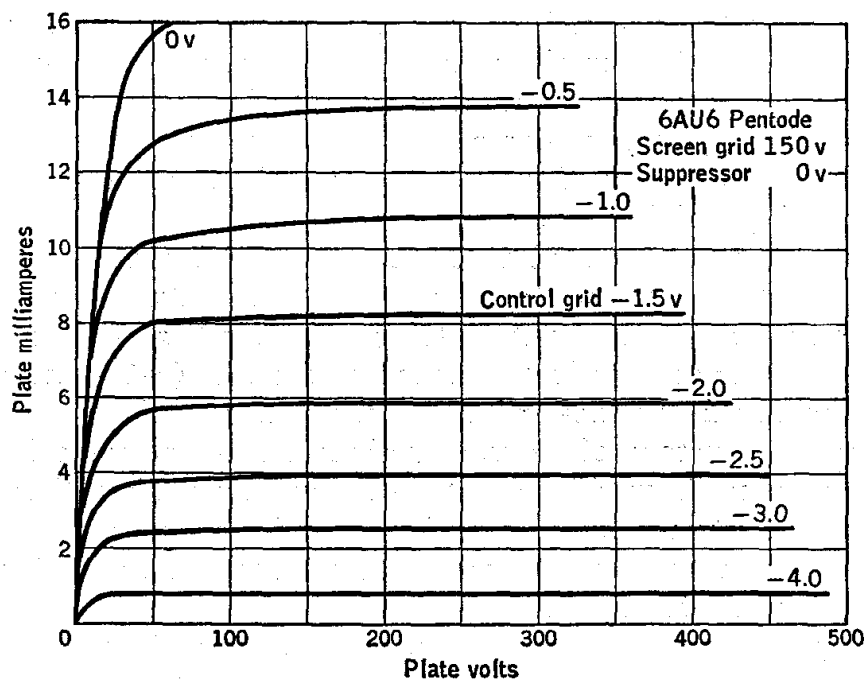


FIG. 173. Characteristic curves for the 6AU6 pentode. Effect of plate voltage and control-grid bias on plate current for constant screen- and suppressor-grid potentials.

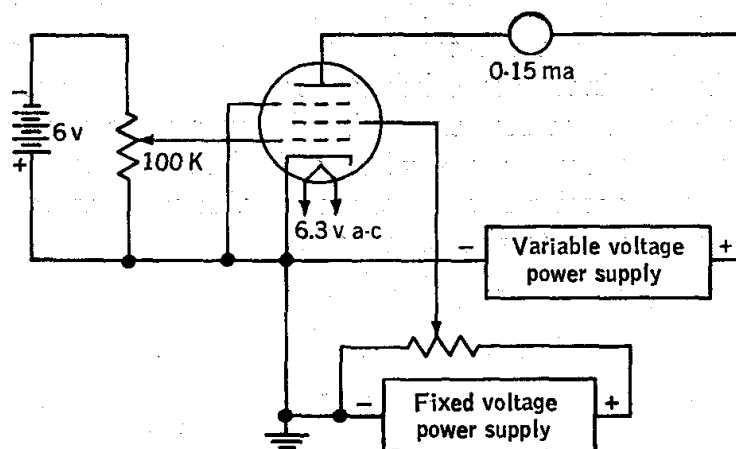


FIG. 174. Circuit for the determination of characteristic curves for a pentode.

separate, nominally equivalent triodes contained in a single miniature glass tube envelope). Pentodes retain the advantage, however, of much reduced interaction between plate and grid circuits and are therefore particularly useful in radiofrequency amplifier circuits.



## SEMICONDUCTOR DEVICES

**Semiconductors.** The energy levels available to electrons in crystalline solids come in *bands* of closely spaced levels. These bands are separated by *energy gaps*, or forbidden zones. The lowest band of interest here is the *valence band*, so named because the electron states concerned are localized in the bonds between pairs of adjacent atoms. Electrons in these states are not mobile except where vacancies exist into which neighboring electrons can move. The next higher of the bands of interest here is the *conduction band*, so named because electrons in this band are highly mobile.

The classification of solids into insulators, semiconductors, and metals is closely related to the width of the energy gap between valence and conduction bands. For insulators, this gap is wide (e.g., 7 electron volts for diamond), for semiconductors, it is intermediate ( $\sim 1$  electron volt), while for metals the valence and conduction bands overlap.

The semiconductors of greatest technical interest are silicon and germanium, both Group IV elements. The valence shells of these atoms contain four electrons, and in a perfect crystal a given atom forms four covalent bonds in a tetrahedral arrangement exactly similar to that of the diamond structure for carbon.

In the pure crystalline state at low temperatures, silicon and germanium are poor conductors. The reason for this is that nearly all the electrons are in the practically filled valence band and hardly any are in the conduction band. If the temperature is raised, an appreciable number of electrons are elevated into the conduction band. At the same time, an equal number of holes is created in the valence band. The resulting material exhibits an increased conductance which is due not only to the motion of *electrons* in the conduction band, but also to the fact that the *holes* in the valence band move when a field is applied. In the pure material, these two species of carriers are equal in number and both make significant contributions to the conductivity.

The addition of small but accurately controlled amounts of specific impurities to a highly purified sample of a semiconductor can have a remarkable effect. Thus, if arsenic is added to germanium, it enters the structure by replacement of germanium atoms. The neutral arsenic atom has five electrons in the valence shell, of which only four are required in bonding to the four neighboring germanium atoms. The fifth electron is quite easily raised to the conduction band. The arsenic is hence called a *donor impurity*, the additional current carriers introduced by the impurity are *negative* (electrons), and the resulting semiconductor is referred to as *n-type germanium*.

A different result is obtained by the addition of indium, for example,

for which the neutral atom has three electrons in the valence shell. When such an atom enters the germanium lattice by substitution and forms four covalent bonds with neighboring atoms, it must capture an electron from an adjacent germanium atom, thus creating a hole. The indium is called an *acceptor* impurity, the current carriers introduced by the impurity are *positive* (holes), and the resulting semiconductor is classified as *p* type.

The general characteristics of semiconductors are treated in the reference works of Shockley<sup>1</sup> and Wright.<sup>2</sup> The most important applications of semiconductors involve the use of appropriate combinations of *p*- and *n*-type materials in diodes and transistors. The theory of operation of these devices is discussed at an introductory level in a number of references.<sup>3</sup>

**Thermistors.** Perhaps the simplest semiconductor device is the thermistor, or thermally sensitive resistor. Thermistors are made from mixtures of various metallic oxides sintered together under controlled conditions to yield a ceramic-like material which has a large negative temperature coefficient of resistance, usually of the order of 4 per cent/°C at room temperature. The resistance  $R$  at temperature  $T$ , to a good approximation, is represented by the relation

$$\log R = \frac{a}{T} + b \quad (74)$$

where  $a$  and  $b$  are constants characteristic of the thermistor.

The combination of high specific resistance, large temperature coefficient, and good stability makes thermistors particularly suitable for use in temperature control and measurement. They can be sealed in glass for protection from corrosive materials, with the resultant element still small enough to give a very rapid response to a change in the temperature of its environment.

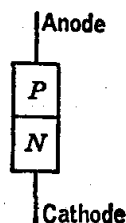
**Diodes.** When a *p*-type crystal and an *n*-type crystal are joined together, a semiconductor *diode* is formed. The labeling of terminals and

<sup>1</sup> Shockley, "Electrons and Holes in Semiconductors," D. Van Nostrand Company, Inc., Princeton, N.J. (1950).

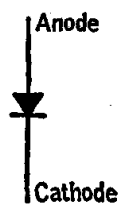
<sup>2</sup> Wright, "Semi-conductors," John Wiley & Sons, Inc., New York (1950).

<sup>3</sup> Coblenz and Owens, "Transistors," McGraw-Hill Book Company, Inc., New York (1955); Riddle and Ristenbatt, "Transistor Physics and Circuits," Prentice-Hall, Inc., Englewood Cliffs, N.J. (1958); "International Rectifier Corporation Engineering Handbook," International Rectifier Corporation, El Segundo, Calif.; Terman, "Electronic and Radio Engineering, 4th ed., McGraw-Hill Book Company, Inc., New York (1955); Greiner, Semiconductor Devices and Applications, McGraw-Hill Book Company, Inc., New York (1961).

the schematic symbol for this device are shown in Fig. 175. Its most important properties are summarized in the current-voltage characteristic, typically of the form shown in Fig. 176. It can be seen that, provided the breakdown voltage is not exceeded, the resistance to current flow in the backward direction is relatively high, while the forward resistance is relatively low. The diode can therefore function as a rectifier, though this is by no means its only use.



(a)



(b)

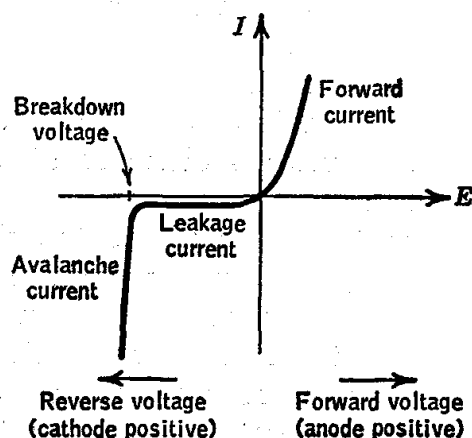


FIG. 175. (a) Semiconductor diode; (b) schematic symbol for semiconductor diode.

FIG. 176. Current-voltage characteristics of *p-n* junction diode.

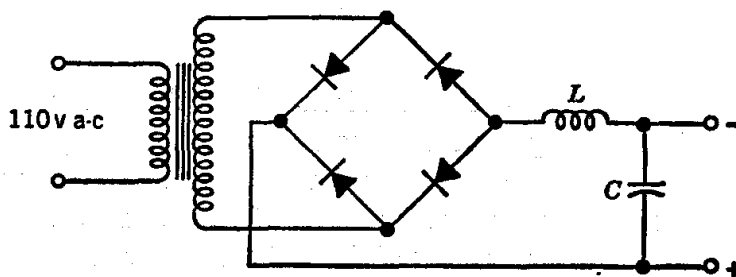


FIG. 177. Bridge rectifier power supply with semiconductor diodes.

Semiconductor diodes of the power-rectifier type have been developed which are very efficient and reliable, and they are coming into widespread use as rectifiers in d-c power supplies. Figure 177 shows a typical bridge rectifier circuit. For either polarity of the a-c voltage at the transformer secondary, current can flow in only one direction through the load; it goes through one pair of diodes during one half-cycle and through the other pair during the other half-cycle. As compared with tubes, semiconductors offer the great advantage in this application of low forward resistance, absence of filament power requirements, and indefinite life—provided the maximum ratings are not exceeded. It is very important that the diodes be mounted on heat-dissipating plates, with ample sur-

face area per diode, and that the reverse voltage rating not be exceeded even momentarily. The air circulation provided by a small blower greatly improves the efficiency of cooling.

A related application is that of low-level detection. Although a bridge arrangement of four diodes may be used, the simple circuit of Fig. 178 is often employed. The output is a voltage which follows the envelope of the input a-c voltage. The time constant  $RC$  is made large compared with the period of the carrier, but small enough to follow the component of highest frequency in the modulation envelope. It becomes obvious on consideration that for proper operation of the circuit in this manner,  $R$  must be large compared with the forward resistance and small compared

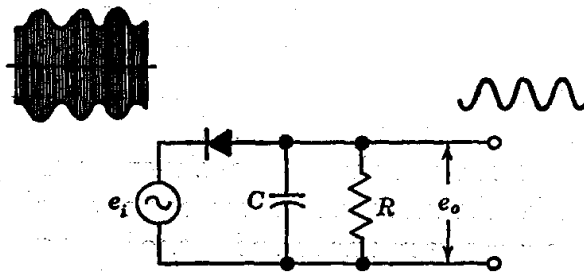


FIG. 178. Diode detector circuit.

with the back resistance of the diode. It is necessary at high frequencies to take into account the shunting effect of the diode-junction capacitance, which effectively appears in parallel with the diode.

The operation of the diode detector is simplest when the amplitude of the input a-c voltage is sufficient to extend into the linear region of the forward-current characteristic (Fig. 176). The diode is then said to act as a *linear detector*; the output voltage varies linearly with the amplitude of the input a-c voltage. An input-voltage level of the order of a volt or so is usually sufficient to ensure linearity. If the amplitude of the input voltage is such that the peaks do not reach beyond the bend of the forward-current-characteristic curve, the diode still functions as a detector, though the detection is not linear. In this region, the diode characteristic is approximated by the series expansion

$$I = aE + bE^2 + \dots \quad (75)$$

If a modulated voltage waveform such as that of Eq. (52) is used, for example, it is not difficult to show that the current contains terms at the frequency  $\omega_m$ , these terms being generated by the term  $bE^2$ . A diode detector operated in this fashion is therefore called a *square-law detector*.

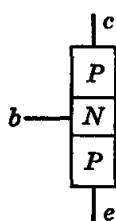
Since the diode presents a highly nonlinear impedance, it is also used

for mixing (i.e., combining two a-c voltages in such a way as to produce sum or difference frequencies) and for harmonic generation.

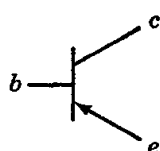
Though most types of diodes are ruined if the breakdown voltage is exceeded, the *Zener diode* is designed to be operated in the avalanche region (Fig. 176). Since the voltage across the diode in this region is nearly constant over a rather wide range of currents, the Zener diode can function as a voltage regulator. The regulating capacity is characterized by the dynamic resistance,  $dE/dI$ , which depends on the operating point. Zener diodes are available for a number of voltages, ranging from a few volts to over a hundred. The voltage stability in many cases is limited by the variation in breakdown voltage with temperature,  $\sim 0.1$  per cent/ $^{\circ}\text{C}$ . For use as reference voltage sources, temperature-compensated units are available having temperature coefficients of the order of 0.001 per cent/ $^{\circ}\text{C}$  over a wide temperature range and offering a fractional stability of  $10^{-5}$  when operated near  $25^{\circ}\text{C}$ ; these units are much more rugged than the conventional Weston standard cell.

When reverse bias (not exceeding the breakdown voltage) is applied to a semiconductor diode, the resistance becomes very high but an appreciable capacitance exists between anode and cathode terminals. Since this capacitance is a function of the voltage, a reverse-biased diode can function as a *voltage-variable capacitor*. Perhaps the most common application

is the control of the frequency of an oscillator by means of an applied voltage.



(a)



(b)

FIG. 179. (a) Structure of *p-n-p* transistor; (b) schematic diagram of *p-n-p* transistor.

**Transistors.** The structure of a *p-n-p* transistor is shown pictorially in Fig. 179. It consists of a very thin layer of *n*-type semiconductor material sandwiched between two *p*-type regions in such a way that two diode-type junctions are formed back to back. The three terminals are designated *emitter*, *base*, and *collector*. The *n-p-n* transistor is similar but with *n* and *p*

interchanged. In the schematic symbol, the emitter terminal is designated with an arrow that shows the direction of easy current flow across the emitter-base junction.

The symmetry which might appear from Fig. 179a to exist is destroyed when the usual biasing potentials are applied. For both *n-p-n* and *p-n-p* types, biasing is such that the base potential is intermediate between that of the other two electrodes, with the normal emitter-base junction biased in the forward direction and the collector-base junction biased in the reverse direction. The resulting current flow for a *p-n-p* transistor under normal bias conditions may be visualized as follows. Current enters through the emitter lead and leaves via the base and collector leads.

The magnitude of the emitter current is then the sum of the magnitudes of the base and collector currents. The current directions are all reversed for the  $n-p-n$  transistor. This flow scheme is easily remembered from the schematic symbols.

The three circuit configurations employed are designated by specifying which of the three electrodes is common to the input and output circuits (Fig. 180). The generally accepted voltage and current sign conventions

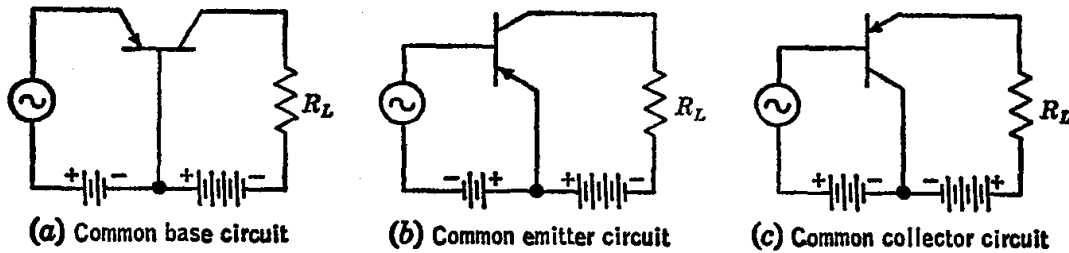


FIG. 180. Circuit configurations for  $p-n-p$  transistors. The analogous arrangements for  $n-p-n$  transistors are the same except for the reversal of all battery polarities.

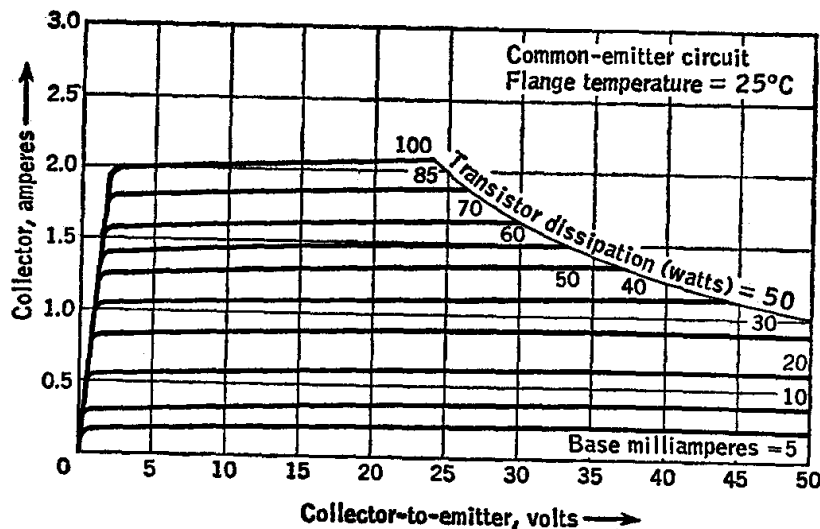


FIG. 181. Characteristic curves for a power transistor, Type 2N1070, common-emitter configuration.

are also based upon Fig. 180. For both  $n-p-n$  and  $p-n-p$  types, the electrode potentials are measured relative to that of the common electrode, if only one subscript is given. (When no configuration is specified, the common-base arrangement is usually to be assumed.) To avoid ambiguity, symbols with two subscripts are often used, such as  $E_{ce}$  for the potential of electrode  $c$  relative to that of  $e$ . In any case, the positive direction for current flow is usually *into* the transistor.

Characteristic curves for the common-emitter configuration are given for a typical power transistor in Fig. 181. Note that over a fairly wide

range of operating conditions, the collector current is determined mainly by  $I_b$  and is relatively insensitive to changes in  $E_{ce}$ . The base-collector current amplification factor  $\beta$  for this configuration is defined by

$$\beta = \left( \frac{\partial I_c}{\partial I_b} \right)_{E_{ce}} \quad (76)$$

Representative values of  $\beta$  range between 20 and 100. Amplification in this configuration then results from the fact that a small change in base current results in a much larger change in collector current.

One form of equivalent circuit for a transistor is the common-base configuration given in Fig. 182. The parameters  $r_b$ ,  $r_e$ ,  $r_c$  are dynamic resistance characteristics of the transistor;  $\alpha$  is the emitter-collector amplification factor,

$$\alpha = - \left( \frac{\partial I_c}{\partial I_e} \right)_{E_{cb}} = \frac{\beta}{\beta + 1} \quad (77)$$

and  $r_m$  is the mutual impedance;  $r_m = \alpha r_c - (1 - \alpha)r_b$ . These parameters are all to be evaluated at the operating point for the given circuit. The equivalent circuit is included here especially to emphasize a few salient facts about transistors: (a) the input impedance may be rela-

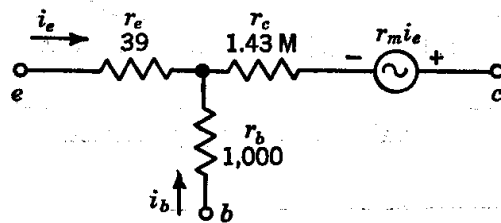


FIG. 182. One form of equivalent circuit for a transistor. Numerical values are for Amperex 2N279, for which  $r_m$  is 1.38 M. Resistances in ohms, with  $M = 10^6$ .

tively low; (b) it depends on the output load impedance; (c) the output impedance depends on the source impedance. In short, the input and output circuits are not nearly as well isolated as for a vacuum-tube circuit. This fact complicates the process of designing transistor circuits.<sup>1</sup>

Transistors are quite rugged mechanically, but are rather easily damaged electrically. The various maximum ratings specified by the manufacturer should be scrupulously respected since there is often little margin left for error. For power transistors, the deratings for higher-temperature operation should not be overlooked, because even if effective cooling is provided, these units are likely to become warm under operating conditions.

<sup>1</sup> A large collection of carefully designed transistor circuits, "Handbook of Selected Semiconductor Circuits," NAVSHIPS 93484, is available from the Superintendent of Documents, U.S. Government Printing Office. Circuit-design principles are also discussed in this reference.

Manufacturer's data sheets often give the values for the so-called  $h$  parameters rather than  $r_b$ ,  $r_e$ ,  $r_c$ , and  $r_m$ . The latter may be calculated from the  $h$  parameters, or alternatively, an equivalent circuit may be constructed directly from the  $h$  parameters. See, for example, the works of Riddle and Ristenbatt, *op. cit.*, Terman (1955), *op. cit.*, and Landee, Davis, and Albrecht, *op. cit.*

Other disadvantages to be mentioned are the temperature dependence of the characteristic curves and the generation of semiconductor noise, which can in some cases be many times larger than the Johnson noise (page 578).

On the other hand, the small size and low power consumption of transistors offer definite advantages for certain applications. For example, a small amplifier or oscillator, together with batteries sufficient to provide operating power for months, can be housed in a single well-shielded box to achieve a high degree of freedom from hum and from interference due to external electrical influences. Such units can also easily be isolated from ground potential.

Both graphical and analytical methods are available for the analysis of standard transistor circuits. The procedures are recognizably analogous to those outlined above for vacuum-tube circuits, but are somewhat more involved because of the greater degree of interaction between input and output circuits. A clear, thorough, and practical introduction to these techniques has been presented by Riddle and Ristenbatt.<sup>1</sup>

## NOISE

**Noise as the Ultimate Limit to Sensitivity.**<sup>2</sup> The ultimate limitation in the accuracy with which an electric current or voltage (or indeed any macroscopic quantity) can be measured, or in the minimum magnitude of voltage or current which can be detected, is set by random fluctuations which are an inherent aspect of the behavior of systems consisting of a large number of (atomic-scale) particles. For example, one may employ an electronic amplifier of high gain to detect or measure a minute unbalance voltage from a Wheatstone bridge. Before the system can give optimum performance, it is necessary to eliminate such factors as poor contacts, effects of variations in power-line voltage, pickup of stray voltages, etc.; with sufficient care, these can all be reduced to a negligible level. But after this has been done, the output of an amplifier of sufficiently high gain will be found to exhibit strictly random fluctuations, which originate from sources located in early stages of the amplifier or in the bridge circuit itself. In this context, such fluctuations are called *noise*.

The general magnitude of noise fluctuations can best be characterized by the mean square noise voltage  $\langle E_n^2 \rangle$  or the rms value  $\langle E_n^2 \rangle^{1/2}$ . It is clear that one cannot expect to detect a signal voltage  $E_s$ , which is less than the

<sup>1</sup> Riddle and Ristenbatt, *op. cit.*

<sup>2</sup> Goldman, *op. cit.*; Van der Ziel, "Noise," Prentice-Hall, Inc., Englewood Cliffs, N.J. (1954).



rms voltage of the accompanying noise; nor, for larger signal voltages, can one expect to be able to measure  $E_s$  with an error less than the rms noise voltage.

**Frequency Distribution of Noise.** Figure 183 shows several samples of noise observed at the output of an amplifier by means of an oscilloscope. Each trace is a photograph of a single sweep. The source of noise in all cases was the same.

In the first case, the frequency range 1 to 25 kc/sec was amplified; in

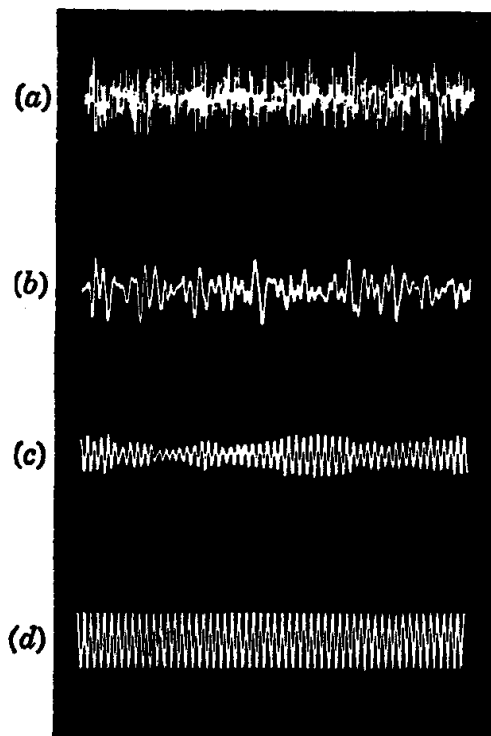


FIG. 183. Oscilloscope photographs showing appearance of noise voltage as a function of time. (a) Passband 1 to 25 kc/sec; (b) passband 1 to 5 kc/sec; (c) passband 50 cycles/sec wide, centered at 5 kc/sec; (d) 5 kc/sec sine wave.

the second case, a low-pass filter was added so that only the range 1 to 5 kc/sec was amplified; in the third case, amplification was restricted to a narrow range, about 50 cycles/sec wide, centered at 5 kc/sec. For comparison, a 5 kc/sec sine wave is shown at (d). The time scale is the same for all four sweeps, but the oscilloscope amplification was increased progressively for traces (a), (b), and (c).

These observations illustrate the fact that a noise voltage can be considered to consist of a large number of Fourier components (page 555), representing a wide range of frequencies, with some components being passed and others being rejected when the noise is put through a frequency-selective network. Though the mathematical analysis of noise is not simple, this notion can be put on a rigorous basis.

**Johnson Noise.** This is the noise, inherent in any resistor, due to

thermal agitation of the electrons. The mean square voltage of noise components due to this cause in the frequency range  $f$  to  $(f + \Delta f)$  in a resistor of resistance  $R$  at temperature  $T$  is given by the Nyquist equation,

$$\langle E_n^2 \rangle = 4kTR\Delta f \quad (78)$$

In any network, the actual resistor may be replaced by its equivalent: a voltage generator  $E_n$  (of zero internal impedance) acting in series with a noiseless resistance  $R$ . For 300°K, the value of  $4kT$  is  $1.65 \times 10^{-20}$  joule.

**Shot-effect Noise.** The tube current of a vacuum tube fluctuates on account of the corpuscular nature of electrons. The resulting noise is called *shot-effect* noise. For a triode, the shot-effect component in the plate current in the frequency range  $f$  to  $(f + \Delta f)$  is given by

$$\langle I_n^2 \rangle = \frac{0.664}{\sigma} 4kT_c g_m \Delta f \cong 4kT_c g_m \Delta f \quad (79)$$

where  $\sigma$  = a parameter characteristic of a given type of tube (with a value typically between 0.5 and 1.0)

$T_c$  = cathode temperature (about 1000°K for oxide-coated cathodes)

$g_m$  = transconductance of the tube

An equivalent circuit for the tube is obtained by placing a current generator  $I_n$  (of infinite internal impedance) in parallel with the tube plate resistance  $r_p$ , which is to be considered noiseless. The shot effect is often the principal source of noise in radiofrequency circuits.

**Flicker-effect Noise.** An additional source of noise in vacuum tubes which is particularly important at audiofrequencies is the flicker effect. This noise arises from slow random fluctuations in the rate of emission of electrons from the cathode and is generally ascribed to processes taking place in the oxide coating. The frequency distribution of this noise is such that the resulting mean square noise current in a small frequency range  $f$  to  $(f + \Delta f)$  goes approximately as  $f^{-1}\Delta f$ . At the lower audiofrequencies, say below 1 kc/sec, the flicker effect usually becomes a more serious source of noise than the shot effect.

**Current Noise.** Noise in excess of the Johnson noise is produced when d-c current passes through a semiconductor or a carbon-composition resistor. The mean square noise voltage generated in this way has approximately a  $1/f$  frequency dependence. In sensitive amplifiers, particularly for the lower audiofrequencies, current noise can be greatly reduced by the use of wire-wound, metal-film, or carbon-film resistors.

**Noise in Transistors.** Noise generated in transistors includes Johnson noise and excess noise, the latter with roughly a  $1/f$  frequency dependence. Transistors therefore tend to have poor noise characteristics at low audiofrequencies. However, improved types are becoming available, and audio amplifiers with reasonably good noise characteristics have been developed.

**Noise Figure.** The noise figure  $F$  of an amplifier compares the actual noise output obtained under specified conditions with that which would be obtained if no noise were generated within the amplifier itself. For the purpose of defining  $F$ , it is assumed that the amplifier input terminals are connected to an external network, or dummy input, which has an impedance matching that of the amplifier input and which generates only

Johnson noise. Then  $F$  is defined as the ratio of the total noise power output of the amplifier to that due to Johnson noise from the dummy input.

**Noise Calculations.** Once the noise *sources* have been characterized, as by Eq. (78) or (79), for example, there remains the problem of determining the noise at the *output* of the system. Though it is difficult to make accurate calculations, it is relatively easy to make estimates which are entirely satisfactory for many purposes.

When random noise from several independent sources is combined, one may add the noise powers, the mean-square noise voltages, or the mean-square noise currents. The first-stage gain is often high enough that noise generated in subsequent stages is negligible.

Consider the case of a linear amplifier. Since the gain is a function of frequency, it is necessary in principle to consider separately the noise in each small frequency range  $\Delta f$ . A means of avoiding this complication in practical calculations is provided by introducing the *bandwidth for noise*  $B$ , defined by

$$\int_0^\infty G^2(f)df = G_0^2 B \quad (80)$$

where  $G(f)$  = voltage or current gain at frequency  $f$ , from the location of the noise source to the output (cf. Fig. 162)

$G_0$  = peak value of  $G(f)$

Equation (80) furnishes the justification for the following procedure, which is often used. The noise generator in the equivalent circuit for the source is considered to have the rms voltage or current corresponding to a frequency range  $\Delta f = B$ ; for example,

$$\langle E_n^2 \rangle = 4kTRB \quad (\text{Johnson noise source}) \quad (81)$$

$$\text{or} \quad \langle I_n^2 \rangle = 4kTg_m B \quad (\text{shot noise source}) \quad (82)$$

The subsequent gain for the rms noise is then taken as  $G_0$ .

In many applications, the task of evaluating the integral in Eq. (80) can be avoided by using the half-power bandwidth  $\mathcal{B}$  (page 558) as an approximation for  $B$ . Actually, for the simple  $LRC$  resonance curve and for a single-section low-pass  $RC$  filter,  $B = (\pi/2)\mathcal{B}$ . For the idealized rectangular response curve (gain constant between frequencies  $f_1$  and  $f_2$ , zero outside this range)  $B$  exactly equals  $\mathcal{B}$ .

A more difficult case, but one of great practical importance, is that of a linear amplifier followed by a detector, the output of which is filtered and then registered by a meter, chart recorder, or other indicating device.<sup>1</sup> Let the noise bandwidth of the amplifier be  $B_a$  and that of the detector-

<sup>1</sup> For theoretical treatments of the response of detector circuits to noise, see Van der Ziel, *op. cit.*, and Goldman, *op. cit.*

filter-indicator system,  $B_i$ . For the purpose of estimating signal-to-noise ratios, the system bandwidth for noise,  $B_n$ , now replaces  $B$  in Eq. (81) or (82). For either a square-law or linear detector with weak signal,

$$B_n \cong \sqrt{B_a B_i} \quad (83)$$

For a phase-sensitive detector, or for a linear detector operated with a strong carrier,

$$B_n \cong \frac{1}{2} B_i \quad (84)$$

Here the designations *weak* and *strong* pertain to a comparison with the rms noise level at the detector input. For both  $B_a$  and  $B_i$ , the approximation  $B \cong \mathfrak{B}$  may be used. For a single-section low-pass  $RC$  filter, the exact value for  $B_i$  is  $1/4RC$ . Ordinarily, since  $B_i \ll B_a$ , much greater noise reduction is obtainable with a phase-sensitive detector than with a simple square-law or linear detector with weak signal, for the same output-response time.

## MEASUREMENTS AND TEST EQUIPMENT

**Multimeters.** Widely used in testing electronic equipment, the multimeter consists of a single d'Arsonval meter mounted, with auxiliary networks, in a portable case. The basic meter is a d-c microammeter, typically 50  $\mu$ a full scale. By means of a number of switch-selected shunts, series resistors, batteries, and a rectifier, this single meter serves for measurement of d-c or a-c voltage, d-c current, or resistance. The accuracy is typically 1 or 2 per cent of full scale.

While this is a versatile and extremely useful instrument, the user should be aware of its major limitations:

1. When used to measure voltage, the meter presents a certain conductance between its leads, so that connecting the meter between two points in a circuit is equivalent to connecting a resistor between these two points. The voltage actually measured by the meter is therefore not the same as the voltage which existed between the same two points before the meter was connected. The meter resistance can be calculated from the "ohms-per-volt" rating  $\lambda$ , which is usually printed on the face of the meter scale. A typical value is  $\lambda = 20,000$  ohms/volt. The input resistance  $R_i$  of the meter is  $R_i = \lambda E_f$ , where  $E_f$  is the *full-scale* voltage for the particular range used.

2. Because of the type of rectifier used, a-c measurements cannot reliably be made at frequencies above the audio range with the multimeters now generally available.

3. For a-c measurements, the meter deflection is determined by the average rectified voltage; the scale calibration in terms of rms values is

correct only for a sinusoidal waveform. The presence of a d-c component also causes error.

4. Resistance measurements may be quite meaningless if the circuit contains voltage sources.

**Vacuum-tube Voltmeters.** The chief limitation of the d'Arsonval meter—that of drawing power from the circuit under test—can be

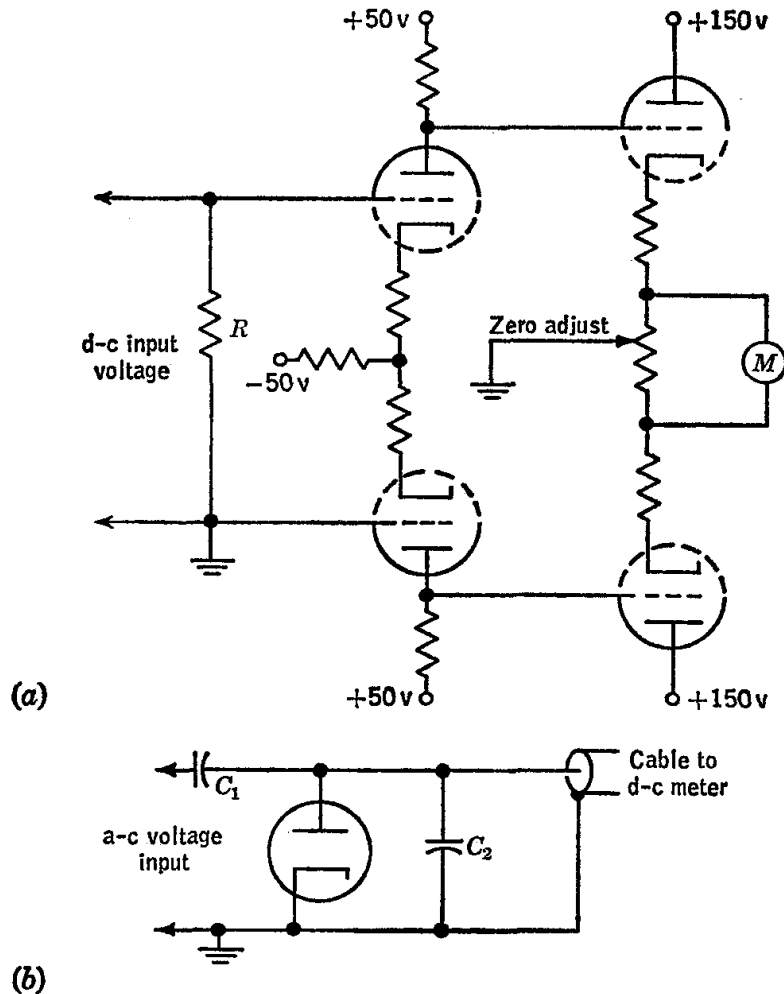


FIG. 184. (a) Simple d-c vacuum-tube voltmeter circuit; (b) diode probe used for a-c voltage measurements.

practically eliminated by the use of vacuum tubes. Figure 184a shows a simple voltmeter circuit which illustrates how this result may be accomplished. With the input leads shorted, the potentiometer is adjusted to bring the meter to zero deflection. When the d-c voltage to be measured is applied to the input terminals, the circuit becomes unbalanced and a deflection of the meter results. The use of two twin-triode tubes in a balanced arrangement helps to reduce drift caused by

variations in  $E_{bb}$  or in filament potential, since to a first approximation these factors affect both triode circuits in the same way and therefore do not alter the meter deflection. The input resistance is high: the upper limit to  $R$  is set by the requirement that grid current produce only a negligible error, and the grid current is quite small since in this circuit the grids are a volt or so negative relative to the cathodes. With this type of circuit, input impedances of the order of 10 to 100 megohms are achieved in modern vacuum-tube voltmeters. The accuracy is typically 1 to 3 per cent of full scale.

Alternating-current voltage measurements are made possible with the addition of a simple diode rectifier (Fig. 184*b*). The diode load circuit is  $R$  and  $C_2$ . Capacitor  $C_1$  blocks direct-current. To avoid error from the use of long leads at high frequencies, the diode circuit is mounted in a small cylindrical housing connected through a cable to the meter itself. Thus the diode can be brought quite close to the circuit point at which the voltage is to be measured. In this way, a-c voltage measurements can be made reliably well into the UHF region (hundreds of megacycles). The input impedance for alternating current for a typical instrument is equivalent to several megohms (dependent on frequency) in parallel with  $1.5 \mu\text{f}$ .

**Potentiometric Instruments.** Modern potentiometric instruments are a far cry from the slide-wire-on-a-meter-stick type and offer accuracy par excellence for measurement of d-c voltages. The use of a potentiometer should always be considered when an accuracy of better than about 1 per cent is desired. The balancing time is of the order of tenths of a second for electronically balanced types, and of course appreciably longer and quite dependent on circumstances for manually operated types. The more accurate instruments in the former class offer five-figure digital readout.

**The Cathode-ray Oscilloscope.** The essential element of the cathode-ray oscilloscope is the oscilloscope tube, whose structure is shown in Fig. 185. It contains an electron gun, which produces a beam of electrons that is directed upon a fluorescent screen at the opposite end of the tube, and deflecting plates,<sup>1</sup> to which voltages may be applied to displace the beam from its equilibrium position. As the beam moves, its path is traced out on the fluorescent screen, where it may be observed or photographed. The electron gun consists of a thermionic emitting cathode, a grid, and two anodes. The grid controls the electron density of the beam and to a lesser extent influences the focusing of the beam by the two anodes which accelerate the electrons toward the screen. The

<sup>1</sup> Magnetic deflection can also be employed, but in practically all laboratory instruments electrostatic deflection is used.

final velocity with which the electrons leave the gun depends upon the potential of the second anode. The intensity of the image is changed by changing the grid voltage, while adjustment of the beam focus is accomplished by changing the potential of the focusing anode. The diaphragms in the electrodes help to keep the beam sharp.

The two sets of deflecting plates in the tube are arranged so that one causes a horizontal deflection of the beam, and hence of the fluorescent spot produced on the screen, and the other a vertical deflection. Because appreciable voltages must be impressed across the plates to produce a large displacement of the beam, amplifiers are provided in the instrument to amplify the actual input voltages. When alternating voltages are applied simultaneously to the two plates, the position of the spot at any time represents the vector sum of the instantaneous values of the

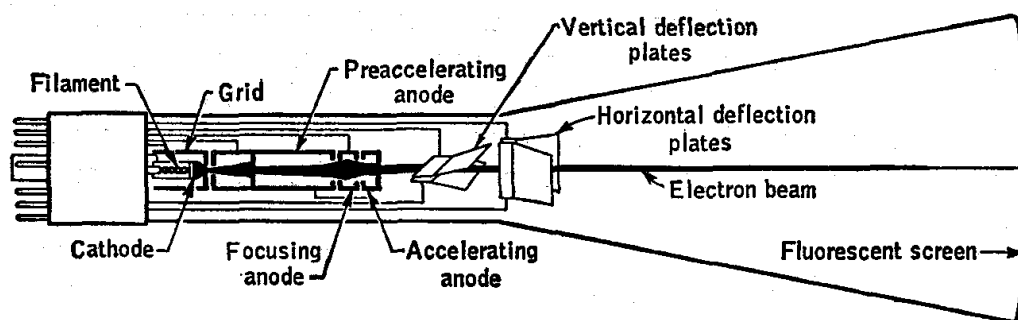


FIG. 185. Electrode arrangement of cathode-ray oscilloscope tube.

voltages applied to the two sets of plates. Because the screen is phosphorescent as well as fluorescent, the motion of the spot produces a line pattern on the screen, the nature of which depends on the wave shapes, amplitudes, and phase relationship of the two voltages.

A major application of the cathode-ray oscilloscope is in showing the appearance of a voltage as a function of the time. For this purpose the beam is periodically swept horizontally across the screen at a uniform rate to a point of maximum displacement, from which it returns practically instantaneously to its zero position; the frequency of this action is termed the *sweep frequency*, and the special type of voltage wave applied to the horizontal plates to produce it is provided by a special variable-frequency oscillator incorporated in the instrument. The unknown voltage is applied to the vertical-deflection plates. If the frequency of the sweep voltage is adjusted to equality with that of the unknown, the pattern on the screen will represent one cycle of the unknown voltage.

The oscilloscope is also useful for the comparison of the frequencies of two voltages. The two voltages are applied simultaneously to the two sets of deflection plates. If the ratio of the frequencies is a rational

number, a closed pattern called a Lissajous figure will result, and from its form the frequency ratio can be determined. An unknown frequency is determined by comparing it with the output of a calibrated variable-frequency oscillator, the frequency of which is adjusted until a simple Lissajous pattern is obtained. In Fig. 186 is shown the pattern for a frequency ratio of 3:2.

The relative phase of two sinusoidal voltages of the same frequency can also be determined. The two signals are applied to the two sets of deflection plates. The vertical and horizontal amplifiers are adjusted as required to give equal deflections for the two signals, if the latter are not equal in amplitude. If the two voltages are in phase, the pattern will be a straight line, making an angle of  $45^\circ$  with the horizontal. If the voltages

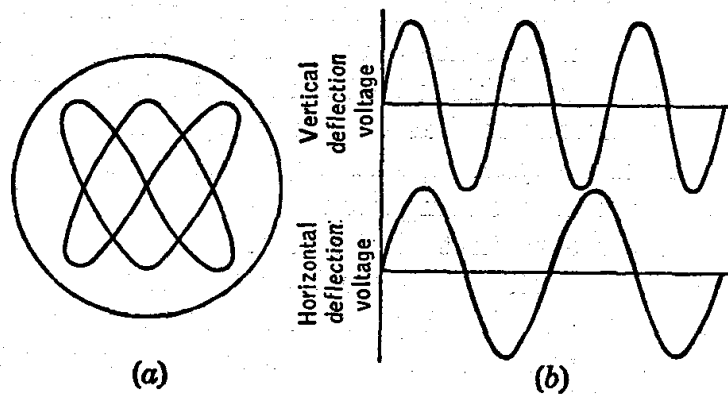


FIG. 186. Typical Lissajous pattern in frequency comparison with the cathode-ray oscilloscope.

are  $90^\circ$  out of phase, the pattern is a circle. For other phase angles the pattern is an ellipse.

The input impedance, deflection sensitivity, and frequency-response (or rise-time) characteristics of an oscilloscope depend entirely on the signal amplifier used. In a typical case, the input impedance may correspond to 2 megohms in parallel with  $20 \mu\mu\text{f}$ . This impedance is high enough so that d-c and audiofrequency circuits are usually not much affected by connection of the oscilloscope leads; however, the effect of the oscilloscope input capacity may be considerable when added to a radio-frequency circuit.

Perhaps the single most common source of confusion for the novice using an oscilloscope is the occurrence of pickup. The term *pickup* refers to a voltage which appears in the circuit of interest (in this case, the oscilloscope leads and input circuit) as a result of coupling with stray magnetic or electrostatic fields. The ubiquitous power-line fields are a frequent source of pickup, which is then called hum pickup. It is



imperative that shielded leads be used if reliable indications are to be obtained for circuits with even moderately high impedances, say above a few thousand ohms.

**Measurement of Resistance, Capacitance, and Inductance.** For many purposes, satisfactory measurements of resistance, capacitance, or inductance can be made with an impedance bridge (page 481) or with a suitable UHF equivalent employing transmission-line techniques. It is important to bear in mind the frequency at which the measurement is made, since the effective values of  $R$ ,  $L$ , and  $C$  are somewhat dependent on frequency. In general, components handbooks or manufacturer's literature should be consulted with regard to the frequency dependence of these parameters for particular types of components.<sup>1</sup>

Capacitors and resistors with the size and accuracy required for most applications are available, but it is often desired to wind a coil either to give a certain value of inductance or to resonate with a given capacitance at a specified frequency. This is best done by trial, with available coil-winding data or equations used as a preliminary guide. A trial coil can be connected across a capacitor, and a grid-dip meter used to find the resonant frequency of the resulting circuit. (The principle of the method is essentially the same as that of the resonance method explained on pages 226–229.) The value of  $L$  can be calculated from the resonant frequency if  $C$  is known. Most physical circuits are actually multiply resonant, so it is wise to make a rough calculation based on the winding data to guard against being led far astray by spurious resonances.

**Measurement of Frequency.** Three important methods for the measurement of frequency will be described, in the order of increasing accuracy.

*Resonance Method.* The signal of unknown frequency is coupled into a resonant  $LC$  circuit, and the capacitance adjusted to produce resonance with the signal. Grid-dip meters are usually designed to be usable in this way, the dial being calibrated directly in frequency units. This method requires an appreciable amount of signal power; an accuracy of several per cent can be expected.

*Heterodyne Frequency Meter.* This instrument contains a variable-frequency, calibrated oscillator, the output of which is mixed with the signal and adjusted to zero beat. The mixing may take place in the frequency meter or in an external circuit, as may be convenient. A crystal-controlled oscillator and harmonic generator are usually included in the

<sup>1</sup> As a rough general rule, the resistance of composition-type and film-type resistors and the capacitance of air, mica, or ceramic capacitors are approximately constant from direct current at least through the radiofrequency region and in some cases even into the UHF region. On the other hand, the effective resistance and inductance of coils and of wire-wound resistors may change considerably over a decade of frequency.

meter to provide a series of closely spaced reference points at which the dial calibration may be checked. The crystal oscillator, in turn, may be adjusted to zero beat with station WWV or a local standard. An accuracy of the order of 0.05 per cent is readily achieved in the measurement of an unknown frequency.

**Counter.** The use of a gated event counter for measurement of frequency is illustrated in the simplified block diagram of Fig. 187. The time-base generator resets the counter electronically to zero and then provides a rectangular pulse, which opens the signal gate for a very precisely controlled period of time, one of the five intervals shown being

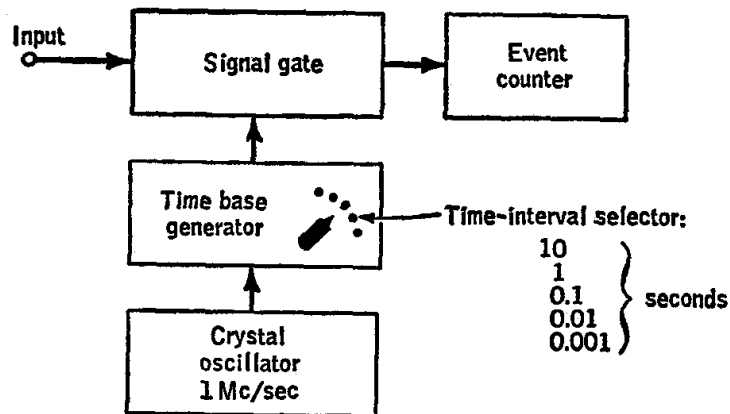


Fig. 187. Block diagram of frequency counter.

selected by a switch. During the open period, the input signal passes through to the counter, and the number of cycles is registered. After a brief waiting period, determined by a circuit within the time-base generator, the cycle is repeated. The frequency of the signal is indicated by the number of counts received during the open period, the decimal-point position depending on the interval time selected.

The accuracy of measurement is determined largely by the accuracy of the oscillator which controls the timing of the time-base generator. Commercially available frequency counters offer an accuracy of 5 parts in  $10^8$ , plus or minus one count.

The *period* of the incoming signal may be measured by having the signal control the gate and counting the time-base pulses. The *time interval* between two incoming pulses can be measured by having the first pulse open the gate and the second close it, the time-base pulses being passed and counted during the open period.

**Time and Frequency Standards.** Broadcasts from the U.S. National Bureau of Standards short-wave radio stations WWV (near Washington, D.C.) and WWVH (Hawaii) provide standard carrier fre-

quency transmissions with various standard audio tones and time signals which are valuable for calibration purposes.<sup>1</sup>

The principal radiofrequency transmissions are at 5, 10, and 15 Mc/sec. The following standard audio and time signals are transmitted as modulation:

1. For certain 2- or 3-min periods, an audiofrequency tone at 600 or 440 cycles/sec is carried as a single upper sideband with power about one-third that of the carrier.
2. One-second time signals are sent as 0.005-sec pulses of 1000-cycles/sec modulation, each pulse consisting of 5 cycles, beginning at the start of a second. These time signals are heard as clicks at 1-sec intervals.
3. During selected 1-min intervals, a special timing code is broadcast which gives the day, hour, minute, and second, coded in binary form. This is heard as a harsh buzzing sound.

The radio- and audiofrequencies as transmitted are held stable to within a few parts in  $10^{10}$ ; an offset of  $-150$  parts in  $10^{10}$  is maintained relative to the atomic frequency standards which constitute the U.S. Frequency Standard. Time intervals as transmitted have the same fractional accuracy, with an additional limitation of  $\pm 1 \mu\text{sec}$ . However, changes in the height of the reflecting layer of the ionosphere produce a Doppler-effect error which limits the accuracy of received signals to about  $3 \times 10^{-7}$ . The Doppler error can be averaged out by extending the measurements over a sufficiently long period of time.

Low-frequency standard signals at carrier frequencies of 60 and 20 kc/sec are transmitted by the National Bureau of Standards Stations WWVB (Boulder, Colo.) and WWVL (Sunset, Colo.), respectively. These transmissions are by ground wave and so avoid the Doppler error.

## MISCELLANEOUS ELECTRONIC CIRCUITS

**Full-wave-rectifier Power Supply.** A typical circuit employed to provide d-c power for vacuum-tube circuits is given in Fig. 188a. It is based on the full-wave-rectifier circuit of Fig. 163c, the output of which is a pulsating voltage equivalent to a steady d-c voltage plus an alternating component called the *ripple voltage*. In this case, the main component of the ripple voltage is at 120 cycles/sec. For the reduction of the ripple component in the output voltage, a two-section filter is employed in the circuit of Fig. 188a.

The operation of the filter can be understood by considering that each section consists of an inductor in series with a capacitor as in Fig. 188b.

<sup>1</sup> The complete schedule of signals transmitted may be obtained from the National Bureau of Standards, Radio Standards Division, Boulder, Colo.

The input voltage  $E_i$  has an a-c component superimposed on a d-c component. The inductor, or *choke*, offers a high impedance to alternating current, while the capacitor offers a low impedance to alternating current; hence only a small fraction of the a-c component appears across

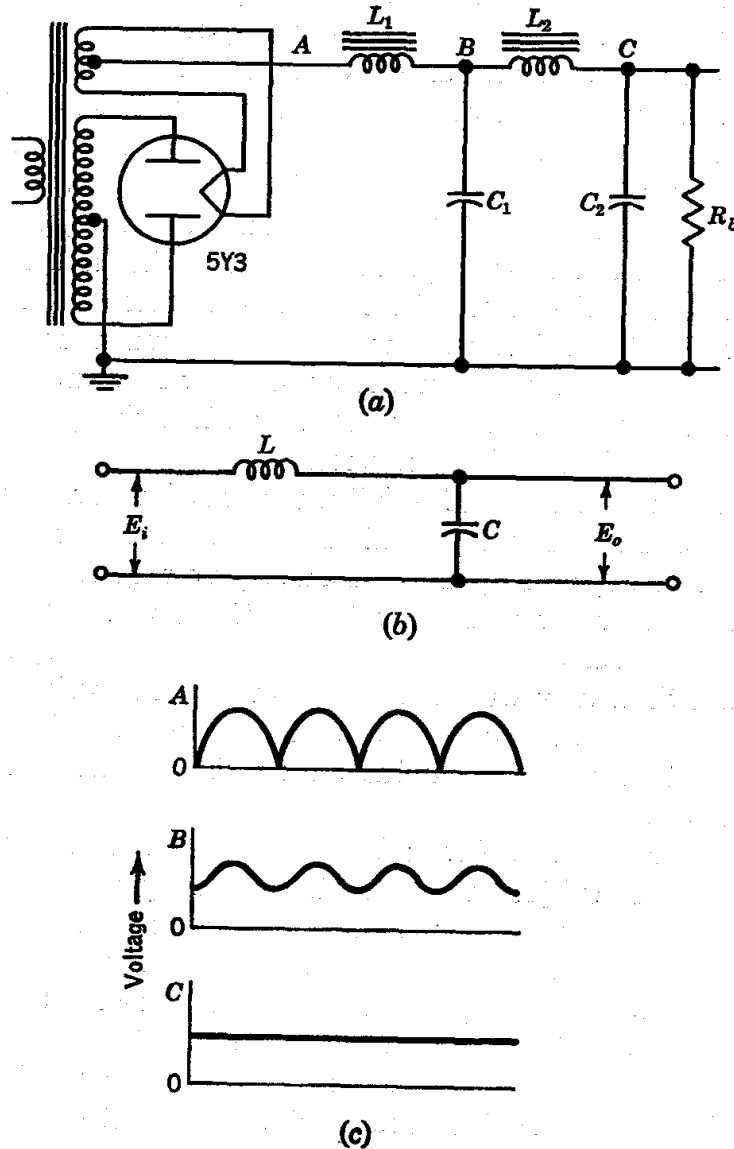


FIG. 188. (a) Direct-current power-supply circuit; (b) LC filter section shown separately with input  $E_i$  and output  $E_o$  indicated; (c) voltage waveforms observed between points A, B, C and ground: A, output of rectifier; B, output of first filter stage; C, output of second filter stage.

the capacitor. On the other hand, most of the d-c input voltage appears across the load, though there is some loss due to the resistance of the choke-coil windings. In the less critical applications, only one filter stage is necessary.

The filter shown is of the *choke-input* type. If the first choke is omitted, there remains a *capacitor-input* filter. The latter yields a higher output voltage, since the capacitor  $C_1$  then becomes charged nearly to the peak rather than the average value of the input voltage. The ripple amplitude also increases. In tube manuals, graphs are often included for rectifier tubes showing the d-c output voltage to be expected for a given a-c input voltage, current drain, and type of filter.

The chokes should always be placed in the lead that is *not* grounded, which is usually (but not necessarily) the positive lead. There is considerable capacitance between the secondary of the power transformer and its primary, one side of which is grounded. This capacitance to ground will bypass some a-c ripple around the chokes if they are put in the grounded side of the filter. In order for the filter to function effectively, the current through it must not fall below a minimum value. The bleeder resistor  $R_b$  provides this minimum current flow and also serves to permit the condensers to discharge rapidly when the power supply is turned off, a safety factor of importance.

The tube illustrated is called a full-wave rectifier and corresponds to two diodes in a single envelope with a common cathode. The output voltage at point  $C$  depends upon the secondary voltage of the transformer and upon the current furnished by the rectifier, which determines the potential drops across the tube and the chokes. The output voltage of the circuit will then vary with fluctuations in the line voltage across the transformer primary and with the current drawn by the load. This undesirable feature may be eliminated by the addition of a voltage-regulating section.

**Alternating-current Voltage Regulators.** The ordinary 110-volt a-c line voltage is subject to fluctuations arising primarily from the changing load on the line. Regulating units of several kinds are available for providing a constant-voltage output at the line frequency. In the selection of an a-c voltage regulator, one should consider the question of stability against variations in load as well as that of stability against fluctuations in line voltage. Electronically controlled regulators are the most versatile, as they provide good regulation against wide variations in either load or line, have a fairly rapid response, and give a sine-wave output with relatively little distortion.

**Direct-current Voltage Regulator.** For sensitive circuits, it is usually necessary to provide a more stable d-c voltage than can be obtained with the circuit of Fig. 188. The usual solution is to add an electronic regulator, illustrated in Fig. 189. The triode  $V_1$ , interposed between the unregulated input voltage and the load, functions as an electronically controlled resistance, which is caused to vary in such a way

as to minimize changes in the output voltage  $E_o$ , whether due to changes in input voltage or to changes in load.

The operation of the circuit is as follows. Resistors  $R_1$  and  $R_2$ , which are chosen for good stability, act as a potential divider to provide a voltage  $E_s$ , which is a fixed fraction of  $E_o$ . Then  $E_s$  is compared with the stable reference voltage  $E_r$ , supplied by a battery, voltage regulator tube (page 592), or Zener diode (page 574). The differential amplifier circuit amplifies the difference  $E_s - E_r$  and causes the grid potential of  $V_1$  to change in a direction opposite to that of any change in  $E_s$ . Therefore, if

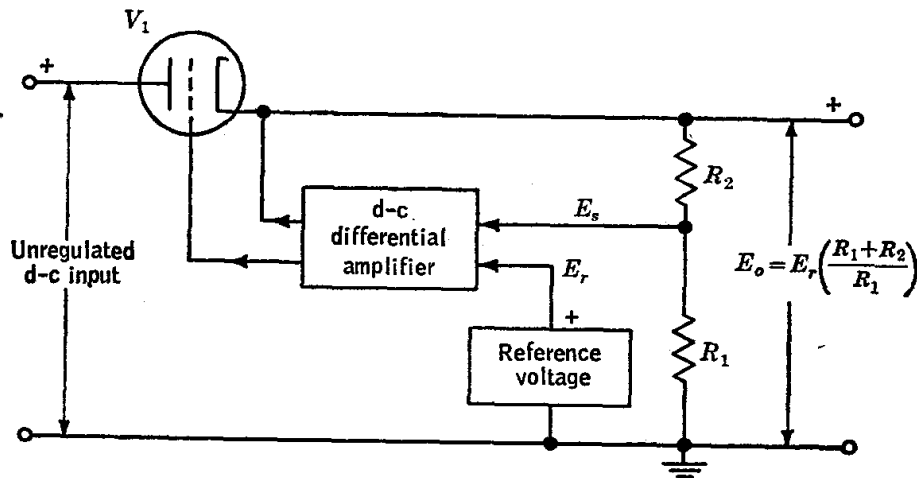


FIG. 189. Diagram illustrating the principle of a typical electronic regulator for a d-c power supply.

$E_o$  should increase, the grid of  $V_1$  is driven in a negative direction by the differential amplifier, the effect being to increase the resistance offered by  $V_1$  to the load current and thus to oppose the original change in  $E_o$ . In essence, then, the regulating circuit functions to keep  $E_s$  equal to  $E_r$ , so that the output voltage is held at the value

$$E_o = E_r \frac{R_1 + R_2}{R_1}$$

The response is rapid enough to minimize hum and other a-c disturbances in the audiofrequency range, as well as to correct for slower variations in output. The quality of the regulation varies considerably with the type of circuit used and the load current drawn, but typically both hum and variations in  $E_o$  due to changes in line voltage and load are reduced to the millivolt level. The limiting factor is often the stability of the reference voltage or of the first tube of the d-c amplifier.

It is worth remembering that this circuit tends to maintain the voltage

constant at the sampling network  $R_1$ ,  $R_2$  rather than at the load. If the load is some distance from the supply, serious deterioration in performance can result from the resistance in the leads or from stray voltages picked up. The remedy for this is to use the technique of "remote sensing," in which two additional leads, adequately shielded, are used between the supply and load, these leads being so arranged that they do not carry the load current, but merely sample the voltage across the load and carry this information to the differential amplifier.

The output voltage can be made continuously variable over a substantial range by introducing a potentiometer into the sampling network so that the ratio  $(R_1 + R_2)/R_1$  becomes adjustable.

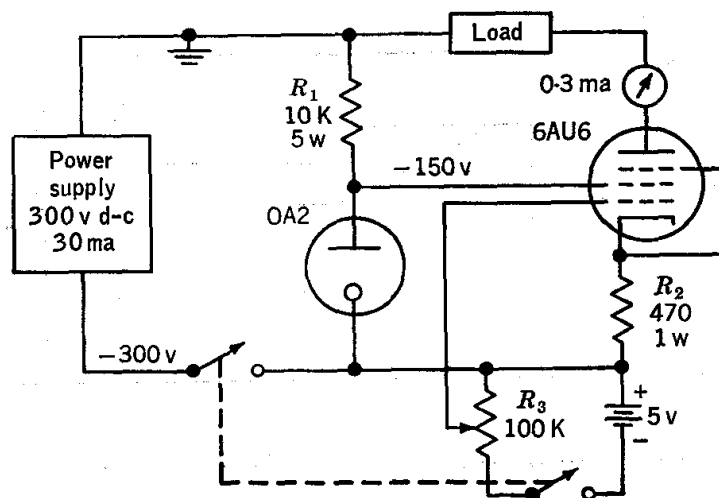


FIG. 190. Circuit diagram for constant current supply.

**Constant Current Supply.** When it is desired to maintain a constant d-c current through a changing resistive load, as in Exp. 28, the circuit of Fig. 190 may be employed. The plate current of the pentode tube is nearly independent of the plate voltage over a fairly wide range of voltages when the control-grid and screen-grid potentials are held constant. (Cf. Fig. 173.) If the load resistance increases, the potential drop across it increases and the plate voltage of the tube decreases, but the resulting change in plate current is small. The current stability is further improved by the presence of the cathode resistor  $R_2$ . The plate current is controlled by adjusting the control-grid bias of the tube, a battery being used to obtain a very stable bias voltage.

Constancy of screen-grid voltage is assured by use of the voltage-regulator tube OA2. This type of tube contains a cold cathode of large area, an anode of small area, and a gas, such as argon, at low pressure. It is found that such a tube exhibits a practically constant potential drop from cathode to anode provided the current lies within limits specified by

the manufacturer. If the voltage across the series combination of  $R_1$  and the tube changes, the current through the tube will change, but the potential drop across it will not. The total change in voltage then appears across  $R_1$ . The resistance of  $R_1$  must be large enough to restrict the maximum current through the  $VR$  tube to a safe value, or the voltage-regulating property of the tube will be lost.

**Vacuum-tube Relay.** A current of the order of several milliamperes is required for the operation of the usual electromagnetically actuated relay. It is often desired to operate such a relay by means of a control device which itself supplies a much smaller current. A common example is the ordinary mercury thermoregulator, the flow of current through which may result in fouling of the capillary due to arcing at the mercury-air interface as contact is made or broken.

Figure 191a shows a typical vacuum-tube relay circuit employed in thermostat regulation. When the regulator contacts are open, the bias on the tube is maintained by the flow of plate current through the cathode resistors  $R_2$  and  $R_3$ . Reference to characteristic curves for a 12AU7 triode shows that the grid bias will be about  $-2.5$  volts, each plate current 5 ma, the plate voltage 100 volts, and the potential drop across the relay coil 50 volts. The relay contacts will hence be closed, and current will flow through the thermostat heater until the regulator contacts are closed by expansion of the mercury. When this occurs, a potential drop of 12 volts is produced across the resistor  $R_1$ ; the grid bias is thus changed to  $-12$  volts, and the plate current of the tube is reduced to zero. The relay contacts are thus opened, and the heating current is turned off. It is to be noted that the maximum current flowing through the mercury interface of the regulator is only  $6 \mu\text{a}$ . The maximum value of  $R_1$  for a particular tube is limited by the possibility of grid current flow. It is not possible to omit  $R_1$ , because in such a case the grid is left floating when the regulator contacts are open, and the performance of the tube becomes erratic.

The analogous circuit employing a transistor is shown in Fig. 191b.

Figure 192 gives complete details for a vacuum-tube relay circuit which has performed very satisfactorily in continuous service over extended periods of time. Semiconductor diodes are used in the bias and plate power supplies. The  $RC$  network in the grid circuit, with a time constant of 1 sec, provides a delay in response sufficient to prevent the occurrence of chattering, which can become a problem with the simpler circuits of Fig. 191.

**Cathode Follower.** Figure 193a shows the actual circuit diagram and equivalent circuit for a cathode follower, a device widely used in modern electronic equipment. The operation of the circuit is easily understood qualitatively: if the input signal  $e_i$  causes the grid potential to increase positively, the tube current  $I_p$  increases; as a result, the cathode potential



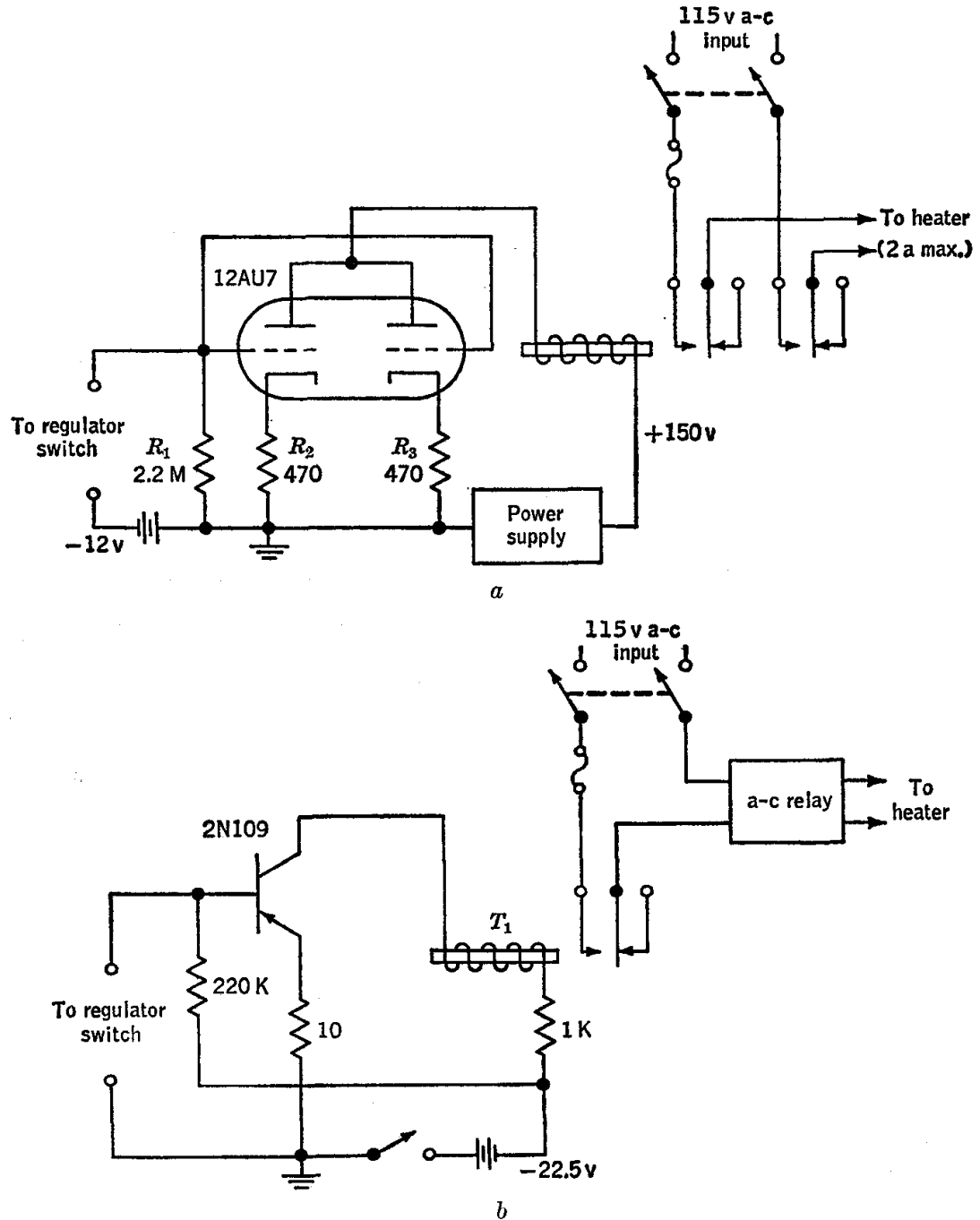


FIG. 191. (a) Vacuum-tube relay circuit. (Potter-Brumfield KCP 11 relay, 5-K, 7.2-ma coil.) (b) transistor-controlled relay circuit. ( $T_1$  = Potter-Brumfield PW5LS, 5-K, 2-ma coil.)

$I_p R_k$  also increases, the cathode thus tending to "follow" the grid. The voltage gain  $e_o/e_i$  may be seen from the equivalent circuit, Fig. 193b, to be

$$\frac{e_o}{e_i} = \frac{\mu R_k}{\mu R_k + r_p + 1} \cong \frac{R_k}{R_k + (r_p/\mu)} \quad (85)$$

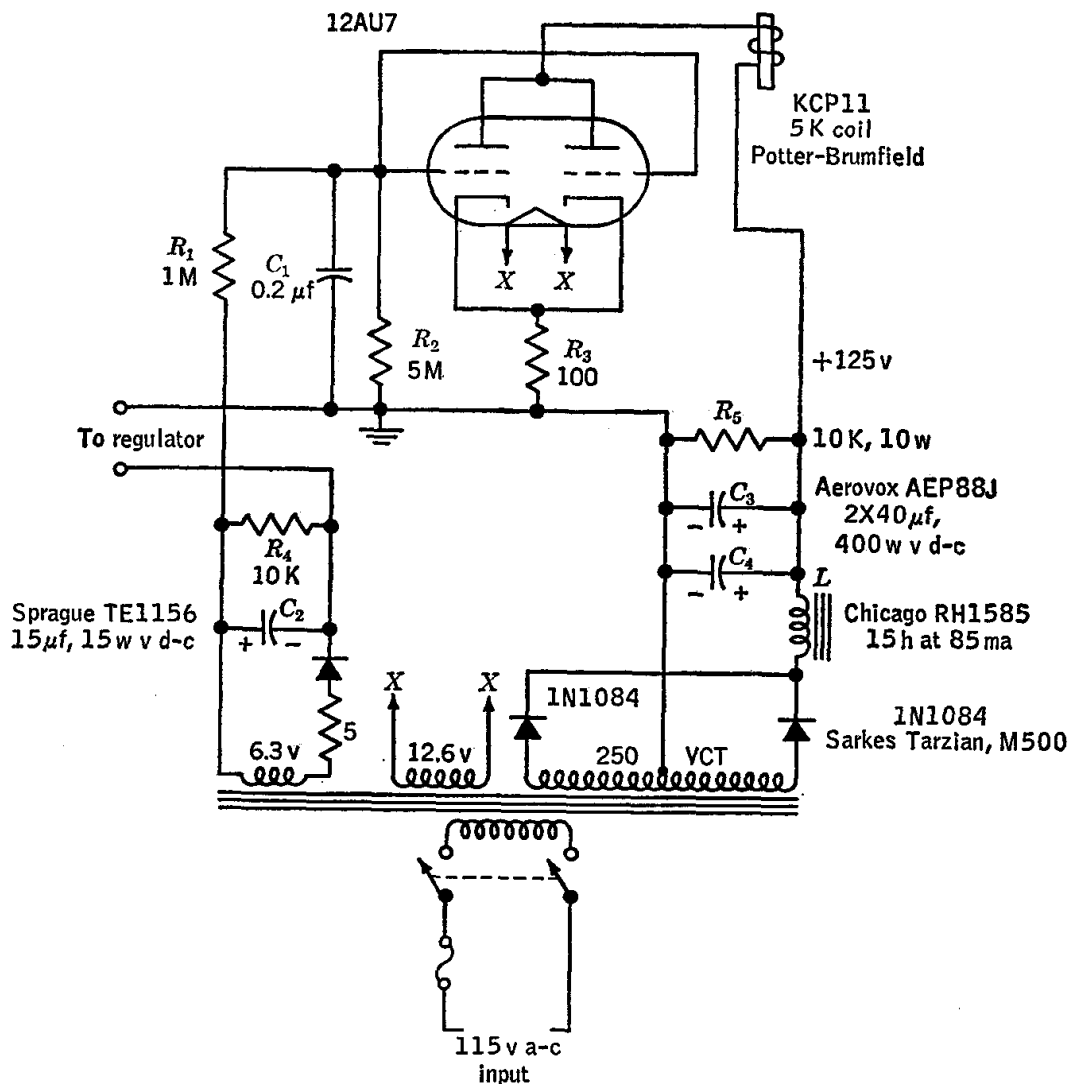


FIG. 192. Thermostat heater control circuit. The relay shown actuates a 115-volt a-c relay (KRP11AG) which in turn actuates another of the same type. The latter switches power to the heaters.

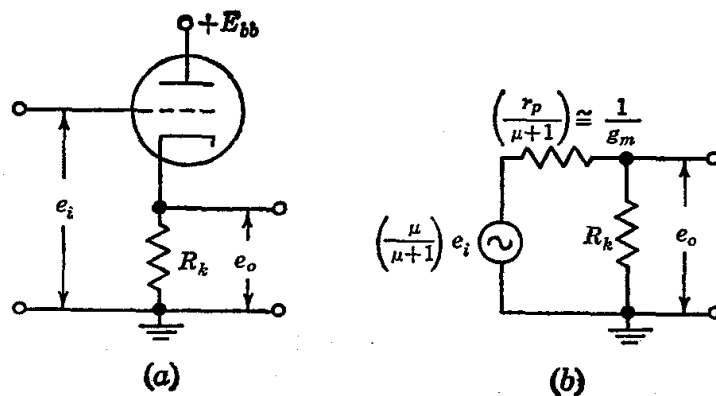


FIG. 193. Cathode follower. (a) Actual circuit; (b) equivalent circuit.

the approximation holding for  $\mu \gg 1$ . The ratio  $e_o/e_i$  is somewhat less than unity, but the power gain is large, as the cathode follower has a relatively high input impedance and low output impedance, the latter typically of the order of a few hundred ohms. Its use is illustrated in Fig. 194. If a load of, say, 10,000 ohms were to be connected at *A*, the gain of the first stage would drop severely; if the same load were connected at *B*, the over-all gain would drop only slightly. Thus the tube functions to supply the current required by a relatively low impedance load.

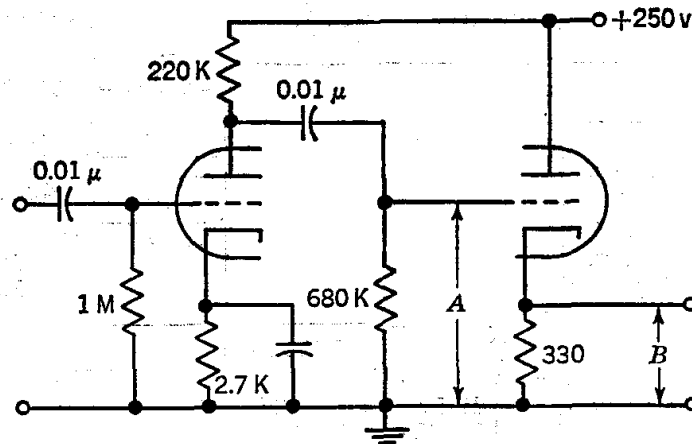


FIG. 194. Triode amplifier and cathode follower.

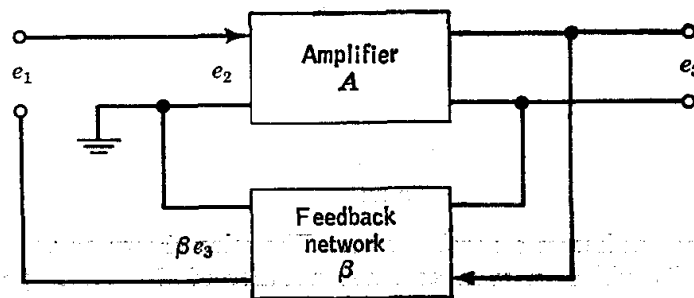


FIG. 195. Amplifier with feedback.

**Amplifier with Feedback.** The term *feedback* refers to the process of deriving from the output of an amplifier stage a voltage, called the *feedback voltage*, and applying it in series with the input signal of the same or an earlier stage. If the phase of the voltage fed back is such as to aid the signal to which it is added, the feedback is called *positive*, or *regenerative*; if the phase is such as to oppose the signal, the feedback is called *negative*, *degenerative*, or *inverse*.

The block diagram of an amplifier with feedback is illustrated in Fig. 195. For simplicity, we shall assume that there is no phase shift in either the amplifier or the feedback network, other than a possible sign

change ( $180^\circ$  shift). The signal input  $e_1$  is applied between the terminals shown. The total input to the amplifier, however, is  $e_2 = e_1 + \beta e_3$ , that is, the sum of the signal plus the feedback voltage  $\beta e_3$ . The amplifier itself has gain  $A$ , meaning  $e_3/e_2$ . The feedback network provides an output which is a certain fraction  $\beta$  of the amplifier output  $e_3$ . Then the definition of  $A$  leads to

$$(e_1 + \beta e_3)A = e_3 \quad (86)$$

whence the over-all gain  $G$ , from signal input terminals to output, is

$$G = \frac{e_3}{e_1} = \frac{A}{1 - \beta A} \quad (87)$$

For the case of negative feedback ( $\beta A$  negative), the gain  $G$  is less than  $A$  in magnitude; with regenerative feedback ( $\beta A$  positive), the gain  $G$  is greater than  $A$  in magnitude. For  $\beta A \cong 1$ , the amplifier becomes quite unstable and may break into oscillation.

In some applications, the feedback network produces a phase shift dependent on frequency. In this case, the quantities  $\beta$  and  $G$  in Eq. (87) become complex.

Three examples of the application of the principle of feedback follow: (a) the use of negative feedback to improve linearity of an amplifier and stability of gain, (b) the use of frequency-selective feedback to create a narrow-band amplifier, and (c) the use of regenerative feedback to convert an amplifier into an oscillator.

**Amplifiers with Negative Feedback.** Inverse feedback is used when it is desired to sacrifice gain in order to reduce distortion in the

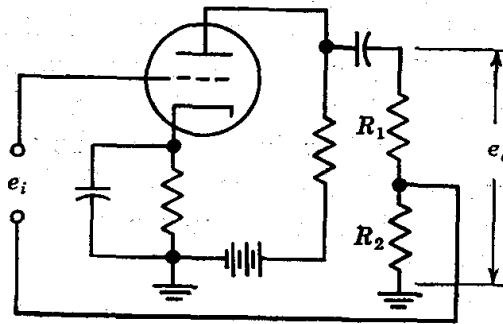


Fig. 196. Amplifier stage illustrating inverse feedback.

output waveform or to improve the constancy of gain. The use of inverse feedback for this purpose is illustrated in the circuit of Fig. 196. The input signal  $e_i$  is applied in series with the fraction<sup>1</sup>  $\beta = R_2/(R_1 + R_2)$

<sup>1</sup> The output impedance of the triode circuit, if not small compared with  $R_1$ , must be taken into account in calculating  $\beta$ . If the impedance of the coupling capacitor is negligible, the output impedance (page 566) of the triode circuit is effectively in series with  $R_1$ .

of the output voltage  $e_o$  of the amplifier stage. Because the plate voltage is decreased by an increase in grid voltage, the output voltage  $e_o$  is  $180^\circ$  out of phase with the input voltage, and hence the feedback is negative. The feedback voltage  $\beta e_o$  is then  $180^\circ$  out of phase with  $e_i$ , so that the signal amplification is reduced.

To see how the advantages mentioned above are obtained, one may apply Eq. (87) to this case. Here  $\beta A$  is negative. For  $|\beta A| \gg 1$ , the over-all signal gain approaches  $-(1/\beta)$ , and thus is determined mainly by the feedback network, and becomes relatively insensitive to the tube characteristics. For example, for  $\beta = \frac{1}{4}$  and  $A = -80$ , the value of  $G$  is  $-3.81$ ; now if  $A$  changes by 10 per cent, perhaps by replacement of the tube,  $G$  changes by only 0.5 per cent.

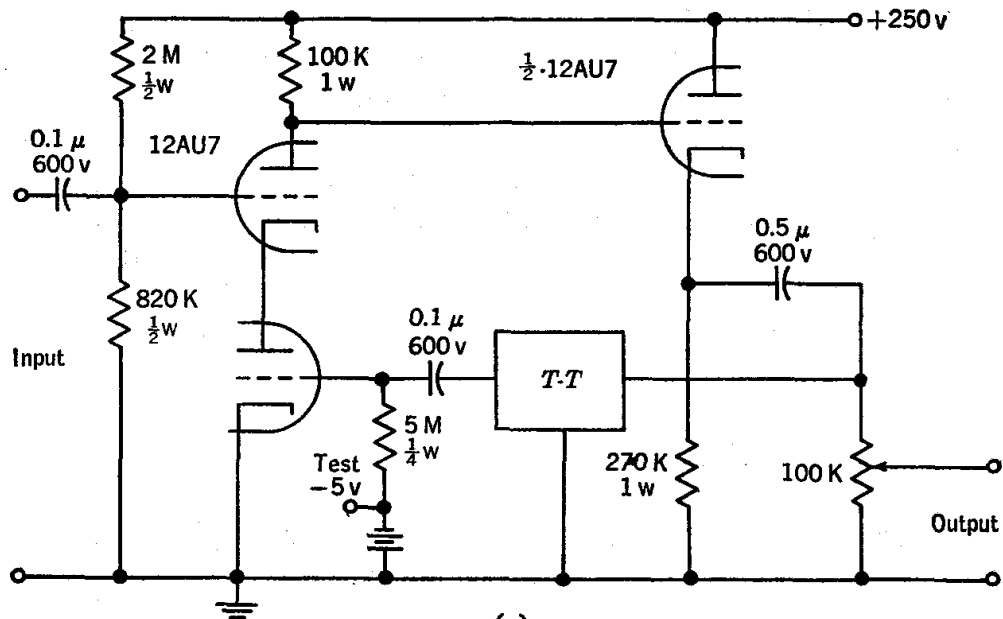
Another way of introducing negative feedback is to omit the cathode bypass capacitor. Since the a-c current through the cathode resistor is the same as that through the plate load impedance, the a-c cathode voltage becomes proportional to the a-c output voltage. Furthermore, this a-c cathode voltage is effectively subtracted from the input signal because the actual input to the tube is the difference between the grid and cathode voltages. The equivalent circuit of Fig. 172 provides the basis for the quantitative treatment of this case.

**Narrow-band (Frequency-selective) Audio Amplifier.** The term narrow-band amplifier refers to a bandpass amplifier of relatively narrow bandwidth. Figure 197a is the diagram of a narrow-band amplifier which employs feedback as a means of achieving frequency selectivity.<sup>1</sup> The twin-T network, Fig. 197b, exhibits a null output at a frequency  $\omega_0 = 2\pi f_0$ , satisfying the condition  $\omega_0^2 = 1/RC$ . The feedback is degenerative, so that the over-all amplifier gain is very low ( $G \ll 1$ ), except for frequencies close to the null frequency  $f_0$  for the twin-T. The resulting amplifier response curve is similar to that of a parallel resonant circuit peaked at  $f_0$ . With the circuit values shown, the gain at the peak frequency is 2, and the value of  $Q$ , the ratio of  $f_0$  to the half-power bandwidth  $\Delta f$ , is 15. The unused half of one twin-triode tube can be used as an amplifier if additional gain is needed.

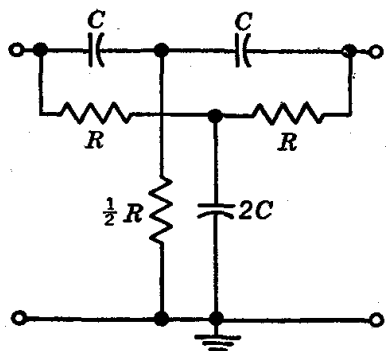
This circuit can be used throughout the audio range. As to the twin-T component sizes,  $C$  should be large enough to minimize effects of variations in stray capacitance, and  $R$  large enough to avoid overloading the cathode follower. A practical realization of the twin-T is shown as Fig. 197c.

**Vacuum-tube Oscillator.** An oscillator circuit is one which converts d-c power into a-c power. The use of feedback with an amplifier to achieve this end is illustrated by the diagram of Fig. 198. Here the

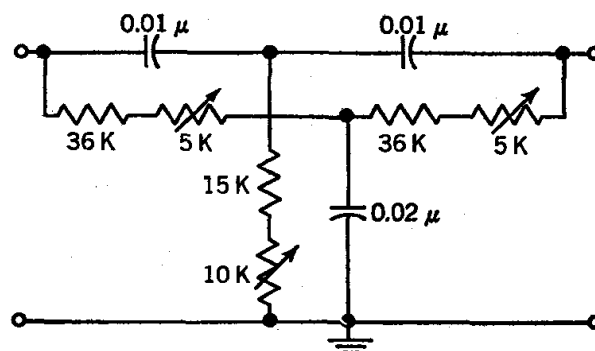
<sup>1</sup> Fleisher in Valley and Wallman (eds.), *op. cit.*



(a)



(b)



(c)

FIG. 197. Frequency-selective amplifier. (a) Circuit diagram of amplifier [adapted from circuit of Fleisher in Valley and Wallman (eds.), "Vacuum Tube Amplifiers," McGraw-Hill Book Company, Inc., New York (1948)]; (b) twin-T network; (c) practical twin-T network, tunable from 380 to 420 cycles/sec.

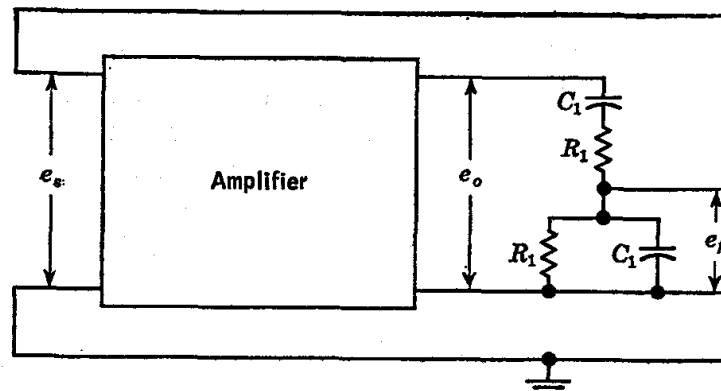


FIG. 198. Schematic diagram of RC-coupled oscillator.

entire grid excitation for the amplifier is derived by feeding back part of the output into the grid circuit. Note that in this case the amplitude and phase of the feedback voltage are dependent on frequency.

The circuit of Fig. 198 falls in the class of feedback circuits illustrated by Fig. 195, but with the signal input terminals shorted together since there is now no external signal. If the oscillations are to be self-sustaining, two conditions<sup>1</sup> must be met at the frequency of oscillation:

1. For Eq. (86) to be satisfied with no external excitation ( $e_1 = 0$ ), a necessary condition is

$$A\beta = 1 \quad (88)$$

2. The total phase shift in the amplifier and feedback network must be  $0^\circ$ .

On the assumption that the amplifier phase shift is negligible, condition 2 is met when the feedback-network phase shift is zero. For the network shown, this happens at only one frequency,<sup>2</sup>  $f = 1/2\pi R_1 C_1$ . This condition therefore determines the frequency of oscillation. Though other types of feedback networks are used for oscillators, all have in common this property, namely, a phase shift strongly dependent on frequency, this being essential for good frequency stability.

For the network shown, the value of  $\beta$  is  $\frac{1}{3}$  when the phase shift is zero, so that Eq. (88) is satisfied for an amplifier gain of 3. In practical terms, the amplifier would be designed to have a small-amplitude gain of somewhat more than 3. The amplitude of oscillations, then, will build up until the nonlinearity in tube characteristics, or some other factor, reduces the gain to a value exactly satisfying Eq. (88). Thus, through the dependence of  $A$  on amplitude, Eq. (88) actually determines implicitly the amplitude of oscillations.

An excellent practical audio-oscillator circuit which employs these principles is shown in Fig. 199. Here degenerative feedback (network  $R_3, R_4, R_5$ , and the lamp  $V_3$ ) is used to stabilize the gain at approximately the value 3. Good amplitude stability is provided by the use of lamp  $V_3$  in the feedback network; if the amplitude increases, the increased a-c power dissipated in the lamp causes the temperature of its filament to increase. The accompanying increase in resistance alters the feedback ratio in such a way as to decrease the gain and thus to oppose the change in amplitude. A better waveform is obtained in this way than if the amplitude is stabilized through nonlinearity in the tube dynamic transfer characteristic.

<sup>1</sup> Both conditions are contained in Eq. (88) if  $A$  and  $\beta$  are considered in general to be complex quantities.

<sup>2</sup> Landee, Davis, and Albrecht, *op. cit.*, Section 6, p. 48.

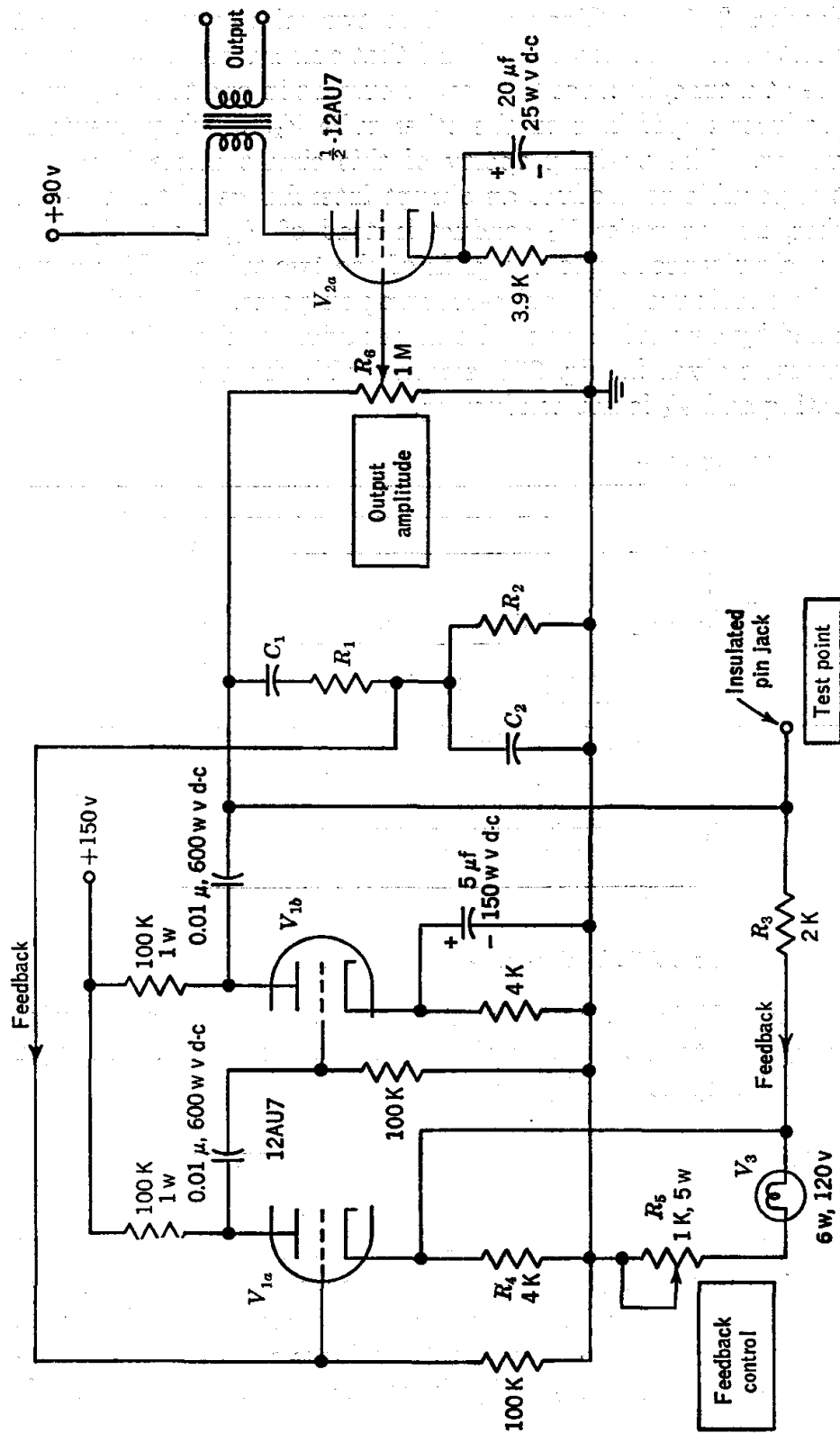


FIG. 199. Circuit of audio oscillator with good waveform and amplitude stability [adapted from circuit of Terman, Buss, Hewlett, and Cahill, *Proc. IRE*, 27, 649 (1939)]. Values of  $R_1$ ,  $R_2$ ,  $C_1$ ,  $C_2$  are chosen for the desired frequency of oscillation. The degenerative feedback control  $R_5$  is adjusted to achieve good amplitude stability consistent with a satisfactory waveform as observed with an oscilloscope connected at the test point. The amplitude is normally about 1 volt rms at this point.



**Eccles-Jordan Trigger Circuit.** When two triodes are connected as in the circuit of Fig. 200, it will be found that current will flow through only one tube at a time, because the flow of current in one tube  $V_1$  automatically produces a grid bias on the other tube  $V_2$ , which prevents it from conducting. The useful property of this circuit arises from the fact that it is possible to produce an abrupt interchange of the roles of the two tubes, i.e., to make  $V_2$  conduct instead of  $V_1$ , by applying a voltage pulse simultaneously to the grids of the two tubes. This property makes the circuit useful for pulse-counting purposes. That this is so may be verified by determining the circuit behavior for the values of the circuit parameters given in Fig. 200, starting with the assumption that  $V_1$  is conducting and  $V_2$  is not conducting.

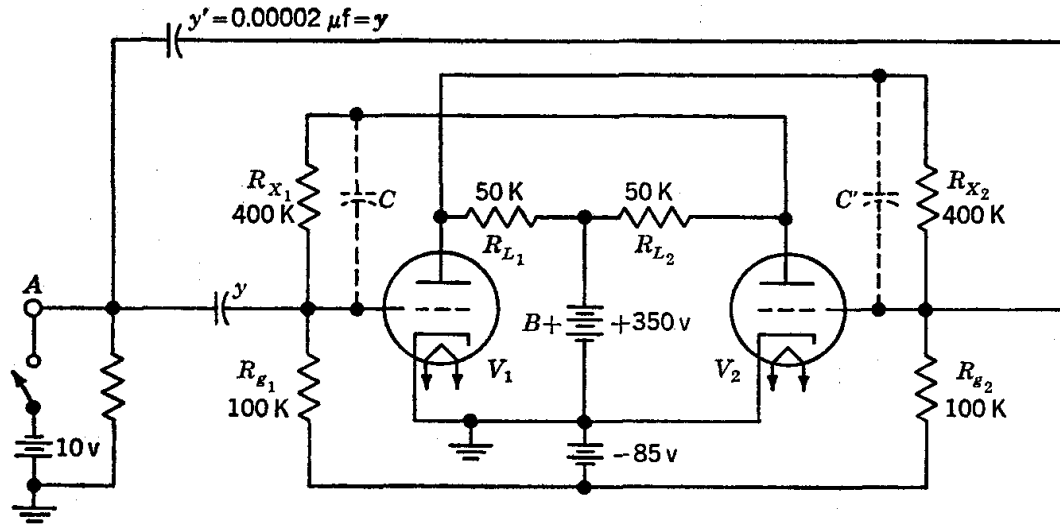


FIG. 200. Eccles-Jordan trigger circuit.

The grid bias of  $V_1$  is obviously equal to  $-85$  volts plus the potential drop across the resistor  $R_{g1}$ . Since there is no current flowing through  $V_2$ , the potential drop across  $R_{g1}$  is given by

$$E_{R_{g1}} = (350 + 85) \times \frac{100,000}{100,000 + 400,000 + 50,000} = 79.2 \text{ volts}$$

The grid bias of  $V_1$  is then equal to  $-5.8$  volts; its plate voltage and plate current  $i_{p1}$  must now be determined. The potential drops across  $R_{g2}$ ,  $R_{x2}$ , and  $R_{L1}$  must add up to 435 volts, since these three resistors are connected in series across the 435-volt total voltage supply. If the current flowing through  $R_{g2}$  and  $R_{x2}$  is  $i_{c2}$ , the current flowing through  $R_{L1}$  is  $i_{c2} + i_{p1}$ , and

$$100,000i_{c2} + 400,000i_{c2} + 50,000(i_{p1} + i_{c2}) = 435 \text{ volts}$$

The additional information required for the determination of the values of the two unknowns  $i_{p_1}$  and  $i_{c_2}$  is provided by the characteristic curves for the 6C5 triode, since the plate voltage for  $V_1$  is  $350 - 50,000(i_{p_1} + i_{c_2})$  volts, and the grid bias of the tube has been determined to be  $-5.8$  volts. It is found that  $i_{p_1}$  is 3.4 milliamp and  $i_{c_2}$  is 0.5 milliamp, corresponding to a plate voltage of 155 volts for  $V_1$  and a drop of 195 volts across  $R_{L_1}$ . Since  $i_{c_2}$  is 0.5 milliamp, the potential drop across  $R_{g_2}$  is 50 volts. The grid bias of  $V_2$  is therefore  $-35$  volts, a value for which the tube cannot conduct, substantiating our previous assumption to this effect. The foregoing calculation shows that  $V_2$  cannot conduct if  $V_1$  is conducting, because the flow of the plate current through the plate load resistor of  $V_1$  automatically produces a grid bias on  $V_2$  which prevents it from conducting.

When the switch is open, the point  $A$  is at ground potential. If the switch is closed,  $A$  becomes negative with respect to ground, and electrons will be repelled from the condensers  $y$  and  $y'$  until the potential drops across them have been increased by 10 volts. The electrons from condenser  $y'$  flow through  $R_X$ , and  $R_{L_1}$  to  $B^+$  and in so doing cause a momentary increase in the grid bias of  $V_2$ , which cannot be made less conducting. The electrons flowing out of condenser  $y$  flow through  $R_X$ , and  $R_{L_1}$ , and hence cause a decrease in the potential drop across  $R_{g_1}$ , increasing the grid bias on  $V_1$  and making it less conducting; as a result, the plate current of  $V_1$  decreases, the potential drop across  $R_{L_1}$  decreases, and the potential drop across  $R_{g_2}$  therefore increases, making the grid bias smaller and rendering the tube  $V_2$  conducting. (Owing to the amplifying properties of the triode, the decrease in the grid bias on  $V_2$  resulting from the decrease in the potential drop across  $R_{L_1}$  more than offsets the increase in grid bias due to the electron flow from  $y'$ .) As  $V_2$  begins to conduct, the drop across  $R_{L_1}$  increases, which increases the grid bias on  $V_1$  still further, and the process continues until  $V_1$  is nonconducting and  $V_2$  alone conducts.

If now the switch is opened, the point  $A$  is returned to ground potential, and a condenser-discharging current flows into  $y$  through  $R_{g_1}$ , momentarily decreasing the bias of  $V_2$ .  $V_1$  then begins to conduct, and the circuit "triggers" again, returning  $V_1$  to the conducting state and  $V_2$  to the nonconducting state. Because this triggering action is positive and rapid, the Eccles-Jordan circuit finds application in the scaling units employed for counting the pulses from Geiger-Müller tubes. With such sharp pulses, the condensers  $C$  and  $C'$  are used to eliminate the influence of the interelectrode capacitances in the triodes on the action of the circuit.

**Pulse-counting, or Scaling, Circuit.** A typical scaling circuit<sup>1</sup> based on the Eccles-Jordan trigger circuit is shown in Fig. 201. It is seen to consist of two stages, or trigger pairs, of the type just considered, con-

<sup>1</sup> Lifschutz and Lawson, *Rev. Sci. Instr.*, **9**, 83 (1938).

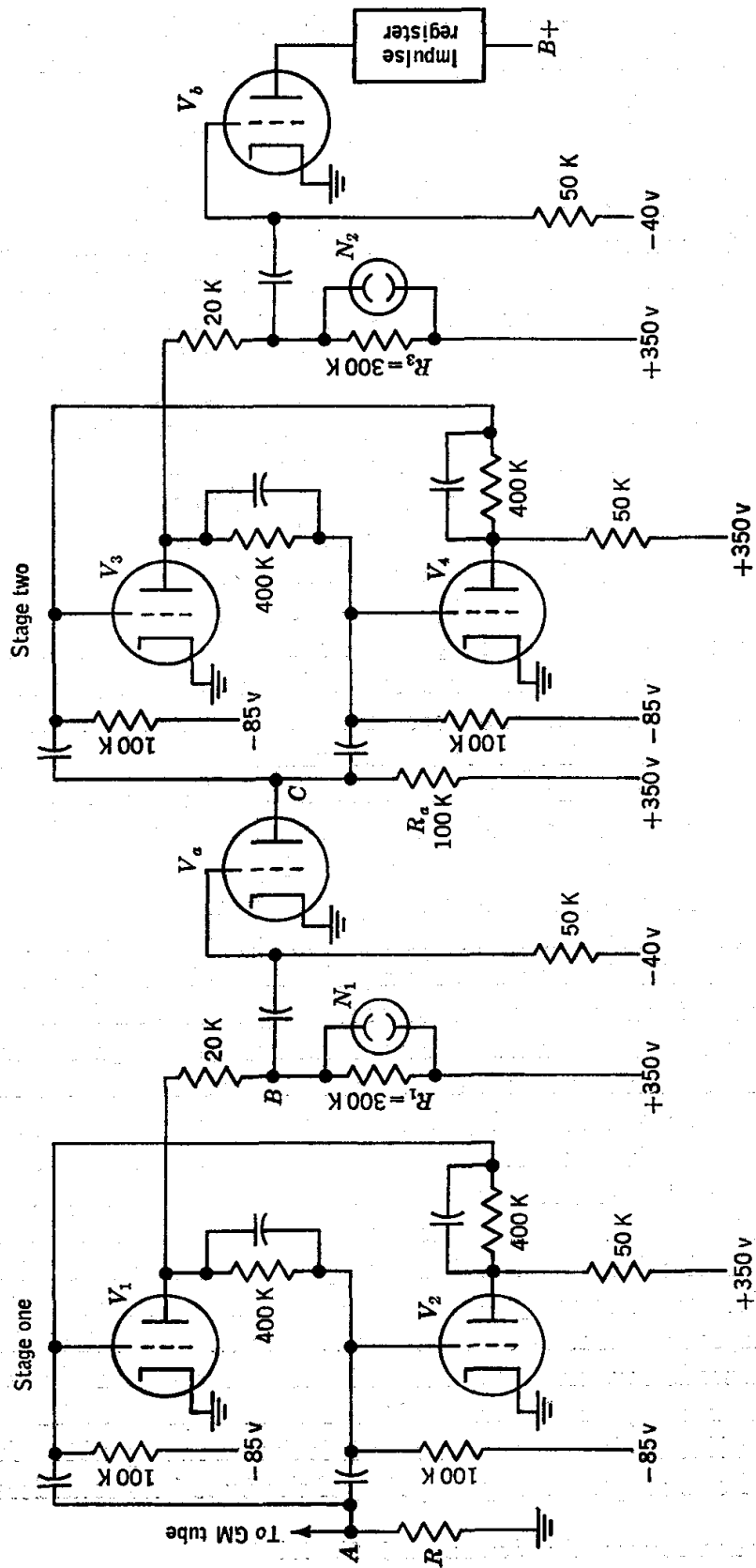


Fig. 201. Scale-of-four counting circuit based on Eccles-Jordan trigger circuit.

ected by an in-between-stage tube whose function is indicated below. In addition, small neon lamps have been placed across a portion of the plate resistor of one tube of each pair to indicate which tube is conducting. These tubes give a visible indication but draw practically no current.

Let us suppose that the tubes  $V_2$  and  $V_4$  are initially in the conducting state. Both neon lights will then be out, since no current will be flowing through the resistors  $R_1$  and  $R_3$ . (This condition may be achieved, for example, by grounding the grids of  $V_2$  and  $V_4$  momentarily.) Let an avalanche of electrons from the Geiger-Müller tube flow through the resistor  $R$  to ground. The point  $A$  will be abruptly driven negative, and a negative pulse will be applied to the grids of  $V_1$  and  $V_2$ ; i.e., the grid bias of each tube will be momentarily increased. As explained above, this will cause the first stage to trigger;  $V_2$  will be cut off, and  $V_1$  will conduct. When  $V_1$  is not conducting, there is no potential drop across  $R_1$ , and the neon lamp  $N_1$  is out. When  $V_1$  abruptly is made to conduct, the flow of plate current through  $R_1$  creates a potential drop which lights  $N_1$ , while the resulting abrupt decrease in potential at point  $B$  sends a negative pulse to the grid of  $V_a$ . Since  $V_a$  is normally nonconducting anyway, this momentary increase in its grid bias has no effect on  $V_a$ , and hence there is no effect on stage 2, where  $V_4$  continues to conduct, with  $V_3$  nonconducting. The first pulse from the Geiger-Müller tube then makes  $V_1$  conduct, lighting  $N_1$ , cuts  $V_2$  off, and has no other effect.

Let a second pulse come from the Geiger-Müller tube. Stage 1 will again be triggered;  $V_2$  will conduct, and  $V_1$  will be cut off. When the plate current of  $V_1$  is cut off,  $N_1$  will go out, and the potential at point  $B$  will rise abruptly, causing a positive pulse at the grid of  $V_a$ , which is thereby momentarily rendered conducting. The resulting momentary flow of plate current through the plate resistor  $R_a$  causes an abrupt decrease of potential at point  $C$ . This in turn causes a negative pulse at the grids of  $V_4$  and  $V_3$ , thus triggering the second stage so that  $V_4$  is cut off and  $V_3$  conducts, lighting neon lamp  $N_2$  and sending a negative pulse to  $V_b$ , which is unaffected. The second pulse thus turns off  $N_1$ , turns on  $N_2$ , and has no further effects.

The third pulse will again trigger stage 1;  $V_1$  is again made conducting,  $N_1$  lights up, and a negative pulse is applied to the grid of  $V_a$ . Since  $V_a$  is unaffected by a negative pulse, stage 2 is not affected by the third pulse, and  $N_2$  also remains on.

A fourth pulse will trigger stage 1, turning  $N_1$  off and applying a positive pulse to the grid of  $V_a$ . This in turn applies a negative pulse to the grids of  $V_3$  and  $V_4$ . The second stage triggers also;  $N_2$  is turned off, and a positive pulse is applied to the grid of  $V_b$ . This results in a momentary flow of plate current through  $V_b$ , and hence through the coil of the electromagnetically actuated mechanical impulse register, which records one

count. The fifth pulse will then light  $N_1$ , the sixth will light  $N_2$  and turn off  $N_1$ , etc.

Because the counter is actuated only by every fourth pulse, this circuit is referred to as a scale-of-four counting circuit.

**Phase-sensitive Detector.** The phase-sensitive detector, illustrated schematically in Fig. 202, has two inputs, a signal input and a reference input. The latter is usually a sine wave,

$$E_r = E_0 \cos 2\pi f_0 t \quad (89)$$

while the signal input is a voltage of the same frequency,

$$E_s = E'_0 \cos (2\pi f_0 t + \varphi_s) = E_1 \cos 2\pi f_0 t + E_2 \sin 2\pi f_0 t \quad (90)$$

often accompanied by noise.<sup>1</sup> It is the function of the phase-sensitive

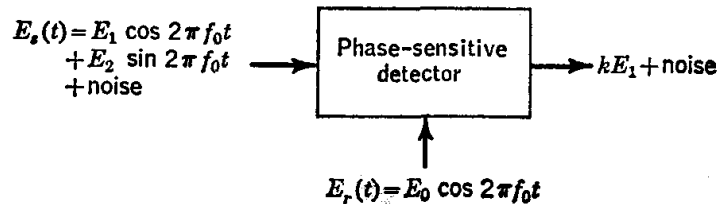


FIG. 202. Diagram illustrating the function of a phase-sensitive detector.

detector to produce an output d-c voltage proportional to the amplitude  $E_1 = E'_0 \cos \varphi_s$  of the *in-phase* component of the signal, while responding as little as possible to the quadrature ( $90^\circ$ ) component and to noise. Of course, it does necessarily respond to noise components with frequencies sufficiently close to  $f_0$ . Many practical phase-sensitive detector circuits also respond to noise components close to integral multiples of  $f_0$ , but this is seldom a disadvantage because the bandwidth of the preceding amplifier can easily be made narrow enough to eliminate noise components at harmonics of  $f_0$ .

Two practical phase-sensitive detector circuits are shown in Fig. 203. In the upper circuit, the reference signal drives a switching relay which feeds the signal alternately to two different points. For the signal component in phase with the reference voltage, the positive half-cycle is always applied to one side and the negative half-cycle to the other. The low-pass filter smooths out the a-c components, and there results a d-c voltage which produces a meter deflection. However, for the sine component of the signal, the switching times are such that no d-c component results in the output, since in this case the switching occurs at the peaks of the signal voltage. For a noise component of frequency  $f_n$ , close to  $f_0$ , the switching occurs at different points on successive cycles; the

<sup>1</sup> Several examples of systems which include phase-sensitive detectors occur in Chap. 26.

resulting output contains no d-c component, but does contain a-c components, some of which are at the frequency  $|f_n - f_0|$ , which may be low enough ( $\approx 1/2\pi RC$ ) to appear at the output of the low-pass filter. The totality of noise components of frequencies close to  $f_0$  in the input therefore produces random low-frequency fluctuations in the output.

With the use of high-speed relays, particularly solid-state types, this and similar circuits are useful in the low audio range, up to several hundred cycles per second. The switching can be accomplished electronically with a twin-triode tube, as in the circuit of Schuster,<sup>1</sup> which,

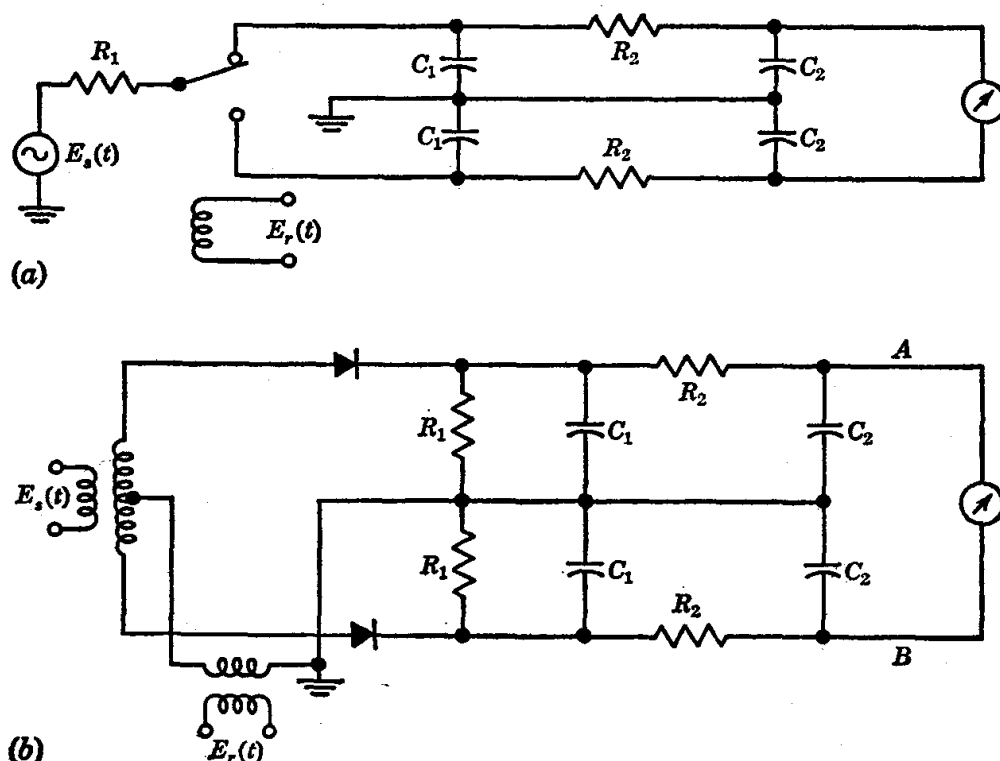


FIG. 203. Practical phase-sensitive detector circuits. (a) Relay type; (b) diode type.

with only minor changes, has been used very successfully at frequencies throughout the range 30 cycles/sec to 100 kc/sec.

Another type of phase-sensitive detector is that of Fig. 203b. To examine its operation, consider first the case in which there is no signal input. Then the reference input, applied through a transformer, is fed to a split load comprising two ordinary diode detector circuits (page 573) in parallel. The output of each is a d-c voltage close to the peak value of the input waveform. If the diodes and other components are suitably matched, the same d-c voltage is developed at point A as at B, and the net voltage difference between these output terminals is zero. The reference voltage is chosen to be rather large, say 5 to 15 volts rms. Now let the

<sup>1</sup> Schuster, *Rev. Sci. Instr.*, 22, 254 (1951).

signal voltage be applied. For proper operation of the detector, this must be much smaller than the reference voltage, perhaps less than a volt. If the signal voltage has the same frequency and phase as the reference, the total voltage (vector sum) applied to one diode circuit is increased, while that applied to the other is decreased, and a d-c voltage unbalance develops at the output terminals *A* and *B*. A signal voltage 90° out of phase with the reference, however, does not produce an output because the vector addition of a small quadrature signal to the large reference voltage produces only a negligible change in amplitude, and hence does not unbalance the two diode circuits. Again, noise components at frequencies  $f_n$  close to  $f_0$  produce a-c components in the output at frequencies  $|f_n - f_0|$ .

### SAFETY PRECAUTIONS

It is particularly important that the safety factor be kept firmly in mind in working on or with electronic circuits, since the hazards involved in any electrical work where high voltages may be present are considerable. A current of as little as 15 milliamp has been known to be fatal, and although such shocks usually are produced by higher-voltage sources, the ordinary 110-volt a-c line voltage has been known to be sufficient. The hazard is especially great when the skin is moist, particularly as a result of perspiration.

Direct-current voltages are also very dangerous. A particular source of trouble arises when, owing to faulty circuit design, no path has been provided for the discharge of high-voltage condensers after the main power switch has been turned off. A good-quality condenser will retain its charge for quite a time if the only discharge path is by slow leakage of current between the terminals. A bleeder resistor across the condenser may be employed to eliminate this difficulty, but it is well to bear in mind that the time constant for discharging may be several minutes, and also that bleeder resistors may fail, or somehow become disconnected. The only safe course is to develop the habit of ensuring the discharge of high-voltage condensers, before working around them, by momentarily placing a screwdriver or other reliable short across the terminals.

It is desirable to employ double-pole switches in a-c or d-c power lines. One side of the 110-volt a-c line is usually at ground potential; if a non-polarized plug is used, with a single-pole switch in the line, there is an even chance that one terminal of the load will be live when the main power switch is off, unless, of course, a transformer is used between line and load.

Alterations of circuits should be carried out only with the primary power source disconnected. In the measurement of voltages, etc., properly insulated test leads must be used.

## Appendix

### ALGEBRA OF COMPLEX NUMBERS

The rules of complex algebra will be stated briefly. A complex number  $c$  may always be written in the form

$$c = a + ib \quad (\text{A1})$$

where  $a$  and  $b$  are real numbers and  $i$  is the pure imaginary unit defined by

$$i^2 = -1 \quad (\text{A2})$$

The rules for manipulation of complex numbers are the same as the usual rules of algebra for real numbers, with  $i$  treated purely as an algebraic symbol, except for use of Eq. (A2). Thus, for example, the sum of two complex numbers

$$c_1 = a_1 + ib_1 \quad (\text{A3})$$

$$c_2 = a_2 + ib_2 \quad (\text{A4})$$

is 
$$c_1 + c_2 = (a_1 + a_2) + i(b_1 + b_2) \quad (\text{A5})$$

The product is

$$c_1 c_2 = (a_1 a_2 - b_1 b_2) + i(a_1 b_2 + a_2 b_1) \quad (\text{A6})$$

and the quotient  $c_1/c_2$  is

$$\begin{aligned} \frac{c_1}{c_2} &= \frac{a_1 + ib_1}{a_2 + ib_2} = \frac{(a_1 + ib_1)(a_2 - ib_2)}{a_2^2 + b_2^2} \\ &= \frac{a_1 a_2 + b_1 b_2}{a_2^2 + b_2^2} + i \frac{a_2 b_1 - a_1 b_2}{a_2^2 + b_2^2} \end{aligned} \quad (\text{A7})$$

In all cases, the resulting complex number has been written explicitly in terms of its real and imaginary parts.

A very useful formula of complex algebra is the Euler equation,

$$e^{ix} = \cos x + i \sin x \quad (\text{A8})$$

Clearly, any complex number  $a + ib$  can be written alternatively in the form  $Ae^{i\varphi}$ , where  $A$  and  $\varphi$  are real, since a solution always exists for the equations

$$Ae^{i\varphi} = A \cos \varphi + i(A \sin \varphi) = a + ib \quad (\text{A9})$$



Complex quantities may be plotted in a plane as shown in Fig. 204, the abscissa and ordinate being the real and imaginary parts, respectively. The graph provides a very helpful means for visualizing the implications of Eq. (A9):  $A$  and  $\varphi$  are the polar coordinates of the point representing a complex number, while  $a$  and  $b$  are the rectangular coordinates of the same point. Multiplication by a real number moves a point directly away from the origin; multiplication by  $e^{i\varphi}$  rotates a point through an angle  $\varphi$  counterclockwise.

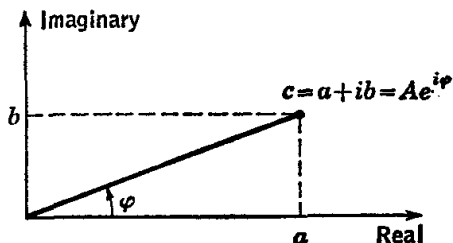


FIG. 204. Graph of complex numbers in a plane. The point indicated for the general complex number  $c = a + ib = Ae^{i\varphi}$  has rectangular coordinates  $(a, b)$  and polar coordinates  $(A, \varphi)$

The complex conjugate  $c^*$  of a complex number  $c$  is obtained by replacing  $i$  by  $-i$  throughout. Thus  $(c^*c)$  is a real number, the square root of which is called the *magnitude*, or *absolute value*, of  $c$ , often represented by the symbol  $|c|$ . Clearly,  $|c| = A$ .

## PHYSICAL-CHEMICAL CONSTANTS

The following tables give the recommended values of the fundamental constants for physical chemistry based upon the reanalysis and reevaluation of experimental values by Cohen, DuMond, Layton, and Rollett.<sup>1</sup> The constants involving moles or equivalent are based on the new atomic-weight scale with  $^{12}\text{C}$  set by definition at 12 atomic mass units.

### VALUES OF THE DEFINED CONSTANTS

Standard gravity.....	980.665 cm sec <sup>-2</sup>
Standard atmosphere.....	1,013,250 dynes cm <sup>-2</sup>
Standard millimeter of mercury pressure.....	$\frac{1}{760}$ atm
Calorie (thermochemical).....	4.1840 joules
	4.18331 int joules
	41.2929 cm <sup>3</sup> atm
	0.0412917 liter atm
Triple point of water <sup>a</sup> .....	273.16
Atomic weight of carbon.....	12.00000

<sup>a</sup> Crittenden, *Science*, 120, 1007 (1954).

<sup>1</sup> *Reviews Modern Phys.*, 27, 363 (1955).

## VALUES OF THE BASIC CONSTANTS

Velocity of light	$c$	$(2.997930 \pm 0.000003) \times 10^{10}$ cm sec <sup>-1</sup>
Planck constant	$h$	$(6.6252 \pm 0.00023) \times 10^{-27}$ erg sec
Avogadro constant	$N$	$(6.0229 \pm 0.00016) \times 10^{23}$ mole <sup>-1</sup>
Faraday constant	$F$	96,491.2 $\pm$ 1.1 coulombs equiv <sup>-1</sup> 23,062 cal volt <sup>-1</sup> equiv <sup>-1</sup>
Absolute temperature of the "ice point," 0°C	$T_{0^\circ\text{C}}$	273.1500 $\pm$ 0.0002°K
Pressure-volume product for 1 mole of a gas at 0° and zero pressure	$(PV)_{T_0^\circ}^{P_0}$	22,413.6 cm <sup>3</sup> atm mole <sup>-1</sup> 22.4130 liter atm mole <sup>-1</sup> 2271.06 $\pm$ 0.04 joules mole <sup>-1</sup>

## VALUES OF THE DERIVED CONSTANTS

Electronic charge	$e = \frac{F}{N}$	$(1.60206 \pm 0.000036) \times 10^{-19}$ coulomb 1.60206 $\times$ 10 <sup>-20</sup> emu 4.8029 $\times$ 10 <sup>-10</sup> esu
Gas constant	$R = \frac{(PV)_{T_0^\circ}^{P_0}}{T_0^\circ}$	1.9872 cal deg <sup>-1</sup> mole <sup>-1</sup> 82.057 cm <sup>3</sup> atm deg <sup>-1</sup> mole <sup>-1</sup> 0.082054 liter atm deg <sup>-1</sup> mole <sup>-1</sup> 8.3143 $\pm$ 0.00034 joules deg <sup>-1</sup> mole <sup>-1</sup>
Boltzmann constant	$k = R/N$	$(1.38044 \pm 0.00007) \times 10^{-16}$ erg deg <sup>-1</sup>

## VALUES OF CERTAIN AUXILIARY RELATIONS

- 1 second (mean solar) = 1.00273791 sidereal seconds
- 1 joule = 0.999835  $\pm$  0.000052 international joule
- 1 ohm = 0.999505  $\pm$  0.000015 international ohm
- 1 ampere = 1.000165  $\pm$  0.000025 international amperes
- 1 volt = 0.999670  $\pm$  0.000029 international volt
- 1 coulomb = 1.000165  $\pm$  0.000025 international coulombs
- 1 watt = 0.999835  $\pm$  0.000052 international watt
- 1 liter = 1000.028  $\pm$  0.004 cm<sup>3</sup>

## REDUCTION OF BAROMETER READINGS ON A BRASS SCALE TO 0°

$$P_0 = P - P \frac{\alpha t - \beta(t - t_s)}{1 + \alpha t}$$

$P_0$  = barometer reading reduced to 0°

$P$  = observed barometer reading

$t$  = centigrade temperature of barometer

$\alpha$  = 0.0001818 = mean cubical coefficient of expansion of mercury between 0 and 35°

$\beta$  = linear coefficient of expansion of scale material,  $18.4 \times 10^{-6}$  for brass

$t_s$  = temperature at which scale was calibrated, normally 20°C

## CORRECTION TO BE SUBTRACTED FROM BAROMETER READINGS

$t, ^\circ\text{C}$	720 mm	730 mm	740 mm	750 mm	760 mm	770 mm	780 mm
15	1.76	1.78	1.81	1.83	1.86	1.88	1.91
16	1.88	1.90	1.93	1.96	1.98	2.01	2.03
17	1.99	2.02	2.05	2.08	2.10	2.13	2.16
18	2.11	2.14	2.17	2.20	2.23	2.26	2.29
19	2.23	2.26	2.29	2.32	2.35	2.38	2.41
20	2.34	2.38	2.41	2.44	2.47	2.51	2.54
21	2.46	2.50	2.53	2.56	2.60	2.63	2.67
22	2.58	2.61	2.65	2.69	2.72	2.76	2.79
23	2.69	2.73	2.77	2.81	2.84	2.88	2.92
24	2.81	2.85	2.89	2.93	2.97	3.01	3.05
25	2.93	2.97	3.01	3.05	3.09	3.13	3.17
26	3.04	3.09	3.13	3.17	3.21	3.26	3.30
27	3.16	3.20	3.25	3.29	3.34	3.38	3.42
28	3.28	3.32	3.37	3.41	3.46	3.51	3.55
29	3.39	3.44	3.49	3.54	3.58	3.63	3.68
30	3.51	3.56	3.61	3.66	3.71	3.75	3.80

## VAPOR PRESSURE OF WATER

$t, ^\circ\text{C}$	$P, \text{ mm Hg}$	$t, ^\circ\text{C}$	$P, \text{ mm Hg}$	$t, ^\circ\text{C}$	$P, \text{ mm Hg}$	$t, ^\circ\text{C}$	$P, \text{ mm Hg}$
0	4.6	26	25.2	40	55.3	90	526.0
5	6.5	27	26.8	45	71.9	95	634.0
10	9.2	28	28.3	50	92.5	96	657.7
15	12.8	29	30.1	55	118.1	97	682.1
20	17.5	30	31.8	60	149.5	98	707.3
21	18.7	31	33.7	65	187.6	99	733.2
22	19.8	32	35.7	70	233.8	100	760.0
23	21.0	33	37.7	75	289.3	101	787.6
24	22.4	34	39.9	80	355.5	102	816.0
25	23.8	35	42.2	85	433.8	103	845.3

## DENSITY OF WATER IN GRAMS PER CUBIC CENTIMETER

Degrees	0	0.1	0.2	0.3	0.4	0.5	0.6	0.7	0.8	0.9
0	0.999841	847	854	860	866	872	878	884	889	895
1	0.999900	905	909	914	918	923	927	930	934	938
2	0.999941	944	947	950	953	955	958	960	962	964
3	0.999965	967	968	969	970	971	972	972	973	973
4	0.999973	973	973	972	972	972	970	969	968	966
5	0.999965	963	961	959	957	955	952	950	947	944
6	0.999941	938	935	931	927	924	920	916	911	907
7	0.999902	898	893	888	883	877	872	866	861	855
8	0.999849	843	837	830	824	817	810	803	796	789
9	0.999781	774	766	758	751	742	734	726	717	709
10	0.999700	691	682	673	664	654	645	635	625	615
11	0.999605	595	585	574	564	553	542	531	520	509
12	0.999489	486	475	463	451	439	427	415	402	390
13	0.999377	364	352	339	326	312	299	285	272	258
14	0.999244	230	216	202	188	173	159	144	129	114
15	0.999099	084	069	054	038	023	007	*991	*975	*959
16	0.998943	926	910	893	877	860	843	826	809	792
17	0.998744	757	739	722	704	686	668	650	632	613
18	0.998595	576	558	539	520	501	482	463	444	424
19	0.998405	385	365	345	325	305	285	265	244	224
20	0.998203	183	162	141	120	099	078	056	035	013
21	0.997992	970	948	926	904	882	860	837	815	792
22	0.997770	747	724	701	678	655	632	608	585	561
23	0.997538	514	490	466	442	418	394	369	345	320
24	0.997296	271	246	221	196	171	146	120	095	069
25	0.997044	018	*992	*967	*941	*914	*888	*862	*836	*809
26	0.996783	756	729	703	676	649	621	594	567	540
27	0.996512	485	457	429	401	373	345	317	289	261
28	0.996232	204	175	147	118	089	060	031	002	*973
29	0.995994	914	885	855	826	796	766	736	706	676
30	0.995646	616	586	555	525	494	464	433	402	371

\* Where values are designated with an asterisk, the first three figures are to be supplied from the zero column in the next lower row.

## CONCENTRATION SCALES

No one concentration scale is well suited to all purposes; the different scales possess advantages or disadvantages as situations change. The mole-fraction scale is useful in theoretical work because it is symmetrical with respect to all components and because several measurable properties of an "ideal" solution are proportional to mole fraction. When transport phenomena are being studied, a volume-based scale such as molarity must be employed as is convenient in analytical chemistry. The molality scale, on the other hand, is useful in dealing with equilibrium phenomena.

In macromolecular chemistry one often works with substances of unknown molecular weight, and the scales grams per milliliter and per 100 ml, weight per cent, and volume fraction find application. The weight per cent scale (along with mole fraction and molality) is independent of temperature and pressure, but it cannot be used in the description of flow processes.

Some definitions for six familiar concentration scales are listed below, where  $g$  = gram,  $M$  = molecular weight of components 1, 2, 3, etc., from  $j$  to  $q$ , and  $n$  = number of moles:

1. Mole fraction

$$X_i = \frac{g_i/M_i}{\sum_{j=1}^q g_j/M_j} = \frac{n_i}{n_1 + n_2 + \cdots + n_q}$$

2. Molality (moles component  $i$  per 1000 g component 1)

$$m_i = \frac{1000g_i}{g_1M_i} = \frac{1000n_i}{n_1M_1}$$

3. Molarity (moles of  $i$  per liter of solution having density  $\rho$ )

$$c_i = \frac{1000\rho g_i/M_i}{\sum_{j=1}^q g_j} = \frac{1000\rho n_i}{n_1M_1 + n_2M_2 + \cdots + n_qM_q}$$

4. Grams  $c$  of component  $i$  per 100 ml of solution

$$c_i = \frac{100\rho g_i}{\sum_{j=1}^q g_j} = \frac{100\rho n_iM_i}{n_1M_1 + n_2M_2 + \cdots + n_qM_q}$$

5. Weight per cent of component  $i$ 

$$w_i = \frac{100g_i}{\sum_{j=1}^q g_j}$$

6. Volume fraction  $\phi$  of component  $i$  ( $\bar{v}$  = partial specific volume in solution)

$$\phi_i = \frac{\rho \bar{v}_i g_i}{\sum_{j=1}^q g_j} = \frac{c_i \bar{v}_i}{100}$$

COLOR-CODE CONVENTIONS FOR  
ELECTRONIC-CIRCUIT COMPONENTS

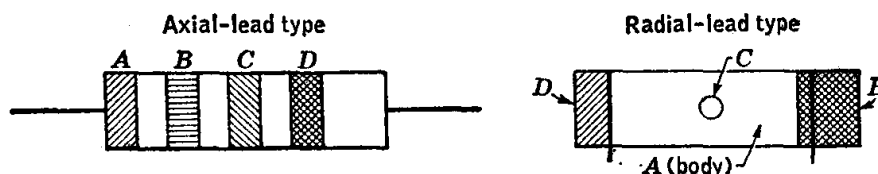
## I. Resistors and Capacitors

## Color Code

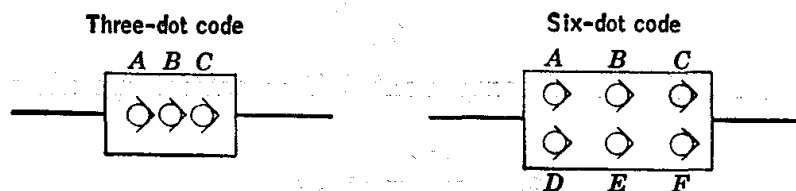
Color	Significant figure	Decimal multiplier	Tolerance, per cent, 1938 RMA standard	Voltage rating, <sup>a</sup> 1938 RMA standard
Black.....	0	1		
Brown.....	1	10	1	100
Red.....	2	100	2	200
Orange.....	3	1,000	3	300
Yellow.....	4	10,000	4	400
Green.....	5	100,000	5	500
Blue.....	6	1,000,000	6	600
Violet.....	7	10,000,000	7	700
Gray.....	8	100,000,000	8	800
White.....	9	1,000,000,000	9	900
Gold.....	...	0.1	± 5	1000
Silver.....	...	0.01	± 10	2000
No color.....	...	.....	± 20	500

<sup>a</sup> Capacitors only.

## Resistors

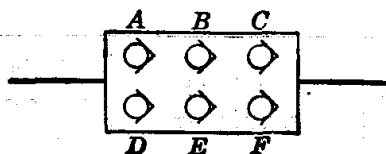


- A. First significant figure, resistance in ohms  
 B. Second significant figure  
 C. Decimal multiplier  
 D. Tolerance

**Fixed Mica Capacitors****1. Radio Manufacturers Association 1938 Standard**

- A. First significant figure  
 B. Second significant figure  
 C. Decimal multiplier  
 500 volts, 20 per cent tolerance only

- A. First significant figure  
 B. Second significant figure  
 C. Third significant figure  
 D. Voltage rating  
 E. Tolerance  
 F. Decimal multiplier

**2. American War Standard and Joint Army-Navy Code**

- A. Always black (mica condenser)  
 B. First significant figure  
 C. Second significant figure  
 D. AWS or JAN characteristic  
 E. Tolerance  
 F. Decimal multiplier

**II. RMA Transformer Color Code****Power transformers:**

- Primary—black  
 High-voltage winding—red; center tap, red and yellow  
 Rectifier filament winding—yellow; center tap, yellow and blue  
 Filament winding No. 1—green; center tap, green and yellow  
 Filament winding No. 2—brown; center tap, brown and yellow  
 Filament winding No. 3—slate; center tap, slate and yellow

**Audio transformers:**

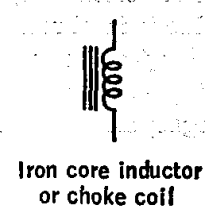
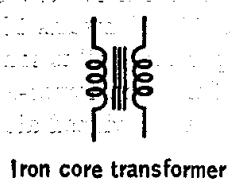
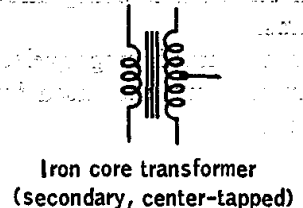
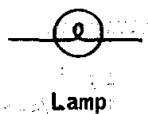
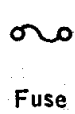
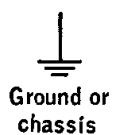
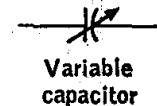
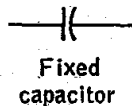
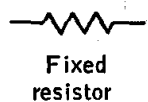
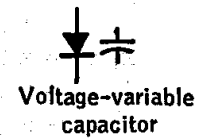
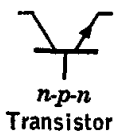
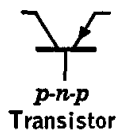
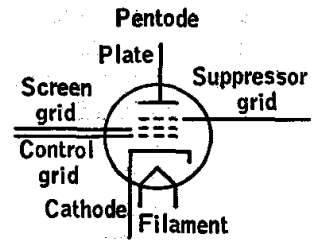
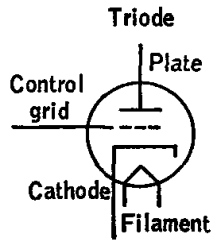
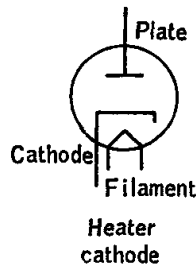
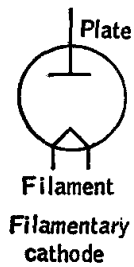
- Blue—plate lead  
 Red—B<sup>+</sup> lead  
 Brown—second plate on push-pull  
 Green—grid lead  
 Black—ground lead  
 Yellow—second grid on push-pull

**Intermediate frequency transformers:**

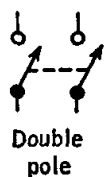
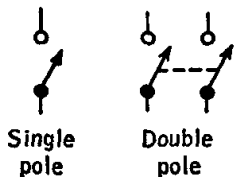
- Blue—plate lead  
 Red—B<sup>+</sup> lead  
 Green—grid lead  
 Black—ground (or AVC)  
 For center-tapped IF transformer, second grid is green-and-black-striped

# SCHEMATIC SYMBOLS FOR ELECTRONIC-CIRCUIT COMPONENTS

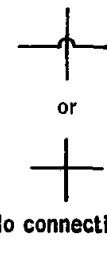
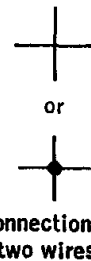
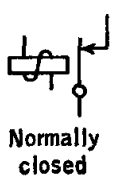
## Diodes



## Switches



## Relays





## COMMON ABBREVIATIONS OF ELECTRONICS

## Units:

a	= ampere
c	= cycle
c/sec	= cycle per second
f	= farad
h	= henry
v	= volt
w	= watt
$\Omega$	= ohm

## Unit prefixes:

p	= pico-	$= 10^{-12}$
$\mu$	= micro-	$= 10^{-6}$
m	= milli-	$= 10^{-3}$
k, K	= kilo-	$= 10^3$
M	= mega-	$= 10^6$
G	= giga-	$= 10^9$

## Miscellaneous:

a-c, A-C	= alternating (i.e., time-dependent, with average value zero)
db	= decibel [measure of relative power: $\text{db} = 10 \log (P_2/P_1)$ ]
d-c, D-C	= direct (i.e., time-independent)
p-p	= peak-to-peak
rms	= root-mean-square (page 544)
VAC	= volts a-c (rms value)
VCT	= volts, center-tapped (transformer winding)

## Examples:

1 $\mu\text{f}$	= 1 pf = 1 micromicrofarad = $10^{-12}$ farad
1 Mc/sec	= 1 megacycle per second = $10^6$ cycles per second
1 KMc/sec	= 1 kilomegacycle per second = $10^9$ cycles per second
1 K	= 1 kilohm = $10^3$ ohms

For *resistances*, the symbol  $\Omega$  is very often omitted, it being understood that the value is in ohms. Thus 100 K means  $10^5$  ohms.

For *frequencies*, the "per second" is sometimes omitted, megacycles per second then being abbreviated as Mc. The lower-case m is sometimes used for mega-, so that megacycles per second is abbreviated also as mc.

## *Index*

- Abbe refractometer, 55, 418
- Absorbancy, 101
- Absorbancy indices, 145
- Absorption and dispersion of radiation, 522
- Absorption coefficient, 529
- Absorption line, 526, 530
- Absorption spectrum, 100
- A-c circuit theory, 543
- Acid catalysis, 140, 143
- Acid dissociation constant, 107
  - apparent, 159
- Actinometer, 339
- Activated complex, 131
- Activation energy, 131
- Activity, 78
- Activity coefficient, 52, 67, 82, 160, 185
- Activity quotient, 185
- Adiabatic calorimeter process, 31
- Adiabatic combustion calorimeter, 16
- Admittance, 548
- Adsorption, 328, 497
  - of gases, 333
- Adsorption isotherms, 333
- Algebra of complex numbers, 609
- Amici prisms, 56
- Amplification, 566
- Amplification factor, 565
- Amplifier, 599
  - narrow-band, 598
- Amplitude-modulated waveform, 556
- Amplitude modulation, 556
- Angstrom unit, 243
- Angular momentum, 262, 281
- Anharmonicity, 257
- Anion-exchange resin, 306, 329
- Anions, 158
- Anisotropic crystals, 237
- Anode, 172
- Anti-Stokes lines, 249
- Apparent dissociation constant, 159
- Apparent equilibrium constant, 93, 206
- Apparent molal volume, 88
- Appendix, 609
- Arcs, 504
- Arrhenius heat of activation, 131
- Arrhenius theory, 159
- Associated liquids, 225
- Association, 111
- Atomic weight, 3
- Audio amplifier, 598
- Audio oscillator, 601
- Avogadro constant, 611
- Axis of rotatory inversion, 288
- Azeotrope composition, 66
  - pressure dependence, 66
- Azeotropes, 53, 66
- Azeotropic composition, 58
- Ballast tank, 41
- Balmer series, 245
- Bandwidth, 520, 539, 551, 558, 559
- Barns, 351
- Barometer corrections, 611, 612
- Barrier-layer cells, 512
- Beckmann thermometer, 431
- Beer-Lambert law, 101
- Benzene purification, 499
- Bernoulli equation, 150
- Berthelot's equation, 13, 43
- Beta particles, 343
- Binary mixture, analysis, 108
- Binary solid-liquid system, 116
- Binary solution, 51
- Boiling point, determination, 445
  - elevation, 73
- Boiling-point constant, 77
- Boiling-point diagram, 58
- Boiling-point elevation constant, 73
- Bolometer, 511, 537
- Boltzmann constant, 45, 611
- Bomb calorimeter, 15, 16
- Born-Oppenheimer approximation, 254
- Bourdon gauge, 442
- Bouyancy correction, 453
- Bragg's law, 290
- Bridge-rectifier power supply, 572
- Bromination of acetone, 143
- Bubble-plate fractionating column, 63
- Buffer capacity, 197
- Buffers, 196, 200
- Calomel electrode, 190
- Calorie, 610
- Calorimeter, 24, 34
- Calorimetry, 437
- Capacitance, 482, 543, 586
- Capacitance measurements, 482

- Capacitors, 615, 616
- Capillary condensation, 33
- Capillary-rise method, 321
- Cathode, 173
- Cathode follower, 593, 595
- Cathode-ray oscilloscope, 583
- Cation-exchange resin, 306, 329
- Cations, 158
- Cell constant, 158, 233
- Cells, with transference, 174
  - without transference, 193, 194, 208
- Center of symmetry, 288
- Centrifugal-distortion coefficient, 257
- Centrifugal-distortion constants, 283
- Centrifugal energy, 256
- Cerenkov radiation, 492
- Characteristic curve of photographic plate, 515
- Characteristic curves, 386, 562, 575
  - for pentode, 569
- Chemical kinetics, 129
- Chemical potential, 51
- Chromatography, 306
- Circuit elements, 548
- Circularly polarized light, 237
- Clapeyron equation, 39
- Clausius-Clapeyron equation, 39, 334
- Coefficient, of expansion, 85
  - of viscosity, 147, 296
- Colligative properties, 301
- Collimator, 243
- Collision diameter, 45
- Color-code conventions, 615
- Combustion heat, 15
- Complex conjugate, 610
- Complexing agent, 307
- Components, 121
- Concentration scales, 614
- Conductance, 136, 137, 157
  - at high frequencies, 483
  - potassium chloride solution, 475
  - pumping systems, 367, 371
- Conductance cell, 163
- Conductance water, 163, 475
- Conduction band, 570
- Conductivity cells, 473, 474
- Constant-boiling composition, 59
- Constant current supply, 592
- Constant-pressure calorimeter, 29
- Constants, physical-chemical, values, 610
- Cooling curves, 116, 118
- Cottrell boiling-point apparatus, 75
- Coulombs, 167
- Coulometer, 476
- Countercurrent-distribution, 112
- Counters, Geiger-Müller, 487, 489
  - neutron, 492
  - proportional, 489
- Counting circuit, 604
- Coupling constants, 271
- Cross section, 351
- Dark reaction, 341
- D'Arsonval galvanometer, 464
- Deadweight gauge, 443
- Degree, of cross linking, 317
  - of dissociation, 96
- Density, 452
- Depolarization factor, 250
- Detector, diode, 573
  - phase-sensitive, 606
- Deuterium oxide, 357, 485
- Developer, 514
- Developing photographic plates, 516
- Dewar flask, 34
- Diamagnetic shielding, 267
- Dielectric constant, 212, 213, 480
  - frequency dependence, 218
  - of polar liquids, 223
  - of a solid, 231
  - static, 214
- Differential distribution curves, 311
- Differential heat of solution, 22, 125, 214
- Diffraction, 288
- Diffraction angles, 294
- Diffusion, 458
  - restricted, 459
  - steady-state, 459
- Diffusion current, 175, 179
- Diffusion pump, 46
- Dilute solution, 81
- Dilution, integral heat, 23
- Diode detector circuit, 573
- Diode rectification, 560
- Diodes, 571
- Dipolar ion, 199
- Dipole moment, 212
  - permanent, 214
- Dispersion curve, 247
- Displacement field vector, 213
- Dissociation of nitrogen tetroxide, 96
- Distillation, azeotropic, 497
  - fractional, 449
  - high-vacuum, 451
- Distilling apparatus, 54
- Distribution coefficient, 110, 308
- Distribution law, 111
- Drop-weight apparatus, 327
- Drop-weight method, 322
- Dropping-mercury electrode, 175
- DuNouy ring-pull apparatus, 325
- Dynamic-transfer characteristic, 564
- Dynamical variable, 264
- Ebullimeters, 446
- Eccles-Jordan trigger circuit, 602
- Eigenvalues, 266
- Electric field, 213
- Electric field strength, 167
- Electric vector, 237
- Electrical conductance, 157
- Electrical energy, 27, 477
  - measurement, 477
- Electrical heating, 37
- Electrical measurements, 463
- Electrical work, 208
- Electrochemical cells, 183, 210
  - thermodynamics, 208

- Electrode potentials, 183
- Electrolysis, 172
- Electrolytic conductance, 471
- Electromagnetic spectrum, 519
- Electromotive force, 183
  - standard, 184
- Electron microscope, 425, 426
- Electronic charge, 611
- Electronic-circuit components, 615, 617
- Electronic potential function, 255
- Electronic regulator, 591
- Electronics, 384, 542
  - abbreviations, 618
  - schematic symbols, 617
- Electroscope, 488
- Element of symmetry, 288
- Elevation of boiling point, 73
- Energy distribution, 343
- Energy-level diagram, 279
- Energy levels, 256
- Enthalpy, of combustion, 15
  - of formation, 21, 31
  - of a solute, 28
  - of sublimation, 49
  - of vaporization, 39
- Enthalpy change, 30
- Entropy of activation, 131
  - for viscous flow, 154
- Entropy change, 66, 202
- Equations for representing data, 409
- Equilibria, heterogeneous, 110
- Equilibrium in solution, 93
- Equilibrium constant, 93, 100, 202
  - apparent, 93, 206
  - thermodynamic, 93
- Equivalent conductance, 158
- Equivalent generators, 552
- Equivalent networks, 549
- Error of counting determinations, 404
- Error function, 394
- Error problems, 414
- Errors of measurement, 393
  - (See also Experimental errors)
- Eutectic point, 118
- Exchange reactions, 357
- Experimental errors, estimation, 396
  - influence on final result, 398
- Extraction, 111
- Eyring equation, 131
- Eyring theory, 153
  
- Falling-ball method, 152
- Falling-ball viscometer, 152, 155
- Falling-drop method, 455
- Faraday, M., 167
- Faraday constant, 611
- Feedback, 596
  - inverse, 597
  - negative, 597
- Fick's laws, 458
- Field-modulation method, 525
- Figure of merit, 540
- Figure axis, 279
- Filters, 590
  - gelatine, 507
  - interference, 507
  - optical, 506
- First law of thermodynamics, 16, 27
- First-order reaction, 129, 140
- Flash photolysis, 505
- Flowmeter, 439, 441
- Force-elongation curve, 316
- Forepump, 368
- Fourier integral analysis, 555
- Fourier series analysis, 555
- Fractional distillation, 60, 449
- Fractionating column, 63
- Freas-type conductance cell, 163
- Free energy, 66, 202
  - of activation for viscous flow, 153
- Free surface energy, 324
- Freezing point, 86, 118
- Freezing-point apparatus, 84
- Freezing-point depression constants, 86
- Freezing-point depression data, 78
- Frequency counter, 587
- Frequency distribution of noise, 578
- Frequency measurement, 586
- Frequency modulation, 557
- Frequency spectrum, 556
- Frequency standards, 587
- Freundlich adsorption isotherm, 330, 333
- Fugacity, 51
- Fugacity coefficient, 51
  
- Galvanometer sensitivity, 180
- Galvanometers, 463
  - amplified, 466
  - period of, 464
  - portable, 465
- Gamma radiation, 493
- Gas, ideal, 3
  - ideal constant, 3
- Gas-adsorption apparatus, 335
- Gas constant, 611
- Gas density, 3
- Gas-density balance, 7
- Gas-saturation method, 59, 448
- Gases, 3, 439
- Gauge, Bourdon, 443
  - deadweight, 443
- Gaussian function, 394
- Geiger-Müller counter, 487, 489
- Geiger-Müller tube, 345
- Gibbs free energy, 66
- Gibbs free-energy change, 96, 208
- Gibbs-Duhem equation, 66
- Gibbs-Helmholtz equation, 96, 209
- Glass electrode, 195
- Glassblowing, 361
- Glycine titration, 200
- Graphs, 408
- Grid, 561
- Guggenheim method, 140
- Gyromagnetic ratio, 266
  
- Hagen-Poiseuille equation, 149
- Half-wave potential, 176

- Hamiltonian operator, 266, 283
- Harmonic generation, 558
- Heat, of combustion, 15
  - of neutralization, 38
  - of reaction in solution, 29
  - of solution, 22
  - of sublimation, 49
  - of vaporization, 43 "
- Heater control circuit, 595
- Height equivalent per theoretical plate, 64
- Herz-Knudsen equation, 45
- Heterodyne-beat method, 212
- Heterodyning, 557
- Heterogeneous equilibria, 110
- High-polymer solutions, 296
- High-resolution NMR spectrum, 275
- High vacuum, 367
- High-vacuum distillation, 451
- Hittorf apparatus, 170
- Hittorf method, 170
- Homogeneous equilibria, 93
- Hot atom, 505
- Hydrogen electrode, 190
- Hydrolysis, 129
- Ice point, 611
- Ideal dilute solution, 81
- Ideal-gas law, 3
- Ideal solution, 52, 81
- Ignition circuit, 18
- Immiscible solvents, 110
- Impedance, 547, 550
  - of network, 548
- Impedance bridge, 234, 481
- Impedance matching, 553
- Induced moment, 215
- Inductance, 482, 543, 586
- Infrared absorption spectrum, 254
- Infrared spectrometer, 534, 538
- Infrared spectrophotometer, 535
- Infrared spectroscopy, 541
- Integral heat, of dilution, 23
  - of solution, 22, 72
- Interfacial tension, 321
- Interferometric methods, 422
- Internal conversion, 355
- Internal energy, 17
- Internal field, 215
- International temperature scale, 428
- Intrinsic viscosity, 296
- Inversion of sucrose, 139
- Ion-exchange column, 309
- Ion-exchange resin, 306
- Ionic mobility, 167
- Ionization chamber, 487
- Ionization gauges, 378
- Irreversible processes, 147
- Isomeric transition, 355
- Isopiestic method, 449
- Isoteric heat of adsorption, 337
- Isotopes, 484
  - stable, 485
- Isotropic crystals, 237
- Isotropic substances, 213
- Johnson noise, 578
- Kinetics, 129
- Knudsen cell, 46
- Knudsen gas, 372
- Knudsen method, 44
- Langmuir adsorption isotherm, 330, 334
- Latent image, 514
- Lattice constant, 290
- Leak detection, 380
- Light scattering, 422
- Light-scattering apparatus, 423
- Light sources, 502
- Liquid-junction potential, 185
- Liquid-vapor equilibrium, 51
- Lissajous pattern, 585
- Littrow mirror, 537
- McLeod gauge, 376
- Macromolecules, 296
- Magnetic coupling, 553
- Magnetic dipole, 263
- Magnetic moment, 263
- Magnetically coupled circuit, 553
- Manometer, 5, 440
  - closed-end, 4, 7, 42
  - open-end, 42
- Mark-Houwink equation, 297
- Mass spectrometry, 485
- Mean activity coefficients, 189
- Mean ionic activity coefficient, 161
- Mercury arc, 502, 503
- Mercury purification, 499
- Mercury thermometers, 429
- Mercury-vapor diffusion pump, 369
- Mercury-vapor lamp, 340
- Method, of averages, 411
  - of least squares, 413
- Methyl red, 107
- Meyer (Victor) method, 9
- Microbar, 367
- Microns, 367
- Microscopy, 424
- Microwave absorption line, 529
- Microwave frequency equipment, 534
- Microwave frequency standard, 533
- Microwave spectrograph, 531
- Microwave spectrometer, 529
- Microwave spectroscopy, 541
- Miller indices, 290
- Mirror plane, 288
- Mixing cell, 106
- Mixing flask, 137
- Mixing waving forms, 557
- Moderators, 352
- Molal boiling-point elevation constant, 73, 77
- Molality, 22, 614
- Molar absorbandy index, 101
- Molar Gibbs free energy, 78
- Molar refraction, error in, 399
- Molar refractivity, 218
- Molar volume, 88
- Molarity, 614

- Mole fraction, 614
- Molecular structure, 254
- Molecular weight, 297
  - apparent, 74
  - average, 96
  - distribution, 302
  - number-average, 301, 302
  - weight-average, 302
- Moment of inertia, 256, 280
- Monochromators, 508
- Monomer unit, 300
- Moving-boundary apparatus, 166, 479
- Moving-boundary method, 165
- Multimeters, 581
  
- Neutron-capture cross section, 351
- Neutron counters, 492
- Newtonian fluid, 148
- Nicol prism, 237
- Nitrogen tetroxide, 96
  - handling, 97
- NMR spectroscopy, 262, 266
- Noise, 577
  - current, 579
  - flicker-effect, 579
  - frequency distribution, 578
  - Johnson, 578, 580
  - shot, 580
  - shot-effect, 579
- Noise figure, 579
- Noise sources, 580
- Normal liquids, 225
- Normal mode of vibration, 250
- Normalized distribution function, 404
- Norton's theorem, 553
- Nuclear chemistry, 484
- Nuclear induction method, 276
- Nuclear magnetic resonance (NMR), 523, 541
- Nuclear-magnetic-resonance spectrometer, 524, 527
- Nuclear-magnetic-resonance spectroscopy, 262, 266
- Nuclear spin angular momentum, 265
- Number-average molecular weight, 301, 302
- Numerical aperture, 424
  
- Oblate, 281
- Oil diffusion pump, 370
- Operators, commutability, 264
- Optical absorbancy, 101
- Optical pyrometers, 436
- Optical rotatory dispersion, 236
- Opticochemical measurements, 418
- Organic yield, 350
- Oscillator, 220, 599
- Oscilloscope, 583
- Oscilloscope photographs, 578
- Oscilloscope tube, 584
- Osmometer, 303, 461
- Osmotic coefficient, 82
- Osmotic pressure, 301, 305, 460
- Ostwald viscometer, 149
  
- Parallel resonant circuit, 550
- Partial molal property, 87
- Partial molal volumes, 88
- Partial molar enthalpy, 33
- Partial molar Gibbs free energy, 78
- Partial-molar-heat capacities, 33
- Particle size distribution, 310
- Pentode, 568
- Per cent transmission, 104
- pH, 196
- Phase diagram, 116
- Phase distribution, 110
- Phase equilibrium, 67
- Phase relationships, 544
- Phase rule, 121
- Phase-sensitive detector, 606
- Phillips gauge, 379
- Photochemistry, 339, 502
- Photoelectric cells, 511
- Photography, 514
- Photohydrolysis of monochloroacetic acid, 339
- Photomultiplier tubes, 512
- Photovoltaic cells, 512
- Physical-chemical constants, 610
- Pirani gauge, 377
- pK value, 198
- Plait point, 122
- Planck constant, 611
- Plane-polarized light, 236, 237
- Platinizing, 192
- Point group, 288
- Poise, 148
- Poiseuille's law, 371
- Polarimeter, 239
- Polarimetry, 426
- Polarizability, 215
- Polarization, 213
- Polarogram, 176
- Polarography, 175
- Potential-energy curve, 255
- Potentiometer, 187, 466
- Potentiometer circuit, 467
- Potentiometers, recording, 468
- Power supply, 588
- Power-supply circuit, 588
- Principal axes, 280
- Probable error, 395
  - of the mean, 395
- Products of inertia, 280
- Prolate, 281
- Propagation of probable errors, 401
- Proportional counter, 487, 489
- Proton relative chemical-shift values, 269
- Pulfrich refractometer, 419
- Pulse counting, 603
- Pulse height, 487
- Pulse-height analyzer, 491
- Pumping speed, 367
- Pumps, 444
- Purification of materials, 495
- Purification methods, 496
- Pycnometers, 90, 452
- Pyrex properties, 361
- Pyrometers, 436, 437

- Quantum yield, 339  
Quinhydrone, 207
- Radiation chemistry, 493  
Radiation dosage, 494  
Radiation safety, 493  
Radicals, production, 505  
Radioactive isotopes, 343  
Radiofrequency spectrometer, 528  
Radioisotopes, 484  
Radium-beryllium source, 352  
Raman apparatus, 251  
Raman effect, 248  
Raman frequency, 249  
Raman frequency shift, 249  
Raman spectrum, 248  
Raman tube, 251  
Ramsay-Young apparatus, 40  
Random errors, 393, 394  
Range of  $\beta$  particles, 343, 347  
Range-energy relation, 348  
Rate, of disintegration, 350  
    of reaction, 129  
Rate law, 144  
Reaction, first-order, 129  
    second-order, 129  
Reaction cells, 513  
Reaction-rate constant, 129  
Rectification, 560  
Reduced mass, 255  
Reduction potential, 206  
Reference electrode, 184  
Refractive index, 55, 419  
    of air, 259  
Refractometer, differential, 420  
    Pulfrich, 419  
Refractometry, 418  
Relative humidity, 13  
Relay, vacuum-tube, 593  
Relay circuit, 594  
Representation of data, 405  
Residuals, 394  
Resistance, 482, 543, 586  
Resistors, 615  
Resolution, 520  
Resolving power, 424  
Resonance apparatus, 227  
Resonance circuit, 229  
Resonance method, 223, 226  
Response time, 520  
Reynolds number, 150, 153  
Ring method, 322  
Rotameter, 440, 441  
Rotary oil pumps, 368  
Rotational coefficient  $B_r$ , 257  
Rotational constants, 283  
Rotational energy levels, 256  
Rotational freedom, 232  
Rotational spectrum, 278  
Rubberlike elasticity, 316  
Rydberg constant, 245
- Safety, 608  
Scattering theory, 289
- Schlieren optical system, 421  
Schlieren techniques, 420  
Scintillation counters, 347, 490  
Scintillation detector, 490  
Second-order reaction, 129, 135  
Sedimentation rate, 310  
Sedimentation-tube assembly, 312  
Selection rules, 258, 286  
Self-absorption curve, 348  
Semiconductor diode, 572  
Semiconductors, 570  
Sensitivity, 520  
Shearing force, 147  
Shielding constant, 267  
Side-band method, 268  
Signal-to-noise ratio, 539  
Significant figures, 404  
Silver-silver chloride electrode, 190  
Single-electrode potentials, 183  
Sinusoidal waveforms, 544  
Sodium chloride purification, 500  
Sodium hydroxide purification, 500  
Soft glass, properties, 361  
Solid-state detectors, 491  
Solubility, 121, 124  
Solute, association, 83  
    dissociation, 83  
Solutions, 51  
    filter, 506  
Space lattice, 289  
Specific conductance, 158  
Specific resistance, 158  
Specific rotation, 240  
Specific viscosity, 296  
Spectrograph, constant-deviation, 244  
Spectrography, 243  
Spectrometer, for high resolution  
    (NMR), 527  
    infrared, 534  
    microwave, 529  
    NMR, 524  
Spectrometer radiofrequency, 522, 528  
Spectrometry, 243  
Spectrophotometer, 103, 104  
Spectrophotometer cell, 106  
Spectroscopic methods, 254  
Spectroscopy, 243, 519  
Spin angular momentum, 265, 266  
Spin-coupling constant, 270  
Spin-spin coupling, 270  
Square wave, 555  
Standard atmosphere, 610  
Standard boiling point, 39  
Standard buffers, 196  
Standard cells, 468  
Standard deviation, 395  
    of the mean, 395  
Standard electrodes, 469  
Standard electromotive force, 184  
Standard entropy change, 202  
Standard-free-energy change, 202  
Standard gravity, 620  
Stark cell, 530  
Stark components, 532

- Stark effect, 278, 530
- Stark-effect modulation spectrometer, 530
- Stark-effect patterns, 286
- Stark splittings, 279
- Staudinger (unit), 296
- Stem correction, 430
- Stokes' law, 310
- Stokes lines, 249
- Sublimation pressure, 44
- Supercooling, 118, 120
- Superheating, 74, 446
- Surface chemistry, 321
- Surface energy, 324
- Surface tension, 321, 457
  - capillary-rise method, 322, 324
  - drop-weight method, 322, 327
  - ring method, 322, 325
- Susceptibility, 213
- Sweep frequency, 584
- Symbols, electronic, 618
  - physical-chemical, 617
- Symmetry, 280
- Symmetry operation, 288
- Systematic errors, 393
- Szilard-Chalmers process, 349
  
- Table, functional, 405
  - statistical, 405
- Taylor series, 79
- Temperature scale, 428
- Ternary diagram, 122
- Test equipment, 581
- Theoretical plate, 61
- Thermal analysis, 120
- Thermal coefficient of expansion, 85
- Thermal, 434
- Thermistor, 25, 83, 571
- Thermochemistry, 15
- Thermocouple, 117, 433, 434
  - types, 435
- Thermocouple calibration, 120
- Thermocouple gauge, 377
- Thermodynamic activity, 52
- Thermodynamic equilibrium constant, 93
- Thermodynamic ionization constant, 160
- Thermodynamics, first law, 16, 27
- Thermometer, Beckmann, 431
  - bimetallic, 431
  - gas, 431
  - mercury, 429
  - resistance, 432
- Thermometry, 428
- Thermopile calibration, 510
- Thermopiles, 508
- Thévenin's theorem, 552
- Three-component system, 121, 122
- Tie line, 121
- Time standards, 587
- Toepler pump, 444
- Torque, 282
- Transconductance, 565
- Transference numbers, 165, 167, 170, 479
- Transformer color code, 616
- Transistors, 574
- Transition probability, 284
- Transpiration method, 448
- Treatment of experimental data, 393
- Triangular diagram, 121
- Triiodide ion, 113
- Triode, 561
- Triode amplifier, 563, 564
- Triode-amplifier circuit, 387, 567
  
- Unit cell, 289
  
- Vacuum gauges, 375, 379
- Vacuum pumps, 368, 374, 444
- Vacuum-tube oscillator, 598
- Vacuum-tube relay, 593
- Vacuum tubes, 559
- Valence band, 570
- van Laar coefficients, 53
- van Laar equations, 53, 68
- van't Hoff equation, 125
- Vapor composition, 65
- Vapor density, 9
- Vapor-liquid graph, 61
- Vapor-pressure apparatus, 41
- Vapor pressures, 39, 447
  - benzene, 59
  - ethanol, 59
- Variance, 121
- Velocity gradient, 147
- Velocity profile, 149
- Vibration-rotation interaction, 257
- Vibrational energy levels, 249, 256
- Victor Meyer apparatus, 10
- Victor Meyer method, 9
- Vigreux column, 63
- Viscometer, 149
- Viscometry, 456
- Viscosity, 147, 296
- Viscosity number, 296
- Voltage regulators, 590
- Voltmeters, 466
- Volume fraction, 615
  
- Wagner grounding circuit, 162
- Washburn correction, 17
- Water, density, 613
  - purification, 499
  - vapor pressure, 612
- Wave number, 243
- Waveforms, 545
- Weight-average molecular weight, 302
- Weight per cent, 615
- Weston cell, 468, 469
- Westphal balance, 454
- Wheatstone bridge, 26, 161, 471
- Wheatstone-bridge circuit, 472
  
- X-ray diffraction, 288
- X-ray powder camera, 293
  
- Zener diode, 574
- Zone refining, 498
- Zwitter ion, 198





